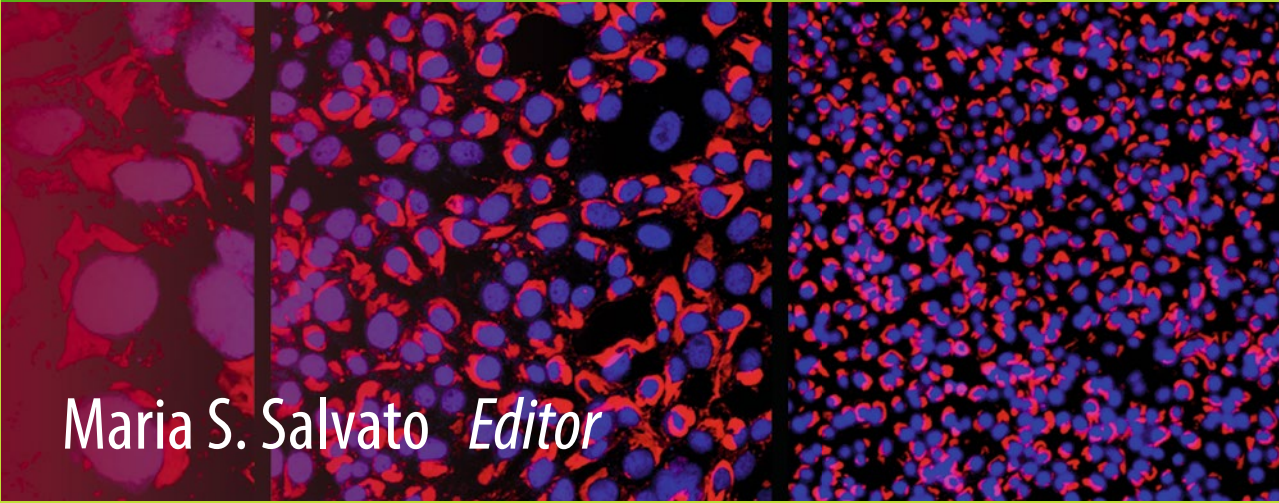


Methods in
Molecular Biology 1604

Springer Protocols



Maria S. Salvato *Editor*

Hemorrhagic Fever Viruses

Methods and Protocols

 Humana Press

METHODS IN MOLECULAR BIOLOGY

Series Editor
John M. Walker
School of Life and Medical Sciences
University of Hertfordshire
Hatfield, Hertfordshire, AL10 9AB, UK

For further volumes:
<http://www.springer.com/series/7651>

Hemorrhagic Fever Viruses

Methods and Protocols

Edited by

Maria S. Salvato

School of Medicine, University of Maryland, Baltimore, MD, USA

 **Humana Press**

Editor

Maria S. Salvato
School of Medicine
University of Maryland
Baltimore, MD, USA

ISSN 1064-3745 ISSN 1940-6029 (electronic)
Methods in Molecular Biology
ISBN 978-1-4939-6980-7 ISBN 978-1-4939-6981-4 (eBook)
DOI 10.1007/978-1-4939-6981-4

Library of Congress Control Number: 2017935485

© Springer Science+Business Media LLC 2018

This work is subject to copyright. All rights are reserved by the Publisher, whether the whole or part of the material is concerned, specifically the rights of translation, reprinting, reuse of illustrations, recitation, broadcasting, reproduction on microfilms or in any other physical way, and transmission or information storage and retrieval, electronic adaptation, computer software, or by similar or dissimilar methodology now known or hereafter developed.

The use of general descriptive names, registered names, trademarks, service marks, etc. in this publication does not imply, even in the absence of a specific statement, that such names are exempt from the relevant protective laws and regulations and therefore free for general use.

The publisher, the authors and the editors are safe to assume that the advice and information in this book are believed to be true and accurate at the date of publication. Neither the publisher nor the authors or the editors give a warranty, express or implied, with respect to the material contained herein or for any errors or omissions that may have been made. The publisher remains neutral with regard to jurisdictional claims in published maps and institutional affiliations.

Cover illustration: Detecting Ebola virus replication by the RNA-FISH method, Lindquist and Schmaljohn, Chapter 14

Printed on acid-free paper

This Humana Press imprint is published by Springer Nature
The registered company is Springer Science+Business Media LLC
The registered company address is: 233 Spring Street, New York, NY 10013, U.S.A.

Preface

Hemorrhagic fever viruses (HFV) include some of the most lethal agents of the microbial world. Disease onset can be rapid and fatal. HFV can be extraordinarily contagious and will spread in hospitals without sophisticated infection control. HFV disease is characterized by a rapid onset of fever, muscle ache, and “flu-like” symptoms, followed by liver necrosis, lymph node depletion, coagulation defects, and organ systems failure. Most people have subclinical HFV infections but the potential for severe disease distinguishes the HFV as a major public health threat. As high level threat agents, there will be unique rules for handling HFV in research settings [1, 2].

Most virology texts do not embrace the classification of “hemorrhagic fever viruses.” According to the rules for virus classification [3], viruses should not be classified according to the diseases they cause since a virus that makes one organism ill might not affect another. The most useful classifications should allude to the structure of the virion or the region where the virus was found. The appellation “hemorrhagic fever virus” is an operational name given to those viruses with unique potential to cause severe vascular leakage disease.

Hemorrhagic fever viruses frequently belong to the taxonomic families *Hantaviridae*, *Nairoviridae*, *Peribunyaviridae*, *Phenuiviridae*, *Arenaviridae*¹, *Flaviviridae*, *Filoviridae* and *Rhabdoviridae*. *Arenaviridae* include the largest number of viruses causing viral hemorrhagic fever (VHF) [4]. The importance of *Arenaviridae* is reflected in this book as 19 of 30 chapters focus on arenaviruses as experimental examples of HVE. This compilation of work from many laboratories makes reference to high-containment facilities and precautions for working with high risk-group agents, even though most of the protocols herein have broad utility and are applicable to less virulent Risk Group 2 agents, as well as to highly virulent Risk Group 4 Select Agents.

In May of 2015, during the height of the Ebolavirus disease outbreak in Western Africa, the world faced the ravages of Ebola virus disease and the toll it took on populations and health care workers who voluntarily entered the danger zones. While it is important to encourage appropriate responses to epidemic disease, this type of information blurs the lines between fearsome natural infections and the attenuated versions that are so necessary for effective biomedical research. For example, Reston virus, so named because it was discovered in a dying monkey colony in Reston Virginia, was later suspected to be an attenuated virus that had co-infected the monkeys with a simian hemorrhagic fever virus [5]. Because it was an ebolavirus, similar in form to the ebolaviruses that ravaged Zaire and Sudan, Reston virus was branded a Risk Group 4 Select Agent. A surveillance team traveled to the Philippines, the origin of the ill-fated monkey colony, to find the source of Reston virus. The virus was not found in bats or rodents, but was detected on farms where both pigs and farmers had been infected [6–8]. As a result, pigs were exterminated and the farmers were quarantined. Since the domestic pigs that became ill were also co-infected with porcine arteriviruses and/or circoviruses, it was not clear that clinical disease was due solely

¹As of June 2017, the former *Bunyaviridae* family is now the order *Bunyavirales* containing the virus families *Hantaviridae*, *Nairoviridae*, *Peribunyaviridae*, *Phenuiviridae* and *Arenaviridae*.

or even mainly to Reston virus infection. Fear instilled by the name “Ebola” may have caused scientists to overlook the potential benefits of having an attenuated virus for vaccine development and even overlooked the contribution of other infectious agents to the disease in Philippine pig farms. These challenges must be met by rigorous studies using commonly accepted practices and standards. This book is intended to help develop a common understanding of how best to approach the study of hemorrhagic fever viruses of many types and in many places.

This book has five parts. The first part on *Surveillance, diagnosis, and classification of hemorrhagic fever viruses* begins by discussing methods used to predict viral pandemics. Following this introductory chapter are two chapters on the methods and strategies for classifying viruses: one describes the open-source software available for classifying sequences obtained during surveillance, and the other describes Pairwise Sequence Comparison (PASC) to help determine genetic distances between taxa. Next, there is a chapter on viral diagnostics with specific methods for antibody capture using Lassa virus antigens. Three chapters address approaches for epidemiological surveillance: one on surveillance of clinical samples, one on field surveillance of arthropod-borne viruses, and the other on surveillance of rodent-borne viruses.

The second part of the book covers *Structural studies and reverse genetics of hemorrhagic fever viruses*. Three chapters describe studies on viral entry and on envelope membrane fusion. One chapter describes assays for glycoprotein function, another, assays for Z matrix protein functions, and two chapters cover the structure and functions of the arenavirus nucleocapsid protein (NP). A chapter on RNA fluorescence *in situ* hybridization (FISH) describes the subcellular localization of viral gene expression. The techniques successfully used to reveal universal budding mechanisms for filoviruses, arenaviruses, and rhabdoviruses are described in a chapter on using virus-like particles to study virus egress. One chapter describes polymerase function of the Crimean-Congo hemorrhagic fever virus, typical of the large multi-functional polymerases of the hemorrhagic fever viruses. Finally, there are two chapters devoted to reverse genetic systems: one for filoviruses and the other giving us two reverse genetic approaches for Pichindé virus.

The third part contains chapters on *In vivo models of hemorrhagic fever virus infection*. The chapter on murine models for VHF describes a quantitative measure for vascular leakage using Evan’s blue dye that could be applied to other animal models of VHF. The authors who gave us a chapter on the guinea pig model for VHF also used this model to test their antibody therapy for Ebola virus infection. A primate model for VHF summarizes the methods used to sample infected rhesus monkeys. Finally, we present a method to obtain a subset of primary human liver cells that can be cultured long term and used for HFV infections.

The fourth part contains *Immune assays and vaccine production for hemorrhagic fever viruses*. The first chapter in this part is a remarkable description of the facilities and procedures used to produce the live attenuated-Junín vaccine against Argentinian hemorrhagic fever. Next is a chapter on detecting virus-antibody immune complexes in secondary dengue infection. The last chapter in this part is on DNA vaccines from a laboratory renowned for promoting such vaccines for a number of hemorrhagic fever viruses.

The fifth and final part describes *Host responses to viral hemorrhagic fever*. First is a method for identifying host restriction factors controlling Junín or dengue virus infection. Then we present two chapters analyzing antivirals: one that determines the life cycle stage blocked by an antiviral, and another that uses high-throughput screening to find antivirals against a retroviral surrogate for a hemorrhagic fever virus. The last chapter is a cell culture method to assess coagulation after HFV infection.

Despite a tremendous amount of interest, there remains a gap between identifying viruses during surveillance and linking these agents to specific disease risks. Viruses that cause hepatitis, like the HFV, carry more risk for the malnourished, the immunosuppressed, or the aged [9] than for the young techies of Silicon Valley. Our goal here is to promote research on the disease mechanisms of HFV by offering detailed instructions on exploring structure/function of viral molecules and assessing virus effects in cell culture and in animal models. Armed with this type of information, we will eventually be able to do more than classify a virus' taxon but also find its actual risk group. Such research will move HFV from the category of bio-terrors to the category of manageable bio-threats.

Baltimore, MD, USA

Maria S. Salvato

References

1. BMBL rules. <http://www.cdc.gov/biosafety/publications/bmbl5/index.htm>. Accessed 10 Aug 2016
2. NIH Guidelines. http://osp.od.nih.gov/sites/default/files/NIH_Guidelines.html. Accessed April 2016
3. ICTV Code. <http://www.ictvonline.org/codeOfVirusClassification.asp>. Accessed Oct 2016
4. Zapata JC, Pauza CD, Djavani MM, Rodas JD, Moshkoff D, Bryant J, Ateh E, Garcia C, Lukashevich IS, Salvato MS (2011) LCMV infection of macaques: a model for Lassa fever. *Antiviral Research* 92 (2):125–138
5. McCormick JB, Fisher-Hoch S (1996) *Level 4 virus hunters of the CDC*. Turner Publishing, Inc, Atlanta p 308, ISBN 1-57036-277-7
6. WHO Reston report April 2009. http://www.who.int/csr/resources/publications/WHO_HSE_EPR_2009_2/en/. Accessed Aug2016
7. Barrette RW, Metwally SA, Rowland JM, Xu L, Zaki SR, Nichol ST, Rollin PE, Towner JS, Shieh WJ, Batten B, Sealy TK, Carrillo C, Moran KE, Bracht AJ, Mayr GA, Sirios-Cruz M, Catbagan DP, Lautner EA, Ksiazek TG, White WR, McIntosh MT (2009) Discovery of swine as a host for the Reston ebolavirus. *Science* 325: 204–206
8. Burk R, Bollinger L, Johnson JC, Wada J, Radoshitzky SR, Palacios G, Bavari S, Jahrling PB, Kuhn JH (2016) Neglected filoviruses. *FEMS Microbiol Rev* 40(4): 494–519
9. Scrimshaw NS, SanGiovanni JP (1997) Synergism of nutrition, infection, and immunity: an overview. *Am J Clin Nutr* 66(2):464S–77S

Contents

<i>Preface</i>	<i>v</i>
<i>Contributors</i>	<i>xiii</i>
PART I SURVEILLANCE, DIAGNOSIS AND CLASSIFICATION OF HEMORRHAGIC FEVER VIRUSES	
1 Global Spread of Hemorrhagic Fever Viruses: Predicting Pandemics	3
<i>Jean-Paul Gonzalez, Marc Souris, and Willy Valdivia-Granda</i>	
2 An Approach to the Identification and Phylogenetic Analysis of Emerging and Hemorrhagic Fever Viruses	33
<i>Francisco J. Díaz, Luis E. Paternina, and Juan David Rodas</i>	
3 Preliminary Classification of Novel Hemorrhagic Fever-Causing Viruses Using Sequence-Based PAirwise Sequence Comparison (PASC) Analysis	43
<i>Yīmíng Bào and Jens H. Kuhn</i>	
4 Epidemiological Surveillance of Viral Hemorrhagic Fevers With Emphasis on Clinical Virology	55
<i>Carolina Montoya-Ruiz and Juan David Rodas</i>	
5 Diagnostics for Lassa Fever: Detecting Host Antibody Responses	79
<i>Maria S. Salvato, Igor S. Lukashevich, Sandra Medina-Moreno, and Juan Carlos Zapata</i>	
6 Sampling Design and Mosquito Trapping for Surveillance of Arboviral Activity	89
<i>Luis E. Paternina and Juan David Rodas</i>	
7 Epidemiological Surveillance of Rodent-Borne Viruses (Roboviruses)	101
<i>Juan David Rodas, Andrés F. Londoño, and Sergio Solari</i>	
PART II STRUCTURAL STUDIES AND REVERSE GENETICS OF HEMORRHAGIC FEVER VIRUSES	
8 Entry Studies of New World Arenaviruses	113
<i>María Guadalupe Martínez, María Belén Forlenza, Nélida A. Candurra, and Sandra M. Cordo</i>	
9 Studies of Lassa Virus Cell Entry	135
<i>Antonella Pasquato, Antonio Herrador Fernandez, and Stefan Kunz</i>	
10 A Cell-Cell Fusion Assay to Assess Arenavirus Envelope Glycoprotein Membrane-Fusion Activity	157
<i>Joanne York and Jack H. Nunberg</i>	
11 Assays to Assess Arenaviral Glycoprotein Function	169
<i>Junjie Shao, Xiaoying Liu, Yuying Liang, and Hinh Ly</i>	

12	Expression and X-Ray Structural Determination of the Nucleoprotein of Lassa Fever Virus	179
	<i>Xiaoxuan Qi, Wenjian Wang, Haohao Dong, Yuying Liang, Changjiang Dong, and Hinh Ly</i>	
13	Assays to Demonstrate the Roles of Arenaviral Nucleoproteins (NPs) in Viral RNA Synthesis and in Suppressing Type I Interferon	189
	<i>Qinfeng Huang, Junjie Shao, Yuying Liang, and Hinh Ly</i>	
14	Intracellular Detection of Viral Transcription and Replication Using RNA FISH	201
	<i>Michael E. Lindquist and Connie S. Schmaljohn</i>	
15	Hemorrhagic Fever Virus Budding Studies	209
	<i>Ronald N. Harty</i>	
16	Roles of Arenavirus Z Protein in Mediating Virion Budding, Viral Transcription-Inhibition and Interferon-Beta Suppression.	217
	<i>Junjie Shao, Yuying Liang, and Hinh Ly</i>	
17	Structure–Function Assays for Crimean–Congo Hemorrhagic Fever Virus Polymerase	229
	<i>Marko Zivcec</i>	
18	Minigenome Systems for Filoviruses	237
	<i>Thomas Hoenen</i>	
19	Establishment of Bisegmented and Trisegmented Reverse Genetics Systems to Generate Recombinant Pichindé Viruses	247
	<i>Rekha Dhanwani, Qinfeng Huang, Shuiyun Lan, Yanqing Zhou, Junjie Shao, Yuying Liang, and Hinh Ly</i>	
PART III IN VIVO MODELS OF HEMORRHAGIC FEVER VIRUS INFECTION		
20	Murine Models for Viral Hemorrhagic Fever.	257
	<i>Rosana Gonzalez-Quintial and Roberto Baccala</i>	
21	Testing Experimental Therapies in a Guinea Pig Model for Hemorrhagic Fever	269
	<i>Gary Wong, Yuhai Bi, Gary Kobinger, George F. Gao, and Xiangguo Qiu</i>	
22	A Primate Model for Viral Hemorrhagic Fever	279
	<i>Maria S. Salvato, Igor S. Lukashevich, Yida Yang, Sandra Medina-Moreno, Mahmoud Djavani, Joseph Bryant, Juan David Rodas, and Juan Carlos Zapata</i>	
23	A Primary Human Liver Cell Culture Model for Hemorrhagic Fever Viruses	291
	<i>Mahmoud Djavani</i>	
PART IV IMMUNE ASSAYS AND VACCINE PRODUCTION FOR HEMORRHAGIC FEVER VIRUSES		
24	Protocol for the Production of a Vaccine Against Argentinian Hemorrhagic Fever	305
	<i>Ana María Ambrosio, Mauricio Andrés Mariani, Andrea Soledad Maiza, Graciela Susana Gamboa, Sebastián Edgardo Fossa, and Alejandro Javier Bottale</i>	

25	Detection of Virus-Antibody Immune Complexes in Secondary Dengue Virus Infection.	331
	<i>Meng Ling Moi, Tomohiko Takasaki, and Ichiro Kurane</i>	
26	Future Approaches to DNA Vaccination Against Hemorrhagic Fever Viruses	339
	<i>John J. Suschak and Connie S. Schmaljohn</i>	
PART V HOST RESPONSES TO VIRAL HEMORRHAGIC FEVER		
27	Identifying Restriction Factors for Hemorrhagic Fever Viruses: Dengue and Junín.	351
	<i>Federico Giovannoni, Jose Rafael Peña Cárcamo, María Laura Morell, Sandra Myriam Cordo, and Cybele C. García</i>	
28	Determining the Virus Life-Cycle Stage Blocked by an Antiviral	371
	<i>Claudia S. Sepúlveda, Cybele C. García, and Elsa B. Damonte</i>	
29	Retrovirus-Based Surrogate Systems for BSL-2 High-Throughput Screening of Antivirals Targeting BSL-3/4 Hemorrhagic Fever-Causing Viruses	393
	<i>Sheli R. Radoshitzky, Veronica Soloveva, Dima Gharaibeh, Jens H. Kuhn, and Sina Bavari</i>	
30	Protocols to Assess Coagulation Following In Vitro Infection with Hemorrhagic Fever Viruses	405
	<i>Melissa L. Tursiella, Shannon L. Taylor, and Connie S. Schmaljohn</i>	
	<i>Index</i>	419

Contributors

- ANA MARÍA AMBROSIO • *Instituto Nacional de Enfermedades Virales Humanas, Dr JI Maiztegui, ANLIS, Pergamino, Provincia de Buenos Aires, Argentina*
- ROBERTO BACCALA • *Department of Immunology and Microbial Sciences, The Scripps Research Institute, La Jolla, CA, USA*
- YIMÍNG BÀO • *Information Engineering Branch, National Center for Biotechnology Information (NCBI), National Library of Medicine (NLM), National Institutes of Health (NIH), Bethesda, MD, USA*
- SINA BAVARI • *United States Army Medical Research Institute of Infectious Diseases (USAMRIID), Fort Detrick, Frederick, MD, USA*
- YUHAI BI • *CAS Key Laboratory of Pathogenic Microbiology and Immunology, Institute of Microbiology, Chinese Academy of Sciences, Beijing, China*
- ALEJANDO JAVIER BOTTALE • *Instituto Nacional de Enfermedades Virales Humanas, Dr JI Maiztegui, ANLIS, Pergamino, Provincia de Buenos Aires, Argentina*
- JOSEPH BRYANT • *University of Maryland School of Medicine, Baltimore, MD, USA*
- NÉLIDA A. CANDURRA • *Laboratorio de Bioquímica y Biología del virus Junín, Departamento de Química Biológica (QB), Facultad de Ciencias Exactas y Naturales (FCEyN), Universidad de Buenos Aires (UBA)-Instituto de Química Biológica de la Facultad de Ciencias Exactas y Naturales (IQUIBICEN)-Consejo Nacional de Investigaciones Científicas y Técnicas (CONICET), Buenos Aires, Argentina*
- SANDRA MYRIAM CORDO • *Laboratorio de Bioquímica y Biología del virus Junín, Departamento de Química Biológica (QB), Facultad de Ciencias Exactas y Naturales (FCEyN), Universidad de Buenos Aires (UBA)-Instituto de Química Biológica de la Facultad de Ciencias Exactas y Naturales (IQUIBICEN)-Consejo Nacional de Investigaciones Científicas y Técnicas (CONICET), Buenos Aires, Argentina*
- ELSA B. DAMONTE • *Laboratorio de Estrategias Antivirales, Departamento de Química Biológica, Facultad de Ciencias Exactas y Naturales (FCEyN), Universidad de Buenos Aires (UBA), Buenos Aires, Argentina; Instituto de Química Biológica de la Facultad de Ciencias Exactas y Naturales (IQUIBICEN), UBA-Consejo Nacional de Investigaciones Científicas y Técnicas (CONICET), Buenos Aires, Argentina*
- REKHA DHANWANI • *La Jolla Institute for Allergy and Immunology, La Jolla, CA, USA*
- FRANCISCO J. DÍAZ • *Grupo de Immunovirología, Facultad de Medicina, Universidad de Antioquia, Medellín, Colombia*
- MAHMOUD DJAVANI • *Institute of Human Virology, University of Maryland School of Medicine, Baltimore, MD, USA*
- CHANGJIANG DONG • *Norwich Medical School, University of East Anglia, Norwich, UK*
- HAOHAO DONG • *Norwich Medical School, University of East Anglia, Norwich, UK*
- ANTONIO HERRADOR FERNANDEZ • *Institute of Microbiology, University Hospital Center, University of Lausanne, Lausanne, Switzerland*
- MARÍA BELÉN FORLENZA • *Laboratorio de Bioquímica y Biología del virus Junín, Departamento de Química Biológica (QB), Facultad de Ciencias Exactas y Naturales (FCEyN), Universidad de Buenos Aires (UBA)-Instituto de Química Biológica de la*

- Facultad de Ciencias Exactas y Naturales (IQUIBICEN)-Consejo Nacional de Investigaciones Científicas y Técnicas (CONICET), Buenos Aires, Argentina*
- SEBASTIÁN EDGARDO FOSSA • *Instituto Nacional de Enfermedades Virales Humanas, Dr JI Maiztegui, ANLIS, Pergamino, Provincia de Buenos Aires, Argentina*
- GRACIELA SUSANA GAMBOA • *Instituto Nacional de Enfermedades Virales Humanas, Dr JI Maiztegui, ANLIS, Pergamino, Provincia de Buenos Aires, Argentina*
- GEORGE F. GAO • *CAS Key Laboratory of Pathogenic Microbiology and Immunology, Institute of Microbiology, Chinese Academy of Sciences, Beijing, China*
- CYBELE C. GARCÍA • *Laboratorio de Estrategias Antivirales, Departamento de Química Biológica, Facultad de Ciencias Exactas y Naturales (FCEyN), Universidad de Buenos Aires (UBA), Buenos Aires, Argentina; Instituto de Química Biológica de la Facultad de Ciencias Exactas y Naturales (IQUIBICEN), UBA-Consejo Nacional de Investigaciones Científicas y Técnicas (CONICET), Buenos Aires, Argentina*
- DIMA GHARAIBEH • *United States Army Medical Research Institute of Infectious Diseases (USAMRIID), Fort Detrick, Frederick, MD, USA*
- FEDERICO GIOVANNONI • *Laboratorio de Estrategias Antivirales, Departamento de Química Biológica (QB), Facultad de Ciencias Exactas y Naturales (FCEyN), Universidad de Buenos Aires (UBA), Instituto de Química Biológica de la Facultad de Ciencias Exactas y Naturales (IQUIBICEN), Consejo Nacional de Investigaciones Científicas y Técnicas (CONICET), Buenos Aires, Argentina*
- JEAN-PAUL GONZALEZ • *Kansas State Univeristy-Center of Excellence for Emerging Zoonotic Animal Diseases, Manhattan, Kansas, USA; Health for Development, Inc., Paris, MD, France*
- ROSANA GONZALEZ-QUINTIAL • *Department of Immunology and Microbial Science, The Scripps Research Institute, La Jolla, CA, USA*
- RONALD N. HARTY • *Department of Pathobiology, School of Veterinary Medicine, University of Pennsylvania, Philadelphia, PA, USA*
- THOMAS HOENEN • *Friederich-Loeffler-Institut, Institute for Molecular Virology and Cell Biology, 17493 Greifswald - Isle of Riems, Germany*
- QINFENG HUANG • *Department of Swine Infectious Diseases, Shanghai Veterinary Research Institute, Chinese Academy of Agricultural Sciences, Shanghai, China*
- GARY KOBINGER • *Special Pathogens Program, National Microbiology Laboratory, Public Health Agency of Canada, Winnipeg, Canada; Department of Medical Microbiology, University of Manitoba, Winnipeg, Canada; Department of Immunology, University of Manitoba, Winnipeg, Canada; Department of Pathology and Laboratory Medicine, University of Pennsylvania School of Medicine, Philadelphia, PA, USA*
- JENS H. KUHN • *Integrated Research Facility at Fort Detrick (IRF-Frederick), Division of Clinical Research (DCR), National Institute of Allergy and Infectious Diseases (NIAID), National Institutes of Health (NIH), Frederick, MD, USA*
- STEFAN KUNZ • *Institute of Microbiology, University Hospital Center, University of Lausanne, Lausanne, Switzerland*
- ICHIRO KURANE • *National Institute of Infectious Diseases, Shinjuku, Japan*
- SHUIYUN LAN • *Cocrystal Pharma, Inc., Tucker, GA, USA*
- YUYING LIANG • *Department of Veterinary and Biomedical Sciences, University of Minnesota, Twin Cities, Saint Paul, MN, USA*
- MICHAEL E. LINDQUIST • *Virology Division, United States Army Medical Research Institute of Infectious Diseases, Fort Detrick, Frederick, MD, USA*

- XIAOYING LIU • *Department of Veterinary and Biomedical Sciences, University of Minnesota, Twin Cities, Saint Paul, MN, USA*
- ANDRÉS F. LONDOÑO • *Grupo de Investigación en Medicina Veterinaria GIVET, Corporación Universitaria Lasallista, Caldas, Colombia*
- IGOR S. LUKASHEVICH • *University of Louisville School of Medicine, Louisville, KY, USA*
- HINH LY • *Department of Veterinary and Biomedical Sciences, University of Minnesota, Twin Cities, Saint Paul, MN, USA*
- ANDREA SOLEDAD MAIZA • *Instituto Nacional de Enfermedades Virales Humanas, Dr JI Maiztegui, ANLIS, Pergamino, Provincia de Buenos Aires, Argentina*
- MAURICIO ANDRÉS MARIANI • *Instituto Nacional de Enfermedades Virales Humanas, Dr JI Maiztegui, ANLIS, Pergamino, Provincia de Buenos Aires, Argentina*
- MARÍA GUADALUPE MARTÍNEZ • *Department of Cell Biology, Albert Einstein College of Medicine, Bronx, NY, USA*
- SANDRA MEDINA-MORENO • *Institute of Human Virology, University of Maryland School of Medicine, Baltimore, MD, USA*
- MENG LING MOI • *Institute of Tropical Medicine, Nagasaki University, Nagasaki, Japan*
- CAROLINA MONTOYA-RUIZ • *Línea de Zoonosis Emergentes y Re-emergentes, Grupo Centauro, Facultad de Ciencias Agrarias, Universidad de Antioquia, Medellín, Colombia*
- MARÍA LAURA MORELL • *Laboratorio de Estrategias Antivirales, Departamento de Química Biológica (QB), Facultad de Ciencias Exactas y Naturales (FCEyN), Universidad de Buenos Aires (UBA), Instituto de Química Biológica de la Facultad de Ciencias Exactas y Naturales (IQUIBICEN), Consejo Nacional de Investigaciones Científicas y Técnicas (CONICET), Buenos Aires, Argentina*
- JACK H. NUNBERG • *Montana Biotechnology Center, University of Montana, Missoula, MT, USA*
- ANTONELLA PASQUATO • *Institute of Microbiology, University Hospital Center, University of Lausanne, Lausanne, Switzerland*
- LUÍS E. PATERNINA • *Grupo Investigaciones Biomédicas, Universidad de Sucre, Sucre, Colombia*
- JOSE RAFAEL PEÑA CÁRCAMO • *Laboratorio de Estrategias Antivirales, Departamento de Química Biológica (QB), Facultad de Ciencias Exactas y Naturales (FCEyN), Universidad de Buenos Aires (UBA), Instituto de Química Biológica de la Facultad de Ciencias Exactas y Naturales (IQUIBICEN), Consejo Nacional de Investigaciones Científicas y Técnicas (CONICET), Buenos Aires, Argentina*
- XIAOXUAN QI • *Norwich Medical School, University of East Anglia, Norwich, UK*
- XIANGGUO QIU • *Special Pathogens Program, National Microbiology Laboratory, Public Health Agency of Canada, Winnipeg, Canada; Department of Medical Microbiology, University of Manitoba, Winnipeg, Canada*
- SHELI R. RADOSHITZKY • *United States Army Medical Research Institute of Infectious Diseases (USAMRIID), Fort Detrick, Frederick, MD, USA*
- JUAN DAVID RODAS • *Línea de zoonosis Emergentes y Re-emergentes, Grupo Centauro, Facultad de Ciencias Agrarias, Universidad de Antioquia, Antioquia, Colombia*
- MARIA S. SALVATO • *Institute of Human Virology, University of Maryland School of Medicine, Baltimore, MD, USA*
- CONNIE S. SCHMALJOHN • *Virology Division, United States Army Medical Research Institute of Infectious Diseases (USAMRIID), Fort Detrick, MD, USA*

- CLAUDIA S. SEPÚLVEDA • *Laboratorio de Estrategias Antivirales, Departamento de Química Biológica, Facultad de Ciencias Exactas y Naturales (FCEyN), Universidad de Buenos Aires (UBA), Buenos Aires, Argentina; Instituto de Química Biológica de la Facultad de Ciencias Exactas y Naturales (IQUIBICEN), UBA-Consejo Nacional de Investigaciones Científicas y Técnicas (CONICET), Buenos Aires, Argentina*
- JUNJIE SHAO • *Department of Veterinary and Biomedical Sciences, University of Minnesota, Twin Cities, Saint Paul, MN, USA*
- SERGIO SOLARI • *Grupo Mastozoología, Instituto de Biología, Universidad de Antioquia, Medellín, Colombia*
- VERONICA SOLOVEVA • *United States Army Medical Research Institute of Infectious Diseases (USAMRIID), Fort Detrick, Frederick, MD, USA*
- MARC SOURIS • *IRD, Laos and Cambodia Representative, Vientiane, Lao PDR*
- JOHN J. SUSCHAK • *Virology Division, United States Army Medical Research Institute of Infectious Diseases (USAMRIID), Fort Detrick, MD, USA*
- TOMOHIKO TAKASAKI • *National Institute of Infectious Diseases, Shinjuku, Japan*
- MELISSA L. TURSIELLA • *Virology Division, United States Army Medical Research Institute of Infectious Diseases (USAMRIID), Fort Detrick, Frederick, MD, USA*
- SHANNON L. TAYLOR • *Virology Division, United States Army Medical Research Institute of Infectious Diseases (USAMRIID), Fort Detrick, Frederick, MD, USA*
- WILLY VALDIVIA-GRANDA • *Orion Integrated Biosciences, New Rochelle, NY, USA*
- WENJIAN WANG • *Norwich Medical School, University of East Anglia, Norwich, UK; Laboratory of Department of Surgery, The First Affiliated Hospital, Sun Yat-sen University, Guangzhou, Guangdong, China*
- GARY WONG • *CAS Key Laboratory of Pathogenic Microbiology and Immunology, Institute of Microbiology, Chinese Academy of Sciences, Beijing, China; Special Pathogens Program, National Microbiology Laboratory, Public Health Agency of Canada and Department of Medical Microbiology, University of Manitoba, Winnipeg, Canada*
- YIDA YANG • *Institute of Infectious Diseases, First Affiliated Hospital, Zhejiang University, Hangzhou, Zhejiang Province, People's Republic of China*
- JOANNE YORK • *Montana Biotechnology Center, University of Montana, Missoula, MT, USA*
- JUAN CARLOS ZAPATA • *Institute of Human Virology, University of Maryland School of Medicine, Baltimore, MD, USA*
- YANQING ZHOU • *College of Animal Science and Technology and Veterinary Medicine, Huazhong Agricultural University, China*
- MARKO ZIVCEC • *Viral Special Pathogens Branch, Centers for Disease Control and Prevention (CDC), Atlanta, GA, USA*

Part I

Surveillance, Diagnosis and Classification of Hemorrhagic Fever Viruses

Chapter 1

Global Spread of Hemorrhagic Fever Viruses: Predicting Pandemics

Jean-Paul Gonzalez, Marc Souris, and Willy Valdivia-Granda

Abstract

As successive epidemics have swept the world, the scientific community has quickly learned from them about the emergence and transmission of communicable diseases. Epidemics usually occur when health systems are unprepared. During an unexpected epidemic, health authorities engage in damage control, fear drives action, and the desire to understand the threat is greatest. As humanity recovers, policy-makers seek scientific expertise to improve their “preparedness” to face future events.

Global spread of disease is exemplified by the spread of yellow fever from Africa to the Americas, by the spread of dengue fever through transcontinental migration of mosquitos, by the relentless influenza virus pandemics, and, most recently, by the unexpected emergence of Ebola virus, spread by motorbike and long haul carriers. Other pathogens that are remarkable for their epidemic expansions include the arenavirus hemorrhagic fevers and hantavirus diseases carried by rodents over great geographic distances and the arthropod-borne viruses (West Nile, chikungunya and Zika) enabled by ecology and vector adaptations. Did we learn from the past epidemics? Are we prepared for the worst?

The ultimate goal is to develop a resilient global health infrastructure. Besides acquiring treatments, vaccines, and other preventive medicine, bio-surveillance is critical to preventing disease emergence and to counteracting its spread. So far, only the western hemisphere has a large and established monitoring system; however, diseases continue to emerge sporadically, in particular in Southeast Asia and South America, illuminating the imperfections of our surveillance. Epidemics destabilize fragile governments, ravage the most vulnerable populations, and threaten the global community.

Pandemic risk calculations employ new technologies like computerized maintenance of geographical and historical datasets, Geographic Information Systems (GIS), Next Generation sequencing, and Metagenomics to trace the molecular changes in pathogens during their emergence, and mathematical models to assess risk. Predictions help to pinpoint the hot spots of emergence, the populations at risk, and the pathogens under genetic evolution. Preparedness anticipates the risks, the needs of the population, the capacities of infrastructure, the sources of emergency funding, and finally, the international partnerships needed to manage a disaster before it occurs. At present, the world is in an intermediate phase of trying to reduce health disparities despite exponential population growth, political conflicts, migration, global trade, urbanization, and major environmental changes due to global warming. For the sake of humanity, we must focus on developing the necessary capacities for health surveillance, epidemic preparedness, and pandemic response.

Key words Viral hemorrhagic fever, Pandemic, Global biosecurity, Predicting epidemic risk (i.e., pathogenic threat and vulnerability)

1 Introduction

1.1 Preamble

Infectious diseases have swept the world, taking the lives of millions of people, causing considerable upheaval, and transforming the future of entire populations. Every year pathogens cause nearly 14 million deaths worldwide, mostly in developing countries. More than 350 infectious diseases have emerged between the 1940s and 2004 [1]. Also among the 500 known arboviruses, only 50 are known to be human pathogens, while the others only infect wild animals and/or arthropods. To anticipate an epidemic one must identify the risk, prepare an appropriate response, and control the disease spread by first identifying the vulnerabilities of the population and circumscribing the potential space into which a disease will extend. When the epidemic expansion risk is identified, adequate information must be communicated to decision makers. Ultimately, an appropriate response will depend on biosurveillance, prevention, sustained data processing, communication, strategic immunization campaigns, resilience, and mitigation strategies.

The viral hemorrhagic fevers (VHFs) are a diverse group of human illnesses caused by RNA viruses including approximately 50 species of the *Arenaviridae*, *Filoviridae*, *Bunyavirales*, *Flaviviridae*, and *Rhabdoviridae* (Table 1). Despite the efforts placed on early detection, viruses like dengue, Ebola, Lassa, Crimean-Congo hemorrhagic fevers continue to threaten the health of millions of people, mostly in areas where demographic changes, and political and socio-economic instability interrupt vaccination campaigns [2]. However, the threat of VHF to global health is increased by intercontinental travel and global trade. Moreover, because of the high case fatality rate of some of these pathogens, such concerns extend to the potential use of these viruses by bio-terrorists [3].

1.2 Historical Perspectives

Global expansion of several diseases is exemplified by the spread of yellow fever from Africa to the Americas, the spread of dengue Fever across continents, and recently, the spread of Ebola virus from the Democratic Republic of the Congo to Western Africa. The concept of an epidemic, as a disease affecting many persons at the same time and spreading from person to person in a locality where the disease was not previously prevalent, was not enunciated until 1854 when John Snow produced his admirable demonstration of the emergence of an infectious disease in an urban area: the emergence of a cholera epidemic in London. At that time, none could clearly comprehend the mechanisms of emergence and spread since the existence of microbes had just been demonstrated by Louis Pasteur in the late 1830s and microbe transmission modes were more speculative than based on medical or scientific facts, until 1876 when Robert Koch demonstrated that bacteria can be transmitted and responsible for diseases. Nowadays, it is extremely difficult to make a retrospective diagnosis of historical pandemics,

Table 1
Most common hemorrhagic fever viruses and their associated disease

Family	Virus	Disease	Origin
<i>Arenaviridae</i>	Junín virus	Argentinian HF ^a	Argentina
<i>Arenaviridae</i>	Whitewater Arroyo virus	Whitewater Arroyo HF	N. America
<i>Arenaviridae</i>	Chapare virus	Chapare HF	Bolivia
<i>Arenaviridae</i>	Guanarito virus	Venezuelan HF	Venezuela
<i>Arenaviridae</i>	Lassa fever virus	Lassa fever	Africa
<i>Arenaviridae</i>	Lujo virus	Lujo HF	Africa
<i>Arenaviridae</i>	Lymphocytic choriomeningitis virus	Lymphocytic choriomeningitis	World
<i>Arenaviridae</i>	Machupo virus	Bolivian HF	Bolivia
<i>Arenaviridae</i>	Sabiá virus	Brazilian HF	Brazil
<i>Filoviridae</i>	Marburgviruses	Marburg virus disease	Africa
<i>Filoviridae</i>	Ebolaviruses ^b	Ebola virus disease	Africa
<i>Flaviviridae</i>	Alkhurma virus	Alkhurma HF	Saudi Arabia
<i>Flaviviridae</i>	Dengue viruses	severe dengue	World
<i>Flaviviridae</i>	Kyasanur Forest disease virus	Kyasanur Forest disease	India
<i>Flaviviridae</i>	virus	Kyasanur Forest disease virus	China
<i>Flaviviridae</i>	Omsk hemorrhagic fever virus	Omsk HF	India
<i>Flaviviridae</i>	Tick-borne encephalitis virus	Tick-borne encephalitis	Eurasia
<i>Flaviviridae</i>	Yellow fever virus	Yellow fever	Africa/S. America
<i>Hantaviridae</i>	Hantaan virus ^c	HF with renal syndrome	World
<i>Hantaviridae</i>	Puumala virus	Nephropathia epidemica	World
<i>Paramyxoviridae</i>	Hendra virus	Hendra virus encephalitis	Australia
<i>Paramyxoviridae</i>	Nipah virus	Nipah virus encephalitis	Asia
<i>Nairoviridae</i>	Crimean-Congo hemorrhagic fever virus	Crimean-Congo HF	Africa/Asia
<i>Peribunyaviridae</i>	Ngari virus	Garissa HF	Africa
<i>Peribunyaviridae</i>	Ilesha virus	Ilesha HF	Africa
<i>Phenuiviridae</i>	Rift Valley fever virus	Rift Valley fever	Africa
<i>Rhabdoviridae</i>	Bas-Congo virus	Bas-Congo HF	Africa

^aHF is hemorrhagic fever

^bEbolaviruses pathogenic for humans include *Bundibugyo*, *Ebola*, *Sudan*, and *Tai Forest viruses*

^cThere are currently 41 species in the *Orthohantavirus* genus. The pathogeny of most of them is unknown

during times when clinical descriptions were rare or lacking accuracy, and the extent of an epidemic was extremely subjective. Thus, it is common to note that the first outbreak described in the Western World was that of the plague of Athens for which Thucydides rather precisely reported the symptoms; today this epidemic has often been attributed to typhus through its clinical picture and epidemic profile [4].

The first historically recorded outbreaks due to viral agents date to antiquity when the Roman armies were returning from distant countries bringing with them “exotic” diseases. Indeed, the rise of a “new” virus is an extremely rare event. Most often, in terms of pathogen emergence, a virus adapts through mutation and selection pressure to a human host causing disease. Presumably, smallpox, measles, and influenza were among the plagues that struck the ancient Latins in gusts of epidemics more or less severe. The Antonin plague that extended from 167 to 172 AD in much of Western Europe, when the troops of Emperor Lucius Verus returned from war against the Parthians, is often attributed to a smallpox pandemic by historians. In the Middle Ages, it seems that smallpox made a return around 541 AD to France, Germany, Belgium, and the British Islands [5]. The acute respiratory infections reported during the winter of 876–877 AD accompanying the return of the Carolingian armies from Italy have been attributed by historians to a flu epidemic. Many soldiers of Charlemagne died then. The disease returned regularly and fiercely in 927 and 1105 AD to the western European peninsula [6, 7] (Table 2).

1.3 Past and Present Viral Pandemics

From the plague (*sensu lato*, including all transmissible diseases) of antiquity, to the severe acute respiratory syndrome that emerged on the eve of the third millennium, pandemics have followed in the history of mankind. As noted by Mirko Grmek, a historian of medicine, it seems that one pandemic will drive in another. If several diseases circulate concomitantly, one of them will take precedence over the other, an epidemic over the previous, and it is more likely that a pandemic will prevail [8]. Plague temporarily replaced the leprosy that appeared in Eurasia for over 50,000 years; during the first millennium, plague was manifested by successive pandemics that crossed continents. During the first half of the past millennium, syphilis started its expansions, crossed oceans, and became global. Tuberculosis originated in Europe more than 15,000 years ago, but it was only at the turn of the seventeenth century that it was considered a pandemic; smallpox was also manifest as epidemics and then was pandemic at its peak in the late nineteenth century, then smallpox persisted until the Jenner area. Although early medical records of smallpox are available (Egypt, China, India), large and devastating epidemics were only identified in the late fifteenth century of the millennium. Smallpox was introduced into the Americas by Spanish settlers in the Caribbean island of Hispaniola in 1492 and arrived in Mexico in 1509. On Hispaniola

Table 2
Viral pandemics

	Disease	Origin	Inception/end	Morbidity/mortality
Measles virus (<i>Paramyxoviridae</i>)	Measles	Asia, Northern Africa	Third century ^a	/200m ^b
Variola virus (<i>Poxviridae</i>)	Smallpox	North Eastern Africa	Tenth century–1979 ^c	50m year/20 m
Yellow fever virus (<i>Flaviviridae</i>)	Yellow fever	Africa	Fourteenth century ^d -	30–70m/year
Influenza A virus (<i>Orthomyxoviridae</i>)	Pandemic flu	Northern China	1580 ^e	/0.023%
Influenza A virus (<i>Orthomyxoviridae</i>)	Russian flu	Uzbekistan	1889–1890	/1m
Poliovirus (<i>Enteroviridae</i>)	Poliomyelitis	Western hemisphere	1900–1960s	/5%
Influenza A virus H1N1 (<i>Orthomyxoviridae</i>)	Spanish flu	US Kansas	1918–1919	/50m
Influenza A virus H2N2 (<i>Orthomyxoviridae</i>)	Asian flu	China	1956–1958	/2m
Marburgviruses (<i>Filoviridae</i>)	Marburg virus disease	Eastern Africa?	1967 ^f	/55%
Influenza A virus H3N2 flu (<i>Orthomyxoviridae</i>)	Hong Kong flu	Hong Kong	1968–1969	/1m
Crimean-Congo hemorrhagic fever virus (<i>Nairoviridae</i>)	Crimean-Congo HF	Central Africa	1969 - ^g	/40%
Lassa virus (<i>Arenaviridae</i>)	Lassa fever	Western Africa	1969 - ^h	
Ebolaviruses (<i>Filoviridae</i>)	Ebola virus disease	Central Africa	1976 - ⁱ	>30,000/50%
HIV-1, -2 (<i>Lentiviridae</i>)	HIV/AIDS	Cameroon	1981–2012	35.3m/25m
Rift Valley fever virus (<i>Phenuiviridae</i>)	Rift Valley fever	North East Africa ^l	1987–2000	/1%
SARS-CoV (<i>Coronavirinae</i>)	SARS ^k	China	2003 -	/36%

(continued)

Table 2 (continued)

	Disease	Origin	Inception/end	Morbidity/mortality
	MERS-CoV (<i>Coronavirinae</i>)	Saudi Arabia	2012 -	/36%
	Ebola virus (<i>Filoviridae</i>)	Guinea (Western Africa)	2014–2016	2000

^a“.” = uncertainty about virus circulation and endemics

^bm = million

^ceradicated

^dc. = century

^eLarge pandemic occurring every 10–30 years

^fWest Germany, Yugoslavia and then discovered in Africa

^gOccurred South of 50 °N latitude then extended to the Western Asia, Balkans, Asia

^hImported cases to Canada, Germany, Israel, Japan, Netherlands, United Kingdom, USA

ⁱContinental sparse repetitive epidemics in different countries, expansion within the African Rain forest

^jExpansion to Western Africa and Western Asia (and also Saudi Arabia, Yemen)

^kSevere acute respiratory syndrome

Island, one third of a million of the inhabitants died of smallpox in the following 20 years. Smallpox devastated the native Amerindian population and was an important factor in the conquest of the Aztecs and the Incas by the Spaniards [9]. In 1545, 8000 children died in Goa, India, from a smallpox epidemic. In Europe, smallpox was a leading cause of death in the eighteenth century, killing an estimated 400,000 Europeans each year [10]. During the twentieth century, it is estimated that smallpox was responsible for 300–500 million deaths. The last known natural case of smallpox occurred in Somalia in 1977 [11].

It is only at the end of the first millennium that all these pathologies were better understood and their infectious origins elucidated. The first pandemic of the twentieth century was attributed to the H1N1 Spanish Flu that emerged in Kansas in 1918. However, this “flu pandemic” is now thought to have had sub-epidemic circulation earlier in France or Germany or even prior emergence in China in 1916 or 1917 [12], and to be exacerbated by concurrent bacterial infections. Although it burned out quickly by 1920, it has been estimated that one third of the world’s population was afflicted; 50 million people died, half of them in the first 25 weeks of the outbreak.

Since the 1960s, the frequency and magnitude of dengue fever epidemics increased dramatically as the viruses and the mosquito vectors have both expanded geographically in pandemic proportions [13] largely extending the pandemic to all the intertropical zone. In the early 1980s, human immunodeficiency viruses (HIV-1 and HIV-2) spread as an acquired immunodeficiency syndrome (AIDS), a pandemic that continues to take its terrible toll at the global level. Since the emergence of AIDS, 78 million people have been infected and 39 million have died. According to World Health

Organization updates, as of June 2015 only 17 million people were accessing antiretroviral treatment and among them, seven of ten pregnant women received treatment.

In 2003, a severe acute respiratory syndrome, SARS, inaugurated the twenty-first century as a first pandemic of the millennium, involving more than 24 countries with secondary epidemic chains in Asia, Europe, North America, South America, and a total of 8098 cases [14].

Ultimately, one of the major characteristics that defines today's pandemics, apart from the introduction of the disease within several continents or the rapid expansion across the administrative borders of countries, is the initiation of locally active transmission of the pathogen. Although, the first Ebola virus disease outbreak of Western Africa was considered a pandemic and witnessed several exported cases with secondary epidemic chains in distant countries of the African continent (i.e., Nigeria, Mali), outside of Africa, exported cases rarely sparked local transmission.

1.4 Understanding the Transition from Outbreak, to Epidemic, to Pandemic.

1.4.1 From Focal to Global

Emergence from a sporadic case to an outbreak, to an epidemic, and ultimately to a pandemic depends upon effective transmission among nonimmune hosts, host availability (density), characteristics of the vector (natural or human made) that would enable it to circumvent distances, and the pathogen infectiousness. All these dynamics are essential for an effective disease transmission and spread. An outbreak is a sudden increase in occurrences of a disease in a particular time and place, more localized than an epidemic. An epidemic occurs as the disease spreads to a large number of people in a given population within a short period of time. To spark an epidemic chain of transmission depends on factors like immune population density, virus infectiousness, promiscuity, vulnerability, etc., while the efficiency of such transmission depends on how many persons will be infected by one person (i.e., the reproductive ratio or R_0). An epidemic event will therefore expand in space (beyond the first cluster of cases) and time (rapid spread). A pandemic is essentially spatial, and represents an epidemic of infectious disease that has spread through human populations across a large region, extensively across two or more continents, to worldwide. However, all these typologies harbor the same fundamentals: emergence from one index case, transmission from one host to another, and spatial expansion. Altogether, an epidemic and a pandemic are respectively a local and a global network of interconnected infectious disease outbreaks (i.e., epidemic chains). Ultimately, understanding how disease (i.e., pathogens) spread in the social system is fundamental in order to prevent and control outbreaks, with broad implications for a functioning health system and its associated costs [15]. Also, after the last case occurs at the end of an epidemic, the goal is to control the risk of transmission for a 21-day time period. This three-week period represents an incubation when the infected subject does not transmit the virus and remains asymptomatic. The "21 days" is based on

experimental methods use in virology to detect virus replication: Influenza virus infected eggs should hatch in 21 days, there is a 21-day limit for an arbovirus to infect a living model (suckling mice, mice, rats, guinea pigs, cell lines). Moreover, most viral infectious diseases have a maximal incubation period of 21 days, with few exceptions (e.g., HIV, and rabies). Ultimately, such 21-day periods multiplied by the potential of a carrier to travel will produce the risk area for the emergence of secondary cases (from a walking distance to the long distances covered by commercial jets). However, it is important to clarify that many VHF including Ebola virus can be carried by an asymptomatic host for several months [16, 17].

1.4.2 Transmission and Spread

The mode of transmission profiles the epidemic pattern of a transmissible disease. It is extremely helpful when a disease emerges to rapidly surmise the mode of transmission and how to respond (e.g., water-borne disease, arthropod-borne disease, human-to-human transmission). Pathogen transmission can be interspecific or hetero-specific, direct or indirect. Direct transmission occurs by close contact with infected biological products (e.g., blood, urine, saliva). Indirect transmission occurs with intermediate hosts such as arthropod vectors (e.g., mosquito, tick) or mammalian vector/reservoir (e.g., rodent, chiropteran) or from infected environmental means (e.g., soil, water, etc.). Mobility and transportation are the main factors for diseases dispersion, as an emblematic example, one can simply show how the 2013–2016 EVD outbreak of Western Africa expanded due to the transportation of patients during their 21-day incubation periods, first by foot-paths, then by motorbike, then taxis and public transportation, finally becoming a global concern with patients traveling by boat or commercial airline [18, 19].

Host population density and promiscuity, crowded places (like schools, markets, mass transportation system) also play an important role in the efficiency of transmission as well as the level of herd immunity (e.g., annual pandemic flu), altogether this gives us the level of population susceptibility (i.e., vulnerability). Environmental factors can also be major drivers of pathogen expansion, for example the emergence of Nipah encephalitis. The Nipah virus, when it emerged for the first time in Malaysia in 1998, was transported by its natural host, a frugivorous chiropteran. A year earlier, an immense forest fire affecting several Indonesian islands had forced the escape of disease-carrying bats that took refuge in Malaysian orchards, planted to nurture newly developed pig farms. Both pigs and farmers became infected and Nipah virus was discovered for the first time. Another classical example, more associated with human environment and behavior, is the old story of the spread of dengue virus via the used tires carrying infected *Aedes aegypti* eggs and transporting dengue across oceans and continents [20].

Understanding the mechanisms of transmission and expansion of disease vectors with respect to the typology (epidemic pattern) of a disease is the ultimate challenge for controlling and preventing

disease. Typologies from human-to-human transmission, zoonotic diseases, arboviruses, water-borne diseases, and others play different roles in the rate of disease spread and need to be clearly understood. Finally, while an epidemic pattern is driven intrinsically by the virus and its vector, the host population, the mode of transmission, and even the human environment (e.g., population density, urbanization, agricultural practices, health system, public health policies) as well as physical environment (season, meteorology, climate changing, latitude, altitude) factor into the rate of disease spread.

1.4.3 *The Virus*

With respect to pandemic risk (the rapidity and area covered by disease), the main characteristics of a virus are found in its environmental persistence while remaining infectious. Environmental persistence depends on: virus structure, enveloped viruses are more sensitive than the naked viruses; its mode of entry into the body of the susceptible subject (transdermal, oral, respiratory); its ability to diffuse out of the body for a sufficient period of time which will, in turn, enable transmission to a greater number of subjects (R_0). Altogether these intrinsic factors link to the infectivity of the virus, indeed, viruses transmitted by aerosol possess certainly the most efficient way to spark an epidemic that increases with population density and vulnerability as well as with the resistance of the virus to environmental factors outside the host cells.

1.4.4 *Hosts*

The cycle of transmission shapes the epidemic in time and spatial dispersion. For example, animal to human zoonoses are dictated by chance encounters between host (population density, animal farming, pets, hunting) and, eventually transmission such as that observed between human and nonhuman primates [21]. Vector-transmitted diseases (i.e., arthropod-borne diseases) depend on the vector ecology (ability to transmit, length of the intrinsic cycle of the virus, trophic preferences, vector density, seasonality, reproduction, breeding sites, food abundance for hematophagous arthropods). Mobility of hosts/vectors that are part of the natural cycle will also play a role in the potential for disease expansion (e.g., mosquito-flying distance, cattle transhumance, human migration). Also, other factors associated with the hosts will render a more efficient transmission: human behaviors like fear/social responses, nosocomial infections, super-spreaders); viruses having multiple natural hosts (vicariates) or vectors; vectors with multiple trophic preferences (e.g., biting cattle, birds, and primates); the incubation period in the vertebrate hosts as well as the intrinsic replication in the arthropod vectors will also intervene; ultimately subclinical infection is also an underestimated factor of virus dispersion and transmission that modifies the epidemiological pattern of disease.

One can distinguish also a typology of communicable diseases that reflects the spatial and temporal mode of transmission including arthropod-borne transmission, human-to-human transmission, human-to-animal (and vice versa) transmitted diseases (i.e., zoo-

noses) including vector and nonvector transmitted diseases, and some other types of environmentally transmitted diseases. All of them represent unique types of transmission and risk of spread with a variable path of time, and also dependent on multiple factors (environment, climate, behavior, etc.).

1.4.5 Territories

We have to consider territories as spaces where disease can potentially expand and that can be characterized by the fundamental factors of emergence and spread: the vulnerability of the population, the level of favorable transmission factors, and the probability for the population to be exposed to the virus. VHF are exemplary for their epidemic patterns of expansion dependent on the above reviewed factors (i.e., fundamentals of emergence) and their epidemiological characteristics (i.e., virus, host, environments). For example, let us consider the control of arenavirus spread by their strong host-species association. On a geological time scale, arenaviruses such as the agent for Argentinian hemorrhagic fever (AHF) coevolved with their natural rodent host and then spread according to the expansion of the rodent host. One host–one virus ultimately produces a localized endemic cycle, the distribution of the disease overlaps the distribution of the rodent host while enzootic patterns appear naturally limited to an ecosystem (e.g., local rodent populations, behaviors, and environmental factors). Hantaviruses also appear as a global complex, resulting from the coevolution of virus and rodent hosts and a global dispersion of generally localized enzootic diseases [22–24]. As for the pandemic risk associated with a natural virus reservoir, chiropterans are unique flying and migratory mammals that have been associated with *flaviviruses* and other viruses of major public health importance [25], their potential as vectors will eventually favor the spread of these viruses into new territories. Also because there is potential for a long coevolution, epidemiological patterns are also dependent on virus-host spillover, host vicariate, and other environmental factors (e.g., climate change and man-made changes in land use). Other arboviruses such as yellow fever virus, dengue virus, as well as West Nile, chikungunya, or Zika viruses show a pandemic risk associated with the existing distribution of their respective arthropod vector, vector density, and ability to transmit virus.

Investigating the fundamental factors of transmission and favorable territories for disease emergence are necessary to evaluate the risk, respond to the epidemic, and control its expansion from an index case to a pandemic. Ultimately, when the fundamentals are understood and epidemic/pandemic risk identified, suitable emergency funding needs to be identified and made available in endemic areas to insure political willingness and community participation. Ultimately, a suitable response will improve biosurveillance, data processing, communication, strategic immunization campaigns, and research for future risk prevention. Several emblematic VHF and their original “epidemiological engineering” are presented in herein.

2 Viral Hemorrhagic Fevers

2.1 *Viral Hemorrhagic Fevers and Hemorrhagic Fever Viruses*

VHF such as Ebola Virus Disease, Lassa fever, Rift Valley fever, or Marburg virus disease are highly contagious and deadly diseases, with potential to become pandemics. Remarkably, VHF are essentially caused by viruses of eight families; *Arenaviridae*, *Filoviridae*, *Hantaviridae*, *Nairoviridae*, *Peribunyaviridae*, *Phenuiviridae*, *Flaviviridae*, and more recently *Rhabdoviridae* [26] (Table 3).

Hemorrhagic fever viruses (HFV) have been classified as “Select Agents” because they are considered to pose a severe threat to both human and animal health due to high mortality rate, human-to-human transmission, and, in some cases, the potential to be aerosolized and used as bioweapons [27]. Each of these HFV shares some common features that define the nosology of the VHF group, from virus structures to the clinical and epidemiological characteristics of their diseases.

Table 3
Viral hemorrhagic fever emergence and pandemics

Date	Disease ^a	Place	Type ^a
3000 BCE ^b	Yellow fever	Africa	E
1976 to date	Yellow fever	Nigeria	LEE
Seventeenth century to 1998	Yellow fever	Brazil	LEE
1952 (1978 ^c)	HFRS	Korea	E
1976	EVD	DRC	E
2014	EVD	Western Africa	P
1967	MVD	Europe	E
1953	DF/DHF	South East Asia	E, LEE
1970s	DF/DHF	Oceania, Central and South America	E, LEE, P
1980s	DF/DHF	Africa	E, LEE, P
1969	Lassa fever	Nigeria	E
1972	Lassa fever	Liberia, Sierra Leone	LEE
Twelfth century (1944 ^d)	CCHF	Central Asia (Crimea)	E
1956	CCHF	Africa (DRC)	E
Mid 1900s	CCHF	Western Asia	LEE

^aE is Emergence; P is Pandemic; LEE is Large Emerging Events

^bFrom the third millennium to the present, multiple outbreaks of yellow fever were recorded in Africa, largely spreading as long-term pandemics to the Americas during the seventeenth century and thereafter

^cHantavirus identified as a hitherto etiologic agent

^dCCHF virus isolation

^eHFRS is hemorrhagic fever with renal syndrome; EVD is Ebola virus disease, DF/DHF is dengue fever/severe dengue; CCHF is Crimean-Congo hemorrhagic fever virus

- HFV are RNA viruses with envelope proteins embedded in a lipid bilayer, they are dependent on their animal and/or insect hosts for survival, and their geographical spread overlaps the areas where their natural hosts live.
- HFV spread person-to-person through direct contact with symptomatic or asymptomatic patients, body fluids, or cadavers.
- VHF can have a zoonotic origin, as when humans have contact with infected livestock via slaughter or consumption of raw meat, unpasteurized milk, bushmeat, inhalation or contact with materials contaminated with excreta from rodents or bats.
- HFV can be vector-borne, i.e., transmitted via rodents, mosquitos, and ticks.
- VHF are zoonotic diseases. Accidental transmission from the natural host to humans can eventually lead to human-to-human transmission, human infection, and sporadic outbreaks.
- With a few noteworthy exceptions (i.e., ribavirin), there is no cure or established drug treatment for VHF, while limited vaccines could be available, including YF, AHF, and RVF (the latter is for animals only).
- VHF have common features: they affect many organs, they damage blood vessels, and they affect the body’s ability to regulate itself. Clinical case definitions describe VHF with at least two of the following clinical signs: hemorrhagic or purpuric rash; epistaxis, hematemesis, hemoptysis, melena, among other hemorrhagic symptoms without known predisposing host factors for hemorrhagic manifestations. In fact, during an epidemic, all infected patients do not show these signs and a specific case definition needs to be defined in accordance with the suspected or proven viral etiology of the disease [28]. Also, VHF pathogenesis encompasses a variety of mechanisms including: (1) alteration of hepatic synthesis of coagulation factors, cytokine storm, increased vascular permeability, complement activation, disseminated intravascular coagulation. Moreover, severe pathogenic syndrome is often supported by an ineffective immunity, high viral loads, and severe plasma leakage and co-infection with other pathogens [29].

2.2 Study Cases: VHF Pandemic Risk Today

The present chapter will mainly focus on the factors that can specifically and eventually contribute to a pandemic risk and how did we learn from historical spread of the VHF.

2.2.1 Yellow Fever Virus, YFV: A Timeless Plague

The yellow fever disease pandemic is thought to have originated in Africa, where the virus emerged in East or Central Africa and spread to Western Africa. In the seventeenth century, it spread to South America through the “triangular” slave trade, after which several major outbreaks occurred in the Americas, Africa, and Europe [30, 31]. The yellow fever vaccine is a fantastic gift from pioneering vac-

cinology; it is efficient, affordable for developing countries, and protects for at least a decade or even life-long. However, YF remains a particular concern at the global level and the number of cases has unexpectedly increased this past decade. Nowadays, YFV causes 200,000 infections and 30,000 deaths every year, with nearly 90% occurring in Africa. Nearly a billion people live in an endemic area [32]. Although YFV is common in tropical areas of South America and Africa, it has never been isolated in Asia [33]. Ultimately, the pandemic risk is there, from the uncontrolled epidemic as for example in the inland remote area of the Brazilian Mato Grosso state, to the recent burst of epidemics in West and Central Africa including Angola, DRC, as well as imported cases in Kenya and China [34, 35]. Indeed, the risk of a pandemic exists if any imported case goes to an area where the fundamentals of emergence are present (i.e., *Aedes aegypti* and a nonimmune human population). For years it has been stressed that YF coverage needs to be exhaustive in the endemic area, and the WHO international health regulations (IHR) need to be strictly respected when peoples are crossing frontiers to or from an endemic area [36].

2.2.2 Dengue Hemorrhagic Fever, DHF: An Expanding Pathogeny

Even though the virus was known to actively circulate in Asia, North America, and Africa 200 years ago, a global pandemic of dengue fever began in Southeast Asia in the 1950s [37, 38]. Dengue virus (DENV) expansion was followed by the emergence of a DHF pandemic that occurred in the late twentieth century (see above, the “tire-mosquito larvae connection”). By the end of the century, DHF emerged in the Pacific and the Americas, and extended to all Asian continents [32]. Lately, in the 1980s, epidemic dengue fever occurs in Africa, with a predominant activity in East Africa, while sylvatic DENV circulation was described in Western Africa [39]. The different dengue virus serotypes spread also independently to all continents. While it is remarkable that infection with one serotype does not provide cross-protective immunity against the others, epidemics caused by multiple serotypes became more frequent, and highly pathogenic DENV were identified [40]. Dengue fever to date has a global distribution with an estimated 2.5 billion people at risk. Yearly, hundreds of thousands of DHF cases occur [32]. Altogether, the requirements for a DHF pandemic are globally present [41]: the highly competent *Aedes aegypti* and *Aedes albopictus* DENV vectors, the globally distributed DENV serotypes and highly pathogenic strains, and finally, climate change that opens new breeding opportunities for these mosquitoes to expand and eventually transmit imported DENV into new populations and territories [42]. Mankind will have to live with this pandemic until the new DENV vaccines can be implemented.

2.2.3 Marburg Virus Disease: A Brief, but Disturbing History

In 1967, an unknown disease was reported by a group of laboratory workers in West Germany and former Yugoslavia [43]. Over the course of 2 months, 31 cases and seven deaths occurred.

Conclusions made by treating physicians at the time (and published shortly thereafter) highlighted the following: high fatality rate, risk of relapse; risk of sexual transmission [38]. A connection was made to infected African primates, *Chlorocebus aethiops*, when laboratory workers were exposed to their imported tissues. It took 43 years to effectively connect Marburg virus, MARV, to a bat, *Rousettus aegyptiacus*, as a natural MARV reservoir in Central Africa [44]. MARV is considered to be extremely dangerous for humans, is classified as a Risk Group 4 Pathogen, and also is listed as a Select Agent; however, the pandemic risk cannot be assessed because only four epidemics have occurred. Although MARV expansion appears to be limited to a few countries in Africa, the recent emergence (estimated at a few decades ago) of a second human pathogenic marburgvirus known as Ravn virus, and the widely distributed Old World rousette fruit bats (*Rousettus* spp.) serving as reservoir for both viruses [45], are two factors that favor pandemic risk.

2.2.4 Ebola Virus Disease: Disconcerting and Cryptic Silent Periods

Although more than 35 years after its emergence from a remote area on the Ebola river in the Central African rain forest, Ebola virus (EBOV) remained hidden in a cryptic natural cycle. Then a series of 23 outbreaks occurred in the large Congolese rain forest of Central Africa [46]. The epidemic risk was always considered to be localized and circumscribed [47]. Then, suddenly without warning, in the late months of 2013, EBOV emerged for the first time in a remote area of Western Africa and sparked an outbreak more massive than ever witnessed before. More than 28,000 people were infected, ten countries recorded cases (transmitted or imported), the pandemic risk raised fear, and WHO declared it as an international health emergency that requires a coordinated global approach [48].

Besides the lack of preparedness of national and international public health systems, the other major factor that played an immense role for the dispersion of EVD in Western Africa was the extreme mobility of village populations. They followed the Kissidougou forest foot-paths to the towns in Guinea using motor-bikes, cars, and other public transportation, then later EVD traveled by plane to the global level. The EVD epidemic went from outbreak to pandemic risk. Like Marburg virus, another member of the *Filoviridae*, Ebola virus, shares bats as a potential virus reservoir, human and nonhuman primates are highly sensitive to the virus, and inter-epidemic periods play an important role since the epidemic silences tend to diminish the attention of health services and increase epidemic risk. In this way, the first Western African EVD epidemic is exemplary for showing the hidden risks contained in the natural cycle of a virus, and the sudden emergence followed by an unprecedented velocity of spreading. In the absence of bio-surveillance, a pandemic risk remains.

2.2.5 Hemorrhagic Fever with Renal Syndrome: No Pandemic Risk but a Recently Growing Ancient Family That Can Still Be Surprising

Hemorrhagic Fever with Renal Syndrome, HFRS, appears first as a global concern of one virus family, several human pathogenic viruses of the genus *Orthohantavirus*, multiple clinical presentations, and different epidemiological patterns [49]. Hantaviruses and HFRS were first described in Asia [50]; nowadays, Hantaviruses are the cause of zoonoses that are expanding worldwide. Indeed, since 1993 when a previously unknown hantavirus was implicated in the first hantavirus pulmonary syndrome (HPS) outbreak in the United States, several other hantavirus infections were reported in western Europe, and then hantaviruses were described in South America. Ultimately, after an early suspicion of the presence of the Hantaviruses in Africa [51], a novel hantavirus, Sangassou virus, was isolated in 2012 in Guinea [52]. Altogether we observed the emergence of the *Hantaviridae* in the Western hemisphere, from the old World to the new World, and recently discovered its first tentative steps on the African continent. With respect to the Orthohantavirus genus, a real pandemic exists even when multiple viruses are involved. Ultimately, as for the *Arenaviridae*, hosts are specific and certainly the major vectors of virus dispersion.

2.2.6 Lassa Fever and Other Arenaviruses: A Global Dispersion with Localized Epidemics

The *Arenaviridae* includes 33 different viral species grouped as Old or New World arenaviruses [53], each is maintained by rodents of individual species as natural reservoir host and as vector for the viruses that are human pathogens. The rodent hosts are chronically infected without obvious illness and they pass virus vertically to their offspring. De facto, the distribution of the virus covers that of its natural hosts but is isolated in an ecosystem generally limited by natural barriers, e.g., mountains, river. A phenomenon in which rodent lineages are naturally infected by a virus and remain in such a limited environment is called “nidality” [54]. This is what it is observed for Argentinian HF, Venezuelan HF, Bolivian HF, and Lassa HF. Regarding the pandemic risk of any of these HF, arenaviruses because of their strict association with their natural hosts, like the hantaviruses, have their expansion potential limited by their natural hosts even though the latter are widely spread and could certainly be infected. Such risk lies in an unexpected encounter between infected and noninfected populations under the pressures of (as yet unknown) factors that favor their migration from enzootic to non-enzootic areas. In that matter, lymphocytic choriomeningitis virus, another member of the *Arenaviridae*, has a worldwide distribution through its domesticated natural host, the ubiquitous house mouse, *Mus musculus*.

2.2.7 Crimean-Congo Hemorrhagic Fever: An Emerging Threat

Although Crimean-Congo hemorrhagic fever, CCHF, is a widespread disease endemic to Africa, the Balkans, Western Asia, and Asian countries south of the 50th parallel North, it is generally transmitted by ticks to livestock or humans and therefore geographically limited to regions where tick vectors feed on humans.

Although the competent ixodid vector is limited, as is the abundance of their natural hosts, climate change modifies the distribution and abundance of tick hosts (i.e., tick abundance) [55]. Additionally the CCHFV pandemic risk is limited by low mobility, geographical repartition, and seasonal activity, although its main natural hosts are widely dispersed from Africa, to Asia and Europe [56]. Ultimately, human-to-human transmission occurs from close contact with the blood, secretions, or other biological fluids of infected persons but these remain rare events with a $R_0 < 1$. Altogether, a CCHF pandemic risk remains hypothetical but underlined by the risk of human-to-human transmission [57].

2.2.8 Rift Valley Fever

As for CCHF, Rift Valley fever, RVF, is first a disease of cattle and illustrates a unique subcontinental zoonotic spread along the path of traditional herders. RVF became a transcontinental risk with trade and transportation when the virus spread from North East Africa to Western Africa, and even to Madagascar [58]. If one considers its pandemic risk, with respect to RVF epidemiology as a mosquito-transmitted disease, two factors have to play concomitantly: the presence of infected cattle (i.e., nonimmune) and competent mosquito abundance, both considered hazards, while concretizing the risks from human vulnerability (nonimmune; mosquito bite; direct exposure to infected blood).

3 Response Preparedness

3.1 Framework

In order to streamline the prevention and the actions to reduce epidemic risk, the various elements involved in an outbreak are here considered from a systemic point of view, considering the risk as the convergence of a hazard and vulnerability:

- The presence of the threat (or “hazard” pathogen, i.e., vector, virus reservoir) is considered to be a necessary—but not sufficient—condition for the development of a disease. It is often known only in terms of probabilities, sometimes very low and therefore often subject to significant random variability in time and space. We often seek to evaluate the spatial and temporal differences of this probability, trying to measure its significance. Sometimes, it only uses one character necessary to the presence of the pathogen or vector (e.g., the presence of water, a minimum temperature, a type of vegetation).
- The susceptibility of the host (which is essentially linked to individual characters, genetic, biological, such as immune status or age) is individual, and often given by a probability.
- Direct exposure of the host to the hazard is an element of active vulnerability, depending on the behavior of the host that increases the likelihood of contact between host and hazard by

exposing it to an environment conducive to his presence (e.g., travel and contacts, professional activities). It also includes all the known “risk” behaviors that increase the likelihood of direct exposure to the hazard.

- Passive vulnerability of the host, which is not directly dependent on the pathology, is not even necessary nor sufficient for pathology, but influences the exposure of the host to the hazard or to protection from the pathology. This protection consists of prophylaxis, access to care, availability of care. It is independent of the real presence of the hazard; the host can be vulnerable without being exposed to the threat. The vulnerability is often defined by several levels (individual, context). It is very often “spatial” as linked to phenomena of segregation or spatial concentration. This is an area primarily studied by geography.

Ultimately, this vision can differentiate what is active, often subject to high variability, random in time and space (the emergence or the presence of hazards is often difficult if not impossible to control) from what is passive, generally situated among more stable population levels (sensitivities, exhibitions, behaviors, and vulnerabilities). This allows for better public health preventive actions, and also to understand rationally crisis situations by preemptively targeting the most important elements of the system in terms of vulnerability, and secondly by optimizing risk reduction (elimination of vectors, vaccinations, quarantine, etc.). In all cases, these actions must be adapted to social contexts to have a real impact on risk behaviors and vulnerabilities that they generate, hence the increasing role of anthropology in the field of health.

To prevent or reduce the epidemic risk, it is necessary to act on each component of this system:

- Reducing the susceptibility of the host (e.g., immunization, vaccination, prophylaxis).
- Reducing host exposure to the pathogen (e.g., vector control, quarantine, exclusion zone).
- Eliminating the pathogen directly (e.g., animal slaughter, disinfection, hygiene), or indirectly (e.g., suppress transmission).
- Reducing host vulnerability (e.g., socio-economic, behavioral, access to health care system).
- Reducing host exposure to emergency condition (e.g., real-time data collection, warning systems for emergency, crisis management, implementation of treatment).

The rapid detection of emergence is the key to controlling the spread of an epidemic. It requires comprehensive monitoring to trigger alerts and all other risk-reducing actions, in particular, reducing the exposure of the host to the pathogen and, if possible,

the elimination of the pathogen. In parallel to the monitoring and warning systems, protocols must always take into account local characteristics of political power and decision-making bodies that could otherwise render ineffective year-long action plans or warning systems (for example, the management of the chikungunya epidemic in Reunion Island was largely impacted by bottlenecks related to local political system) [59].

3.2 Global Surveillance and Data Collection

Biosurveillance and efficiency in data collection and management will be the technical keys for prevention (early detection of epidemic risk) and forecasting epidemic emergence and spread (i.e., analyzing the data in near real time taking into account the vulnerability of a given population). Also, this can be achieved only by exhaustive capacity building (human and technical) mostly in the more vulnerable developing countries but also where the most advanced technology needs to be developed. Networking biosurveillance systems are a major undertaking from regional to global, involving politics and diplomacy. Taking in account the local characteristics of political structures and decision systems is fundamental.

Despite our current recognition of the risks posed by emerging and re-emerging infectious diseases to global public health and stability, reliable structured data remains a major gap in our ability to measure (and therefore manage) globally infectious diseases. WHO has long served as an information hub for infectious disease events worldwide; however, extracting quantitative data from WHO information bulletins (*Weekly Epidemiological Record* and the more recent *Disease Outbreak News alerts*) proves to be a time-consuming effort with limited results in terms of operability, and exists more for the record and future analysis. The current proliferation of geospatial information tools (i.e., Geographical Information System, GIS) and stepwise advances in data extraction capabilities have made it possible to develop robust, systematic databases facilitating anomaly detection (like clusters), infectious disease models (and model evaluation), and apples-to-apples comparisons of historic infectious disease events worldwide. However, biosurveillance capabilities—the key to global prevention and health security—remain inadequate to support true early detection and response. Increased access to technology, rapidly developing communications infrastructures, smartphone usage for suspected-case reporting, and global networks of (formal and informal) disease surveillance practitioners provide an explosive opportunity to patch and improve surveillance networks. The challenge is to leverage all these developments, implement technical and capacity building where needed, before the next epidemic with global impact emerges.

Several organizations have developed systems to collect epidemic information and facilitate rapid response: WHO has the Department of Pandemic and Epidemic Diseases (PED) that

develops mechanisms to address epidemic diseases, thereby reducing their impact on affected populations and limiting their international spread. Among them some have self-explanatory titles: the Battle against Respiratory Viruses (BRaVe); Early Warning and Response systems for Epidemics in emergency (EWARE); Emerging and Dangerous Pathogens Laboratory Network (EDPLN); International Coordinating Group for access to vaccines for epidemics (ICG); Global Infection Prevention and Control Network; (GIPCN); Global Influenza Surveillance and Response System (GISRS); Global Leptospirosis Environmental Action Network (GLEAN); Meningitis Environmental Risk Information Technologies (MERIT); Weekly Epidemiological Record (WER); Emerging Diseases Clinical Assessment and Response Network (EDCARN). Global commitment to these efforts will insure their readiness in times of need.

3.3 Emergency Funding for Outbreaks, Epidemics, and Pandemics

Most certainly and most importantly, any preparedness and response requires emergency funding [60]. It has been estimated that if the Ebola virus disease response started 2 months earlier, it could have reduced the total number of deaths by 80% in Liberia and Sierra Leone [61]. We learned from this last EVD epidemic that in March 2015, the African Union's Minister of Finance requested the African Risk Capacity (ARC) Agency to help Member States to better plan, prepare, and respond to devastating outbreaks by developing new applications for financial tools, like insurance, that can significantly improve the speed of funds to affected countries and shorten the time between event and response. The Agency is now developing an outbreak and epidemic insurance product primarily based on responsibly and timely budget reallocation; however, viruses do not wait. Moreover, the World Bank's Pandemic Emergency Facility is designed to finance surge capacity and support international government partners to actively participate to the response. Ultimately, epidemics are not one-off events, but rather demonstrate financial patterns similar to other natural catastrophes. As natural catastrophes, large epidemics can be insured by creating financial mechanisms to facilitate the movement of critical resources within affected countries and ultimately manage the spread of disease and minimizing macroeconomic impact [62].

3.4 Tools and Strategies for a Global Prevention of Pandemic Risk

Classical tools and strategies for predicting epidemics encompass human disease surveillance (e.g., public health and hospital statistics) and, sometimes, environmental surveys (e.g., climate, el Niño, earthquake, tsunami); also more recently complying with One Health concept, human and veterinary health as well environmental risk factors have been reunited in a comprehensive approach of Public Health risk (i.e., outbreak, epidemic risks). However, this heuristic approach of health remains limited to specific diseases and territories and does not apply as a global predictor of pandemics.

First, historical data is the only available objective view of past epidemics and pandemics, needs to be collected, formatted, corrected, and analyzed. This will be the foundation of the different tools and strategies described below. In that matter, with respect to the depth of the past data available, time series of disease observation, modern tools such as Internet Search Data have actually led to the development of several specific sites (e.g., Google Flu and Dengue) [63], whose search-term reports have correlated strongly with incidence estimates in several public health reports in Europe, Asia, and the U.S. However, even though such tools can complement classical disease surveillance, most of these sites are geographically limited and cannot be used for live monitoring of epidemic risk and for Neglected Tropical Disease Surveillance [64, 65]. However, from such historical and live-collected data, health alert systems can be implemented, and prediction models can be developed. Moreover, thanks to the spatial analyses, combining multiple data sources will provide the ultimate tools for live-mapping an outbreak, which will lead to an efficient response when tools and strategy have been specifically identified (i.e., sufficient and available in-country health system resources and funding; identifying variations in pathogen sequences that contribute to R_0 and pathogenicity; monitoring population movement; etc.).

3.4.1 “Big Data” Analysis

The amount of data being digitally collected and stored is exponentially accumulating. It is estimated that, as of September of 2016, the World Wide Web reached 5.02 billion pages containing eight zettabytes of accessible data, and the accumulation of information is growing around 40% every year [66]. This situation has generated much discussion about how to use the unprecedented availability of information and computational resources and the sophistication of new analytic and visualization algorithms for decision-making to reduce the impact of infectious diseases. In fact, it is argued that the paradigm of “Big Data” will change not only the way business and research is done, but significantly improve the understanding of factors leading to the emergence of infectious diseases. Big Data could lead to the implementation of a decentralized biosurveillance enterprise allowing organizations and individuals to take full advantage of a large collection of disparate, unstructured qualitative, and quantitative datasets. With the proper integration and the right analytics, Big Data could find unusual data trends leading to better pathogen detection systems, as well as therapeutic and prophylactic countermeasures. However, the impact of these analyses and forecasts depends not only on how the data is collected, ingested, disambiguated and processed, but also on how it is relayed in different operational contexts to users with different backgrounds and understandings of technology. While impressive in data mining capabilities, real-time content analysis of social media data misses much of the factual complexity.

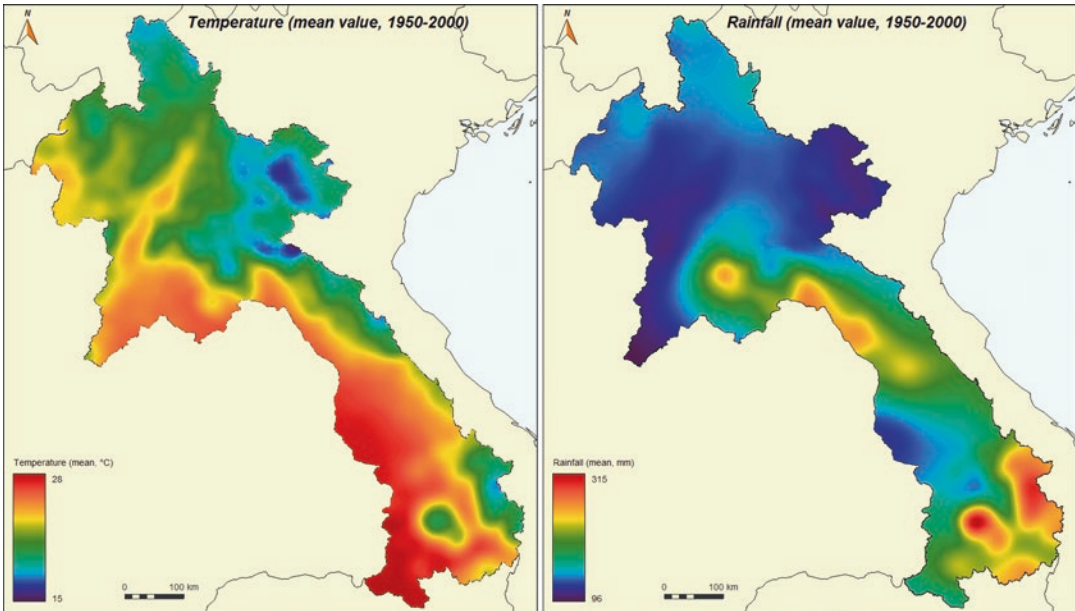


Fig. 1 Mapping environmental factors that have a major impact on insect vector population (i.e., mosquitoes and ticks). This map of Laos constitutes the basis of a risk map showing part of the hazards contributing to virus vector density that could be matched with human density and pathogen prevalence leading to a risk map (spatial risk) and eventually extended through seasonality (temporal risk). Mean temperature and mean rainfalls are interpolated as climatic conditions, as environmental factors influencing the presence of mosquitoes

Quality issues within freeform user-provided hashtags and biased referencing can significantly undermine our confidence in the information obtained to make critical decisions about the natural versus intentional emergence of a pathogen.

3.4.2 Spatial Analysis

Risk factors associated with a health event in a population are often linked to environmental factors (Fig. 1). They are also linked to spatial relationships between individuals, especially for infectious diseases. The geographical distribution of these phenomena reflects spatial relationships. Beyond “classic” epidemiology mainly based on statistical analysis, using the location and spatial distribution is essential in the understanding of health events and analysis of their mechanisms.

Spatial analysis in epidemiology is a method to help determine the location (georeferenced) of risk factors. It allows one to identify the spatial and temporal differentiation in the distribution of events, using their location in time and space. When the location is available, with precision for each studied object (i.e., individuals or geographical units), it is possible to:

- Characterize the overall spatial distribution, using synthetic indices on the absolute position of an object, on the average spatial arrangement of objects or their values (grouping/

dispersion, spatial dependence, variogram measure of Auto-correlation Space).

- Look for characteristics of the overall shape of the phenomenon (tendency, shape), and search for a theoretical spatial distribution, or for a process to model the observed spatial distribution.
- Look for unusual places (geographical centers and source sites; aggregates; exclusions; hot spots, cold spots), and to study the spatial relationships at the individual level.
- Conduct spatiotemporal analysis: search index cases, reconstruction of paths, diffusion models, models of extinction, etc.
- Spatial analysis allows the development of applications for modeling epidemics, preparing warning systems, as well as crisis management systems, risk prevention and analysis systems, and vaccination campaigns. Many tools for biomonitoring and prevention of epidemic risk have been developed (Fig. 2), as well as software tools to:
 - (a) Visualize spatial distributions.
 - (b) Synthesize and analyze position and spatial relationships between events (continuity, consolidation, attraction-repulsion, shape, centrality, displacement, diffusion processes).
 - (c) To analyze the relationship between spatial distribution of attributed values and environmental characteristics of the phenomenon (environmental correlations).
 - (d) To model the phenomena of emergence, dissemination, extinguishment of an epidemic.

Cluster detection, space-time analysis, and spatial integration with environmental and demographic data are widely used in such warning systems.

3.4.3 Genomic-Based Biosurveillance

Multiple and complex factors are associated with the emergence and impact of pathogens in a given geographical area. Therefore, public health analysts are confronted with the task to identify the likely, and unlikely, consequences and alternative critical outcomes of a given VHF outbreak. This requires the ability to monitor in near real time the dynamics of the geographical dissemination of these viruses in villages, cities, countries, continents, or the globe using new analytical techniques within the emerging field of *genomic-based biosurveillance*. This concept integrates microbial genotyping, next generation sequencing, metagenomics, big data and database analytics, and contextualized visualization to identify, characterize, and attribute known and unknown pathogens and generate estimates of how different contingencies will affect their impact [67]. A genomic-based biosurveillance system includes

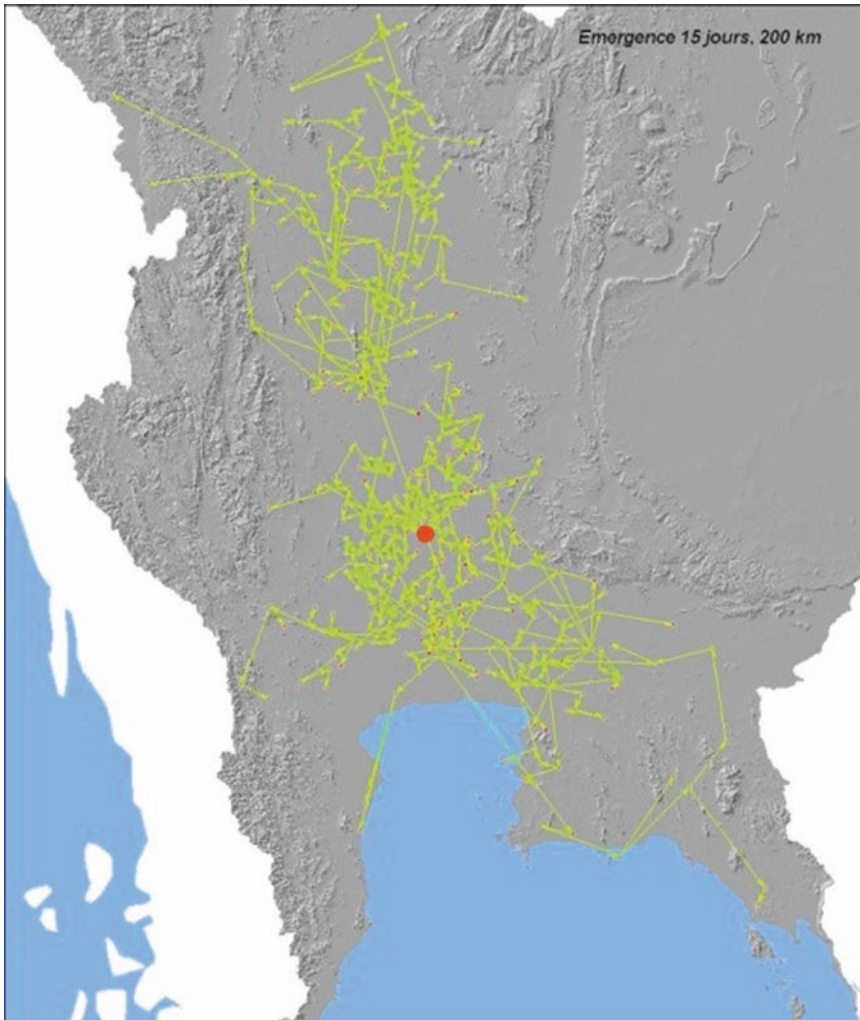


Fig. 2 From the point of emergence of H5N1 to the pathways of spread: The exemplary case of the highly pathogenic avian influenza virus H5N1 in Thailand. From the emergence of one imported case (*red-filled circle*), the pathway direction (*arrowed green lines*) of H5N1 infection in farms (*yellow points*) is reconstituted, using dates of infection and distance between farms. Results show local spread with time-to-time medium distance jumps

powerful microbial genomic characterization to rapidly identify a pathogen [67]. This characteristic makes a genomic-based biosurveillance a useful approach not only for public health but serves as a deterrence tool for intentional biological weapon development and deployment. The initial step consists of integration of signals generated by molecular-based assays and next generation DNA sequencing and unbiased microbial characterization for pathogen source tracing, attribution and forensics. While each of these techniques has been discussed in the literature in detail [68], the integration of this information can yield a more extended view of the scale of a pathogen outbreak. The development of high-throughput

DNA sequencing technologies (i.e., DNA and cDNA forms of RNA viral genomes) is allowing the genomic characterization of previously unknown pathogens without relying on prior reference molecular information [69, 70]. This information is available within days, and even hours, of sample collection, and well before the development of animal infection models. Because of their portability, this technology will become widely used in the next 5 years in routine clinical settings. However, to be clinically and epidemiologically relevant, DNA sequences must be rapidly and effectively translated into actionable information defining pathogen characteristics (i.e., virulence or drug resistance), it must point to a source of origin, and discriminate a natural event from a manmade release [71]. While some government agencies are considering use of genomic information to develop next generation Level-0 and Level-1 detection/surveillance devices [72, 73], there is no reference database where researchers can retrieve standardized genomic signatures and motif fingerprints to develop primer-, probe-, and antibody-based detection technology using reference moieties. The impact of genomic-based biosurveillance in public health and biodefense will not be fully realized until addressing the current impracticality of transferring the terabytes of genomic data generated by DNA sequencing devices to a centralized architecture performing analysis operations, as that might take hours or even days. Therefore, a new paradigm could emerge from encouraging the development of decentralized algorithms that first determine in situ the presence of pathogen-specific genomic signatures or motif fingerprints, summarize and relay the results into an operational biosurveillance metadata format for contextualized decision support.

3.4.4 Database Management and Geographical Information System (GIS)

The localized data management, time, and space required for spatial analysis is performed by geographic information systems (GIS). These are computer systems that manage large volumes of data and easily use the location to perform spatial analysis. Most GIS are not limited to data management functions, but also integrate multiple analysis tools, data transformation, and cartographic representation. These are for the most part complex applications with enormous features. The “GIS” designation covers a wide variety of software projects built according to different technical options, functionality, and diverse performances. A GIS is essentially a management tool (structure, organization, entry, storage), an analytical tool (statistical and geographical treatment, spatial analysis), and a communication tool (data visualization, descriptive mapping, thematic mapping, atlas). It is also a tool that allows the use of a spatial model for the simulation of a process, such as the development of an epidemic. GIS facilitates the interface between modeling and simulation program, and the geographic database, and can ultimately take over the whole of access to spatial information

needed by the modeling program. The GIS should thus be at the heart of organizing the collection and processing of monitoring data. To ensure the management of this system, it is important to set up a body specifying all the collection, validation, processing and dissemination of information and results (alerts, risk modeling, near real-time dissemination of results). This body must be proposed and validated by political authorities, preemptively, to avoid further blockage and to ensure effectiveness in situations of epidemic crisis.

3.4.5 *Mathematical Modeling*

Mathematical modeling is a mathematical formulation of a parameter or risk; it depends on identified or hypothesized risk factors whose coefficients are determined by a statistical or heuristic analysis from historical or observed data with the use of R_0 , as a basic reproduction rate, to timely and spatially predict the spread-speed of an emerging outbreak. Spatial-temporal modeling of health events can be seen as the final stage of the analysis. It is different from statistical modeling. Despite using risk factors, it considers the epidemic phenomenon as a whole, taking into account the spatial relationships between agents (hosts, vectors, reservoirs, and pathogens), between individuals, and relationships between individuals and their environment. This model is thus useful for understanding and anticipating the epidemics, and can be generally used to classify individuals in different states (susceptible, infected, sick healed, immune) and to model the major phenomena that can change the state of an individual. However, when a model takes into account many phenomena, it can quickly become very complex. The vast majority of models are simplifications of assumed reality. Two broad categories of methods are usually developed in modeling:

- A deterministic approach, based on differential equations whose coefficients are adjusted from observed data, or monitoring data from epidemics. In this model, one can introduce stochastic types of components in the coefficients, studying the variability of observed data. Taking no account of spatial relationships is difficult in these models, which deal in general populations, not individuals.
- A nondeterministic approach, which is based on agents whose behavior is described by expertly determined rules (multi-agent models). The status of each agent is calculated at each time step, from its behavior, environment, and relations between the agent and all other agents. These models take into account a more realistic description of the phenomenon, near the complex system finely describing reality. They allow us to consider spatial relationships in each time step. These models require intensive calculation, and their use is made possible by development of the power of computer calculations.

4 Conclusion

Let us first honestly address the fundamental questions about epidemics and preparedness: What did we learn from all the past epidemics, what will we remember in times of need? Are we prepared for the worst of these hypothetical pandemics abundantly illustrated in the cinema and unfortunately sometimes overwhelmed when reality goes beyond fiction? Certainly, we are not “globally” prepared, unfortunately, at that scale, the immense natural and human disparities do not permit it, but we do our best in our own societies. The concept of disease emergence, born only at the end of the twentieth century, is a societal marker, our desire to be on alert, understand and predict epidemics. Ultimately, there are a few, but necessary and difficult goals to reach for the prevention and control of any epidemic, also these goals are part of the development of our societies, as well as for education, they become part of the well-being for all: First, beyond understanding transmission, is needed a clear understanding of the epidemiological pattern and the spread of a given disease, before it is too late; then, which is certainly one of the more complex and costly things to achieve, is having an efficient health system to respond to an epidemic and an operational network to respond at the regional and global levels; and last but certainly not a least, having identified funding for any public health emergency will be crucial to changing our world. Perhaps, in a shrinking global community, after too many Ebola virus disease outbreaks, we will learn and be prepared for future epidemic challenges? The progress made, mostly by computer sciences in the overall analysis of health data, should serve as a tool in the prevention of major epidemics. Let us ultimately use our predictions of pandemic risk to meet and unite beyond the current frontiers of political and social wills.

Acknowledgments

W.A. Valdivia-Granda has been funded by the Department of Homeland Security and the Department of Defense. We are grateful to Sarah Cheeseman Barthel, Director, Data Acquisition & Management Metabiota, Inc., for her review and input of the section on “global surveillance and data collection.”

References

1. Dawson PM et al (2015) Epidemic predictions in an imperfect world: modelling disease spread with partial data. *Proc R Soc B* 282(1808):20150205
2. Debré P, Gonzalez JP (2013) Vie et mort des épidémies. *O J Med*, p 285
3. Beeching NJ, Dance DAB, Miller ARO, Spencer RC (2002) Biological warfare and bioterrorism. *Br Med J* 324(7333):336–339
4. Thucydides (2016) The history of the Peloponnesian War (english trans. by Richard Crawley). The Internet classics archive. <http://classics.mit.edu//pelopwar.html>
5. Biraben JN (1995) Les maladies en Europe: équilibre et ruptures de la pathocénose. In: MD Grmek (ed) *Histoire de la pensée médicale en Occident*, t.1, Seuil, 1995, p. 283–310.

6. Berche P (2012) Faut-il encore avoir peur de la grippe. *Histoire des pandémies*, Odile Jacob 2012:80–81
7. Littman RJ, Littman ML (1973) Galen and the Antonine plague author(s). *The Am Jof Philol* 94(3):243–255
8. Grmek MD (1997) *Histoire de la Pensée Médicale en occident—tome 2, de la renaissance aux Lumières*. Le Seuil, Paris
9. Fenner F (1988) Smallpox and its eradication (history of international public health, no 6). World Health Organization, Geneva
10. Stanley et al. (2010) The smallpox pandemic of 1870–1874.
11. Simmons BJ, Falto-Aizpurua LA, Griffith RD, Nouri K (2015) Smallpox: 12,000 years from plagues to eradication: a dermatologic ailment shaping the face of society. *JAMA Dermatol* 151(5):521. doi:10.1001/jamadermatol.2014.4812
12. Ferguson NM et al (2006) Strategies for mitigating an influenza pandemic. *Nature* 442(7101):448–452
13. Gubler DJ (2011) Dengue, urbanization and globalization: the unholy trinity of the 21st century. *Trop Med Health* 39(4 Suppl):3–11. doi:10.2149/tmh.2011-S05
14. Hughes JM (2004) SARS: an emerging global microbial threat. *Trans Am Clin Climatol Assoc* 115:361–372. discussion 372–374
15. Valdano E et al (2015) Predicting epidemic risk from past temporal contact data. *PLoS Comput Biol* 11(3):1004152
16. Bellan SE, Pulliam JR, Dushoff J, Meyers LA (2014) Ebola control: effect of asymptomatic infection and acquired immunity. *Lancet* 384(9953):1499–1500. doi:10.1016/S0140-6736(14)61839-0
17. Akerlund E, Prescott J, Tampellini L (2015) Shedding of Ebola virus in an asymptomatic pregnant woman. *N Engl J Med* 372(25):2467–2469. doi:10.1056/NEJMc1503275
18. Wauquier N, Bangura J, Moses L, Humarr Khan S, Coomber M, Lungay V, Gbakie M, Sesay MS, Gassama IA, Massally JL, Gbakima A, Squire J, Lamin M, Kanneh L, Yillah M, Kargbo K, Roberts W, Vandi M, Kargbo D, Vincent T, Jambai A, Guttieri M, Fair J, Souris M, Gonzalez JP (2015) Understanding the emergence of Ebola virus disease in sierra leone: stalking the virus in the threatening wake of emergence. *PLoS Curr* 2015; 7:pil:ecurrents.outbreaks.9a6530ab7bb9096b34143230ab01cdef. doi:10.1371/currents.outbreaks.9a6530ab7bb9096b34143230ab01cdef
19. Spengler JR, Ervin ED, Towner JS, Rollin PE, Nichol ST (2016) Perspectives on West Africa Ebola virus disease outbreak, 2013–2016. *Emerg Infect Dis* 22(6):956–963. doi:10.3201/cid2206.160021
20. Reiter P (1998) *Aedes albopictus* and the world trade in used tires, 1988–1995: the shape of things to come? *J Am Mosq Control Assoc* 14:83–94
21. Gonzalez JP, Prugnonne F, Leroy E (2013) Men, primates, and germs: an ongoing affair. *Curr Top Microbiol Immunol* 365:337–353. doi:10.1007/82_2012_304
22. Yashina LN, Abramov SA, Gutorov VV, Dupal TA, Krivopalov AV, Panov VV, Danchinova GA, Vinogradov VV, Luchnikova EM, Hay J, Kang HJ, and Yanagihara R (2010) Seewis virus: phylogeography of a Shrew-Borne hantavirus in Siberia, Russia. *Vector Borne Zoonotic Dis* 10(6):585–591. doi:10.1089/vbz.2009.0154 PMID: PMC2979336
23. Gonzalez JP (1996) Coevolution of rodent and viruses: arenaviruses and hantaviruses. In: M. Ali Ozcel (ed) *New dimension in parasitology*. *Acta Parasitol Turcica* 20(Supp 1): 617–638
24. Gonzalez JP, Jean MD (1999) The arenavirus and rodent coevolution process: a global view of a theory. In: JF Saluzzo, B Dodet (eds) *Factors in the Emergence and control of rodent-borne diseases*. Elsevier, Paris, pp 39–42
25. Drexler JF, Seelen A, Corman VM, Fumie Tateno A, Cottontail V, Melim Zerbinati R, Gloza-Rausch F, Klose S, Adu-Sarkodie Y, Oppong SK, EKV K, Osterman A, Rasche A, Adam A, Müller MA, Ulrich RG, Leroy EM, Lukashev AN, Drosten C (2012) Bats worldwide carry hepatitis E virus-related viruses that form a putative novel genus within the family *Hepeviridae*. *J Virol* 86(17):9134–9147. doi:10.1128/JVI.00800-12
26. Grard G, Fair JN, Lee D, Slikas E, Steffen I, Muyembe JJ, Sittler T, Veeraraghavan N, Ruby JG, Wang C, Makuwa M, Mulembakani P, Tesh RB, Mazet J, Rimoin AW, Taylor T, Schneider BS, Simmons G, Delwart E, Wolfe ND, Chiu CY, Leroy EM (2012) A novel rhabdovirus associated with acute hemorrhagic fever in Central Africa. *PLoS Pathog* 8(9): 1002924
27. Federal Select Agent program: Select Agent and toxins list. <http://www.selectagents.gov/SelectAgentsandToxinsList.html>. Accessed Aug 2016
28. WHO recommended surveillance standards WHO/CDS/CSR/ISR/99.2 <http://www.who.int/csr/resources/publications/surveillance/whocdscsr992syn.pdf>. Accessed Aug 2016

29. Paessler S, Walker DH (2013) Pathogenesis of the viral hemorrhagic fevers. *Annu Rev Pathol* 8:411–440. doi:[10.1146/annurev-pathol-020712-164041](https://doi.org/10.1146/annurev-pathol-020712-164041)
30. Oldstone M (2009) Viruses, plagues, and history: past, present and future. Oxford University Press, Oxford, pp 102–104
31. WHO (2014) Yellow fever fact sheet N°100. World Health Organization, Geneva
32. Garske T, Van Kerkhove MD, Yactayo S, Ronveaux O, Lewis RF et al (2014) Yellow fever in Africa: estimating the burden of disease and impact of mass vaccination from outbreak and serological data. *PLoS Med* 11(5):e1001638. doi:[10.1371/journal.pmed.1001638](https://doi.org/10.1371/journal.pmed.1001638)
33. Gubler DJ (2004) The changing epidemiology of yellow fever and dengue, 1900 to 2003: full circle? *Comp Immunol Microbiol Infect Dis* 27(5):319–330
34. Grobbelaar AA, Weyer J, Moolla N, Jansen-van-Vuren P, Moises F, Paweska JT (2016) Resurgence of yellow fever in Angola, 2015–2016. *Emerg Infect Dis* 22(10):1854–1855. doi:[10.3201/eid2210.160818](https://doi.org/10.3201/eid2210.160818)
35. Simons H, Patel D (2016) International health regulations in practice: focus on yellow fever and poliomyelitis. *Hum Vaccin Immunother* 12(10):2690–2693
36. Burki T (2016) Yellow fever in Africa: a disaster waiting to happen. *Lancet Infect Dis* 16(8):896–897. doi:[10.1016/S1473-3099\(16\)30224-9](https://doi.org/10.1016/S1473-3099(16)30224-9)
37. Gubler DJ, Clark GG (1995) Dengue/dengue hemorrhagic fever: the emergence of a global health problem. *Emerg Infect Dis* 1(2):55–57
38. Delaporte (1874) Rapp. au ministre de la marine. *J offic* 2 avr 1874, p. 2546, 2e col
39. LeDuc JW, Esteves K, Gratz NG (2004) Dengue and dengue haemorrhagic fever. In: Murray CJ, Lopez AD, Mathers CD (eds) *The global epidemiology of infectious diseases, Global burden of disease and injury series*, vol 4. World Health Organization, Geneva, pp 219–242
40. Gubler DJ (1988) Dengue. In: Monath TPM (ed) *Epidemiology of arthropod-borne viral disease*. CRC Press, Boca Raton (FL), pp 223–260
41. Halstead SB (1992) The XXth century dengue pandemic: need for surveillance and research. *Rapp Trimest Statist Sanit Mondo* 45: 292–298
42. Gubler DJ, Trent DW (1994) Emergence of epidemic dengue/dengue hemorrhagic fever as a public health problem in the Americas. *Infect Agents Dis* 2:383–393
43. Siegert R, Shu HL, Slenczka W, Peters D, Müller G (2009) Zur Ätiologie einer unbekanntem, von Affen ausgegangenen menschlichen Infektionskrankheit. *Deutsch Med Wochenschr* 92(51):2341–2343. doi:[10.1055/s-0028-1106144](https://doi.org/10.1055/s-0028-1106144)
44. Towner JS, Amman BR, Sealy TK, Carroll SAR, Comer JA, Kemp A, Swanepoel R, Paddock CD, Balinandi S, Khristova ML, Formenty PB, Albarino CG, Miller DM, Reed ZD, Kayiwa JT, Mills JN, Cannon DL, Greer PW, Byaruhanga E, Farnon EC, Atimmedi P, Okware S, Katongole-Mbidde E, Downing R, Tappero JW, Zaki SR, Ksiazek TG, Nichol ST, Rollin PE (2009) Isolation of genetically diverse Marburg viruses from Egyptian fruit bats. *PLoS Pathog* 5(7):1000536
45. Paweska JT, Jansen-Van-Vuren P, Masumu J, Lemana PA, Grobbelaar AA, Birkhead M, Cliff S, Swanepoel R, Kemp A (2012) Virological and serological findings in *Rousettus aegyptiacus* experimentally inoculated with vero cell-adapted hogan strain of Marburg virus. *PLoS One* 7(9):45479. doi:[10.1371/journal.pone.0045479](https://doi.org/10.1371/journal.pone.0045479)
46. Jean-Paul G, Herbreteau V, Morvan J, Leroy E (2005) Ebola virus circulation in Africa: a balance between clinical expression and epidemiological silence. *Bull Soc Pathol Exotiq* 98(3):210–217
47. Leroy EM, Gonzalez JP, Baize S (2011) Ebola and Marburg haemorrhagic fever viruses: major scientific advances, but a relatively minor public health threat for Africa. *Clin Microbiol Infect* 17(7):964–976
48. Gostin LO, Lucey D, Phelan A (2014) The Ebola epidemic: a global health emergency. *JAMA* 312(11):1095–1096. doi:[10.1001/jama.2014.11176](https://doi.org/10.1001/jama.2014.11176)
49. Kulzer P, Schäfer RM, Heidland A (1993) Hantavirus infections 1993: endemic or unrecognized pandemic? *Dtsch Med Wochenschr* 118(42):1546–1546
50. Johnson KM (2001) Hantaviruses: history and overview. *Curr Top Microbiol Immunol* 256(256):1–14. doi:[10.1007/978-3-642-56753-7_1](https://doi.org/10.1007/978-3-642-56753-7_1)
51. Gonzalez JP, McCormick JB, Baudon D, Gautun JP, Meunier DY, Dournon E, Georges AJ (1984) Serological evidence for Hantaan-related virus in Africa. *Lancet* 2: 1036–1037
52. Klempa B, Witkowski PT, Auste B, Koivogui L, Fichet-Calvet E, Strecker T, Ter Meulen J, Krüger DH (2012) Sangassou virus, the first hantavirus isolate from Africa, displays genetic and functional properties distinct from those of other murinae-associated hantaviruses. *J Virol* 86(7):3819–3827. doi:[10.1128/JVI.05879-11](https://doi.org/10.1128/JVI.05879-11)

53. Radoshitzky SR, Bào Y, Buchmeier MJ, Charrel RN, Clawson AN, Clegg CS, DeRisi JL, Emonet S, Gonzalez JP, Kuhn JH, Lukashevich IS, Peters CJ, Romanowski V, Salvato MS, Stenglein MD, de la Torre JC (2015) Past, present, and future of arenavirus taxonomy. *Arch Virol* 160(7):1851–1874
54. Salazar-Bravo J, Dragoo JW, Bowen MD, Peters CJ, Ksiazek TG, Yates TL (2002) Natural nidality in Bolivian hemorrhagic fever and the systematics of the reservoir species. *Infect Genet Evol* 1(3):191–199
55. Medlock JM, Hansford KM, Bormane A et al (2013) Driving forces for changes in geographical distribution of *Ixodes ricinus* ticks in Europe. *Parasit Vectors* 6:1. doi:10.1186/1756-3305-6-1
56. Spengler JR, Bergeron É, Rollin PE (2016) Seroepidemiological studies of Crimean-Congo hemorrhagic fever virus in domestic and wild animals. *PLoS Negl Trop Dis* 10(1):e0004210. doi:10.1371/journal.pntd.0004210
57. Ergonul O (2012) Crimean-Congo hemorrhagic fever virus: new outbreaks, new discoveries. *Curr Opin Virol* 2:215–220. doi:10.1016/j.coviro.2012.03.001
58. Nanyingi MO, Munyua P, Kiama SG, Muchemi GM, Thumbi SM, Bitek AO, Bett B, Muriithi RM, Njenga MK (2015) A systematic review of rift valley fever epidemiology 1931–2014. *Infect Ecol Epidemiol* 5:28024
59. Soumahoro MK, Boelle PY, Gaüzere BA, Atsou K, Pelat C, Lambert B, La Ruche G, Gastellu-Etchegorry M, Renault P, Sarazin M, Yazdanpanah Y, Flahault A, Malvy D, Hanslik T (2011) The chikungunya epidemic on La Réunion Island in 2005–2006: a cost-of-illness study. *PLoS Negl Trop Dis* 5(6):e1197. doi:10.1371/journal.pntd.0001197
60. National Academies of Sciences, Engineering, and Medicine (2016) Global health risk framework: pandemic financing: workshop summary. The National Academies Press, Washington, DC. doi:10.17226/21855.
61. Beavogui M and Madsbjerg S. African risk capacity. Executive perspective: outbreak and epidemic insurance, new solution to an old problem. The Rockefeller Foundation, 27 Sept 2016. <http://sustainability.thomsonreuters.com/2016/09/27/executive-perspective-outbreak-and-epidemic-insurance-new-solution-to-an-old-problem/>. Accessed Aug 2016
62. Gonzalez JP. UNESCO. From the Ebola river to the Ebola virus disease pandemic: what have we learned? <http://www.sciforum.hu/programme/speakers-and-abstracts/gonzalez-jean-paul.html>. Accessed Aug 2016
63. <http://www.google.org/flutrends/about/>. Accessed Aug 2016
64. Chan EH et al (2011) Using web search query data to monitor dengue epidemics: a new model for neglected tropical disease surveillance. *PLoS Negl Trop Dis* 5(5):e1206
65. Gluskin RT, Johansson MA, Santillana M, Brownstein JS (2014) Evaluation of internet-based dengue query data: google dengue trends. *PLoS Negl Trop Dis* 8(2):e2713. doi:10.1371/journal.pntd.0002713
66. <http://www.worldwidewebsite.com>. Accessed Aug 2016
67. Valdivia-Granda WA (2013) Biosurveillance enterprise for operational awareness, a genomic-based approach for tracking pathogen virulence. *Virulence* 4(8):745–751
68. Valdivia-Granda WA (2010) Bioinformatics for biodefense: challenges and opportunities. *Biosec Bioterr Biodef Strat Pract Sci* 8(1):69–77
69. Gallego B et al (2009) Biosurveillance of emerging biotreats using scalable genotype clustering. *J Biomed Inform* 42(1):66–73
70. Ronald D, Fricker J, Banschbach D (2012) Optimizing biosurveillance systems that use threshold-based event detection methods. *Inf Fusion* 13(2):117–128
71. Valdivia-Granda W (2012) Biodefense oriented genomic-based pathogen classification systems: challenges and opportunities. *J Bioterr Biodef* 3(1):2–9
72. Jenkins WO et al. (2012) Biosurveillance observations on BioWatch generation-3 and other federal efforts: testimony before the subcommittees on emergency preparedness, response, and communications and Cybersecurity, infrastructure protection, and security technologies, committee on house homeland security, house of representatives, in testimony GAO-12-994 T. US Govt Accountability Office, Washington, DC
73. Jenkins WO, United States. Congress. House (2012) Committee on Homeland Security. Subcommittee on Emergency Preparedness Response and Communications., United States. Congress. House. Committee on Homeland Security. Subcommittee on Cybersecurity Infrastructure Protection and Security Technologies., United States. Government Accountability Office: Biosurveillance observations on BioWatch Generation-3 and other federal efforts: testimony before the Subcommittees on Emergency Preparedness, Response, and Communications and Cybersecurity, Infrastructure Protection, and Security Technologies, Committee on House Homeland Security, House of Representatives. In: *Testimony GAO-12-994 T*. U.S. Govt. Accountability Office, Washington, DC

An Approach to the Identification and Phylogenetic Analysis of Emerging and Hemorrhagic Fever Viruses

Francisco J. Díaz, Luis E. Paternina, and Juan David Rodas

Abstract

An important aspect of virological surveillance is the identification of the detected viruses. Broad surveillance, that typically employs deep sequencing of collected tissue samples, provides the investigator with many sequence files constructed from overlapping stretches of DNA sequences. Directed surveillance for viruses of a specific taxonomic group provides the investigator with sequence files from cDNA amplified using specific primers to conserved viral regions. Here we will describe general approaches to identify hemorrhagic viral agents through phylogenetic analysis of cDNA sequences obtained during surveillance activities.

Key words Hemorrhagic viruses, Phylogenetics, Databases, Alignment, Genetic trees, Bioinformatics

1 General Introduction

Viral hemorrhagic fevers (VHF) refer to a group of diseases caused by agents from different RNA viral families. The term “viral hemorrhagic fever” is used to describe the multisystem syndrome characterized by impairment of the vascular system, sometimes accompanied by hemorrhage (bleeding). Although the bleeding by itself is rarely the cause of death, and some types of hemorrhagic fever viruses can cause relatively mild illnesses, some of these viruses cause severe, life-threatening disease [1].

Viral hemorrhagic fevers share several features: (1) they all are produced by enveloped RNA viruses; (2) they are all zoonotic, involving transmission by insects, ticks, rodents, bats, or other wild or domestic reservoirs; (3) they are geographically restricted to the areas where their hosts live; (4) humans are usually incidental hosts that are sporadically infected, but in some cases, they can also transmit these viruses to other humans; and (5) outbreaks cannot be easily predicted, and there are very few antiviral treatments and

vaccines available [1]. So far, most of the agents associated with HF have been found within the following four viral families:

Filoviridae: Ebola and Marburg virus diseases

Arenaviridae: Lassa fever, Lujo, Guanarito, Machupo, Junín, Sabiá, and Chapare viruses

Bunyavirales: Rift Valley fever (mosquito-borne), Crimean-Congo hemorrhagic fever, and hantaviruses

Flaviviridae: Dengue, yellow fever, Omsk hemorrhagic fever, Kyasanur Forest disease, and Alkhurma viruses [2]

Here we will describe freely available programs to align your DNA sequence obtained from surveillance activities with reference sequences deposited in public databases like GenBank; we will describe how to analyze your sequence files in order to get phylogenetic trees for viral agent identification with brief notes about the utility of this work in epidemiological studies (e.g., mapping vector population spread and epidemic start sites).

2 Materials

Besides the sequences, the only other “materials” required for phylogenetic sequence analyses are the appropriate computer hardware and software: a sequence database and one or more phylogenetic packages.

1. Sequence databases. The major sequence database is GenBank, maintained at the National Center for Biotechnology Information (NCBI), Bethesda, Maryland, available at <http://www.ncbi.nlm.nih.gov/genbank/> [3]. The European (EMBL) and Japanese (DDBJ) bioinformatic databases are equivalent to GenBank since these three organizations exchange data on a daily basis. Several manuals and tutorials are available at the GenBank web site to get started and to understand the resources of the site. Another useful database for research in hemorrhagic fever viruses is the Virus Pathogen Resource (ViPR) available at <http://www.viprbrc.org/>. This is a more curated database focused on virus families; among them are *Flaviviridae*, *Togaviridae*, *Arenaviridae*, former *Bunyaviridae*, *Filoviridae*, and others. Besides serving as a repository of sequence data, the site provides several analytical tools for sequence alignment, similarity searches, phylogenetic reconstruction, sequence variation, and more [4].
2. Phylogenetic software. Many computer programs have been developed to perform phylogenetic and related sequence analyses and have been made available. A comprehensive list of them with comments about their uses and links to their web sites is maintained by Professor Joseph Felsenstein at the University of Washington [5]. Most of these are specialized

programs that perform specific analyses, making it necessary to combine them with other programs; so they will not be described here. We recommend MEGA (Molecular Evolutionary Genetic Analysis) software for beginners, a multipurpose, user-friendly, and free software that allows one to perform the full process of bioinformatic and evolutionary analysis of nucleic acid and protein sequences in a single platform. The program includes sufficient help, tutorials, and examples to allow the user to develop familiarity. MEGA is updated frequently; here version 6.0, described in reference [6], will be used in its more basic form. A detailed guide to its use is provided in the book *Phylogenetic Trees Made Easy* [7].

3 Method

The protocol that follows assumes that you have amplified viral sequences, either directly from a patient, host, or environmental sample or from a virus isolate.

1. **Obtain one or several genomic sequences** of your samples or isolates either by direct sequencing a PCR product or from a cloned sequence (*see Note 1*). Assemble the products of individual sequencing reactions into a single “contig,” and edit conflicting bases or segments. Save your sequence in FASTA format in a plain text editor. Alternatively, sequences obtained by deep (next-generation) sequencing could be used.
2. **Search for homologous sequences** in GenBank. Go to the BLAST page of NCBI (<http://blast.ncbi.nlm.nih.gov/Blast.cgi>), and select *nucleotide blast*. Copy and paste your sequence in the Enter Query Sequence window. In Choose Search Set/Database, choose Others “Nucleotide collection (nr/nt)”. In Program Selection, select Optimize for “Somewhat similar sequences (blastn)”. Check the “Show results in a new window” and click on the BLAST button. The search could take 1 min or more. Look in the Graphic Summary to get a quick idea of the coverage and identity of the homologous sequences found or “hits.” Scroll down to the Description section. It is a table with the 100 closest sequences to your query. The first of these hits gives you the identity of the virus in most of the cases. The columns at the right give some metrics showing how well each hit matches to the query sequence. The “Query cover” and “Ident” columns give a percent value of the coverage and identity. The “E-value” is the probability of having this match just by chance. Select the sequences you wish to include in the analysis by checking them at the left. How many and which sequences to select depend on the scope of the analysis, either limited to strains of the same virus or different

species within a genus or a family. As a rule of thumb, avoid selecting sequences with very similar names or with identical E-values because they are probably redundant sequences. Also avoid selecting sequences with a low coverage (say, less than 60–70%). Go back to the top of the table and click on Download and then on FASTA (aligned sequences) to get the dataset of sequences in a text file. Open the dataset with a text editor, include query sequence and (optional) other less closely related sequences to be used as “outgroups” in the analysis. Edit sequence names to a short and meaningful sentence like “Lujovirus South Africa 2008” and save it with .fas extension, say “newseq.fas” (*see Note 2*).

3. **Align the sequences.** Open MEGA and note the menu options. Follow this path Align → Edit/Build Alignment → Create New DNA alignment → DNA. The “Alignment Explorer” window will open. Here click the “Open” icon to browse, and open your dataset file. Move your mouse over the toolbar buttons above to know what their functions are. Align the DNA sequences using either Clustal W or MUSCLE. In the window that appears, accept (OK/Compute) the alignment default parameters, unless you have a good reason to modify them. Alignment may take some minutes depending on the size and complexity of your dataset. Visually check the quality of the alignment. If this is satisfactory, go to the Data menu and select “Save session”. The program will assign the “.mas” extension (e.g., Newseq.mas). Go back to the Data menu and select Export Alignment → MEGA format. Save this as suggested (e.g., Newseq.meg), and minimize the Alignment Explorer to return to the main menu. Next, use the Data function in the toolbar to open the .meg file you just created. Now you can use the “TA” button to open the “Sequence Explorer” or go directly to the next step.
4. **Select a substitution model.** From MEGA main menu, select Models → “Find best DNA/protein model (ML)”. In the incoming window, accept the default Analysis Preferences and compute. These steps may take some minutes depending on your dataset and your computer. It yields a table showing how different substitution models fit to your dataset sorted by the Bayesian information criteria (BIC). The first (upper) model is recommended for the next step (*see Note 3*).
5. **Perform the phylogenetic analysis.** With the *.meg file still open, go to the Phylogeny function in Mega main menu, and select Construct/test Neighbor-joining tree. Other methods could also be used, but we recommend trying neighbor-joining first to get a quick phylogenetic tree that could be improved later. In the opening Analysis Preferences window, select the

following options. Test of Phylogeny: Bootstrap method. No. of Bootstrap replications: 1000. Substitution type: nucleotide. Model/method: the model selected in **step 4**. Rates among sites: If the model selected in **step 4** included a +G (e.g., TN93+G), then choose Gamma distributed, and type the value in the (+G) column of the table in the next option (Gamma Parameter); otherwise (e.g., TN93 or TN93+I), select Uniform rates in Rates among Sites. Pattern among Lineages: Same (Homogeneous). Gaps/Missing Data Treatment: Partial deletion. Site Coverage Cutoff (%): 95. Finish with \sqrt Compute. The analysis could take a few seconds or several minutes depending on the dataset (*see Note 4*).

6. **Edit and interpret the phylogenetic tree.** When the analysis is finished, a phylogenetic tree will appear in a new window. Move the mouse over the icons in the left and upper bars to explore the editing options available. Look for the out-group sequence(s) in the tree, and click on the branch that leads to it (them); go to the “Place Root on Branch” icon on the left bar, and click on it to place the root properly. Observe the tree carefully. Terminal branches that are too short or too long could indicate redundant sequences or misaligned sequences, respectively. Decide which sequences should be removed and which others are missing, according to your knowledge of the species or genus. Go back to the dataset obtained in **step 2** and modify it properly. When ready, repeat **steps 3–6** until you are satisfied with the tree (*see Note 5*).
7. **Consider post-phylogenetic analyses.** Molecular epidemiological study of viruses uses several analytical tools including phylogenetic, phylogeographic, and phylodynamic analyses. The aforementioned stepwise protocol for genetic analysis is the basis of virus evolutionary genetics. Phylogenetic analysis of viral sequences proceeds as outlined in Fig. 1, and each of the steps is described in the protocol with some important notes about it. One of the most prolific uses of such genetic analyses lies in the field of phylogeography. The phylogeographic analysis focuses on the coupled study of the distribution/dispersion process of organisms and their genetic variation. There are several classic examples of phylogeography of hemorrhagic viruses that have provided useful information about their evolution and dispersion patterns [8, 9].

This kind of work has enabled the mapping of origin points for outbreaks [10] and the dispersion patterns of hemorrhagic fever viruses in their reservoirs [11], and more recently, in conjunction with experimental methods, virologists are trying to make predictions about the future fitness and molecular evolution of some emerging/reemerging viruses [12].

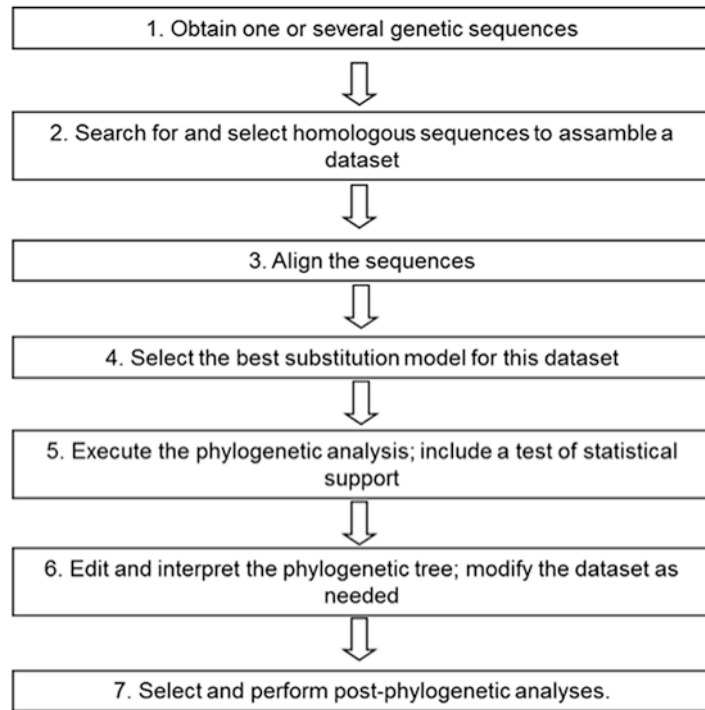


Fig. 1 Steps in a phylogenetic study

4 Notes

1. Both second-generation automated sequencing and third-generation (deep) sequencing technologies are useful for molecular epidemiology purposes. The former can be accomplished by direct sequencing of RT-PCR products or by sequencing recombinant clones of retro-transcribed genomic sequence; this latter variant, however, is not recommended since it could randomly select for sequences that do not represent the majority of the viral population; these sequences could also exhibit additional mutations introduced during the amplification process. On the other hand, direct sequencing yields the consensus sequence of the viral population in the isolate or in the sample. It is worth noting, however, that primers used in diagnostic PCR are not always satisfactory for molecular epidemiology work, since they are often designed to amplify short, well-conserved genomic segments with few variable sites on them. These sequences are good enough for identifying viral species and often for subtyping/genotyping too. However, most powerful phylogenetic and phylodynamic analyses require large alignments of sequences with many variable sites to produce robust, well-supported statistical inferences. The longer

the sequenced segment, the better. Accordingly, sequences of 500 nucleotides or more are sufficient for most analyses, but longer segments are needed when several isolates of an epidemic cluster or from a single endemic site are being studied. Therefore, additional primer pairs amplifying long or contiguous segments are usually required.

Third-generation sequencing technologies are more promising since they allow one to obtain longer, frequently complete, genomic sequences of viral isolates. They also help to identify viral sequences of non-previously identified viruses from clinical or from complex environmental samples [13]. Technical and financial issues still preclude the use of these technologies on a routine basis in most places, but these obstacles could be overcome soon due to the rapid development of these technologies.

2. The first analysis performed on a genomic sequence usually consists of searching for identical or similar sequences in a large bioinformatic database like GenBank, maintained at the National Center for Biotechnology Information (NCBI), Bethesda, Maryland, available at <http://www.ncbi.nlm.nih.gov/nucore/> [3]. BLAST (Basic Local Alignment Search Tool) is the resource available at GenBank for such searches. The “blastn” algorithm, which compares your own (query) nucleotide sequence with all nucleic acid sequences in the database, in sense and antisense directions, is the basic method for searching, but many other algorithms like megablast, blastp, blastx, and others are available for more refined searches in nucleotide and protein databases. Several manuals and tutorials are available at <http://www.ncbi.nlm.nih.gov/genbank/> to get started and gain understanding about the resources of the site. BLAST outputs include a table with the description, accession number, percent identity, probability (E-value) of a false-positive hit, and other measures of the most similar sequences. Graphic summaries, alignments, taxonomy reports, several downloading formats, as well as links to the original publication and other resources are also available.
3. When you are performing the substitution model selection, please have in mind that the substitution model option in MEGA only explores the 24 most common substitution patterns, while specialized software for this purpose such as jModelTest has approximately 88 models with other models in development. Because MEGA only works with 24 substitution patterns, just substitution models listed in MEGA are allowed. Model selection: MEGA software typically orders the substitution models according to the highest BIC; however, it also provides AIC and log likelihood for the same substitution model. You need to choose the best model for your data according to your criteria (BIC, AIC, AICc, log likelihood).

4. MEGA offers several kinds of analysis that range from similarity analysis based on dendrograms such as UPGMA, minimum evolution, and neighbor joining up to analysis of characters such as maximum parsimony and maximum likelihood. The tree reconstruction method chosen by the scientist will determine the type of tree that you can obtain, and concordance among them is expected; however, because of the different principles in which they lie on, it is possible to obtain different genetic trees (tree topology, branch length, branch support). Further information about the different methods is provided with examples in *Molecular Evolution and Phylogenetics* [14] and *Phylogenetic Trees Made Easy* [7].

When you are running your phylogenetic analysis, the most common setting for bootstrapping procedure is 1,000. The bootstrapping is a nonparametric procedure used for assessment of confidence of genetic clustering. In this case, it is used as an estimator for branch support. The result of bootstrap will be a number between zero to a hundred, and the higher the bootstrap (closest to 100), the better supported is your cluster/clade. However, it is important to mention that only the highest values of bootstrap are considered to be good evidence for cluster/clade support and values below 70 are considered non-conclusive support for branches [15].

5. Once you have obtained your tree, you can save this output in *.mts format that allows the saving of not only the phylogenetic tree but also the setup information of the whole analysis (just like a Log file). This information of the analysis contains the substitution model, the options for treatment of gaps, the support method, the number of sites used in the analysis, and the sites used (first + second + third or otherwise).

References

1. CDC (2013) Viral hemorrhagic fevers. CDC Fact Sheet 1–3. doi: [10.1111/j.1749-6632.2009.05106.x](https://doi.org/10.1111/j.1749-6632.2009.05106.x)
2. Knust B (2016) Chapter 3: viral hemorrhagic fevers. In: Barrett GW (ed) Centers for disease control and prevention: CDC health information for international travel. Oxford University Press, New York, pp 3–6
3. Benson DA, Cavanaugh M, Clark K, Karsch-Mizrachi I, Lipman DJ, Ostell J, Sayers EW (2013) GenBank. *Nucleic Acids Res* 41:36–42. doi:[10.1093/nar/gks1195](https://doi.org/10.1093/nar/gks1195)
4. Pickett BE, Sadat EL, Zhang Y, Noronha JM, Squires RB, Hunt V, Liu M, Kumar S, Zaremba S, Gu Z, Zhou L, Larson CN, Dietrich J, Klem EB, Scheuermann RH (2012) ViPR: an open bioinformatics database and analysis resource for virology research. *Nucleic Acids Res* 40:593–598. doi:[10.1093/nar/gkr859](https://doi.org/10.1093/nar/gkr859)
5. Felsenstein J (1995) University of Washington. <http://evolution.genetics.washington.edu/phylip/software.html>. Accessed 4 Sept 2016
6. Tamura K, Stecher G, Peterson D, Filipski A, Kumar S (2013) MEGA6: molecular evolutionary genetics analysis version 6.0. *Mol Biol Evol* 30:2725–2729. doi:[10.1093/molbev/mst197](https://doi.org/10.1093/molbev/mst197)
7. Hall BG (2011) *Phylogenetic trees made easy*, 4th edn. Sinauer Associates Inc., Sunderland
8. Beck A, Guzman H, Li L, Ellis B, Tesh RB, Barrett AD (2013) Phylogeographic reconstruction of African yellow fever virus isolates indicates recent simultaneous dispersal into east and west Africa. *PLoS Negl Trop Dis* 7(3):31910. doi:[10.1371/journal.pntd.0001910](https://doi.org/10.1371/journal.pntd.0001910)

9. Rico-Hesse R, Harrison LM, Salas RA, Tovar D, Nisalak A, Ramos C, Boshell J, de Mesa MT, Nogueira RM, da Rosa AT (1997) Origins of dengue type 2 viruses associated with increased pathogenicity in the Americas. *Virology* 230:244–251. doi:[10.1006/viro.1997.8504](https://doi.org/10.1006/viro.1997.8504)
10. Zehender G, Ebranati E, Shkjezi R, Papa A, Luzzago C, Gabanelli E, Lo Presti A, Lai A, Rezza G, Galli M, Bino S, Ciccozzi M (2013) Bayesian phylogeography of Crimean-Congo hemorrhagic fever virus in Europe. *PLoS One* 8(11):e79663. doi:[10.1371/journal.pone.0079663](https://doi.org/10.1371/journal.pone.0079663)
11. Olayemi A, Obadare A, Oyeyiola A, Igbokwe J, Fasogbon A, Igbahenah F, Ortsega D, Asogun D, Umeh P, Vakkai I, Abejegah C, Pahlman M, Becker-Ziaja B, Günther S, Fichet-Calvet E (2016) Arenavirus diversity and phylogeography of *Mastomys natalensis* rodents, Nigeria. *Emerg Infect Dis* 22:687–690. doi:[10.3201/eid2204.150155](https://doi.org/10.3201/eid2204.150155)
12. Tsetsarkin KA, Chen R, Yun R, Rossi SL, Plante KS, Guerbois M, Forrester N, Perng GC, Sreekumar E, Leal G, Huang J, Mukhopadhyay S, Weaver SC (2014) Multi-peaked adaptive landscape for chikungunya virus evolution predicts continued fitness optimization in *Aedes albopictus* mosquitoes. *Nat Commun* 5:1–14. doi:[10.1038/ncomms5084](https://doi.org/10.1038/ncomms5084)
13. Palacios G, Druce J, Du L, Tran T, Briese T, Conlan S, Quan PL, Hui J, Marshall J, Simons JF, Egholm M, Paddock CD, Shieh WJ, Goldsmith CS, Zaki SR, Catton M, Lipkin WI (2008) A new arenavirus in a cluster of fatal transplant-associated diseases. *N Engl J Med* 358:991–998. doi:[10.1056/NEJMoa073785](https://doi.org/10.1056/NEJMoa073785)
14. Nei M, Kumar S (2000) *Molecular evolution and phylogenetics*, 2nd edn. Oxford University Press, Oxford
15. Anisimova M, Gil M, Dufayard JF, Dessimoz C, Gascuel O (2011) Survey of branch support methods demonstrates accuracy, power, and robustness of fast likelihood-based approximation schemes. *Syst Biol* 60:685–699. doi:[10.1093/sysbio/syr041](https://doi.org/10.1093/sysbio/syr041)

Preliminary Classification of Novel Hemorrhagic Fever-Causing Viruses Using Sequence-Based PAirwise Sequence Comparison (PASC) Analysis

Yīmíng Bào and Jens H. Kuhn

Abstract

During the last decade, genome sequence-based classification of viruses has become increasingly prominent. Viruses can be even classified based on coding-complete genome sequence data alone. Nevertheless, classification remains arduous as experts are required to establish phylogenetic trees to depict the evolutionary relationships of such sequences for preliminary taxonomic placement. Pairwise sequence comparison (PASC) of genomes is one of several novel methods for establishing relationships among viruses. This method, provided by the US National Center for Biotechnology Information as an open-access tool, circumvents phylogenetics, and yet PASC results are often in agreement with those of phylogenetic analyses. Computationally inexpensive, PASC can be easily performed by non-taxonomists. Here we describe how to use the PASC tool for the preliminary classification of novel viral hemorrhagic fever-causing viruses.

Key words Pairwise sequence comparison analysis, PASC, Species demarcation, VHF, Viral hemorrhagic fever, Virus classification, Virus taxonomy

1 Introduction

The International Committee on Taxonomy of Viruses (ICTV) is responsible for the classification of viruses into taxa, such as orders, families, subfamilies, genera, or species [1]. Official classification is a relatively lengthy process mediated by ICTV Study Groups responsible for specific viral families [1]. In the past, classification was based predominantly on morphological properties of virions, their serological relationships, virus host range, pathogenicity, and genome organization. Therefore, official classification of viruses was often delayed for years until these properties were described in the scientific literature.

The number of viral genome sequences in public databases, such as the US National Center for Biotechnology Information (NCBI) database GenBank [2], has increased dramatically in recent years due to the development of novel sequencing technologies

and methods and to increased interest in viral (meta)genomic sequencing efforts [3]. The ICTV reacted to this development by, in principle, permitting classification of viruses based on coding-complete genome sequence data alone. However, classification was not accelerated as experts were required to establish phylogenetic trees, and such trees were then validated by ICTV Study Groups to depict the evolutionary relationships of such sequences. This type of analysis is usually computationally expensive, and the interpretation of the results is not straightforward. Consequently, the backlog of unclassified viruses continues to increase exponentially [3].

For more rapid preliminary classification based on sequence classification, several virus classification tools based on pairwise sequence comparison have been brought forward [4, 5]. These tools include, for instance, PAirwise Sequence Comparison (PASC), DivErsity pArtitioning by hieRarchical Clustering (DEmARC) [6], and sequence demarcation tool (SDT) [7] analyses.

Here we describe the use of the PASC tool for preliminary virus classification because a nonexpert user-friendly PASC software tool is available open-access at the web site of NCBI [8]. In the improved version of the PASC tool [4, 8], pairwise sequence identities among input sequences are calculated by a combined Basic Local Alignment Search Tool (BLAST)-based alignment method. The distribution of these pairwise identities is represented by a histogram/plot (Fig. 1) showing numbers of sequence pairs at each percentage of pairwise identities. The percentages at the gaps between the peaks on the histogram can be used as demarcation criteria for different taxa.

The NCBI PASC tool has been preloaded with genomic sequences of all known viral hemorrhagic fever-causing viruses. Consequently, the sequence of a putative novel viral hemorrhagic fever-causing virus can be easily compared directly to genomic sequences already analyzed by PASC. The PASC result will provide a strong indication of the probability that the virus at hand is a member of existing species or requires classification into a novel species in existing higher taxa or establishment of novel higher taxa. This PASC-based preliminary classification can then be used as the basis for a formal taxonomic proposal (“TaxoProp”) for submission to the ICTV for official classification of the novel virus [9].

2 Materials

1. Viral genome sequences used in PASC are directly obtained from the NCBI viral genome resource [10], and taxonomy information associated with the genomes is obtained from the NCBI taxonomy database [11] [note that the NCBI taxonomy database is built on, but is not yet identical with, ICTV taxonomy].

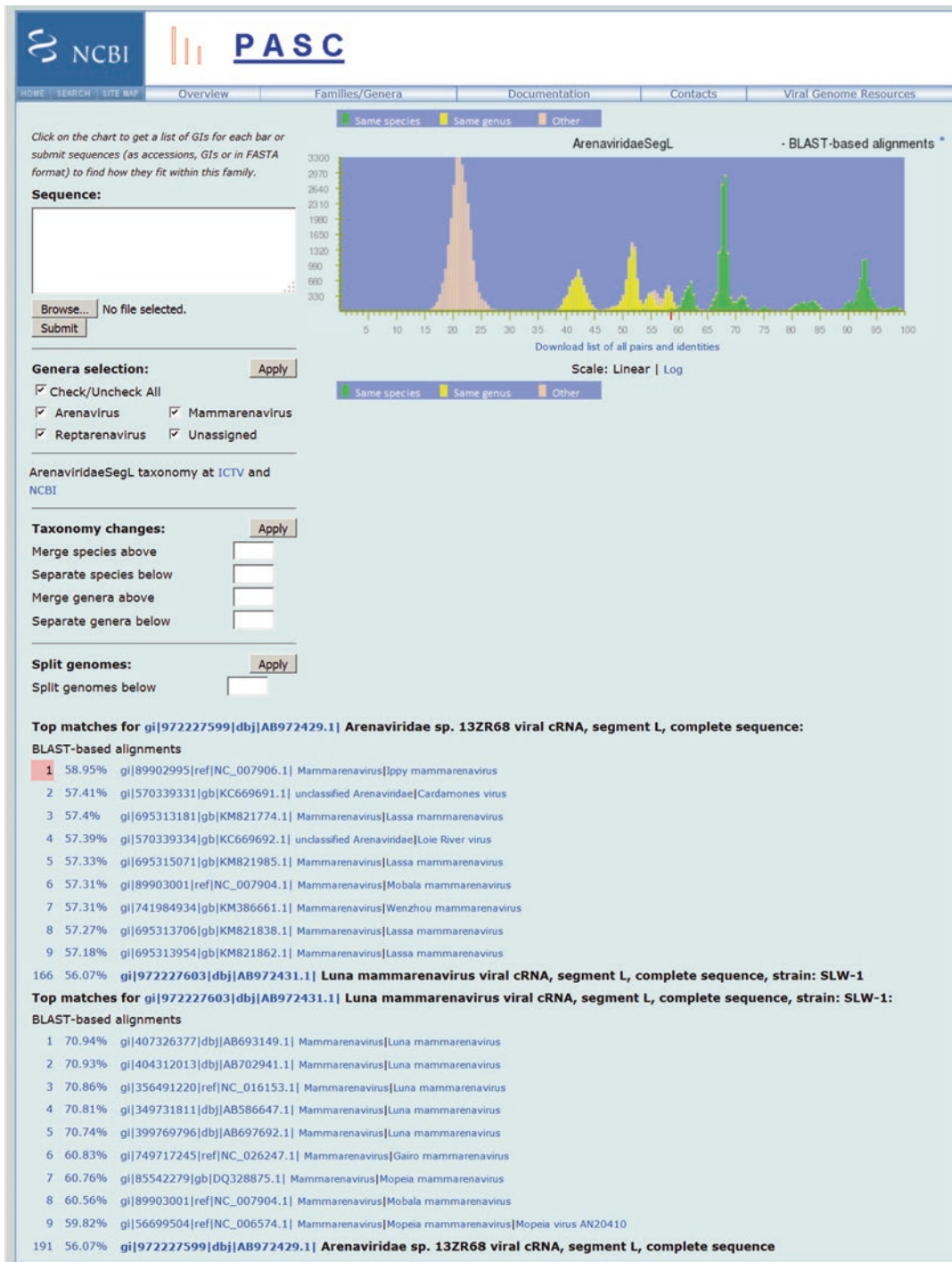


Fig. 1 Screenshot of the “ArenaviridaeSegL” (=Arenaviridae L segment) PASC user interface showing PASC results for GenBank sequences AB972429.1 (unclassified mammarenavirus “sp. 13ZR68”) and AB972431.1 (Luna virus SLW-1 [currently assigned to the species *Luna mammarenavirus*] [16])

2. Input viral genome sequences to be analyzed by PASC are those either deposited in GenBank [2] or provided by the user in FASTA format [12, 13].

3 Methods

1. On the PASC webpage [8], select the virus “Family/Genera” tab, and click on the taxon the putative novel virus belongs to based on preliminary sequence analyses (e.g., BLAST of polymerase chain reaction [PCR]-derived genomic fragment sequences). In the case of a (suspected) segmented or polypartite virus genome, separate PASC results are created for each segment (e.g., L segment of members of the *Arenaviridae* or M segment of members of the *Bunyavirales*), and sequences of the appropriate segment are used for comparison. After selecting a taxon, the user will enter into the PASC user interface (Fig. 1).
2. In the “Sequence:” input box of the interface, specify the query genome using either its Accession or GI number if the genomic sequence of the putative novel virus is present in GenBank, or copy/paste the sequence in FASTA format into the box. Alternatively, upload a file containing the sequence by clicking the “Browse” button underneath the “Sequence:” input box. Use only coding-complete genomes [14, 15] as query sequences [in the absence of a viral isolate in tissue culture, the ICTV currently hesitates to consider classifying a virus based on genomic sequences that are less than coding-complete]. Add up to 50 sequences in one submission.
3. Click the “Submit” button and wait for a list of pairwise identities, from the highest to the lowest, between this input genome and (1) the rest of input genomes (if more than one are retrieved) in bold (*see* Fig. 1), and (2) five to ten of the closest matches to existing genomes within the chosen taxon not in bold.
4. Locate the top hit among the existing genomes to the input genome. If only one input genome is queried, locate the first one on the list. If more than one input genome is queried, locate the first genome not highlighted in bold.
 - (a) For virus families with already established PASC-derived taxon demarcation criteria (e.g., *Arenaviridae* [16], *Filoviridae* [17]), compare the percentage identity between the input sequence and the top hit with the established taxon demarcation criteria cutoffs, and then determine the taxonomic placement of the new virus (*see* **Notes 1** and **2**).
 - (b) For virus families with not-yet-established PASC-derived taxon demarcation criteria (e.g., *Bunyavirales*, *Rhab-*

doviridae), locate the percentage identity between the input sequence and the top hit on the graph of the PASC result (upper right-hand corner). If the identity value is located in the region with predominantly green peaks, then the examined virus may belong to the same species as the top hit. If the identity value is located in a yellow area, then the examined virus may belong to a different species but to the same genus as the top hit. If the identity value is found in the brown area, then the examined virus may have to be assigned to a novel genus (*see* **Notes 3–5**).

4 Notes

1. For example, in Fig. 1, the percentage identity between the first input sequence (unclassified mammarenavirus “sp. 13ZR68” L segment, GenBank #AB972429.1) and its top species hit (*Ippy mammarenavirus*, Ippy virus L segment, RefSeq #NC_007906.1) is 58.95% (red bar on the x -axis of the PASC plot). This value is less than the currently agreed-upon mammarenavirus L segment species cutoff of 76% and greater than the currently agreed-upon arenavirus L segment genus cutoff of 35% [16]. Therefore, “sp. 13ZR68” may have to be assigned to a novel species but in the same genus that includes *Ippy mammarenavirus* (genus *Mammarenavirus*) if a similar divergence is measured for the “sp. 13ZR68” S segment. Similarly, the second input sequence (*Luna mammarenavirus*, Luna virus SLW-1L segment, GenBank #AB972431.1) is only 70.94% identical to its top hit (*Luna mammarenavirus*, Luna virus LSK-2, GenBank #AB693149.1), and therefore this virus may have to be assigned to a novel species but in the same genus that includes *Luna mammarenavirus* (genus *Mammarenavirus*) if a similar divergence is measured for the “Luna virus LSK-2” S segment. The percentage identity between the two input sequences is 56.07%, therefore confirming that both input sequences belong to two different species in the same genus.
2. **Establishing demarcation criteria**—A gap between the peaks in a PASC plot may serve as a demarcation criterion for taxonomic ranks. In the case of agreement between NCBI taxonomy and ICTV taxonomy, a gap between peaks in green and yellow colors may be used as the species demarcation cutoff, and a gap between peaks in yellow and brown colors may be used as the genus demarcation cutoff. PASC plots may suggest different possibilities for taxon demarcation cutoffs that could be chosen by the user, but it is ultimately the role of the ICTV to formally establish such criteria, taking into account other

Table 1
Species and genus demarcation criteria suggested by PASC analyses for families with viral hemorrhagic fever-causing members

Virus family	Species cutoff	Genus cutoff	References
<i>Filoviridae</i>	64–77% ^a	42–46% ^a	[17]
<i>Arenaviridae</i> L segment (mammarenaviruses only)	76%	30–33%	[16]
<i>Arenaviridae</i> S segment (mammarenaviruses only)	80%	30–40%	[16]
<i>Rhabdoviridae</i>	73% ^a	43% ^a	N/A
<i>Flaviviridae</i>	N/A ^{a,b}	N/A ^{a,b}	N/A
<i>Bunyavirales</i> L segment	N/A ^a	21–35% ^a	N/A
<i>Bunyavirales</i> M segment	N/A ^{a,b}	N/A ^{a,b}	N/A
<i>Bunyavirales</i> S segment	N/A ^{a,b}	N/A ^{a,b}	N/A

^aThese cutoffs are purely based on PASC analyses and have not been accepted by ICTV Study Groups or the ICTV

^bNot available (N/A) because different species cutoffs have been used for divergent genera included in these families

biological properties of a particular virus. Species and genus demarcation criteria based primarily on PASC (and supplemented by additional biological data) were thus far established for two viral families with viral hemorrhagic fever-causing members: *Arenaviridae* [16] and *Filoviridae* [17]. In the case of *Arenaviridae*, PASC-derived taxon demarcation criteria have been accepted by the ICTV *Arenaviridae* Study Group and are therefore part of official taxonomy. ICTV acceptance of PASC demarcation criteria for *Filoviridae* has not yet occurred, although the currently used sequence-based taxon demarcation criteria for members of that family [18] are very close to those suggested by PASC analysis [17]. PASC analysis is able to suggest demarcation cutoffs for some other virus families (e.g., *Rhabdoviridae*), but not for others (e.g., *Flaviviridae*) because the members of different genera in a particular family may have evolved at very different rates and therefore may require vastly different species cutoffs (Table 1).

- For example, Fig. 2 shows PASC analysis of the coding-complete genome of Bas-Congo virus (GenBank # JX297815.1), an unclassified rhabdovirus suspected to cause viral hemorrhagic fever in humans [19]. The complete genome of Bas-Congo virus is 36.2% identical to the top hit (species *Tibrogargan tibrovirus*, Tibrogargan virus, RefSeq #NC_020804.1). Since this value is located in the region of brown peaks, Bas-Congo virus may be considered as the member of a novel rhabdoviral genus rather than a member of the genus *Tibrovirus* [note, though, that Bas-Congo virus shares

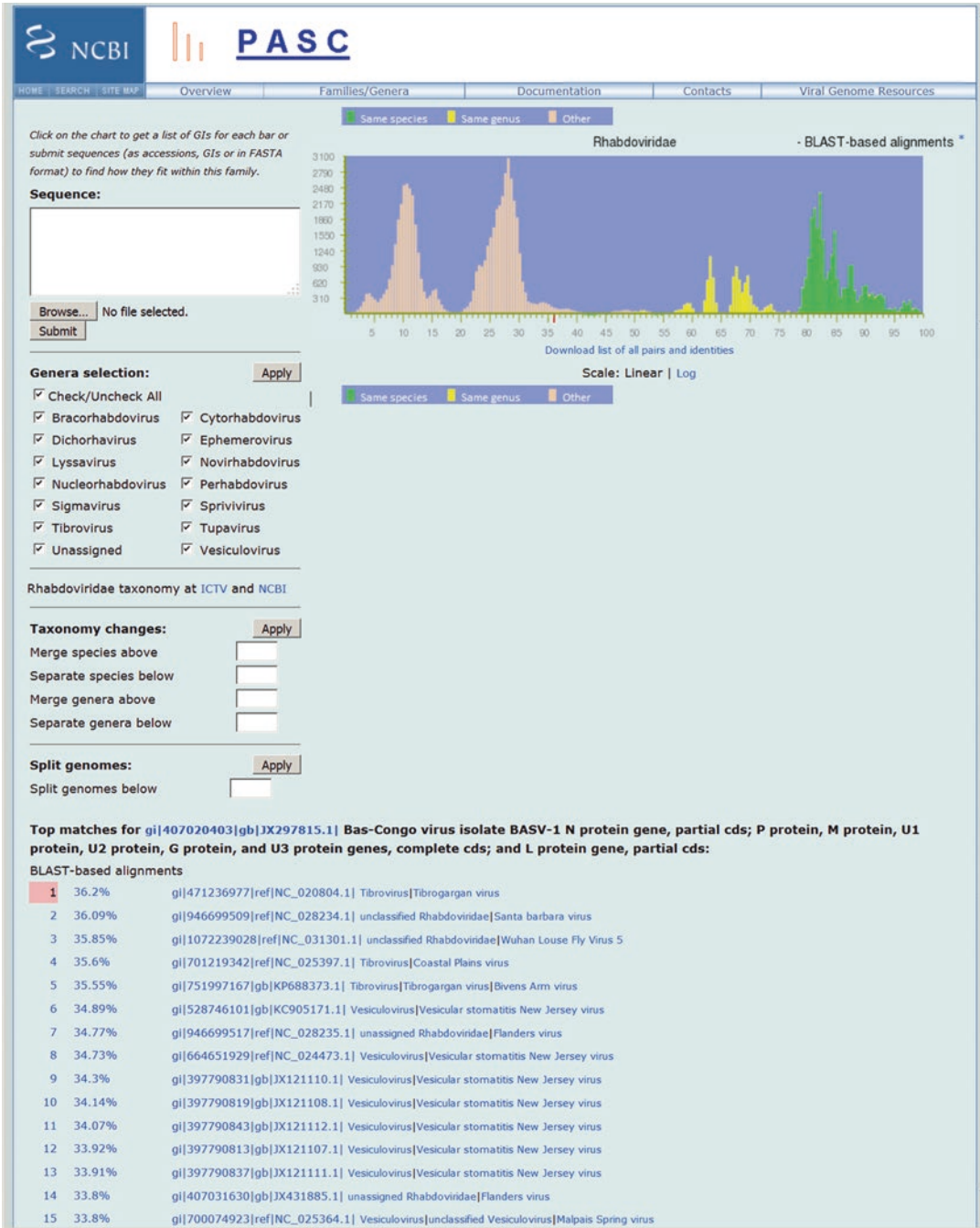


Fig. 2 Screenshot of the “*Rhabdoviridae*” PASC user interface showing PASC results for GenBank sequence JX297815.1 (unclassified rhabdovirus Bas-Congo virus)

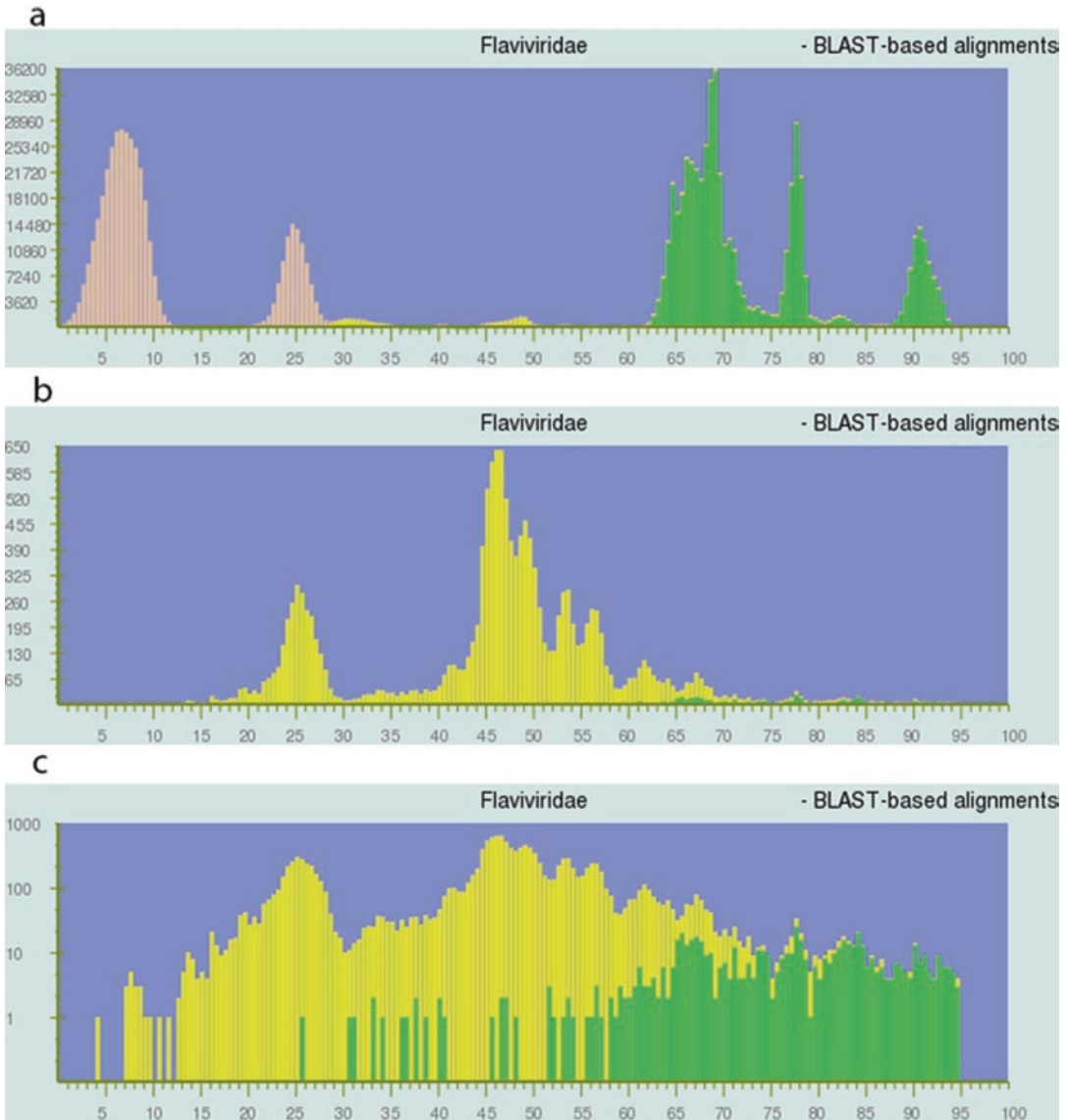


Fig. 3 Screenshot of the “*Flaviviridae*” PASC user interface showing PASC results for the entire family (a), the genus *Flavivirus* in linear scale (b), and the genus *Flavivirus* in log scale (c)

numerous properties with various tibroviruses, suggesting that Bas-Congo virus could nevertheless be considered a member of the genus *Tibrovirus* despite the PASC result].

- 4. Dealing with complications**—Three colors are used to label viral genome sequence pairs that have different taxonomic relationships. The green, yellow, and brown bars in the PASC plots represent pairs of genomes that are assigned to the same species, different species belonging to the same genus, and different genera, respectively, in the current NCBI taxonomy

database [11]. Ideally, each peak in a PASC plot is depicted in only one color because the viruses contributing to each peak should belong to the same taxonomic lineage.

However, the occurrence of different colors in the same peak is not uncommon. For instance, in a PASC analysis of the family *Flaviviridae* (Fig. 3a), green can be found in the predominantly yellow peak at the region of 65–68% identities when only one of the included genera, *Flavivirus*, is analyzed (Fig. 3b; see also Note 5). If that analysis is switched from linear to log scale (Fig. 3c), a small number of yellow dots are visible in the region greater than 75% identity. Two main reasons for different colors in the same peak are: (1) Some of the analyzed virus genomes were assigned to the incorrect lineage in the NCBI taxonomy database. For instance, the small yellow dots at the 90% identity value in Fig. 3c represent the identity between RefSeq #NC_027709.1 (Spanish goat encephalitis virus) and #NC_001809 (louping ill virus). Virus genomes with identities around 90% mostly belong to the same species as indicated by the green color. The publication associated with the genome record #NC_027709 also contains the suggestion that Spanish goat encephalitis virus and louping ill virus both belong to the same species *Louping ill virus* [20]. However, in the NCBI taxonomy database, Spanish goat encephalitis virus is listed as an unclassified species different from *Louping ill virus*. If the Spanish goat encephalitis virus genome is assigned to the species *Louping ill virus*, the dot at the 90% value would be in green. (2) In the case of many viruses, criteria other than sequence identities are used for species demarcation. For instance, the currently recognized four dengue viruses (dengue virus 1–4) have been assigned officially to a single species (*Dengue virus*), even though their genome identities are as low as those between members belonging to separate species in the genus *Flavivirus*. This inconsistency is the reason why the 68% identity value in Fig. 3c is comprised of both green (representing genome pairs assigned to the same species [*Dengue virus*] between dengue virus 1 [GenBank #EF457905.1] and dengue virus 2 [GenBank #EF105379.1]) and yellow (representing genome pairs assigned to separate species, i.e., those of Japanese encephalitis virus [GenBank # HM596272.1, species *Japanese encephalitis virus*] and West Nile virus [GenBank # DQ176636.2, species *West Nile virus*]). Consequently, use of PASC analysis is limited in the case of the genus *Flavivirus* until taxonomic inconsistencies are removed by the ICTV *Flaviviridae* Study Group.

5. **Selecting individual genera**—When a novel virus is known to belong to an existing genus, all other genera of the family can be unchecked from the “Genera selection” section below the “Sequence:” input box on the PASC user interface page. For

example, compare Fig. 3a, which shows PASC results for the entire family *Flaviviridae*, to Fig. 3b, c, which show results only for the flaviviral genus *Flavivirus*, but not those for the flaviviral genera *Hepacivirus*, *Pegivirus*, and *Pestivirus*. A new input sequence will then only be compared to existing sequences belonging to viruses assigned to the selected genus, therefore reducing computation time. This calculation shortcut is particularly helpful in the case of families represented by a large number of genomes (compare the number of total genome pairs in Fig. 3a to b/c). Taking this shortcut is also necessary when different species demarcation cutoffs are used for different genera in one family (e.g., *Flavivirus* versus *Hepacivirus*).

Acknowledgments

We thank Vyacheslav Chetvernin for developing and maintaining the PASC tool. We also thank Laura Bollinger of the IRF-Frederick for critically editing this manuscript.

This work was funded in part through Battelle Memorial Institute's prime contract with the US National Institute of Allergy and Infectious Diseases (NIAID) under Contract No. HHSN272200700016I. A subcontractor to Battelle Memorial Institute who performed this work is J.H.K., an employee of Tunnell Government Services, Inc. This research was also supported in part by the Intramural Research Program of the National Institutes of Health, National Library of Medicine (Y.B.). Opinions expressed here are our own and do not reflect the view of the NIH, the Department of Health and Human Services, or the US government.

References

1. International Committee on Taxonomy of Viruses (ICTV) (2016) International Committee on Taxonomy of Viruses. <http://www.ictvonline.org/>
2. National Center for Biotechnology Information (NCBI) (2016) GenBank. <http://www.ncbi.nlm.nih.gov/genbank/>
3. Brister JR, Ako-Adjei D, Bao Y, Blinkova O (2015) NCBI viral genomes resource. *Nucleic Acids Res* 43(Database issue):D571–D577. doi:10.1093/nar/gku1207
4. Bao Y, Chetvernin V, Tatusova T (2014) Improvements to pairwise sequence comparison (PASC): a genome-based web tool for virus classification. *Arch Virol* 159(12):3293–3304. doi:10.1007/s00705-014-2197-x
5. Bao Y, Kapustin Y, Tatusova T (2008) Virus classification by PAirwise Sequence Comparison (PASC). In: Mahy BWJ, van Regenmortel MHV (eds) *Encyclopedia of virology*, vol 5, 3rd edn. Elsevier, Oxford, UK, pp 342–348
6. Lauber C, Gorbalenya AE (2012) Partitioning the genetic diversity of a virus family: approach and evaluation through a case study of picornaviruses. *J Virol* 86(7):3890–3904. doi:10.1128/JVI.07173-11
7. Muhire BM, Varsani A, Martin DP (2014) SDT: a virus classification tool based on pairwise sequence alignment and identity calculation. *PLoS One* 9(9):e108277. doi:10.1371/journal.pone.0108277
8. National Center for Biotechnology Information (NCBI) (2016) PASC. <http://www.ncbi.nlm.nih.gov/sutils/pasc/viridty.cgi?textpage=overview>

9. International Committee on Taxonomy of Viruses (ICTV) (2016) Taxonomy Proposal Templates. <https://talk.ictvonline.org/files/taxonomy-proposal-templates/>
10. National Center for Biotechnology Information (NCBI) (2016) Viral Genomes. <http://www.ncbi.nlm.nih.gov/genome/viruses/>
11. National Center for Biotechnology Information (NCBI) (2016) Taxonomy. <http://www.ncbi.nlm.nih.gov/taxonomy>
12. Pearson WR (2014) BLAST and FASTA similarity searching for multiple sequence alignment. *Methods Mol Biol* 1079:75–101. doi:10.1007/978-1-62703-646-7_5
13. Pearson WR (2016) Finding protein and nucleotide similarities with FASTA. *Curr Protoc Bioinformatics* 53:3.9.1–3.9.25. doi:10.1002/0471250953.bi0309s53
14. Ladner JT, Beitzel B, Chain PS, Davenport MG, Donaldson EF, Frieman M, Kugelman JR, Kuhn JH, O’Rear J, Sabeti PC, Wentworth DE, Wiley MR, Yu GY, The Threat Characterization Consortium, Sozhamannan S, Bradburne C, Palacios G (2014) Standards for sequencing viral genomes in the era of high-throughput sequencing. *mBio* 5(3):e01360–e01314. doi:10.1128/mBio.01360-14
15. Ladner JT, Kuhn JH, Palacios G (2016) Standard finishing categories for high-throughput sequencing of viral genomes. *Rev Sci Tech* 35(1):43–52. doi:10.20506/rst.35.1.2416
16. Radoshitzky SR, Bao Y, Buchmeier MJ, Charrel RN, Clawson AN, Clegg CS, DeRisi JL, Emonet S, Gonzalez J-P, Kuhn JH, Lukashevich IS, Peters CJ, Romanowski V, Salvato MS, Stenglein MD, de la Torre JC (2015) Past, present, and future of arenavirus taxonomy. *Arch Virol* 160(7):1851–1874. doi:10.1007/s00705-015-2418-y
17. Bao Y, Chetvernin V, Tatusova T (2012) PAirwise Sequence Comparison (PASC) and its application in the classification of filoviruses. *Viruses* 4(8):1318–1327. doi:10.3390/v4081318
18. Kuhn JH, Becker S, Ebihara H, Geisbert TW, Johnson KM, Kawaoka Y, Lipkin WI, Negredo AI, Netesov SV, Nichol ST, Palacios G, Peters CJ, Tenorio A, Volchkov VE, Jahrling PB (2010) Proposal for a revised taxonomy of the family *Filoviridae*: classification, names of taxa and viruses, and virus abbreviations. *Arch Virol* 155(12):2083–2103. doi:10.1007/s00705-010-0814-x
19. Grard G, Fair JN, Lee D, Slikas E, Steffen I, Muyembe J-J, Sittler T, Veeraraghavan N, Ruby JG, Wang C, Makuwa M, Mulembakani P, Tesh RB, Mazet J, Rimoin AW, Taylor T, Schneider BS, Simmons G, Delwart E, Wolfe ND, Chiu CY, Leroy EM (2012) A novel rhabdovirus associated with acute hemorrhagic fever in Central Africa. *PLoS Pathog* 8(9):e1002924. doi:10.1371/journal.ppat.1002924
20. Mansfield KL, Morales AB, Johnson N, Ayllón N, Höfle U, Alberdi P, Fernández de Mera IG, García Marín JF, Gortázar C, de la Fuente J, Fooks AR (2015) Identification and characterization of a novel tick-borne flavivirus subtype in goats (*Capra hircus*) in Spain. *J Gen Virol* 96(Pt 7):1676–1681. doi:10.1099/vir.0.000096

Epidemiological Surveillance of Viral Hemorrhagic Fevers With Emphasis on Clinical Virology

Carolina Montoya-Ruiz and Juan David Rodas

Abstract

This article will outline surveillance approaches for viral hemorrhagic fevers. Specific methods for surveillance of clinical samples will be emphasized. Separate articles will describe methods for surveillance of rodent-borne viruses (reoviruses) and arthropod-borne viruses (arboviruses). Since the appearance of hantaviruses and arenaviruses in the Americas, more than 30 different species in each group have been established, and therefore they have become the most frequently emerging viruses. Flaviviruses such as yellow fever and dengue viruses, although easier to recognize, are also more widely spread and therefore considered a very important public health issue, particularly for under-developed countries. On the other hand, marburgviruses and ebolaviruses, previously thought to be restricted to the African continent, have recently been shown to be more global. For many of these agents virus isolation has been a challenging task: trapping the specific vectors (mosquitoes and ticks), and reservoirs (rodents and bats), or obtaining the samples from suspected clinical human cases demands special protective gear, uncommon devices (respirators), special facilities (BSL-3 and 4), and particular skills to recognize the slow and inapparent cytopathic effects in cell culture. Alternatively, serological and molecular approaches have been very helpful in discovering and describing newly emerging viruses in many areas where the previous resources are unavailable. Unfortunately, in many cases, detailed studies have been performed only after outbreaks occur, and then active surveillance is needed to prevent viral dissemination in human populations.

Key words Zoonotic viruses, Clinical samples, Hemorrhagic fevers, Diagnostics

1 Introduction

1.1 Surveillance of Clinical Samples for RNA Viruses

Ambitious attempts at broad microbial surveillance are currently being carried out on our oceans and in the air of our cities. Surveillance of our oceans involves passing liters of liquid through graded filters that capture different sizes of microbes, followed by extraction and high-throughput cDNA sequencing of microbial nucleic acids [1]. Surveillance of air involves capture of microbes onto adsorbent surfaces, elution of microbes from these surfaces, and then cDNA sequencing [2]. In contrast to those global efforts to catalogue environmental microbes, we focus here on the surveillance of those RNA viruses that occasionally infect human

beings, but are more often carried by rodents or insects. Although most infections in the carrier host have little pathology, human infection can cause severe disease and is, therefore, a public health concern.

The usual progression of events is that an “outbreak” of disease such as viral hemorrhagic fever (VHF) is followed by epidemiological surveillance of the likely viral zoonotic reservoirs and by retrospective surveillance of stored clinical samples. In order to conserve resources, our surveillance focused first on detecting infectious virus, viral sequences, and viral antigens in clinical samples. Our accompanying articles on surveillance of rodent-borne and insect-borne viruses describe the use of Global Information Systems (GIS) to systematize surveillance over large geographic regions.

1.2 Common Features of Viral Hemorrhagic Fevers

Viral hemorrhagic fevers (VHF) encompass a group of diseases caused by agents from different RNA viral families. The term “viral hemorrhagic fever” is used to describe the multisystem syndrome characterized by impairment of the vascular system accompanied by hemorrhage (bleeding). Although the bleeding by itself is rarely the cause of death, and some types of hemorrhagic fever viruses cause relatively mild illnesses, many of these viruses cause severe, life-threatening disease [3].

Viral hemorrhagic fevers share several features, among others: (1) they all are produced by enveloped-RNA viruses, (2) they are all of zoonotic nature that involves transmission by insects, ticks, rodents, bats, or other wild and domestic reservoirs; (3) these viruses tend to be geographically restricted to the areas where their hosts live, (4) humans are usually incidental hosts that are sporadically infected, but in some cases, they can also transmit these viruses to other humans; (5) outbreaks cannot be easily predicted, and there are very few antiviral treatments or vaccines available for these viral agents [3].

1.3 Case Definitions for Epidemiological Surveillance

All VHF present with fever (body temperature over 40 °C), and one or more of the following **clinical findings**: severe headache, muscle pain, erythematous maculopapular rash on the trunk with fine desquamation 3–4 days after rash onset, vomiting, diarrhea, pharyngitis, abdominal pain, bleeding not related to injury, retrosternal chest pain, proteinuria, and thrombocytopenia [3, 4]. As part of the **laboratory criteria** for diagnosis, VHF blood or tissue samples may also carry one or more of these signs: viral antigens [detectable by immunohistochemistry or enzyme-linked immunosorbent assay (ELISA)], infectious virus (detectable by cell culture), and viral RNA sequences [detectable by reverse transcription-polymerase chain reaction (RT-PCR)] [4]. From an **epidemiological perspective**, valid **linkages** (or **risk factors**) could be: (1) contact with blood or other body fluids of a patient with VHF,

(2) residence in/or travel to a VHF endemic area, (3) work in a laboratory that handles VHF specimens, (4) work in a laboratory that handles bats, rodents, or primates from endemic areas, and (5) sexual intercourse with a confirmed acute or convalescent VHF case within 10 weeks of that person's onset of symptoms [4]. Finally, for the purpose of classification, a **suspected case** is the one that meets the **clinical and epidemiologic linkage criteria**, and a **confirmed case** is the one that meets the **clinical and laboratory criteria** [4].

1.4 Virological Surveillance

Viral hemorrhagic fevers (VHF) are caused by enveloped RNA viruses of zoonotic origin and transmitted by mosquitoes, ticks, rodents, bats, or domestic animals. So far, most of the viral agents associated with these HF have been found within the following four virus families: filoviruses, including marburgviruses and ebolaviruses (that are thought to be primarily bat-borne), arenaviruses, including Lassa fever, Lujo, Guanarito, Machupo, Junín, Sabiá, and Chapare viruses (that are primarily rodent-borne), bunyaviruses, including Rift Valley fever (mosquito-borne), Crimean-Congo hemorrhagic fever (tick-borne), and hantaviruses (rodent-borne), and the flaviviruses, including dengue and yellow fever viruses (mosquito-borne), Omsk hemorrhagic fever, Kyasanur Forest disease, and Alkhurma viruses (tick-borne) [5].

VHF caused by arena- and hantaviruses are usually diagnosed by RT-PCR or by using antigen-capture ELISA. There are also ELISA and Indirect Fluorescent Antibody tests for serology detection, used to detect IgM or a fourfold rise in IgG, but it is a widely known fact that some agents causing HF, such as arenaviruses, elicit antibodies too late to be useful for clinical diagnosis. Viral isolation is also a possibility, but in many cases this technique requires skillful laboratory personal and high-containment (BSL-3/4) facilities, which makes it impractical for most developing countries in Africa, Asia, and South America where the majority of these cases occur. Currently, the attenuated vaccine against Argentinian hemorrhagic fever is the only VHF vaccine available to protect laboratory workers and to prevent VHF caused by arenaviruses. Also, few antiviral drugs (ribavirin and convalescent serum) are available to treat patients in case of accidental infection [6].

1.5 Practical Concerns for Surveillance

In surveillance studies the goal is to collect and keep samples in good condition for isolation of virus and RNA. Although the containment requirements for Risk Group 3/4 agents are very high, viral isolation is useful for obtaining biological material to perform subsequent genetic and serological viral characterization [7–9]. The main precaution that has to be taken during field and clinical studies is to maintain the cold chain, because it avoids the reduction of viral titer or RNA degradation. Consequently, all biological samples obtained during fieldwork must be shipped in dry ice,

liquid nitrogen, or RNALater, and once at the laboratory, they must be stored in liquid nitrogen or $-130\text{ }^{\circ}\text{C}$ (or at least $-80\text{ }^{\circ}\text{C}$) freezer. The $-20\text{ }^{\circ}\text{C}$ freezer is feasible for a short time storage (no more than 24 h), and sometimes cold packs could be used for serum samples or during short field sampling (also under 24 h) [7]. However, the best option to keep blood, tissues, urine, and ectoparasites cold during field sampling is liquid nitrogen [10].

Another requirement for classical virological surveillance is to reduce the bacterial contamination when obtaining samples, because this avoids the further need to filter material for cell culture in the viral isolation procedure. To reduce bacterial contamination, tissues should be stored in sterile tubes with screw caps or placed in sterile cryovials, and quickly put into liquid nitrogen. Necropsy material must be sterilized and working environments should be kept as clean as possible. When planning to isolate virus, different types of samples could be used to inoculate several types of cell cultures and laboratory animals. Samples to be used depend on the suspected virus, and could come from blood, mammalian tissues, arthropod organs, or excreta of mammals or insects.

2 Materials

2.1 *Virus Isolation from Clinical Samples*

1. Clinical blood and serum samples (mainly from suspected virus infections) or tissues (postmortem cases, and endothelial cell infections).
2. Histopaque is a sterile solution of polysucrose and sodium diatrizoate adjusted with a specific density to provide viscosity gradients for cell isolation. Histopaque-1077 has a density of 1.077 g/ml facilitating the recovery of viable lymphocytes and other mononuclear cells from small volumes of whole primate blood. Histopaque-1083 allows recovery of viable mononuclear cells from rats, mice, and other small mammals, Histopaque-1119 is commonly used for the recovery of mononuclear cells and granulocytes [11, 12].
3. Low-speed centrifuge capable of generating $400 \times g$.
4. 15 ml plastic centrifuge tubes.
5. Vero E6 cells are used for hantavirus, arenavirus, flavivirus, and filovirus isolation because they have a defect in interferon production.
6. Culture flasks.
7. Phosphate-buffered saline (PBS): 137 mM NaCl, 2.7 mM KCl, 10 mM Na_2HPO_4 , 2 mM KH_2PO_4 , pH 7.4.
8. Maintenance medium for Vero cells: MEM with 2% fetal bovine serum, 1% penicillin, 1% streptomycin, 1% sodium pyruvate, and 7.5% bicarbonate.

9. Incubator with 37 °C and 5% CO₂.
10. Glass spheres are used to lyse the cells at the end of each passage to store supernatants with lysed cells.
11. Polyethylene glycol (PEG) 6000, 8000, or 40,000 Da powder for precipitating virus from solution.
12. Amicon Ultra-4 filter units (Millipore) for concentrating virus-containing fluid.
13. Biosafety cabinet for tissue culture.

2.2 RNA Isolation from Clinical Samples

1. Common RNA-isolation kits contain a reagent for disrupting cells and RNA-protein complexes: TRIzol[®] Reagent (Thermo Fisher), QIAzol[®] Lysis Reagent (Qiagen), and TRI Reagent[®] (Sigma) [13–17] all contain a monophasic solution of phenol and guanidine isothiocyanate designed to facilitate lysis of fatty tissues and inhibit RNases.
2. Chloroform is used to separate the TRIzol/sample mixtures into phases.
3. 100% isopropanol and ethanol (used at 70% and 96–99%).
4. 1.5 ml plastic tubes.
5. Micro-centrifuge for high-speed (14,000 × *g*) spins of samples with less than 2 ml volume.
6. Manual of mechanical homogenizer.
7. The other alternative methodology to do the RNA isolation is the Silica (glass-particle)-based kits. These are suitable for serum, plasma, milk, urine, meconium, nasal fluids, swab-eluted fluids, and whole blood and are designed for a sample volume of less than 500 µl. These kits contain disruptive agents like TRIzol and, additionally, silica that adsorbs nucleic acids. Examples of kits are: PureLink[®] Viral RNA/DNA Kits (Life Technologies), QIAamp[®] Viral RNA (Qiagen), and High Pure Viral Nucleic Acid Kit (Roche). They have been used for dengue virus detection in serum samples and hantavirus detection in saliva and urine samples [15, 18, 19].

2.3 RT-PCR for Virus Genome Detection

1. Samples of purified RNA.
2. Kit to make cDNA, usually containing random hexameric primers and poly dT to amplify the RNA, and some type of reverse transcriptase, buffers, and nucleotide solutions.
3. Forward and reverse primers to amplify conserved regions of the viral genome.
4. Heat-resistant DNA polymerase for PCR.
5. Thermal cycler.

Table 1
Concentration of agarose gel needed to resolve different sizes of cDNA

Agarose concentration (w/v)	Fragment size resolved
0.3%	5–60 kb
0.5%	1–30 kb
0.7%	0.8–12 kb
1.0%	0.5–10 kb
1.2%	0.4–7 kb
1.5%	0.2–3 kb
2.0%	0.1–2 kb

2.4 Agarose Gels to Separate Viral Nucleic Acids or RT-PCR Products

1. Buffers for gel electrophoresis: 10× Tris-Borate-EDTA (TBE) buffer: 108 g Tris base (890 mM), 55 g boric acid (890 mM), 40 ml EDTA (0.5 M), add H₂O up to 1 L (pH 8.0). 50× Tris-Acetate-EDTA (TAE) buffer: 242 g Tris base, 57.1 ml glacial acetic acid (40 mM Tris Acetate), 32.7 g Na₂EDTA (2 mM), H₂O to 1 L, pH 8.0.
2. Electrophoresis equipment: there are many options available for horizontal setups; some of the most commonly used are from Berkeley and Bio-Rad.
3. Agarose gel could be used to analyze DNA fragments between 0.1 and 25 kb (Table 1).
4. Gel Loading buffer: 20% Ficoll-400, 0.1 M disodium EDTA (pH 8.0), 1.0% sodium dodecyl sulfate, 0.25% bromophenol blue, 0.25% Xylene cyanol [20].
5. 0.5 µg/ml ethidium bromide (EtBR) is an intercalating agent used to stain nucleic acid. Since it is a carcinogen, inactivate it by combining it with activated carbon (100 mg of activated carbon/100 ml of EtBr in solution). [21].
6. UV trans-illuminator.

2.5 ELISA for Serological Surveys of Antibody Responses to Virus Infection

In the specific case of the *Orthobantavirus* genus, several types of recombinant antigens for hantaviruses of different species have been used in the format of ELISA assays [22–24]. Commercial kits are available for highly endemic Flaviviruses like yellow fever and dengue. Here, we list two major types of ELISA, the indirect ELISA that detects host antibodies to virus (Table 2) and those (sandwich ELISA) that directly detect viral antigens (Table 3).

Indirect ELISA vary in the type of antigen used to capture antibodies, e.g., infected cell lysates or recombinant proteins [24, 25]. The following components are employed in one example of in-house ELISA to detect host antibodies to hantaviruses.

Table 2
Commercial ELISA kits for detection of antibodies against VHF

Virus antigen	Isotype	Methodology	Supplier	Commercial name
Dengue (serotype 1-4)	human IgG	Indirect ELISA assay	Focus	Dengue Virus IgG DxSelect™
Dengue (serotype 1-4)	human IgG	Indirect ELISA assay	Abcam	Anti-Dengue virus IgG Human ELISA (ab108728)
Dengue (serotype 1-4)	human IgG	Indirect ELISA assay	Mybiosource	Dengue virus IgG, ELISA
Dengue (serotype 1-4)	human IgG	Indirect ELISA assay	Panbio	Panbio® Dengue IgG Indirect ELISA: Dengue
Dengue (serotype 1-4)	human IgG	Indirect ELISA assay	Sigma-Aldrich	Dengue Virus IgM ELISA (SE120042)
Dengue (serotype 1-4)	human IgG	Indirect ELISA assay	Calbiotech	Dengue Virus IgG ELISA
Dengue (serotype 1-4)	human IgM	Capture ELISA assay	Focus	Dengue Virus IgM Capture DxSelect™
Dengue (serotype 1-4)	human IgM	Indirect ELISA assay	Abcam	Anti-Dengue virus IgM Human ELISA (ab108729)
Dengue (serotype 1-4)	human IgM	Indirect ELISA assay	Sigma-Aldrich	Dengue Virus IgM ELISA (SE120043)
Dengue (serotype 1-4)	human IgM	Indirect ELISA assay	Calbiotech	Dengue Virus IgM ELISA
Yellow fever	human IgG	Indirect ELISA assay	Mybiosource	Human yellow fever virus (YFV) antibody (IgG) ELISA
Yellow fever	human IgG	Double-antigen sandwich	Mybiosource	Qualitative Human Yellow Fever IgG (YFV-IgG) ELISA
Yellow fever	human IgM	Double-antigen sandwich	Mybiosource	Yellow fever virus (YFV) antibody (IgM), ELISA
Cocktail of recombinant nucleoproteins ^a	human IgG	Indirect ELISA assay	Focus	Hantavirus IgG DxSelect™
Cocktail of recombinant nucleoproteins ^a	human IgM	Indirect ELISA assay	Focus	Hantavirus IgM DxSelect™
Rift Valley fever	IgG ^b	Competitive ELISA	ID.Vet	ID Screen® Rift Valley Fever Competition Multi-species
Rift Valley fever	IgM ^b	Capture ELISA assay	ID.Vet	ID Screen® Rift Valley Fever IgM Capture

^aMultiple species of IgG or IgM are available

^bViral antigens on ELISA plates: Hantaan, Seoul, Puumala, Dobrava and Sin Nombre

Table 3
Commercial kits for detection of viral antigens

Virus antigen	Sample	Methodology	Company	Commercial name
Detection of Human Ebola Virus	Serum, plasma, tissue homogenate	Sandwich ELISA assay	MybioSource	Qualitative Human Ebola Virus (EV) ELISA Kit
Dengue NS1 Antigen	Serum	Sandwich ELISA assay	Focus	Dengue NS1 Antigen DxSelect™
Human Marburg virus	Serum, plasma, tissue homogenate	Sandwich ELISA assay	MybioSource	Qualitative Human Marburg Virus (MV) ELISA Kit
Lassa virus nucleoprotein	Serum	Immunoblot	Corgenix	ReLASV® Antigen Rapid Test for Lassa fever diagnosis
VP40 Ebola virus antigen	Whole blood and plasma	Rapid chromatographic immunoassay	Corgenix	ReEBOVTM Antigen Rapid Test

1. Clinical plasma or serum samples to be surveyed. Positive control serum and uninfected (negative) controls should be available to include in the ELISA.
2. 96-well flat-bottomed ELISA plates.
3. Viral antigen, which could be infected cell lysate or recombinant proteins [24, 25], this ELISA protocol was used for recombinant hantavirus nucleocapsid protein [22–24].
4. Phosphate-buffered saline (PBS): 137 mM NaCl, 2.7 mM KCl, 10 mM Na₂HPO₄, 2 mM KH₂PO₄ pH 7.4.
5. PBS-T is ELISA wash: 0.05% Tween-20 in PBS.
6. ELISA blocking buffer: PBS-T with 3% bovine serum albumin (BSA).
7. Secondary antibody conjugated with peroxidase or alkaline phosphatase: i.e., peroxidase-labeled goat anti-human IgG (H + L) antibody (KPL) for patient sera, and horseradish peroxidase (HRP)-labeled goat anti-*Peromyscus leucopus* IgG (H + L) secondary antibody (KPL) for *Peromyscus* rodent sera.
8. A peroxidase substrate: o-phenylenediamine dihydrochloride (OPD).
9. An incubator at 37 °C.
10. ELISA plate reader capable of reading 450 nm wavelength.

2.6 Immunofluorescence (IF) Microscopy

1. Glass microscope slides with wells and coverslips.
2. Cultured cells infected with a specific agent (positive controls) and cultured cells infected with unknown agents such as surveillance samples.
3. Phosphate-buffered saline (PBS): 137 mM NaCl, 2.7 mM KCl, 10 mM Na₂HPO₄, 2 mM KH₂PO₄, pH 7.4.
4. Primary hantavirus antibody or sera against hantavirus (Sin Nombre virus recombinant hyperimmune mouse ascitic fluid, HMAF).
5. Fluorescein isothiocyanate (FITC)-conjugated goat anti-mouse IgG, a secondary antibody conjugated with fluorochrome.
6. Acetone and 100% ethanol.
7. Evans-blue dye in water (1:10,000 w/v) to enhance visualization of nuclear antibodies.
8. Glass spheres to help collect cell lysates (Add the glass spheres and PBS to the culture flask and shake them on the monolayer).
9. Oil immersion microscope.
10. Clear nail polish to seal coverslips.
11. Biosafety cabinet for tissue culture (Type II laminar flow).

2.7 Neutralization (NT) Assay

1. 6-well plates.
2. Type II Biosafety cabinet (laminar flow) for tissue culture.
3. Incubator: 37 °C, 5% CO₂.
4. 10 × 100 mm sterile serial-dilution tubes.
5. Serum dilution medium: Eagle's minimal essential medium (EMEM), 2% heat-inactivated fetal bovine serum (FBS), 1% Penn/strep, 1% L-glutamine, and 1% sodium bicarbonate.
6. Agarose overlay medium: 4 g of agarose per 200 ml of sterile water. This is microwaved until it dissolves and maintained in a warm water bath to allow it to cool to 40 °C before combining with enriched EMEM and adding to cells. The EMEM should be 200 ml: 10% FBS, 2× nonessential amino acids, 2% Penn/strep, 2% L-glutamine, and 20 mM HEPES.
7. Vero cells.
8. Neutral red vital stain.
9. Temperature-regulated water bath.

2.8 Western Blot (WB)

1. SDS PAGE (*see* polyacrylamide gel).
2. Colorimetric kit BCIP-NBT Solution Kit.
3. Skim milk.

4. Nitrocellulose or polyvinylidene difluoride (PDVF) membrane. The PDVF membrane should be activated by immersion in methanol 100% for 5 or 10 min.
5. Electrophoresis apparatus.
6. Primary antibody: human sera. Secondary antibody: (HRPO)-conjugated goat anti-human IgG antibody.
7. Tris-buffered saline with Tween-20 (TBST) buffer: 20 mM Tris adjusted to pH 7.5, 150 mM NaCl, 0.1% Tween-20.
8. Blocking buffer for the WB: TBST containing 5% skim milk powder.
9. Transfer buffer: 25 mM Tris, 190 mM glycine, 20% methanol, adjust the pH to 8.3.

2.9 Sodium Dodecyl Sulfate-Polyacrylamide Gel Electrophoresis (SDS-PAGE)

1. SDS sample buffer: 0.0625 M Tris-HCl (pH 6.8), 2% SDS, 10% glycerol, 5% β -mercaptoethanol, 0.001% bromophenol blue.
2. 5 \times Running buffer: 15.1 g Tris-base, 72.0 g glycine, 5.0 g SDS, H₂O to 1000 ml. Dilute to make 1 \times or 2 \times working solutions, as appropriate.
3. Coomassie blue stain is commonly used at the end of a gel run when you want to confirm protein migration. Coomassie stain (0.025% dye): 200 ml acetic acid, 0.5 g Coomassie blue G-250 dye, 1800 ml H₂O.
4. Destaining buffer: 30% methanol, 10% glacial acetic acid in water.
5. Prestained protein ladder for molecular weight marking.
6. Gel apparatus and power supply.

3 Methods

3.1 Protocol for Virus Isolation from Tissues, Clinical Serum, or Blood Samples

Whole blood samples can either be allowed to coagulate for serum isolation, or they can be collected with anti-coagulant and layered on the top of a density medium like Histopaque-1077, and spun for 30 min, 400 $\times g$, at room temperature. The cloudy layer above the medium/Histopaque interface is mostly lymphocytes and monocytes (PBMC) and the clearer layer above that is plasma. Serum, plasma, and PBMC fractions can be immediately processed for virus assays or frozen for later use.

3.1.1 Virus Isolation from Tissue and Sera Sample

The protocol is adapted for hantavirus isolation from frozen tissues and yellow fever or dengue isolation from human sera [26–28].

1. For hantavirus isolation approximately 50 and 100 mg of tissue are homogenized in PBS (concentration of 10% w/v). When attempting yellow fever or dengue isolation, one should

dilute the human sera 1:10 in PBS solution (without magnesium and calcium).

2. Inoculate all the tissue suspensions onto a monolayer of Vero E6 cells grown in 12.5-cm² plastic culture flasks (confluence >80%). For yellow fever or dengue virus isolation, inoculate 100 µl of the diluted sample in confluent monolayers of Vero cells in 12.5 cm² plastic culture flasks.
 3. The flask inoculated with the sample is incubated for 60 min at 37 °C in a humidified atmosphere with 5% CO₂ (the cultures are briefly rocked every 15 min).
 4. Remove the excess of inoculated suspension and 7.0 ml or 15 ml of maintenance medium is added to each flask.
 5. The monolayers are maintained under a fluid overlay and incubated under the same conditions as **step 3**.
 6. On day 7 post-inoculation, half of the monolayer overlay is replaced with fresh maintenance medium. Observe the flask for cytopathic effects (CPE). Yellow fever grows quickly during the first inoculation, but hantavirus isolation, usually takes long time and requires up to three blind passages to detect the virus. In both cases, the cytopathic effect could be hard to see, for this reason the final detection is normally performed with IF.
 7. At day 13 or 14 for hantavirus isolation, or 7–10 days for yellow fever or dengue virus, scrape-off or glass-bead agitate the cells and collect them with the supernatant (approximately 7 ml) and add 1.5 ml of this suspension to a fresh monolayer of Vero E6 cells, for a “blind” passage using the same methodology as used for the first inoculation. Observe the flask for CPE (*see Note 1*).
 8. At the end of the virus isolation, virus may be concentrated from media by either high-speed centrifugation (3 h at 150,000 × *g*), precipitation using PEG, or collected on filters with pore sizes smaller than the virus particles (*see Note 2*). For virus precipitation, add 7–8% (w/v) PEG powder to a conical tube containing virus-media, mix it well, let it sit at 4 °C for 3 h to overnight, and spin at low speed (400 × *g*) in the cold to collect the precipitate. Resuspend the virus pellet in PBS (using a tenth of the original media volume) and dialyze this against PBS to remove the PEG [29]. Virus can also be concentrated by spinning onto small-pore filters, such as Amicon filters or Macrosep filtration devices (Pall).
1. Viral cultures preserved in an uninterrupted cold chain or using a chemical stabilizer (such as RNAlater from Qiagen, Life Technologies) could be used to isolate RNA and perform genetic characterizations.

3.2 Isolating and Quantifying Viral RNA (See Note 3)

2. Add 1 ml TRIzol[®] Reagent per 50–100 mg of tissue sample or add 0.75 ml of TRIzol[®] per 0.25 ml of sample ($5\text{--}10 \times 10^6$ cells from tissue).
3. Homogenize sample using a mechanical or manual homogenizer.
4. Shake tube vigorously by hand for 15 s.
5. Incubate for 2–3 min at room temperature.
6. Centrifuge the sample at $12,000 \times g$ for 15 min at 4 °C. The mixture separates into a lower red phenol-chloroform phase, an interphase, and a colorless upper aqueous phase. RNA remains in the aqueous phase.
7. Separate the RNA into an aqueous phase by adding a one-third volume of chloroform, agitating the sample for 30 s, and then spinning for 2 min in the microcentrifuge.
8. Place the upper or aqueous phase containing the RNA in a new tube.
9. Add 0.5 ml of 100% isopropanol to the aqueous phase, mix well, and leave on ice for at least 15 min.
10. Centrifuge at $12,000 \times g$ for 10 min at 4 °C.
11. Decant the supernatant (*see Note 4*).
12. Add 1 ml of 75–70% ethanol per 1 ml of TRIzol[®] used.
13. Vortex the sample a few seconds and centrifuge the tube at $7500 \times g$ for 5 min at 4 °C.
14. Air dry the RNA pellet for 5–10 min. Do not dry the pellet by vacuum centrifuge.
15. Resuspend the RNA in 10–50 μ l nuclease-free water and freeze until further use.

3.3 Reverse Transcription and Polymerase Chain Reaction (RT-PCR)
(*See Note 5*)

The PCR assay is a good tool for epidemiological surveillance because it can be performed at biosafety level-2 and allows the genetic characterization and identification of the circulating agents.

1. Quantify RNA by spectrophotometry at 260/280 nm wavelengths.
2. Using a cDNA-making kit, combine the viral RNA with random hexanucleotide primers and polydT to amplify the RNA in the presence of buffer, reverse transcriptase, and nucleotide solutions.
3. Using a PCR kit, combine an aliquot of cDNA from the previous step with forward and reverse primers to amplify conserved regions of the viral genome.
4. Place the mixture in a thermal cycler to produce amplicons (amplified cDNA segments) of the viral genome.

3.4 Agarose Gel to View PCR Products (Amplicons) (See Note 6)

1. After conventional PCR, the DNA products (or amplicons) can be run on an agarose gel to detect their size and sometimes identify them by hybridization.
2. The usual buffers to run and prepare agarose gels are TBE (tris-borate-EDTA) and TAE (Tris-acetate-EDTA). Although TAE has a lower buffering capacity than TBE, TAE should be used when DNA gel purification is performed for subsequent procedures such as sequencing, whereas TBE is more appropriate during extended electrophoresis (longer than 30 min).
3. Make a 1.5 or 2% agarose gel to resolve PCR amplicons. This can be stained with EtBR and photographed, or alternatively, blotted to a nitrocellulose filter and hybridized to DNA probes.
4. To purify DNA from gels, there are also many kits available, i.e., QIAquick® Gel Extraction Kit (Qiagen). The procedures for agarose gel variations and protocols to purify DNA from gels are available on Bench Guide, Qiagen [30].

3.5 Serological Surveillance

The **ELISA** is a good tool for epidemiological surveillance studies of animal reservoirs and humans. The detection of IgG antibodies is indirect evidence of circulation of virus of interest or closely related viruses, and the detection of IgM is indicative of recent infections. Unfortunately, most viruses that cause hemorrhagic fevers emerge at brief and unexpected intervals; so commercial reagents are not available. Currently, there are many studies that use recombinant antigens because they could be produced in BSL-2 laboratories, unlike cell lysates of some hemorrhagic viruses that require higher biosecurity levels. As an example of the indirect ELISA protocol to detect IgG antibodies, we describe the assay that uses recombinant nucleocapsid protein expressed by *E. coli*. The protocol described here is similar to those published for Sin Nombre and Andes hantaviruses [22, 24] (see **Notes 7 and 8**).

1. Recombinant viral nucleocapsid protein (rNp) expressed by *E. coli* is diluted in PBS to a concentration of 1 µg/ml as capture antigen.
2. Add 100 µl per well of the recombinant protein dilution and incubate overnight at 4 °C (for all the incubations it is necessary to use a humid chamber (a box with a wet towel) to avoid plate evaporation).
3. Wash the plate three times with PBS-T.
4. Plates are blocked with PBS-T containing a nonspecific protein like BSA or nonfat dry milk powder using 100 or 150 µl per well for 1 h at 37 °C.
5. Wash plates three times with PBS-T.
6. The patient or rodent sera under surveillance are diluted 1:200 with PBS-T containing nonspecific protein and 100 µl of these dilutions is added per well of the plate for 1–3 h at 37 °C.

7. Wash the plate three times with PBS-T.
8. Dilute the conjugated antibody with PBS-T and add 100 μ l of the dilution per well for 1 h at 37 °C. (Antibody dilutions could be in the range of 1:1000 to 1:20,000).
9. Wash the plate three times with PBS-T.
10. Prepare the substrate for the color reaction with o-phenylenediamine dihydrochloride (OPD) according to the manufacturer's instructions, add 100 μ l per well, and allow it to develop for 10–15 min.
11. Measure the absorbance at 450 nm using a plate spectrophotometer.

**3.6 Immunofluorescence (IF)
Microscopy to Detect
Virus Antigens or
Antibodies**

IF is a serological technique that can be set up for both antibody detection and viral antigen detection (*see Note 9*). This technique has some limitations for antibody detection in comparison to other serological assays because cell-culture slides must be produced, sometimes necessitating high-containment facilities. In some epidemiological studies, this technique is used to support the results obtained with other serological assays such as ELISA and Western Blot [31–34]. IF is very commonly used for antigen detection to confirm results of viral isolation. Depending on the availability of a primary antibody from infected animal or human cases, and the respective secondary antibody, virus infection of the original culture could be detected [35, 36]. The following protocols were described by Powers et al. to detect Rio Mamore hantavirus and Wuff et al. to detect Marburg infection [35, 37].

1. At the end of the first passage of the virus isolation assay, cells from the monolayer are scraped with glass spheres, using a small amount of PBS for cell dilution.
2. Clean the glass microscope slides briefly with ethanol.
3. Drop the cell suspension into the wells of the microscope slide, and let them air-dry in the biosafety cabinet.
4. Fix the cells with cold acetone for 1–10 min and store at –80 °C or –20 °C until performing the serological assay.
5. Before using the stored slides, they should be washed in PBS three times for 5 min.
6. To block unspecific binding, incubate the slide with PBS-T-BSA for 10 min at room temperature.
7. Decant the blocking solution and wash the cells three times in PBS-T, 5 min per wash.
8. Incubate with the primary antibody: in the case of hantavirus infection it is Sin Nombre virus recombinant hyper-immune mouse ascitic fluid (HMAF) in PBS-T with 1% BSA in a humidified chamber for 1 h at room temperature or 4 °C for

several hours. In the case of Marburg infection it is guinea pig immune serum prepared against Marburg virus (the primary antibodies in both cases are not commercial reagents; therefore, this usually is prepared in the laboratory or obtained by donations). When the IF is performed to evaluate serum samples from patients as primary antibody, each slide must have positive and negative control sera and the patient's samples must be used in different dilutions ranging from 1:20 to 1:160.

9. Decant the mixture with the primary antibody solution and wash the cells three times in PBS-T, 5 min each wash.
10. Incubate the cells with the secondary antibody, in case of hantavirus detection it is FITC-conjugated goat anti-mouse IgG in PBS-T with 1% BSA in a humidified chamber for 1 h at room temperature in the dark. In case of Marburg infection it is the same preparation FITC-conjugated anti-guinea pig.
11. Decant the mixture of the secondary antibody solution and wash three times with PBS-T for 5 min each in the dark.
12. Mount coverslips with a drop of mounting medium.
13. Seal coverslip with nail polish to prevent drying and movement under the microscope.
14. Read the slides under the fluorescence microscope.
15. Store slides in the dark at -20°C or 4°C .

3.7 Neutralization (NT) Test

The *in vitro* NT test consists of mixing serum samples with a certain amount of a titered virus stock, and then inoculating this mixture onto cell culture monolayers with a semisolid media. A serum sample with NT activity will reduce the capacity of your virus stock to cause CPE in cell culture. In epidemiological surveillance, the neutralization assay is very useful because, normally, the other serological tests have a high cross-reactivity among viruses of different species within the same genus, for this reason it is difficult to determine which virus is the etiological agent. The neutralizing antibodies are more specific for viruses, for example the dengue neutralizing antibodies can differentiate among different serotypes, making this technique essential for determining which serotypes circulate in a given area [38, 39]. Otherwise, the neutralization assay only identifies antibodies that block the virus entrance to the host cell; for that reason this technique is also useful in estimating vaccine efficacy [38]. Nevertheless, the NT also has some disadvantages for its application in epidemiological surveillance: it requires more time to perform than other serological tests and requires a cell culture laboratory with the appropriate biosafety level (BSL) according to the risk group of each agent [NIH Guidelines http://osp.od.nih.gov/sites/default/files/NIH_Guidelines.html].

The following protocol for a DENV NT test is simplified from the world health organization protocol [38].

1. Heat inactivate all sera to be assayed in a 56 °C water bath for 30 min.
2. Prepare serial 1:2 dilutions of test sera and positive and negative control sera in serum diluent (MEM). To the first tube of each dilution series, and to each of the five other tubes in the series, add 250 µl of diluent. Then prepare 1:10 dilution and the next tube 1:20, and so on.
3. Prepare all the control sera at the same dilutions as the clinical sera under surveillance.
4. Rapidly thaw the virus vial of the appropriate serotype, in a 37 °C water bath and then place it immediately on ice.
5. Place the same volume of the diluted virus stock into each of the serum dilution tubes, including controls for a final virus concentration of approximately 50 PFU/ 0.2 ml.
6. Mix the virus + serum well by gentle vortexing and incubate the tubes in a 37 °C water bath for 1 h.
7. Label 6-well plates containing confluent Vero cell monolayers for inoculation and remove all culture supernatants, being careful to prevent the monolayers from becoming dry.
8. Add 200 µl of the virus-serum mixture and inoculate this into each of the two wells of a properly prepared 6-well plate. Distribute the inoculum by rocking the plate back and forth and from side to side.
9. Incubate the inoculated plates at 37 °C for 1 h in a 5% CO₂ incubator to allow for virus absorption. Be sure that the plates are level so that the cell monolayers do not become dry. Rock the plates at regular intervals to maintain moisture on the cell sheets.
10. After the incubation period, remove the inoculum and add 2.5 ml of agarose-containing overlay medium to each well.
11. To mix the **first overlay medium** with equal volume of 2% agarose solution immediately prior to use (*see* Subheading 2) (*see* **Note 10**).
12. Set the plates at room temperature for 15–20 min to allow the agarose to solidify.
13. Incubate the plates upside down to minimize water condensation in the wells in a 37 °C, 5% CO₂ incubator for 5 days (depending on virus strain) to allow virus plaques to develop.
14. After the previously determined incubation time (e.g., 5 days) prepare the second overlay containing the vital stain neutral red. Add 2 ml of the second overlay to each well.

15. To make the **second overlay medium**, do exactly as for the first, but add neutral red to a final concentration of 0.5%. Allow the agar solution to cool as for the first overlay, then add the neutral red (which should be at room temperature) right before use.
16. Set the plates at room temperature for 15–20 min to allow the agarose to solidify.
17. Incubate the plates, same environment as above, for a minimum of 18 h or up to 48 h to allow the cells to maximally take up neutral red stain.
18. Place the stained 6-well plates on a light box. Using a counting pen, count the plaques. For a valid assay the negative control should contain a minimum of 30 plaques. As plaque overlap would be caused by excessive numbers of plaques it must be avoided.

3.8 Western Blots (WB) to Detect Viral Antigens (See Note 11)

Western blots give information about the specific proteins that are recognized by antibodies and require separation of antigen proteins on a SDS-PAGE in discernible bands corresponding to their molecular weight. WB is useful in epidemiological surveillance to detect antibodies in patients and animals to confirm the result of the ELISA commonly used in screening, e.g., for Ebola, Crimean-Congo, and Seoul virus [40–42]. Similar to the ELISA, the antigens for the WB could be recombinant proteins or native antigens. In the case of antibody detection, recombinant antigens are more often used to reduce the background reactivity to other cellular components [40–42]. WB is advantageous for epidemiological surveillance, because in rapid assays for field studies, antigens can be preloaded onto membranes to detect specific antibodies using colorimetric systems that do not require special equipment [43]. For example, there is a WB protocol to detect Crimean-Congo hemorrhagic fever virus (CCHFV) antibodies [41, 44, 45].

1. Load more than 1 µg of the recombinant Np in each well of the gel, this protein will be prepared in sampling buffer (*see* Subheading 2.9) and boiled for 10 min.
2. Run the gel for 2 h at approximately 120 V.
3. Transfer the proteins to a nitrocellulose membrane. For this procedure place the gel and membrane onto the transfer sandwich according to the electrophoresis apparatus manufacturer's recommendations. Place the cassette in the transfer tank immersed in transfer buffer. Transfer overnight in a cold room at a constant current of 10 mA.
4. The membrane with the proteins is blocked by incubating in TBST with 5% skim milk for 1 h at room temperature.

5. Wash the membrane three times with TBST, for 5 min each time.
6. Incubate the blots with human sera (1:100) dilution in TBST solution for 1 h at room temperature.
7. Wash three times again with TBST/5 min each.
8. Incubate the blots with the secondary antibody; in this case, it is horseradish peroxidase (HRPO)-conjugated goat anti-human IgG antibody (1:2000) in TBST solution.
9. Wash the membrane twice with (TBS)/5 min each.
10. The positive signal will be detected using the colorimetric kit (BCIP-NBT Solution Kit).

3.9 SDS- Polyacrylamide Gel Electrophoresis (SDS-PAGE) for WB

Denaturing polyacrylamide gels are useful for identifying proteins and evaluating their integrity. In epidemiological surveillance, the Western Blot is the most common application for this kind of gel. By heating the sample under denaturing and reducing conditions, proteins become unfolded and coated with SDS detergent molecules, acquiring a high net negative charge that is proportional to the length of the polypeptide chain [30]. Use 15% acrylamide for proteins between 12 and 43 kDa, 10% for proteins between 16 and 68 kDa, 7.5% for proteins between 36 and 94 kDa, and 5% for proteins between 57 and 212 kDa. Complete protocols to make these gels are available in [44].

1. After preparing the polymerized polyacrylamide gel, protein samples are mixed in equal volume proportion with SDS sample buffer, and boiled for 10 min.
2. After vortexing and heating the protein samples (for denaturation), these are loaded onto a gel previously immersed in running buffer. The running conditions for proteins in a range of 10–100 kDa are approximately 120 V for 2 h.
3. For gel staining, immerse the gel in Coomassie stain for at least 30 min and then immersed in destaining buffer to get rid of the excess dye until the proteins are clearly visible. A different method is used for silver staining to detect low abundance proteins (*see Note 12*) [46].

4 Notes

1. **During virus isolation assays** it is necessary to have a negative control (non-inoculated monolayer of cells), because you need to check the contamination of cultures and this allows the comparison between the inoculated and non-inoculated monolayers to detect CPE.

2. Normally after a successful virus isolation, the concentration (or titer) of isolated virus is low, so to get a concentrated stock it is recommended to use Amicon filters or PEG precipitation.
3. During virus amplification in culture, supernatants of each passage could also be processed for RNA isolation or for rt-PCR to detect viral nucleic acid. Additionally, cells fixed in the monolayer could be scraped to make slides for immunofluorescence for evaluating virus infection.
4. If you have so little starting material that you do not expect to see RNA pellets, add 1 μg of glycogen to your aqueous phases. Glycogen is inert in subsequent polymerase reactions, but it helps to precipitate RNA and makes a visible pellet. Glycogen can be purchased as a powder (e.g., Oyster glycogen from Sigma), suspended in sterile water, phenol extracted, ethanol precipitated, and stored frozen at 1 mg/ml.
5. PCR has many different purposes in surveillance studies. PCR is often used for the detection of an unknown virus because it is possible to use primers for a conserved sequence of a suspected virus genus and get the first viral sequence. For example, “universal” primers were designed for the arenavirus genus [47]. Another strategy to get unknown viral sequence is what is called “primer walking.” For this technique, different oligonucleotides are designed taking into account the alignment of related viruses, and after the first sequence is obtained, it is used to design oligonucleotides to get a new fragment and the procedure continues in this way [48].
6. Real-time PCR (rt-PCR), also known as quantitative rt-PCR or qPCR, is a variation on the conventional Reverse Transcription-PCR (RT-PCR). Quantitative PCR has become widely used in epidemiological surveillance and clinical studies because its setup takes less time than the conventional PCR and it is more sensitive for deducing relative concentrations of viral RNA with respect to host mRNA [49]. It is more often used in research related with diagnostics of known viral infections, but is not a good choice to get viral sequences because the amplicon sizes are too short. There is a TaqMan format of qPCR that uses specific probes to identify different viral serotypes, i.e., Alm et al. tested human samples using a specific probe for each dengue serotype [50].
7. **IgG ELISA:** To perform each ELISA assay it is necessary to use at least one positive and some negative controls to detect any variation in the reactivity. The concentration of the recombinant antigen and the dilution of the secondary antibody should be standardized to reduce the background in the negative controls and to optimize the signal in the positive controls.

The usual concentration of recombinant antigens is between (1–10 $\mu\text{g}/\text{ml}$) [24, 51], and the concentration of the secondary antibody is highly dependent on the commercial brand with normal values usually found between 1/1000 and 1/20,000.

There are different commercial reagents for development of color reaction, among them, TMB and ABTS (KPL), which could have different sensitivities, depending on the specific needs.

8. **ELISA for IgM detection:** In epidemiology, surveillance with IgM tests is less commonly used than the IgG test. IgM is regularly known as a short-lived response and tests are more often employed for diagnosis of clinical cases, particularly to detect patients with a recent infection [52, 53]. Considerations are similar to those for the IgG ELISA protocol; however, the antibody-capture methodology is more commonly used for the IgM assay with some additional variations. It is also necessary to adjust the concentration of the captured antibody.
9. **Indirect immunofluorescence assay (IIF):** For the cell fixation, use ice-cold methanol or 3–4% paraformaldehyde in PBS pH 7.4 for 15 min and room temperature. The advantage of acetone fixation is that a permeabilization protocol is not required to detect intracellular antigens. If you do not use acetone, the permeabilization protocol consists of incubating the samples for 10 min with PBS containing 0.25% Triton X-100 (or 100 μM digitonin or 0.5% saponin). However, permeabilization is not appropriate for the use of cell-surface antigens since it destroys membranes. As for other serological assays, the dilution of primary and secondary antibody should be standardized. In case the IF slides cannot be used immediately, they should be stored at $-80\text{ }^{\circ}\text{C}$. For better distinction of the cell nucleus add Evans blue dye to the solution of the secondary antibody.
10. **Neutralization (NT) tests:** When the virus is added to dilute sera it is necessary to be very careful to avoid contamination. Add the virus first to the negative control dilution, and then to test sera, and finally to the positive controls; avoid contaminating the pipette with sera. Hot agarose in the first overlay medium kills the cells, so be sure that this solution cools before adding it to the cell monolayer.
11. **Western Blots:** The transfer of proteins, blocking and incubation with the primary antibody can be carried out at room temperature or $4\text{ }^{\circ}\text{C}$ (avoiding protein degradation). To corroborate successful protein transfer, the membrane can be temporally stained with Red Ponceau that can be washed off to allow reuse of the membrane for the WB.

For verification, positive and negative control human sera should be tested under the same conditions in each WB. The time it takes to transfer proteins can be reduced by using low current, but this should be standardized for proteins with different sizes.

12. **SDS-PAGE for Western Blots:** It is recommended that two identical SDS-PAGE gels are prepared, one to transfer the proteins to the membrane for WB and another to stain with Coomassie for protein visualization. In the staining and destaining procedures, it is necessary to avoid evaporation; otherwise the gel could break. Silver staining is a long procedure but is more sensitive than Coomassie blue.

References

1. Williamson SJ, Allen LZ, Lorenzi HA, Fadrosh DW, Brami D, Thiagarajan M, McCrow JP, Tovchigrechko A, Yooseph S, Venter JC (2012) Metagenomic exploration of viruses throughout the Indian Ocean. *PLoS One* 7:e42047. doi:10.1371/journal.pone.0042047
2. Yooseph S, Andrews-Pfannkoch C, Tenney A, McQuaid J, Williamson S, Thiagarajan M, Brami D, Zeigler-Allen L, Hoffman J, Goll JB, Fadrosh D, Glass J, Adams MD, Friedman R, Venter JC (2013) A metagenomic framework for the study of airborne microbial communities. *PLoS One* 8:e81862. doi:10.1371/journal.pone.0081862
3. CDC (2013) Viral hemorrhagic fevers. CDC Fact Sheet 1–3. doi: 10.1111/j.1749-6632.2009.05106.x
4. CDC (2011) VHF 2011 case definition CSTE position statement-laboratory criteria for diagnosis epidemiologic linkage. 1–3
5. Knust B (2016) Chapter 3 viral hemorrhagic fevers. In: Brunette GW (ed) *Centers Dis. Control Prev. CDC Heal. Inf. Int. Travel* 2016. Oxford University Press, New York
6. CFSPH Iowa State University (2010) Viral hemorrhagic fevers caused by arenaviruses. *Cent food Secur Public Heal* 1–9
7. Witkowski PT, Kallies R, Hoveka J, Auste B, Ithete NL, Šoltys K, Szemes T, Drosten C, Preiser W, Klempa B, Mfunne JK, Kruger DH (2015) Novel arenavirus isolates from Namaqua rock mice, Namibia, Southern Africa. *Emerg Infect Dis* 21:1213–1216. doi:10.3201/eid2107.141341
8. Safronetz D, Sogoba N, Lopez JE, Maiga O, Dahlstrom E, Zivcec M, Feldmann F, Haddock E, Fischer RJ, Anderson JM, Munster VJ, Branco L, Garry R, Porcella SF, Schwan TG, Feldmann H (2013) Geographic distribution and genetic characterization of Lassa virus in sub-Saharan Mali. *PLoS Negl Trop Dis* 7:e2582. doi:10.1371/journal.pntd.0002582
9. Kariwa H, Yoshikawa K, Tanikawa Y, Seto T, Sanada T, Saasa N, Ivanov LI, Slonova R, Zakharycheva TA, Nakamura I, Yoshimatsu K, Arikawa J, Yoshii K, Takashima I (2012) Isolation and characterization of hantaviruses in Far East Russia and etiology of hemorrhagic fever with renal syndrome in the region. *Am J Trop Med Hyg* 86:545–553. doi:10.4269/ajtmh.2012.11-0297
10. Monath TP, Newhouse VF, Kemp GE, Setzer HW, Cacciapuoti A (1974) Lassa virus isolation from *Mastomys natalensis* rodents during an epidemic in Sierra Leone. *Science* 185:263–265. doi:10.1126/science.185.4147.263
11. Frei M (2014) *Biofiles*. Sigma-Aldrich 6: 17–21
12. McCall MD, Maciver AH, Pawlick R, Edgar R, Shapiro AM (2011) Histopaque provides optimal mouse islet purification kinetics: comparison study with Ficoll, iodixanol and dextran. *Islets* 3:144–149
13. Montoya-Ruiz C, Cajimat MN, Milazzo ML, Diaz FJ, Rodas JD, Valbuena G, Fulhorst CF (2015) Phylogenetic relationship of Necocli virus to other South American Hantaviruses (*Bunyaviridae: Hantavirus*). *Vector Borne Zoonotic Dis* 15:438–445. doi:10.1089/vbz.2014.1739
14. Lwande OW, Lutomiah J, Obanda V, Gakuya F, Mutisya J, Mulwa F, Michuki G, Chepkorir E, Fischer A, Venter M, Sang R (2013) Isolation of tick and mosquito-borne arboviruses from ticks sampled from livestock and wild animal hosts in Ijara District, Kenya. *Vector Borne Zoonotic Dis* 13:637–642. doi:10.1089/vbz.2012.1190

15. Klungthong C, Gibbons RV, Thaisomboonsuk B, Nisalak A, Kalayanarooj S, Thirawuth V, Nutkumhang N, Mammen MP Jr, Jarman RG (2007) Dengue virus detection using whole blood for reverse transcriptase PCR and virus isolation. *J Clin Microbiol* 45:2480–2485. doi:[10.1128/JCM.00305-07](https://doi.org/10.1128/JCM.00305-07)
16. Gäumann R, Mühlemann K, Strasser M, Beuret CM (2010) High-throughput procedure for tick surveys of tick-borne encephalitis virus and its application in a national surveillance study in Switzerland. *Appl Environ Microbiol* 76:4241–4249. doi:[10.1128/AEM.00391-10](https://doi.org/10.1128/AEM.00391-10)
17. Wilson WC, Romito M, Jaspersen DC, Weingartl H, Binopal YS, Maluleke MR, Wallace DB, van Vuren PJ, Paweska JT (2013) Development of a Rift Valley fever real-time RT-PCR assay that can detect all three genome segments. *J Virol Methods* 193:426–431. doi:[10.1016/j.jviromet.2013.07.006](https://doi.org/10.1016/j.jviromet.2013.07.006)
18. Pettersson L, Klingström J, Hardestam J, Lundkvist A, Ahlm C, Evander M (2008) Hantavirus RNA in saliva from patients with hemorrhagic fever with renal syndrome. *Emerg Infect Dis* 14:406–411. doi:[10.3201/eid1403.071242](https://doi.org/10.3201/eid1403.071242)
19. Godoy P, Marsac D, Stefas E, Ferrer P, Tischler ND, Pino K, Ramdohr P, Vial P, Valenzuela PD, Ferrés M, Veas F, López-Lastra M (2009) Andes virus antigens are shed in urine of patients with acute hantavirus cardiopulmonary syndrome. *J Virol* 83:5046–5055. doi:[10.1128/JVI.02409-08](https://doi.org/10.1128/JVI.02409-08)
20. Voytas D (2000) UNIT 2.5A resolution and recovery of large section DNA fragments. In: Ausubel FM, Brent R, Kingston RE et al (eds) *Curr Protoc. Mol. Biol.* Wiley, New York
21. Lunn G, Lawler G (2002) Appendix H Safe Use of Hazardous Chemicals. In: Ausubel FM, Brent R, Kingston RE et al (eds) *Curr. Protoc. Mol. Biol.* Wiley, New York
22. Schlegel M, Tegshduuren E, Yoshimatsu K, Petraityte R, Sasnauskas K, Hammerschmidt B, Friedrich R, Mertens M, Groschup MH, Arai S, Endo R, Shimizu K, Koma T, Yasuda S, Ishihara C, Ulrich RG, Arikawa J, Köllner B (2012) Novel serological tools for detection of Thottapalayam virus, a Soricomorpha-borne hantavirus. *Arch Virol* 157:2179–2187. doi:[10.1007/s00705-012-1405-9](https://doi.org/10.1007/s00705-012-1405-9)
23. Koma T, Yoshimatsu K, Taruishi M, Miyashita D, Endo R, Shimizu K, Yasuda SP, Amada T, Seto T, Murata R, Yoshida H, Kariwa H, Takashima I, Arikawa J (2012) Development of a serotyping enzyme-linked immunosorbent assay system based on recombinant truncated hantavirus nucleocapsid proteins for New World hantavirus infection. *J Virol Methods* 185:74–81. doi:[10.1016/j.jviromet.2012.06.006](https://doi.org/10.1016/j.jviromet.2012.06.006)
24. Koma T, Yoshimatsu K, Pini N, Safronetz D, Taruishi M, Levis S, Endo R, Shimizu K, Yasuda SP, Ebihara H, Feldmann H, Enria D, Arikawa J (2010) Truncated hantavirus nucleocapsid proteins for serotyping Sin Nombre, Andes, and Laguna Negra hantavirus infections in humans and rodents. *J Clin Microbiol* 48:1635–1642. doi:[10.1128/JCM.00072-10](https://doi.org/10.1128/JCM.00072-10)
25. Ksiazek TG, Peters CJ, Rollin PE, Zaki S, Nichol S, Spiropoulou C, Morzunov S, Feldmann H, Sanchez A, Khan AS (1995) Identification of a new North American hantavirus that causes acute pulmonary insufficiency. *Am J Trop Med Hyg* 52:117–123
26. Onyango CO, Ofula VO, Sang RC, Konongoi SL, Sow A, De Cock KM, Tukei PM, Okoth FA, Swanepoel R, Burt FJ, Waters NC, Coldren RL (2004) Yellow fever outbreak, imatong, Southern Sudan. *Emerg Infect Dis* 10:1063–1068
27. Milazzo ML, Duno G, Utrera A, Richter MH, Duno F, de Manzione N, Fulhorst CF (2010) Natural host relationships of hantaviruses native to western Venezuela. *Vector Borne Zoonotic Dis* 10:605–611. doi:[10.1089/vbz.2009.0118](https://doi.org/10.1089/vbz.2009.0118)
28. Medina F, Medina JF, Colón C, Vergne E, Santiago GA, Muñoz-Jordán JL (2012) Dengue virus: isolation, propagation, quantification, and storage. *Curr Protoc Microbiol*. doi:[10.1002/9780471729259.mc15d02s27](https://doi.org/10.1002/9780471729259.mc15d02s27)
29. Lewis GD, Metcalf TG (1988) Polyethylene glycol precipitation for recovery of pathogenic viruses, including hepatitis A virus and human rotavirus, from oyster, water, and sediment samples. *Appl Environ Microbiol* 54:1983–1988
30. Qiagen (2009) Bench guide plasmid DNA genomic DNA and RNA. Qiagen
31. Witkowski PT, Leendertz SA, Auste B, Akoua-Koffi C, Schubert G, Klempa B, Muyembe-Tamfum JJ, Karhemere S, Leendertz FH, Krüger DH (2015) Human seroprevalence indicating hantavirus infections in tropical rainforests of Côte d'Ivoire and Democratic Republic of Congo. *Front Microbiol* 6:1–6. doi:[10.3389/fmicb.2015.00518](https://doi.org/10.3389/fmicb.2015.00518)
32. Goeijenbier M, Hartskeerl RA, Reimerink J, Verner-Carlsson J, Wagenaar JF, Goris MG, Martina BE, Lundkvist Å, Koopmans M, Osterhaus AD, van Gorp EC, Reusken CB (2014) The hanta hunting study: underdiagnosis of puumala hantavirus infections in symptomatic non-travelling leptospirosis-suspected patients in the Netherlands, in 2010 and April to November 2011. *Eurosurveillance* 19:1–10

33. Emmerich P, Günther S, Schmitz H (2008) Strain-specific antibody response to Lassa virus in the local population of west Africa. *J Clin Virol* 42:40–44. doi:10.1016/j.jcv.2007.11.019
34. Papa A, Sidira P, Larichev V, Gavrilova L, Kuzmina K, Mousavi-Jazi M, Mirazimi A, Ströher U, Nichol S (2014) Crimean-Congo hemorrhagic fever virus, Greece. *Emerg Infect Dis* 20:288–290. doi:10.3201/cid2002.130690
35. Powers AM, Mercer DR, Watts DM, Guzman H, Fullhorst CF, Popov VL, Tesh RB (1999) Isolation and genetic characterization of a hantavirus (*Bunyaviridae: Hantavirus*) from a rodent, *Oligoryzomys microtis* (Muridae), collected in northeastern Peru. *Am J Trop Med Hyg* 61:92–98
36. Hetzel U, Sironen T, Laurinmäki P, Liljeroos L, Patjas A, Henttonen H, Vaheri A, Artelt A, Kipar A, Butcher SJ, Vapalahti O, Hepojoki J (2013) Isolation, identification, and characterization of novel arenaviruses, the etiological agents of bovid inclusion body disease. *J Virol* 87:10918–10935. doi:10.1128/JVI.01123-13
37. Wulff H, Slenczka W, Gear JHS (1978) Early detection of antigen and estimation of virus yield in specimens from patients with Marburg virus disease. *Bull World Health Organ* 56:633–639
38. World Health Organization (2007) Guidelines for plaque reduction neutralization testing of human antibodies to dengue viruses. http://apps.who.int/iris/bitstream/10665/69687/1/who_ivb_07.07_eng.pdf
39. Leslie T, Martin NJ, Jack-Roosberg C, Odongo G, Beausoleil E, Tuck J, Raviprakash K, Kochel TJ (2014) Dengue serosurvey in Sint Eustatius. *PLoS One* 9:1–5. doi:10.1371/journal.pone.0095002
40. Jayme SI, Field HE, de Jong C et al (2015) Molecular evidence of Ebola Reston virus infection in Philippine bats. *Virol J* 12:107. doi:10.1186/s12985-015-0331-3
41. Xia H, Li P, Yang J, Pan L, Zhao J, Wang Z, Li Y, Zhou H, Dong Y, Guo S, Tang S, Zhang Z, Fan Z, Hu Z, Kou Z, Li T (2011) Epidemiological survey of Crimean-Congo hemorrhagic fever virus in Yunnan, China, 2008. *Int J Infect Dis* 15:e459–e463. doi:10.1016/j.ijid.2011.03.013
42. Costa F, Porter FH, Rodrigues G, Farias H, de Faria MT, Wunder EA, Osikowicz LM, Kosoy MY, Reis MG, Ko AI, Childs JE (2014) Infections by *Leptospira interrogans*, Seoul virus, and Bartonella spp. among Norway rats (*Rattus norvegicus*) from the urban slum environment in Brazil. *Vector Borne Zoonotic Dis* 14:33–40. doi:10.1089/vbz.2013.1378
43. Hjelle B, Jenison S, Torrez-Martinez N, Herring B, Quan S, Polito A, Pichuanes S, Yamada T, Morris C, Elgh F, Lee HW, Artsob H, Dinello R (1997) Rapid and specific detection of Sin Nombre virus antibodies in patients with hantavirus pulmonary syndrome by a strip immunoblot assay suitable for field diagnosis. *J Clin Microbiol* 35:600–608
44. Gallagher SR (2008) UNIT 7.3 SDS-polyacrylamide gel electrophoresis (SDS-PAGE), Current protocols essential laboratory techniques. Wiley, Hoboken
45. Wei PE, Luo YJ, Li TX, Wang HL, Hu ZH, Zhang FC, Zhang YJ, Deng F, Sun SR (2010) Serial expression of the truncated fragments of the nucleocapsid protein of CCHFV and identification of the epitope region. *Virol Sin* 25:45–51. doi:10.1007/s12250-010-3067-7
46. Chevallet M, Luche S, Rabilloud T (2006) Silver staining of proteins in polyacrylamide gels. *Nat Protoc* 1:1852–1858. doi:10.1038/nprot.2006.288
47. Ledesma J, Fedele CG, Carro F, Lledó L, Sánchez-Seco MP, Tenorio A, Soriguer RC, Saz JV, Domínguez G, Rosas MF, Barandika JF, Gegúndez MI (2009) Independent lineage of lymphocytic choriomeningitis virus in wood mice (*Apodemus sylvaticus*), Spain. *Emerg Infect Dis* 15:1677–1680. doi:10.3201/eid1510.090563
48. Yadav PD, Vincent MJ, Nichol ST (2007) Thottapalayam virus is genetically distant to the rodent-borne hantaviruses, consistent with its isolation from the Asian house shrew (*Suncus murinus*). *Virol J* 4:80. doi:10.1186/1743-422X-4-80
49. Jääskeläinen AJ, Moilanen K, Aaltonen K, Putkuri N, Sironen T, Kallio-Kokko H, Vapalahti O (2015) Development and evaluation of a real-time EBOV-L-RT-qPCR for detection of Zaire ebolavirus. *J Clin Virol* 67:56–58. doi:10.1016/j.jcv.2015.04.003
50. Alm E, Lindegren G, Falk KI, Lagerqvist N (2015) One-step real-time RT-PCR assays for serotyping dengue virus in clinical samples. *BMC Infect Dis* 15:493. doi:10.1186/s12879-015-1226-z
51. Li G, Pan L, Mou D, Chen Y, Zhang Y, Li X, Ren J, Wang P, Zhang Y, Jia Z, Huang C, Sun Y, Yang W, Xiao SY, Bai X (2006) Characterization of truncated hantavirus nucleocapsid proteins and their application for serotyping. *J Med Virol* 932:926–932. doi:10.1002/jmv
52. Kuchuloria T, Imnadze P, Chokheli M, Tsertsvadze T, Endeladze M, Mshvidobadze

- K, Clark DV, Bautista CT, Abdel Fadeel M, Pimentel G, House B, Hepburn MJ, Wölfel S, Wölfel R, Rivard RG (2014) Viral hemorrhagic fever cases in the country of Georgia: Acute Febrile Illness Surveillance Study results. *Am J Trop Med Hyg* 91:246–248. doi:[10.4269/ajtmh.13-0460](https://doi.org/10.4269/ajtmh.13-0460)
53. Klempa B, Koulemou K, Auste B, Emmerich P, Thomé-Bolduan C, Günther S, Koivogui L, Krüger DH, Fichet-Calvet E (2013) Sero-epidemiological study reveals regional co-occurrence of Lassa- and hantavirus antibodies in Upper Guinea, West Africa. *Tropical Med Int Health* 18:366–371. doi:[10.1111/tmi.12045](https://doi.org/10.1111/tmi.12045)

Diagnostics for Lassa Fever: Detecting Host Antibody Responses

Maria S. Salvato, Igor S. Lukashevich, Sandra Medina-Moreno, and Juan Carlos Zapata

Abstract

There are two types of viral diagnostics: (1) those that detect components of the pathogen (like viral RNA or proteins) and (2) those that detect host molecules that rise or fall as a consequence of pathogen infection (like anti-viral antibodies or virus-induced inflammatory cytokines). Quantitative PCR to detect Lassa RNA, and clinical chemistry to detect high liver enzymes (AST/ALT) are commonly used to diagnose Lassa fever. Here, we discuss the various types of diagnostics for Lassa fever and the urgent need for early diagnosis. We also describe a protocol for using the attenuated Lassa vaccine candidate, ML29, as an antigen for detecting Lassa-specific antibodies. Since antibodies are developed late in the progression of Lassa fever disease, this is not an early diagnostic, but is more useful in surveillance of the population to determine the sero-prevalence of antibodies to Lassa virus (LASV), and to define treatment options for people in close contact with a Lassa-infected person.

Key words Lassa diagnosis, Host-response diagnostics, ML29 antigen, Early diagnosis, Antibody response, Surveillance

1 Introduction

Differential diagnosis for Lassa fever (LF) includes malaria, dengue fever, Ebola virus disease, typhoid fever, gastroenteritis, pneumonia, influenza, and many other infections beginning with flu-like symptoms. In the endemic areas of Western Africa, it is hard to arrive at an etiologic diagnosis due to a lack of convenient diagnostic laboratories. The early flu-like signs can rapidly progress to more specific manifestations like facial edema, petechial rash, and sore throat [1]. Table 1 describes the progression of Lassa fever (LF) obtained by blood exposure, for example by needle stick from a viremic patient, and the types of diagnostics that can be used at the different stages of disease.

Table 1
Diagnosis of Lassa fever: progression of host responses and virus replication

Disease → Progression	Day 1–4	Day 5–9	Day 7–15	Day 10–20
<i>Detect host response</i>				
Mild infection	Early innate immune response	You might note mild signs: headache, weakness, myalgia. Strong CMI ^a .	CTL assay or T cell proliferation assay detects strong CMI	ELISA to detect Lassa virus-specific IgM or IgG is clearly positive.
Severe infection	Transcriptome ^b : Drop in PTGS2, & NR4A2. Kinomics shows low signaling.	Late innate response, weak CTL response. Disease signs = fever, high liver enzymes, low blood pressure.	Signs = pharyngitis, petechial rash, vascular leakage, facial edema. High liver enzymes: ALT/AST >5X normal.	Signs = kidney failure. Deafness, possibly hemorrhage. ELISA might detect antiviral antibodies, but they are weak.
<i>Detect virus, virus protein, or virus RNA</i>				
	No detectable virus until d3 or d4.	<ul style="list-style-type: none"> – Virus plaque assay detects peak viremia. – qRT-PCR detects viral RNA – Immunohistochemistry detects viral antigens in tissues – Antigen capture ELISA detects viral antigen – Western blot or Rapid detects viral protein. 	<p>In a mild infection, viral components decrease due to good immune response.</p> <p>In a severe infection, viral components remain high, virus >10⁴ infectious units/ml.</p>	<p>In a mild infection, disease signs disappear and the patient becomes well.</p> <p>In a severe infection, 16% of hospitalized cases succumb to death. For those who recover, virus RNA persists for months.</p>

^aCMI means cell-mediated immunity or immunity that does not involve antibodies. It is detectable by T cell proliferation to antigen (detecting CD4 responses), by cytotoxic T cell assays (Fluor- or chromium-release due to virus-specific lysis of infected cells; secretion of cytokines like IFN- γ in response to viral antigens; tetramer-binding assays), and by assays for activated phagocytes

^bTranscriptome analysis of macaques with viral hemorrhagic fever showed dramatic drops in gene expression of PTGS2 (encoding COX2) and Nuclear Receptor 4A2 (NR4A2; responsible for up-regulating retinoic acid receptors) [2]

There are no commercially available diagnostic assays for detecting the pre-viremic or incubation phase of LASV infection. Early diagnosis of LF is crucial for initiating treatment, implementing preventive measures, and contact-tracing possible disease carriers [3]. Host responses to infection during the incubation phase could conceivably contribute to predicting clinical disease. Studies

in rhesus monkeys infected with lymphocytic choriomeningitis virus (LCMV) [2] or people infected with influenza A virus [4, 5] established patterns of virus-specific host responses occurring before viremia. A goal for this work has been to develop diagnostic chips that will measure changes in host gene expression that are predictive of disease onset. Unfortunately, despite a great deal of research investment into predictive chips, no such diagnostics are currently available due to the great person-to-person variation in disease susceptibilities and immune responses.

The problem of human variation could be solved by an intense effort to classify people into transcriptome types. For example, after characterizing the blood transcriptome of 1000 healthy people and hierarchical clustering of their profiles, it may be possible to determine whether the clustering follows any external characteristics, such as age, gender, ethnicity, body mass index, etc. Should the clustering allow a classification of the 1000 subjects into a limited number of “groups,” then each individual could belong to a group and have a healthy comparator when they become ill. Biomarker chip analysis relies on comparison to an appropriate healthy control, so either a healthy person from your “group” can serve as your comparator when you get sick, or you can rely on your own “healthy profile” to compare to your “sick profile.” When we profiled macaques it was possible to use their pre-infection bloods as the “healthy control” and our results were very consistent for each animal. Based on NHP studies, a severe drop in mRNA for COX2 or NR4A2 and a rise in mRNA for fibronectin1, CD14, or chemokine receptor CCR2 occurred before viremia rose enough to be detectable by conventional diagnostics [2]. In human beings we would expect this drop or rise to occur with respect to the expression of those genes in a healthy comparator. If the sick person fits this profile, they would be likely to be harboring a virulent case of LFD.

LASV isolation is the “gold standard” for LF diagnosis, but it must be done in high containment Biosafety Level-4 (BSL-4) facilities and requires several days for completion [3]. Most diagnostics for LF detect the proteins or nucleic acids of LASV. A new “lateral flow immunoassay” detects the LASV nucleocapsid protein (NP) in serum samples and was developed by the Hemorrhagic Fever Virus Consortium with Corgenix Medical Corporation, CO, USA [6]. This approach uses immobilized antibodies to capture virus antigens, and is probably the most rapid and cost-effective type of early diagnostic.

Reverse transcription-PCR (RT-PCR) proved useful for LASV detection with 100% sensitivity [7, 8]. By using specific primers for a conserved region in the S segment, up to 79% positive predictive value was achieved, compared with 21% for Indirect immunofluorescence assay (IFA). Testing of three sequential samples after admission increased the positive predictive value to 100%

compared with 52% for IFA [9]. Later, these protocols were optimized by including real-time PCR assays [10], second rounds of amplification (nested PCR) [11], targeting several sites on the L segment [12] or combining PCR with sequencing [13]. With PCR there are issues of strain variation (nucleotide mismatching), cross-contamination, and high implementation costs in resource-limited settings [13].

Late-stage diagnostics are also available. Virus neutralization tests, reversed passive hemagglutination and inhibition, and complement fixing antibody detections were some of the first LASV diagnostics, but detectable antibodies appear late after infection and are primarily useful for surveillance [14–17]. IFA can be used for LF antibody detection (an increase of more than four times in IgG-LASV titers, IgG of <1:256 on admission, or IgM-LASV titer of <1:4 is considered positive) however; specificity is low in populations with small apparent risk of infection and does not distinguish between LASV strains. IFA detects antibodies 7–10 days after the onset of illness, 3–4 days faster than the cytopathic effects (CPE) seen by virus isolation [1, 18, 19]. ELISA (Enzyme-Linked Immunosorbent Assay) was developed for detecting LASV-IgM and IgG and antigen. This test improved sensitivity and specificity, however, early detection was not improved unless antigen assays were used that were positive on the day of patient admission [6, 20–26]. The antigen used in antibody-capture ELISA is important: GP is “type specific” or more species-specific, and NP is “group specific” or more broadly cross-reactive; so antigen that consists of whole virions (like the ML29-attenuated reassortant virus [25]) should have the broadest capacity to detect antibodies from a wide variety of LASV isolates. Other studies showed increased sensitivity or specificity by combining IgM and antigen assays, but detection has rarely been fast enough for patients to initiate therapy and survive. Molecular methods such as Western Blot analysis have also been tried for detecting NP and envelope glycoprotein-2 (GP2) antibodies [20]. With the use of this technique, it was possible to detect both IgG and IgM against NP in acute samples with very low positive predictive value (53.6%) but high negative predictive value (93%) [27].

Here, we describe the use of an attenuated Lassa vaccine candidate as an inexpensive antigen for performing antibody-detecting ELISA. 96-well polystyrene plates are coated with viral antigen, and then the patient serum or plasma is added to each well. If the patient sample contains anti-Lassa antibodies, they will bind the antigen and be detected by an enzyme-linked secondary antibody. This antibody mediates a color change in the wells upon the addition of a substrate such as TMB. Such an inexpensive assay will establish the sero-prevalence of Lassa exposure in a given population and help in assessing the need for developing clinical capacity

and outbreak preparedness, as well as to guide the treatment to people in close contact with a confirmed LF case.

Clinical and laboratory diagnosis of LASV has been improved during the last 20 years by the introduction of new antibody or nucleic acid detection assays. The new technologies shorten the time between infection and diagnosis but fail to detect infection during the incubation period. Thus, there are important opportunities for more advanced LF diagnostics that incorporate early patterns of host responses with pathogen detection.

2 Materials

1. ML29 antigen: ML29 virus is a reassortant between Lassa and Mopeia viruses containing the NP and GP from LASV, and the Z and L genes from Mopeia virus. Non-infectious antigen is derived from a stock of ML29 that is 10^7 plaque forming units/ml and, inactivated by sonication for five 3-second bursts at maximum intensity in a cup sonicator (*see Note 1*).
2. ELISA plates: 96-well flat-bottomed plastic microtiter plates.
3. Phosphate buffer saline (PBS) pH 7.4.
4. Coating Buffer (100 mM Bicarbonate buffer, pH 9.6): 1.59 g Na_2CO_3 , 2.93 g NaHCO_3 , add distilled water to 1 l; pH 9.6 by adding dilute NaOH or HCL as needed. Alternative: Carbonate-Bicarbonate Buffer Capsules (e.g., from Sigma).
5. Blocking Buffer: 10% nonfat dry milk (NFDM) in PBS. Dry milk prevents nonspecific binding of detection antibodies to the multiwell plate surfaces (*see Note 2*).
6. Wash Buffer: 0.05% Tween-20 (polysorbate 20) in PBS. Tween detergent will prevent nonspecific antibody binding.
7. Distilled or deionized water. Poor quality water can cause high background or high optical density readings.
8. Sample Dilution Buffer: 10% NFDM, 0.05% Tween-20, in PBS.
9. Serum or plasma samples: unknown patient samples; patient samples known to be Lassa-infected (positive controls); uninfected patient samples (negative controls).
10. Secondary antibody conjugates: Goat, sheep, rat, or mouse anti-human IgG conjugated with peroxidase enzyme can be used. Each of them has to be optimized for this procedure.
11. 3,3',5,5'-Tetramethylbenzidine (TMB; substrate for the peroxidase enzyme that is linked to the secondary antibody).
12. TMB Stop Solution: Stops the enzyme-substrate reaction and color development.

13. Single-channel and multi-channel pipets.
14. Barrier pipette tips 5–1000 μ l to avoid cross-contaminations.
15. Serological plastic pipettes 5, 10, and 25 ml.
16. Reagent reservoirs.
17. Conical centrifuge tubes (15 ml and 50 ml).
18. 14 ml polypropylene round-bottom tubes.
19. Assorted clean/sterile glassware (e.g., beakers, flasks).
20. Non-powdered gloves; nitrile recommended.
21. Aluminum foil.
22. Optical tape (plate covers).
23. Safety glasses.
24. Timer.
25. Vortex mixer.
26. Magnetic stirrer and stir bar.
27. 37 °C incubator.
28. 2–8 °C refrigerator.
29. –20 °C freezer.
30. –80 °C freezer (for long-term storage of patient samples).
31. Class II biological safety cabinet.

3 Method

1. To coat 96-well plates with antigen, first dilute ML29 antigen 1:100 in Coating Buffer (10 ml/plate). Then vortex the solution 5 s, add 100 μ l/well, incubate plates for 3 h 37 °C (or alternatively 4 °C overnight).
2. To block the plates, prepare fresh Blocking Buffer (25 ml/plate). Stir it for 30 min to make sure NFDM is all dissolved.
3. After coating is completed, remove the plates from the incubator and aspirate the antigen from the wells. This can be done manually using a multichannel pipet or with automated or semi-automated washer such as the NUNC Immuno™ Wash 12 aspirator. After aspiration, wells should not dry before the addition of the next reagent.
4. Wash plates six times with Wash Buffer using the semi-automated washer or multichannel pipet. Soak plates 2 min between washes.
5. Remove residual wash fluid by tapping inverted plate on absorbent paper.
6. Add 250 μ l Blocking Buffer to all wells of the plate and incubate overnight at 4 °C (or 3 h at 37 °C).

7. Dilute patient samples 1:100 in Sample Dilution Buffer in 1.5 ml Eppendorf tubes. Make enough dilute sample to place 100 μ l per well. Your positive and negative controls should have been pretested. In our case, our positive control worked best at a dilution of 1:200 and the negative control at 1:100.
8. Remove the blocked plates from 37 °C incubator or 4 °C refrigerator.
9. Aspirate the Blocking Solution with a semi-automated washer or a multichannel pipet.
10. Wash plates six times with Wash Buffer, soaking 2 min between washes.
11. Remove residual wash fluid from wells by tapping inverted plate on absorbent paper.
12. Add 100 μ l per well of diluted samples to the 96-well plate. Figure 1 shows an example of plate design.
13. Incubate plates in 37 °C incubator for 1 h. Plates can be stacked and covered with foil or optical tape plate-covers.
14. Remove plates from incubator but do not dump their contents, instead be careful to aspirate the samples from the wells

Date: _____

anti-IgG Lot # and dilution: _____

Operator: _____

Expiration date: _____

	1	2	3	4	5	6	7	8	9	10	11	12
A	1			8			15			22		
B	2			9			16			23		
C	3			10			17			24		
D	4			11			18			25		
E	5			12			19			26		
F	6			13			20				NEGATIVE	
G	7			14			21				POSITIVE	
H	BLANK											

Positive control ID: _____

NOTES: _____

Positive control preparation date: _____

Positive control dilution: _____

Sign: _____ Date: _____

Fig. 1 Sample layout for a 96-well plate ELISA to test 26 unknown sera in triplicate. The plate includes a negative control in triplicate, a positive control in triplicate and 12 blank wells (*buffer instead of serum*). Relevant information about the assay should be documented according to Good Lab Practices

so as to prevent cross-contamination. Wash plates six times with Wash Buffer, soaking 2 min between washes. Remove residual fluid from wells by tapping inverted plate on absorbent paper.

15. Dilute anti-human IgG antibody conjugate in Sample Dilution Buffer (1:2500 dilution). Dilution should occur in two stages: 1:100 dilution first, vortex, and then 1:25 dilution, vortex. You will need 10 ml per plate. Add 100 μ l of secondary antibody conjugate to each well of the plate.
16. Incubate plates in 37 °C incubator for 1 h. Plates can be stacked and covered with foil or optical tape plate-covers.
17. Remove plates from incubator. Be careful to aspirate the samples from the wells so as to prevent cross-contamination (do not dump their contents). Wash plates six times with Wash Buffer, soaking 2 min between washes. Remove residual fluid from wells by tapping inverted plate on absorbent paper.
18. Bring the TMB to room temperature 15 min before using it. The TMB will usually not work well after its expiration date. Add 100 μ l per well.
19. Cover plates with foil and incubate them in the dark for 15 min at room temperature.
20. Stop color development by adding 100 μ l per well of TMB Stop Solution. Add this slowly and carefully so as to prevent making bubbles (that cause the plate-reader to make incorrect readings). Change tips between rows and use barrier tips to prevent cross-contaminating wells.
21. Turn on the microplate reader 20 min before use, so it is warmed up. Place each plate in the reader at 450 nm with zero reference filter (depending on the ELISA reader). Read plate within 15 min after final incubation.

4 Notes

1. If the starting titer of the virus to be used as antigen is less than 10^7 , use Amicon filters to concentrate the stock.
2. The Carnation-Nestle brand is a soluble particulate-milk preparation that causes no clumping. Some other milk brands produce fine powders that clump, are less soluble, and contribute to high backgrounds.

References

1. McCormick JB, King IJ, Webb PA, Johnson KM, O'Sullivan R, Smith ES, Trippel S, Tong TC (1987) A case-control study of the clinical diagnosis and course of Lassa fever. *J Infect Dis* 155:445–455
2. Djavani MM, Crasta OR, Zapata JC, Fei Z, Folkerts O, Sobral B, Swindells M, Bryant J, Davis H, Pauza CD, Lukashevich IS, Hammamieh R, Jett M, Salvato MS (2007) Early blood profiles of virus infection in a

- monkey model for Lassa fever. *J Virol* 81:7960–7973
3. Bausch DG, Rollin PE, Demby AH, Coulibaly M, Kanu J, Conteh AS, Wagoner KD, McMullan LK, Bowen MD, Peters CJ, Ksiazek TG (2000) Diagnosis and clinical virology of Lassa fever as evaluated by enzyme-linked immunosorbent assay, indirect fluorescent-antibody test, and virus isolation. *J Clin Microbiol* 38:2670–2677
 4. Zaas AK, Chen M, Varkey J, Veldman T, Hero AO 3rd, Lucas J, Huang Y, Turner R, Gilbert A, Lambkin-Williams R, Oien NC, Nicholson B, Kingsmore S, Carin L, Woods CW, Ginsburg GS (2009) Gene expression signatures diagnose influenza and other symptomatic respiratory viral infections in humans. *Cell Host Microbe* 6:207–217
 5. Woods CW, McClain MT, Chen M, Zaas AK, Nicholson BP, Varkey J, Veldman T, Kingsmore SF, Huang Y, Lambkin-Williams R, Gilbert AG, Hero AO 3rd, Ramsburg E, Glickman S, Lucas JE, Carin L, Ginsburg GS (2013) A host transcriptional signature for presymptomatic detection of infection in humans exposed to influenza H1N1 or H3N2. *PLoS One* 8:e52198
 6. Grove JN, Branco LM, Boisen ML, Muncy IJ, Henderson LA, Schieffellin JS, Robinson JE, Bangura JJ, Fonnies M, Schoepp RJ, Hensley LE, Seisay A, Fair JN, Garry RF (2011) Capacity building permitting comprehensive monitoring of a severe case of Lassa hemorrhagic fever in Sierra Leone with a positive outcome: case report. *Virol J* 8:314
 7. Lunkenheimer K, Hufert FT, Schmitz H (1990) Detection of Lassa virus RNA in specimens from patients with Lassa fever by using the polymerase chain reaction. *J Clin Microbiol* 28:2689–2692
 8. Trappier SG, Conaty AL, Farrar BB, Auperin DD, McCormick JB, Fisher-Hoch SP (1993) Evaluation of the polymerase chain reaction for diagnosis of Lassa virus infection. *Am J Trop Med Hyg* 49:214–221
 9. Demby AH, Chamberlain J, Brown DW, Clegg CS (1994) Early diagnosis of Lassa fever by reverse transcription-PCR. *J Clin Microbiol* 32:2898–2903
 10. Drosten C, Gottig S, Schilling S, Asper M, Panning M, Schmitz H, Gunther S (2002) Rapid detection and quantification of RNA of Ebola and Marburg viruses, Lassa virus, Crimean-Congo hemorrhagic fever virus, Rift Valley fever virus, dengue virus, and yellow fever virus by real-time reverse transcription-PCR. *J Clin Microbiol* 40:2323–2330
 11. Lukashevich IS, Carrion R Jr, Salvato MS, Mansfield K, Brasky K, Zapata J, Cairo C, Goicochea M, Hoosien GE, Ticer A, Bryant J, Davis H, Hammamieh R, Mayda M, Jett M, Patterson J (2008) Safety, immunogenicity, and efficacy of the ML29 reassortant vaccine for Lassa fever in small non-human primates. *Vaccine* 26:5246–5254
 12. Vieth S, Drosten C, Lenz O, Vincent M, Omilabu S, Hass M, Becker-Ziaja B, ter Meulen J, Nichol ST, Schmitz H, Gunther S (2007) RT-PCR assay for detection of Lassa virus and related old world arenaviruses targeting the L gene. *Trans R Soc Trop Med Hyg* 101:1253–1264
 13. Panning M, Emmerich P, Olschlager S, Bojenko S, Koivogui L, Marx A, Lugala PC, Gunther S, Bausch DG, Drosten C (2010) Laboratory diagnosis of Lassa fever, Liberia. *Emerg Infect Dis* 16:1041–1043
 14. Bloch A (1978) A serological survey of Lassa fever in Liberia. *Bull World Health Organ* 56:811–813
 15. Arnold RB, Gary GW (1977) A neutralization test survey for Lassa fever activity in Lassa, Nigeria. *Trans R Soc Trop Med Hyg* 71:152–154
 16. Goldwasser RA, Elliott LH, Johnson KM (1980) Preparation and use of erythrocyte-globulin conjugates to Lassa virus in reversed passive hemagglutination and inhibition. *J Clin Microbiol* 11:593–599
 17. Tomori O, Johnson KM, Kiley MP, Elliott LH (1987) Standardization of a plaque assay for Lassa virus. *J Med Virol* 22:77–89
 18. Wulff H, Lange JV (1975) Indirect immunofluorescence for the diagnosis of Lassa fever infection. *Bull World Health Organ* 52:429–436
 19. Van der Waals FW, Pomeroy KL, Goudsmit J, Asher DM, Gajdusek DC (1986) Hemorrhagic fever virus infections in an isolated rainforest area of Central Liberia. Limitations of the indirect immunofluorescence slide test for antibody screening in Africa. *Trop Geogr Med* 38:209–214
 20. Lukashevich IS, Clegg JC, Sidibe K (1993) Lassa virus activity in Guinea: distribution of human antiviral antibody defined using enzyme-linked immunosorbent assay with recombinant antigen. *J Med Virol* 40:210–217
 21. Niklasson BS, Jahrling PB, Peters CJ (1984) Detection of Lassa virus antigens and Lassa virus-specific immunoglobulins G and M by enzyme-linked immunosorbent assay. *J Clin Microbiol* 20:239–244

22. Jahrling PB, Niklasson BS, McCormick JB (1985) Early diagnosis of human Lassa fever by ELISA detection of antigen and antibody. *Lancet* 1:250–252
23. Ivanov AP, Tkachenko EA, van der Groen G, Butenko AM, Konstantinov OK (1986) Indirect immunoenzyme method for the laboratory diagnosis of Lassa and Ebola hemorrhagic fevers. *Vopr Virusol* 31:186–190
24. Barber GN, Clegg JC, Lloyd G (1990) Expression of the Lassa virus nucleocapsid protein in insect cells infected with a recombinant baculovirus: application to diagnostic assays for Lassa virus infection. *J Gen Virol* 71(Pt 1):19–28
25. Lukashevich IS, Patterson J, Carrion R, Moshkoff D, Ticer A, Zapata J, Brasky K, Geiger R, Hubbard GB, Bryant J, Salvato MS (2005) A live attenuated vaccine for Lassa fever made by reassortment of Lassa and Mopeia viruses. *J Virol* 79:13934–13942
26. Emmerich P, Thome-Bolduan C, Drosten C, Gunther S, Ban E, Sawinsky I, Schmitz H (2006) Reverse ELISA for IgG and IgM antibodies to detect Lassa virus infections in Africa. *J Clin Virol* 37:277–281
27. Ter Meulen J, Koulemou K, Wittekindt T, Windisch K, Strigl S, Conde S, Schmitz H (1998) Detection of Lassa virus antinucleoprotein immunoglobulin G (IgG) and IgM antibodies by a simple recombinant immunoblot assay for field use. *J Clin Microbiol* 36:3143–3148

Sampling Design and Mosquito Trapping for Surveillance of Arboviral Activity

Luís E. Paternina and Juan David Rodas

Abstract

Mosquitoes are the most important vectors for arboviral human diseases across the world. Diseases such as Dengue Fever (DF), West Nile Virus (WNV), Yellow Fever (YF), Japanese Encephalitis (JE), Venezuelan Equine Encephalitis (VEE), and St. Louis Encephalitis (SLE), among others, have a deep impact in public health. Usually mosquitoes acquire the arboviral infection when they feed on viremic animals (birds or mammals), so their infection can be detected along the year or in short periods of time (seasons). All of this depends on the frequency and seasonality of the encounters between viremic animals and vectors.

With the convergence of several phenomena like the increasing traveling of human populations, globalization of economy and more recently the global warming, the introduction of nonendemic arbovirus into new areas has become the current scenario. As examples of this new social and environmental frame we can mention the outbreak of West Nile Virus in North America in the late 1990s and more recently the outbreaks of chikungunya and Zika virus in the Americas. The present chapter deals with one of the first steps in the development of research studies and diagnosis programs, the surveillance of arboviruses in their vectors, the sampling design and mosquito trapping methods. The chapter also includes some important considerations and tips to be taken into account during the mosquito fieldwork.

Key words GIS, Mosquitoes, Sampling, Trapping methods, Arbovirus, Surveillance

1 Introduction

Global warming is already extending the geographical range of mosquitoes and ticks that harbor and transmit arboviruses, resulting in outbreaks of dengue fever and yellow fever in new locations [1]. Here we describe the use of geographic information systems (GIS) in sampling design for vector surveillance, and we describe collection and processing of insect vectors in fieldwork conditions.

1.1 Sampling Design for Vector Surveillance Using Geographic Information Systems (GIS)

The search of arboviruses through mosquito sampling is usually performed as a result of the notification of viral infection in humans or animals in endemic or enzootic areas. However, in areas where arboviruses have not yet been detected in mosquitoes, a random

and uniform sampling design helps to systematize the study of arbovirus and vector distribution.

This methodology should reduce systematic errors in vector sampling and maximize the chances of finding arboviral agents in nature using a spatially variable approach. A wide variety of software exists for GIS analyses to help with the spatial design of sampling. The best known of these is ArcGis (property of ESRI Company); however, free software from the Open Source Geospatial Foundation (OSGeo) such as GRASS GIS and QGIS are also available.

Here, we focus on the software QGIS, which is now widely used among private and official institutions around the world as an alternative to ArcGis software. The increasing popularity of QGIS lies in its free distribution under a General Public License (GPL) and the availability of hundreds of plugins for geo-processing, geo-spatial statistics, and handling and analysis of processed layers and remote sensor images.

The random or uniform sampling design is meant to make a relatively unbiased sampling of vector/reservoir populations in a defined zone. Both methodologies allow the creation of points over the area of interest where the trapping of vectors will be carried out. It is important to emphasize that these methodologies are popular in ecological analyses in order to establish comparisons between areas or search for specific events in wildlife populations, but it is uncommon in investigations of zoonotic diseases.

The planning of trap distribution for collections of zoonotic vectors is an important element in the surveillance of hemorrhagic fevers caused by arboviruses and reoviruses [2, 3]. Unfortunately, examples of successful random or uniform sampling designs for the surveillance of arboviral diseases are not very common in the literature, because they require a large economic and logistic effort. However, there are several examples that show how a good sampling design can provide answers to very important questions on the dynamics of hemorrhagic diseases. One very successful example of the sampling design for arboviral surveillance is the work of a Brazilian team that studies the dengue fever vector [4]. They found strong spatial-temporal correlations between the abundance of *Aedes aegypti* females with cluster of cases in Belo Horizonte (Minas Gerais, Brazil) using a uniform sampling design based on city blocks [4]. Another example is the surveillance of arboviruses in well characterized areas or Australia using modern techniques of sampling with monitoring of frequent vector population [5–7].

It is important to mention that GIS is not only useful for sampling design purposes or for the retrospective study of disease patterns, it is also used for real time surveillance of arboviral diseases and for modeling of disease and forecasting [2, 8–10]. For example, the Georgia Department of Public Health sponsors the Arboviral Query and Mapping Tool website. This platform provides information

about arboviral activity by years in this part of the USA. In Australia for example, the New South Wales Arbovirus Surveillance Program provides weekly reports about arbovirus activity (<http://medent.usyd.edu.au/arbovirus/>) with detailed environmental information and mosquitoes/arbovirus detection.

As the GIS technologies become more common because of the globalization of computational mobile systems (cell phones, tablets, and personal computers), these tools can be a great source of data for monitoring mosquitoes for hemorrhagic fever surveillance programs across the world.

1.2 Preferred Collection Methods

For purposes of arbovirus surveillance and detection in mosquitoes, scientists take advantage of the common knowledge about the positive phototaxis and CO₂-tropism shown by insects, their ecology and habitat preferences [11]. Consequently, mosquito collection is usually performed with light traps (such as the CDC Light Traps or Shannon Light traps) or the traditionally used “oral aspirators” for the search of insects in their resting places. However, using these two generic strategies only a small fraction of the fauna of insects that may be involved in transmission cycles of arboviral agents can be studied [12, 13].

Since many of the insect-borne viral agents that cause hemorrhagic diseases have genetic material based on RNA [13], insects must be kept alive until they arrive at the laboratory and are either processed immediately or preserved in the cold chain. In this way, we can guarantee the integrity of the genetic material for detection and further isolation and characterization of the arboviral agent [5, 14, 15]. In the mosquito-trapping scheme, the collection method is particularly important, since this determines the amount and richness of the mosquito community that is being sampled [16]; this is why there are many different strategies for trapping insects.

Several factors influence mosquito trapping in terms of quantity (number of mosquitoes/night) or quality (richness or diversity of the caught fauna), the choice of the collection method is particularly important because is one of the determining factors of the diversity of samples for the future arboviral testing. Here we present a synopsis of the main categories of trapping methods with some notes about their use in field-work (Table 1). In spite of the many methods available for mosquito trapping, the CDC Light Trap remains as the standard and is one of the most widely used methods because it allows the collection of a considerable amount of mosquitoes during the night by using the positive phototaxis exhibited by many groups of mosquitoes. Nevertheless this positive phototaxis can be variable among different groups of mosquitoes. Here, we describe the standard collection of mosquitoes in field work, presenting CDC Light traps guidelines for surveillance of arboviruses with successful results in the Old World and in the Americas [5, 17–21].

Table 1
Evolution of mosquito trapping methods commonly used for the surveillance of arboviruses

Methods	Environment	Main purpose	Performance and notes	References
Oral aspirators	Indoor/outdoor	Resting and blood-seeking mosquitoes	Low performance, time-consuming and uneven population sampling of unfed and fed mosquitoes.	[11, 25]
Animal-Baited Trap	Outdoor	Blood-seeking female	Low performance.	[11, 26]
Light Traps	Indoor/outdoor	Mainly blood-seeking and blood-fed mosquitoes	High performance, uneven population sampling.	[11, 17–19, 21, 28]
CO ₂ -baited Light Traps	Indoor/outdoor	Mainly blood-seeking and blood-fed females	Very high performance, uneven population sampling.	[11, 21, 27–30]
Resting Site Traps (RST)	Outdoor mainly	Mainly blood-fed and gravid females	High performance, more even population sampling because of the relative unbiased method.	[30–32]
Passive Box Traps (PBT)	Outdoor mainly	Mainly blood-fed and gravid females	High performance, more even population sampling because of the relative unbiased method.	[23, 27]
CO ₂ -baited PBT	Outdoor mainly	Mainly blood-fed and blood-seeking females	High performance, uneven population sampling because of the relative biased method.	[23, 33]
Honey-FTA® Card in PBT	Outdoor mainly	Blood-fed and blood-seeking females	High performance, more even population sampling because of the relative unbiased method.	[7, 23, 24]

A typical arbovirus life cycle vectored by mosquitoes begins when the mosquito feeds on viremic mammals or birds. Because of this, blood-fed and nonnulliparous females are usually the preferred target of the sampling methods [13]. These guidelines are applicable to many arboviral agents transmitted by mosquitoes. Nevertheless, not all mosquitoes are equally attracted by the CDC Light Trap, and sometimes the use of a bait (CO₂ and other attractants) and oral aspirator collection at resting places would be helpful in the trapping of mosquitoes of exotic species.

The systematic search for blood-fed and gravid females has facilitated the detection and discovery of multiple arboviral agents. New methods have been developed specifically for capture and surveillance of other zoonotic agents [6, 22]. As an example, in recent years we have seen the monitoring of Japanese Encephalitis Virus using Passive Box Trapping (PBT) in Australia. This trapping system allows the evaluation of infection by arboviral agents in the captured mosquito population, and an estimation of vector abundance [23].

Later modifications of this methodology allowed the inclusion of FTA[®] cards (nucleic acid-binding paper) soaked with honey in the Passive Box Trap (Honey-FTA PBT) in order to get a very high performance passive trap for mosquitoes with a preservation system for arboviral RNA. In this particular case the FTA[®] is used to bind the nucleic acid (RNA or DNA) when the arbovirus-infected mosquito regurgitates the virus while it is consuming the honey [7, 24]. Then, the FTA cards are used for detection and characterization of the viral RNA obtained from mosquitoes. This FTA-PBT coupled technology must be evaluated in some other scenarios for the validation of the methodology; however, this trapping method represents a major breakthrough in arboviral surveillance for the identification of active risk transmission in endemic conditions, and for the research of arboviral agents in new areas. Further reading about other mosquito-sampling methods (past and current methodologies) are available from the classical text in medical entomology, *Mosquito Ecology* [11].

2 Materials

2.1 Use of Geographic Information Systems (GIS) in Surveillance Design

1. Laptop or desktop computer: we do not need an expensive computer; just make sure that your equipment is good enough to work with videos or images.
2. QGIS software: a copy of the software can be freely downloaded from <http://qgis.org/es/site/forusers/download.html>.
3. Shapefile: a shapefile (.shp, is a vector file) of your study area that will be helpful in order to limit the number and the extent of the sampling design.

4. Point Sampling Tool plugin for QGIS: this tool will generate points in the shapefile space according to our needs, in random or uniform ways.

2.2 Trapping Mosquitoes in Fieldwork

1. CDC Light Traps: CDC Light Traps are commercially available in many entomological stores, as an example you can obtain traps at Bioquip (Cat. 2836BQ). Traps are commonly provided with one collection bag, you will need one bag per trapping night for each CDC Light Trap.
2. Forceps: straight, curved, and featherweight forceps are commercially available.
3. Chill table: commercially available, it is better to have a portable unit in order to facilitate the transportation of the equipment.
4. GPS: Precise equipment is required; the technical specifications of the equipment tell you the error in the estimation of the spatial position.
5. Plastic microtubes: 1.5 or 2 mm polypropylene microtubes are commercial available and are used to store individual insects.
6. RNALater (optional): Use this reagent only if you are not planning to use liquid nitrogen for preservation of mosquitoes. This is highly recommended when you are collecting mosquitoes in remote locations.

3 Methods

3.1 Use of GIS to Design Surveillance Strategy

1. Install the stand-alone version of the latest QGIS from their official website; this may take a few minutes after the download of the software (*see Note 1*).
2. Once you have installed the software, in the “Complement” menu of the main panel of QGIS, select “Manage and install complements”. In the new panel, please look for the “Point Sampling Tool” and select it for installation (*see Note 2*).
3. Import a shapefile of your study area into QGIS; we use the shapefile of US counties (scale 500k, 1:500.000) obtained from the Cartographic Boundary Shapefiles Database of the USA Census Bureau (https://www.census.gov/geo/maps-data/data/cbf/cbf_counties.html). Once you have imported your shapefile into QGIS, the software will ask you about the Coordinate Reference System (CRS); we use for this example the WGS84 (also known as EPSG: 4326). After this you will see your data (in our case the US counties map) on the main screen of QGIS.
4. To generate the points over the study area, go to “Vector” menu, then to “Research Tools” submenu and finally, to

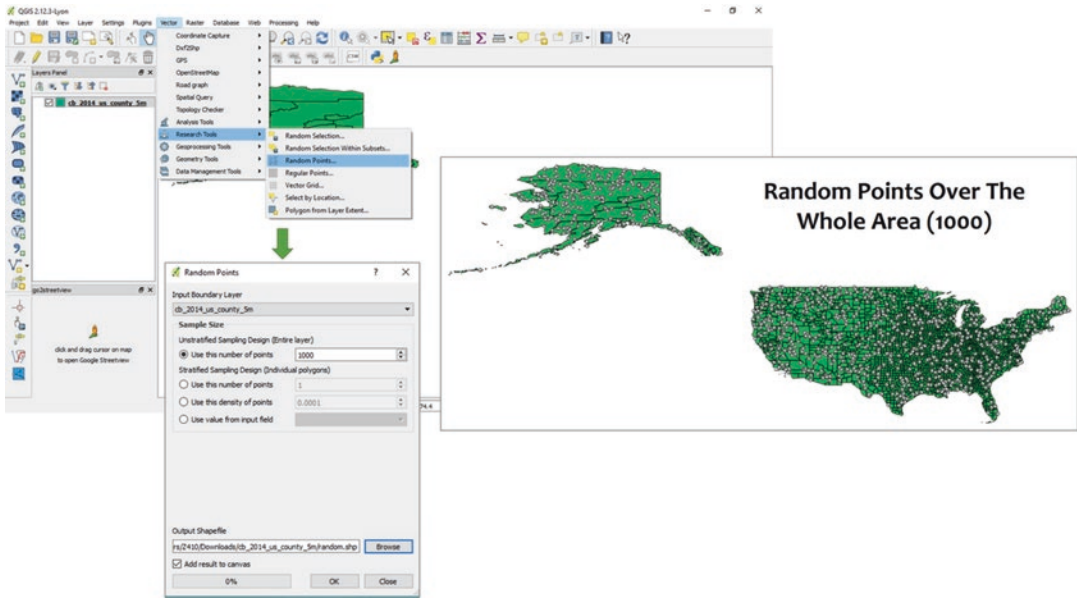


Fig. 1 Sampling points generated using an unstratified sampling design in QGIS 2

“Random Points”. Using this procedure you can generate sampling points in two different ways: (1) random points over the area or (2) evenly distributed points over the study area. The selection of a random or uniform sampling algorithm depends on the purpose of the vector sampling (Fig. 1).

5. For the random generation of points you will need to provide the number of points to be created, this number depends on the number of trapping stations that you can use, e.g., 100 mosquito traps, 300 Sherman traps (for rodents), and 150 tomahawks (for rodents). Then, once you have provided the number or points in the “Unstratified Sampling Design”, the software will make a new layer (vector layer) containing the points required.
6. One can also “Stratify” the number of points that cover a shapefile, meaning that one can create a certain number of points according to each hierarchy of the shapefile (country, state, cities) using the first option under the “Stratified Sampling Design” submenu. In this particular case, we want 1 point for each polygon inside our US shape file (Fig. 2).
7. To create a uniform sampling design, one must select the “Regular Points” option in the “Research Tools” submenu. These settings will produce a desired number of points evenly distributed in your shape file. One can set the number of points for convenience or get an unknown number of points by choosing the “spacing point” option.
8. You are now ready to distribute traps and plan your collections.

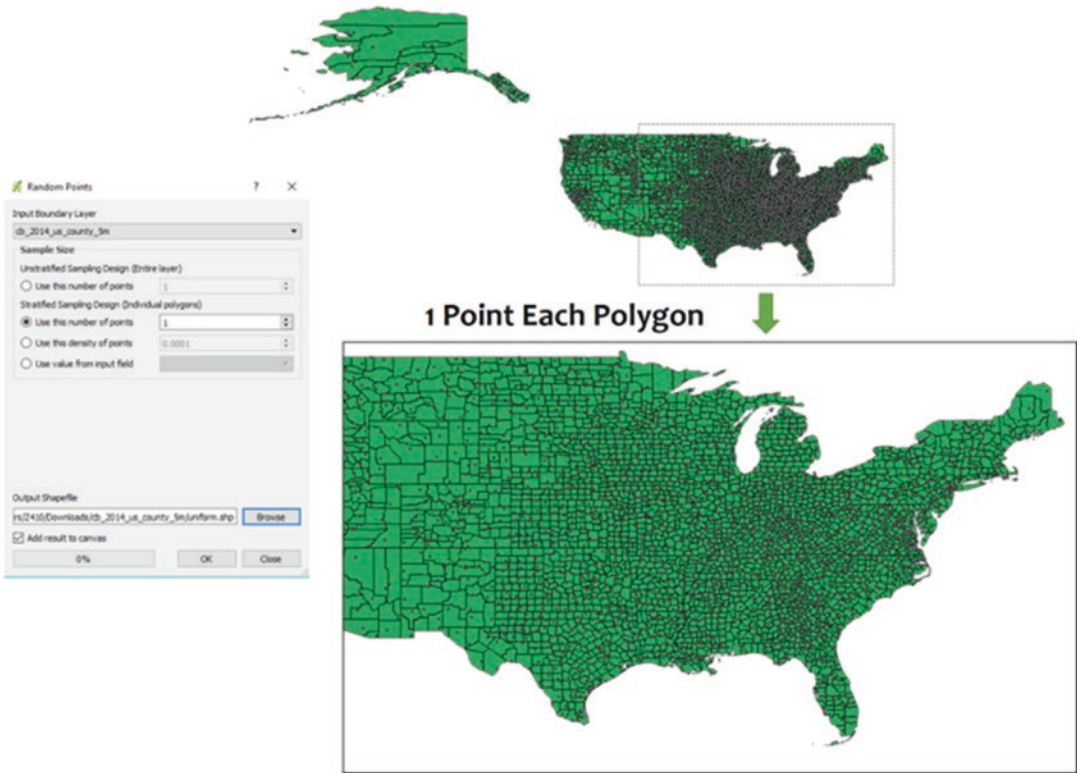


Fig. 2 Stratified sampling points design in QGIS 2.12

3.2 Field Trapping of Mosquitos

1. Select the points for the installation of light traps using the criteria of your convenience (canopy density, distance to forest patch, and distance to rivers, among many other criteria) and taking into consideration the ecology of the mosquito community that you want to sample. The trapping grid must be defined before the fieldwork, the trapping points can be randomly distributed over the study area or following a trapping grid defined by the scientist (lineal, radial, and small windows, among others) (*see Note 3*) (Fig. 3).
2. Make sure that the installed traps are at least 1.5 m above the ground level. Take into consideration that mosquito community may have a vertical stratification and at this ground level the canopy mosquitoes are not typically collected (*see Note 4*).
3. Usually the sampling of mosquitoes takes from 18:00 to 6:00, after this time detach the collection bag and close the open side. The bags must be handled carefully to avoid any possible damage to mosquitoes. Once you have collected the bag, you must replace it the collection bag with a new one (*see Note 5*).



Fig. 3 Examples of trapping sites using two light trap methodologies. (a) A CDC trap installed on a secondary tropical dry forest. (b) Shannon trap installed in a secondary tropical dry forest

4. Carefully place the mosquitoes of a single collection bag in one (or several) Petri dish. Each petri dish will be placed on the chilling plate and checked under the stereomicroscope in order to sort the mosquitoes according to species (or genera if you have trouble in the species identification process) using the proper taxonomic keys. A very useful and interactive mosquito identification key is provided by the Walter Reed Biosystematic Unit (http://www.wrbu.org/VecID_MQ.html) (*see Note 6*).
5. Each pool of sorted insects must be gently transferred to microtubes with RNALater (or empty cryovials if you are using a liquid nitrogen tank for mosquito preservation and transport). The pool size may vary between 2 and 50 insects, it depends entirely of the mosquito abundance and general size of the insects, some insects can be small as *Uranotaenia* (Culicinae, Uranotaeniini) or as large as *Mansonia* (Culicinae, Mansoniini) (*see Note 7*).
6. If you are not planning to do RNA extraction immediately, save your samples at -80°C until the performance of the nucleic acid extraction protocol. The samples must be preserved in cold chain in order to guarantee the quality and integrity of viral RNA for detection and characterization purposes.

4 Notes

1. This software is completely free (free software policy of the Open Source Initiative) and it is very intuitive. QGIS was created by the Open Source Geospatial Foundation (OSGeo), there are documentation and support (commercial and community-based support) for its use in Linux, Windows, and

- Mac. You can get further information about the software at <http://www.qgis.org>.
2. There are thousands of additional plugins for every task in QGIS; so, feel free to navigate among the plugins if you have other needs to cover.
 3. The prior definition of trapping scheme (random trap distribution or in a predefined grid) is important for a good spatial representation of the studied area. Mark the spatial position of every CDC light trap with your GPS, this will allow you to locate quickly your traps in the field and allow you to determine if there are ecological patterns of mosquito and arboviral distribution in a posterior analysis. The accuracy of the GPS device normally range from ~10 ft to 3 in. Select GPS equipment according to your needs and budget.
 4. Usually the batteries that power your trap must be protected from the rain and wild animals, use a blanket or a battery bag (or a plastic battery box) to protect it from any damage.
 5. Collection of mosquitoes must be done preferentially over at least 3 days, it is preferable longer sessions (more than 3 days) of trapping in order to get a better representation of the mosquito community. Make sure that you have enough batteries for the fieldwork, always test the battery power between trapping nights.
 6. The sorting and proper identification of mosquitoes is critical for the understanding of transmission cycles of arboviral agents. The identification of mosquitoes is usually a challenging task, and it is more challenging in field conditions, currently the identification of mosquitoes related with the transmission of arboviral agents can be done also through the analysis of mitochondrial Cytochrome B (CytB) or Cytochrome c Oxidase I (COI) DNA sequences.
 7. If you are not planning to do RNA extraction immediately, save your samples at -80°C until the performance of the nucleic acid extraction protocol. The samples must be preserved in cold chain in order to guarantee the quality and integrity of viral RNA for detection and characterization/isolation purposes.

References

1. Shuman EK (2010) Global climate change and infectious diseases. *N Engl J Med* 362: 1061–1063
2. Tami A, Grillet ME, Grobusch MP (2016) Applying Geographical Information Systems (GIS) to arboviral disease surveillance and control: a powerful tool. *Travel Med Infect Dis* 14:9–10. doi:10.1016/j.tmaid.2016.01.002
3. Clements ACA, Pfeiffer DU (2009) Emerging viral zoonoses: frameworks for spatial and spatiotemporal risk assessment and resource planning. *Vet J* 182:21–30. doi:10.1016/j.tvjl.2008.05.010
4. de Melo DPO, Scherrer LR, Eiras ÁE (2012) Dengue fever occurrence and vector detection by larval survey, ovitrap and mosquiTRAP: a space-time clusters analysis. *PLoS One*. doi:10.1371/journal.pone.0042125
5. Van den Hurk AF, Nisbet DJ, Foley PN et al (2002) Isolation of arboviruses from mosquitoes

- (Diptera: Culicidae) collected from the Gulf Plains region of northwest Queensland, Australia. *J Med Entomol* 39:786–792. doi:[10.1603/0022-2585\(2002\)039\[0786:IOA FMD\]2.0.CO;2](https://doi.org/10.1603/0022-2585(2002)039[0786:IOA FMD]2.0.CO;2)
6. Van Den Hurk AF, Hall-Mendelin S, Johansen CA et al (2012) Evolution of mosquito-based arbovirus surveillance systems in Australia. *J Biomed Biotechnol*. doi:[10.1155/2012/325659](https://doi.org/10.1155/2012/325659)
 7. Flies EJ, Toi C, Weinstein P et al (2015) Converting mosquito surveillance to arbovirus surveillance with honey-baited nucleic acid preservation cards. *Vector Borne Zoonotic Dis* 15:397–403. doi:[10.1089/vbz.2014.1759](https://doi.org/10.1089/vbz.2014.1759)
 8. Konrad SK, Zou L, Miller SN (2013) A geographical information system-based web model of arbovirus transmission risk in the continental United States of America. *Geospat Health* 7:157–159
 9. Lozano Fuentes S, Wedyan F, Hernandez Garcia E et al (2013) Cell phone-based system (Chaak) for surveillance of immatures of dengue virus mosquito vectors. *J Med Entomol* 50:879–889. doi:[10.1603/ME13008](https://doi.org/10.1603/ME13008)
 10. Faulde MK, Spiesberger M, Abbas B (2012) Sentinel site-enhanced near-real time surveillance documenting West Nile virus circulation in two *Culex* mosquito species indicating different transmission characteristics. *J Egypt Soc Parasitol* 42:461–474
 11. Silver JB (2008) Mosquito ecology - field sampling methods, 2nd edn. doi:[10.1007/978-1-4020-6666-5](https://doi.org/10.1007/978-1-4020-6666-5)
 12. Sánchez-Seco MP, Rosario D, Quiroz E et al (2001) A generic nested-RT-PCR followed by sequencing for detection and identification of members of the alphavirus genus. *J Virol Methods* 95:153–161. doi:[10.1016/S0166-0934\(01\)00306-8](https://doi.org/10.1016/S0166-0934(01)00306-8)
 13. Conway MJ, Colpitts TM, Fikrig E (2014) Role of the vector in arbovirus transmission. *Annu Rev Virol* 1:71–88. doi:[10.1146/annurev-virology-031413-085513](https://doi.org/10.1146/annurev-virology-031413-085513)
 14. Bryant JE, Crabtree MB, Nam VS et al (2005) Short report: isolation of arboviruses from mosquitoes collected in Northern Vietnam. *Am J Trop Med Hyg* 73:470–473. [pii]: 73/2/470
 15. Turell MJ, O'Guinn ML, Jones JW et al (2005) Isolation of viruses from mosquitoes (Diptera: Culicidae) collected in the Amazon Basin region of Peru. *J Med Entomol* 42:891–898. doi:[10.1603/0022-2585\(2005\)042\[0891:IOVFMD\]2.0.CO;2](https://doi.org/10.1603/0022-2585(2005)042[0891:IOVFMD]2.0.CO;2)
 16. Acuff VR (1976) Trap biases influencing mosquito collections. *Mosq News* 36:51–53
 17. Hoyos-López R, Uribe Soto SI, Rúa-Uribe G, Gallego-Gómez JC (2015) Molecular identification of Saint Louis encephalitis virus genotype IV in Colombia. *Mem Inst Oswaldo Cruz* 110:719–725. doi:[10.1590/0074-02760280040](https://doi.org/10.1590/0074-02760280040)
 18. Hoyos-López R, Uribe Soto SI, Gallego-Gómez JC (2015) Evolutionary relationships of West Nile virus detected in mosquitoes from a migratory bird zone of Colombian Caribbean. *Virol J* 12:80. doi:[10.1186/s12985-015-0310-8](https://doi.org/10.1186/s12985-015-0310-8)
 19. Vázquez A, Sánchez-Seco M-P, Palacios G et al (2012) Novel flaviviruses detected in different species of mosquitoes in Spain. *Vector Borne Zoonotic Dis* 12:223–229. doi:[10.1089/vbz.2011.0687](https://doi.org/10.1089/vbz.2011.0687)
 20. Sánchez-Seco MP, Rosario D, Domingo C et al (2005) Generic RT-nested-PCR for detection of flaviviruses using degenerated primers and internal control followed by sequencing for specific identification. *J Virol Methods* 126:101–109. doi:[10.1016/j.jviromet.2005.01.025](https://doi.org/10.1016/j.jviromet.2005.01.025)
 21. Calzolari M, Zé-Zé L, Růžek D et al (2012) Detection of mosquito-only flaviviruses in Europe. *J Gen Virol* 93:1215–1225. doi:[10.1099/vir.0.040485-0](https://doi.org/10.1099/vir.0.040485-0)
 22. Ritchie SA, van den Hurk AF, Zborowski P et al (2007) Operational trials of remote mosquito trap systems for Japanese encephalitis virus surveillance in the Torres Strait, Australia. *Vector Borne Zoonotic Dis* 7:497–506. doi:[10.1089/vbz.2006.0643](https://doi.org/10.1089/vbz.2006.0643)
 23. Ritchie SA, Cortis G, Paton C et al (2013) A simple non-powered passive trap for the collection of mosquitoes for arbovirus surveillance. *J Med Entomol* 50:185–194. doi:[10.1603/ME12112](https://doi.org/10.1603/ME12112)
 24. Hall-Mendelin S, Ritchie SA, Johansen CA et al (2010) Exploiting mosquito sugar feeding to detect mosquito-borne pathogens. *Proc Natl Acad Sci* 107:11255–11259. doi:[10.1073/pnas.1002040107](https://doi.org/10.1073/pnas.1002040107)
 25. Ramesh D, Muniaraj M, Samuel PP et al (2015) Seasonal abundance & role of predominant Japanese encephalitis vectors *Culex tritaeniorhynchus* & *Cx. gelidus* Theobald in Cuddalore district, Tamil Nadu. *Indian J Med Res* 142:23. doi:[10.4103/0971-5916.176607](https://doi.org/10.4103/0971-5916.176607)
 26. Mitchell CJ, Darsie RF Jr, Monath TP, Sabattini MS, Daffner J (1985) The use of an animal-baited net trap for collecting mosquitoes during western equine encephalitis investigations in Argentina. *J Am Mosq Control Assoc* 1: 43–47
 27. Johnson BJ, Kerlin T, Hall-Mendelin S et al (2015) Development and field evaluation of the sentinel mosquito arbovirus capture kit (SMACK). *Parasit Vectors* 8:509. doi:[10.1186/s13071-015-1114-9](https://doi.org/10.1186/s13071-015-1114-9)

28. Pezzin A, Sy V, Puggioli A et al (2016) Comparative study on the effectiveness of different mosquito traps in arbovirus surveillance with a focus on WNV detection. *Acta Trop* 153:93–100. doi:[10.1016/j.actatropica.2015.10.002](https://doi.org/10.1016/j.actatropica.2015.10.002)
29. Drago A, Marini F, Caputo B et al (2012) Looking for the gold standard: assessment of the effectiveness of four traps for monitoring mosquitoes in Italy. *J Vector Ecol* 37:117–123. doi:[10.1111/j.1948-7134.2012.00208.x](https://doi.org/10.1111/j.1948-7134.2012.00208.x)
30. L'Ambert G, Ferré JB, Schaffner F, Fontenille D (2012) Comparison of different trapping methods for surveillance of mosquito vectors of West Nile virus in Rhône Delta, France. *J Vector Ecol* 37:269–275. doi:[10.1111/j.1948-7134.2012.00227.x](https://doi.org/10.1111/j.1948-7134.2012.00227.x)
31. Panella NA, Crockett RJK, Biggerstaff BJ, Komar N (2016) Novel device for collecting resting mosquitoes. *J Am Mosq Control Assoc* 27:323–325. doi:[10.2987/09-5900.1](https://doi.org/10.2987/09-5900.1)
32. Williams GM, Gingrich JB (2007) Comparison of light traps, gravid traps, and resting boxes for West Nile virus surveillance. *J Vector Ecol* 32:285–291
33. van den Hurk AF, Hall-Mendelin S, Townsend M, Kurucz N, Edwards J, Ehlers G, Rodwell C, Moore FA, McMahon JL, Northill JA, Simmons RJ, Cortis G, Melville L, Whelan PI, Ritchie SA (2014) Applications of a sugar-based surveillance system to track arboviruses in wild mosquito populations. *Vector Borne Zoonotic Dis* 14:66–73

Epidemiological Surveillance of Rodent-Borne Viruses (Roboviruses)

Juan David Rodas, Andrés F. Londoño, and Sergio Solari

Abstract

This article will outline surveillance approaches for rodent-borne viruses (roboviruses). We present a synopsis of the main categories of trapping methods with some notes about their use in fieldwork. We also describe the types of laboratory analysis commonly used in Robovirus surveillance.

Key words Zoonotic viruses, Roboviruses

1 Introduction

Here, we describe our methods for trapping and processing rodent samples in our surveillance for rodent-borne viruses (roboviruses), some of which cause viral hemorrhagic fever (VHF). Our methods have also been discussed in previous publications [1, 2]. Although lymphocytic choriomeningitis virus (LCMV), the prototype arenavirus that infects *Mus musculus* was discovered in the 1930s [3], it was not until the 1960s that other important members of the same family that cause VHF were isolated in South America: Junín virus carried by *Calomys musculinus* was isolated in Argentina, and Machupo virus was isolated from *Calomys callosus* in Bolivia [4, 5]. Later on in the 1980s, Guanarito virus, the etiologic agent of Venezuelan hemorrhagic fever, was detected in *Sigmodon alstoni* [6], highlighting the importance of small mammals as viral reservoirs. Moreover, Hemorrhagic Fever with Renal Syndrome (HFRS), clinically described in the 1950s in South Korea, was also rodent-borne, although the Hantaan virus (*Hantaviridae* family) was not isolated until the 1970s from striped field mice, *Apodemus agrarius* [7]. Later, the Sin Nombre Virus (SNV), carried by the deer mouse *Peromyscus maniculatus*, caused the first outbreak of Hantavirus Pulmonary Syndrome (HPS) in North America (USA) in 1993 [8], and Choclo virus produced some fatal cases in 2000 in

Panama [9] increasing the interest in developing techniques for active surveillance and viral isolation from field rodents on the American continent.

2 Materials

Materials and tools required for trapping small vertebrate mammals could be divided into different tasks: field trapping, safety utensils and reagents, manipulation devices for obtaining biological samples and preserving museum specimens, and equipment for storage and transportation.

2.1 Field Trapping

1. The most common traps for hunting small mammals in virology field studies are folding Sherman live traps (8 × 9 × 23 cm, H.B. Sherman Trap Company, Tallahassee, FL, USA) and Tomahawk traps (14 × 14 × 40 cm, Tomahawk Trap Company, Tomahawk, WI, USA) (*see Note 1*).
2. Trap bait is most frequently a mixture of peanut butter and oat flakes (*see Note 2*).
3. Brilliant colored flag tape is useful for labeling the sites where traps are placed to ease the finding, checking, and recovery of all trap stations [10].
4. A large sack (or shoulder bag) is an appropriate mean for transporting the traps [11].

2.2 Biosafety Equipment for Capturing and Handling Small Wild Mammals

1. Heavy rubber or leather gloves.
2. Long-sleeved shirt, long pants, socks, and lace-up shoes with shoe covers.
3. Disposable surgeon's gown that ties in the back (or disposable overalls), a powder air-purifying respirator (PAPR), or half-faced respirator/goggles with HEPA filter.
4. Reagents required for sampling are 10% bleach, 70% ethanol, Lysol (or any other similar disinfectant), 10% formalin (for tissue preservation), methoxyfluorane or its inexpensive substitute isofluorane (gaseous anesthetics), ketamine:xylazine (10:1, parenteral anesthetics), sodium phenobarbital (0.1 ml of 350 mg/ml, for euthanasia), heparin, and filter paper (e.g., Nobuto strips used to adsorb and preserve blood at room temperature for later antibody testing) [11] (*see Notes 3 and 4*).

2.3 Sample Collection

1. Plastic collection bags, zip-lock bags, indelible markers, soap for washing hands and wash water, clipboard, paper, pencils, gauze, cotton balls, surgical gloves, paper towels, bucket to clean the traps and the utensils, squeeze bottle, alcohol burner, matches or lighter, dissecting scissors and forceps, twist-ties, 1 cc syringes

with 22-G needles, 3 cc syringes, capillary tubes, and sharps-disposal containers. Also for rodent identification: spring scales (100 and 1000 g) and a small ruler (30 cm) or tape-measure (100 cm or longer) for specimens measurements [11].

2.4 Storage and Transportation of Rodent Samples

1. Red-cap tubes (for collecting serum).
2. Freezing-resistant screw tubes or cryovials, racks, and freezer boxes for samples.
3. Polystyrene dry ice container (or a dry-ice cooler) or a small liquid nitrogen tank.
4. Cleaning brushes, buckets, autoclave tape, and biohazard bags [11].

2.5 Other Conveniences for a Field Trip

1. A tent, folding table, chairs (or stools).
2. Flashlights, magnifying lens, drinking water, maps.
3. Insect repellent and a first aid kit (*see Note 5*).

2.6 Hantavirus Isolation from Rodent Tissue

A protocol for hantavirus isolation from frozen rodent tissues has been described [12].

1. Frozen rodent tissues that have been cut into approximately 1 g pieces.
2. Histopaque-1083 density gradients for recovery of viable mononuclear cells from rats, mice, and other small mammals,
3. Low-speed centrifuge capable of generating $400 \times g$.
4. 15 ml plastic centrifuge tubes.
5. Vero E6 cells are used for hantavirus, arenavirus, flavivirus, and filovirus isolation because they have a defect in interferon production.
6. Culture flasks.
7. Phosphate-buffered saline (PBS): 137 mM NaCl, 2.7 mM KCl, 10 mM Na_2HPO_4 , 2 mM KH_2PO_4 , pH 7.4.
8. Maintenance medium for Vero cells: MEM with 2% fetal bovine serum, 1% penicillin, 1% streptomycin, 1% sodium pyruvate, and 7.5% bicarbonate.
9. Incubator with 37 °C and 5% CO_2 .
10. Glass spheres are used to lyse the cells at the end of each passage in order to store supernatants with lysed cells.
11. Polyethylene glycol (PEG) 6000, 8000, or 40,000 Da powder for precipitating virus from solution.
12. Amicon Ultra-4 filter units (Millipore) for concentrating virus-containing fluid.
13. Biosafety cabinet for tissue culture.

3 Methods

3.1 Trapping

Animals

1. Select the points for the installation of traps with the aid of free or private mapping systems (Google Earth, Bing Maps, QGIS or ArcGis) (*see Note 6*).
2. Before the trapping expedition check integrity and functionality of equipment (respirators, filters, batteries, traps, etc.), label all traps, prepare enough bait for at least 2 days, and labels for cryovials.
3. Once in the field, traps should be evenly distributed, preferably through a transect arrangement [13], placing all baited traps before dark in delineated areas out of sight of roads, sidewalks, paths, livestock, or human activity. Traps should be placed in the field for collection of wild rodents and, for synanthropic rodents, they should be placed close to houses, buildings, and shelters. Well-placed traps will enhance your chances of success [10]. Place traps near evidence of rodent activity, borrows, brush piles, fallen logs, or abandoned items that could provide shelter, and set each line in a different habitat type (house, fenceline, pasture etc.). Avoid locating traps in direct sunlight, particularly during summer, and, during winter, add cotton balls as nesting material. Some good outdoor places to install traps include: near bushes in the peri-domestic area, near barns, shelters and stables, within the crops and inside the storage places for cereal and grains (*see Note 7*) and Figs. 1 and 2.
4. Mark the beginning and the end of each trap line with a flagging tape (in bushy and weedy areas it may be necessary to mark the location of each trap), and place 10–20 traps on a line with 5–10 m intervals [13]. Be careful to make traps as level as possible, and check the trigger mechanism for adjustment and sensitivity; for a greater success, traps should be set to go off at the slightest touch [14].
5. Make a local topographic map of the trap lines (number and type placed in each line) and make an habitat assessment for each trap line, recording the location with GPS coordinates (when possible).
6. Check traps early the next morning wearing protective gear (long pants, long-sleeved shirt, heavy shoes, and heavy rubber gloves). If the trap was visited but empty, consider it dirty and place it in a double plastic bag for decontamination and validation of functionality, and replace it with a clean trap.
7. If a trap is closed, lift it and check it carefully, with your arms extended and being aware of wind direction (away from you). If a nontarget animal has been captured (toad or a bird), release the animal, reset the trap, or collect it for decontamination. When the trap contains a target rodent, mark it with date,



Fig. 1 Trap Placement. (a) Outdoor sites to place Tomahawk and Sherman traps. Traps must be placed close to bushes and around the houses. (b) Indoor sites to place Tomahawk and Sherman traps. When indoors, traps should be placed in the proximity of crevices and holes in the wall and wherever there is evidence of rodent presence (bitten materials and remains of food or feces)

time, line number and habitat, place it in a bag, and tie it twice and leave it on the ground to be collected after you finish checking the line. Traps can only be reopened after wearing protective clothing (PAPR or half-faced respirator/goggles with HEPA filter).

8. When trap success appears to be 10% or better, traps may be left in the same location for a second night.
9. Place traps on plastic bags in the vehicle and transport them to the processing site, then wash rubber gloves with soap and water, remove gloves, and wash hands [11].

3.2 Processing Trapped Animals

1. The site for animal processing should be secluded (away from human or livestock activity), but preferably outdoors. If indoors, the floor should be easily disinfected and have windows for ventilation.
2. Everyone should wear surgeon's gowns or disposable overalls, shoe covers, double latex gloves, safety goggles, and respirator with HEPA filter. Tasks such as anesthetizing, weighing, measuring, doing necropsy, data recording, and decontamination should be performed by at least two technicians.

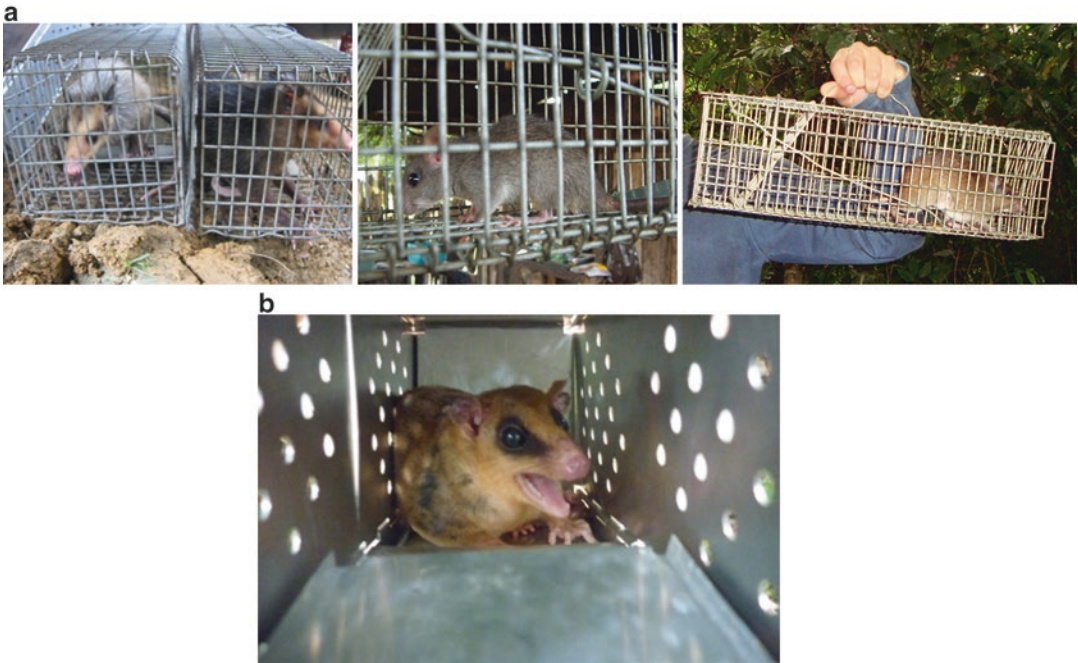


Fig. 2 Examples of trapped animals. (a) Specimens of field and synanthropic rodents collected with Tomahawk traps. Opossums (*Didelphis*), rats (*Rattus*) and spiny rats (*Proechimys*) fit well in this type of device. (b) Specimens of field mammals collected with Sherman traps (*Marmosa isthmica*). These traps are good for catching small mammals such as rodents, small marsupials, some wild rodents (*Peromyscus*, *Zygodontomys*, and others), and the domestic mouse (*Mus musculus*)

3. Set up the processing table with all the required materials before starting. After that, place a cotton soaked in anesthetic (methoxyfluorane or isofluorane) within a plastic anesthesia bag, fix the bag to the front of the trap, and release the mammal from the first trap. When hard to perform, include the entire trap in a bigger anesthesia bag, or inject the rodent intradermally with ketamine: xylazine (10:1), 0.02–0.05 cc/20–40 g mouse or 0.1–0.3 cc/200–400 g rat.
4. When the animal becomes motionless, remove it from the bag, place it on a clean surface, and begin assessment and processing.
5. The first step will be to weigh, measure, and assess the animal before bleeding it (Fig. 3). Take standard measurements (total length, tail length, right hind foot, ear); record presence of ectoparasites and reproductive data.
6. Bleeding can be performed from the retroorbital plexus with a heparinized capillary or by intracardiac puncture.
7. Before performing necropsy, make sure the animal has died from exsanguination, anesthetic overdose, carbon dioxide asphyxiation, or cervical dislocation. Subsequently, an abdomi-



Fig. 3 Morphometric measurements for rodent classification: body length, tail length, foot length, ear length

nal incision is made to obtain lung, heart, liver, kidney, and spleen samples, which are immediately stored in liquid nitrogen. Samples are transported from the field to the laboratory in liquid nitrogen and are subsequently stored in $-80\text{ }^{\circ}\text{C}$ (or $-130\text{ }^{\circ}\text{C}$) ultra-freezer.

8. Finally, skin is prepared and carcasses and skulls are stored in 70% alcohol for species identification at a mammal-collection laboratory [11, 15].
9. Virus isolation from tissue has been well described elsewhere and is beyond the scope of the current chapter [16–18]. In general, frozen tissues are weighed, cut into 1 g pieces, and then processed for virus isolation or for RNA extraction. In this way, you can record the amount of virus or viral RNA per gram of tissue.
10. Isolate virus from tissue by dis-associating cells and co-cultivating them with Vero cells for a plaque assay or for using immune-fluorescent antiviral antibodies to quantify the number of infected cells per gram of tissue.

11. Isolate RNA from tissues using reagents that disrupt cells and RNA-protein complexes like phenol-quantidine isothiocyanate mixtures.
12. Subject the RNA to qPCR to amplify specific viral sequences using defined primers, or subject it to broader analyses like deep sequencing to reveal the spectrum of microbial genomes represented in your samples.

4 Notes

1. Although small Sherman live traps are standard, longer models may be more effective [19].
2. Other items (raisin, bacon, fruit essences, seeds) can be used depending on the ecology of the focal species [14].
3. Some researchers use 90% ethanol for field storage of tissues and specimens, and then change specimens to 70% ethanol for definitive storage.
4. People conducting fieldwork could be exposed not only to rodent-borne viruses (arena or hantavirus), through their excreta (urine, feces, and saliva), but also to many other zoonotic infections from the same secretions (such as leptospira) or through their ectoparasites (ticks, fleas, lice, or mites that carry agents such as *Rickettsia*, *Borrelia*, and *Yersinia* among others). Be careful at all times, wear protective clothing, and strive for BSL-3/4 practices.
5. Scientists interested in this kind of work should get all the necessary trapping/collecting permits and approved protocols for wild mammal collection and handling.
6. Accessibility of the trap site will also determine the number of traps available [10].
7. Presence and abundance of field mice, rats, and other small mammals near human settlements can be detected by recent evidence of their activity such as chewed food, fecal deposits, bitten cables, gnawed wood, and holes in the walls among others.

References

1. Londoño AF, Díaz FJ, Agudelo-Flórez P, Levis S, Rodas JD (2011) Genetic evidence of hantavirus infections in wild rodents from northwestern Colombia. *Vector Borne Zoonotic Dis* 11:701–708. doi:[10.1089/vbz.2010.0129](https://doi.org/10.1089/vbz.2010.0129)
2. Quintero JC, Londoño AF, Díaz FJ, Agudelo-Flórez P, Arboledo M, Rodas JD (2013) Ecoepidemiología de la infección por rickettsias en roedores, ectoparásitos y humanos en el noroeste de Antioquia, Colombia. *Biomedica* 33(S1):2–9. doi:[10.7705/biomedica.v33i0.735](https://doi.org/10.7705/biomedica.v33i0.735)
3. Armstrong C, Lillie RD (1934) Experimental lymphocytic choriomeningitis of monkeys and mice produced by a virus encountered in studies of the 1933 St Louis encephalitis epidemic. *Public Health Rep* 49:1019. doi:[10.2307/4581290](https://doi.org/10.2307/4581290)

4. Maiztegui JI (1975) Clinical and epidemiological patterns of Argentine haemorrhagic fever. *Bull World Health Organ* 52:567–575
5. Johnson KM, Kuns ML, Mackenzie RB, Webb PA, Yunker CE (1966) Isolation of Machupo virus from wild rodent *Calomys callosus*. *Am J Trop Med Hyg* 15:103–106
6. Tesh RB, Jahrling PB, Salas R, Shope RE (1994) Description of Guanarito virus (*Arenaviridae: Arenavirus*), the etiologic agent of Venezuelan hemorrhagic fever. *Am J Trop Med Hyg* 50:452–459
7. Lee HW, Lee PW, Johnson KM (1978) Isolation of the etiologic agent of Korean hemorrhagic fever. *J Infect Dis* 137:298–308. doi:10.1016/j.jviromet.2009.04.006
8. Schwarz TF, Zaki SR, Morzunov S, Peters CJ, Nichol ST (1995) Detection and sequence confirmation of Sin Nombre virus RNA in paraffin-embedded human tissues using one-step RT-PCR. *J Virol Methods* 51:349–356
9. Vincent MJ, Quiroz E, Gracia F, Sanchez AJ, Ksiazek TG, Kitsutani PT, Ruedas LA, Tinnin DS, Caceres L, Garcia A, Rollin PE, Mills JN, Peters CJ, Nichol ST (2000) Hantavirus pulmonary syndrome in Panama: identification of novel hantaviruses and their likely reservoirs. *Virology* 277:14–19. doi:10.1006/viro.2000.0563
10. Barnett A, Dutton J (1995) Expedition field techniques small mammals (excluding bats), 2nd edn. Royal Geographical Society, London
11. Mills JN, Childs JE, Ksiazek T, Peters CJ (1995) Methods for trapping and sampling small mammals. In: CDC, US DHHS PHS. Forces, Armed Management, Pest, pp 1–54
12. Milazzo ML, Duno G, Utrera A, Richter MH, Duno F, De Manzione N, Fulhorst CF, de Manzione N (2010) Natural host relationships of hantaviruses native to western Venezuela. *Vector Borne Zoonotic Dis* 10:605–611. doi:10.1089/vbz.2009.0118
13. Pearson DE, Ruggiero LF (2003) Transect versus grid trapping arrangements for sampling small-mammal communities. *Wildl Soc Bull* 31:454–459. doi:10.2307/3784324
14. Voss RS, Emmons LH (1996) Mammalian diversity in neotropical lowland rainforests: a preliminary assessment. *Bull AMNH* 120:1–115
15. Mills JN, Yates TL, Childs JE, Parmenter RR, Ksiazek TG, Rollin PE, Peters CJ (1995) Guidelines for working with rodents potentially infected with hantavirus. *J Mammal* 76:716–722. doi:10.2307/1382742
16. Elliott LH, Ksiazek TG, Rollin PE, Spiropoulou CF, Morzunov S, Monroe M, Goldsmith CS, Humphrey CD, Zaki SR, Krebs JW (1994) Isolation of the causative agent of hantavirus pulmonary syndrome. *Am J Trop Med Hyg* 51:102–108
17. Fulhorst CF, Monroe MC, Salas RA, Duno G, Utrera A, Ksiazek TG, Nichol ST, de Manzione NM, Tovar D, Tesh RB (1997) Isolation, characterization and geographic distribution of Caño Delgadito virus, a newly discovered South American hantavirus (family *Bunyaviridae*). *Virus Res* 51:159–171
18. Powers AM, Mercer DR, Watts DM, Guzman H, Fulhorst CF, Popov VL, Tesh RB (1999) Isolation and genetic characterization of a hantavirus (*Bunyaviridae: Hantavirus*) from a rodent, *Oligoryzomys microtis* (Muridae), collected in northeastern Peru. *Am J Trop Med Hyg* 61:92–98
19. Slade NA, Eifler M, Gruenhagen ND (1993) Differential effectiveness of standard and long Sherman live-traps in capturing small mammals. *J Mammal* 74:156–161. doi:10.2307/1381915

Part II

Structural Studies and Reverse Genetics of Hemorrhagic Fever Viruses

Entry Studies of New World Arenaviruses

**María Guadalupe Martínez, María Belén Forlenza, Nélide A. Candurra,
and Sandra M. Cordo**

Abstract

Identification of cell moieties involved in viral binding and internalization is essential since their expression would render a cell susceptible. Further steps that allow the uncoating of the viral particle at the right subcellular localization have been intensively studied. These “entry” steps could determine cell permissiveness and often define tissue and host tropism. Therefore applying the right and, when possible, straightforward experimental approaches would shorten avenues to the complete knowledge of this first and key step of any viral life cycle. Mammarenaviruses are enveloped viruses that enter the host cell via receptor-mediated endocytosis. In this chapter we present a set of customized experimental approaches and tools that were used to describe the entry of Junín virus (JUNV), and other New World mammarenavirus members, into mammalian cells.

Key words Virus, Receptor recognition, Endocytosis pathways

1 Introduction

Viral entry into the host cell is a key step in the infection cycle. The entry process involves an initial interaction between a virus and attachment factor(s) and/or receptors, leading to virus internalization, release of the genome, and subsequent infection. Thus, addressing the mechanisms used for viruses during early steps of infection is fundamental to determining virus tropism and developing novel antiviral therapies.

The study and characterization of viral entry requires a combination of techniques that allow the specific measurement of viral binding to its receptor together with the involvement of different, and perhaps novel, internalization pathways. Measuring direct virus binding to cells requires the optimization of methods to label and purify viral particles (i.e., radioisotope or fluorescent conjugation). Indirect detection by fluorophore-conjugated antibodies is also possible with minor downstream steps. However, multiple approaches are necessary to cover uncertainties of a single virus-bound readout.

When the specific receptor used by the virus is known, a wider variety of tools become available, such as transient expression of the specific receptor in receptor-negative cell lines.

To determine the internalization pathway(s) and cellular structures involved in virus entry, different and complementary approaches are available. Drugs or small molecules specifically targeting gene product functions are commonly used and rely on the previously proven specificity of each compound. Additionally, genetic tools such as dominant-negative protein expression have been widely used during the last decades.

Direct visualization of the viral entry process can be achieved by electron microscopy (EM). Some endocytic structures are easily identified by EM due to their distinct morphology (i.e., clathrin-coated pits). For other not-so-morphologically-distinct structures, immuno-EM is necessary, labeling both the virus particle and the cell structure of interest with specific antibodies. However, labeling with gold-conjugated antibodies depends on the existence of a strong and specific antibody-antigen interaction.

JUNV is the causative agent of Argentinian hemorrhagic fever. For decades it has been locally studied, and in recent years it gained worldwide attention due to its relevance as a bioterrorism agent. Thus, according to the National Institute for Allergy and Infectious Diseases (NIAID, USA) and its Biodefense program, arenaviruses like Junín virus is a Category A Priority Pathogen.

Here we described our experience in establishing and optimizing methods to determine key features of JUNV entry into host cells. We have used JUNV or JUNV glycoprotein complex (GPC)-pseudotyped particles to study their ability to be recognized by the human C-type lectins hDC- or hL-SIGN. These findings provided evidence that hDC- and hL-SIGN can mediate the entry of JUNV into cells, in the absence of its specific cellular receptor hTfR1, suggesting an important role in virus infection. Using radioactive virus-binding assays, we showed that JUNV infects polarized lines preferentially through the apical surface [1]. Also performing the above-described studies, we have successfully defined cytoskeleton components essential for virus entry [2]. Our studies demonstrated that early JUNV infection of Vero cells relies on both an intact actin network and a dynamic microtubule network.

Our findings have shown that clathrin-mediated endocytosis is the main JUNV internalization pathway into Vero cells [3] (Fig. 1). Virus entry was dependent on dynamin 2 GTPase and EPS15. In addition, we have shown that after virus internalization, JUNV traffics through Rab5 (early) and Rab7 (late) endosomes in its pH-dependent entry [4]. Taken together, our experimental designs and protocols allowed us to explore a broad spectrum of JUNV entry features. From new putative attachment factors/receptor

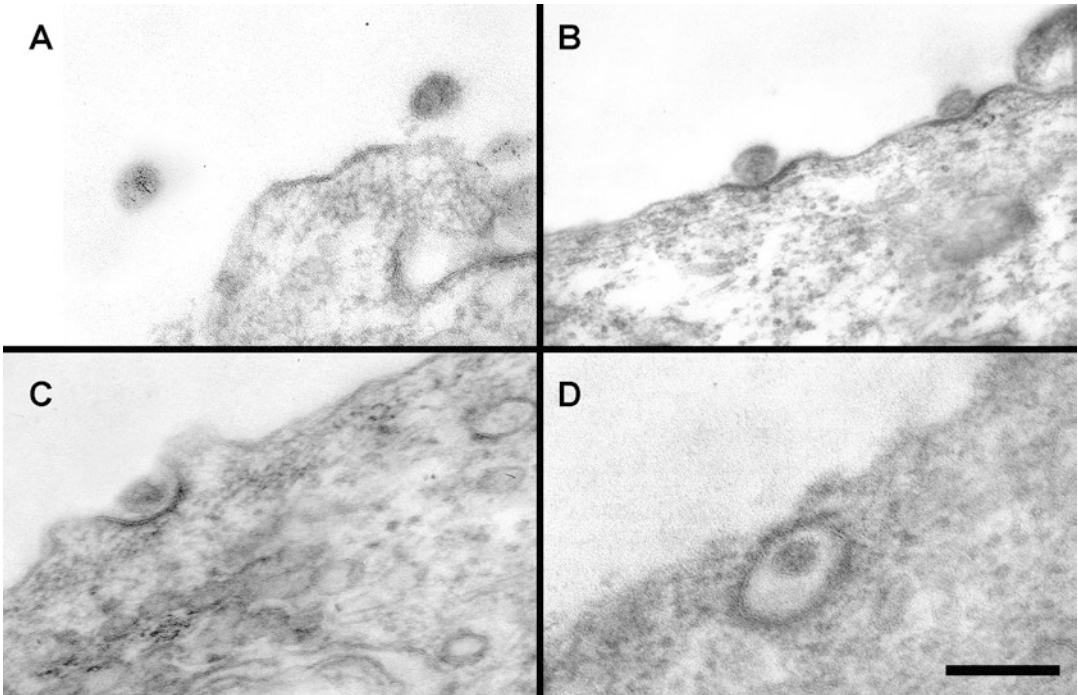


Fig. 1 Ultrastructural analysis of JUNV entry into Vero cells via clathrin-coated vesicles. Vero cells were incubated with concentrated JUNV for 60 min at 4 °C. Infection was initiated by shifting the temperature to 37 °C. After 15 min at 37 °C, cells were washed in PBS and fixed in 1.5% glutaraldehyde. Thin sections were made for ultrastructural analysis by transmission EM. **(a)** Population of JUNV outside Vero cells. **(b)** Binding of JUNV particles at the plasma membrane of Vero cells. **(c)** Uptake of JUNV by clathrin-coated pits. **(d)** JUNV is internalized within a clathrin-coated vesicle. Bar: 200 nm

molecules to cellular pathways used during internalization, all these features are essential to complete the gap in our knowledge about JUNV infection of specific cells.

2 Materials

2.1 Strains of Viruses, VLP, Cells, and Media Used in Entry Assays

1. Naturally attenuated Junín virus strain: IV was propagated in Vero cells at BSL-2 containment [5]. JUNV stock titers between 2×10^6 and 1×10^7 PFU/mL were aliquoted and stored at -80 °C.
2. Pseudotyped virion suspensions expressing the JUNV envelope glycoprotein were produced in 293T cells as described in Subheading 3.6. [6]. Pseudotyped stock titers in Vero cells were between 1×10^7 and 5×10^7 RLU/mL.
3. Vero cells (ATCC CCL81) were cultured at 37 °C in Dulbecco's Modified Eagle's Medium (DMEM) containing 5% fetal bovine serum (FBS), 100 U penicillin/mL, and 100 µg streptomycin/mL.

4. 293T (ATCC CRL-11268), BHK-21 (ATCC CCL10), and 3T3 cells (ATCC CCL1658), and 3T3-derived hDC-SIGN and hL-SIGN cells (NIAID AIDS Research and Reference Reagent Program) were grown in DMEM containing 10% FBS.
5. CHO-TRVb cell cultures (devoid of detectable cell-surface TfR) provided by Dr. Colin Parrish (James A. Baker Institute for Animal Health, Cornell University) were grown in Ham's F12 containing 10% FBS. All cell cultures were grown under 5% CO₂ in humidified incubator.

2.2 Viral Attachment and Adsorption Studies

2.2.1 Quantifying Virus Binding Using Radiolabeled Virions

1. Purified, [³⁵S]methionine-labeled JUNV stock: 5 × 10⁷ PFU/mL, 1 × 10⁸ dpm/mL produced as described in [7].
2. 24-well plates.
3. Phosphate-buffered saline (PBS).
4. Blocking solution: PBS containing 1% FBS, 0.1% glucose, and 0.5% BSA.
5. Lysis buffer: 0.1 M NaOH containing 1% SDS.
6. Scintillation fluid: dissolve 10g of PPO (2,5-diphenyloxazole) and 150 mg of POPOP 1,4-bis[-2(5-phenyloxazole)-benzene] in 237 mL of Triton X-100. Complete with toluene to 1 L. Filter the scintillation fluid to remove any particles and store in a brown bottle to prevent deterioration by light.
7. Liquid scintillation counter.

2.2.2 Quantifying Virus Binding Using Non-radiolabeled Virions

1. Purified non-radiolabeled stock or JUNV pseudotyped particle suspensions.
2. 24-well plates.
3. PBS.

2.2.3 Imaging Virus Binding by Confocal Microscopy

1. Purified non-radiolabeled JUNV stock.
2. 24-well plates.
3. Blocking solution: 4% BSA in PBS.
4. Anti-JUNV antibody GB03-BE08 (for antibody details, *see* Table 1).
5. Rabbit anti-hDC-SIGN antibody.
6. Anti-hTfR1 antibody.
7. Reagents for IF listed in Subheading 2.5.
8. Confocal microscope (Olympus FV 1000 or similar).

Table 1
Antibodies and their specificities

Antibody/Compound	Characteristics	Working concentration (dilution)	Time of incubation	Refs./Provider
IC06-BE10	Monoclonal anti- JUNV against the NP protein	4 µg/mL (1/250)	60 min at 37 °C/ ON at 4 °C	[8]
GB03-BE08	Monoclonal anti- JUNV against the GPC protein	4 µg/mL (1/250)	60 min at 37 °C/ ON at 4 °C	
anti- JUNV rabbit	Rabbit anti- JUNV polyclonal serum	1/50	60 min at 37 °C/ ON at 4 °C	[9]
P5D4	Monoclonal anti- VSV antibody	10 µg/mL (1/100)	60 min at 37 °C/ ON at 4 °C	Sigma Aldrich
I3-6800	Monoclonal anti- hTRF1 antibody	5 µg/mL (1/100)	60 min at 37 °C/ ON at 4 °C	Zymed
T-5158	Monoclonal anti α-tubulin antibody clon B512	25 µg/mL (1/200)	60 min at 37 °C/ ON at 4 °C	Sigma Aldrich
DC-SIGN (D7F5C) XP	Rabbit anti hDC-SIGN monoclonal antibody	1/200	60 min at 37 °C/ ON at 4 °C	Cell Signaling
9E9A8	Monoclonal anti hDC-SIGN antibody	5 µg/mL (1/300)	60 min at 37 °C/ ON at 4 °C	NIAID AIDS
97526	Polyclonal anti- hDC-SIGN antibody	1/300	60 min at 37 °C/ ON at 4 °C	Abcam
58603	Polyclonal anti hL-SIGN antibody	2 µg/mL (1/300)	60 min at 37 °C/ ON at 4 °C	Abcam

(continued)

Table 1
(continued)

Antibody/Compound	Characteristics	Working concentration (dilution)	Time of incubation	Refs./Provider
14EG7	Monoclonal anti-hDC/L-SIGN antibody	2 µg/mL (1/300)	60 min at 37 °C/ ON at 4 °C	NIAID AIDS
anti- mouse AF 488	Goat anti- mouse	0.2 µg/mL (1/1000)	60 min at 37 °C	Molecular probes
anti- rabbit AF 555	Goat anti- rabbit	0.2 µg/mL (1/1000)	60 min at 37 °C	Molecular Probes
Anti-mouse AF 568	Goat anti- mouse	0.2 µg/mL (1/1000)	60 min at 37 °C	Molecular probes
Phalloidin- FITC	actin staining	10 µg/mL	60 min at 37 °C	Sigma-Aldrich
Transferrin-TRITC	Transferrin TRITC-acoplated	20 µg/mL	60 min at 37 °C	Sigma-Aldrich
Choleric toxin-TRITC	β-subunit choleric toxin TRITC-acoplated	0.5 µg/mL	60 min at 37 °C	Sigma-Aldrich
DAPI	nuclear staining	1 µg/mL	5 min at room temperature	Sigma Aldrich
Hoechst 33342	nuclear staining	1 µg/mL	5 min at room temperature	Sigma-Aldrich

2.3 Viral Internalization Studies

2.3.1 Quantifying Virus Internalization Using Radiolabeled Virions

1. Proteinase K solution: 1 mg/mL proteinase K in PBS.
2. PMSF solution: 1 mM PMSF in PBS containing 3% BSA.
3. Reagents listed in Subheading [2.2.1](#).

2.3.2 Quantifying Virus Internalization Using Non-radiolabeled Virions

1. TRIzol (Invitrogen).
2. Isopropanol (analytic grade).
3. Chloroform (analytic grade).
4. 75% ethanol solution.
5. Bi-distilled nuclease-free water.
6. Real mix (Biodynamics, Argentina).
7. dNTPs 10 mM (Biodynamics, Argentina).
8. Moloney murine leukemia virus reverse transcriptase (M-MLV RT; Promega).
9. 1 µg or 50 pmol random primers (Biodynamics, Argentina).
10. Primer ZF: 5'-ATGGGCAACTGCAACGGGGCATC-3'.
11. Primer ZR: 5'-GTTGCCATCAATGACCCCTTCA-3'.
12. Primer GAPDH-F151 (Invitrogen): 5'-GTTGCCATCAATGACCCCTTCA-3'.
13. Primer GAPDH-R339 (Invitrogen): 5'-CAGCCTTCTCCATGGTGGTG-3'.
14. Thermocycler equipment (e.g., iCycler iQ Bio-Rad and its software iQ5 2.1.97.1001).
15. cDNA premix (per reaction): 3 µg RNA, 1 µg or 50 pmol random primers, enough nuclease-free water to complete 10 µL per reaction.
16. cDNA Mix (per reaction): 1 µL 10 mM dNTPs, 1 µL M-MLV RT, 4 µL nuclease-free water.
17. Reagents listed in Subheading [2.3.1](#).

2.3.3 Reagents and Materials Used for Electron Microscopy

1. 24-well plates.
2. Ice-cold 1.5% glutaraldehyde in 0.2 M phosphate buffer pH 7.2.
3. 0.2 M phosphate buffer.
4. 0.32 M sucrose solution.
5. 1.5% osmium tetroxide.
6. Graded ethanol solution.
7. Uranyl acetate.
8. Epon 812 resin (TAAB).
9. Diamond knife.

10. Reynold's solution.
11. C10 Zeiss electron microscope.
12. Kodak 4489 film.

2.4 Viral Entry Inhibition Studies

2.4.1 Cell Viability Assay

1. 5 mg/mL MTT [3-(4,5-dimethylthiazol-2-yl)-2,5-diphenyl tetrazolium bromide] stock solution dissolved in DMSO or PBS (Sigma-Aldrich). Store at -20°C in the dark.
2. 96-well plates.
3. Graded ethanol solution.
4. Spectrophotometer: reading at 570 nm and background at 630–690 nm.

2.4.2 Receptor-Specific Modulators

1. Mannan (Sigma-Aldrich) stock solution 50 mM in sterile water.
2. 24-well plates.
3. Anti-JUNV SA02-BG12 antibody (for antibody details, *see* Table 1).
4. Anti-hDC-SIGN 9E9A8 antibody.
5. Anti-hDC-/L-SIGN 14EG7 antibody.
6. Anti-hDC-SIGN 97526.
7. Anti-VSV P5D4 antibody.
8. Anti-mouse AF 488 antibody.
9. cDNA3.1-hDC-SIGN and pcDNA3.1-hL-SIGN constructs (NIAID AIDS).
10. pcDNA3.1 plasmids expressing different transferrin receptors: pcDNA3.1-hTfR1 (*Homo sapiens*), pcDNA3.1-fTfR1 (*Felis catus*), pcDNA3.1-cTfR1 (*Canis lupus familiaris*), and pcDNA3.1-mTfR1 (*Mus musculus*). All are provided by Dr. Colin Parrish, James A. Baker Institute for Animal Health, Cornell University.

2.4.3 Endocytic Pathway-Affecting Compounds

1. Pharmacological compounds (*see* Table 2).
2. 24-well plates.
3. Maintenance medium (MM): complete DMEM containing 1.5% FBS.
4. Serum-free DMEM.
5. Anti-JUNV IC06-BE10 antibody.
6. Anti-mouse AF 568 antibody.
7. Transferrin-TRITC.
8. β -Subunit cholera toxin-TRITC (*see* Note 1).
9. Reagents for IF are listed in Subheading 2.5. Antibodies and fluorescent marker details are in Table 1.
10. Olympus BX51 microscope.

Table 2
Entry and cytoskeleton inhibitors and their specificities

	Inhibitor compound ^a	Working concentration ranges	Time of incubation	Refs.
<i>Entry step affected</i>				
Acid pH-dependant entry	Ammonium chloride	5–10 mM	30 min + virus adsorption	[10]
	Concanamycin A (ConcA)	5–10 nM	60 min + virus adsorption	^b
Dinamin-dependant endocytosis	Dynasore (Dyn)	90–150 μM		
Clathrin-mediated endocytosis	Clorpromazine (CPZ) (<i>see Note 21</i>)	20–50 μM	120 min + virus adsorption	[3, 4]
Cholesterol-dependant entry	Nistatin (NT)	70–120 μM	120 min	[3, 4]
	Methyl-β-cyclodextrin (MβCD)	5–10 μM	30 min	^b
<i>Cytoskeleton component affected</i>				
Actin (polymerization)	Citochalasin D (CitD)	1–2 μM	30 min + virus adsorption	[2]
	Latrunculin A (LatA)	1–5 μM		
Actin (depolymerization)	Jasplakinolide (Jas)	0.5 μM		
Microtubules (polymerization)	Nocodazole (Noc)	20–40 μM		
Microtubules (depolymerization)	Paclitaxel (Pac)	40–100 μM		

^aAll compounds used in Table 2 were acquired from Sigma-Aldrich

^bUnpublished data

2.4.4 Cytoskeleton-Affecting Compounds

1. Inhibitory compounds (*see* Table 2).
2. 24-well plates.
3. Anti-tubulin T-5158 antibody.
4. Anti-JUNV IC06-BE10 antibody.
5. Anti-mouse AF 568 antibody.
6. Phalloidin-FITC.

2.4.5 Dominant-Negative Constructions Inhibiting Virus Entry

1. Plasmids encoding wt or dominant-negative constructions of EPS15 (GFP-EΔ95-295) [11], dynamin 2 (GFP-K44A) [12], and Rab5 (GFP-S34 N) [13] fused to GFP.
2. Lipofectamine 2000 (Invitrogen).
3. OptiMEM media (Invitrogen).
4. Anti-JUNV IC06-BE10 antibody.

5. Anti-mouse AF 568 antibody.
6. Transferrin-TRITC.
7. Reagents for IF listed in Subheading 2.5 and antibodies and fluorescent markers details in Table 1.
8. Olympus BX51 microscope.

2.5 Immunofluorescence (IF) and Light Microscopy

1. PBS.
2. 0.2% Triton X-100 solution in PBS.
3. 16% paraformaldehyde (PFA) solution (Electron Microscopy Sciences). Prepare a 4% working solution by dilution 1:4 in PBS.
4. Blocking solution: Prepare a 2% (g/v) stock solution of porcine skin gelatin in PBS (10× solution). Autoclave and keep sterile. Prepare a working blocking solution (1×) by making a 1/10 dilution of the 10× stock.
5. 2 mg/mL poly-L-lysine (PLL, Sigma-Aldrich) stock solution in water is used to coat coverslips. Filter to sterilize. Put 1 mL aliquots into sterile microcentrifuge tubes and store at -20°C . To make a working stock, thaw and dilute 1:100 to 20 $\mu\text{g}/\text{mL}$ in sterile water (*see Note 2*).
6. 12 mm round glass coverslips (thickness #1.5).
7. Mounting solution: Prolong diamond antifade medium (Molecular Probes).
8. DAPI or Hoechst (*see Note 3*).
9. Anti-JUNV IC06-BE10.
10. Anti-JUNV polyclonal serum.
11. Anti-tubulin T-5158 antibody.
12. Rabbit anti-hDC-SIGN antibody.
13. Phalloidin-FITC, transferrin-TRITC, cholera toxin-TRITC.
14. Anti-mouse AF 488, anti-mouse AF 568, and anti-rabbit AF 555.
15. Fluorescence microscope equipped with lamp and filters for excitation and detection of triple-stained samples (BFP/GFP/RFP). High-sensitivity camera and objectives with magnification of 20× or 10× and 60× or 100× (*see Note 4*).

2.6 Plaque-Forming Unit (PFU) Assay

1. Vero cell cultures.
2. 24-well plates.
3. 1.4% methylcellulose solution (Sigma-Aldrich) (*see Notes 5 and 6*).
4. MM of 2× concentration.
5. Plaque semisolid medium: composed of half parts of 1.4% methylcellulose and 2× MM.
6. 10% paraformaldehyde.

7. Crystal violet solution: dissolve 1 g crystal violet in 10 mL of 96% ethanol, and then complete up to 100 mL with distilled water.
8. Bench transilluminator.

2.7 Pseudotyped Virion Production

1. 293T cell cultures.
2. 24-well plate.
3. MLV-based transfer vector encoding luciferase.
4. MLV Gag-Pol packaging construct.
5. pEGFP-C1 (Clontech) or pcDNA3.1(-) plasmid (Invitrogen).
6. Codon-optimized version of GPC of Junín virus strain IV GenBank: DQ272266.3 (GeneArt) subcloned into the pcDNA3.1 expression plasmid (Invitrogen).
7. pcDNA3.1 expression plasmid encoding VSV-G as a control.
8. TurboFect Transfection Reagent (Thermo Fisher).
9. 0.45- μm pore-sized membrane filter (Sarstedt).
10. Luciferase Assay Kit (Promega).
11. GloMax 20/20 Luminometer (Promega).

3 Methods

3.1 Viral Attachment Studies

In the following experimental approaches, use the JUNV-susceptible cell line of your choice and change the culture media accordingly.

3.1.1 Quantifying Radiolabeled JUNV Particle Binding

1. Plate around 1×10^5 cells (i.e., Vero) per well in 24-well plates to a 90-100% confluency.
2. Pretreat cells with blocking solution (*see* Subheading 2.2.1) at 37 °C for 1 h to avoid nonspecific binding.
3. Infect cells at MOI of 1 with 100 μL of radiolabeled virus (200,000 dpm) per well routinely; each condition is done in duplicate; take this into account when preparing radiolabeled stock (*see* Note 7).
4. Incubate for 60 min at 4 °C.
5. Wash cells extensively with cold PBS and lyse in 500 μL lysis buffer per well and dissolve in scintillator solution (*see* Subheading 2.3.1).
6. Quantify cell-associated [^{35}S]-radioactivity using a liquid scintillation counter.
7. Determine total amount of cell-associated dpm in control infected cells vs. treated-infected cells. Values may also be expressed as percentages.

3.1.2 Quantifying Non-radiolabeled JUNV Particle Binding

1. Proceed as in Subheading 3.1.1 from 1 to 4 but using non-radiolabeled virus stock.
2. Wash cells extensively with cold PBS and lyse in 500 μ L of PBS per well by freezing and thawing twice.
3. Quantify the amount of infectious bound virus by standard PFU assay (*see* Subheading 3.4).

3.1.3 Determining Virus Binding by Confocal Microscopy

1. Plate around 1×10^5 cells (i.e., 3T3-DC-SIGN, Vero) per well in 24-well plates to a 90–100% confluency.
2. If target cells express both TfRI and DC-SIGN, preincubate cells with anti-hTfRI antibody for 1 h at 4 °C (blocking one of the two molecules would allow detecting and binding to one another).
3. Infect the cultures with 100 μ L of JUNV (MOI of 5) diluted in MM and in the presence of blocking agent (*see* Note 8), during 1 h at 4 °C and continuously shaking.
4. Wash gently the cultures three times with cold PBS and incubate with primary antibodies dilutions (*see* Table 1 and Note 9) for 1 h at 4 °C, continuously shaking.
5. Wash gently three times with cold PBS and then incubate for 20 min with PFA 4% at room temperature (RT) (*see* Note 10).
6. Wash three times with PBS at RT.
7. Process the cultures for IF assay to detect JUNV-GPI and DC-SIGN (*see* Subheading 3.5). Use confocal microscopy to detect adsorbed particles and DC-SIGN in membrane (*see* Notes 11 and 12).

3.2 Viral Internalization Studies

3.2.1 Quantifying Radiolabeled JUNV Particle Internalization

For the internalization assay, follow instructions as in Subheading 3.1. After virus adsorption at 4 °C for 1 h, incubate cells at 37 °C for 1 h to allow virus penetration.

1. Wash cultures with PBS and treat with proteinase K solution to remove external adsorbed virus.
2. Stop protease treatment by adding PMSF solution for 3 min at RT.
3. Follow **steps 5 and 6** to quantify internalized radiolabeled virus.

3.2.2 Quantifying Non-radiolabeled JUNV Particle Internalization

Proceed as in Subheading 3.2.1 and alternatively wash and lyse infected cultures in TRIzol buffer (according to the manufacturer's instructions) and continue as follows:

1. Extract total RNA by adding 0.2 mL of chloroform per mL of TRIzol. Mix vigorously by hand for 15 s and centrifuge at $12,000 \times g$ in a bench centrifuge, 15 min at 4 °C.

2. Take upper phase containing total RNA and transfer to a sterile tube to precipitate RNA by adding 0.5 mL of isopropanol per mL of TRIzol. Incubate samples at RT for 10 min and centrifuge at $12,000 \times g$, 15 min at 4 °C.
3. Remove and discard gently all supernatant and wash pellet once with 1 mL of 75% ethanol per mL of TRIzol. Mix by vortexing and centrifuge at not more than $7,500 \times g$ for 5 min at 4 °C.
4. Air-dry the RNA for 10–20 min and resuspend in 50 μ L of RNase-free water (*see Note 13*). Incubate for 10 min at 55–60 °C and store at –80 °C until use.
5. Generate the cDNA using the following procedure: Prepare the cDNA premix and cDNA reaction mix from Subheading 2.3.2. Mix together the cDNA premix with the cDNA reaction mix, vortex, and centrifuge for a spin and incubate for 2 h at 42 °C. Store at –80 °C until use.
6. Quantification of the amount of cell-bound viral RNA was performed by qRT-PCR employing TaqMan technology as follows:
 - (a) Amplify the cDNA PCR using specific viral gene primers (*see Subheading 2.3.2*).
 - (b) Amplify housekeeping mRNA using gene-specific primers (*see Subheading 2.3.2*).
 - (c) Normalize average viral RNA Ct values to the average Ct values of GAPDH, and set $\Delta\Delta$ Ct-based fold-change calculations relative to untreated virus infected, determining the Ct values using software indicated (*see Note 14*).

3.2.3 Electron Microscopy Readout

1. Plate around 5×10^5 cells (i.e., 3T3-DC-SIGN, Vero) per well in a 6-well plate to a 90–100% confluency.
2. Infect the cultures with 100 μ L of JUNV (MOI of 50) for 1 h at 4 °C.
3. Expose the cultures to 37 °C for 15 min.
4. Wash the cells three times with cold PBS.
5. Fix the cultures with 1.5% glutaraldehyde in 0.2 M phosphate buffer pH 7.2 during 4 h at RT.
6. Wash the cultures overnight in a 0.32 M sucrose in 0.1 M phosphate buffer solution at 4 °C.
7. Resuspend the cells and centrifuge at $500 \times g$ for 10 min. Add 1.5% osmium tetroxide overnight at 4 °C for the post-fixation.
8. Dehydrate the cultures in ethanol solutions followed with propylene oxide.

9. Embed the cells in Epon resin and let it polymerize for 2 days at 70 °C.
10. Take ultrathin sections with a diamond knife.
11. Stain with 2% uranyl acetate and then with Reynold's solution.
12. Take micrographs with Zeiss electron microscope using Kodak 4489 film.

3.3 Using Inhibitors to Determine Cellular Components Involved in Virus Entry

3.3.1 Measuring Cell Viability

The inhibitory effect of any experimental condition or compound on virus internalization can be measured by different experimental approaches. Initially it is important to establish the nontoxic range of a chosen compound for a particular cell line.

1. Plate around 2×10^4 cells (i.e., Vero, 3T3) in a 96-well plate to a 90–100% confluency (*see Note 15*).
2. Prepare a gradient of compound concentrations to a total of 600 μL each (in the corresponding cell culture medium).
3. Remove growth medium and add 100 μL per well of the compound concentration to be tested. Add 100 μL per well of culture medium to control wells (*see Note 16*).
4. Incubate the plate for the time chosen to be tested.
5. Add 10 μL of MTT stock solution to each well and incubate 2 h at 37 °C.
6. Remove the supernatants and add 200 μL of ethanol to each well to solubilize the formazan crystals by vigorous shaking.
7. Measure absorbance in a microplate reader at 595 nm.
8. Calculate CC_{50} as the compound concentration necessary to reduce cell viability by 50%.

3.3.2 Modulating Virus Receptor-Specific Recognition

Inhibition of Virus Infection by C-Type Lectin-Binding Compounds

1. Plate around 1×10^5 cells (i.e., 3T3 or 3T3-derived hDC-SIGN and hL-SIGN cells) per well in 24-well plates to a 90–100% confluency (containing a coverslip for determination of viral infection by IF, *see Subheading 3.5*).
2. Prepare dilutions of the blocking agent of interest in DMEM 5% FBS in sterile plastic tubes. Use concentrations ranging from 50 to 100 $\mu\text{g}/\text{mL}$ for mannan or 20 $\mu\text{g}/\text{mL}$ of anti-DC-/L-SIGN blocking antibodies.
3. Gently remove the media from the cells in the 24-well plate and replace 300 μL of the media with the blocking agent or DMSO as a control.
4. Incubate 60 min at 37 °C.
5. Prepare virus dilutions in media for viral infection (MM warmed up at 37 °C) to a final MOI of 1 and add the appropriate concentration of the blocking agent. Gently remove the

media from the cells and replace it with the media containing the compound and the virus (100 μ L).

6. Incubate for 60 min at 37 °C.
7. Gently remove the infectious media from the cells; do two very gentle washes with warm PBS.
8. Add 500 μ L of warm DMEM 5% FBS media/well. Incubate for 24 h at 37 °C.
9. At 24-h post-infection, collect the supernatants in sterile plastic tubes.
10. Clarify supernatants by centrifugation at 10,000 $\times g$, 10 min at 4 °C. Transfer the supernatant to a new sterile tube (*see* **Note 17**).
11. Virus yields will be determined by plaque assays in Vero cells (*see* Subheading 3.4).
12. For virus infection determination by IF, after the two washes, add 500 μ L of warm DMEM 5% FBS media/well.
13. At 24-h post-infection, wash cells on the coverslips two times with warm PBS and fix and permeabilize cells for IF.
14. Follow protocol for indirect IF in Subheading 3.5 for the detection of infected cells.
15. Calculate mean of positive cells in three independent experiments as indicated in Subheading 3.5.

Pseudotype Transduction of Cells Expressing Different Tfr1

1. Transfect 3T3 cells using Lipofectamine following manufacturers' recommendation. Use 500 ng of plasmid coding for transferrin receptor (*see* Subheading 2.4.2) and pEGFP-C1 as a control.
2. In parallel, transfect 3T3 cells control or stably 3T3DC- or L-SIGN with 500 ng of plasmid coding for transferrin receptors.
3. At 24 h after transfection, plate transfected cells in 24-well plates.
4. Transduce with 1×10^6 RLU of pseudotyped virion suspension (*see* Subheading 3.6) the next day at 37 °C for a minimum of 4 h.
5. Remove the inoculum and measure luciferase activity at 48 h post-transduction using a Luciferase Assay Kit (according to manufacturer's recommendation) and a GloMax 20/20 Luminometer.

3.3.3 Endocytic Pathway-Affecting Compounds

1. Plate around 1×10^5 cells (i.e., Vero, 3T3, TRVb) in a 24-well plate to 90–100% confluency per well (containing a coverslip for determination of viral infection by IF, *see* Subheading 3.5).
2. Treat with the corresponding concentration and time according to the drug (*see* Table 2) at 37 °C.

3. Remove the medium and infect with 100 μL of JUNV (MOI of 0.1) for 1 h at 37 °C in the presence of the same concentration of drug diluted in MM (*see* **Notes 18** and **19**).
4. After removing the inoculum, change the MM for fresh MM at 24 h at 37 °C.
5. Collect the supernatant to determine virus yields by PFU assay as in Subheading **3.4**.
6. Wash the cells three times with PBS for 5 min, fix them with PFA 4% for 10 min at room temperature, and then permeabilize with Triton X-100 0.2% for the same period of time. Process the cells for IF assay to detect NP (*see* Subheading **3.5** and Table **1**) and quantify the effect of compounds on virus entry (*see* **Notes 20** and **21**).

3.3.4 Inhibition of Virus Infection by Cytoskeleton-Disrupting Compounds

1. Plate 1×10^5 Vero cells in a 24-well plate (containing PLL-coated coverslips for determination of viral infection by IF; *see* Subheading **3.5**).
2. Prepare compound solutions in sterile plastic tubes in increasing concentrations, diluted in DMEM 5% FBS (*see* Table **2**).
3. Gently remove the media from the cells in the 24-well plate and replace 300 μL of media with the compounds or DMSO as a control.
4. Incubate 30 min at 37 °C.
5. Prepare virus dilutions in media for viral infection (MM warmed up at 37 °C) to a final MOI of 1 and add the appropriate concentration of the compound. Gently remove the media from the cells and replace with the media containing the compound and the virus (100 μL).
6. Incubate for 60 min at 37 °C.
7. Gently remove the infectious media from the cells; do two very gentle washes with warm PBS.
8. Add 500 μL of warm DMEM 5% FBS media/well. Incubate for 24 h at 37 °C.
9. At 24-h post-infection, collect the supernatants in sterile plastic tubes. Clarify supernatants by centrifugation at $500 \times g$, 10 min at 4 °C. Transfer the supernatant to a new sterile tube (*see* **Note 17**).
10. Virus yields will be determined by plaque assays in Vero cells (*see* Subheading **3.4**).
11. Wash the cells three times with PBS for 5 min, fix them with 4% PFA for 10 min at room temperature, and permeabilize with Triton X-100 0.2% for the same period of time. Process the cells for IF assay to detect NP (*see* Subheading **3.5** and Table **1**) and quantify the effect of compounds on virus entry (*see* **Notes 22** and **23**).

3.3.5 Dominant-Negative Mutations to Inhibit Virus Entry into Endosomes

1. Plate around 5×10^4 cells (i.e., Vero, 3T3) in a 24-well plate to 50–70% confluency.
2. Add 300 μL of OptiMEM solution and keep the cultures at 37 °C (*see Note 24*).
3. Mix 1 μg of plasmid DNA with 40 μL of OptiMEM for 10 min at room temperature (*see Notes 25 and 26*).
4. Mix 1 μL of Lipofectamine with 50 μL of OptiMEM per tube and incubate for 10 min at room temperature.
5. Add 50 μL of Lipofectamine mix prepared in **step 4** to each tube containing the plasmid mix in **step 3**, and incubate for 20 min at room temperature.
6. Add 100 μL of the mix containing the DNA-Lipofectamine complexes to the cells and incubate to 37 °C during 6 h. Then, replace with maintenance medium and incubate for 18 h.
7. Infect the cultures with 100 μL of JUNV (MOI of 1) for 1 h at 37 °C.
8. Remove the inoculum and add fresh MM for 24 h more.
9. Wash the cultures three times with PBS.
10. Fix the cultures with 4% PFA in PBS at room temperature for 10 min and then permeabilize them using 0.2% Triton X-100 in PBS for 10 min.
11. Process the cultures for IF assays to detect NP (*see Subheading 3.5*).

3.4 Plaque-Forming Unit (PFU) Assay

1. Collect the supernatant (1 mL) of each sample that needs PFU determination.
2. Incubate Vero cells until 80% confluency with 100 μL of serial dilutions (1/10–1/10,000) of the supernatants in MM at 37 °C for 1 h. Make duplicates for each dilution (*see Note 27*).
3. Remove the inoculum, wash, and add semisolid medium (*see Subheading 2.6*). Incubate for 7 days at 37 °C.
4. Fix the monolayers by adding 10% PFA for 30 min, wash exhaustively with tap water, and stain for 30 min with crystal violet solution. Wash again as before and let the plate air-dry.
5. Count the number of plaques in each well by using a bench transilluminator.
6. Calculate the PFU/mL using the following formula:
$$\text{PFU/mL} = X/V \times \text{Dil}$$

References: X , plaque number per well; V , volume of inoculum; Dil , dilution used.

3.5 Immunofluorescence Microscopy Readout

1. To prepare PLL-coated coverslips: in the tissue culture hood, put sterile round coverslips into 24-well plates. Add 0.5 mL PLL working stock/well and swirl to cover. Leave at room temperature for 20 min. Aspirate and let dry in hood with lid off.
2. Grow the cells on the PLL-coated coverslips, treat or infect them, and after the indicated time, wash three times with PBS during 5 min.
3. Fix the cultures using 4% PFA for 20 min at room temperature.
4. Add 0.2% Triton X-100 in PBS when permeabilization is required (*see* **Notes 28** and **29**).
5. Incubate the coverslips with the blocking solution (*see* Subheading **2.6**) for 1 h at 37 °C (*see* **Note 30**).
6. Wash the cultures three times (5 min each wash) with PBS.
7. Incubate the cultures with the primary antibody (*see* **Table 1**), repeat the washing steps, and incubate with the second antibody 1 h at 37 °C (*see* **Table 1**).
8. Wash the cultures as in **step 7** and incubate with DAPI in PBS during 5 min.
9. Wash the cultures three times with PBS and then once using ultrapure water (5 min each wash).
10. Mount the glass coverslips with the mounting solution.
11. Calculate the mean of positive cells in three independent experiments. Quantify the number of JUNV positive cells over total cells in 20 randomly chosen optical fields for each experiment. Express values as a percentage of the corresponding control.

3.6 Production of Pseudotyped Virions

1. Plate 5×10^5 293T cells/well in 0.5 mL of DMEM 10% FBS in a 6-well plate and culture overnight at 37 °C.
2. Co-transfect 293T cells, at a ratio of 1:1:1, with an MLV-based transfer vector encoding luciferase [14], an MLV Gag-Pol packaging construct, and an envelope glycoprotein-expressing vector (pcDNA3.1-JUNVGPC) or VSV-G as a control by using TurboFect, as recommended by the manufacturer.
3. Incubate cells at 37 °C for 48 h. Collect the supernatants, filter them through 0.45 μm pore-sized membranes, and store at -80 °C. Determine titers by luciferase assay in Vero cells.

4 Notes

1. TRITC and FITC conjugates can be replaced by AF 568 or AF 488.
2. Keep it on ice while you work with PLL working solution.

3. Both DAPI and Hoescht are amenable for nuclear staining.
4. Epifluorescence or confocal microscopes are both amenable for the readout in Subheading 3.5.
5. All the solutions should be prepared in cell culture quality water.
6. Prepare 1.4% methylcellulose solution in cell culture quality water. Agitate vigorously and autoclave.
7. To test the effect of a compound on virus adsorption infect in the presence or absence of the compound.
8. During infection and antibody incubations, always keep the anti-transferrin receptor antibody in the media to study DC-SIGN-associated binding.
9. Prepare primary and secondary antibody dilutions in the blocking solution (*see* Subheading 2.2.3).
10. For IF assays, the 4% PFA must be prepared fresh.
11. For staining two components, incubate at the same time with both antibodies prepared in 4% BSA in PBS.
12. As a control for nonspecific secondary staining, perform the same protocol without adding the primary antibody. Instead, incubate cells with the blocking solution for the same period of time.
13. Alternatively use 0.5% SDS solution by pipetting the solution up and down.
14. Δ Ct: calculate the difference between viral media values and cellular media values. $\Delta\Delta$ Ct: difference between the Δ Ct in the infected condition and the Δ Ct of the uninfected condition.
15. Each condition needs six replicates or more, so a standard test including ten different compound concentrations and proper controls will require a complete microplate.
16. Strong pipetting should be avoided to prevent cell detachment.
17. The samples can be stored at -80 °C for later determination of virus yield.
18. For NT and M β CD which present virucidal activity, wash the cells three times with PBS and infect without the compound.
19. Stock solution of compounds used in Subheading 3.3.3 should be prepared in DMSO solvent with the exception of M β CD which can be dissolved in water. Working solutions should be prepared in MM with the exception of M β CD and NT which may be prepared in a serum-free media.
20. As a control for compound activity, use the endocytic markers instead of the virus suspension. Incubate with transferrin-TRITC (clathrin-dependent internalization) or cholera toxin-TRITC (cholesterol-dependent internalization) for 20 or 30 min each after treatments with the compounds.

Internalization of endocytic markers should be inhibited by the specific treatments and conditions.

21. Pitstops 1 and 2 are novel compounds designed to inhibit clathrin-mediated endocytosis. Pitstop 2 is used more frequently owing to its cell permeability whereas Pitstop 1 retains value as an *in vitro* chemical probe, and it can be used for *in-cell* experiments if it is introduced by microinjection [15].
22. To verify the effect of the compounds in the cell cytoskeleton, incubate the cells with phalloidin-FITC for actin filament detection or with anti-tubulin antibody for microtubule detection.
23. 90 min after the treatments with the compounds, evaluate the recovery of the actin and microtubule distribution, by IF assay.
24. Transfection protocol in Subheading 3.3.5 was done following manufacturer's recommendations.
25. For control assays, use a plasmid with the same backbone expressing GFP.
26. To control the effect of dominant-negative constructions, incubate the transfected cells with transferrin-TRITC for 20 min. The transferrin internalization should be inhibited in cells expressing the dominant-negative proteins.
27. Do not allow the cells to dry out and agitate inoculum by swirling the plate every 15 min.
28. For membrane IF studies, do not use **step 4** in Subheading 3.5.
29. By **step 4** it is possible to save the plate containing the fixed cultures at -20°C during 1 week. Make sure they were completely dried before freezing them.
30. During culture incubations with antibodies or blocking solutions, use humid incubator chambers to prevent evaporation of the antibody solution.

References

1. Cordo SM, Cesio y AM, Candurra NA (2005) Polarized entry and release of Junín virus, a new world arenavirus. *J Gen Virol* 86:1475–1479
2. Martínez MG, Cordo SM, Candurra NA (2008) Involvement of cytoskeleton in Junín virus entry. *Virus Res* 138:17–25
3. Martínez MG, Cordo SM, Candurra NA (2007) Characterization of Junín arenavirus cell entry. *J Gen Virol* 88:1776–1784
4. Martínez MG, Forlenza MB, Candurra NA (2009) Involvement of cellular proteins in Junín arenavirus entry. *Biotechnol J* 4:866–870
5. Contigiani MS, Sabattini MS (1977) Virulencia diferencial de cepas de virus Junín por marcadores biológicos en ratones y cobayos. *Medicina (B Aires)* 37:244–251
6. Martínez MG, Bialecki MA, Belouzard S, Cordo SM, Candurra NA, Whittaker GR (2013) Utilization of human DC-SIGN and L-SIGN for entry and infection of host cells by the new world arenavirus, Junín virus. *Biochem Biophys Res Commun* 441:612–617
7. Damonte EB, Mersich SE, Candurra NA (1994) Intracellular processing and transport of Junín virus glycoproteins influences virion infectivity. *Virus Res* 34:317–326
8. Sanchez A, Pifat D, Kenyon RH, Peters CJ, McCormick JB, Kiley MP (1989) Junín virus monoclonal antibodies: characterization and

- cross-reactivity with other arenaviruses. *J Gen Virol* 70:1125–1132
9. Damonte EB, Mersich SE, Candurra NA, Coto CE (1986) Cross reactivity between Junín and Tacaribe viruses as determined by neutralization test and immunoprecipitation. *Med Microbiol Immunol* 175:85–88
 10. Castilla V, Mersich SE, Damonte EB (1991) Lysosomotropic compounds inhibiting the multiplication of Junín virus. *Rev Argent Microbiol* 23:86–89
 11. Benmerah A, Bayrou M, Cerf-Bensussan N, Dautry-Varsat A (1992) Inhibition of clathrin-coated pit assembly by an EPS15 mutant. *J Cell Sci* 112:1303–1311
 12. Damke H, Baba T, Warnock DE, Schmid SL (1994) Induction of mutant dynamin specifically blocks endocytic coated vesicle formation. *J Cell Biol* 127:915–934
 13. Li G, Stahl PD (1993) Structure-function relationship of the small GTPase rab5. *J Biol Chem* 15:24475–24480
 14. Negre D, Mangeot PE, Duisit G, Blanchard S, Vidalain PO, Leissner P, Winter AJ, Rabourdin-Combe C, Mehtali M, Moullier P, Darlix JL, Cosset FL (2000) Characterization of novel safe lentiviral vectors derived from simian immunodeficiency virus (SIVmac251) that efficiently transduce mature human dendritic cells. *Gene Ther* 7:1613–1623
 15. Robertson MJ, Deane FM, Stahlschmidt W, von Kleist L, Haucke V, Robinson PJ, McCluskey A (2014) Synthesis of the Pitstop family of clathrin inhibitors. *Nat Protoc* 9:1592–1606

Studies of Lassa Virus Cell Entry

Antonella Pasquato, Antonio Herrador Fernandez, and Stefan Kunz

Abstract

Host cell entry is the first and most fundamental step of every virus infection and represents a major barrier for zoonotic transmission and viral emergence. Targeting viral entry appears further as a promising strategy for therapeutic intervention. Several cellular receptors have been identified for Lassa virus, including dystroglycan, TAM receptor tyrosine kinases, and C-type lectins. Upon receptor binding, LASV enters the host cell *via* a largely unknown clathrin- and dynamin-independent endocytotic pathway that delivers the virus to late endosomes, where fusion occurs after engagement of a second, intracellular receptor, the late endosomal/lysosomal resident protein LAMP1. Here, we describe a series of experimental approaches to investigate LASV cell entry and to test candidate inhibitors for their action at this early and decisive step of infection.

Key words Lassa virus, Viral entry, Receptor, Endocytosis, Endosome, Inhibitor

1 Introduction

1.1 *Lassa Virus Receptors and Cell Entry*

Host cell attachment and subsequent entry are the first steps of Lassa virus (LASV) infection and represent crucial determinants for zoonotic transmission, tissue tropism, and disease potential. Targeting viral entry is a promising strategy for therapeutic intervention as it allows blocking the pathogen before it can take control over the host cell. The first receptor for LASV was identified as dystroglycan (DG), a ubiquitously expressed conserved cellular receptor for extracellular matrix (ECM) proteins [1]. Expressed in most developing and adult tissues, DG provides a molecular link between the ECM and the actin cytoskeleton and serves as a receptor for LASV, Mopeia, Mobala, some isolates of lymphocytic choriomeningitis virus (LCMV), and Clade C New World arenaviruses [1, 2]. Initially synthesized as a single precursor polypeptide, DG core protein is processed into the N-terminal α -DG and the transmembrane β -DG [3]. Binding of LASV and ECM proteins to DG critically depends on posttranslational modification by the glycosyltransferase LARGE gene product

that adds [-3-xylose- α 1,3-glucuronic acid- β 1-] copolymer polysaccharides to the α -DG moiety in a tissue-specific manner [4–9]. A recent genome-wide haploid screen revealed that LASV strikingly mimics the molecular mechanisms of receptor recognition of host-derived ECM proteins [10].

More recently, the Tyro3/Axl/Mer (TAM) receptor tyrosine kinases Axl and Tyro3 and the C-type lectins DC-specific ICAM-3-grabbing nonintegrin (DC-SIGN) and LSECtin have been identified as candidate LASV receptors [11, 12]. Based on their known expression patterns, DC-SIGN and LSECtin may contribute to LASV entry in some cell types [13], but their exact role is currently unclear [12]. The TAM kinases Tyro3 and Axl are broadly expressed conserved receptors for the phosphatidylserine (PS)-binding serum protein Gas6 that is involved in removal of apoptotic cells. Over the past years, TAM kinases have been implicated in viral entry *via* “apoptotic mimicry,” which is characterized by recognition of PS displayed on the viral lipid envelope by cellular PS receptors [14]. The co-expression of DG with TAM receptors on many human cell types implicated in LASV infection [15] suggests complex receptor use.

Arenaviruses, including LASV, enter the host cell *via* receptor-mediated endocytosis with subsequent transport to late endosomal compartments, where fusion occurs at low pH [16, 17]. Initial studies suggested that Old World arenaviruses enter *via* an unknown clathrin- and dynamin-independent pathway [18–20]. Recent genome-wide RNA interference (RNAi) silencing screens identified sodium-hydrogen exchanger (NHE, also known as the ATP6 family of ATPases) as host factors involved in the multiplication of the prototypic Old World arenavirus LCMV [21]. In a follow-up study, de la Torre and colleagues validated NHE as entry factors for arenaviruses and provided a first link between arenavirus entry and macropinocytosis [22].

Upon internalization, LASV is rapidly delivered to late endosomes, passing through the multivesicular body and hijacking the endosomal sorting complex required for transport (ESCRT) [19]. At the late endosome, LASV dissociates from DG under low pH and engages the late endosomal/lysosomal resident protein LAMP1, which serves as an intracellular secondary receptor required for subsequent fusion [23]. Engagement of LAMP1 by LASV, combined with low pH (<5.0), triggers fusion of the viral membrane with the limiting membrane of the late endosome by the fusion-active viral glycoprotein (GP2), creating a “fusion pore” [24]. By an unknown mechanism of “uncoating”, the viral ribonucleoprotein (RNP) comprised of viral RNA, NP, and L is released from the capsid and enters the cytosol to initiate viral transcription and replication.

1.2 BSL-2 Surrogate Viruses to Study LASV Entry

Since LASV is a BSL-4 pathogen, work with the live virus is restricted to high-containment facilities, which is a challenge. To study LASV host cell binding and entry in the context of productive arenavirus

infection, a recombinant LCMV expressing the complete envelope glycoprotein (GPC) of LASV (rLCMV-LASVGP) has been generated using LCMV reverse genetics [25]. As viral entry is exclusively mediated by the viral envelope, the rLCMV-LASVGP chimera represents a suitable model for LASV entry studies that has been widely used for the characterization of LASV cell tropism *in vitro* [18, 19, 26, 27] and *in vivo* [28, 29]. The original version of rLCMV-LASVGP contains the core of the LCMV isolate ARM53b [18], and newer variants contain the core of LCMV Clone 13 [28, 29]. Since the viral GPC represents only circa 15% of the viral genome and LASV virulence is largely determined by the L segment encoding the RNA-dependent RNA polymerase L, rLCMV-LASVGP are generally considered as BSL-2 pathogens for tissue culture work described in the following sections. Recent infection studies in mice revealed an attenuated phenotype of rLCMV-LASVGP when compared to the parental LCMV isolates [29]. Recombinant LCMV expressing the G protein of vesicular stomatitis virus (rLCMV-VSVG) that differs in receptor use and entry [30] represents a control virus for many applications also *see Note 1*.

Enveloped viruses can incorporate foreign glycoproteins in their envelope by the process of pseudotyping. Several pseudotype platforms have been established for LASV, including recombinant vesicular stomatitis virus (VSV) [31], murine retroviruses [32], and human immunodeficiency virus (HIV)-1 [33]. Recombinant VSV pseudotyped with LASVGP is generated by infection of cells with recombinant VSV whose G protein has been replaced by enhanced green fluorescent protein (EGFP) (rVSV- Δ G*) and providing recombinant LASVGP *in trans* [34]. The resulting rVSV- Δ G*-LASVGP pseudotypes are capable of entering susceptible target cells and undergoing viral replication and transcription without cell-to-cell propagation. Different formats of retroviral pseudotypes exist for LASV. The most widely used are retroviral pseudotypes based on Moloney murine leukemia virus (MLV) [32, 35] and HIV-1 [33]. In both systems, recombinant LASVGP is co-expressed with a replication-deficient retroviral genome bearing an EGFP or luciferase reporter in packaging cell lines providing the missing retroviral components. Upon cell entry these retroviral pseudotypes can integrate into the host cell genome and express the reporter gene in the absence of productive viral infection.

1.3 Studying Different Steps of LASV Entry

The kinetics of viral attachment and entry is crucial for the efficiency of zoonotic transmission of the virus and spread within the host organism. To obtain an estimate of the on-rate of virus-receptor attachment, the simple assay described in Subheading 3.3 can be employed. Briefly, virus is added to confluent cells at low multiplicity in the cold, allowing receptor binding without internalization. At different time points, unbound virus is removed by washing and cells shifted to 37 °C to allow entry of attached virus.

After 1 h, cells are treated with the lysosomotropic agent ammonium chloride to prevent further entry *via* pH-dependent fusion. When added to cells, ammonium chloride raises the endosomal pH within seconds and blocks further low pH-dependent cellular processes without causing overall cytotoxicity [36, 37].

To monitor internalization of viruses, many sophisticated protocols have been developed. In the context of arenavirus entry, we recommend a modified version of a well-established assay originally developed by the Helenius laboratory to study cell entry of polyomaviruses [38, 39] described in Subheading 3.4. Briefly, purified virus is labeled with the reagent N-hydroxysulfosuccinimide (Sulfo-NHS-SS)-biotin, resulting in a biotin label that is cleavable by reducing agents. As long as the virus stays bound to the cell surface, the biotin label can be cleaved efficiently with the potent, membrane-impermeable reducing agent Tris(2-carboxyethyl) phosphine (TCEP). Once internalized *via* endocytosis, the biotin-labeled virus is protected from TCEP and retains its biotin moiety after exposure of cells to TCEP. Internalized virus can then be detected specifically by immunoprecipitation of LASV GP2, followed by detection of biotin label using streptavidin-HRP. This assay allows semiquantitative detection of arenavirus internalization [26, 38].

To assess how fast the virus escapes from late endosomes, the time required to become resistant to ammonium chloride is determined (Subheading 3.5). Briefly, virus is added to cells in the cold to allow receptor binding without internalization. The temperature is then shifted to 37 °C and ammonium chloride added at the different time points and left throughout the experiment. Since ammonium chloride depletes the endosomal proton gradient within seconds, this method allows a fairly accurate determination of the kinetics of endosomal escape.

Unwanted off-target effects of candidate inhibitors are frequently a significant concern in viral entry studies. To preferably target cell entry and to minimize the duration of drug exposure, we recommend the experimental setup schematically shown in Fig. 1a (Subheading 3.6.3). Briefly, cells are pretreated for 30–60 min with candidate inhibitors, followed by virus infection at low multiplicity in the presence of drug. After 1 h, drug is washed out using medium containing ammonium chloride to block further entry. Productive infection is then detected by immunofluorescence or detection of reporter activity. The assay outlined in Fig. 1a gives the first hints about the mechanism of action of a candidate entry inhibitor. Classical time-of-addition experiments can discriminate between effects on entry and subsequent replication/transcription of the virus, but cannot discriminate inhibition of pre-fusion steps of entry from fusion and early post-fusion events, like viral uncoating. The “postentry” assay outlined in Fig. 1b (Subheading 3.6.4) addresses this issue by synchronizing

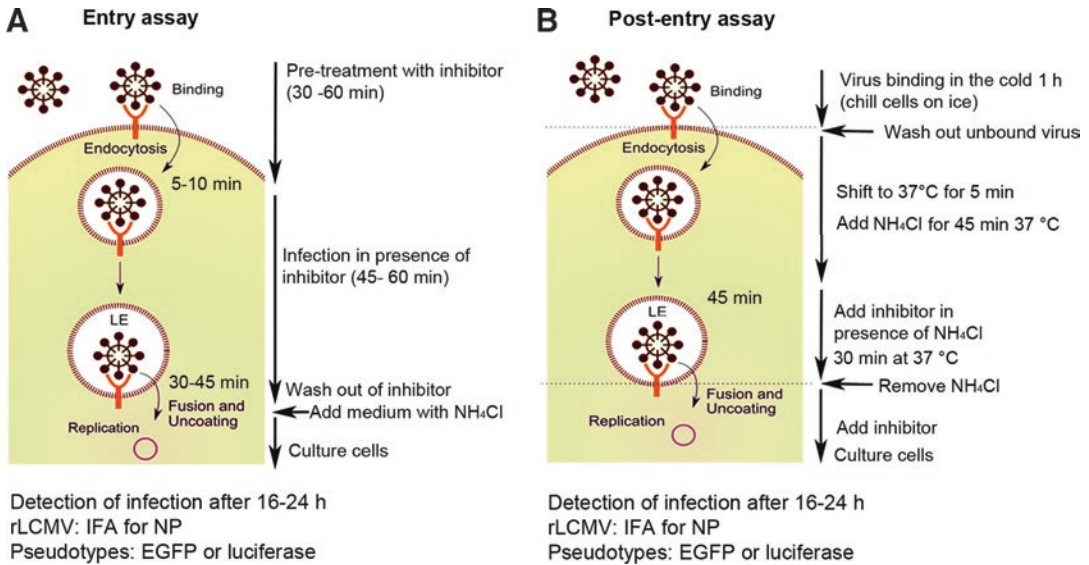


Fig. 1 Assays to study the effects of candidate inhibitors on LASV entry. (a) Schematic representation of the entry assay (Subheading 3.6.3). (b) The assay format to detect effects on fusion and “postentry” steps of infection (Subheading 3.6.4). For details, please *see text*

virus escape from late endosomes with the drug treatment and may represent an alternative to classical time-of-addition studies. Originally developed for influenza A virus, this assay format is suitable for LASV and other late-fusing viruses with low fusion pH [40]. Briefly, virus is attached in the cold, followed by entry for 45 min in the presence of ammonium chloride. This allows the virus to proceed to late endosomes without undergoing fusion (Fig. 1b). Candidate inhibitors are added in the presence of ammonium chloride for another 30 min, followed by washout of ammonium chloride in the presence of drug. Due to the small volume of endosomes, removal of the lysosomotropic agent restores the endosomal proton gradient within a few minutes, allowing the virus to undergo fusion, uncoating, and early replication in the presence of drugs.

2 Materials

2.1 Cell Lines and Culture Media

- A549 cells:** The human epithelial cell line A549 (ATCC: CCL-185) is used to study LASV entry. It represents a good model for epithelial cells that are important targets of arenaviruses in vivo. A549 culture medium: Dulbecco’s Modified Eagle Medium (DMEM), 1× penicillin-streptomycin (Pen/Strep), 1× L-glutamine (Gln), 10% (w/v) FBS.
- VeroE6 cells:** The VeroE6 (ACTT: CRL-1586) cell line is a clone of Vero 76 and derives from kidney epithelial cell extracts

of the African green monkey *Chlorocebus aethiops*. It is often used for detecting viral plaque-forming units (PFU) used in titration. Vero cell culture medium: DMEM, 1× Pen/Strep, 1× L-Gln, 10% (w/v) FBS.

3. **BHK-21 cells:** The baby hamster kidney (BHK)-21 cell line (ATCC: CCL-10) was created from a 1-day-old newborn hamster. They are frequently used for the production of recombinant LCMV viruses. BHK cell culture medium: DMEM, 1× Pen/Strep, 1× L-Gln, 13 mL 20% glucose, 25 mL 2× tryptone-peptone broth (TPB), 10% (v/v) FCS. To avoid acidification during long culture times, use 20 mM HEPES buffer in addition to the CO₂.
4. **GP2-293[®] cells:** HEK293-based retroviral packaging cell line from Clontech stably expressing the MLV-derived gag and pol gene. GP2-293 allows the packaging of any MLV-based vector containing the appropriate packaging signal. 293 cell culture medium: DMEM, 1× Pen/Strep, 1× L-Gln, 10% FCS.

2.2 Antibodies

1. Monoclonal antibody 113 is anti-LCMV NP, purified IgG in PBS [41].
2. Monoclonal antibody 83.6 is mouse anti-LCMV GP. It recognizes a highly conserved epitope in GP2 of LASV and is used as purified IgG in PBS [42].
3. Horseradish peroxidase (HRP) conjugated polyclonal goat anti-mouse IgG (Dako).
4. Rhodamine Red-X-AffiniPure Goat Anti-Mouse IgG (H + L) (Jackson ImmunoResearch).

2.3 Transfection and Virus Entry Analysis

1. Dulbecco's Modified Eagle Medium (DMEM) (Gibco[®] Life Technologies).
2. Hank's Balanced Salt Solution (HBSS) (Gibco[®] Life Technologies).
3. Penicillin/streptomycin stock solution (10,000 U/mL), 100× (Gibco[®] Life Technologies)
4. CellTiter-Glo[®] Luminescent Cell Viability Assay Kit (Promega).
5. Polyethylene glycol (PEG) 8000.
6. Nuclear dye 4',6-diamidino-2-phenylindole (DAPI) (Molecular Probes).
7. N-hydroxysulfosuccinimide (Sulfo-NHS-SS)-biotin (Pierce).
8. Tris(2-carboxyethyl)phosphine (TCEP) (Sigma).
9. Protein G conjugated to Sepharose 4B (Sigma).
10. Lipofectamine 2000 (Invitrogen).
11. SuperSignal West Femto Maximum Sensitivity Substrate (Pierce).

12. Slide-A-Lyzer Cassette with 100 kDa cutoff (Pierce).
13. TNE: 10 mM Tris-HCl, pH 7.5, 100 mM NaCl, 1 mM EDTA.
14. Renografin-60: 520 mg/mL diatrizoate meglumine (Sigma), 80 mg/mL sodium diatrizoate (Sigma), 3.2 mg/mL sodium citrate, 0.4 mg/mL EDTA, in distilled water, pH 7.4.
15. IFA staining buffer: PBS, 1% (v/v) FCS, 0.1% (w/v) saponin.
16. PBS-CM: PBS supplemented with 0.5 mM CaCl₂ and 1 mM MgCl₂.
17. Quenching solution: 50 mM glycine, 150 mM NaCl, 1 mM MgCl₂, 0.1 mM CaCl₂, adjusted to pH 8.0.
18. TCEP reaction buffer: 15 mM TCEP, 50 mM HEPES, pH 7.5, 150 mM NaCl, 1 mM CaCl₂, 1 mM MgCl₂.
19. Lysis buffer: 1% (w/v) Triton X-100, 0.05% (w/v) SDS, 50 mM Tris-HCl, pH 7.5, 150 mM NaCl, 1 mM EDTA, 1 mM phenylmethylsulfonyl fluoride (PMSF), protease inhibitor complex to be added immediately before use (cOmplete, Roche).

3 Methods

3.1 Production of rLCMV-LASVGP: A BSL-2 Surrogate for LASV

3.1.1 Production of Recombinant LCMV Variants

The following production protocol has been modified from the classical protocol established for LCMV [43] and is suitable for the production of rLCMV stocks with volumes of up to several liters.

1. Seed 2×10^6 BHK-21 cells in a 75 cm² flask the day before infection and culture them in BHK-21 medium (*see* below). Cells will double once and grow to 60–70% confluency.
2. 16–24 h post seeding, thaw aliquots of viruses at 37 °C in the water bath and keep them on ice during the experiment. After use, viruses can be refrozen, which results in reduction of titers by circa 50%.
3. Use rLCMV-LASVGP and rLCMV-VSVG at multiplicity of infection (MOI) = 0.01. Mix the viral stock with fresh medium to a final 5 mL volume in a 15 mL Falcon[®] tube.
4. Remove medium from the flask and add inocula. Incubate for 1 h at 37 °C and 5% (v/v) CO₂. Flasks are moved every 10 min to ensure optimal infection.
5. Remove inocula and add 15 mL of pre-warmed BHK-21 medium supplemented with 5% tryptone-peptone broth (Sigma) and 20 mM HEPES to increase viral production efficiency and avoid excessive acidification.
6. Incubate 48–72 h at 37 °C and 5% (v/v) CO₂.

7. Collect and pool supernatants in 15 mL Falcon tubes.
8. Centrifuge aliquots at $3,100 \times g$ Heraeus Labofuge 400 swinging rotor 75008179 for 5 min at 4 °C to remove cells and cellular debris.
9. Collect clear supernatants into new 15 mL tubes.
10. Aliquot supernatants in 2 mL cryovials and keep 500 μ L to perform virus titers. Do not overfill the tube that can explode when the volume increases during freezing.
11. Freeze aliquots of crude viral stocks at -80 °C. Warning: each thawing will reduce the viral titers of about 50%.

3.1.2 Virus Purification

The following purification protocol has been modified from Dutko et al. [43]. We recommend at least 100 mL of crude virus stock (please see above) as starting material:

1. Thaw crude virus stock rapidly in 37 °C water bath. Centrifuge at $3,100 \times g$ for 5 min at 4 °C and add 6.5 g PEG/100 mL cleared supernatant.
2. Stir solution overnight at 4 °C using a magnetic stirrer.
3. Transfer solution to 50 mL sealable centrifuge buckets (Sorvall) and spin at $7,649 \times g$ for 30 min (Sorvall centrifuge, SS34 rotor).
4. Discard supernatant and resuspend the pellet in 5–10 mL of TNE.
5. Prepare a discontinuous Renografin-60 gradient: 1 mL 50% Renografin-60/TNE + 2 mL 40% Renografin-60/TNE and 3 mL 10% Renografin-60/TNE in SW41 ultracentrifuge tubes.
6. Carefully load resuspended virus in TNE on the gradient. Centrifuge at $217,000 \times g$ for 90 min in a SW41 swing-out rotor. Purified virus appears as a whitish band at the interface of Renografin-60 40% and 10%.
7. Collect the purified virus with a sterile Pasteur pipette. Warning: do not use a syringe to perforate the tube.
8. Resuspend the collected virus in TNE.
9. Dialyze overnight against 5 l PBS (two changes) using a Slide-A-Lyzer Cassette (Pierce) with 100 kDa cutoff.
10. Aliquot the virus in cryovials and store at -80 °C.

3.1.3 Determination of rLCMV Titers by Immunofocus Assay

Determination of infectious virus titers for LCMV is normally done *via* plaque assay. However, plaques formed by rLCMV-LASVGP and rLCMV-VSVG are difficult to reveal, and we recommend immunofocus assay (IFA) as an alternative.

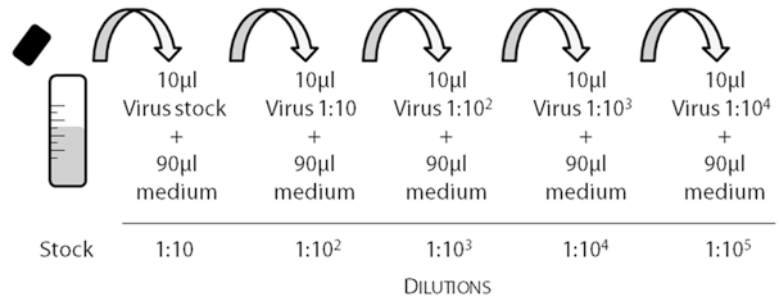


Fig. 2 Schematic representation of serial dilution of the viral stock. For details, please see text

1. Seed 2×10^4 VeroE6 cells per well in a 96-well tissue culture plate and grow into closed monolayers at 37 °C and 5% (v/v) CO₂.
2. The following day, prepare tenfold serial virus dilutions using complete medium as shown in Fig. 2.
3. Infect VeroE6 cells with virus dilutions and incubate for 45 min at 37 °C and 5% (v/v) CO₂.
4. Remove inoculum and add fresh complete medium.
5. Incubate for 16 h at 37 °C and 5% (v/v) CO₂.
6. Remove media and wash two times with 200 µL/well PBS.
7. Fix cells with 100 µL/well 2% (v/v) formaldehyde in PBS. Incubate for 15 min in the dark at room temperature (RT).
8. Remove fixation solution and wash twice with 200 µL/well PBS.
9. Remove PBS and permeabilize cells with 100 µL/well IFA staining buffer. Incubate 15 min at RT.
10. Remove permeabilization solution and add 100 µL/well of primary antibody: mAb 113 anti-LCMV NP [41] 1:200 in IFA staining buffer. Incubate 1 h at RT.
11. Remove primary antibody solution and wash cells twice with 200 µL/well PBS.
12. Add 100 µL/well of secondary antibody, Rhodamine Red-X-conjugated goat anti-mouse IgG, 1:100 in IFA staining buffer. Incubate 45 min at RT. Protect from light.
13. Remove secondary antibody and wash cells twice with 200 µL/well PBS. Keep 100 µL/well PBS and store the plate at 4 °C in the dark (wrap in aluminum foil). Fluorescence can be examined over several weeks.
14. Count NP-positive cells under a fluorescence microscope.

15. Choose the dilution where you can count 50–200 cells/well. Score infected foci as one infectious event.
16. Calculate titers using the following formula: *(Number of infected cells) × (fold dilution) PFU/100 μL*.
17. Expected titers of crude stocks: rLCMV-LASVGP: 10^7 – 10^8 PFU/mL, rLCMV-VSVG: 10^5 – 10^6 PFU/mL.

3.2 Production of Pseudotypes for LASV Entry Studies

3.2.1 Production of VSV Pseudotypes

Recombinant vesicular stomatitis virus (VSV) strains pseudotyped with LASVGP or VSVG are generated using a protocol modified from [44].

1. Plate 4×10^5 HEK293T cells in M6 tissue culture plates coated with poly-L-lysine ($2 \mu\text{g}/\text{cm}^2$) for 16–24 h reaching 60–70% confluency.
2. Transfect expression plasmids pC-LASVGP, pC-VSVG, or pC-EGFP using Lipofectamine 2000.
3. For transfection, the following mixture is prepared (amounts per well):
 - 2 μg DNA dissolved in 100 μL Opti-MEM serum-free medium.
 - Mix well (10 s vortex).
 - Dissolve 10 μL Lipofectamine in 100 μL Opti-MEM.
 - Mix DNA/Opti-MEM with Lipofectamine/Opti-MEM (10 s vortex).
 - Incubate for 15–30 min at room temperature.
 - Add 800 μL of Opti-MEM.
 - Mix well (pipette up and down three times).
 - Remove medium from cells and wash cells twice in Opti-MEM
 - and add the DNA/Lipofectamine mixture.
 - Incubate for 4 h at 37 °C, 5% (v/v) CO₂.
 - Remove DNA/Lipofectamine mixture and add 4 mL medium/well to cells.
4. Incubate plates at 37 °C, 5% (v/v) CO₂ for 24–32 h to allow recombinant glycoprotein expression.
5. Infect the transfected cells with rVSV-ΔG*-VSVG at MOI of 3–5 to assure that >98% of cells are infected.
6. Wash cells extensively (>5 times) with pre-warmed medium without FBS. *Note: this is essential to lower contamination with the input rVSV-ΔG*-VSVG virus.*
7. Incubate infected cells at 37 °C, 5% (v/v) CO₂ for further 24 h.

8. Collect and pool supernatants.
9. Clear supernatants by low-speed centrifugation ($430 \times g$, 5 min, 4°C).
10. Aliquot the supernatants into 2 mL cryovials (1.2 mL/vial).
11. Freeze aliquots at -80°C .
12. Expected titers: rVSV- ΔG^* -VSVG: 10^7 – 10^8 PFU/mL, rVSV- ΔG^* -LASVGP: 10^5 – 10^6 PFU/mL.

3.2.2 Production of Retroviral Pseudotypes

Different formats of retroviral pseudotypes exist for LASV. Here, we describe the production of retroviral pseudotypes based on MLV [32, 35].

1. For MLV pseudotype production, the packaging cell line GP2-293[®] cells stably expressing MLV gag and pol is used.
2. Seed 4×10^5 GP2-293[®] cells/well in M6 tissue culture plates coated with poly-L-lysine ($2 \mu\text{g}/\text{cm}^2$) for 16–24 h, reaching 60–70% confluency.
3. Transfect expression plasmids for viral GPs (pC-LASVGP, pC-VSVG, or pC-EGFP control) together with the MLV genomic plasmid pLZRS-Luc-gfp using Lipofectamine 2000.
4. $2 \mu\text{g}$ of each plasmid DNA is dissolved in 100 μL Opti-MEM serum-free medium and transfection performed as described above (point 3).
5. After incubation of the DNA/Lipofectamine mix with the cells at 37°C , 5% (v/v) CO_2 for 4 h, remove media, wash cells twice with serum-free medium, and add fresh complete medium (4 mL/well).
6. Collect and pool supernatants.
7. Clear supernatants by low-speed centrifugation ($430 \times g$, 5 min, 4°C).
8. Aliquot the supernatants into 2 mL cryovials (1.2 mL/vial).
9. Freeze aliquots at -80°C .
10. Expected titers: rMLV-LASVGP: 10^5 – 10^6 PFU/mL, rMLV-LASVGP: 10^7 PFU/mL.

3.2.3 Concentration of MLV Pseudotypes

The method is adapted from [45] and allows recovery of infectivity close to 100%.

1. Clarify supernatants by centrifugation ($490 \times g$, 5 min, 4°C).
2. Transfer supernatants in new tubes and discard pellet. Supernatants can be kept on ice for up to 24 h.
3. Ultracentrifuge supernatants (35–40 mL/tube) at $112,000 \times g$ at 4°C for 2 h using a SW28 rotor.
4. Discard supernatants after centrifugation.

5. Wash pellet twice with serum-free medium, followed by additional centrifugation $112,000\times g$ at 4°C .
6. Discard the washing medium and resuspend pellets overnight in $1\times$ HBSS on ice in a closed vial on a shaker.
7. Aliquot the purified virus ($50\ \mu\text{L}/\text{cryovial}$) and store the aliquots at -80°C .

3.2.4 Determination of Pseudotype Titers

Determination of infectious pseudotype titers makes use of the EGFP reporter gene present in the genome of recombinant VSV and MLV vectors.

1. Seed 2×10^4 VeroE6 cells per well in a 96-well tissue culture plate and grow into closed monolayers.
2. On the following day, prepare tenfold serial dilutions using complete medium (Fig. 2).
3. Infect VeroE6 cells with pseudotype dilutions and incubate them for 1 h.
4. Remove inoculum and add fresh complete medium.
5. Incubate for 16–24 h.
6. Remove media and wash two times with $200\ \mu\text{L}/\text{well}$ PBS.
7. Fix cells with $100\ \mu\text{L}/\text{well}$ 2% (v/v) formaldehyde in PBS. Incubate for 15 min in the dark at RT.
8. Remove fixation solution and wash twice with $200\ \mu\text{L}/\text{well}$ PBS.
9. Count EGFP-positive cells under a fluorescence microscope.
10. Choose the dilution where you can count 50–200 cells/well. Score infected foci as one infectious event.

3.3 Assay to Assess Virus-Cell Attachment Kinetics

The protocol described below is suitable for use with rLCMV-LASVGP as well as VSV and MLV pseudotypes and provides a good estimate on the kinetics of virus-cell attachment with a resolution in the range of minutes (*see Note 2*).

1. Seed cells of interest, e.g., A549 cells, in a 96-well tissue culture plate (2×10^4 cells/well) to obtain confluent monolayers after 16–24 h.
2. Remove medium and add fresh complete medium ($100\ \mu\text{L}/\text{well}$) supplemented with 20 mM HEPES, pH 7.5.
3. Dilute virus in cold complete medium containing 20 mM HEPES at 2000 PFU/mL, corresponding to 200 PFU/ $100\ \mu\text{L}$ added per well, resulting in an MOI of circa 0.01.
4. Remove medium and add virus inocula to cells in the cold (4°C) allowing receptor binding without internalization.
5. At different time points (0, 2, 5, 10, 15, 20, 30, 45, and 60 min), remove inocula and wash twice with $200\ \mu\text{L}/\text{well}$ cold serum-free medium to remove unbound virus.

6. Add 200 μL /well fresh medium supplemented with 10% (w/v) FBS.
7. Immediately shift cell to 37 °C to allow entry of attached virus particles.
8. After 45 min, add 20 mM ammonium chloride to the culture medium to prevent further entry via low pH fusion.
9. For rLCMV, productive entry is quantified after 16 h by detection of LCMV Nucleoprotein (NP) in IFA as described in Subheading 3.1.3. VSV and MLV pseudotypes expressing EGFP can be detected by direct fluorescence microscopy.
10. Plot infection versus time to obtain virus-binding curves. The time of half-maximal attachment of the virus correlates with the on-rate of virus-receptor binding.

3.4 Assay to Monitor Virus Internalization

This protocol is suitable for rLCMV and any other virus that can be purified and concentrated. However, in our experience, it is challenging in the context of VSV and MLV pseudotypes. The reasons are the markedly lower titers and impurities in the preparations (*see Notes 3–5*).

3.4.1 Preparation of Biotinylated rLCMV-LASVGP

1. Use a concentrated Renografin-purified stock of rLCMV-LASVGP (*see* Subheading 3.1.1). Dilute virus to 5×10^8 PFU/mL in PBS-CM and keep in the cold.
2. Freshly prepare the stock solution by dissolving 5.56 mg of Sulfo-NHS-SS-biotin in 100 μL DMSO (final concentration 100 mM) 15–20 min before use.
3. Add Sulfo-NHS-SS-biotin to the virus in cold PBS-CM at a final concentration of 1 mM.
4. Incubate for 1 h at RT by end-over-end rotation in a 15 mL Falcon® tube.
5. Quench reaction by adding cold quenching solution for 10 min.
6. Dialyze overnight against PBS using a Slide-A-Lyzer Cassette (100 kDa cutoff).
7. Test the efficiency of labeling by incubating a sample of the biotinylated virus with 15 mM TCEP or reaction buffer for 30 min. Treatment should result in a loss of >95% of the biotin label assessed by Western blot using streptavidin-HRP for detection.
8. Determine the titer of the labeled virus using IFA (Subheading 3.1.1). Loss of infectivity during the labeling procedure is minimal. When compared to the original virus stock, biotin labeling should not reduce infection by more than 50%, i.e., we expect titers of $2\text{--}3 \times 10^8$ PFU/mL.
9. Aliquot biotinylated virus in cryovials and store them at -80 °C. The biotin label is stable over several years.

3.4.2 Virus Internalization Assay

1. Seed $4\text{--}6 \times 10^5$ cells/well in M6 plates to obtain confluent monolayers after 16–24 h. Cells will double during this period resulting in a density of 10^6 cells/well.
2. Remove culture medium.
3. Wash twice with 2 mL of cold HBSS.
4. Chill plate on ice for 5 min.
5. Dilute NHS-SS-biotinylated virus to 10^8 PFU/mL in HBSS and chill on ice.
6. Add cold solution containing the virus to cells (1 mL/well, MOI = 100).
7. Incubate cells for 1 h on ice under gentle shaking.
8. Wash cells with 2×2 mL cold HBSS to remove unbound virus.
9. Shift the cells to 37 °C by adding 4 mL/well pre-warmed complete medium to induce virus internalization.
10. Remove medium after the desired time points (e.g., 0, 2, 5, 10, 15, 20, 30, and 60 min) and chill cells on ice.
11. Add 2 mL/well of TCEP (15 mM) in TCEP reaction buffer on ice for 30 min. Apply the solution twice. TCEP is highly reactive in the cold and does not penetrate the cell membrane under these conditions.
12. Discard TCEP solution.
13. Wash cells three times with 15 mL cold HBSS.
14. Quench the remaining TCEP with 100 mM aqueous solution of iodoacetamide (Sigma) for 10 min on ice.
15. Remove solution and lyse cells with 1 mL/well of lysis buffer for 30 min at 4 °C.
16. Clear lysates by centrifugation at $11,700 \times g$ and 4 °C for 10 min and add unlabeled purified LCMV (10^7 PFU/mL final concentration) as a carrier. At this point, lysates can be processed further to immunoprecipitation (IP) of LASV GP2 (please see below), or they can be frozen and stored at -20 °C for several months.

3.4.3 Detection of Biotinylated LASV GP2

Detection of biotinylated LASV GP2 is performed by immunoprecipitation of total LASV GP2 with a specific mAb 83.8 recognizing a highly conserved epitope [42].

1. Immobilization of the antibody prior to addition of the antigen in question enhances the efficiency of the precipitation. For immobilization put 20 μ L of a 1:1 suspension of protein G conjugated to Sepharose 4B (Sigma) in PBS at the bottom of a 1.5 mL Eppendorf tube. Add 10 μ g of purified mAb 83.6

and incubate at room temperature for 30 min. Antibody is ready for use. If not used immediately, store on ice for up to several hours.

2. Incubate lysates immobilized mAb 83.6 overnight at 4 °C.
3. Wash Sepharose beads four times with lysis buffer.
4. Elute bound LCMV GP2 by boiling the antibody matrix in SDS-polyacrylamide gel electrophoresis (PAGE) sample buffer (nonreducing) for 5 min.
5. Separate immunoprecipitated proteins by SDS-PAGE.
6. Blot proteins to nitrocellulose, and detect biotinylated GP2 by streptavidin-HRP (1:5000) using SuperSignal West Femto Maximum Sensitivity Substrate and enhanced chemiluminescence (ECL).

3.5 Determination of the Kinetics of Endosomal Escape of the Virus

The following protocol is suitable to assess endosomal escape kinetics for LASV, rLCMV-LASVGP, as well as VSV and MLV pseudotypes.

1. Seed 2×10^4 cells/well in a 96-well plate to obtain confluent monolayers after 16–24 h.
2. Chill cell monolayers on ice for 30 min.
3. Dilute virus in cold complete medium containing 20 mM HEPES at 2000 PFU/mL.
4. Add 200 PFU virus in 100 μ L per well, corresponding to an MOI of circa 0.01.
5. Incubate plate on ice for 1 h.
6. Wash cells twice with 200 μ L/well of cold PBS to remove unbound virus.
7. Shift cells quickly to 37 °C by adding 100 μ L/well warm complete medium.
8. At different time points (0, 2, 5, 10, 15, 20, 30, 45, and 60 min), add 20 mM ammonium chloride (final concentration) to prevent virus entry via low pH fusion.
9. Incubate cells at 37 °C for 16–24 h in the presence of ammonium chloride.
10. For rLCMV, productive entry is quantified after 16 h by detection of LCMV NP in IFA (Subheading 3.1.1), and VSV and MLV pseudotypes expressing EGFP can be detected by direct fluorescence.
11. Plot infection versus time to obtain the curves of ammonium chloride resistance. The time of half-maximal virus infection correlates to the half-time of endosomal escape. For late-fusing viruses like LASV, this is typically in the range of 20–40 min.

3.6 Assays to Study Inhibitors of LASV Cell Entry

3.6.1 Preparation of Inhibitors for Entry Studies

1. Choose a suitable solvent to dissolve candidate inhibitors. A common solvent used for hydrophobic compounds is DMSO. For hydrophilic compounds, PBS or saline can be used.
2. Test solvent toxicity on your cells of choice. Typically, up to 2 (v/v) % DMSO are well tolerated by most cell lines.
3. Prepare dilutions using sterile solvents applying aseptic procedures.
4. Store inhibitor stocks and dilutions preferentially in opaque vials to avoid drug degradation by light exposure and store at $-20\text{ }^{\circ}\text{C}$ unless specified otherwise.

3.6.2 Evaluation of Inhibitor Cytotoxicity

Prior to testing the inhibitory potency on a specific virus/cell system, compounds must be analyzed for their cytotoxicity that can greatly vary depending on the cell type and the assay format used. Compounds and concentrations that reduce cell viability by $>20\%$ are normally discarded.

1. Seed 2×10^4 cells/well in a 96-well white plate with transparent bottom to obtain confluent monolayers after 16–24 h.
2. On the day of toxicity testing, prepare inhibitor dilutions using the appropriate solvent. Make sure that each drug dilution has the same volume.
3. Remove media and add 100 μL of fresh media supplemented with the indicated drug concentrations.
4. Expose cells to inhibitors at $37\text{ }^{\circ}\text{C}$ for the time you have planned for the experiments, e.g., 16–24 h for entry or postentry studies.
5. Add 100 μL of reagent from the CellTiter-Glo[®] Luminescent Cell Viability Assay Kit.
6. Incubate cells 10 min at room temperature.
7. Read luminescence with a luminescence reader. Luminescence is proportional to the cellular ATP concentration.

3.6.3 Effects of Inhibitors on LASV Entry

This assay examines effects of candidate inhibitors on LASV entry and early postentry steps of infection and is schematically shown in Fig. 1a (*see Note 6*).

1. Seed 2×10^4 cells/well in a 96-well plate to obtain confluent monolayers after 16–24 h. Perform triplicate experiments using at least three different drug concentrations to detect dose-response effects.
2. On the day of the experiment, prepare inhibitor dilutions using the appropriate solvent. Make sure that each drug dilution has the same volume.

3. Pretreat cells with inhibitors at the indicated concentrations for 30 min (fast-acting compounds) up to 60 min (slow-acting compounds) at 37 °C. Use the solvent vehicle alone as negative control.
4. Remove media and add virus (200 PFU/well) in 100 µL in the presence of inhibitors.
5. Incubate cells at 37 °C for 45 min–1 h.
6. Remove inocula and wash cells three times with 200 µL/well pre-warmed serum-free medium containing 20 mM ammonium chloride.
7. Add 200 µL/well of pre-warmed complete media supplemented with 20 mM ammonium chloride.
8. For rLCMV, productive entry is quantified after 16 h by detection of LCMV NP in IFA (Subheading 3.2.1), and VSV and MLV pseudotypes expressing EGFP can be detected by direct fluorescence.
9. Plot infection versus drug concentrations to obtain information on the dose-response characteristic. If significant inhibition without dose dependence is observed, we recommend using inhibitors at higher dilution, to exclude saturation effects.

3.6.4 Effects of Inhibitors on Fusion and Post-fusion Steps of Infection

This assay allows excluding observed drug effects in Subheading 3.6.4 on viral fusion and early post-fusion events of infection (Fig. 1b) (*see Note 7*).

1. Seed 2×10^4 cells/well in a 96-well plate to obtain confluent monolayers after 16–24 h. Perform at least triplicate experiments.
2. Chill cell monolayers on ice for 30 min.
3. Dilute virus in cold complete medium containing 20 mM HEPES at 2000 PFU/mL.
4. Add 200 PFU virus in 100 µL per well, corresponding to an MOI of circa 0.01.
5. Incubate plate on ice for 1 h.
6. Wash cells twice with 200 µL/well of cold PBS to remove unbound virus.
7. Shift cells quickly to 37 °C by adding 100 µL/well warm complete medium supplemented with 20 mM ammonium chloride. Incubate for 45 min. This allows the virus to enter cells and to progress to late endosomes, without undergoing fusion.
8. In the meantime, prepare inhibitor dilutions using the appropriate solvent. Make sure that each drug dilution has the same volume. Dilute drugs at the required concentrations in complete medium supplemented with 20 mM ammonium chloride. Include solvent vehicle controls.

9. Remove medium from cells and add medium containing drugs in the presence of 20 mM ammonium chloride. Incubate cells at 37 °C for 30 min. This allows the drug to exert its inhibitory function while the virus is blocked at the level of the late endosome.
10. Remove inocula and wash three times with pre-warmed serum-free medium without ammonium chloride.
11. Add 100 µL/well of pre-warmed complete media supplemented with drugs.
12. Incubate cells at 37 °C for 16 h.
13. For rLCMV, productive entry is quantified after 16 h by detection of LCMV NP in IFA (Subheading 3.1.3), and VSV and MLV pseudotypes expressing EGFP can be detected by direct fluorescence.

4 Notes

1. Several BSL-2 surrogates have been established for LASV entry studies, including recombinant LCMV (rLCMV-LASVGP) and pseudotype platforms, based on replication-deficient VSV and retroviral vectors. Depending on the planned applications, some restrictions do apply. Due to the high conservation of the replication/transcription machinery between LCMV and LASV, rLCMV-LASVGP allows one to study LASV entry in the context of productive arenavirus infection. Both LASV and LCMV form spherical enveloped particles with a median size of 100 nm that are decorated with densely packed GP spikes. The size, geometry, and arrangement of GP of rLCMV-LASVGP are therefore similar to authentic LASV. In contrast, VSV pseudotypes of arenaviruses adopt the characteristic bullet shape and size of VSV that varies considerably from arenaviruses. Lentiviral particles (MLV, HIV-1) are more similar in size and shape to arenaviruses, but may vary in the density of arenavirus GP displayed at the surface.
2. The assay to monitor virus-cell attachment (Subheading 3.3) is suitable to study the attachment of LASV to its receptor(s) in a semiquantitative manner. If present, functionally glycosylated DG mediates rapid virus attachment via a lectin-type binding that is of high affinity and shows little temperature dependence. However, it is currently unknown whether DG serves primarily as an attachment factor, similar to glycosaminoglycans for other viruses, or if it functions as an authentic entry receptor. The kinetics of viral attachment does, therefore, not necessarily correlate with the kinetics of internalization assessed by Subheading 3.4.
3. The assay to monitor virus internalization (Subheading 3.4) is suitable for LCMV, recombinant LCMV, and any other arenavirus that can be purified and concentrated to the necessary

degree. However, in our experience, the adaptation of the assay to VSV and MLV pseudotypes has not been possible. The reasons are likely the markedly lower virus titers and impurities in the preparations.

4. In the virus internalization assay (Subheading 3.4), biotinylation is used to selectively label internalized virus. This would in theory allow fractionation by precipitation of biotinylated proteins by streptavidin-conjugated agarose, followed by detection of LASV GP2 in a Western blot with mAb 83.6 to GP2. However, this alternative approach did not work in our hands. It is important to add unlabeled purified rLCMV-LASVGP as carrier for the IP with mAb 83.6 to achieve the necessary efficiency of the IP approach. A high-sensitivity ECL kit is required to detect biotinylated GP2 derived from internalized virus.
5. The assay to monitor virus internalization (Subheading 3.4) cannot discriminate between virus entering into “dead-end” pathways and virus particles that will exit from the late endosome and establish productive infection. This is a limitation that has to be kept in mind.
6. In the LASV entry assay (Subheading 3.6.3, Fig. 1a), off-target effects of inhibitors or candidate drugs are a major concern. To circumvent this problem, drugs are washed out with medium containing ammonium chloride. Most experimental inhibitors show full reversibility and can be efficiently washed out. This markedly reduces overall toxicity and unwanted effects on postentry steps of viral infection. Even in case of irreversible inhibitors, washout allows one to replenish the drug target over time, which frequently alleviates toxicity problems.
7. In the LASV “postentry” assay (Subheading 3.6.4, Fig. 1b), washout of ammonium chloride restores the low luminal pH of the late endosome within a few minutes. The wash steps have to be performed rapidly to prevent reversion of drug action. If drugs with known high off-rates are used, compounds should be added to the wash buffer to avoid false-negative results.

References

1. Cao W, Henry MD, Borrow P, Yamada H, Elder JH, Ravkov EV, Nichol ST, Compans RW, Campbell KP, Oldstone MB (1998) Identification of alpha-dystroglycan as a receptor for lymphocytic choriomeningitis virus and Lassa fever virus. *Science* 282:2079–2081
2. Spiropoulou CF, Kunz S, Rollin PE, Campbell KP, Oldstone MB (2002) New World arenavirus clade C, but not clade A and B viruses, utilizes alpha-dystroglycan as its major receptor. *J Virol* 76:5140–5146
3. Barresi R, Campbell KP (2006) Dystroglycan: from biosynthesis to pathogenesis of human disease. *J Cell Sci* 119:199–207
4. Kanagawa M, Saito F, Kunz S, Yoshida-Moriguchi T, Barresi R, Kobayashi YM, Muschler J, Dumanski JP, Michele DE, Oldstone MB et al (2004) Molecular recognition by LARGE is essential for expression of functional dystroglycan. *Cell* 117:953–964
5. Kunz S, Rojek JM, Kanagawa M, Spiropoulou CF, Barresi R, Campbell KP, Oldstone MB

- (2005) Posttranslational modification of alpha-dystroglycan, the cellular receptor for arenaviruses, by the glycosyltransferase LARGE is critical for virus binding. *J Virol* 79:14282–14296
6. Rojek JM, Spiropoulou CF, Campbell KP, Kunz S (2007) Old world and clade C new world arenaviruses mimic the molecular mechanism of receptor recognition used by alpha-dystroglycan's host-derived ligands. *J Virol* 81:5685–5695
 7. Goddeeris MM, Wu B, Venzke D, Yoshida-Moriguchi T, Saito F, Matsumura K, Moore SA, Campbell KP (2013) LARGE glycans on dystroglycan function as a tunable matrix scaffold to prevent dystrophy. *Nature* 503:136–140
 8. Inamori K, Yoshida-Moriguchi T, Hara Y, Anderson ME, Yu L, Campbell KP (2012) Dystroglycan function requires xylosyl- and glucuronyltransferase activities of LARGE. *Science* 335:93–96
 9. Yoshida-Moriguchi T, Campbell KP (2015) Matriglycan: a novel polysaccharide that links dystroglycan to the basement membrane. *Glycobiology* 25:702–713
 10. Jae LT, Raaben M, Riemersma M, van Beusekom E, Blomen VA, Velds A, Kerkhoven RM, Carette JE, Topaloglu H, Meinecke P et al (2013) Deciphering the glycosylome of dystroglycanopathies using haploid screens for Lassa virus entry. *Science* 340:479–483
 11. Shimojima M, Stroher U, Ebihara H, Feldmann H, Kawaoka Y (2012) Identification of cell surface molecules involved in dystroglycan-independent Lassa virus cell entry. *J Virol* 86:2067–2078
 12. Goncalves AR, Moraz ML, Pasquato A, Helenius A, Lozach PY, Kunz S (2013) Role of DC-SIGN in Lassa virus entry into human dendritic cells. *J Virol* 87:11504–11515
 13. Van Breedam W, Pohlmann S, Favoreel HW, de Groot RJ, Nauwynck HJ (2014) Bitter-sweet symphony: glycan-lectin interactions in virus biology. *FEMS Microbiol Rev* 38:598–632
 14. Amara A, Mercer J (2015) Viral apoptotic mimicry. *Nat Rev Microbiol* 13:461–469
 15. Lemke G, Burstyn-Cohen T (2010) TAM receptors and the clearance of apoptotic cells. *Ann N Y Acad Sci* 1209:23–29
 16. Cosset FL, Marianneau P, Verney G, Gallais F, Tordo N, Pecheur EI, ter Meulen J, Deubel V, Bartosch B (2009) Characterization of Lassa virus cell entry and neutralization with Lassa virus pseudoparticles. *J Virol* 83:3228–3237
 17. Klewitz C, Klenk HD, ter Meulen J (2007) Amino acids from both N-terminal hydrophobic regions of the Lassa virus envelope glycoprotein GP-2 are critical for pH-dependent membrane fusion and infectivity. *J Gen Virol* 88:2320–2328
 18. Rojek JM, Sanchez AB, Nguyen NT, de la Torre JC, Kunz S (2008) Different mechanisms of cell entry by human-pathogenic old world and new world arenaviruses. *J Virol* 82:7677–7687
 19. Pasqual G, Rojek JM, Masin M, Chatton JY, Kunz S (2011) Old world arenaviruses enter the host cell via the multivesicular body and depend on the endosomal sorting complex required for transport. *PLoS Pathog* 7:e1002232
 20. Quirin K, Eschli B, Scheu I, Poort L, Kartenbeck J, Helenius A (2008) Lymphocytic choriomeningitis virus uses a novel endocytic pathway for infectious entry via late endosomes. *Virology* 378:21–33
 21. Panda D, Das A, Dinh PX, Subramaniam S, Nayak D, Barrows NJ, Pearson JL, Thompson J, Kelly DL, Ladunga I et al (2011) RNAi screening reveals requirement for host cell secretory pathway in infection by diverse families of negative-strand RNA viruses. *Proc Natl Acad Sci U S A* 108:19036–19041
 22. Iwasaki M, Ngo N, de la Torre JC (2014) Sodium hydrogen exchangers contribute to arenavirus cell entry. *J Virol* 88:643–654
 23. Jae LT, Raaben M, Herbert AS, Kuehne AI, Wirchnianski AS, Soh TK, Stubbs SH, Janssen H, Damme M, Saftig P et al (2014) Virus entry Lassa virus entry requires a trigger-induced receptor switch. *Science* 344:1506–1510
 24. Nunberg JH, York J (2012) The curious case of arenavirus entry, and its inhibition. *Virus* 4:83–101
 25. Sanchez AB, de la Torre JC (2006) Rescue of the prototypic arenavirus LCMV entirely from plasmid. *Virology* 350:370–380
 26. Moraz ML, Pythoud C, Turk R, Rothenberger S, Pasquato A, Campbell KP, Kunz S (2013) Cell entry of Lassa virus induces tyrosine phosphorylation of dystroglycan. *Cell Microbiol* 15:689–700
 27. Rojek JM, Moraz ML, Pythoud C, Rothenberger S, Van der Goot FG, Campbell KP, Kunz S (2012) Binding of Lassa virus perturbs extracellular matrix-induced signal transduction via dystroglycan. *Cell Microbiol* 14:1122–1134
 28. Lee AM, Cruite J, Welch MJ, Sullivan B, Oldstone MB (2013) Pathogenesis of Lassa fever virus infection: I. Susceptibility of mice to recombinant Lassa Gp/LCMV chimeric virus. *Virology* 442:114–121
 29. Sommerstein R, Ramos da Palma J, Olschlager S, Bergthaler A, Barba L, Lee BP, Pasquato A, Flatz L (2014) Evolution of recombinant lymphocytic choriomeningitis virus/Lassa virus

- in vivo highlights the importance of the GPC cytosolic tail in viral fitness. *J Virol* 88: 8340–8348
30. Pinschewer DD, Perez M, Sanchez AB, de la Torre JC (2003) Recombinant lymphocytic choriomeningitis virus expressing vesicular stomatitis virus glycoprotein. *Proc Natl Acad Sci U S A* 100:7895–7900
 31. Kunz S, Rojek JM, Perez M, Spiropoulou CF, Oldstone MB (2005) Characterization of the interaction of Lassa fever virus with its cellular receptor alpha-dystroglycan. *J Virol* 79:5979–5987
 32. Reignier T, Oldenburg J, Noble B, Lamb E, Romanowski V, Buchmeier MJ, Cannon PM (2006) Receptor use by pathogenic arenaviruses. *Virology* 353:111–120. Epub 2006 Jun 2021
 33. Larson RA, Dai D, Hosack VT, Tan Y, Bolken TC, Hruby DE, Amberg SM (2008) Identification of a broad-spectrum arenavirus entry inhibitor. *J Virol* 82:10768–10775
 34. Takada A, Robison C, Goto H, Sanchez A, Murti KG, Whitt MA, Kawaoka Y (1997) A system for functional analysis of Ebola virus glycoprotein. *Proc Natl Acad Sci U S A* 94:14764–14769
 35. Rojek JM, Spiropoulou CF, Kunz S (2006) Characterization of the cellular receptors for the South American hemorrhagic fever viruses Junin, Guanarito, and Machupo. *Virology* 349:476–491
 36. Ohkuma S, Poole B (1978) Fluorescence probe measurement of the intralysosomal pH in living cells and the perturbation of pH by various agents. *Proc Natl Acad Sci U S A* 75:3327–3331
 37. Ohkuma S, Poole B (1981) Cytoplasmic vacuolation of mouse peritoneal macrophages and the uptake into lysosomes of weakly basic substances. *J Cell Biol* 90:656–664
 38. Rojek JM, Perez M, Kunz S (2008) Cellular entry of lymphocytic choriomeningitis virus. *J Virol* 82:1505–1517
 39. Pelkmans L, Puntener D, Helenius A (2002) Local actin polymerization and dynamin recruitment in SV40-induced internalization of caveolae. *Science* 296:535–539
 40. Banerjee I, Miyake Y, Nobs SP, Schneider C, Horvath P, Kopf M, Matthias P, Helenius A, Yamauchi Y (2014) Influenza A virus uses the aggresome processing machinery for host cell entry. *Science* 346:473–477
 41. Buchmeier MJ, Lewicki HA, Tomori O, Oldstone MB (1981) Monoclonal antibodies to lymphocytic choriomeningitis and pichindé viruses: generation, characterization, and cross-reactivity with other arenaviruses. *Virology* 113:73–85
 42. Weber EL, Buchmeier MJ (1988) Fine mapping of a peptide sequence containing an antigenic site conserved among arenaviruses. *Virology* 164:30–38
 43. Dutko FJ, Oldstone MB (1983) Genomic and biological variation among commonly used lymphocytic choriomeningitis virus strains. *J Gen Virol* 64:1689–1698
 44. Perez M, Watanabe M, Whitt MA, de la Torre JC (2001) N-terminal domain of Borna disease virus G (p56) protein is sufficient for virus receptor recognition and cell entry. *J Virol* 75:7078–7085
 45. Beyer WR, Westphal M, Ostertag W, von Laer D (2002) Oncoretrovirus and lentivirus vectors pseudotyped with lymphocytic choriomeningitis virus glycoprotein: generation, concentration, and broad host range. *J Virol* 76:1488–1495

A Cell-Cell Fusion Assay to Assess Arenavirus Envelope Glycoprotein Membrane-Fusion Activity

Joanne York and Jack H. Nunberg

Abstract

For many viruses that enter their target cells through pH-dependent fusion of the viral and endosomal membranes, cell-cell fusion assays can provide an experimental platform for investigating the structure-function relationships that promote envelope glycoprotein membrane-fusion activity. Typically, these assays employ effector cells expressing the recombinant envelope glycoprotein on the cell surface and target cells engineered to quantitatively report fusion with the effector cell. In the protocol described here, Vero cells are transfected with a plasmid encoding the arenavirus envelope glycoprotein complex GPC and infected with the vTF7-3 vaccinia virus expressing the bacteriophage T7 RNA polymerase. These effector cells are mixed with target cells infected with the vCB21R-lacZ vaccinia virus encoding a β -galactosidase reporter under the control of the T7 promoter. Cell-cell fusion is induced upon exposure to low-pH medium (pH 5.0), and the resultant expression of the β -galactosidase reporter is quantitated using a chemiluminescent substrate. We have utilized this robust microplate cell-cell fusion assay extensively to study arenavirus entry and its inhibition by small-molecule fusion inhibitors.

Key words Arenavirus, Envelope glycoprotein, Membrane fusion, Syncytium formation, Cell-cell fusion, Endosome, Fusion inhibitor

1 Introduction

The defining function of the viral envelope glycoprotein is to orchestrate fusion of the viral and cellular membranes, thereby promoting release of the virion core into the cell to initiate viral replication. Classically, enveloped viruses have been subdivided into those that fuse at the plasma membrane in response to receptor binding (such as HIV-1 and the paramyxoviruses) and those that undergo receptor-mediated endocytosis and fuse upon exposure to acidic pH in the maturing endosome. Many of the hemorrhagic fever viruses surveyed in this volume belong to this latter group, with membrane fusion taking place in endosomal and lysosomal compartments, removed from facile experimental manipulation. For the majority of these viruses whose envelope

glycoproteins normally traffic to the cell surface for virion assembly, this process of pH-induced endosomal fusion can be readily studied using the surrogate of cell-cell fusion. First noted as syncytium formation among Sindbis virus-infected cells exposed to acidic pH (“fusion-from-within” [1]), these systems have evolved with emerging technology to serve as robust platforms for structure-function studies of membrane-fusion activity. Modern assays typically utilize effector cells expressing the envelope glycoprotein and target cells engineered to quantitatively report fusion of the two. It is important to bear in mind that these assays do not necessarily recapitulate all aspects of virus entry within the endocytic pathway. Specifically, the possible role of secondary receptors and endolysosomal proteases needs to be considered. Nonetheless, these simple biosafe assays can provide a reliable quantitative read-out of membrane-fusion activity.

We have utilized cell-cell fusion assays extensively to study arenavirus entry and its inhibition by small-molecule fusion inhibitors. Arenaviruses enter the host cell through pH-dependent fusion of the viral and endosomal membranes, a process mediated by the viral envelope glycoprotein complex GPC [2]. GPC is synthesized as a precursor that trimerizes and is cleaved by the cellular S1P/SKI-1 protease [3–5] to generate the mature receptor-binding (GP1) [6, 7] and transmembrane fusion (GP2) [8–11] subunits. Unlike other class I fusion proteins, GPC retains a 58 amino-acid residue signal peptide as a third, noncovalently associated subunit in the mature complex [12–14]. This stable signal peptide (SSP) contains two hydrophobic regions that span the membrane to form a hairpin structure [15], with a central external loop that interacts with the membrane-proximal ectodomain of GP2 to sense acidic pH and trigger membrane fusion [16, 17]. SSP association is also required for transit of the GP1-GP2 precursor through the Golgi, and thus for proteolytic maturation and transport to the cell surface for virion assembly [18]. Several chemically distinct classes of small-molecule fusion inhibitors have been demonstrated to act through the pH-sensing SSP-GP2 interface to antagonize the effect of acidic pH in activating GPC membrane fusion [19].

The GPC-mediated cell-cell fusion assay used in our laboratory was developed through the modification of the recombinant vaccinia virus-based fusion reporter assay described by Nussbaum, Broder, and Berger in 1994 to study HIV-1 Env [20]. In brief, Vero cells are infected with a recombinant vaccinia virus expressing the bacteriophage T7 RNA polymerase and transfected with a pcDNA-based plasmid encoding GPC. These cells are mixed with target cells infected with another recombinant vaccinia virus encoding a β -galactosidase reporter under the control of the T7 promoter. Antiviral drugs are used to block production of progeny vaccinia viruses and thereby prevent cross-infection of effector and target cells. Cell-cell fusion is induced upon exposure of the

coculture to acidic medium (pH 5.0), and the resultant expression of the β -galactosidase reporter is quantitated using a chemiluminescent substrate. A version of this assay that eliminates the use of BSL-2 recombinant vaccinia viruses has also been described [21].

2 Materials

2.1 Cell Culture

1. Vero-76 African green monkey (*Chlorocebus aethiops*) kidney cells (ATCC CRL-1587).
2. Recombinant vaccinia virus vTF7-3 (NIH AIDS Reagent Program, Division of AIDS, NIAID, catalog #356, contributed to the AIDS Reagent Program by Dr. Thomas R. Fuerst and Dr. Bernard Moss; *see Note 1*).
3. Recombinant vaccinia virus vCB21R Lac-Z (NIH AIDS Reagent Program, Division of AIDS, NIAID, catalog # 3365, contributed to the AIDS Reagent Program by Dr. Christopher C. Broder, Paul E. Kennedy, and Dr. Edward A. Berger; *see Note 1*).
4. Falcon™ 96-well clear flat-bottom cell-culture microplates (Corning).
5. Dulbecco's Modified Eagle Medium (DMEM), high glucose, pyruvate (Gibco) is used in a variety of formulations. Growth Medium for the Vero cells is DMEM with 10% heat-inactivated fetal bovine serum (FBS) and 1× L-glutamine. For routine cell passage, we also include 1× Pen Strep. Infection Medium is DMEM with 2% FBS and 1× L-glutamine. Serum-free medium (SFM) contains only the additional 1× L-glutamine. The Post-Transfection Addition medium is prepared using Infection Medium made to 20% FBS and 10 μ M araC. Low-pH Pulse Medium is adjusted to final pH just prior to use and consists of DMEM with 5% FBS, 1× L-glutamine, 10 μ M araC, 100 μ g/ml rifampicin plus 10 mM PIPES, and 10 mM HEPES, prewarmed and titrated to pH 5.0 using concentrated HCl.
6. 10,000 U/ml (100× Pen-Strep) Penicillin-Streptomycin (Gibco).
7. 200 mM (100×) L-Glutamine (Gibco).
8. 0.05% trypsin-EDTA (Gibco).
9. 1 mg/ml poly-D-lysine in H₂O (10× stock) (Sigma).
10. 10× Dulbecco's phosphate-buffered saline (DPBS), no calcium or magnesium (Gibco). Dilute this to make a 1× solution.
11. 10 mM (1000× stock) cytosine β -D-arabinofuranoside (araC) in H₂O (Sigma).
12. 100 mg/ml rifampicin in DMSO (1000× stock) (Sigma).
13. Opti-MEM Reduced Serum Medium (Gibco).

14. Lipofectamine 2000 Transfection Reagent (Invitrogen).
15. 0.5 M PIPES (1,4-piperazinediethanesulfonic acid) brought to pH ~ 7 by titration with concentrated NaOH (Sigma).
16. 1 M HEPES [4-(2-hydroxyethyl)-1-piperazineethanesulfonic acid] (Gibco).
17. Plasmid encoding expression of envelope glycoprotein: For expression of GPC, we typically utilize the minimal T7 promoter present in pcDNA3.1 vectors (Invitrogen) (*see* **Notes 2** and **3**).
18. Monoclonal antibodies to Junin GPC [22] are available through BEI Resources, an NIH/NIAID-funded repository of reagents for biodefense and emerging infectious disease research (www.beiresources.org). We typically use monoclonal antibody QC03-BF11 for immunohistochemical staining of GPC (catalogue # NR-43775).

2.2 Quantitation of β -Galactosidase Fusion Reporter

1. Galacto-Light Plus™ β -Galactosidase Reporter Gene Assay System (Applied Biosystems T1007). This kit contains Lysis Solution, Galacton-Plus substrate, Reaction Buffer Diluent, and light emission Accelerator-II.
2. 96-Well White Opaque Plates (Costar™, Corning).
3. Protease inhibitors (Roche) for use with Galacto-Light Plus Lysis Solution:
 - 1 mg/ml Leupeptin in H₂O (1000× stock).
 - 1 mg/ml Pepstatin in MeOH (1000× stock).
 - 1 mg/ml Aprotinin in H₂O (1000× stock). These three protease inhibitors are added to Lysis Solution just before use to make 1× in each.
4. SpectraMax L microplate Luminometer; 1 channel and at least one injector (Molecular Devices).

3 Methods

3.1 Generation of GPC-Expressing Effector Cells

1. Vero cells are typically split 1:4, and given fresh Growth Medium, one day prior to use in the assay.
2. On Day 1, harvest cells with trypsin-EDTA. Centrifuge and resuspend in Growth Medium without Pen-Strep.
3. Seed 1.5×10^6 cells in 5 ml to a 6 cm culture dish and incubate overnight at 37 °C in a CO₂ incubator. With losses sustained in subsequent steps, one 6 cm dish provides enough effector cells for ~20 cocultures in the 96-well microplate used in the assay. Set up and combine multiple 6 cm dishes if more wells are required for any effector-cell population.
4. Reseed extra cells to a flask for generating target cells on the following day (Subheading 3.2).

5. On Day 2, pretreat effector cells with 10 μM araC for 2 h at 37 $^{\circ}\text{C}$ to block DNA replication and late-gene expression of the vTF7-3 vaccinia virus (*see* **Note 4**). To each 6 cm dish containing 5 ml Growth Medium, add 5 μl of the 1000 \times araC stock and swirl.
6. vTF7-3 is used at a multiplicity of infection (moi) of 2 to infect effector cells. Assuming that the cells have doubled overnight: 3×10^6 cells \times 2 = 6×10^6 pfu vTF7-3 per 6 cm dish. Quickly thaw pre-titered vTF7-3 stock in 37 $^{\circ}\text{C}$ water bath and vortex vigorously to disaggregate.
7. From each 6 cm dish, remove Growth Medium and replace with 750 μl Infection Medium containing additional 10 μM araC and 6×10^6 pfu vTF7-3. Again, vortex vigorously to disaggregate virus. Incubate for 30 min in a CO_2 incubator at 37 $^{\circ}\text{C}$, swirling every 10 min.
8. During incubation with vTF7-3, prepare for plasmid transfection. With our pcDNA3.1-based GPC expression plasmids, we use a total of 2 μg DNA per transfection (2 μg plasmid expressing full-length GPC or a 3:1 mixture of GP1-GP2 and SSP plasmids—*see* **Note 3**). Dilute 2 μg DNA in 500 μl Opti-MEM. Separately, dilute 20 μl Lipofectamine 2000 in 500 μl Opti-MEM and let it sit for 5 min at room temperature. Combine DNA and Lipofectamine 2000 solutions and incubate for 20 min at room temperature.
9. Aspirate vaccinia virus-containing medium from cells and wash twice with serum-free medium. Refeed with 2 ml SFM containing 10 μM araC. Add DNA-Lipofectamine 2000 complex dropwise to culture; rock dish to distribute evenly. Return to incubator for 3 h.
10. After 3 h, add 2 ml of Post-Transfection Addition medium to each dish to bring the final concentration of FBS to 8% and araC to 8 μM . Incubate overnight.

3.2 Generation of Target Cells

1. During the 3 h incubation in transfection medium (Subheading **3.1, step 9**), prepare vCB21R Lac-Z-infected target cells using cells reserved the previous day (Subheading **3.1, step 4**).
2. Harvest cells with trypsin-EDTA, wash with DPBS, and resuspend in SFM to count. Add 5×10^6 cells for each full 96-well microplate to be seeded to a 50 ml conical tube and pellet.
3. Infect cells with vCB21R Lac-Z using an moi of 2: 5×10^6 cells \times 2 = 10^7 pfu. Quickly thaw pre-titered vCB21R Lac-Z stock in 37 $^{\circ}\text{C}$ water bath and vortex vigorously to disaggregate. Resuspend pelleted cells (Subheading **3.2, step 2**) in 1 ml of Infection Medium containing 10^7 pfu vCB21R Lac-Z. Vortex

vigorously. Incubate for 90 min in CO₂ incubator at 37 °C, swirling every 20 min.

4. Fill conical tube with SFM and wash twice by centrifugation to remove free virus. Resuspend cell pellet and adjust to 0.4×10^6 cells/ml in Growth Medium with 100 µg/ml Rifampicin. Seed 100 µl (40,000 cells) per well in a 96-well flat-bottom microplate and culture overnight. Optionally, use poly-D-lysine to precoat wells (*see Note 5*).

3.3 Coculture of Effector and Target Cells

1. On Day 3, harvest effector cells from 6 cm dish (Subheading 3.1, step 10). Remove medium and wash once with 3–5 ml DPBS. Cells could exhibit significant cytopathic effect and may not adhere strongly to the dish (*see Note 5*). Use caution when washing; pipet using the walls of the dish. If some cells are inadvertently dislodged in the DPBS wash, save wash into 15 ml conical collection tube.
2. Remove cells from dish by incubating with 2 ml of pre-warmed 0.5 mM EDTA in DPBS for ~5 min at 37 °C. Gently pipet up and down to disrupt cell clumps and save to collection tube. Rinse dish with DPBS and combine to fill collection tube.
3. Pellet cells and wash in 10 ml SFM before resuspending in 2 ml Growth Medium containing 10 µM araC and 100 µg/ml rifampicin. Adjust to 0.4×10^6 cells/ml.
4. Carefully remove medium from 96-well microcultures containing vCB21R Lac-Z-infected target cells, and add 100 µl of the resuspended effector cells per well (40,000 cells; 1:1 effector cells to target cells) (*see Note 6*).
5. Reseed additional effector cells in a separate microplate to determine transfection efficiency by immunochemical staining. Monoclonal antibodies directed to JUNV GPC typically detect GPC expression in $\geq 70\%$ of the cells. Poor or variable transfection efficiencies will reduce the reliability of the assay.
6. Centrifuge microplate at $\sim 16 \times g$ for 3 min to facilitate cell settling and cell-cell contact. Incubate for 3 h at 37 °C to allow cells to adhere.

3.4 Exposure of Coculture to Acidic pH Medium to Induce Cell-Cell Fusion

1. During the 3-h incubation (Subheading 3.3, step 6), prepare the Low-pH Pulse Medium (*see Notes 7 and 8*).
2. Pipet all medium from cocultures and replace with 100 µl of Pulse Medium, pre-warmed to 37 °C. Tilt plate to ensure all of the neutral medium is removed prior to the addition of the Pulse Medium, and work carefully so that the cell monolayer is neither disturbed nor allowed to dry out.
3. Incubate for 20 min at 37 °C in a CO₂ incubator. In general, maximal cell-cell fusion can be induced using significantly shorter exposures (≥ 5 min).

4. Carefully remove Pulse Medium and replace with 100 μl of Growth Medium containing 10 μM araC and 100 $\mu\text{g}/\text{ml}$ rifampicin.
5. Incubate for 5 h to allow for mixing of cell contents and induction of the β -galactosidase fusion reporter. In some instances, syncytium formation can be detected microscopically within 15 min (*see Note 9*).

3.5 Chemi-luminescence Detection of the β -Galactosidase Fusion Reporter

1. The Galacto-Light Plus™ β -Galactosidase Reporter Gene Assay System is used to detect β -galactosidase expression, as described by the manufacturer.
2. Carefully remove medium from wells and add 60 μl of the kit Lysis Solution to which protease inhibitors have been added.
3. Incubate at room temperature for 10 min, and pipet up and down to ensure complete solubilization.
4. Remove 20 μl to wells in a Corning 3912 96-well white opaque microplate. The remaining lysates can be frozen for back-up analysis. To each well, add 70 μl of the Reaction Buffer Diluent with Galacton-Plus substrate. Incubate in the dark at room temperature for 1 h.
5. Turn on SpectraMax L luminometer and program the following parameters for injection of the kit Accelerator-II enhancer and luminescence detection: room temperature, no shaking, endpoint integration time 1.6 s; P-injector for Accelerator-II, volume 100 μl , delay 1.3 s, speed 270 $\mu\text{l}/\text{s}$.
6. Place white opaque microplate into luminometer, run pre-programmed protocol and record luminescence. Output relative light units (RLUs) can be exported to Excel or GraphPad Prism for subsequent analyses.

3.6 Considerations on Controls, Replicates, and Expected Results

1. A variety of negative controls can be used to establish a “no fusion” background: (1) mock transfection/no envelope glycoprotein, (2) envelope glycoprotein but mock-pulsed with neutral medium, (3) if SSP and the GP1-GP2 precursor are to be co-expressed to reconstitute GPC, SSP can be omitted to block maturation and transport to the cell surface. As illustrated in the example below (Fig. 1), background is typically $\sim 1 \times 10^5$ RLUs relative to the JUNV GPC signal of $\sim 1 \times 10^7$ RLU. The absolute number of RLUs is dependent on the instrument and assay system used. In our hands, the signal from LASV GPC is generally lower ($\sim 2 \times 10^6$ RLU; *see Note 8*).
2. We typically prefer to run six to eight replicate wells, although reliable preliminary information can be obtained using as few as two to three replicates. The range of replicate RLUs should be within twofold (*see Fig. 1*).

no SSP															
– control		wt	mut 1	mut 2	mut 3	mut 4	mut 5	mut 6	mut 7	mut 8	mut 9	mut 10			
		1	2	3	4	5	6	7	8	9	10	11	12		
A	103091	1.14e 7	125915	159998	1.97e 6	385103	134015	137826	123516	1.30e 7	159887	194677			
B	94635	1.19e 7	125700	101773	2.04e 6	395058	83192	141647	144701	1.21e 7	215790	138235			
C	111676	1.18e 7	124831	132428	1.39e 6	208968	116455	132124	134421	1.10e 7	205349	153328			
D	109570	1.14e 7	222897	102430	1.69e 6	133523	142616	138907	158410	1.20e 7	189504	164127			
E	97605	1.12e 7	138323	100044	2.52e 6	169368	137398	143662	110580	1.13e 7	209058	189703			
F	90098	8.51e 6	136721	92916	1.87e 6	257223	95156	116019	121002	1.20e 7	309684	168715			
G	151363	1.18e 7	113362	124743	1.67e 6	382431	115296	103888	148108	1.08e 7	205508	134792			
H	98545	1.31e 7	132575	186031	2.74e 6	330082	140820	126147	118214	1.42e 7	170075	189177			
Mean	107,073	11,390,000	140,041	125,045	1,986,000	282,719	120,619	130,027	132,369	12,060,000	208,107	166,594			
SEM	6,827	459,978	12,162	12,162	159,045	36,957	7,847	4,927	5,923	397,714	16,097	8,275			

Fig. 1 Representative results from cell-cell fusion assays of wild-type (wt) JUNV GPC and 10 SSP mutants (mut 1–10). JUNV GPC was reconstituted by co-expression of SSP and the GP1-GP2 precursor (with CD4 signal peptide), and the assay background was determined by omitting SSP (no SSP, – control). Each column contains eight replicates. Mean values and standard errors of the mean (SEM) are indicated below

4 Notes

1. The recombinant vaccinia viruses vTF7-3 and vCB21R Lac-Z are derived from the non-highly-attenuated WR strain of vaccinia virus. These viruses are handled using Biosafety Level 2 facilities and practices, and prior vaccination is recommended for laboratory workers [23]. We have investigated a version of this assay that does not utilize recombinant vaccinia viruses, using instead T7 polymerase-expressing BHK-21 cells (BSR-T7 [24]) and a T7 promoter-based β -galactosidase expression plasmid [21]. This assay is less robust than the vaccinia virus-based assay and may benefit from further optimization.
2. GPC is very poorly expressed using the human cytomegalovirus immediate-early promoter and enhancer engineered into pcDNA plasmids. By using the vTF7-3 vaccinia virus-encoded T7 polymerase, we take advantage of the strong T7 promoter and the mRNA capping and polyadenylation activities of vaccinia virus for rapid and high-level production of GPC mRNA in the cytoplasm of transfected cells. Any promoter that results in adequate envelope glycoprotein expression should suffice for the assay, although timing may need to be modified to accommodate nuclear expression of the transfected plasmid.
3. SSP can be co-expressed with the GP1-GP2 precursor (directed to the ER via a heterologous signal peptide) to reconstitute the tripartite GPC complex [13, 25]. We utilize the conventional

signal peptide of human CD4. This approach obviates concerns regarding incomplete cleavage of SSP in wild-type and mutant GPCs [12, 14, 26] and generally results in slightly higher levels of membrane-fusion activity than the full-length GPC construct (unpublished).

4. AraC is used with the effector cells to block replication of vaccinia virus DNA, thereby preventing the production of progeny viruses. Similarly, rifampicin is used with target cells to inhibit formation of mature virion particles [27]. Together, these reagents prevent cross-infection between effector and target cells, and hence unwanted fusion-independent expression of the β -galactosidase reporter. Inadequate control of vaccinia virus production is manifest in an elevated background level of β -galactosidase expression. Histochemical staining of test cocultures using X-gal substrate [13] would reveal individual cells with intense color.
5. Vaccinia-infected effector and target cells typically display significant cytopathic effect that can compromise adhesion to the culture substrate. In some cases, precoating the 96-well microculture dish with poly-D-lysine can help. In general, extreme care must be taken in all medium changes of the 96-well microcultures to minimize cell loss. Uneven cell loss between wells will render quantitation of cell-cell fusion difficult.
6. To assess inhibition of cell-cell fusion by small-molecule fusion inhibitors or monoclonal antibodies, serial dilutions of these reagents can be added to the coculture just prior to or with the effector cells. Appropriate dilutions are prepared in separate round-bottom microplates and transferred to the adhered target cells or mixed with effector cells. For tightly bound inhibitors and monoclonal antibodies that target the prefusion form of GPC, the reagent need not be present in the Pulse Medium or subsequently to achieve maximal effect [19]. By contrast, a monoclonal antibody directed to the fusion peptide of JUNV GPC, which is only exposed upon pH-induced fusion activation, needs to be present in the Pulse Medium to inhibit cell-cell fusion [28].
7. The Low-pH Pulse Medium is not strongly buffered and should be prepared just prior to use. Care should be taken to remove all neutral medium from wells prior to the addition of the Pulse Medium to maintain the predetermined pH, while working quickly to prevent cells from drying out.
8. In studies to determine the pH profile for optimal fusion activation, the Pulse Medium can be adjusted within the range of pH 4.0–7.0. We typically use increments of 0.5 pH units. The point of maximal cell-cell fusion by JUNV GPC varies from 5.0 to 5.5 in independent assays. In contrast to published

reports [29], we find that LASV GPC displays the same optimal pH as JUNV GPC [30]. However, cell-cell fusion by LASV GPC appears less robust than that by JUNV GPC, with a ~20-fold dynamic range in this assay relative to the ~100-fold range typically seen with JUNV GPC. This may reflect a requirement by LASV GPC for the interaction with LAMP1 in the endolysosome [31].

9. If the RLU signal is low when assayed after 5 h, extending the coculture overnight may increase β -galactosidase accumulation without an undue increase in background.

Acknowledgments

Our studies of arenavirus membrane fusion and its inhibition have been funded over the past decade by the National Institutes of Health through the following research grants: R21 AI059355, U54 AI065357 (Rocky Mountain Center for Excellence in Biodefense and Emerging Infectious Diseases; John Belisle, Colorado State University), R01 AI074818, R01 AI093387 (Partnerships for Biodefense; Sean Amberg, SIGA Technologies), and R21 AI120490.

References

1. Mann E, Edwards J, Brown DT (1983) Polycaryocyte formation mediated by Sindbis virus glycoproteins. *J Virol* 45:1083–1089
2. Di Simone C, Zandonatti MA, Buchmeier MJ (1994) Acidic pH triggers LCMV membrane fusion activity and conformational change in the glycoprotein spike. *Virology* 198:455–465
3. Lenz O, ter Meulen J, Klenk H-D, Seidah NG, Garten W (2001) The Lassa virus glycoprotein precursor GP-C is proteolytically processed by subtilase SKI-1/S1P. *Proc Natl Acad Sci U S A* 98:12701–12705
4. Beyer WR, Popplau D, Garten W, von Laer D, Lenz O (2003) Endoproteolytic processing of the lymphocytic choriomeningitis virus glycoprotein by the subtilase SKI-1/S1P. *J Virol* 77:2866–2872
5. Kunz S, Edelmann KH, de la Torre J-C, Gorney R, Oldstone MBA (2003) Mechanisms for lymphocytic choriomeningitis virus glycoprotein cleavage, transport, and incorporation into virions. *Virology* 314:168–178
6. Radoshitzky SR, Abraham J, Spiropoulou CF, Kuhn JH, Nguyen D et al (2007) Transferrin receptor 1 is a cellular receptor for New World haemorrhagic fever arenaviruses. *Nature* 446:92–96
7. Cao W, Henry MD, Borrow P, Yamada H, Elder JH et al (1998) Identification of alpha-dystroglycan as a receptor for lymphocytic choriomeningitis virus and Lassa fever virus. *Science* 282:2079–2081
8. York J, Agnihothram SS, Romanowski V, Nunberg JH (2005) Genetic analysis of heptad-repeat regions in the G2 fusion subunit of the Junin arenavirus envelope glycoprotein. *Virology* 343:267–279
9. Eschli B, Quirin K, Wepf A, Weber J, Zinkernagel R et al (2006) Identification of an N-terminal trimeric coiled-coil core within arenavirus glycoprotein 2 permits assignment to class I viral fusion proteins. *J Virol* 80:5897–5907
10. Igonet S, Vaney MC, Vohnrein C, Bricogne G, Stura EA et al (2011) X-ray structure of the arenavirus glycoprotein GP2 in its postfusion hairpin conformation. *Proc Natl Acad Sci U S A* 108
11. Parsy ML, Harlos K, Huiskonen JT, Bowden TA (2013) Crystal structure of Venezuelan hemorrhagic fever virus fusion glycoprotein reveals a

- class I postfusion architecture with extensive glycosylation. *J Virol* 87:13070–13075
12. Eichler R, Lenz O, Strecker T, Garten W (2003) Signal peptide of Lassa virus glycoprotein GP-C exhibits an unusual length. *FEBS Lett* 538:203–206
 13. York J, Romanowski V, Lu M, Nunberg JH (2004) The signal peptide of the Junín arenavirus envelope glycoprotein is myristoylated and forms an essential subunit of the mature G1-G2 complex. *J Virol* 78:10783–10792
 14. York J, Nunberg JH (2007) Distinct requirements for signal peptidase processing and function of the stable signal peptide (SSP) subunit in the Junin virus envelope glycoprotein. *Virology* 359:72–81
 15. Agnihothram SS, York J, Trahey M, Nunberg JH (2007) Bitopic membrane topology of the stable signal peptide in the tripartite Junín virus GP-C envelope glycoprotein complex. *J Virol* 81:4331–4337
 16. York J, Nunberg JH (2006) Role of the stable signal peptide of the Junín arenavirus envelope glycoprotein in pH-dependent membrane fusion. *J Virol* 80:7775–7780
 17. York J, Nunberg JH (2009) Intersubunit interactions modulate pH-induced activation of membrane fusion by the Junin virus envelope glycoprotein GPC. *J Virol* 83:4121–4126
 18. Agnihothram SS, York J, Nunberg JH (2006) Role of the stable signal peptide and cytoplasmic domain of G2 in regulating intracellular transport of the Junin virus envelope glycoprotein complex. *J Virol* 80:5189–5198
 19. York J, Dai D, Amberg SA, Nunberg JH (2008) pH-induced activation of arenavirus membrane fusion is antagonized by small-molecule inhibitors. *J Virol* 82:10932–10939
 20. Nussbaum O, Broder CC, Berger EA (1994) Fusogenic mechanisms of enveloped-virus glycoproteins analyzed by a novel recombinant vaccinia virus-based assay quantitating cell fusion-dependent reporter gene activation. *J Virol* 68:5411–5422
 21. Messina EL, York J, Nunberg JH (2012) Dissection of the role of the stable signal peptide of the arenavirus envelope glycoprotein in membrane fusion. *J Virol* 86:6138–6145
 22. Sanchez A, Pifat DY, Kenyon RH, Peters CJ, McCormick JB et al (1989) Junin virus monoclonal antibodies: characterization and cross-reactivity with other arenaviruses. *J Gen Virol* 70:1125–1132
 23. Centers for Disease Control and Prevention (2009) In: Wilson DE, Chosewood LC (eds) Biosafety in microbiological and biomedical laboratories. HHS, Washington, DC
 24. Buchholz UJ, Finke S, Conzelmann KK (1999) Generation of bovine respiratory syncytial virus (BRSV) from cDNA: BRSV NS2 is not essential for virus replication in tissue culture, and the human RSV leader region acts as a functional BRSV genome promoter. *J Virol* 73:251–259
 25. Eichler R, Lenz O, Strecker T, Eickmann M, Klenk HD et al (2003) Identification of Lassa virus glycoprotein signal peptide as a trans-acting maturation factor. *EMBO Rep* 4:1084–1088
 26. Froeschke M, Basler M, Groettrup M, Dobberstein B (2003) Long-lived signal peptide of lymphocytic choriomeningitis virus glycoprotein pGP-C. *J Biol Chem* 278:41914–41920
 27. Hraby DE, Lynn DL, Kates JR (1980) Identification of a virus-specified protein in the nucleus of vaccinia virus-infected cells. *J Gen Virol* 47:293–299
 28. York J, Berry JD, Ströher U, Li Q, Feldmann H et al (2010) An antibody directed against the fusion peptide of Junin virus envelope glycoprotein GPC inhibits pH-induced membrane fusion. *J Virol* 84:6119–6129
 29. Klewitz C, Klenk HD, ter Meulen J (2007) Amino acids from both N-terminal hydrophobic regions of the Lassa virus envelope glycoprotein GP-2 are critical for pH-dependent membrane fusion and infectivity. *J Gen Virol* 88:2320–2328
 30. Lee AM, Rojek JM, Spiropoulou CF, Gundersen AT, Jin W et al (2008) Unique small molecule entry inhibitors of hemorrhagic fever arenaviruses. *J Biol Chem* 283:18734–18742
 31. Jae LT, Raaben M, Herbert AS, Kuehne AI, Wirchnianski AS et al (2014) Virus entry. Lassa virus entry requires a trigger-induced receptor switch. *Science* 344:1506–1510

Chapter 11

Assays to Assess Arenaviral Glycoprotein Function

Junjie Shao, Xiaoying Liu, Yuying Liang, and Hinh Ly

Abstract

Arenaviruses, such as Lassa virus (LASV) and Pichindé virus (PICV), are enveloped viruses with a bi-segmented ambisense RNA genome. The large (L) genomic segment encodes the Z matrix protein and the L RNA-dependent RNA polymerase, whereas the small (S) genomic segment encodes the nucleoprotein (NP) and the glycoprotein precursor complex (GPC). GPC is processed by signal peptidase in the endoplasmic reticulum into the stable signal peptide (SSP) and GP1/GP2, which is further cleaved by the Golgi-resident subtilisin kexin isozyme-1 (SKI-1)/site-1 protease (S1P) into the cellular receptor-recognition subunit GP1 and the transmembrane subunit GP2, which helps promote the membrane fusion reaction to allow virus entry into the cell. This article describes assays to assess PICV GPC expression, proteolytic processing, fusion function, and GPC-mediated virus-like particle (VLP) entry into cells under tissue-culture conditions.

Key words Arenavirus, Lassa virus (LASV), Pichindé virus (PICV), Glycoprotein precursor complex, GPC, Cell entry, Receptor recognition, Cell membrane fusion

1 Introduction

The first step of arenavirus infection is mediated by cellular attachment and internalization. Arenavirus utilizes its envelop glycoprotein as its receptor-binding protein [1]. During infection of the host cells, arenaviral glycoprotein is expressed as a single polypeptide called glycoprotein precursor complex (GPC), which undergoes cellular proteolytic cleavages, myristoylation, and glycosylation to produce the individual GP1 (cellular receptor-binding subunit), GP2 (membrane fusion subunit), and SSP (stable signal peptide), which together assemble into the mature trimeric complex that is inserted into the membrane of the budding virions [2–7]. The envelope glycoprotein (GPC) mediates entry of the virus into host cell via specific recognition by the different cellular protein receptors. Pathogenic New World arenaviruses (e.g., Junín virus) bind the host cell transferrin receptor 1 (TfR1) through the GP1 receptor-binding subunit of GPC [8, 9], whereas Old World arenaviruses [e.g., LASV and lymphocytic choriomeningitis virus

(LCMV)], as well as several nonpathogenic New World viruses, use the cellular α -dystroglycan protein for uptake into the endosome [10, 11]. Fusion reaction of the viral and cellular membranes is activated by low pH in the endosome and is promoted by the GP2 subunit of GPC [12, 13]. Here, we described several methods to analyze GPC functions, including GPC expression and proteolytic cleavage, pH-dependent membrane fusion, and virus-like particle (VLP) entry into cells under tissue-culture conditions. A comprehensive level of understanding of arenaviral glycoprotein functions will aid in the development of the much needed vaccine and antivirals against deadly human arenaviruses, such as LASV that is responsible for hundreds of thousands of annual human infections and thousands of deaths in several endemic countries in Western Africa [14].

2 Materials

1. Plasmids: pCAGGS-GPC plasmid, which contains the PICV glycoprotein gene; pT7-Fluc contains the Firefly luciferase reporter gene under the T7 promoter (obtained from Jack H. Nunberg, University of Montana); pE-GFP, a lentivirus transfer plasmid containing e-GFP (pHR-CMV-eGFP), lentivirus packaging plasmid (pCMV-dR8.2), lentivirus VSV-G plasmid (pCMV-VSV-G). pCMV-EGFP, a plasmid expressing eGFP under CMV promoter. p β -gal, a plasmid expressing β -gal under CMV promoter.
2. BSRT7-5 cells, obtained from K. Conzelmann at Ludwig-Maximilians-Universität, Germany. These cells were originally derived from BHK-21 cells that were transformed to constitutively express the T7 RNA polymerase [15]. BSRT7-5 cells were cultured in Dulbecco's Modified Eagle Medium (DMEM) supplemented with 10% fetal bovine serum (FBS), 1 mg geneticin per ml, and 50 mg penicillin and streptomycin per ml.
3. 293T cells, a highly transfectable cell line originally derived from human embryonic kidney, were cultured in Dulbecco's Modified Eagle Medium (DMEM) supplemented with 10% fetal bovine serum (FBS), 50 mg penicillin and streptomycin per ml.
4. DMEM (Sigma), MEM (Invitrogen), FBS (Sigma), Penicillin and Streptomycin (Invitrogen), Geneticin (Invitrogen), trypsin-EDTA (Invitrogen), PBS (Sigma).
5. 2 \times Laemmli Sample Buffer (Bio-Rad).
6. Polyacrylamide gel solutions: Resolving gel: 3.3 ml Acrylamide/Bis-acrylamide (30% solution, Sigma), 2.5 ml Resolving buffer (Bio-Rad), 4.1 ml water, 100 μ l 10% SDS, 50 μ l APS (Sigma), 5 μ l TEMED (Sigma). Stacking gel: 1.3 ml

Acrylamide/Bis-acrylamide (30% solution, Sigma), 2.5 ml Stacking buffer (Bio-Rad), 6.1 ml water, 100 μ l 10% SDS, 100 μ l 10% APS (Sigma), 10 μ l TEMED (Sigma).

7. Mini-PROTEAN® Tetra Cell Systems.
8. Molecular weight markers (Bio-Rad).
9. PVDF or Nitrocellulose membranes (Millipore).
10. Tris-buffered saline (TBS) (pH = 7.4, Fisher Scientific).
11. 5% nonfat milk (in TBS).
12. Guinea pig anti-PICV serum.
13. 4% paraformaldehyde (PFA) (Fisher Scientific).
14. IFA blocking buffer: 200 mM glycine, 2% BSA, 2% goat serum in PBS.
15. IRDye-labeled anti-guinea pig antibody (Licor).
16. Firefly luciferase assay kit (Promega) and cell-culture lysis reagent (Promega).
17. Ultracentrifuge (Beckman Coulter).
18. 2.5 M calcium chloride (CaCl_2) (Fisher Scientific).
19. 2 \times HBS: 50 mM HEPES, 280 mM NaCl, 1.5 mM Na_2HPO_4 , pH 7.10.
20. Acidic DMEM (pH 5.0 adjusted by adding HCl) (*see Note 1*).
21. Polybrene, a cationic polymer used to enhance lentiviral transduction (Sigma).
22. Power supply: PowerEase 500 (Thermo Fisher).
23. Trans-blot Turbo Blotting system (Bio-Rad).
24. Odyssey imaging system (Licor).
25. Fluorescence-activated cell sorter (FACS) (Becton Dickinson).
26. Synergy 2 plate reader (BioTeK).
27. Fluorescence microscope (Nikon).
28. Beta-Galactosidase Assay 2 \times Buffer: 200 mM sodium phosphate buffer (pH 7.3), 2 mM MgCl_2 , 100 mM beta-mercaptoethanol, 1.33 mg/ml ONPG.

3 Methods

3.1 Intracellular GPC Expression and Processing

1. Seed 293T cells into 6-well plates at 6×10^5 cells/well with complete DMEM.
2. In the morning of the day of transfection, replace culture medium with an equal aliquot of fresh complete DMEM.
3. Prepare DNA and calcium chloride mix fresh as follows:

2 μ l	pCAGGS-GPC (1 μ g/ μ l).
10 μ l	2.5 M CaCl ₂ .
88 μ l	water.

1–2 h post-medium replacement, add 100 μ l of 2 \times HBS into DNA mix above. Incubate the final DNA mix at ambient temperature for 4 min and then add it dropwise into wells. 6 h post-transfection, replace the medium with fresh complete DMEM and continue to culture in a CO₂ incubator at 37 °C.

- 48 h post-transfection, aspirate the medium, and lyse cells by adding 200 μ l of lysis buffer for 10 min on ice. Concentrate the cell lysates by centrifugation at 15,000 $\times g$ for 3 min, collect the supernatants, and mix them with 2 \times Laemmli Sample Buffer.
- 20 μ l samples were loaded into SDS-PAGE gel with molecular weight marker. The samples were separated at a constant 100 V for 1–1.5 h.
- Transfer the proteins from gel to either nitrocellulose or PVDF membrane by Trans-blot Turbo Blotting system (Bio-Rad) following the manufacturer's instructions.
- Block the membrane with 5% nonfat milk-TBS for 1 h at ambient temperature and then incubate it with guinea pig anti-PICV serum overnight at 4 °C. The next day, wash the membrane in TBS three times and incubate with IRDye-labeled anti-guinea pig antibody for 1 h at ambient temperature. Then wash the membrane with TBS three times at ambient temperature and then scan and analyze it with an Odyssey imaging system (*see Note 2*).

3.2 Cell-Surface GPC Expression

- Follow steps 1–3 of Subheading 3.1.
- 48 h post transfection, the cell medium was aspirated off, and cells were washed once with PBS. Then, the cells were trypsinized with trypsin-EDTA and concentrated by centrifugation at 120 $\times g$ for 5 min. The cells were washed once with PBS.
- Fix the cells with 4% PFA for 5 min. Wash the cells once with PBS and block them with IFA-blocking buffer for 1 h at 4 °C. Then incubate the cells with guinea pig anti-PICV serum overnight at 4 °C.
- The following day, wash cells with PBS three times and incubate with Alexa Fluor® 488 dye-labeled goat anti-guinea pig antibody for 1 h at ambient temperature. Wash cells with PBS three times and analyze by FACS (*see Note 3*).

3.3 GPC

Fusion Assays

3.3.1 eGFP-Based Assay

1. 293T cells were seeded for 18–24 h before transfection in a 12-well plate at a density of 3×10^5 cells/well. 1–2 h before transfection, the medium was replaced by fresh complete DMEM.
2. Prepare DNA and calcium chloride mix as follows:

2 μ l	pCAGGS-GPC (1 μ g/ μ l).
1 μ l	pCMV-EGFP (1 μ g/ μ l).
5 μ l	2.5 M CaCl ₂ .
42 μ l	nuclease-free water.

1–2 h after medium replacement, 100 μ l of 2 \times HBS was added into DNA mix above. The final mix was incubated at ambient temperature for 4 min and then dropwise added into wells. 6 h post transfection, the medium was replaced by a fresh aliquot of complete DMEM and continued to culture in CO₂ incubator at 37 °C.

3. 36 h post transfection, replace the medium with acidic DMEM (pH = 5.0) (*see Note 1*), incubate cells for 5 min at 37 °C, in a CO₂ incubator, and replace with an aliquot of complete DMEM for an additional 12 h of incubation at 37 °C.
4. 48 h post transfection, the supernatants were aspirated off, and cells were washed once with PBS. 4% PFA was used to fix the cells for 5 min. Cells were washed once with PBS.
5. Cells were analyzed by fluorescence microscopy (*see Note 4*).

3.3.2 Luciferase-Based Assay

1. 293T cells were seeded into 12-well plates at 3×10^5 cells/well with complete DMEM.
2. In the morning of the day of transfection, culture medium was replaced by an equal aliquot of fresh complete DMEM.
3. Prepare DNA and calcium chloride mix as follows:

2 μ l	pCAGGS-GPC (1 μ g/ μ l).
1 μ l	pT7-Fluc (100 ng/ μ l).
1 μ l	p β -gal (50 ng/ μ l).
5 μ l	2.5 M CaCl ₂ .
41 μ l	nuclease-free water.

1–2 h after medium replacement, 100 μ l of 2 \times HBS was added into DNA mix above. The final mix was incubated at ambient temperature for 4 min and then dropwise added into wells. 6 h post transfection, the medium was replaced by a fresh aliquot of complete DMEM and continued to culture in CO₂ incubator at 37 °C for 18 h.

4. 24 h post transfection, 293T cells were mixed with BSR-T7 cells (at 1:1 ratio) in 12 wells and cultured for 12 h. 36 h post transfection, the medium of the mixed cells was replaced with acidic DMEM (pH = 5.0) (*see Note 1*) and incubated for 5 min and then replaced by fresh complete DMEM for additional 12 h of culturing.
5. 48 h post transfection, the supernatants were aspirated off, and cells were washed once with PBS. Cells were lysed with cell-culture lysis reagent.
6. The firefly luciferase was analyzed by firefly luciferase assay kit according to the manufacturer's instructions. Briefly, 20 μl of cell lysis was mixed with 100 μl of firefly luciferase assay reagent in 96-well plates. The light production was measured by a plate reader (*see Note 5*). To measure the transfection efficiency, 50 μl of cell lysis was mixed with 50 μl of Beta-Galactosidase Assay 2 \times Buffer for 10 min and the reaction was stopped by adding 150 μl of 1 M Tris-HCl (pH = 8.0). Use the plate reader to analyze the samples at the absorbance of 420 nm. The fusion activity was calculated by taking the ratio of firefly luciferase over beta-gal activities.

3.4 GPC-Mediated Virus-Like Particle (VLP) Entry Assay

3.4.1 GPC VLP Production

1. 293T cells were seeded into 10 cm dish at 3×10^6 cells/dish with complete DMEM.
2. In the morning of the day of transfection, culture medium was replaced by an equal aliquot of fresh complete DMEM.
3. Prepare DNA and calcium chloride mix as follows:

100 μl of DNA mix (for one 6-well plate transfection) contains:	
5 μl	pCAGGS-GPC (1 $\mu\text{g}/\mu\text{l}$).
10 μl	lentivirus packaging plasmid (1 $\mu\text{g}/\mu\text{l}$).
15 μl	pHR'-eGFP (1 $\mu\text{g}/\mu\text{l}$).
50 μl	2.5 M CaCl_2 .
420 μl	nuclease-free water.

- 1–2 h after medium replacement, 500 μl of 2 \times HBS was added into the DNA mix above. The final mix was incubated at ambient temperature for 4 min and then dropwise added into dish. 6 h post-transfection, the medium was replaced by fresh complete DMEM and cultured in CO_2 incubator at 37 $^\circ\text{C}$ for 48 h.
4. 48 and 72 h post-transfection, supernatants were collected and filtered through a 0.45 μm filter and then concentrated by ultracentrifuge at $140,000 \times g$ for 2 h. The concentrated VLPs were resuspended in 300 μl PBS and stored at -80°C .

3.4.2 GPC-Mediated VLP Entry Assay

1. 293T cells were seeded in a 12-well plate at 2×10^5 cells/well with complete DMEM.
2. 16–20 h after seeding, the cell medium was replaced with a fresh aliquot of complete DMEM. Concentrated VLP (100 μ l) (*see* Subheading 3.4, **step 1** above) was mixed with 8 μ g polybrene and dropwise added into wells.
3. 6–8 h post transduction, the cell medium was replaced with a fresh aliquot of the complete DMEM.
4. 48 h post transduction, the cell medium was aspirated off, and cells were washed once with PBS. Then, the cells were trypsinized with trypsin-EDTA and concentrated by centrifugation at $120 \times g$ for 5 min. The cells were washed with PBS once and fixed with 4% PFA for 5 min. The cells were washed once with PBS and then analyzed by microscopy (*see* **Note 6**) or by FACS (*see* **Note 7**).

4 Notes

1. Arenavirus GPC-mediated membrane fusion is pH-dependent. It is critical to prepare acidic DMEM media with accurate pH by using a pH meter.
2. Western blots were used to monitor PICV GPC expression and processing into GP1 and GP2 (Fig. 1). The full-length GPC precursor is approximately 70 kDa, whereas the processed gene products are 37 kDa and 35 kDa, respectively. The higher than expected molecular weight of the proteins based on their amino acid compositions and the fuzziness of the bands are due to different amounts of N-linked glycosylation.

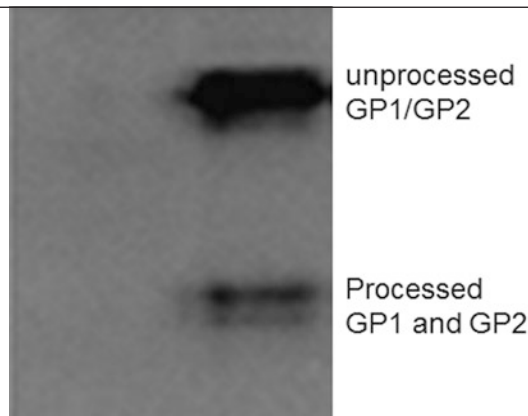


Fig. 1 Western blot showing PICV GPC expression and proteolytic processing. *Left lane* contains cell lysate of the mock transfection with an empty plasmid. *Right lane* shows the unprocessed GP1/2 (*top band*) and processed GP1/GP2 (*bottom bands*)

3. Flow cytometry was used to detect PICV GP expression on the cell surface (Fig. 2). A typical transfection resulted in 44% of the cells expressing GP on their surfaces.
4. GPC fusion function was assessed by the observation of syncytia in cell culture. Fig. 3A shows eGFP-expressing cellular syncytia formation in GPC-transfected cells (right panel) but not in mock-transfected cells (left panel).
5. GPC fusion function was assessed by the detection of luciferase in cells. Fig. 3B shows T7 promoter-driven Fluc expression, which indicates the GP-mediated cell-cell fusion between 293T cells and the BSR-T7 cells.

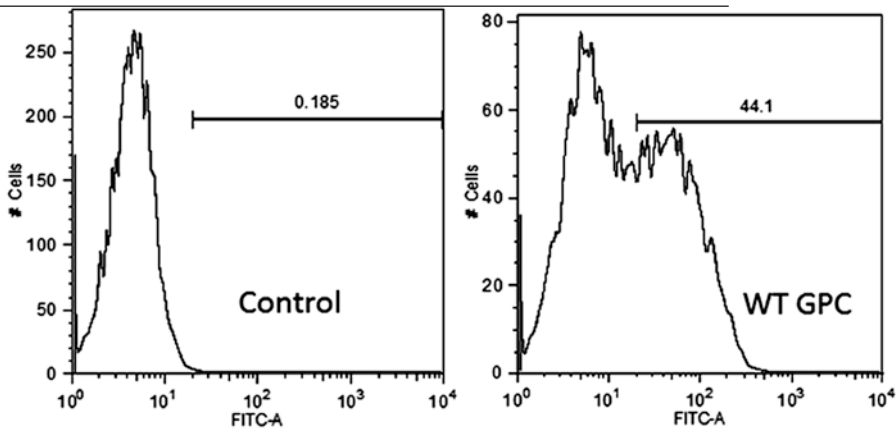


Fig. 2 GPC cell surface expression analysis. FACS analysis shows virtually no GPC expression on the surface of the mock-transfected 293T cells as a control (*left panel*) and 44.1% of GPC expression on the surface of 293T cells transfected with a plasmid expressing the GPC (*right panel*)

a

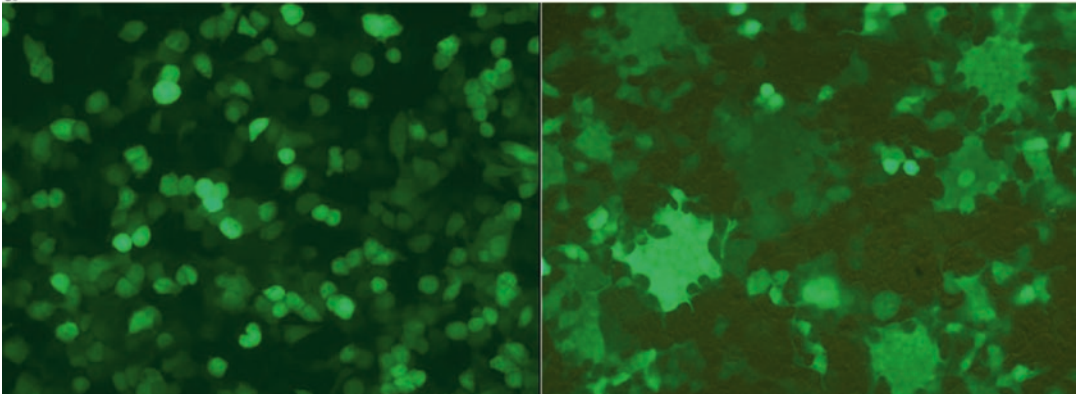


Fig. 3 (A) GPC fusion function. *Right panel* shows syncytia of cells expressing eGFP under the condition of GPC gene expression. *Left panel* is a negative control that shows no evidence of cell-to-cell membrane fusion

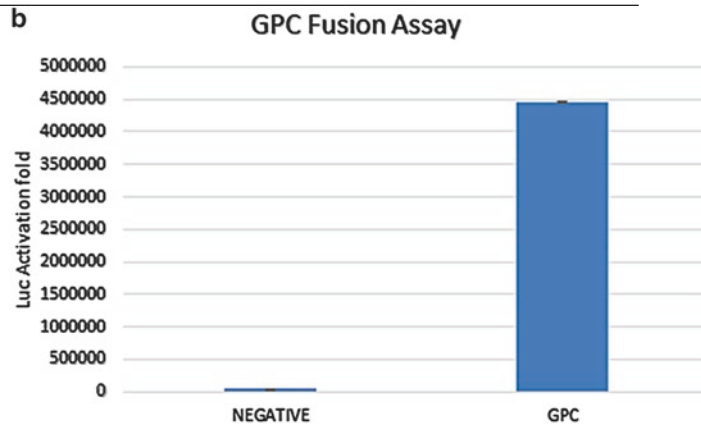


Fig. 3 (B) GPC fusion function. Luciferase assays show no activity in the empty-plasmid-transfected (negative) control cells, whereas high luciferase activity in cells that have been fused as a result of GPC expression

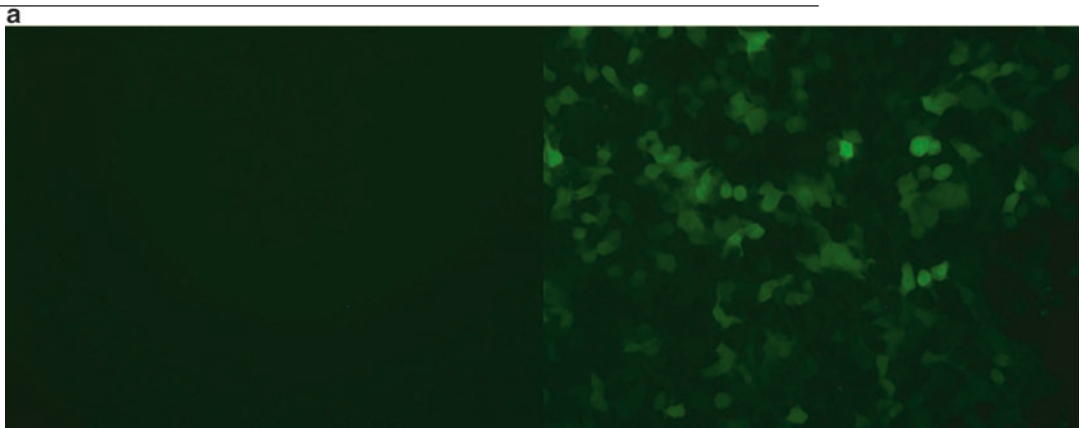


Fig. 4 (A) GPC-mediated VLP entry. Fluorescence microscopy shows no eGFP expression in control 293T cells that have been mock-transduced (*left*), and high eGFP expression in 293T cells that have been infected with VLPs carrying the GPC (*right*)

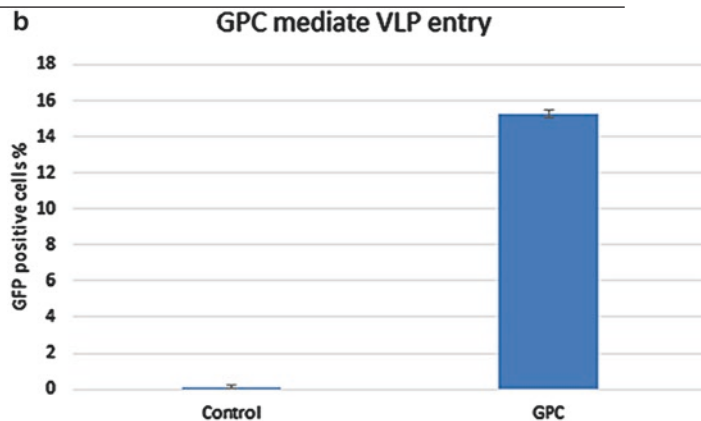


Fig. 4 (B) GPC-mediated VLP entry. FACS analysis shows no eGFP expression in control 293T cells that have been mock-transduced, and high eGFP expression in 293T cells that have been infected with VLPs carrying the GPC

6. GP-mediated VLP entry was monitored by microscopy of eGFP expression in infected cells (Fig. 4A).
7. VLP entry could also be monitored by flow cytometry showing the percentage of eGFP-positive cells (Fig. 4B).

Acknowledgments

This work was supported in part by the NIAID/NIH through the new-direction awards mechanism of the SERCEB grant (U54-AI057157) to YL and HL, and by the NIAID/NIH R01 grants AI083409 to YL and AI093580 to HL.

References

1. Salvato MS, Clegg JCS, Buchmeier MJ, Charrel RN, Gonzalez JP, Lukashevich IS, Peters CJ, Romanowski V (2011) In: King AM, Lefkowitz E, Adams MJ, Carstens EB (eds) Ninth report of the international committee on taxonomy of viruses. Elsevier Academic Press, London
2. Borrow P, Oldstone MB (1992) Characterization of lymphocytic choriomeningitis virus-binding protein(s): a candidate cellular receptor for the virus. *J Virol* 66:7270–7281
3. Lenz O, ter Meulen J, Klenk HD, Seidah NG, Garten W (2001) The Lassa virus glycoprotein precursor GP-C is proteolytically processed by subtilase SKI-1/S1P. *Proc Natl Acad Sci U S A* 98:12701–12705
4. Beyer WR, Popplau D, Garten W, von Laer D, Lenz O (2003) Endoproteolytic processing of the lymphocytic choriomeningitis virus glycoprotein by the subtilase SKI-1/S1P. *J Virol* 77:2866–2872
5. Kunz S, Edelmann KH, de la Torre JC, Gorney R, Oldstone MB (2003) Mechanisms for lymphocytic choriomeningitis virus glycoprotein cleavage, transport, and incorporation into virions. *Virology* 314:168–178
6. Eichler R, Lenz O, Strecker T, Eickmann M, Klenk HD, Garten W (2003) Identification of Lassa virus glycoprotein signal peptide as a trans-acting maturation factor. *EMBO Rep* 4:1084–1088
7. York J, Romanowski V, Lu M, Nunberg JH (2004) The signal peptide of the *Junin arenavirus* envelope glycoprotein is myristoylated and forms an essential subunit of the mature G1-G2 complex. *J Virol* 78:10783–10792
8. Abraham J, Kwong JA, Albarino CG, Lu JG, Radoshitzky SR, Salazar-Bravo J, Farzan M, Spiropoulou CF, Choe H (2009) Host-species transferrin receptor 1 orthologs are cellular receptors for nonpathogenic new world clade B arenaviruses. *PLoS Pathog* 5:e1000358
9. Radoshitzky SR, Abraham J, Spiropoulou CF, Kuhn JH, Nguyen D, Li W, Nagel J, Schmidt PJ, Nunberg JH, Andrews NC, Farzan M, Choe H (2007) Transferrin receptor 1 is a cellular receptor for New World haemorrhagic fever arenaviruses. *Nature* 446:92–96
10. Spiropoulou CF, Kunz S, Rollin PE, Campbell KP, Oldstone MB (2002) New World arenavirus clade C, but not clade A and B viruses, utilizes alpha-dystroglycan as its major receptor. *J Virol* 76:5140–5146
11. Cao W, Henry MD, Borrow P, Yamada H, Elder JH, Ravkov EV, Nichol ST, Compans RW, Campbell KP, Oldstone MB (1998) Identification of alpha-dystroglycan as a receptor for lymphocytic choriomeningitis virus and Lassa fever virus. *Science* 282:2079–2081
12. Di Simone C, Zandonatti MA, Buchmeier MJ (1994) Acidic pH triggers LCMV membrane fusion activity and conformational change in the glycoprotein spike. *Virology* 198:455–465
13. York J, Agnihotram SS, Romanowski V, Nunberg JH (2005) Genetic analysis of heptad-repeat regions in the G2 fusion subunit of the *Junin arenavirus* envelope glycoprotein. *Virology* 343:267–274
14. McLay L, Ansari A, Liang Y, Ly H (2013) Targeting virulence mechanisms for the prevention and therapy of arenaviral hemorrhagic fever. *Antiviral Res* 97:81–92
15. Buchholz UJ, Finke S, Conzelmann KK (1999) Generation of bovine respiratory syncytial virus (BRSV) from cDNA: BRSV NS2 is not essential for virus replication in tissue culture, and the human RSV leader region acts as a functional BRSV genome promoter. *J Virol* 73:251–259

Chapter 12

Expression and X-Ray Structural Determination of the Nucleoprotein of Lassa Fever Virus

Xiaoxuan Qi, Wenjian Wang, Haohao Dong, Yuying Liang, Changjiang Dong, and Hinh Ly

Abstract

We describe methods to express the nucleoprotein (NP) of Lassa fever virus (LASV) in *E. coli*, to purify and crystallize it using the sitting-drop vapor diffusion method. The crystals were screened using Rigaku micro-007 X-ray generator and a dataset was collected at a resolution of 2.36 Å. The crystals belong to space group P3, with the unit cell parameters $a = b = 176.35$ Å, $c = 56.40$ Å, $\alpha = \beta = 90^\circ$, and $\gamma = 120^\circ$. Using the X-ray diffraction method, we constructed a three-dimensional structure of the LASV NP that should aid in the development of novel therapeutic strategies against this virus, for which vaccine and effective treatment modalities are currently unavailable.

Key words Lassa virus, Nucleoprotein, X-ray structure, Large-scale expression, Arenavirus

1 Introduction

Arenaviruses are enveloped, single-stranded ambisense RNA viruses that are geographically, phylogenetically, and serologically divided into two subgroups, the New World and the Old World viruses [1]. Lassa virus (LASV) is an Old World member of the *Arenaviridae* family. It causes Lassa fever (LF), which is an endemic disease in Western African countries like Nigeria, Guinea, Liberia, and Sierra Leone. Lassa fever causes up to 500,000 infections per year and 5000 deaths annually in endemic areas [2]. With the ease of modern means of traveling, Lassa cases have also been reported in America, Europe, Canada, and Japan [3, 4]. Due to the high mortality rate, the ease of human-to-human transmission, and the lack of effective treatments, the Lassa fever virus is categorized by the US Centers for Disease Control and Prevention (CDC) as a Category A Agent, which requires its handling in proper biocontainment (BSL-4) facility and implicates it as a potential bioterror agent [5].

The LASV genome comprises a small RNA segment of 3.4 kb (S-RNA) and a large RNA segment of 7.2 kb (L-RNA). Each segment is reported to encode two viral genes separated by an intergenic region. The S-RNA encodes the nucleoprotein (NP, 64 kDa) and a glycoprotein precursor complex GPC, which is cleaved into two viral glycoproteins GP1 (42 kDa) and GP2 (38 kDa) by the cellular SKI-1/SIP subtilase [6]. The L-RNA encodes the RNA-dependent RNA polymerase (L, 200 kDa) and a small RING finger protein (Z, 11 kDa).

The NP protein interacts with the viral RNA forming a ribonucleoprotein (RNP) complex, which is required for viral RNA transcription and replication. In addition, the NP protein from Lassa fever virus is reported to interact with the Z protein, and possibly also with host cell factors to regulate human immune responses to viral infection [7, 8]. Studies from our laboratory and others have recently shown that LASV NP contains 3'-5' exoribonuclease function that degrades potential pathogen-associated molecular pattern (PAMP) RNAs and results in the suppression of the host's innate immunity [9–11]. With NP playing many crucial roles in mediating virus and host cellular functions, understanding the structure and function of this protein will greatly facilitate the development of therapeutic strategies against this and other deadly viruses in this family. Here, we describe detailed methods of expression, purification, and structural determination of the LASV NP.

2 Materials

2.1 Plasmids and Bacterial Cells

1. pLOU3 vector, which is a derivative plasmid of the pMAL-C4X vector (New England Biolab), contains the LASV NP gene. In this construct, the NP gene is cloned immediately downstream of the Tobacco Etch virus (TEV) proteinase cleavage site, which is preceded by a 6His-tag at the N-terminus of the maltose binding protein (MBP). This protein expression cassette is placed under the control of an isopropyl- β -D-thiogalactopyranoside (IPTG)-inducible (*lacIq*) promoter.
2. *E. coli* Rosetta strain, expressing codons abundant in humans, was transformed with recombinant plasmids.
3. Bacterial growth medium is Luria Broth (LB) with antibiotics: LB liquid medium with 50 μ g/ml Ampicillin and 34 μ g/ml Chloramphenicol.
4. IPTG is a structural mimic of galactose and binds to the Lac Repressor to induce Beta-galactosidase or the protein expression cassette, MBP—TEV cleavage—NP_{LASV}, described in Subheading 2.1, item 1.

5. Amylose-binding buffer: 10% glycerol, 20 mM Tris pH 7.5, 0.2 M NaCl, 1 mM EDTA is supplemented with 2 protease inhibitor tablets, 1 μ M DNase, and 1 mM phenylmethylsulfonyl fluoride (PMSF).

2.2 Protein Expression and Purification

1. Shaker-incubator (Multitron standard, INFORS HT) for growth of bacteria.
2. Spectrophotometer (SmartSpec 3000).
3. High-performance centrifuge (Beckman J-20 Avanti™).
4. *E. coli* cell disruptor (Ts series 1.1 KW and Constant Systems LTD).
5. Amylose resin for affinity isolation of proteins bound to Maltose Binding Protein.
6. Amylose-binding buffer: 1/50 PBS, 50 mM Tris-HCl, 0.5 mM EDTA, 1 mM DTT, 0.3 M NaCl, 10% glycerol.
7. Amylose elution buffer: 10% glycerol, 20 mM Tris pH 7.5, 0.2 M NaCl, 1 mM EDTA, and 10 mM Maltose.
8. 3 mg/ml TEV protease for cleaving the expressed protein.
9. TEV cleavage buffer: 1/50 PBS, 50 mM Tris-HCl, 0.5 mM EDTA, 1 mM DTT, 0.3 M NaCl, and 10% glycerol. This is used with the Desalting column (Hiprep 26/10).
10. ÄKTA purifier 10, a rapid protein liquid chromatography system.
11. 96-Deep-well block for fraction collection.
12. Gel filtration column (Hiload 16/600 Superdex 200).
13. Gel filtration buffer: 20 mM Tris pH 7.5, 0.3 M NaCl, 10% glycerol.
14. -80 °C freezer (U535 Innova).
15. Mass spectroscopy (Q-Star MS/MS micromass MALDI-TOF).
16. Precast electrophoresis gels (NuPAGE 4–12% Bis-Tris gels).
17. 20 \times electrophoresis running buffer (NuPAGE®MES, NP0002).
18. Electrophoresis power supply (PowerEase 500).
19. SDS-PAGE unstained protein standards (Mark12).
20. Coomassie stain (SimplyBlue™ Safe stain).
21. Microwave oven.

2.3 Crystallization and Crystal Screening

1. Crystallization conditions were screened on 2-well MRC plates (SW2T-PS/1-100) with the sitting drop vapor diffusion method.
2. The crystallization drops were built using protein crystallization robot Honeybee system (model 961, Isogen Life Sciences).

3. Crystallization screen PEG/ION (# HR2-126, Hampton Research).
4. Lithium-Polyethylene glycol (Li-PEG) solutions for protein crystallization were #1Li-PEG: 0.2 M LiCl, 20% PEG3350 at 20 °C. After optimization, hexagonal prism crystals were grown in #2Li-PEG: 0.2–0.3 M LiCl and 12–16% PEG3350 at 20 °C. For cryopreservation of crystals we used #3Li-PEG:15% glycerol, 0.2 M LiCl, 16% PEG3350.

2.4 X-Ray Diffraction

1. MicroMax-007 HFM fine focus X-ray generator and the CCD detector Saturn 944+ (Rigaku).
2. ACTOR™ crystal sample changing robot (Rigaku).
3. The data were indexed and scaled using HKL2000 package [12].

3 Methods

3.1 Protein Expression and Purification

1. The recombinant plasmid was transformed into *E. coli* Rosetta strain using the conventional heat-shock transformation method [13].
2. A single bacterial colony was picked and inoculated into 500 ml LB growth medium.
3. Cells were incubated at 37 °C in a shaker-incubator with constant agitation at 200 rpm overnight.
4. The overnight culture was then transferred into 10 l of the LB bacterial growth medium.
5. The culture was incubated at 37 °C with shaking at 200 rpm for about 2 h.
6. The expression of the recombinant NP protein was induced by the addition of IPTG to a final concentration of 0.03 mM when the OD₆₀₀ of the cell culture reached 0.6 (*see Note 1*).
7. The cell culture was kept at 20 °C overnight with shaking at 200 rpm (*see Note 1*).
8. Cells were harvested by centrifugation at 8000 × *g* for 10 min at 4 °C in the J-20 centrifuge.
9. The cell pellet collected from 10 l culture was resuspended in 100 ml of Amylose-binding buffer.
10. Cells were lysed by a cell disruptor at 30 KPsi.
11. The sample was centrifuged in the J-20 centrifuge at maximum speed of 48,254 × *g* for 30 min to remove cellular debris.
12. The supernatant was applied onto the amylose resin column.
13. The column was washed using a 10-column volume of the Amylose-binding buffer (*see Note 2*).

14. The fusion protein was eluted from the column with the Amylose elution buffer.
15. The protein elution buffer was changed to TEV cleavage buffer using the Hiprep desalting column.
16. Fractions containing HisMBP-NP were pooled and the fusion protein was cleaved by incubating with 1 ml His-tagged TEV protease at room temperature overnight (*see* **Notes 2** and **3**).
17. The sample was then applied onto the amylose resin again to remove the MBP.
18. Figure 1 shows the whole protein lysate that contains the Lassa NP-MBP fusion protein, MBP-NP fusion protein purified through the amylose column, and the NP protein after it has been cleaved off from the MBP-NP fusion protein by the Tev proteinase.
19. The flow-through sample was concentrated into 5 ml and applied onto a Hiload 16/600 Superdex 200 gel filtration column, which was equilibrated using the gel filtration buffer and the ÄKTA purifier 10 chromatography system.

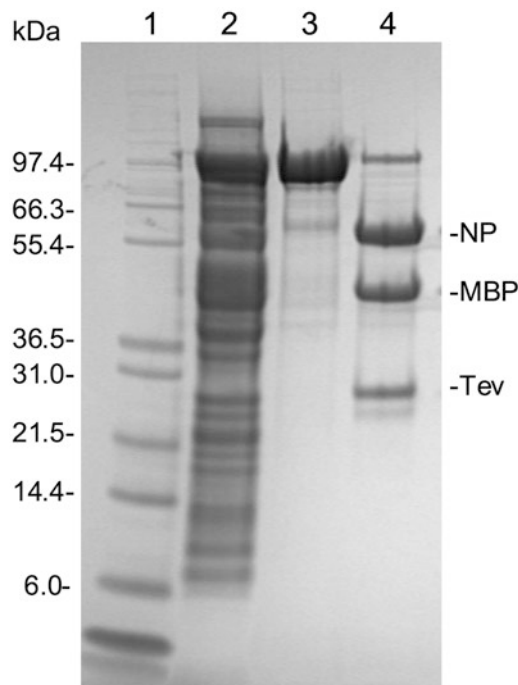


Fig. 1 MBP-NP fusion was purified with an amylose column and the fusion protein was cleaved by Tev proteinase. *Lane 1* is protein molecular weight standard; *Lane 2* shows whole protein lysate of the supernatant; *Lane 3* shows MBP-NP fusion purified by the amylose column; *Lane 4* shows NP protein that is cleaved from the MBP-NP fusion protein by the Tev proteinase

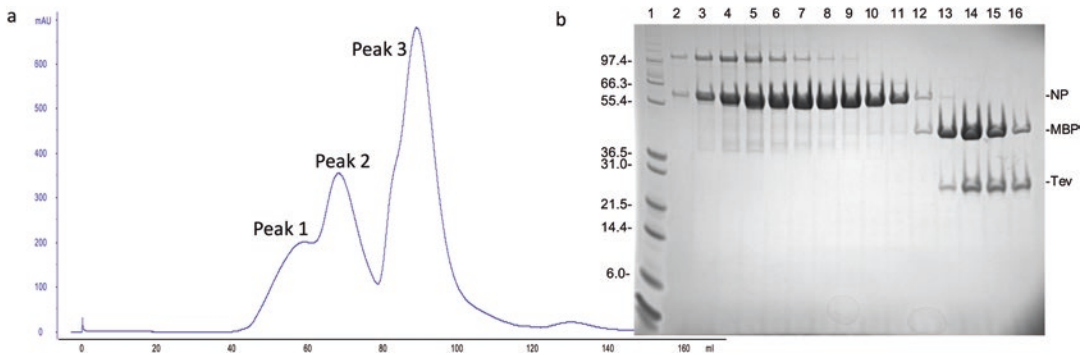


Fig. 2 LASV NP protein was purified by the gel filtration column. (a) Photograph of the gel filtration profile. There are three major peaks: *peak 1* shows aggregation of NP proteins, *peak 2* shows the NP protein alone, and *peak 3* shows NP fusion with MBP. (b) Protein purity was checked by SDS-PAGE electrophoresis. Lane 1, protein molecular weight standard; Lanes 2–6 are elution samples from *peak 1*; Lanes 7–11 are elution samples from *peak 2*; Lanes 12–16 are elution samples from *peak 3*

20. Figure 2 shows Lassa NP protein purified by gel filtration column to homogeneity.
21. The flow rate was 1 ml/min controlled by the ÄKTA purifier 10, and protein peaks were monitored at optical density 280 nm.
22. All elution solutions were collected by the fraction collection of the ÄKTA purifier 10 using the 96-deep-well block.
23. The fractions containing purified NP protein were pooled and concentrated to 7 mg/ml and stored in a -80°C freezer.
24. The protein's identity and integrity were checked by mass spectroscopy and separated by SDS-PAGE.
25. The SDS-PAGE were carried out using precast gels and the PowerEase 500 power supply according to the manufacturer's instruction.
26. The protein molecular marker was used to size the recombinant protein.
27. The SDS-PAGE gels were stained with Coomassie for 10 min.
28. The SDS-PAGE gels were destained by putting the gels in a beaker with water and by boiling for 5 min using a conventional microwave oven.

3.2 Crystallization

1. Crystallization conditions were screened on 2-well plates with the sitting drop vapor diffusion method.
2. The drops were built with $0.15\ \mu\text{l}$ of the protein and $0.15\ \mu\text{l}$ of the mother liquid using two different protein concentrations (7 mg/ml and 3.5 mg/ml), with $100\ \mu\text{l}$ of mother liquid in each reservoir.

3. The initial crystals were formed in #1Li-PEG solution at 20 °C after 7 days. After optimization, hexagonal prism crystals were grown in #2Li-PEG solution at 20 °C for 5 days.
4. Figure 3 shows the purified NP forming crystals with a dimension of 0.2 × 0.2 × 0.6 mm, which are suitable for X-ray diffraction. In order to confirm that the crystals contain the full-length NP protein, a single crystal was picked up and washed three times in the cryoprotectant solution, and dissolved in SDS-loading buffer for SDS-PAGE analysis. The result showed that there was a single band corresponding to the full-length NP protein, implicating its absolute purity and integrity.

3.3 X-Ray Data Collection

1. The crystals were cryoprotected with #3Li-PEG.
2. The crystals were screened using the Rigaku X-ray generator, detector, and robot.
3. One of the crystals was selected and the data generated from it were collected at oscillation angle 0.1° and 100 s exposure per frame with 60 mm of distance from crystal to detector, using the Cu radiation with the wavelength of 1.5418 Å.
4. A total of 1000 frames were reordered. The data were indexed and scaled as described [12] and Table 1.
5. Figure 4 shows the three-dimensional structure of the LASV NP that was built using ARP/wARP automatically and Coot by hands (*see Note 4*).

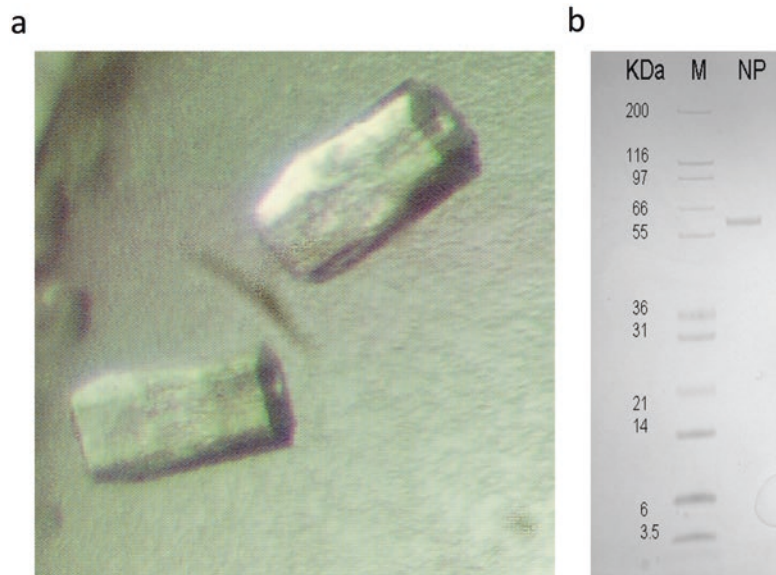


Fig. 3 Photograph of crystals of Lassa NP protein and SDS-PAGE photograph of the NP from the crystals. **(a)** Crystals of the NP protein. **(b)** SDS-PAGE of the NP from the crystals. *Lane 1* shows the protein molecular weight standard; *Lane 2* shows the NP from the crystals

Table 1**Data collection and structure determination statistics**

Data collection	In house data collection	Samarium peak	Samarium inflection	Samarium remote	Native data
Wavelength (Å)	1.5418	1.83	1.84	1.45	0.979
Resolution (Å)	50–2.36 (2.40–2.36)	57.86–2.50 (2.53–2.50)	57.95–2.50 (2.53–2.50)	58.00–2.50 (2.53–2.50)	47.63–1.80(1.81–1.80)
Space group	P3	P3	P3	P3	P3
Cell dimensions (Å, °)	a = b = 176.35, c = 56.40; $\alpha = \beta = 90, \gamma = 120$	a = b = 176.75, c = 56.35; $\alpha = \beta = 90, \gamma = 120$	a = b = 177.01, c = 56.45; $\alpha = \beta = 90, \gamma = 120$	a = b = 177.20, c = 56.54; $\alpha = \beta = 90, \gamma = 120$	a = b = 177.16, c = 56.49; $\alpha = \beta = 90, \gamma = 120$
Unique reflections	41,405 (1998)	68,131(2042)	68,424(2029)	68,691(2057)	184,629(5543)
Redundancy	5.4 (3.9)	5.5(5.4)	5.5(5.4)	5.6(5.5)	5.6(5.5)
Completeness (%)	99.7 (97.1)	100(100)	100(100)	100(100)	99.7(99.0)
I/ σ (I)	27.6 (7.2)	15.3(4.0)	13.6(2.6)	15.5(3.3)	16.4(4.2)
R _{merge}	0.057 (0.166)	0.062(0.342)	0.066(0.541)	0.06(0.433)	0.073(0.393)
Anomalous completeness		97.1(92.6)	97.1(93.2)	99.1(97.4)	
Structure refinement					
R _{factor}					0.1781
R _{free}					0.2014
Rmsd bonds (Å) / Angles(°)					0.04/2.62
					96.83
PDB code					3MWP

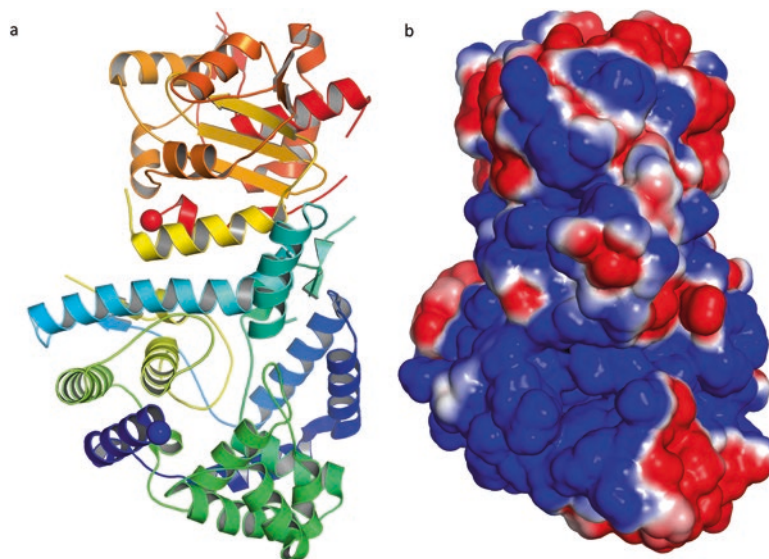


Fig. 4 Three-dimensional structure of LASV NP. **(a)** The protomer structure of NP presented in cartoon. **(b)** Electrostatic potential map of the protomer structure of NP

4 Notes

1. It is important to express the MBP-NP fusion protein at 20 °C, and to use 0.03 mM IPTG concentration for the induction as this condition will produce more soluble MBP-NP fusion protein. Using higher IPTG or higher temperature for protein expression will produce more MBP-NP fusion into inclusion bodies.
2. In all the sample buffer and purification buffers, 10% glycerol is required to stabilize the protein in the buffers.
3. It is important to use TEV proteinase at 1:500 ratio of proteinase/protein to make sure the cleavage should be slow to prevent protein precipitation. To reduce the protein precipitation, dilution of the protein sample to 2 mg/ml is required.
4. The crystals were heavily twinned, and the structure as determined in the space group of P321, but the structure was refined in the space group of P3. During the structure refinement, both the R_{factor} and R_{free} could not be reduced once reached to 0.3 and 0.35 in the space group of P321, respectively.

Acknowledgments

We thank Dr. Louise Major for providing the pLou3 plasmid, Dr. Catherine Botting for assistance with mass spectroscopy, Dr. Zaitsev Slava for helping with data collection, and Dr. Bjoern

Meyer for prompt editorial assistance. This work was supported in part by the NIAID/NIH through the new-direction awards mechanism of the SERCEB grant (U54-AI057157) to YL and HL, by the NIAID/NIH R01 AI083409 to YL, R01 AI093580 and R56 AI091805 to HL, and the Medical Research Council grant (G1100110/1) to CJD.

References

1. Charrel RN, de Lamballerie X, Emonet S (2008) Phylogeny of the genus Arenavirus. *Curr Opin Microbiol* 11(4):362–368
2. Khan SH, Goba A, Chu M, Roth C, Healing T, Marx A, Fair J, Guttieri MC, Ferro P, Imes T, Monagin C, Garry RF, Bausch DG, Mano River Union Lassa Fever Network (2008) New opportunities for field research on the pathogenesis and treatment of Lassa fever. *Antiviral Res* 78(1):103–115
3. Kitching A, Addiman S, Cathcart S, Bishop L, Krahe D, Nicholas M, Coakley J, Lloyd G, Brooks T, Morgan D, Turbitt D. (2009) A fatal case of Lassa fever in London, January 2009 *Euro Surveill.* 14(6). pii: 19117.
4. Haas WH, Breuer T, Pfaff G, Schmitz H, Köhler P, Asper M, Emmerich P, Drosten C, Gölnitz U, Fleischer K, Günther S (2003) Imported Lassa fever in Germany: surveillance and management of contact persons. *Clin Infect Dis* 36(10):1254–1258
5. Illick MM, Branco LM, Fair JN, Illick KA, Matschiner A, Schoepp R, Garry RF, Guttieri MC (2008) Uncoupling GP1 and GP2 expression in the Lassa virus glycoprotein complex: implications for GP1 ectodomain shedding. *Virology* 375:161
6. Lenz O, ter Meulen J, Klenk HD, Seidah NG, Garten W (2001) The Lassa virus glycoprotein precursor GP-C is proteolytically processed by subtilase SKI-1/S1P. *Proc Natl Acad Sci U S A* 98(22):12701–12705
7. Eichler R, Strecker T, Kolesnikova L, ter Meulen J, Weissenhorn W, Becker S, Klenk HD, Garten W, Lenz O (2004) Characterization of the Lassa virus matrix protein Z: electron microscopic study of virus-like particles and interaction with the nucleoprotein (NP). *Virus Res* 100(2):249–255
8. Mahanty S, Hutchinson K, Agarwal S, McRae M, Rollin PE, Pulendran B (2003) Cutting edge: impairment of dendritic cells and adaptive immunity by Ebola and Lassa viruses. *J Immunol* 170(6):2797–2801
9. Qi X, Lan S, Wang W, Schelde LM, Dong H, Wallat GD, Ly H, Liang Y, Dong C (2010) Cap binding and immune evasion revealed by Lassa nucleoprotein structure. *Nature* 468(7325):779–783
10. Huang Q, Shao J, Lan S, Zhou Y, Xing J, Dong C, Liang Y, Ly H (2015) In vitro and in vivo characterizations of pichinde viral nucleoprotein exoribonuclease functions. *J Virol* 89(13):6595–6607
11. Hastie KM, Kimberlin CR, Zandonatti MA, MacRae IJ, Saphire EO (2011) Structure of the Lassa virus nucleoprotein reveals a dsRNA-specific 3' to 5' exonuclease activity essential for immune suppression. *PNAS* 108(6):2396–2401
12. Otwinowski Z, Minor W (1997) Processing of X-ray diffraction data collected in oscillation mode. *Methods Enzymol* 276:307–326
13. Maniatis T, Fritsch EF, Sambrook J (1982) *Molecular cloning: a laboratory manual*. Cold Spring Harbor University Press, Cold Spring Harbor, NY

Assays to Demonstrate the Roles of Arenaviral Nucleoproteins (NPs) in Viral RNA Synthesis and in Suppressing Type I Interferon

Qinfeng Huang, Junjie Shao, Yuying Liang, and Hinh Ly

Abstract

Arenaviruses, such as Lassa virus (LASV) and Pichindé virus (PICV), are enveloped viruses with a bisegmented ambisense RNA genome. The large (L) genomic segment encodes the Z matrix protein and the L RNA-dependent RNA polymerase, whereas the small (S) genomic segment encodes the nucleoprotein (NP) and the glycoprotein (GPC). The NP encapsidates viral genome, is required for viral transcription and replication, and acts as a type I interferon (IFN) antagonist. This article describes assays to demonstrate that NP contains 3'-5' exoribonuclease (RNase) activity to degrade modeled RNA of the pathogen-associated molecular pattern type and suppresses the IFN β promoter-driven luciferase reporter gene. The minigenomic (MG) assay is used to assess the role of NP in replicating and transcribing a viral promoter-driven luciferase reporter gene. These powerful assays demonstrate the versatility of NP in mediating viral replication as well as in modulating host innate immune responses.

Key words Lassa virus, Nucleoprotein, Arenavirus

1 Introduction

Lassa virus (LASV) is responsible for an estimated 300,000–500,000 infections and ~5000 deaths annually in several countries in Western Africa [1, 2]. There are currently no FDA-licensed vaccines or therapeutics to treat or protect against Lassa and other arenavirus infections. A hallmark of Lassa infection is the generalized immune suppression that leads to high levels of viremia in severe and lethally infected patients. Two of the four arenavirus-encoded proteins, namely, the nucleoprotein (NP) and the RING finger Z protein, have recently been described as type I interferon (IFN) antagonists that contribute to the general immunosuppression observed during the course of arenavirus infection [3–7]. A better understanding of how arenaviruses evade host immune surveillance will offer important insights for the development of effective preventative and treatment options.

Toward this goal, we have developed several new research tools and methods, including the development of the *in vitro* NP ribonuclease (NP RNase) assay to assess the NP 3'-5' exoribonuclease function, the interferon-beta (IFN β) promoter-driven luciferase reporter assay to assess the role of NP in suppressing the IFN β promoter, and the LASV minigenome (MG) assay to evaluate LASV polymerase function in mediating transcription and replication of a model arenaviral genomic RNA template [8]. We describe herein detailed protocols for these assays. With NP playing many crucial roles in mediating virus and host immune functions, understanding the biological function of this protein will greatly facilitate the development of therapeutic strategies against LASV and other deadly viruses in the *Arenaviridae*.

2 Materials

2.1 Protein Expression and Purification

1. pLOU3 vector, which is a derivative plasmid of the pMAL-C4X vector (New England Biolab), contains the LASV NP gene. In this construct, the NP gene is cloned immediately downstream of the tobacco etch virus (TEV) proteinase cleavage site, which is preceded by a 6His-tag at the N-terminus of the maltose-binding protein (MBP). This protein expression cassette is placed under the control of an isopropyl-beta-D-thiogalactopyranoside (IPTG)-inducible (*lacIq*) promoter.
2. *E. coli* Rosetta strain that expresses codons abundant in humans was transformed with recombinant plasmids.
3. Bacterial growth medium is Luria broth (LB) with antibiotics: LB liquid medium with 50 $\mu\text{g}/\text{ml}$ ampicillin and 34 $\mu\text{g}/\text{ml}$ chloramphenicol.
4. IPTG, a structural mimic of galactose, binds to the *lac* repressor to induce beta-galactosidase (β -gal) or the protein expression cassette, MBP-TEV cleavage-NPV_{LASV}.
5. Shaker-incubator.
6. Spectrophotometer.
7. J-20 ultracentrifuge.
8. *E. coli* cell disruptor.
9. Amylose resin for affinity isolation of proteins bound to MBP.
10. Amylose binding buffer: 10% glycerol, 20 mM Tris pH 7.5, 0.2 M NaCl, 1 mM EDTA. This buffer is supplemented with two protease inhibitor tablets, 1 μM DNase and 1 μM phenylmethylsulfonyl fluoride (PMSF).
11. Amylose elution buffer: 10% glycerol, 20 mM Tris pH 7.5, 0.2 M NaCl, 1 mM EDTA, 10 mM maltose.
12. 3 mg/ml TEV protease for cleaving the expressed protein.

13. ÄKTA purifier 10 or similar instrument to control the flow rate of the columns.
14. Desalting column (e.g., HiPrep 26/10).
15. Gel filtration column (e.g., Sephacryl S-200).
16. Gel filtration buffer: 20 mM Tris pH 7.5, 0.3 M NaCl, 10% glycerol.
17. -80°C freezer.
18. Mass spectroscopy (Q-Star MS/MS Micromass MALDI-TOF).
19. Precast 4–12% Bis-Tris polyacrylamide gels.
20. Power supply.
21. Unstained protein standards.
22. DNase.
23. Phenylmethylsulfonyl fluoride (PMSF) and other protease inhibitors.
24. Binding buffer: 1/50 PBS, 50 mM Tris-HCl, 0.5 mM EDTA, 1 mM DTT, 0.3 M NaCl, 10% glycerol.
25. TEV cleavage buffer: 1/50 PBS, 50 mM Tris-HCl, 0.5 mM EDTA, 1 mM DTT, 0.3 M NaCl, 10% glycerol. This is used with the desalting column.

2.2 NP Ribonuclease (RNase) Assay

1. Nucleoprotein (NP): *see* Subheading 3.1 for NP purification method.
2. PCR thermal cycler.
3. Microcentrifuge.
4. T4 polynucleotide kinase.
5. Radioisotope (γ -ATP) to radiolabel the RNA oligonucleotide substrate.
6. RNA oligo (5'-AGUAGAAACAAGGCC-3') to serve as RNase substrate.
7. Illustra MicroSpin G25 desalting column.
8. 17% polyacrylamide gel solution containing urea (25 ml): 2.5 ml of 10 \times TBE, 10.5 g urea, 10.6 ml of 40% acrylamide, and 11.9 ml ddH₂O. Add 10 μ l of TEMED and 80 μ l of 30% APS just before pouring.
9. Ambion T7 MEGAscript Kit for T7 polymerase-driven in vitro transcription.
10. Water bath.
11. Electrophoresis autoradiography cassette.
12. X-ray film.
13. Vertical gel electrophoresis apparatus.

14. Power supply.
15. X-ray film developer.
16. 10× RNase buffer: 25 mM Tris-HCl, pH 7.5, 10 mM NaCl, 15 mM KCl, 1 mM MnCl₂, and 0.1 mg/ml bovine serum albumin (BSA).

2.3 Minigenome (MG) Assay and IFN β Promoter-Driven Luciferase Reporter Assay

1. Plasmids: NP and L gene were cloned into pCAGGS mammalian vector under CMV promoter [3]. IFN β promoter-directed LUC plasmid was used for NP-induced interferon suppression assay. MGLF7-5Rluc3 plasmid was used for minigenome assay. β -Galactosidase (β -gal) plasmid was used for normalizing luciferase activity.
2. 293T cell line was cultured in Dulbecco's Modified Eagle Medium (DMEM), supplemented with 10% fetal bovine serum (FBS), 50 mg penicillin, and streptomycin per ml.
3. Plate reader (e.g., Synergy 2 by BioTeK).
4. Lipofectamine 2000 (or other transfection reagent).
5. DEPC water.
6. 2× HEPES buffered saline (HBS): 50 mM HEPES, 280 mM NaCl, 1.5 mM Na₂HPO₄, pH = 7.10.
7. Beta-galactosidase (β -gal), Firefly and Renilla luciferase assay kits.
8. 2.5 M calcium chloride stock solution.
9. Sendai virus, Cantell strain (ATCC, VR907).

3 Methods

3.1 Protein Expression and Purification

1. The recombinant plasmid was transformed into *E. coli* Rosetta strain using the conventional heat-shock transformation method [9].
2. A single colony was picked and inoculated into 500 ml LB bacterial growth medium.
3. Cells were incubated at 37 °C in a shaker-incubator with constant agitation at 200 rpm overnight.
4. The overnight culture was then transferred into 10 l of the LB bacterial growth medium.
5. The culture was incubated at 37 °C with shaking at 200 rpm for about 2 h.
6. Expression of the recombinant NP protein was induced by the addition of IPTG to a final concentration of 0.03 mM when the OD₆₀₀ of the cell culture reached 0.6 (see Note 1).
7. The cell culture was kept at 20 °C overnight with shaking at 200 rpm (see Note 1).

8. Cells were harvested by centrifugation at $8000 \times g$ for 10 min at 4°C in the J-20 centrifuge.
9. The cell pellet collected from 10 l culture was resuspended in 100 ml of amylose binding buffer.
10. Cells were lysed by a cell disruptor at 30 KPsi.
11. The sample was centrifuged in the J-20 centrifuge at maximum speed of $48 \times g$ for 30 min to remove cellular debris.
12. The supernatant was applied onto the amylose resin column.
13. The column was washed using a 10-column volume of the amylose binding buffer (*see Note 2*).
14. The fusion protein was eluted from the column with the amylose elution buffer.
15. The protein elution buffer was changed to TEV cleavage buffer using the HiPrep desalting column.
16. Fractions containing HisMBP-NP were pooled and the fusion protein was cleaved by incubating with 1 ml His-tagged TEV protease at room temperature overnight (*see Notes 2 and 3*).
17. The sample was then applied onto the amylose resin again in order to remove the MBP.
18. The flow-through sample was concentrated into 5 ml and applied onto a HiLoad 16/600 Superdex 200 gel filtration column, which was equilibrated using the gel filtration buffer and the ÄKTA purifier 10 chromatography system.
19. The flow rate was 1 ml/min controlled by the ÄKTA purifier 10, and protein peaks were monitored at optical density of 280 nm.
20. All elution solutions were collected by the fraction collection of the ÄKTA purifier 10 using the 96-deep-well block.
21. The fractions containing purified NP protein were pooled and concentrated to 7 mg/ml and stored in a -80°C freezer.
22. The protein's identity and integrity were checked by mass spectroscopy and proteins were separated by SDS-PAGE.
23. The SDS-PAGE was carried out using precast gels and the PowerEase 500 Power Supply according to the manufacturer's instruction.
24. The protein molecular marker was used to size the recombinant protein.
25. The SDS-PAGE gels were stained with Coomassie dye for 10 min.
26. The SDS-PAGE gels were destained by putting the gels in a beaker with water and boiling for 5 min using a conventional microwave oven.

3.2 NP Ribonuclease (RNase) Assay

1. The 15-nt RNA oligo (*see* Subheading 2.2) was 5' end labeled with γ - ^{32}P ATP in a polynucleotide kinase reaction as follows:

9.5 μl	DEPC-treated water
2 μl	RNA oligo (100 pmol)
5 μl	γ - ^{32}P ATP (25 pmol, 3uCi/pmol, 10uCi/ μl)
2 μl	10 \times kinase buffer
1.5 μl	RNase-free T4 PNK

Sample was incubated at 37 °C for 1 h, then at 95 °C for 2 min. Sample was collected by centrifugation at 13.4 $\times g$ for 1 min. 20 μl DEPC-treated water was added.

2. The unincorporated γ - ^{32}P ATP was eliminated by passing the radiolabeled RNA sample through the Illustra MicroSpin G25 desalting spin column.
3. The γ - ^{32}P -labeled RNA oligo was mixed with fivefold amount of unlabeled RNA oligos of either the same or the complementary sequence, heat denatured at 95 °C for 5 min, and slowly cooled to room temperature in order to form single-stranded RNA (ssRNA) or double-stranded RNA (dsRNA) substrates.
4. The exoribonuclease reaction containing 1 pmol of radiolabeled RNA substrates in either ss or ds form and various concentrations of NP protein in an RNase buffer was incubated at 37 °C for 60 min as follows:

5 μl	DEPC-treated water
1 μl	γ - ^{32}P -labeled RNA oligos
1 μl	10 \times RNase buffer
1 μl	Recombinant LASV NP protein at various concentrations

Sample was incubated at 37 °C for 1 h, 1 μl 0.5 M EDTA was added, and 10 μl formamide loading buffer was also added. The reaction was terminated by heating the sample to 95 °C for 10 min and immediately chilled on ice. Sample was collected by microcentrifugation at 13.4 $\times g$ for 1 min.

5. Prepare denaturing polyacrylamide gel solution.
6. Pre-electrophorese gel at 150 V for 30 min. Use 0.5 \times TBE in upper and lower reservoirs of the gel box.
7. Samples were loaded into wells and were separated at 150 V for 3 h.

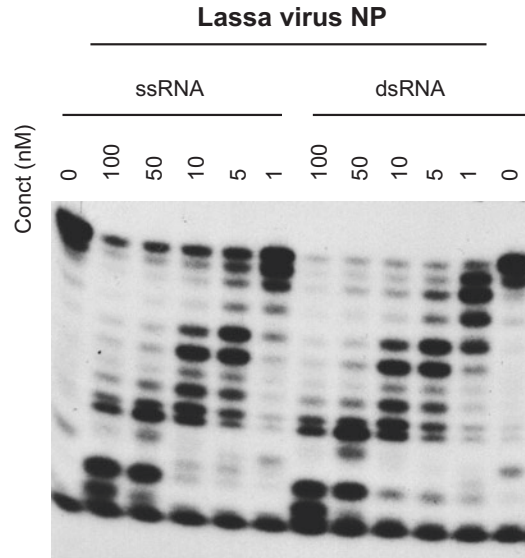


Fig. 1 Cleavage of ssRNA and dsRNA by purified LASV NP. 5'- γ - ^{32}P -labeled ssRNA or dsRNA were used as substrates for cleavage by different concentrations of the purified LASV NP

8. The gel was placed onto a spent film backing and covered with plastic wrap and exposed to an X-ray film with an intensifying screen at $-80\text{ }^{\circ}\text{C}$ freezer.
9. The film was developed in the film developer to visualize RNA cleavage activities (*see Note 4*).
10. As an example of results from this assay, purified LASV NP protein was able to cleave both ss and ds RNAs (Fig. 1). The laddering effects are due to the different efficiencies of RNA cleavage induced by different concentrations of the LASV NP.

3.3 Minigenome (MG) Assay

This assay is meant to measure expression of viral genes from a “minigenome” construct, and it occurs in four stages: (1) the minigenome plasmid is RNA transcribed *in vitro*; (2) 293T cells are transfected with plasmids expressing the viral NP and L genes; (3) 24 h later, these same 293T cells are transfected with the minigenome RNA; and (4) the cells are assessed for luciferase expression. The first stage is covered in **steps 1–8**, the second stage in **steps 9–14**, the third stage in **steps 15–21**, and the fourth stage in **steps 22–24**.

1. Prior to RNA transcription, the plasmid MGLF7-5Rluc3 was linearized by digestion with Nhe I restriction enzyme.
2. DNA was extracted by phenol/chloroform and isopropanol precipitated using the standard technique [9].
3. Transcription reaction was assembled at room temperature according to Ambion MEGAscript[®] Kit manual. Calculate the volume of nuclease-free water necessary to bring the total volume

to 20 μl , and to this amount add 2 μl ATP, 2 μl CTP, 2 μl GTP, 2 μl UTP, 2 μl 10 \times reaction buffer, 1 μg linearized template DNA, and 2 μl enzyme mix.

4. Sample was incubated at 37 $^{\circ}\text{C}$ for 4 h.
5. 115 μl nuclease-free water and 15 μl ammonium acetate stop solution were added.
6. RNA was extracted by phenol/chloroform and isopropanol precipitated using the standard technique [9].
7. Carefully discard the precipitating solution and the RNA was resuspended in 80 μl of DEPC-treated water.
8. RNA was quantified and adjusted to a concentration of 1 $\mu\text{g}/\mu\text{l}$.
9. Prior to plasmid transfection, 293T cells were seeded into 24-well plates at 1×10^5 cells/well that contains 0.5 ml of DMEM with 10% FBS and 50 $\mu\text{g}/\text{ml}$ of penicillin and streptomycin.
10. In the morning of the day of transfection, a fresh aliquot of the cell media was added to the 293T cell culture.
11. DNA and calcium phosphate mixture was prepared at room temperature so that each of the 25 μl of DNA mix (for one 24-well transfection) contains:

1 μl	β -gal reporter plasmid (50 ng/ μl)
1 μl	pCAGGS-NP plasmid (250 ng/ μl)
1 μl	pCAGGS-L plasmid (500 ng/ μl)
2.5 μl	2.5 M calcium chloride stock solution
19.5 μl	Water

12. To prepare triplicates for each test condition, mix as follows:

3 μl	β -gal reporter plasmid (50 ng/ μl)
3 μl	pCAGGS-NP plasmid (250 ng/ μl)
3 μl	pCAGGS-L plasmid (500 ng/ μl)
7.5 μl	2.5 M calcium chloride stock solution
58.5 μl	Water

13. Into each tube of DNA/calcium phosphate mixture (25 \times 3 = 75 μl), add 75 μl of 2 \times HBS. Gently mix sample by vortexing using the lowest speed setting. Add the mixture dropwise using a pipetman into each well of cells (48 μl of sample into each well of the 24-well plate) (*see Note 5*).
14. Incubated cells in a 37 $^{\circ}\text{C}$ CO₂ incubator for 24 h.

15. 4 h before RNA transfection, an aliquot of fresh antibiotics-free DMEM medium was used to replace the overnight cell culture medium.
16. For each well, 1 μg of in vitro-transcribed RNA (*see Note 6*) was diluted into 25 μl OptiMEM[®] I Medium.
17. For each well, 1 μl of Lipofectamine[™] 2000 was diluted into 25 OptiMEM[®] I Medium and incubated for 5 min at room temperature.
18. The diluted RNA was added into diluted Lipofectamine[™] and incubated at room temperature for no more than 10 min.
19. RNA-Lipofectamine[™] 2000 complexes were directly added to each well containing cells and mixed gently by rocking the plate back and forth. The cells were incubated at 37 °C in a CO₂ incubator.
20. The cell medium was replaced by fresh DMEM medium (10% FBS) at 6 h post transfection.
21. 24 h post RNA transfection, cells were washed once by PBS. Then cells were lysed by lysis buffer for Renilla luciferase assay.
22. 20 μl of cell lysate was used for Renilla luciferase assay and another 50 μl of cell lysate was used for β -gal assay according to manufacturer's instructions.
23. Renilla luciferase activity is normalized by dividing the Renilla luciferase reading by the β -gal reading. The minigenome replication activity is represented by the folds of the normalized Renilla luciferase activity with respect to that of the control.
24. In MG assay (Fig. 2), cotransfection of PICV NP and L expression plasmids into 293T cells was able to replicate and transcribe the transfected PICV minigenome (MG) expressing the Renilla luciferase reporter gene. P2 and P18 indicate that the NP and L genes are from different PICV strains.

3.4 IFN β Promoter-Driven Luciferase Reporter Assay

1. 293T cells were seeded into 24-well plates at 1×10^5 cells/well with complete DMEM.
2. In the morning of the day of transfection, culture media was replaced by an equal aliquot of fresh media.
3. Prepare 25 μl DNA and calcium phosphate mix for each well of a 24-well transfection plate as follows:

1 μl	β -gal reporter plasmid (50 ng/ μl)
1 μl	IFN β promoter-driven luc reporter plasmid (100 ng/ μl)
1 μl	pCAGGS-NP plasmid (10–1000 ng/ μl)
2.5 μl	2.5 M calcium chloride stock solution
19.5 μl	Water

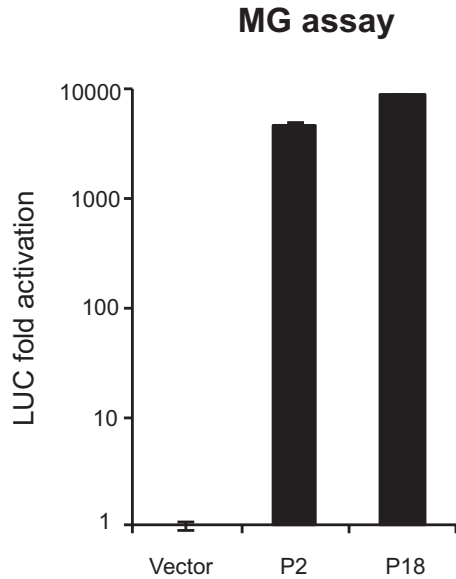


Fig. 2 NP and L protein can replicate and transcribe the viral minigenome (MG). Cotransfection of PICV NP and L expression plasmids into 293T cells was able to replicate and transcribe the transfected PICV minigenome (MG) expressing the Renilla luciferase reporter gene. P2 and P18 indicate that the NP and L genes are from different PICV strains

Prepare triplicates for each test condition as follows:

3 μ l	β -gal reporter plasmid (50 ng/ μ l)
3 μ l	IFN β promoter-driven luc reporter plasmid (100 ng/ μ l)
3 μ l	pCAGGS-NP plasmid (10–1000 ng/ μ l)
7.5 μ l	2.5 M calcium chloride stock solution
58.5 μ l	Water

4. Into each tube of DNA/calcium phosphate mixture ($25 \times 3 = 75 \mu$ l), add 75μ l $2\times$ HBS, vortex using very low speed to mix, and add the mixture to three wells of cells (48μ l per well) as shown in Subheading 3.3.
5. 24 h post transfection, media was replaced by fresh complete DMEM and cells were infected with Sendai virus (SeV) at MOI of 1. Cells were continued in culture for 24 h at 37°C in a CO_2 incubator.
6. Interferon promoter activity was assessed by performing the Firefly luciferase assay using a kit from Promega.
7. An example of results from this assay can be seen in Fig. 3. Sendai virus (SeV) infection of 293T cells was able to stimulate

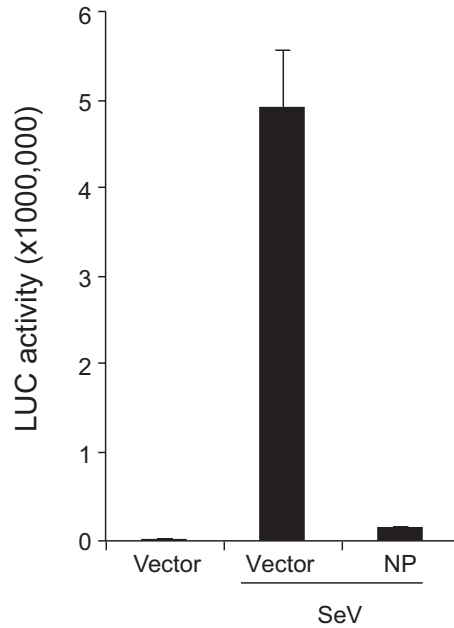


Fig. 3 IFN β promoter-driven luciferase reporter assay to demonstrate the role of LASV NP in suppressing this promoter activity. Sendai virus (SeV) infection of 293T cells was able to stimulate the IFN β promoter activity to express a high level of the Firefly luciferase reporter gene, whereas the LASV NP expression suppresses this promoter activity. Empty vector was used as a control

the IFN β promoter activity to express a high level of the Firefly luciferase reporter gene, whereas the LASV NP expression suppresses this promoter activity. Empty vector was used as a control.

4 Notes

1. It is important to express the MBP-NP fusion protein at 20 °C and to use 0.03 mM IPTG concentration for the induction as this condition will produce more soluble MBP-NP fusion protein. Using higher IPTG or higher temperature for protein expression will produce more MBP-NP fusion into inclusion bodies. In all the sample buffer and purification buffers, 10% glycerol is required to stabilize the protein in the buffers.
2. It is important to use TEV proteinase at 1:500 ratio of proteinase/protein to make sure the cleavage should be slow to prevent protein precipitation.
3. To reduce the protein precipitation, dilution of the protein sample to 2 mg/ml is required.

4. With new isotope, it usually took 3–6 h of exposure of the X-ray film at -80°C .
5. For calcium phosphate transfection, DNA/calcium phosphate mixture was directly added to the cells, dropwise, uniformly and gently over the surface of the monolayer of the cells. It is important to add the precipitate to the cells within 5 min of adding the $2\times$ HBS. If waiting for more than 5 min, the precipitate will be too large and can be toxic to cells.
6. Separate $1\ \mu\text{g}$ of in vitro transcribed RNA in a 1% agarose gel to check for the integrity of the RNA prior to its use in transfection.

Acknowledgments

This work was supported in part by the NIAID/NIH through the new direction awards mechanism of the SERCEB grant (U54-AI057157) to YL and HL, and by the NIAID/NIH R01 grants AI083409 to YL and AI093580 to HL, and by R56 grant AI091805 to HL.

Reference

1. McCormick JB, Fisher-Hoch SP (2002) Lassa fever. *Curr Top Microbiol Immunol* 262:75–109
2. Gunther S, Lenz O (2004) Lassa virus. *Crit Rev Clin Lab Sci* 41:339–390
3. Meyer B, Ly H (2016) Inhibition of innate immune responses is key to pathogenesis by arenaviruses. *J Virol* 90:3810–3818
4. Qi X, Lan S, Wang W, Schelde LM, Dong H, Wallat GD, Ly H, Liang Y, Dong C (2010) Cap binding and immune evasion revealed by Lassa nucleoprotein structure. *Nature* 468:779–783
5. Xing J, Chai Z, Ly H, Liang Y (2015) Differential inhibition of macrophage activation by lymphocytic choriomeningitis virus and pichindé virus is mediated by the Z protein N-terminal domain. *J Virol* 89:12513–12517
6. Xing J, Ly H, Liang Y (2015) The Z proteins of pathogenic but not nonpathogenic arenaviruses inhibit RIG-I-like receptor-dependent interferon production. *J Virol* 89:2944–2955
7. Fan L, Briese T, Lipkin WI (2010) Z proteins of new world arenaviruses bind RIG-I and interfere with type I interferon induction. *J Virol* 84:1785–1791
8. Lan S, McLay Schelde L, Wang J, Kumar N, Ly H, Liang Y (2009) Development of infectious clones for virulent and avirulent pichindé viruses: a model virus to study arenavirus-induced hemorrhagic fevers. *J Virol* 83:6357–6362
9. Maniatis T, Fritsch EF, Sambrook J (1982) *Molecular cloning: a laboratory manual*. Cold Spring Harbor University Press, Cold Spring Harbor

Intracellular Detection of Viral Transcription and Replication Using RNA FISH

Michael E. Lindquist and Connie S. Schmaljohn

Abstract

Many hemorrhagic fever viruses require BSL-3 or BSL-4 laboratory containment for study. The necessary safety precautions associated with this work often contribute to longer assay times and lengthy decontamination procedures. Here we will discuss recent advances in RNA fluorescence in situ hybridization (FISH) that not only allow entirely new investigations into the replication of these viruses but also demonstrate how this method can be applied to any virus with a known sequence and how it can be rapidly performed to minimize time spent in high containment. We have adapted existing protocols for mRNA detection with appropriate changes for examining viruses in a variety of containment laboratories (Shaffer et al., PLoS One 8:e75120, 2013; Raj et al., Nat Methods 5:877–879, 2008).

Key words Viral RNA detection, RNA FISH, RNA localization, TurboFISH, Hemorrhagic fever virus replication

1 Introduction

RNA FISH was developed as a method to visualize cellular RNA by binding a fluorescently labeled oligonucleotide probe to a complementary target sequence. Unfortunately, early methods for RNA FISH required long staining times, and the sensitivity was often not adequate to detect single molecules of RNA. A breakthrough in this technique was achieved when researchers showed that multiple probes could bind to a single RNA and the cumulative result of multiple binding events enabled the visualization of diffraction-limited, single-molecule RNA spots [1, 2]. In this system, each oligonucleotide probe is tagged with a fluorophore and is complementary to a unique region of the target. Probe sets typically contain about 50 probes, enabling a much greater signal-to-noise ratio than previous methods. Probe sets are designed using freely available software to minimize cross-reactivity to other targets, to prevent probe overlap, and to minimize binding to predicted secondary structures. Multi-target probe sets enable single-molecule resolution of host

mRNAs using a 63–100× oil objective lens to achieve such resolution. However, viral RNA tends to cluster in specific subcellular sites (e.g., viral replication factories). Thus, while true single-molecule resolution may not be achievable due to the aggregation of multiple RNAs at one site, the combined signal intensity of these molecules is much greater than a single RNA and can be imaged using low-objective microscope lenses. Detection of viral RNA is therefore much more robust than host RNA and has resulted in the development of a variety of useful assays for virus detection. For hemorrhagic fever viruses with segmented genomes such as Crimean-Congo hemorrhagic fever virus and Lassa fever virus, multiplexed RNA detection can simultaneously detect multiple genomic segments. In addition, probe sets can be designed to detect positive and negative sense RNA, which in some instances can delineate between genomic RNA, viral mRNA, or viral cRNA. We and others have expanded this technique to use in virus-infected tissue sections, high-throughput imaging, and flow cytometry-based assays [3]. Detection of viral RNA allows for in-depth interrogation of the subcellular sites of viral replication, and such experiments will help further examine the mechanisms by which viruses replicate, assemble, and traffic through the cell. An additional benefit of this method is that the robust and quick staining methods described here enable rapid detection of virus infection that is useful for screening assays (Fig. 1).

2 Materials

1. Probe sets composed of approximately 50 unique oligonucleotide probes, each 20–25 nucleotides in length, are typically delivered as dried stocks. Reconstitute the probes in TE buffer to a final concentration of 25 μM . Probe stocks should be aliquoted and frozen at $-20\text{ }^{\circ}\text{C}$.
2. Fixation buffers: 3.7% formalin solution (37% formalin diluted in PBS) or methanol. Make fresh for each experiment.
3. Permeabilization buffer: 70% ethanol.
4. Hybridization buffer: Add 1 mL deionized formamide (*see Note 1*) and 1 mL 20× saline-sodium citrate (SSC) to 8 mL of nuclease-free water. Add 1 g of dextran sulfate and mix for 10 min at room temperature. Aliquot and store the hybridization buffer at $4\text{ }^{\circ}\text{C}$.
5. Wash buffer: Add 20 mL of formamide and 20 mL of 20× SSC to 260 mL of nuclease-free water. Wash buffer can be kept at room temperature.
6. Surfaces for cell growth: Cells can be grown on glass coverslips (#1.0 thickness recommended) placed in 24-well plates,

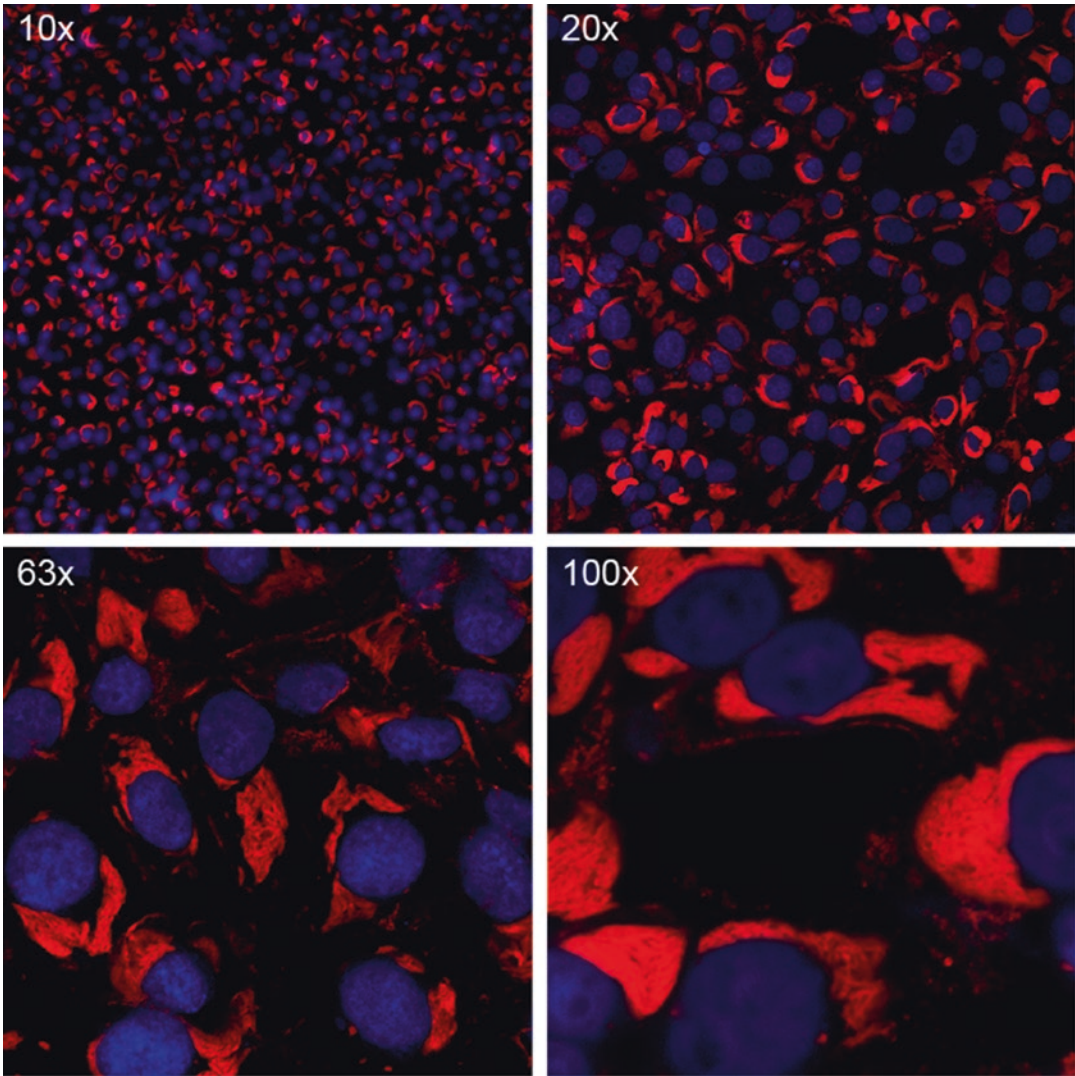


Fig. 1 Vero cells infected with Ebola virus were fixed in methanol. Viral RNA (*red*) was detected using a 5 min RNA FISH incubation with hybridization buffer containing RNA FISH probes and DAPI. Cells were imaged on a confocal microscope with a 10× air objective (*top left*), a 20× air objective (*top right*), a 63× oil objective (*bottom left*), or a 100× oil objective

chambered coverslips, or 96-well flat bottom plates suitable for microscopy (e.g., Greiner CELLSTAR 96-well plates).

7. Microscope objectives: For screening purposes we recommend a 20× objective. For experiments designed to examine subcellular RNA localization, we recommend a 63× oil objective.
8. Immunostaining blocking buffer: 5% bovine serum albumin (nuclease-free) diluted in PBS.
9. Antibodies for detecting protein targets.
10. DAPI staining solution: 4',6-diamidino-2-phenylindole (DAPI) diluted to 5 ng/mL in wash buffer or PBS.

3 Methods

3.1 Probe Sets

Design probe sets appropriate for your target(s) of interest. Typically probe sets contain approximately 50 individual oligonucleotide probes. Probe sets with fewer probes may still yield adequate signal. Enter the target sequence in 5'-3' orientation into a probe generator such as the Stellaris Probe Designer (*see Note 2*). For multiplexed probe detection, ensure that each probe set is tagged with a different fluorophore.

3.2 Cell Culture and Infection Conditions

Cells must be plated on an appropriate substrate for subsequent microscopy. For the best resolution, we recommend plating the cells on glass coverslips (#1.0). For testing or processing large numbers of samples, we recommend microscopy-grade 96-well plates (*see Note 3*). Infect cells with chosen multiplicity of infection (MOI). We have found that depending on the virus, viral RNA is detectable within a few hours of infection.

3.3 Choices for Fixation and Staining

The first method uses formaldehyde fixation followed by ethanol permeabilization. We find this method is preferable when the samples will also be immunostained. The second method, termed “turboFISH,” uses methanol as a fixative and permeabilizing reagent [4]. This method significantly reduces the time required to complete the assay but also requires larger concentration of probe.

3.4 Formaldehyde Fixation

1. Rinse samples with PBS 1–2 times before fixing.
2. Remove the PBS and add enough 3.7% formalin fixation buffer to cover the cells.
3. Incubate at room temperature for 10 min.
4. Remove formalin and rinse the cells 1–2 times in PBS.
5. Remove PBS and replace with ethanol. Incubate cells in ethanol for at least 1 h at 4 °C (*see Note 4*).
6. Remove the probe sets from –20 °C and thaw at room temperature. Once thawed, vortex the probes for a few seconds and briefly centrifuge.
7. Remove hybridization buffer from 4 °C and equilibrate to room temperature.
8. In a fume hood, aspirate ethanol from samples and replace with a generous amount of 10% formamide wash buffer (500 µL/well in 24-well plates).
9. Prepare the hybridization buffer by adding probe stock solution to the buffer. Each probe set must be empirically tested for the optimal concentration, but we recommend starting with a 1:100 dilution of probe in hybridization buffer (0.25 µM).

10. Remove the wash buffer from the wells and add enough probe-hybridization buffer to cover the sample. For samples grown on coverslips, we recommend 100 μL of buffer to be added to the sample. Then carefully cover the sample with a second coverslip to evenly spread the hybridization buffer and to inhibit evaporation (*see Note 5*).
11. Wrap the sample in aluminum foil and place in a humidified 37 °C incubator for at least 4 h or incubate overnight for convenience.
12. Remove the hybridization buffer from the samples and replace with 10% formamide wash buffer (*see Note 6*). If a secondary coverslip was used, carefully remove the top coverslip using tweezers.
13. Incubate the plate at 37 °C for 20–30 min (*see Note 7*). Preferably rock the plates at a low speed (50 RPM). After 30 min, replace wash buffer with fresh wash buffer and incubate an additional 20–30 min.
14. Remove the wash buffer and rinse the cells twice with 2 \times SSC buffer.
15. If co-immunostaining is desired, we recommend minimizing antibody staining times. We generally block and perform primary and secondary antibody incubations at 37 °C for 30 min each when possible. Use nuclease-free BSA or an alternative blocking buffer to minimize degradation of RNA targets.
16. Once the staining is completed, submerge the samples in 3.7% formalin for 24 h in order to ensure complete virus inactivation (*see Note 8*).
17. Once the samples have been removed from containment, carefully decant the formalin. Rinse the samples 2–3 times with PBS.
18. Remove the coverslips from the wells using tweezers. Place the coverslips on glass slides using an appropriate mounting media. We prefer VECTASHIELD HardSet mounting medium as it rapidly dries.
19. After 15–20 min, ensure the mounting media is dry and begin to image the samples (*see Note 9*).

3.5 Methanol Fixation

1. Prior to fixation: Place methanol at –20 °C for about 30 min (or until ice cold), place wash buffer at 37 °C, allow hybridization buffer to equilibrate to room temperature, and thaw, vortex, and centrifuge probes as discussed in Subheading 3.4.
2. In a fume hood, set a hot plate to 37 °C. Alternatively, a 37 °C incubator can be used.
3. Rinse samples with PBS 1–2 times.

4. Remove PBS and add ice-cold methanol to the samples (enough to cover each sample).
5. Place samples at -20°C for 10 min (*see Note 10*).
6. While samples are fixing, prepare the hybridization buffer by adding 2–5 μL of probes to 100 μL of hybridization buffer (0.5–2.5 μM) for each well.
7. When fixation is complete, aspirate the methanol from the samples and add 100 μL of hybridization buffer to each sample.
8. Wrap the sample in aluminum foil and place on the 37°C hot plate. Allow hybridization to proceed for at least 5 min.
9. Remove the hybridization buffer and replace with prewarmed wash buffer. Incubate at 37°C for 1 min.
10. Remove the wash buffer and replace with fresh wash buffer. Repeat wash step twice.
11. Rinse cells 2–3 times with $2\times$ SSC buffer.
12. Process samples for complete inactivation, removal from containment, mounting, and imaging as discussed in Subheading 3.4.

4 Notes

1. All work with formamide should be performed in a fume hood. Be sure to discard used formamide properly.
2. We frequently use sequences obtained from GenBank. However, we have found that the orientation and proper RNA species (cRNA versus genomic RNA) is not always properly labeled. For each sequence, we advise you to verify the sequence is correct.
3. When using 96-well plates, we recommend avoid using the edge wells as these wells tend to dry out more quickly than the interior wells.
4. Cells can be stored in ethanol for several days. Since ethanol tends to evaporate quickly, we recommend adding an excess of ethanol and wrapping the samples in paraffin to slow evaporation when permeabilizing the cells for longer times.
5. For samples grown in 96-well plates, we recommend at least 50 μL of probe-hybridization buffer to prevent a surface tension meniscus from forming and causing the middle of the well to dry out.
6. DAPI can be added to the formamide wash buffer or hybridization buffer when nuclear staining is desired.
7. Always ensure minimal light exposure to the samples once the RNA FISH staining has begun.

8. When using coverslips, be certain to keep the plates facing upward to prevent the coverslips from floating out of their appropriate well.
9. We recommend imaging the samples immediately after the mounting medium has hardened. Samples may be stored at 4 °C for prolonged use, but RNA FISH signal tends to fade more rapidly than immunostaining.
10. If a -20C freezer is not available when performing the methanol fixation, we recommend placing the samples on ice. Alternatively, the fixation can be performed at room temperature if necessary.

Acknowledgments

Opinions, interpretations, conclusions, and recommendations are those of the authors and are not necessarily endorsed by the US Army. We thank Ron Cook and Marc Beal of Biosearch Technologies, Inc., for helping in the design and procurement of Stellaris FISH probes. We thank Dr. Arjun Raj (University of Pennsylvania) for previous protocols.

References

1. Raj A, van den Bogaard P, Rifkin SA, van Oudenaarden A, Tyagi S (2008) Imaging individual mRNA molecules using multiple singly labeled probes. *Nat Methods* 5:877–879. doi:[10.1038/nmeth.1253](https://doi.org/10.1038/nmeth.1253)
2. Femino AM, Fay FS, Fogarty K, Singer RH (1998) Visualization of single RNA transcripts in situ. *Science* 280:585–590
3. Jambo KC, Banda DH, Kankwatira AM, Sukumar N, Allain TJ, Heyderman RS, Russell DG, Mwandumba HC (2014) Small alveolar macrophages are infected preferentially by HIV and exhibit impaired phagocytic function. *Mucosal Immunol* 7:1116–1126. doi:[10.1038/mi.2013.127](https://doi.org/10.1038/mi.2013.127)
4. Shaffer SM, Wu MT, Levesque MJ, Raj A (2013) Turbo FISH: a method for rapid single molecule RNA FISH. *PLoS One* 8:e75120. doi:[10.1371/journal.pone.0075120](https://doi.org/10.1371/journal.pone.0075120)

Chapter 15

Hemorrhagic Fever Virus Budding Studies

Ronald N. Harty

Abstract

Independent expression of the VP40 or Z matrix proteins of filoviruses (marburgviruses and ebolaviruses) and arenaviruses (Lassa fever and Junín), respectively, gives rise to the production and release of virus-like particles (VLPs) that are morphologically identical to infectious virions. We can detect and quantify VLP production and egress in mammalian cells by transient transfection, SDS-PAGE, Western blotting, and live cell imaging techniques such as total internal reflection fluorescence (TIRF) microscopy. Since the VLP budding assay accurately mimics budding of infectious virus, this BSL-2 assay is safe and useful for the interrogation of both viral and host determinants required for budding and can be used as an initial screen to identify and validate small molecule inhibitors of virus release and spread.

Key words Budding, Ebola virus, VLPs, VP40, Matrix protein, TIRF

1 Introduction

Members of the *Filoviridae* and *Arenaviridae* families are important pathogens of humans and animals that can cause sporadic and deadly outbreaks of hemorrhagic fever in many countries [1–5]. Filoviruses and select arenaviruses have been classified by the CDC as category A bioterrorism agents and high priority pathogens, for which there are no FDA-approved vaccines [6–10]. One roadblock to achieving a better understanding of the molecular aspects of filovirus and arenavirus pathogenesis has been the inherent difficulty in studying these pathogens under BSL-4 conditions. The virus-like particle (VLP) budding assay has helped to circumvent this roadblock. As VLP budding accurately recapitulates critical steps of authentic live filovirus or arenavirus budding, but can be carried out under BSL-2 conditions, it provides a safe, novel, and innovative system to interrogate host interactors that influence the budding process and to test/validate new therapeutics that block virus egress. Indeed, our understanding of the budding process and identification of important virus–host interactions that contribute to efficient

virus egress has progressed rapidly over the last decade, in part, due to the use of VLP budding assays [11–36]. Our model Ebola VP40 VLP budding assay is described below.

2 Materials

1. pCAGGS vector containing full-length Ebola virus VP40 gene (eVP40) or GFP fused to the N-terminus of EBOV VP40 (GFP-eVP40).
2. HEK293T cells.
3. DMEM (Life Technologies), 10% fetal calf serum (HyClone), 1× pen/strep.
4. Rabbit polyclonal antiserum raised against Ebola virus VP40 peptide (Cocalico Biologicals; PA).
5. Lipofectamine reagent (Invitrogen) (*see Note 1*).
6. Opti-MEM (Life Technologies) and fetal calf serum (HyClone).
7. RIPA buffer: 50 mM Tris [pH 8.0], 150 mM NaCl, 1.0% NP-40, 0.5% deoxycholate, and 0.1% sodium dodecyl sulfate (SDS).
8. STE buffer for VLPs: 0.01 M Tris-HCl [pH 7.5], 0.01 M NaCl, and 0.001 M EDTA [pH 8.0].
9. For electrophoresis of proteins: 5X loading buffer: 1.5 M Tris-HCl, pH 6.8; 0.5 M DTT, 10% SDS, 0.5% bromophenol blue, and 50% glycerol.
10. Leica DMI6000 microscope with a 100× (1.46 NA) oil immersion objective lens and a Photometrics Evolve 512 Camera (Tucson, AZ).
11. Mattek dishes were used in a heated, humidified environmental chamber (PECON Incubator PM 2000 RBT, PECON CO₂-Controller 2000 with Humidifier, Heating Insert P 2000, Germany) (*see Note 2*).
12. Fluorescence observed by setting 488 nm total internal reflection fluorescence (TIRF) laser excitation to a maximum depth of 90 nm. Images were collected at 10 s intervals with Leica LASX software. TIRF microscopy was performed at the Penn Vet Imaging Core (PVIC) directed and managed by Drs. B. Freedman and G. Ruthel, respectively.
13. All small molecule compounds (e.g., compound 4) were >95% pure, were suspended in DMSO at appropriate concentrations, and were stored at −20 °C (*see Note 3*).

3 Methods

3.1 Transient Transfection

Day 1—Seed HEK293T cells in collagen-coated 6-well plate (1×10^6 /well) and incubate at 37 °C overnight.

Day 2—Mix 0.5 μg (*see Note 4*) of the eVP40 plasmid with 10 μl of the Lipofectamine reagent, and add the mixture to the cells for 6 h in Opti-MEM media. Replace media with new Opti-MEM with or without budding inhibitors and incubate at 37 °C for 24 h.

3.2 Harvest Cell Extracts and VLPs

1. VLPs—Remove culture media and centrifuge at $351 \times g$ for 10 min to remove cellular debris.
2. Layer media onto a 20% sucrose cushion in STE buffer, and centrifuge at $220,000 \times g$ for 2 h at 4 °C to harvest VLPs. Suspend the VLP pellet in 20–40 μl of STE buffer overnight at 4 °C (*see Fig. 1*).
3. Cells—Add 300 μl of RIPA buffer to the cells and centrifuge at $9,500 \times g$ at 4 °C for 5 min.

3.3 SDS-PAGE, Western Blotting, and Protein Quantification

1. Quantify protein using Bio-Rad Protein Assay kit, and use 10% polyacrylamide gel.
2. Mix 10–50 μg of cell lysates with protein loading buffer and microfuge 10 s.
3. Heat samples at 95 °C for 5 min, put quickly on ice for 3 min, microfuge for 10 s, and load samples on the gel.
4. Transfer proteins to nitrocellulose membrane (80 V) for 1.5–2 h.
5. Rinse the membrane gently in PBS-T, and then block it with PBS-T plus 5% milk for 1–3 h at RT or overnight at 4 °C (*see Note 5*).
6. Incubate filter with primary antibody (Ab), diluted appropriately in PBS-T plus 2% milk, for 1–2 h at RT with gentle shaking.

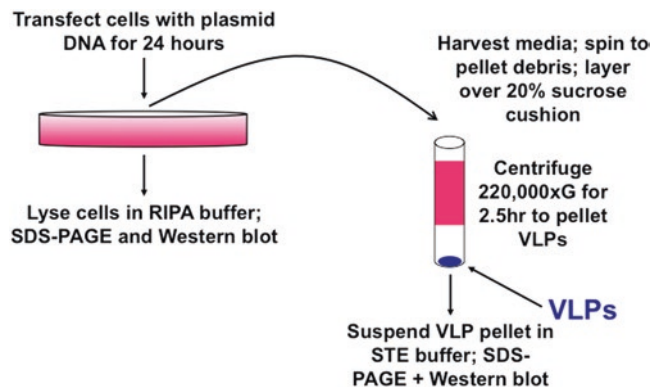


Fig. 1 Overview of VLP budding assay

7. Wash the blot 3× for 10 min each in washing buffer (PBS-T) with shaking.
8. Incubate filter with secondary Ab, diluted appropriately in PBS-T, for 1 h at RT.
9. Wash the blot 3× for 10 min each in washing buffer (PBS-T) with shaking.
10. Drain washing buffer, add ECL solution (Amersham), and develop film for 30 s to 1 min.
11. Quantify protein bands using NIH ImageJ software.

3.4 Live Cell Imaging Using TIRF Microscopy

1. Seed HEK293T cells at 0.5×10^6 cells/ml on a #1.5 cover glass bottom culture dish (Mattek Corporation, Ashland MA, USA), and incubate at 37 °C, 5% CO₂ overnight.
2. The next morning, transfect cells as above with 0.5 µg of GFP-eVP40 plasmid using Lipofectamine for 6 h, and then replace the media with fresh Opti-MEM (Thermo Fisher).
3. Place the Mattek dish in a heated, humidified environmental chamber, and maintain the cells at 37 °C, 5% CO₂ for the duration of imaging (6–24 h post transfection).
4. Visualize the cells (*see* Fig. 2) using a Leica microscope with a 100× oil immersion objective lens and a Photometrics Evolve 512 Camera. The GFP-eVP40 fluorescence at the plasma membrane was observed by setting 488 nm total internal reflection fluorescence (TIRF) laser excitation to a maximum depth of 90 nm, and images were acquired at 10 s intervals with Leica LASX software.

3.5 Inhibition of VLP Budding Using Small Molecule Inhibitors

Transfection and budding assays with inhibitors were performed as described above. Inhibitors were dissolved in DMSO to produce stock concentrations of 100 mM, and inhibitors were diluted in DMSO (0.03–1.0 µM) and added directly into the media for the duration of the experiment (*see* Note 6).

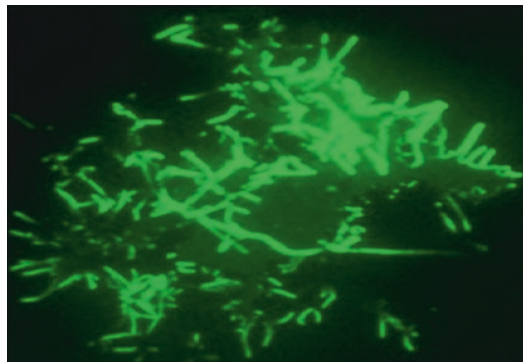


Fig. 2 TIRF microscopy image of HEK293T cells expressing VLP-like projections of GFP-eVP40 at the plasma membrane

4 Notes

1. This reagent routinely allowed for efficient transfection of HEK293T cells; however, other transfection reagents can be used as well.
2. The heated stage and humidified environment is critical for long-term imaging (e.g., 24 h).
3. It is important to check the compounds for purity (e.g., by HPLC), for solubility in DMSO, and for cytotoxicity using a standard MTT or XTT assay. Multiple freeze-thaw cycles of the compounds should be avoided.
4. While we routinely use 0.5 μ g of eVP40 plasmid DNA for transfection, the general rule of thumb is to use the least amount plasmid that allows detectable protein expression.
5. In general, 30–60 min of incubation time for the nitrocellulose filter and washing buffer or antibody solution is sufficient; however, one can incubate overnight for these steps if it is more convenient.
6. Always use DMSO alone as a negative control.

Acknowledgments

I would like to thank past and present members of the lab who contributed to this work. This work was supported in part by NIH grants to R.N.H.

References

1. Ascenzi P, Bocedi A, Heptonstall J, Capobianchi MR, Di Caro A, Mastrangelo E, Bolognesi M, Ippolito G (2008) Ebola virus and Marburgvirus: insight into the *Filoviridae* family. *Mol Aspects Med* 29:151–185. doi:[10.1016/j.mam.2007.09.005](https://doi.org/10.1016/j.mam.2007.09.005)
2. Bray M, Murphy FA (2007) Filovirus research: knowledge expands to meet a growing threat. *J Infect Dis* 196(Suppl 2):S438–S443. doi:[10.1086/520552](https://doi.org/10.1086/520552)
3. Casillas AM, Nyamathi AM, Sosa A, Wilder CL, Sands H (2003) A current review of Ebola virus: pathogenesis, clinical presentation, and diagnostic assessment. *Biol Res Nurs* 4:268–275
4. Feldmann H, Klenk HD, Sanchez A (1993) Molecular biology and evolution of filoviruses. *Arch Virol Suppl* 7:81–100
5. Peters CJ, Khan AS (1999) Filovirus diseases. *Curr Top Microbiol Immunol* 235:85–95
6. Bausch DG, Sprecher AG, Jeffs B, Boumandouki P (2008) Treatment of Marburg and Ebola hemorrhagic fevers: a strategy for testing new drugs and vaccines under outbreak conditions. *Antiviral Res* 78:150–161. doi:[10.1016/j.antiviral.2008.01.152](https://doi.org/10.1016/j.antiviral.2008.01.152)
7. Bray M, Paragas J (2002) Experimental therapy of filovirus infections. *Antiviral Res* 54:1–17
8. Adalja AA, Henderson DA (2014) Optimization of interventions in Ebola: differential contagion. *Biosecure Bioterror* 12:299–300. doi:[10.1089/bsp.2014.0925](https://doi.org/10.1089/bsp.2014.0925)
9. Marzi A, Feldmann H, Geisbert TW, Falzarano D (2011) Vesicular stomatitis virus-based vaccines for prophylaxis and treatment of filovirus infections. *J Bioterror Biodef* S1(4):2157–2526-S1-004. doi:[10.4172/2157-2526.S1-004](https://doi.org/10.4172/2157-2526.S1-004)
10. Kuhn JH, Dodd LE, Wahl-Jensen V, Radoshitzky SR, Bavari S, Jahrling PB (2011) Evaluation of perceived threat differences posed by filovirus variants. *Biosecure Bioterror* 9:361–371. doi:[10.1089/bsp.2011.0051](https://doi.org/10.1089/bsp.2011.0051)

11. Okumura A, Rasmussen AL, Halfmann P, Feldmann F, Yoshimura A, Feldmann H, Kawaoka Y, Harty RN, Katze MG (2015) Suppressor of cytokine signaling 3 is an inducible host factor that regulates virus egress during Ebola virus infection. *J Virol* 89:10399–10406. doi:[10.1128/JVI.01736-15](https://doi.org/10.1128/JVI.01736-15)
12. Han Z, Madara JJ, Liu Y, Liu W, Ruthel G, Freedman BD, Harty RN (2015) ALIX rescues budding of a double PTAP/PPEY L-domain deletion mutant of Ebola VP40: a role for ALIX in Ebola virus egress. *J Infect Dis* 212(Suppl 2):S138–S145. doi:[10.1093/infdis/jiu838](https://doi.org/10.1093/infdis/jiu838)
13. Han Z, Madara JJ, Herbert A, Prugar LI, Ruthel G, Lu J, Liu Y, Liu W, Liu X, Wrobel JE, Reitz AB, Dye JM, Harty RN, Freedman BD (2015) Calcium regulation of hemorrhagic fever virus budding: mechanistic implications for host-oriented therapeutic intervention. *PLoS Pathog* 11:e1005220. doi:[10.1371/journal.ppat.1005220](https://doi.org/10.1371/journal.ppat.1005220)
14. Stahelin RV (2014) Membrane binding and bending in Ebola VP40 assembly and egress. *Front Microbiol* 5:300. doi:[10.3389/fmicb.2014.00300](https://doi.org/10.3389/fmicb.2014.00300)
15. Lu J, Han Z, Liu Y, Liu W, Lee MS, Olson MA, Ruthel G, Freedman BD, Harty RN (2014) A host-oriented inhibitor of Junin Argentine hemorrhagic fever virus egress. *J Virol* 88:4736–4743. doi:[10.1128/JVI.03757-13](https://doi.org/10.1128/JVI.03757-13)
16. Han Z, Lu J, Liu Y, Davis B, Lee MS, Olson MA, Ruthel G, Freedman BD, Schnell MJ, Wrobel JE, Reitz AB, Harty RN (2014) Small-molecule probes targeting the viral PPxY-Host Nedd4 interface block egress of a broad range of RNA viruses. *J Virol* 88:7294–7306. doi:[10.1128/JVI.00591-14](https://doi.org/10.1128/JVI.00591-14)
17. Lu J, Qu Y, Liu Y, Jambusaria R, Han Z, Ruthel G, Freedman BD, Harty RN (2013) Host IQGAP1 and Ebola virus VP40 interactions facilitate virus-like particle egress. *J Virol* 87:7777–7780. doi:[10.1128/JVI.00470-13](https://doi.org/10.1128/JVI.00470-13)
18. Warfield KL, Aman MJ (2011) Advances in virus-like particle vaccines for filoviruses. *J Infect Dis* 204(Suppl 3):S1053–S1059. doi:[10.1093/infdis/jir346](https://doi.org/10.1093/infdis/jir346)
19. Makino A, Yamayoshi S, Shinya K, Noda T, Kawaoka Y (2011) Identification of amino acids in Marburg virus VP40 that are important for virus-like particle budding. *J Infect Dis* 204(Suppl 3):S871–S877. doi:[10.1093/infdis/jir309](https://doi.org/10.1093/infdis/jir309)
20. Liu Y, Lee MS (2011) Olson MA and Harty RN (2011) bimolecular complementation to visualize filovirus VP40-host complexes in live mammalian cells: toward the identification of budding inhibitors. *Adv Virol* 2011:341816. doi:[10.1155/2011/341816](https://doi.org/10.1155/2011/341816)
21. Liu Y, Cocka L, Okumura A, Zhang YA, Sunyer JO, Harty RN (2010) Conserved motifs within Ebola and Marburg virus VP40 proteins are important for stability, localization, and subsequent budding of virus-like particles. *J Virol* 84:2294–2303. doi:[10.1128/JVI.02034-09](https://doi.org/10.1128/JVI.02034-09)
22. Groseth A, Wolff S, Strecker T, Hoenen T, Becker S (2010) Efficient budding of the taci-like virus matrix protein z requires the nucleoprotein. *J Virol* 84:3603–3611. doi:[10.1128/JVI.02429-09](https://doi.org/10.1128/JVI.02429-09)
23. Dolnik O, Kolesnikova L, Stevermann L, Becker S (2010) Tsg101 is recruited by a late domain of the nucleocapsid protein to support budding of Marburg virus-like particles. *J Virol* 84:7847–7856. doi:[10.1128/JVI.00476-10](https://doi.org/10.1128/JVI.00476-10)
24. Okumura A, Pitha PM, Harty RN (2008) ISG15 inhibits Ebola VP40 VLP budding in an L-domain-dependent manner by blocking Nedd4 ligase activity. *Proc Natl Acad Sci U S A* 105:3974–3979. doi:[10.1073/pnas.0710629105](https://doi.org/10.1073/pnas.0710629105)
25. Yamayoshi S, Kawaoka Y (2007) Mapping of a region of Ebola virus VP40 that is important in the production of virus-like particles. *J Infect Dis* 196(Suppl 2):S291–S295. doi:[10.1086/520595](https://doi.org/10.1086/520595)
26. McCarthy SE, Johnson RF, Zhang YA, Sunyer JO, Harty RN (2007) Role for amino acids 212KLR214 of Ebola virus VP40 in assembly and budding. *J Virol* 81:11452–11460. doi:[10.1128/JVI.00853-07](https://doi.org/10.1128/JVI.00853-07)
27. Han Z, Harty RN (2007) Influence of calcium/calmodulin on budding of Ebola VLPs: implications for the involvement of the Ras/Raf/MEK/ERK pathway. *Virus Genes* 35:511–520. doi:[10.1007/s11262-007-0125-9](https://doi.org/10.1007/s11262-007-0125-9)
28. Urata S, Noda T, Kawaoka Y, Yokosawa H, Yasuda J (2006) Cellular factors required for Lassa virus budding. *J Virol* 80:4191–4195. doi:[10.1128/JVI.80.8.4191-4195.2006](https://doi.org/10.1128/JVI.80.8.4191-4195.2006)
29. Johnson RF, Bell P, Harty RN (2006) Effect of Ebola virus proteins GP, NP and VP35 on VP40 VLP morphology. *Virol J* 3:31. doi:[10.1186/1743-422X-3-31](https://doi.org/10.1186/1743-422X-3-31)
30. Kallstrom G, Warfield KL, Swenson DL, Mort S, Panchal RG, Ruthel G, Bavari S, Aman MJ (2005) Analysis of Ebola virus and VLP release using an immunocapture assay. *J Virol Methods* 127:1–9. doi:[10.1016/j.jviromet.2005.02.015](https://doi.org/10.1016/j.jviromet.2005.02.015)
31. Han Z, Harty RN (2005) Packaging of actin into Ebola virus VLPs. *Virol J* 2:92. doi:[10.1186/1743-422X-2-92](https://doi.org/10.1186/1743-422X-2-92)
32. Swenson DL, Warfield KL, Kuehl K, Larsen T, Hevey MC, Schmaljohn A, Bavari S, Aman MJ (2004) Generation of Marburg virus-like particles

- by co-expression of glycoprotein and matrix protein. *FEMS Immunol Med Microbiol* 40:27–31
33. Yasuda J, Nakao M, Kawaoka Y, Shida H (2003) Nedd4 regulates egress of Ebola virus-like particles from host cells. *J Virol* 77:9987–9992
 34. Licata JM, Simpson-Holley M, Wright NT, Han Z, Paragas J, Harty RN (2003) Overlapping motifs (PTAP and PPEY) within the Ebola virus VP40 protein function independently as late budding domains: involvement of host proteins TSG101 and VPS-4. *J Virol* 77:1812–1819
 35. Harty RN, Brown ME, Wang G, Huibregtse J, Hayes FP (2000) A PPxY motif within the VP40 protein of Ebola virus interacts physically and functionally with a ubiquitin ligase: implications for filovirus budding. *Proc Natl Acad Sci U S A* 97:13871–13876. doi:[10.1073/pnas.250277297](https://doi.org/10.1073/pnas.250277297)
 36. Johnson KA, Taghon GJ, Scott JL, Stahelin RV (2016) The Ebola Virus matrix protein, VP40, requires phosphatidylinositol 4,5-bisphosphate (PI(4,5)P2) for extensive oligomerization at the plasma membrane and viral egress. *Sci Rep* 6:19125. doi:[10.1038/srep19125](https://doi.org/10.1038/srep19125)

Roles of Arenavirus Z Protein in Mediating Virion Budding, Viral Transcription-Inhibition and Interferon-Beta Suppression

Junjie Shao, Yuying Liang, and Hinh Ly

Abstract

The smallest arenaviral protein is the zinc-finger protein (Z) that belongs to the RING finger protein family. Z serves as a main component required for virus budding from the membrane of the infected cells through self-oligomerization, a process that can be aided by the viral nucleoprotein (NP) to form the viral matrix of progeny virus particles. Z has also been shown to be essential for mediating viral transcriptional repression activity by locking the L polymerase onto the viral promoter in a catalytically inactive state, thus limiting viral replication. The Z protein has also recently been shown to inhibit the type I interferon-induction pathway by directly binding to the intracellular pathogen-sensor proteins RIG-I and MDA5, and thus inhibiting their normal functions. This chapter describes several assays used to examine the important roles of the arenaviral Z protein in mediating virus budding (i.e., either Z self-budding or NP-Z budding activities), viral transcriptional inhibition in a viral minigenome (MG) assay, and type I IFN suppression in an IFN- β promoter-mediated luciferase reporter assay.

Key words Arenavirus, Lassa virus, Pichindé virus, Matrix protein, RING protein, Virus budding, Interferon suppression, Transcription inhibition

1 Introduction

The *Arenaviridae* consists of a large group of bisegmented single-stranded ambisense RNA viruses that can cause significant morbidity and mortality in humans. Lassa virus and Lujo virus (LUJV), found in Africa, and several other arenaviruses found in South America can cause severe hemorrhagic fever (HF). There are currently limited prevention and treatment modalities against these pathogenic arenaviruses. The only available vaccine (Candid #1) has been developed and used extensively to prevent Argentinian hemorrhagic fever (AHF) caused by Junín virus (JUNV) [1]. Ribavirin, a guanosine analog, has been used in treating arenaviral HF with mixed success and significant toxicity [2].

The arenaviral genome is composed of two segments: the L (large) segment encodes the Z matrix protein and the L polymerase protein, while the S (small) segment encodes the glycoprotein (GPC) and nucleoprotein (NP). The smallest arenaviral protein of 90–99 amino acids in size, depending on the virus, is the zinc-finger protein (Z) that belongs to the RING finger protein family [3]. Like other known RING finger proteins [4], the arenavirus Z protein has been shown to interact with many cellular proteins, including but not necessarily limited to the promyelocytic leukemia protein (PML), eukaryotic elongation factor 4E (eIF4E) or components of the endosomal sorting complexes required for transport (ESCRT) [4, 5]. In addition to interacting with cellular proteins, Z also interacts with the arenaviral L protein to latch the protein onto the genome in order to ensure that the L polymerase is incorporated into virion particles [6]. The interaction between Z and the L polymerase of the Tacaribe virus (TCRV) appears to be essential for mediating viral transcriptional repression activity [7]. Z appears to lock the L polymerase onto the viral promoter in a catalytically inactive state, thus limiting viral replication [6, 8, 9].

Z also serves as a main component required for viral budding by oligomerizing and forming the viral matrix of progeny virus particles [4]. The Z homo-oligomerization process is likely important for its function in virion budding [10]. A crystal structure of a dodecamer form of the LASV Z protein has recently been solved [11]. It shows a ring-like structure of Z with highly basic residues, including a Lys–Trp–Lys triad in the center, as important for Z oligomerization. It is important to note that arenaviral NP protein appears to be required for efficient Z-mediated budding activity of the Tacaribe virus (TCRV) [12] and Pichindé virus (PICV) [13] possibly through specific NP–Z interactions [14, 15].

Arenaviral Z protein has also recently been shown to inhibit the type I interferon-induction pathway by directly binding to the N-terminal CARD domain of the intracellular pathogen-sensor proteins RIG-I and MDA5 [16]. Z proteins from all known pathogenic arenaviruses [e.g., LASV, LUJV, JUNV, Machupo (MACV), Sabiá (SABV), Chapare (CHPV), Guanarito (GTOV), and Dandenong (DANV)] as well as the relatively low pathogenic lymphocytic choriomeningitis virus (LCMV) are able to bind to RIG-I as well as MDA5 and thus, suppress the production of interferon-beta (IFN- β). In contrast, Z proteins of many known nonpathogenic arenaviruses do not bind to RIG-I or MDA5 and fail to inhibit the IFN induction pathway [16]. The fact that this small Z protein plays multiple roles in arenaviral replication and in modulating host immune responses to viral infection highlights the importance of this viral protein as a potential target for antiviral drug development. This chapter describes several assays used to

examine the important roles of the arenaviral Z protein in mediating virus budding (i.e., either Z self-budding or NP-Z budding activities), viral transcriptional inhibition in a viral minigenome (MG) assay, and type I IFN suppression in an IFN- β promoter-mediated luciferase reporter assay.

2 Materials

1. Cells: Human kidney epithelial 293T cells are grown in DMEM supplemented with 10% FBS and 50 μ g of penicillin–streptomycin/ml.
2. Plasmids: For PICV Z protein and NP expression constructs, genes are amplified from the respective plasmid of the full-length PICV L or S segment using primers containing hemagglutinin (HA) or Myc tag at the C terminus, and cloned into the pCAGGS expression vector. IFN- β promoter-directed LUC plasmid is used for a Z-induced interferon suppression assay. MGLF7-5Rluc3 plasmid is used for minigenome assay. pSV- β -Galactosidase Control Vector is purchased from Promega. Human RIG-I N terminal domain (RIG-iN) and LASV Z gene (with HA tag) are cloned into the pCAGGS vector as previously described [16].
3. Assay kits for beta-galactosidase, firefly luciferase, and Renilla luciferase.
4. Promega cell culture lysis 5 \times reagent.
5. Lipofectamine 2000.
6. PCR thermal cycler.
7. Microcentrifuge.
8. Ultracentrifuge.
9. Water bath.
10. Enhanced chemiluminescence (ECL) kit to detect bands in Western blots.
11. ECL detection device (Thermo).
12. Polyethylene glycol (PEG).
13. Plate reader.
14. 2 \times HBS: 50 mM HEPES, 280 mM NaCl, 1.5 mM Na₂HPO₄, pH 7.10.
15. 2.5 M calcium chloride stock solution.
16. RIPA buffer: 10 mM Tris–HCl (pH 8.0), 1 mM EDTA, 0.5 mM EGTA, 1% Triton X-100, 0.1% sodium deoxycholate, 0.1% SDS, 140 mM NaCl.

3 Methods

3.1 Z Self-Budding Assay

1. 293T cells are seeded in 10 cm tissue culture dish at 3×10^6 /dish with complete DMEM.
2. On the morning of the day of transfection, replace cell-culture media with an equal aliquot of fresh complete DMEM.
3. Prepare plasmids and calcium chloride mix fresh as follows:

10 μ l	pCAGGS-PICV-Z-HA plasmid (1 μ g/ μ l)
50 μ l	2.5 M calcium chloride
440 μ l	Water

Add 500 μ l 2 \times HBS to above mixture while vortexing at the lowest speed setting for 10 s. The mixture is added dropwise using a pipetman into dish. Media are replaced with same amount of complete DMEM 6 h post-transfection.

4. Forty-eight hours post-transfection, supernatants are collected and centrifuged at $15,000 \times g$ for 10 min at 4 $^{\circ}$ C. The budded VLP in the cleared supernatants are precipitated with 8% PEG 8000, 0.5 M sodium chloride, collected after centrifugation at $15,000 \times g$ for 15 min, and lysed in RIPA buffer.
5. Cell lysates and the budded VLP are analyzed on a 15% sodium dodecyl sulfate–polyacrylamide gel (SDS-PAGE) and Z proteins are detected by Western blotting with the anti-HA antibody.
6. Figure 1 shows results of the wild-type PICV Z self-budding as VLP.

3.2 NP-Z Budding Assay

1. 293T cells are seeded in a 10 cm tissue culture dish at 3×10^6 /dish with complete DMEM.
2. On the morning of the day of transfection, replace culture media with an equal aliquot of fresh complete DMEM.
3. Prepare plasmids and calcium chloride mix fresh as follows:

10 μ l	pCAGGS-PICV-NP plasmid (1 μ g/ μ l)
10 μ l	pCAGGS-PICV-Z-HA plasmid (1 μ g/ μ l)
50 μ l	2.5 M calcium chloride
440 μ l	Water

Add 500 μ l 2 \times HBS into above mixture by vortexing using the lowest speed setting for 10 s. The mixture is added dropwise using a pipetman into dish. Media are replaced with same amount of complete DMEM 6 h post-transfection.

4. Forty-eight hours post-transfection, supernatants are collected and centrifuged at $15,000 \times g$ for 10 min at 4 $^{\circ}$ C. The budded

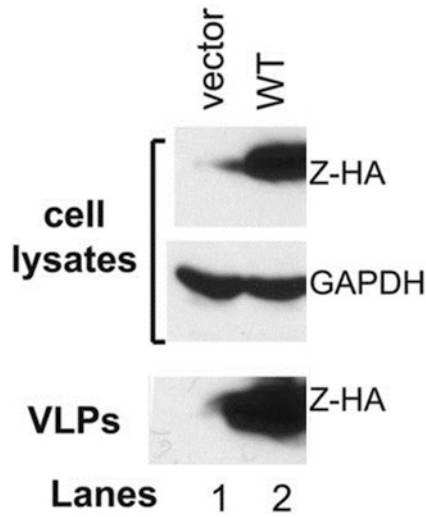


Fig. 1 Analysis of the self-budding activity of the wild-type PICV Z protein. 293T cells were transfected with an empty vector (*lane 1*) or the WT PICV Z expression vector (*lane 2*). Expressions of HA-tagged Z proteins (Z-HA) along with GAPDH as loading control in the cell lysates were analyzed by Western blot. Virus supernatants (VLP) were collected, precipitated by PEG-8000, separated on 15% SDS-PAGE, and analyzed by Western blot

VLP in the cleared supernatants are precipitated with 8% PEG-8000, 0.5 M sodium chloride, collected after centrifugation at $15,000 \times g$ for 15 min, and lysed by RIPA buffer. Cell lysates and the budded VLP are analyzed on a 15% sodium dodecyl sulfate (SDS)-polyacrylamide gel and detected for Z and NP proteins by Western blotting with the anti-HA antibody and rabbit anti-PICV NP sera, respectively (*see Note 1*).

- Figure 2 shows results of NP incorporation into the Z-mediated VLP.

3.3 IFN- β Promoter-Driven Luciferase Reporter Assay

- 293T cells are seeded into 12 well-plate at 3×10^5 /well with complete DMEM.
- In the morning of the day of transfection, culture media are replaced by an equal aliquot of fresh media.
- Prepare DNA and calcium phosphate mix as follows:

1 μ l	pSV- β -Galactosidase plasmid (50 ng/ μ l)
1 μ l	IFN- β promoter reporter plasmid (100 ng/ μ l)
1 μ l	pCAGGS-PICV-Z-HA or pCAGGS-LASV-Z-HA plasmid (1 μ g/ μ l)
1 μ l	pCAGGS-RIG-iN plasmid (50 ng/ μ l)
5 μ l	2.5 M calcium chloride
47 μ l	Water

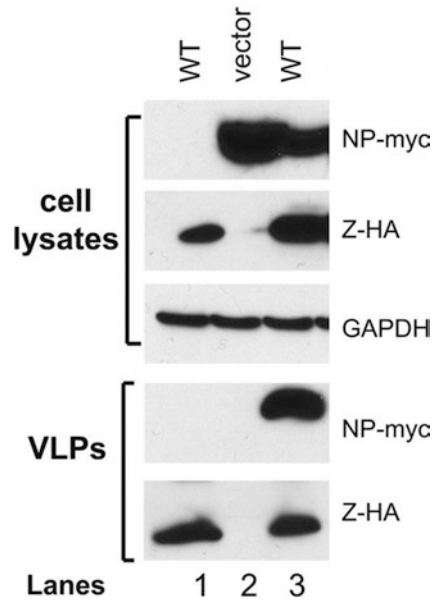


Fig. 2 NP incorporation into Z-mediated VLP formations. 293T cells were transfected with WT PICV Z protein expression vector (*lanes 1 and 3*), empty vector (*lane 2*), and with the NP expression vector (*lanes 2 and 3*). The amounts of VLP released into the supernatants were analyzed by Western blot against Z and NP proteins on 15% SDS-PAGE along with GAPDH as loading control in the cell lysates

To prepare triplicates for each test condition, mix as follows:

3 μ l	pSV- β -galactosidase plasmid (50 ng/ μ l)
3 μ l	IFN- β promoter reporter plasmid (100 ng/ μ l)
3 μ l	pCAGGS-PICV-Z-HA plasmid or pCAGGS-LASV-Z-HA plasmid (1 μ g/ μ l)
15 μ l	2.5 M calcium chloride
141 μ l	Water

Into each tube of DNA–calcium phosphate mixture, add 75 μ l 2 \times HBS, vortex using very low speed to mix, and add the mixture to three wells of cells (98 μ l per well).

- Twenty-four hours post-transfection, the supernatants are aspirated and cells are lysed by 100 μ l of Luciferase Cell Culture Lysis 1 \times Reagent. 20 μ l of cell lysate is used for firefly luciferase assay and another 50 μ l of cell lysate is used for β -gal assay according to manufacturer's instructions.
- The firefly luciferase activity is normalized by dividing the Firefly luciferase reading by the β -gal reading. The IFN- β promoter activity is represented by the folds of the normalized firefly luciferase activity of the test to that the control (*see Note 2*).

6. Figure 3 shows results of the LASV Z-mediated suppression of the IFN- β promoter activity.

3.4 Z-Mediated Viral Minigenome (MG) Replication and Transcription Assay

3.4.1 *In Vitro* RNA Transcription

1. The plasmid MGLEF7-5Rluc3 is linearized by digestion with Nhe I restriction enzyme.
2. DNA is extracted by standard phenol/chloroform and isopropanol precipitation.
3. Transcription reaction is assembled at room temperature according to Ambion MEGAscript[®] Kit manual. Calculate the volume of nuclease-free water to bring the total volume to 20 μ l, and to this amount add 2 μ l ATP, 2 μ l CTP, 2 μ l GTP, 2 μ l UTP, 2 μ l 10 \times reaction buffer, 1 μ g linearized template DNA, and 2 μ l enzyme mix.
4. Sample is incubated at 37 $^{\circ}$ C for 4 h.
5. A hundred and fifteen microliters of nuclease-free water and 15 μ l ammonium acetate stop solution are added.
6. RNA is extracted by phenol–chloroform and isopropanol-precipitated using the standard technique.
7. Carefully discard the precipitating solution and the RNA is resuspended in 80 μ l of DEPC-treated water.
8. RNA is quantified and adjusted to a concentration of 1 μ g/ μ l (*see Note 3*).

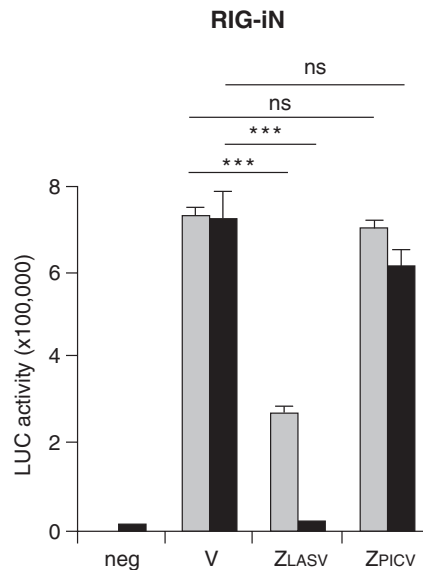


Fig. 3 Z-mediated suppression of the IFN- β promoter-driven luciferase reporter activity. LASV Z, but not PICV Z, inhibits RIG-iN-induced IFN- β activation in a luciferase (LUC)-based promoter assay. 293T cells were transfected with two different concentrations [100 ng (*gray bars*) and 1000 ng (*black bars*)] of either an empty vector (V) or Z plasmids (LASV or PICV) together with IFN- β -LUC, β -Gal, and RIG-iN plasmids. *Neg* negative control (no RIG-iN transfection)

3.4.2 Plasmid Transfection

1. 293T cells are seeded into 24-well plates at 1×10^5 cells/well that contains 0.5 ml of DMEM with 10% FBS and 50 $\mu\text{g}/\text{ml}$ of penicillin and streptomycin.
2. On the morning of the day of transfection, a fresh aliquot of the cell media is added to the 293T cell culture.
3. DNA and calcium phosphate mixture is prepared at room temperature as follows:

Each of the 25- μl of DNA mix (for one 24-well transfection) contains:

1 μl	Beta-gal reporter plasmid (50 ng/ μl)
1 μl	pCAGGS-PICV-Z-HA plasmid (1 $\mu\text{g}/\mu\text{l}$)
1 μl	pCAGGS-NP plasmid (250 ng/ μl)
1 μl	pCAGGS-L plasmid (500 ng/ μl)
2.5 μl	2.5 M calcium chloride
18.5 μl	Water

To prepare triplicates for each test condition, make a mixture as follows:

3 μl	Beta-gal reporter plasmid (50 ng/ μl)
3 μl	pCAGGS-PICV-Z-HA plasmid (1 $\mu\text{g}/\mu\text{l}$)
3 μl	pCAGGS-NP plasmid (250 ng/ μl)
3 μl	pCAGGS-L plasmid (500 ng/ μl)
7.5 μl	2.5 M calcium chloride
55.5 μl	Water

Into each tube of DNA–calcium phosphate mixture ($25 \times 3 = 75 \mu\text{l}$), add 75 μl of 2xHBS. The sample is gently mixed by vortexing using the lowest speed setting. The mixture is added dropwise using a pipetman into each well of cells (48 μl of sample into each well of the 24-well plate).

4. Cells are incubated in a 37 °C CO₂ incubator for 24 h.

3.4.3 RNA Transfection at 24 h After Plasmids Transfection

1. Four hours before transfection, an aliquot of fresh antibiotics-free DMEM is used to replace the overnight cell culture media.
2. For each well, 1 μg of in vitro-transcribed RNA (*see Note 3*) is diluted into 25 μl Opti-MEM® I Medium.
3. For each well, 1 μl of Lipofectamine™ 2000 is diluted into 25 μl Opti-MEM® I Medium and incubated for 5 min at room temperature.
4. The diluted RNA is added to diluted Lipofectamine™ and incubated at room temperature for no more than 10 min.

5. RNA–Lipofectamine™ 2000 complexes are directly added to each well containing cells and mixed gently by rocking the plate back and forth. The cells are incubated at 37 °C in a CO₂ incubator.
6. The cell medium is replaced by fresh DMEM medium (10% FBS) at 6 h post-transfection.
7. Twenty-four hours post-RNA transfection, cells are washed once by PBS. Then cells are lysed by lysis buffer for Renilla luciferase assay.

3.4.4 Renilla Luciferase

Assay

1. Twenty microliters of cell lysate is used for Renilla luciferase assay and another 50 µl of cell lysate is used for β-gal assay according to manufacturer's instructions.
2. Renilla luciferase activity is normalized by dividing the Renilla luciferase reading by the β-gal reading. The minigenome replication activity is represented by the folds of the normalized Renilla luciferase activity of the test to that of the control.
3. Figure 4 shows results of Z-mediated viral minigenome inhibition.

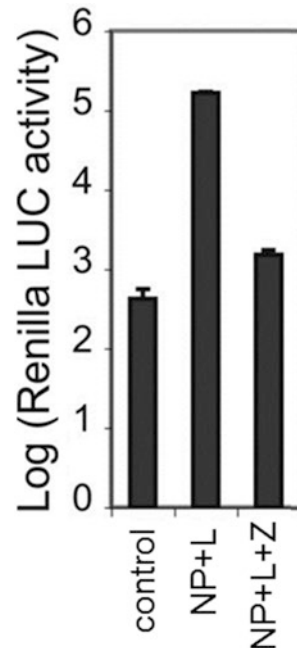


Fig. 4 Z-mediated inhibition of viral RNA synthesis. PICV Z protein was examined for its ability to inhibit viral RNA transcription in the minigenome assay. Control reaction contains the minigenomic RNA and the NP-expressing plasmid only, whereas other reactions also contain other protein-expressing plasmids (i.e., either L-expressing plasmid or L- and Z-expressing plasmids). Results shown are the average of at least three independent experiments with error bars representing standard deviations

4 Notes

1. Western blot analyses are conducted using rabbit sera raised against specific short peptides within the NP protein as previously described [17]. Peptide sequences and limited aliquots of the rabbit sera are available upon request.
2. When performing the IFN- β promoter assay, the amount of RIG-iN and Z plasmid is critical. Low Z and RIG-iN protein expression will lead to unreliable IFN- β readings.
3. The integrity of the RNA needs to be validated by agarose gel electrophoresis prior to use in the transfection reaction.

Acknowledgments

This work was supported in part by the NIAID/NIH through the new-direction awards mechanism of the SERCEB grant (U54-AI057157) to Y.L. and H.L., by the NIAID/NIH R01 AI083409 to Y.L., and R01 AI093580 and R56 AI091805 to H.L.

References

1. Maiztegui JI, KT MK Jr, Barrera Oro JG, Harrison LH, Gibbs PH, Feuillade MR, Enria DA, Briggiler AM, Levis SC, Ambrosio AM, Halsey NA, Peters CJ (1998) Protective efficacy of a live attenuated vaccine against Argentine hemorrhagic fever. AHF Study Group. *J Infect Dis* 177:277–283
2. Gunther S, Lenz O (2004) Lassa virus. *Crit Rev Clin Lab Sci* 41:339–390
3. Salvato MS, Shimomaye EM (1989) The completed sequence of lymphocytic choriomeningitis virus reveals a unique RNA structure and a gene for a zinc finger protein. *Virology* 173:1–10
4. Fehling SK, Lennartz F, Strecker T (2012) Multifunctional nature of the arenavirus RING finger protein Z. *Virus* 4:2973–3011
5. Dwyer EJC, Lai HK, MacDonald RC, Salvato MS, Borden KLB (2000) The lymphocytic choriomeningitis virus RING protein Z associates with eukaryotic initiation factor 4E and selectively represses translation in a RING-dependent manner. *J Virol* 74:3293–3300
6. Kranzusch PJ, Whelan SP (2011) Arenavirus Z protein controls viral RNA synthesis by locking a polymerase-promoter complex. *Proc Natl Acad Sci U S A* 108:19743–19748
7. Wilda M, Lopez N, Casabona JC, Franze-Fernandez MT (2008) Mapping of the tacaribe arenavirus Z-protein binding sites on the L protein identified both amino acids within the putative polymerase domain and a region at the N terminus of L that are critically involved in binding. *J Virol* 82:11454–11460
8. Cornu TI, de la Torre JC (2001) RING finger Z protein of lymphocytic choriomeningitis virus (LCMV) inhibits transcription and RNA replication of an LCMV S-segment minigenome. *J Virol* 75:9415–9426
9. Lopez N, Jacamo R, Franze-Fernandez MT (2001) Transcription and RNA replication of tacaribe virus genome and antigenome analogs require N and L proteins: Z protein is an inhibitor of these processes. *J Virol* 75:12241–12251
10. Kentsis A, Gordon RE, Borden KL (2002) Self-assembly properties of a model RING domain. *Proc Natl Acad Sci U S A* 99:667–672
11. Hastie KM, Zandonatti M, Liu T, Li S, Woods VL Jr, Sapphire EO (2016) Crystal structure of the oligomeric form of Lassa virus matrix protein Z. *J Virol* 90:4556–4562
12. Groseth A, Wolff S, Strecker T, Hoenen T, Becker S (2010) Efficient budding of the tacaribe virus matrix protein Z requires the nucleoprotein. *J Virol* 84:3603–3611
13. Wang J, Danzy S, Kumar N, Ly H, Liang Y (2012) Biological roles and functional mechanisms of arenavirus Z protein in viral replication. *J Virol* 86:9794–9801

14. Capul AA, de la Torre JC, Buchmeier MJ (2011) Conserved residues in Lassa fever virus Z protein modulate viral infectivity at the level of the ribonucleoprotein. *J Virol* 85:3172–3178
15. Casabona JC, Levingston Macleod JM, Loureiro ME, Gomez GA, Lopez N (2009) The RING domain and the L79 residue of Z protein are involved in both the rescue of nucleocapsids and the incorporation of glycoproteins into infectious chimeric arenavirus-like particles. *J Virol* 83:7029–7039
16. Xing J, Ly H, Liang Y (2015) The Z proteins of pathogenic but not nonpathogenic arenaviruses inhibit RIG-I-like receptor-dependent interferon production. *J Virol* 89:2944–2955
17. Liang Y, Lan S, Ly H (2009) Molecular determinants of Pichindé virus infection of guinea pigs—a small animal model system for arenaviral hemorrhagic fevers. *Ann N Y Acad Sci* 1171(Suppl 1):E65–E74

Structure–Function Assays for Crimean–Congo Hemorrhagic Fever Virus Polymerase

Marko Zivcec

Abstract

The recently developed Crimean–Congo hemorrhagic fever virus (CCHFV) reverse genetics systems have paved the way for experiments looking to identify and characterize the roles played by viral and cellular proteins in the CCHFV life cycle. In particular, the development of the noninfectious minigenome and virus-like particle (VLP) systems is a tremendous technological advance, as these systems allow for precisely targeting proteins or nucleic acids and measuring the effects these mutations or treatments have on viral life cycle stages. Importantly, these systems can be used at low-containment levels. Presented are the materials and methods currently available to study CCHFV transcription, replication, and translation in the context of a minigenome or VLP.

Keywords CCHFV, Minigenome, VLP, Reverse-genetics, Transcription, Replication, Polymerase

1 Introduction

Reverse genetics systems have been extensively used to elucidate mechanisms of transcription, replication, and particle assembly of clinically and agriculturally important viruses [1]. Recently, several reverse genetics platforms for studying Crimean–Congo hemorrhagic fever virus (CCHFV) have been developed [2–5]. While studying infectious, recombinant, and/or naturally occurring CCHFV isolates reflects the entire viral replication cycle *in vitro*, such studies are cumbersome and do not allow for the examination of individual steps in the viral life cycle. Conversely, life cycle modeling systems, such as minigenome and virus-like particle (VLP) systems, may be used to dissect parts of the viral life cycle in bio-safety level 2 (BSL-2) facilities. Here, we present the use of minigenomes and VLPs for studying the CCHFV transcription cycle.

The recently described minigenome and transcriptionally and entry-competent VLPs (tecVLPs) can be produced from highly transfectable cell lines, and can enter into and produce a luciferase signal in several cell lines [3, 5]. The generated tecVLPs can

subsequently enter into both efficiently and poorly transfectable cells. Using a combination of luciferase and quantitative RT-PCR (qRT-PCR) approaches, tecVLPs allow for the study of CCHFV transcription, replication, and translation in multiple cell types.

In practice the systems are complimentary to one another and can be used to dissect and study each of the steps in the complete CCHFV replication cycle, without the burden of using infectious CCHFV. In studies in which cell-to-cell spread is not required the minigenome system can be used while the tecVLP system can be used for studies in which targeting cell-to-cell spread is essential. Furthermore the systems allow for the testing of inhibitors of CCHFV transcription, replication, translation, protein maturation, particle assembly, budding, and entry in a BSL-2 setting, thus accelerating the rate of discovery of novel CCHFV therapeutics.

2 Materials

2.1 CCHFV Minigenome and tecVLP Generation

2.0.1 Cells, Media, and Lysis Buffers

1. Maintenance media for BSR-T7 cells: DMEM supplemented with 1 mM sodium pyruvate, 1% penicillin–streptomycin, and 5% fetal bovine serum (GE Life Sciences; *see Note 1*).
2. Maintenance media for HuH7 cells: DMEM supplemented with 10% fetal bovine serum, 1 mM sodium pyruvate, 1% penicillin–streptomycin, and 1% nonessential amino acids (*see Note 1*).
3. Transfection medium: OptiMEM (Thermo Fisher Scientific).
4. Cell lysis buffer for RNA extraction is fully constituted Lysis Binding Solution mixed with 100% isopropanol at a volume ratio of 11:9, respectively (Thermo Fisher Scientific).
5. Cell lysis buffer for luciferase assay: Nano-Glo[®] Luciferase Assay Buffer or 1× Passive Lysis Buffer (Promega).

2.1.1 Transfection with CCHFV-Replication and -Helper Plasmids

1. Prepare the following endotoxin-free and sequence-confirmed plasmids for transfection (*see Note 2*): pCAGGS-T7, encodes a bacteriophage T7 RNA polymerase; pCAGGS-NP, encodes CCHFV nucleocapsid protein; pCAGGS-GPC, encodes CCHFV glycoprotein precursor protein; pCAG-LCK-L, encodes CCHFV RNA-dependent RNA polymerase; pLCK-L-NanoLuc, encodes the CCHFV L segment minigenome [5].
2. LT1 transfection reagent (Mirus Bio).

2.2 CCHFV Minigenome RNA Extraction, qRT-PCR, and Luciferase Assay

1. MagMax RNA extraction kit (Thermo Fisher Scientific; *see Note 3*).
2. MagMax Express-96 Magnetic Particle Processor.
3. Baseline-ZERO DNase (Epicentre Bio, Madison, WI) or equivalent dual action DNase.

4. SuperScript III Platinum One-Step qRT-PCR Kit (Thermo Fisher Scientific) Master mix (per reaction): 12.5 μL 2 \times Reaction Mix, 0.5 μL primer/probe master mix, 0.5 μL SuperScript III RT/Platinum Taq mix, and 6.5 μL nuclease-free water.
5. Assemble the following NanoLuc luciferase Taqman primers and probes (all from TIB Molbiol): NLucF, AGGTGGTGTACCCTGTGGAT; NLucR, ACGGCGATGCCTTCATAC; NLucPr, 6FAM-TGATCCTGCACTATGGCACACTGG--BBQ (*see Note 3*).
6. Appropriate cell type-specific qRT-PCR internal control primers (*see Note 4*).
7. Nano-Glo Luciferase Assay System (Promega; *see Note 5*).

3 Methods

3.1 CCHFV Minigenome Assay

1. Prepare BSRT7 or HuH7 cells in 6-well plates to reach 60–90% confluence on the day of transfection (*see Note 6*).
2. Equilibrate plasmids to room temperature and mix thoroughly by shaking or pipetting. Briefly centrifuge the tubes to collect the plasmids.
3. For minigenomes, in a small sterile vial, mix: 1000 μg pCAGGS-NP, 500 μg pCAG-LCK-L, 1000 μg pCAGGS-T7, and 250 μg pLCK-L-NanoLuc per well of cells to be transfected. Record the total plasmid volume (*see Note 7*). Optionally, you could add 50 μg of firefly luciferase-expressing plasmid, e.g., pGL4.53[luc2/PGK] Vector (Promega).
4. For tecVLPs, in a small sterile vial, mix: 1000 μg pCAGGS-NP, 2500 μg pCAGGS-GPC, 500 μg pCAG-LCK-L, 1000 μg pCAGGS-T7, and 250 μg pLCK-L-NanoLuc per well of cells to be transfected. Record the total volume of plasmids (*see Note 7*).
5. For control cells, in a small sterile vial, mix: 1000 μg pCAGGS-T7, 250 μg pLCK-L-NanoLuc, and 1500–4000 μg pCAGGS per well of cells to be transfected (these serve as the background control or calibrator cells). Record the total plasmid volume (*see Note 7*).
6. For transfecting plasmid mixtures into cells, in another tube, mix: 250 μL OptiMEM and 9 μL (for minigenomes) or 15 μL (for tecVLP) LT1 transfection reagent per well of cells to be transfected (*see Note 7*). Incubate at room temperature for 1–5 min.
7. Combine the plasmid mixtures from Subheading 3.1, step 3, or Subheading 3.1, step 4, and from Subheading 3.1, step 5

with the mixture from Subheading 3.1, **step 6** and mix thoroughly. Incubate at room temperature for 20–30 min.

8. While the transfection reagent and plasmids are incubating, label the plates to be transfected.
9. For minigenomes, add (259 + volume of combined plasmids) μL of transfection mixture to cells in a circular motion, and incubate the cells overnight at 37 °C in a humidified incubator.
10. For tecVLPs, add (265 + volume of combined plasmids) μL of transfection mixture to cells in a circular motion, and incubate the cells overnight at 37 °C in a humidified incubator.
11. The following day, remove transfection reagent and replace with fresh media.
12. Incubate the transfected cells for 1 (minigenome) or 2 (tecVLP) more days.
13. For minigenomes, remove media and lyse the cells with lysis buffer appropriate for application, or freeze at ≤ -20 °C.
14. For tecVLPs, collect media on day 3–4 post transfection. Filter the collected media through 0.22 μm pore-size filter, or centrifuge briefly (5–10 min at 1000–2000 $\times g$) prior to freezing at ≤ -80 °C.
15. tecVLP concentration may be quantified using a modified tissue culture infectious dose 50% (TCID₅₀) assay [5] or qRT-PCR (*see Note 8*).

3.2 TecVLP Entry into Target Cells

1. Prepare cell line of interest prior to thawing tecVLP stocks (*see Note 9*). If testing compounds or otherwise treating target cells, treat as necessary (e.g., transfect with siRNA or pretreat with inhibitor, if using).
2. Thaw tecVLP stocks and dilute as necessary with DMEM or other media.
3. Add 10–100 μL tecVLP stock per 0.3 cm² of target cells and incubate at 37 °C in a humidified incubator for 1 h to overnight.
4. Wash recipient cells 2–3 times with PBS or plain cell medium, and incubate overnight in fresh medium. Alternatively, wash recipient cells 2–3 times with PBS prior to harvesting cells with the desired lysis method (for RNA isolation or luciferase assay).

3.3 Luciferase Assays

Follow manufacturer's instructions (Nano-Glo Luciferase Assay System, Promega), or see below.

1. Optional: partially remove supernatant from transfected or tecVLP-treated cells to use less lysis buffer per well.
2. Add a volume of fully reconstituted Nano-Glo Luciferase Assay Substrate equal to the volume of supernatant in each well, and

incubate at room temperature for ≥ 10 min but ≤ 2 h with shaking; shake occasionally by hand or constantly with a shaker (*see Note 10*).

3. If using clear tissue culture plates, after the incubation step, mix thoroughly and pipette cells into opaque white or black plates. If using opaque tissue culture plates, simply proceed to plate reader.
4. Set gain and read plate. Due to the strength of the NanoLuc signal, transfected cells may have to be diluted to prevent overloading the instrument sensors.

3.4 RNA Extraction for qRT-PCR

1. Use MagMax RNA extraction kit and MagMAX™ Express-96 Magnetic Particle Processor or equivalent according to manufacturer's instructions.
2. Treat purified RNA with a dual action DNase, for 30–120 min according to manufacturer's instructions.
3. Reextract RNA to remove DNase, as it would negatively affect PCR, by using MagMax RNA extraction kit and MagMAX™ Express-96 Magnetic Particle Processor or equivalent according to manufacturer's instructions.

3.5 One-Step qRT-PCR

1. Dilute qRT-PCR primers and probe to create a primer/probe master mix with a final concentration of 20 μM for each primer and 10 μM for the probe.
2. Set up qRT-PCR using SuperScript III Platinum One-Step qRT-PCR Kit reagents or equivalent (*see Note 7*).
3. Add 20 μL of Superscript master mix to each well of qRT-PCR plate and 5 μL of DNase-treated purified RNA.
4. Briefly, gently tap or centrifuge the qRT-PCR plate prior to placing the plate into Applied Biosystems 7300 Real-Time PCR System instrument.
5. Cycle as follows: 15 min at 50 °C, 2 min at 95 °C, followed by 40 cycles of 15 s at 95 °C and 30 s at 60 °C. Take readings at the 60 °C step.
6. Analyze by appropriate software and standardize to calibrator cells (cells transfected with only pCAGGS-T7 and pLCK-L-NanoLuc) using the ΔC_T or $\Delta\Delta C_T$ method, depending on whether internal gene primers and probe are used [6] (*see Note 11*).

$$\Delta C_T = (C_{T\text{minigenome}} - C_{T\text{calibrator}}).$$

$$\Delta\Delta C_T = (C_{T\text{minigenome}} - C_{T\text{minigenome internal control gene}}) - (C_{T\text{calibrator}} - C_{T\text{calibrator internal control gene}}).$$

Fold change over calibrator cell lines is calculated as $2^{-\Delta C_T}$ or $2^{-\Delta\Delta C_T}$.

4 Notes

1. Make sure that cells are growing rapidly and are free of common laboratory contaminants, like mycoplasma or Sendai virus. Cell preparations that grow slowly will be difficult to transfect.
2. Ensure that plasmids are prepared using high-quality, endotoxin-free preparations, or are treated with endotoxin removal reagents. We use NucleoBond Xtra EF kit from Macherey-Nagel (Bethlehem, PA, USA) to generate endotoxin-free plasmids. In addition, confirm all plasmid sequences and determine the concentrations of all plasmids in solution.
3. Any reliable commercial transfection, RNA extraction, DNase, and qRT-PCR reagents will probably be effective, but the protocol may need to be adapted for each substitution. For qRT-PCR probes, dyes other than 6FAM may be used and quenchers other than BlackBerry Quencher (BBQ) may be used. However the use of other dark quenchers such as Black Hole Quencher is recommended.
4. Ensure that the internal housekeeping gene control for qRT-PCR, whether it is commercial or designed in-house, is a validated primer/probe combination targeting a gene that does not readily change due to transfection. Use a housekeeping gene such as β -actin, ribosomal protein(s), or cellular RNA polymerases. Validate internal control genes by transfecting with DNA plasmids and determining the C_T of the housekeeping gene. Select the gene that fluctuates the least. In hamster tissues, we found that the gene ribosomal protein L18 served as an effective internal control gene [7] however whether this gene can be used for other viruses is uncertain.
5. Luciferase reagents other than Nano-Glo will likely yield poor results.
6. When seeding cells for transfection, we typically seed 0.5×10^6 to 1.0×10^6 cells/well (9.6 cm^2) the day before transfection.
7. Whenever preparing master mixes or stocks for multiple wells, always include enough components for an extra half reaction, or 5% more (whichever is larger), to ensure sufficient volume to transfect each well.
8. If desired, tecVLP can be concentrated by centrifugation on a 100 kDa cutoff Amicon column or equivalent, for 5–30 min at $\leq 1500 \times g$. Concentration should be done after filtration or clarification but before freezing at $\leq -80 \text{ }^\circ\text{C}$.
9. tecVLPs may be used on several cell types without special pre-treatment [5].

10. Plate rockers will not adequately mix the NanoLuc Assay reagents in 96-well plates, and therefore use of shakers, or shaking by hand, is advised.
11. Use ΔC_T to measure the relative levels of NanoLuc RNA present in cell supernatants while using the ΔC_T or $\Delta\Delta C_T$ when investigating transfected cells.

Acknowledgements

The author would like to thank Tatyana Klimova and Cesar Albarino for critical editing of the manuscript. The findings and conclusions in this report are those of the authors and do not necessarily represent the official position of the Centers for Disease Control and Prevention.

References

1. Hoenen T, Groseth A, de Kok-Mercado F et al (2011) Minigenomes, transcription and replication competent virus-like particles and beyond: reverse genetics systems for filoviruses and other negative stranded hemorrhagic fever viruses. *Antivir Res* 91:195–208. doi:[10.1016/j.antiviral.2011.06.003](https://doi.org/10.1016/j.antiviral.2011.06.003)
2. Devignot S, Bergeron E, Nichol S et al (2015) A virus-like particle system identifies the endonuclease domain of Crimean-Congo hemorrhagic fever virus. *J Virol* 89:5957–5967. doi:[10.1128/JVI.03691-14](https://doi.org/10.1128/JVI.03691-14)
3. Bergeron E, Albariño CG, Khristova ML, Nichol ST (2010) Crimean-Congo hemorrhagic fever virus-encoded ovarian tumor protease activity is dispensable for virus RNA polymerase function. *J Virol* 84:216–226. doi:[10.1128/JVI.01859-09](https://doi.org/10.1128/JVI.01859-09)
4. Bergeron É, Zivcec M, Chakrabarti AK et al (2015) Recovery of recombinant Crimean Congo hemorrhagic fever virus reveals a function for non-structural glycoproteins cleavage by Furin. *PLoS Pathog* 11:e1004879. doi:[10.1371/journal.ppat.1004879](https://doi.org/10.1371/journal.ppat.1004879)
5. Zivcec M, Metcalfé MG, Albariño CG et al (2015) Assessment of inhibitors of pathogenic Crimean-Congo hemorrhagic fever virus strains using virus-like particles. *PLoS Negl Trop Dis* 9:e0004259. doi:[10.1371/journal.pntd.0004259](https://doi.org/10.1371/journal.pntd.0004259)
6. Livak KJ, Schmittgen TD (2001) Analysis of relative gene expression data using real-time quantitative PCR and the 2(-Delta Delta C(T)) method. *Methods* 25:402–408. doi:[10.1006/meth.2001.1262](https://doi.org/10.1006/meth.2001.1262)
7. Zivcec M, Safronetz D, Haddock E et al (2011) Validation of assays to monitor immune responses in the Syrian golden hamster (*Mesocricetus auratus*). *J Immunol Methods* 368:24–35. doi:[10.1016/j.jim.2011.02.004](https://doi.org/10.1016/j.jim.2011.02.004)

Minigenome Systems for Filoviruses

Thomas Hoenen

Abstract

Filoviruses are among the most pathogenic viruses known to man, and work with live viruses is restricted to maximum containment laboratories. In order to study individual aspects of the virus life cycle outside of maximum containment laboratories, life cycle modeling systems have been established, which use reporter-encoding miniature versions of the viral genome called minigenomes. With basic minigenome systems viral genome replication and transcription can be studied, whereas more advanced systems also allow us to model other aspects of the virus life cycle outside of a maximum containment laboratory. These systems, therefore, represent powerful tools to study the biology of filoviruses, and for the screening and development of antivirals.

Key words Ebolaviruses, Marburgviruses, Filoviruses, Reverse genetics, Life cycle modeling system, Minigenome system

1 Introduction

Ebolaviruses and marburgviruses are the main members of the family *Filoviridae*. Most of these viruses, with the notable exception of the Reston virus, cause severe hemorrhagic fevers in humans with high case fatality rates. While the last few years have seen remarkable progress in the development of vaccines and antiviral treatments [1], at this time none of these countermeasures are approved for use in humans. Filoviruses are, therefore, generally considered to fall into the highest risk group of infectious disease agents, and work with live viruses is restricted to maximum containment biosafety level 4 (BSL-4) facilities. This constitutes a considerable obstacle to research on these viruses, as there are only a handful of these facilities available worldwide, and work in them is rather cumbersome. However, the development of filovirus minigenome systems, which are an example of reverse-genetics based life cycle modeling systems, at the end of the last century by Becker and Mühlberger [2, 3] has made it possible to study aspects of the virus life cycle under BSL-1 or 2 conditions (depending on local regulations—see **Note 1**).

Minigenomes are miniature versions of the viral genome in which the viral open reading frames and most noncoding regions have been removed and replaced with a reporter open reading frame (Fig. 1) [4]. However, the noncoding terminal leader and trailer regions, which carry all the signals necessary for the minigenome to be recognized as an authentic template for viral genome replication and transcription by the polymerase complex, are retained. The minigenome RNA is transcribed from an expression plasmid (initial transcription) either by exogenous T7-polymerase,

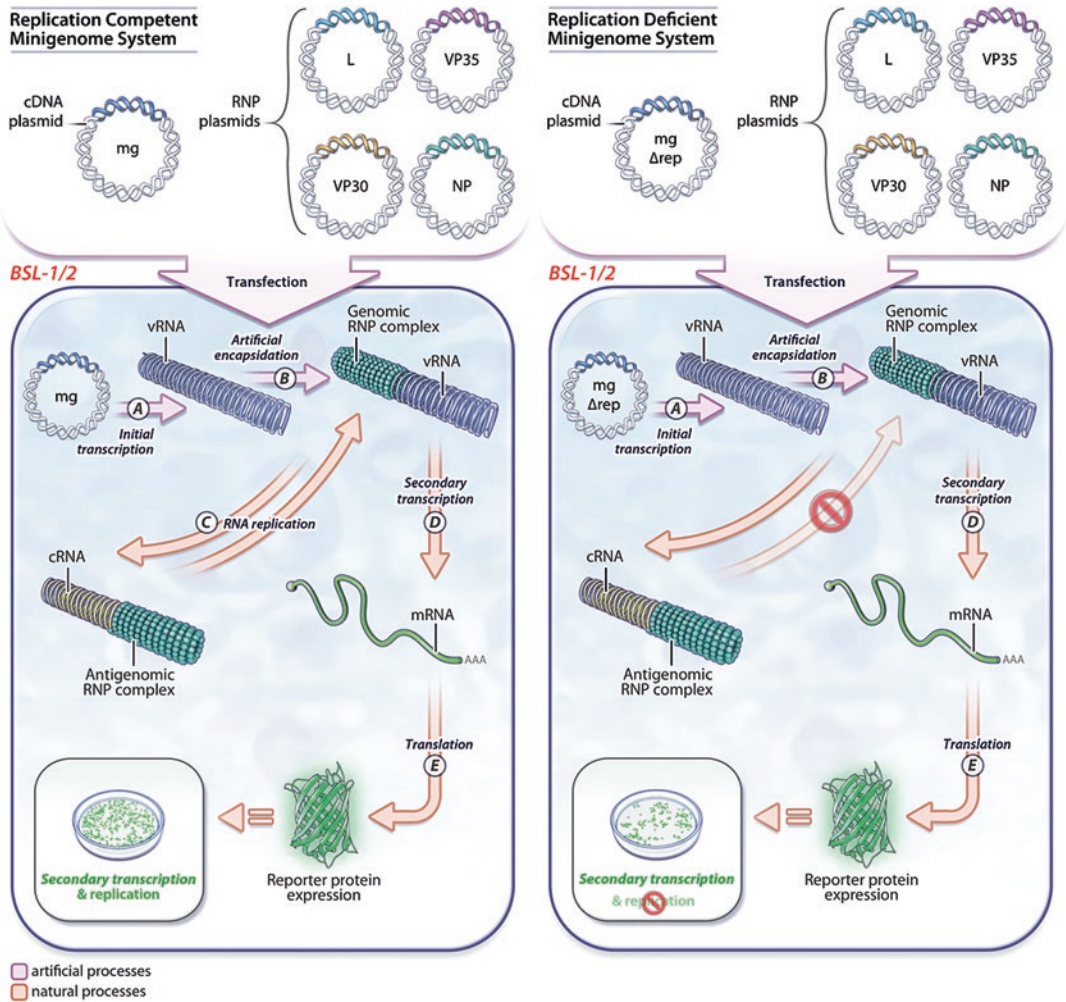


Fig. 1 Schematic of replication-competent and replication-deficient minigenome systems. Cells are transfected with a minigenome plasmid (mg) and the RNP plasmids encoding L, VP35, VP30, and NP. Initial transcription (a) either by cellular Poll or by T7 RNA polymerase provided from a plasmid (not shown) results in a “naked” minigenome (vRNA), which is subsequently encapsidated (b) and can then serve as a template for genome replication (c) and transcription (d), in case of a replication-competent minigenome, or just transcription (d) in case of a replication-deficient minigenome. This results in production of reporter protein (e). Reprinted from [4] with permission from Elsevier

or by cellular RNA-polymerase I [5, 6] (*see Note 2*). Depending on the expression strategy, it can become necessary to include ribozyme sequences at the ends of the transcripts to ensure authentic RNA termini (*see Note 3*). The “naked” initial minigenome transcript is then illegitimately encapsidated by the coexpressed filovirus nucleoprotein NP, and these encapsidated vRNA minigenomes then serve as templates for genome replication and transcription by the ribonucleoprotein complex proteins NP, L (viral polymerase), VP35 (polymerase cofactor), and in the case of ebolaviruses also VP30. The role of VP30 in these processes has been the subject of extensive studies, and it has been shown that VP30 is required for ebolavirus minigenome transcription, but not for replication [3, 7]. Specifically, VP30 is required to overcome a secondary structure at the beginning of the first viral gene during transcription [8]; however, it also seems to play a role in the regulation of genome replication vs. genome transcription [9, 10].

Minigenome replication results in the accumulation of vRNA copies as well as cRNA antigenomes, while transcription leads to the generation of reporter mRNAs and ultimately reporter activity, which reflects both minigenome replication and transcription. In order to differentiate between these two processes, replication-deficient minigenomes have been developed [7]. These constructs carry a deletion in the antigenomic replication promoter, so that vRNA minigenomes can still be transcribed into mRNAs and copied into cRNA antigenomes, but these cRNAs can no longer be copied into progeny vRNA minigenomes, thus abolishing minigenome replication.

In addition to classical monocistronic minigenomes polycistronic minigenomes have also been developed. Bicistronic minigenomes, which carry two reporter open reading frames, have been used to study the role of noncoding and intergenic regions for the regulation of replication and transcription [11, 12], and also to study cotranscriptional mRNA-editing, during which the virus polymerase inserts nontemplated nucleotides at a specific editing site in the GP gene [13]. Further, tetracistronic minigenomes that encode a single reporter and the viral proteins VP40 (matrix protein, responsible for virion morphogenesis and budding), GP_{1,2} (glycoprotein, responsible for virion attachment and entry), and VP24 (nucleocapsids-associated protein) have been developed [14], and can be used to model virtually the complete virus life cycle over multiple infectious cycles under BSL-1 or 2 conditions (*see Note 1*).

As reporter proteins a number of different proteins have been used. Initial work used chloramphenicol acetyltransferase (CAT); however, nowadays luciferases or in some cases fluorescent proteins are used almost exclusively, since they are much easier to use and quantitate. This has made it possible to adapt minigenome

assays for high-throughput applications such as antiviral screening [6, 15].

Here, we will provide details on the use of an ebolavirus monocistronic minigenome with a Renilla luciferase reporter to model genome replication and transcription, and a Firefly luciferase as a control reporter to assess cell viability and effects on plasmid-driven gene expression. For further information on the use of the multicistronic minigenomes the interested reader is referred elsewhere [11–13, 16].

2 Materials

1. HEK 293 cells (*see Note 4*).
2. Dulbecco's Modified Eagle's Medium (DMEM) with 10% (v/v) or 5% (v/v) fetal bovine serum (FBS, heat-inactivated 30 min at 56 °C) and 1% L-glutamine (Q, 2 mM) and 1% penicillin–streptomycin (PS, 100 U/mL). These two formulations will be referred to as DMEM_{10%} and DMEM_{5%}.
3. Opti-MEM (Thermo Fisher Scientific).
4. 6-well or 96-well plates—if using 96-well plates multichannel pipettes and reagent troughs.
5. DNA plasmids pCAGGS-NP, pCAGGS-VP35, pCAGGS-VP30, pCAGGS-L, pCAGGS-T7, pCAGGS-luc2 (Firefly luciferase), pCAGGS-GFP (or another fluorescent protein), p1cis-vRNA-Rluc.
6. Transit-LT1 transfection reagent (Mirus Bio).
7. GloLysis buffer, BrightGlo and RenillaGlo reagent (Promega).
8. Opaque white or black 96-well plates.
9. Luminometer capable of reading 96-well plates.

3 Methods

3.1 Minigenome Assay in 6-Well Format

1. Split 293 cells (*see Note 4*) into 6-well plates in a volume of 2 mL DMEM_{10%} per well for a confluency of ~50% on the next day (*see Note 5*). Incubate cells at 37 °C and 5% CO₂ in a humidified incubator.
2. Pipette DNA following the amounts in Table 1 into a 1.5 mL reaction tube (*see Note 6*). Prepare a negative control by replacing the pCAGGS-L plasmid with an expression plasmid for GFP or another fluorescent reporter, or with empty pCAGGS vector.
3. Add 100 µL/well Opti-MEM to the tube. Vortex, and briefly spin down. Add 2.8 µL/well Transit LT1 to the tube (vortex gently prior to use). Vortex gently, and incubate for 15–30 min.

Table 1
DNA amounts for transfection

Plasmid	Amount per well (6-well format) (ng)	Amount per well (96-well format) (ng)
pCAGGS-NP	125	6.9
pCAGGS-L (or GFP)	1000	55.6
pCAGGS-VP35	125	6.9
pCAGGS-VP30	75	4.2
pCAGGS-T7	250	13.9
pCAGGS-luc2	25	1.4
p1cis-vRNA-RLuc	250	13.9

4. In the meantime, change the medium on the cells to 2 mL DMEM_{5%}.
5. After 15–30 min, mix the formed transfection complexes gently by pipetting, and add 100 μ L/well dropwise to the cells. Try to cover the whole well with the droplets.
6. Rock the plates from side to side, and back and forth—do not rotate or swirl the plates, to avoid uneven distribution of the transfection complexes. Return cells to the incubator.
7. After 24 h, change the medium to 3 mL DMEM_{5%}. If you have substituted L against a fluorescent reporter in the negative control, check for fluorescence to obtain an estimate for the efficiency of transfection (this should be >50%). Return cells to the incubator.
8. After an additional 24 h (48 h post transfection), take off the supernatant, and add 200 μ L/well 1 \times GloLysis buffer to each well. Incubate for 10 min at room temperature.
9. Set pipette to 100 μ L, and wash the cells into the GloLysis buffer (*see Note 7*). Then transfer the lysates into a 1.5 mL tube.
10. Spin down the lysates for 3 min at 10,000 $\times g$ and 4 $^{\circ}$ C, and transfer the supernatants to a fresh tube, avoiding to disturb the pellet of cell debris. Continue in Subheading 3.3.

3.2 Minigenome Assay in 96-Well Format

1. Split 293 cells (*see Note 4*) into 96-well plates in a volume of 100 μ L DMEM_{10%} for a confluency of ~50% on the next day (*see Note 5*). Incubate cells at 37 $^{\circ}$ C and 5% CO₂ in a humidified incubator.

2. Pipette DNA following the amounts in Table 1 into a 1.5 mL reaction tube (*see* **Notes 6** and **8**). Prepare a negative control by replacing the pCAGGS-L plasmid with an expression plasmid for GFP or another fluorescent reporter, or with empty pCAGGS vector.
3. In a biosafety cabinet, add 10 μL /well Opti-MEM to the tube. Vortex, and briefly spin down. Add 0.45 μL /well Transit LT1 to the tube (vortex gently prior to use). Vortex gently, and incubate for 15–30 min.
4. In the meantime, change the medium on the cells to 30 μL DMEM_{5%}.
5. After 15–30 min, add 60 μL /well DMEM_{5%} to the transfection complexes, and mix by pipetting or inverting. Add 70 μL of the diluted transfection complexes to the cells.
6. Rock the plates from side to side, and back and forth—do not rotate or swirl the plates, to ensure even distribution of the transfection complexes. Return cells to the incubator.
7. After 24 h, change the medium to 200 μL DMEM_{5%}. If you have substituted L for a fluorescent reporter in the negative control, check for fluorescence to obtain an estimate for the efficiency of transfection (this should be >50%). Return cells to the incubator.
8. After an additional 24 h (48 h post transfection), take off the supernatant, and add 100 μL /well 1 \times GloLysis buffer to the well. Incubate for 10 min. Continue in Subheading 3.3.

3.3 Measuring Reporter Activity

1. Thaw 40 μL /well BrightGlo reagent and prepare 40 μL /well RenillaGlo reagent (thaw RenillaGlo buffer, and add 1% of RenillaGlo substrate).
2. For each sample, pipet 40 μL BrightGlo reagent into an opaque white or black (*see* **Note 9**) 96-well plate, and pipet 40 μL RenillaGlo reagent into an opaque 96-well plate (*see* **Note 10**).
3. Add 40 μL of sample to a well with BrightGlo reagent, and 40 μL of sample to a well with RenillaGlo reagent. Be careful not to carry over anything between the two different wells (i.e., do not reuse the same tip for pipetting the same sample into different reagents).
4. After 5–10 min, measure the reporter activity in a luminometer. Generally, an integration time of 0.5–1 s should provide sufficiently strong signals (*see* **Note 11**). While the absolute values are dependent on the plate color and on the specific luminometer used, positive (+L) controls should be 100–1000 fold stronger than the negative (–L) controls.
5. Normalize Renilla values to Firefly values to compensate for slight differences in plasmid-driven gene expression, or report both values independently (*see* **Note 12**).

4 Notes

1. Regulations for the biosafety classification of minigenome systems vary from country to country. One factor contributing to these differences in assessment is the classification of the mammalian cells in which these systems are used. For example, in the USA, 293 cells, which are the most commonly used cell type in minigenome systems, are considered Risk Group 2, so that minigenome systems have to be used under BSL-2 conditions, whereas in Germany the same cells are considered Risk Group 1, and thus minigenome systems in Germany are considered safe for use under biosafety level 1 conditions.
2. Principally, it should also be possible to use cellular Pol II for initial transcription, as has been done for other negative sense RNA viruses [17, 18]. However, to the best of our knowledge, such a system has not yet been published for filoviruses.
3. In order to ensure an authentic 3' transcript end, in case of T7- and Pol II-driven transcription the hepatitis delta virus (HDV) ribozyme should be used. Additionally, in order to ensure an authentic, uncapped 5' end in case of Pol II-driven initial transcription, a hammerhead ribozyme sequence should be used. For Pol I-driven initial transcription no ribozyme sequences are required to ensure authentic genome ends.
4. While 293 cells are most often used for minigenome assays due to their good transfectability, other mammalian cells (e.g., Huh7, A549, or Vero cells) can also be used for this assay. For Vero cells the ratio of transfection reagent to DNA should be doubled.
5. Determine the optimal ratio for splitting cells empirically—a good starting point is usually about 1:3 for 6-well plates, and 1:4 for 96-well plates.
6. In our experience, this step can be done outside a biosafety cabinet without jeopardizing the experiment (particularly since the preparation of plasmid DNA is also performed outside a biosafety cabinet). However, it is a reasonable precaution to use filter tips, and to limit the time tubes are kept open to a minimum. All other steps (with the exception of cell harvest and measuring of luciferase activity) should be performed in a biosafety cabinet.
7. Make sure that this is done as uniformly as possible for different wells, in order to ensure an even degree of lysis among the wells.
8. In 96-well format, volumes become so low that it becomes virtually impossible to transfect single wells. Therefore, work

with mastermixes for at least three identical wells. Always set up mastermixes for more wells than you eventually need (i.e., prepare a mastermix for at least four wells if you want to use it for three wells, or for larger numbers of wells prepare mastermix for 110% of wells).

9. While white plates can result in about $30 \times$ stronger signals than black plates, they also tend to be more susceptible to problems with cross talk. For this reason, and because signals produced by this minigenome system tend to be rather high, in most cases the use of black plates is preferable.
10. Cross talk between wells can be an issue, particularly since the Firefly luciferase values tend to be much higher than the Renilla luciferase values. Therefore, it makes sense to cluster all the Renilla wells and all the Firefly wells, but keep at least one empty row between them.
11. Ensure that values are in the linear range of your luminometer; otherwise dilute the samples in PBS.
12. Normalization to a control reporter can be somewhat problematic: If differences in the control reporter activity between wells are due to slight experimental variations during sample harvest, one can assume that the relationship between the effect on the control reporter activity and the minigenome reporter activity is linear, making normalization a valid procedure to compensate for this. Similarly, if differences in control reporter activity between wells are due to differences in cell number (e.g., because of slight experimental variations during cell seeding, or toxicity of tested compounds), normalization is valid. However, if such differences are due to different efficacies of plasmid-driven gene expression between different wells, the effect on control reporter activity is not in a linear relationship to the effect on minigenome reporter activity [7], so that it is better to report both Firefly and Renilla luciferase activity independently rather than to normalize results.

Acknowledgments

The author is grateful to Allison Groseth for critical reading of the manuscript, and to Marie Luisa Schmidt for technical help in refining some of the protocols.

References

1. Mendoza EJ, Qiu X, Kobinger GP (2016) Progression of Ebola therapeutics during the 2014–2015 outbreak. *Trends Mol Med* 22(2):164–173. doi:[10.1016/j.molmed.2015.12.005](https://doi.org/10.1016/j.molmed.2015.12.005)
2. Muhlberger E, Lotfering B, Klenk HD, Becker S (1998) Three of the four nucleocapsid proteins of Marburg virus, NP, VP35, and L, are sufficient to mediate replication and transcription of Marburg virus-specific monocistronic minigenomes. *J Virol* 72(11):8756–8764
3. Muhlberger E, Weik M, Volchkov VE, Klenk HD, Becker S (1999) Comparison of the transcription and replication strategies of marburg virus and Ebola virus by using artificial replication systems. *J Virol* 73(3):2333–2342
4. Hoenen T, Groseth A, de Kok-Mercado F, Kuhn JH, Wahl-Jensen V (2011) Minigenomes, transcription and replication competent virus-like particles and beyond: reverse genetics systems for filoviruses and other negative stranded hemorrhagic fever viruses. *Antivir Res* 91(2):195–208. doi:[10.1016/j.antiviral.2011.06.003](https://doi.org/10.1016/j.antiviral.2011.06.003)
5. Groseth A, Feldmann H, Theriault S, Mehmetoglu G, Flick R (2005) RNA polymerase I-driven minigenome system for Ebola viruses. *J Virol* 79(7):4425–4433. doi:[10.1128/JVI.79.7.4425-4433.2005](https://doi.org/10.1128/JVI.79.7.4425-4433.2005)
6. Jasenosky LD, Neumann G, Kawaoka Y (2010) Minigenome-based reporter system suitable for high-throughput screening of compounds able to inhibit ebolavirus replication and/or transcription. *Antimicrob Agents Chemother* 54(7):3007–3010. doi:[10.1128/AAC.00138-10](https://doi.org/10.1128/AAC.00138-10)
7. Hoenen T, Jung S, Herwig A, Groseth A, Becker S (2010) Both matrix proteins of Ebola virus contribute to the regulation of viral genome replication and transcription. *Virology* 403(1):56–66. doi:[10.1016/j.virol.2010.04.002](https://doi.org/10.1016/j.virol.2010.04.002)
8. Weik M, Modrof J, Klenk HD, Becker S, Muhlberger E (2002) Ebola virus VP30-mediated transcription is regulated by RNA secondary structure formation. *J Virol* 76(17):8532–8539
9. Modrof J, Muhlberger E, Klenk HD, Becker S (2002) Phosphorylation of VP30 impairs Ebola virus transcription. *J Biol Chem* 277(36):33099–33104. doi:[10.1074/jbc.M203775200](https://doi.org/10.1074/jbc.M203775200)
10. Biedenkopf N, Hartlieb B, Hoenen T, Becker S (2013) Phosphorylation of Ebola virus VP30 influences the composition of the viral nucleocapsid complex: impact on viral transcription and replication. *J Biol Chem* 288(16):11165–11174. doi:[10.1074/jbc.M113.461285](https://doi.org/10.1074/jbc.M113.461285)
11. Neumann G, Watanabe S, Kawaoka Y (2009) Characterization of ebolavirus regulatory genomic regions. *Virus Res* 144(1–2):1–7. doi:[10.1016/j.virusres.2009.02.005](https://doi.org/10.1016/j.virusres.2009.02.005)
12. Brauburger K, Boehmann Y, Tsuda Y, Hoenen T, Olejnik J, Schumann M, Ebihara H, Muhlberger E (2014) Analysis of the highly diverse gene borders in Ebola virus reveals a distinct mechanism of transcriptional regulation. *J Virol* 88(21):12558–12571. doi:[10.1128/JVI.01863-14](https://doi.org/10.1128/JVI.01863-14)
13. Mehedi M, Hoenen T, Robertson S, Ricklefs S, Dolan MA, Taylor T, Falzarano D, Ebihara H, Porcella SF, Feldmann H (2013) Ebola virus RNA editing depends on the primary editing site sequence and an upstream secondary structure. *PLoS Pathog* 9(10):e1003677. doi:[10.1371/journal.ppat.1003677](https://doi.org/10.1371/journal.ppat.1003677)
14. Watt A, Moukambi F, Banadyga L, Groseth A, Callison J, Herwig A, Ebihara H, Feldmann H, Hoenen T (2014) A novel life cycle modeling system for Ebola virus shows a genome length-dependent role of VP24 in virus infectivity. *J Virol* 88(18):10511–10524. doi:[10.1128/JVI.01272-14](https://doi.org/10.1128/JVI.01272-14)
15. Hoenen T, Feldmann H (2014) Reverse genetics systems as tools for the development of novel therapies against filoviruses. *Expert Rev Anti-Infect Ther* 12(10):1253–1263. doi:[10.1586/14787210.2014.948848](https://doi.org/10.1586/14787210.2014.948848)
16. Hoenen T, Watt A, Mora A, Feldmann H (2014) Modeling the lifecycle of Ebola virus under biosafety level 2 conditions with virus-like particles containing tetracistronic minigenomes. *J Vis Exp* 91:52381. doi:[10.3791/52381](https://doi.org/10.3791/52381)
17. Martin A, Staeheli P, Schneider U (2006) RNA polymerase II-controlled expression of antigenomic RNA enhances the rescue efficacies of two different members of the *Mononegavirales* independently of the site of viral genome replication. *J Virol* 80(12):5708–5715. doi:[10.1128/JVI.02389-05](https://doi.org/10.1128/JVI.02389-05)
18. Inoue K, Shoji Y, Kurane I, Iijima T, Sakai T, Morimoto K (2003) An improved method for recovering rabies virus from cloned cDNA. *J Virol Methods* 107(2):229–236

Establishment of Bisegmented and Trisegmented Reverse Genetics Systems to Generate Recombinant Pichindé Viruses

Rekha Dhanwani, Qinfeng Huang, Shuiyun Lan, Yanqing Zhou, Junjie Shao, Yuying Liang, and Hinh Ly

Abstract

Pichindé virus (PICV), isolated from rice rats in Colombia, South America, is an enveloped arenavirus with a bisegmented RNA genome. The large (L) genomic segment encodes the Z matrix protein and the L RNA-dependent RNA polymerase, whereas the small (S) genomic segment encodes the nucleoprotein (NP) and the glycoprotein (GPC). This article describes the successful development of reverse genetics systems to generate recombinant PICV with either a bisegmented or trisegmented genome. We have successfully demonstrated that these systems can generate high-titered and genetically stable replication-competent viruses from plasmid transfection into appropriate cell lines. These systems demonstrate the power and versatility of reverse genetic technology to generate recombinant arenaviruses for use in pathogenesis studies and as new viral vaccine vectors.

Key words Arenavirus, Reverse genetics, Pichindé virus

1 Introduction

Pichindé virus (PICV) is an enveloped RNA virus, belonging to the *Arenaviridae*. The genome of PICV, like those of other known arenaviruses, consists of two single-stranded ambisense RNAs: the large (L) segment of ~7.2 kb and the small (S) segment of ~3.4 kb [1]. The L RNA segment encodes the RNA-dependent RNA polymerase L protein in a negative orientation and a small multifunctional Z protein in a positive sense. The S RNA segment encodes another multifunctional protein known as the nucleoprotein (NP) in a negative orientation and the envelope glycoprotein precursor GPC in a positive sense (Fig. 1a). At both ends of each of the genome segments, there are 19 nucleotides (nt) that are imperfectly complementary to each other and are predicted to form the panhandle structures that serve as the *cis*-acting elements required

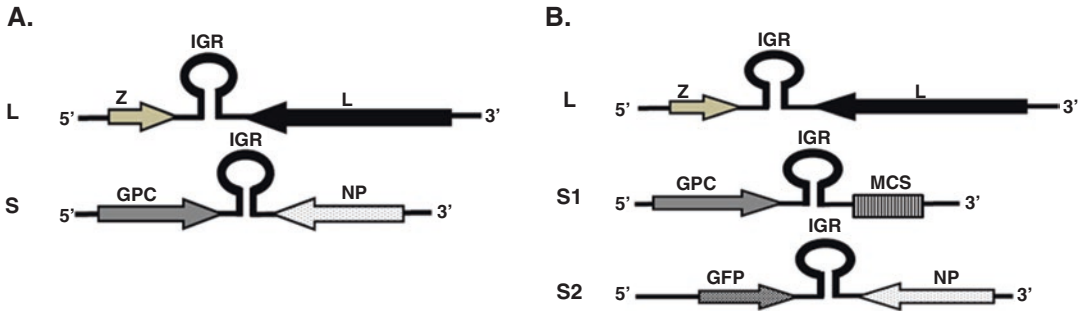


Fig. 1 Schematic diagram of the bisegmented and trisegmented PICV reverse genetics systems: **(a)** Wild-type (WT) bisegmented rP18 PICV genome composed of L and S segments. **(b)** Trisegmented rP18tri PICV genome composed of L, S1, and S2 segments encoding eGFP reporter gene. *IGR* intergenic region, *NP* nucleoprotein, *GPC* glycoprotein complex, *eGFP* green fluorescence protein, *MCS* multiple cloning site

for viral RNA transcription and replication. A unique feature of the arenavirus genomic RNA is the noncoding intergenic regions (IGR) located between the two open reading frames. The IGRs range from 59 to 217 nt in length and are predicted to form 1–3 energetically stable stem-loop structures that are proposed to contribute to the termination of transcription.

The first molecular clone of arenavirus was developed for the prototype lymphocytic choriomeningitis virus (LCMV) [2, 3]. This reverse genetics (RG) system has served as an invaluable tool to study the biological functions of arenavirus proteins and viral RNA elements (e.g., IGR). In this chapter, we describe two different RG systems for PICV. The bisegmented RG system generates recombinant PICV with two genomic RNA segments (L and S), whereas the trisegmented RG system produces viruses with three segments (L and S1 and S2) (Fig. 1b). A similar strategy to generate the trisegmented genome of LCMV has also been recently developed by Emonet and colleagues [4]. In our studies, we have shown that recombinant PICV generated from the bisegmented RG system can recapitulate the parental (stock) viruses in terms of viral growth kinetics in vitro and virulence in vivo [5, 6]. On the other hand, recombinant PICV generated from the trisegmented RG systems are highly attenuated and therefore can be used as vaccine vectors to deliver foreign antigens [7].

2 Materials

2.1 Plasmids, Cell Lines, and Media

1. Plasmids: pUC19-HDVT7t vector are used for cloning PICV genome L segment and S segment, respectively [4]. NP and L gene are cloned into pCAGGS mammalian vector under CMV promoter.

2. Cell lines: BSRT7-5 cells, which constitutively express the T7 RNA polymerase, have been obtained from K. Conzelmann at Ludwig-Maximilians-Universität, Germany. BHK21 cells are used for PICV amplification. Vero cells are used for PICV plaque assay.
3. Culture media: BSRT7-5 cells are cultured in Dulbecco's Modified Eagle Medium (DMEM) supplemented with 10% fetal bovine serum (FBS), 1 mg geneticin per mL, and 50 mg penicillin and streptomycin per mL. BHK21 cells are cultured in Dulbecco's Modified Eagle Medium (DMEM) supplemented with 10% fetal bovine serum (FBS), and 50 mg penicillin and streptomycin per mL. Vero cells are cultured in minimal essential medium (MEM) supplemented with 10% fetal bovine serum (FBS), and 50 mg penicillin and streptomycin per mL.
4. Opti-MEM (Invitrogen) for use in transfections and for culturing transfected cells.

2.2 Reagents and Buffers

1. Lipofectamine 2000 (Invitrogen).
2. Neutral red dye (Sigma).
3. Phosphate Buffer Saline (PBS) (Sigma).
4. Geneticin G418 (Gibco).
5. 2% agar solution: Dissolve 2 g of agar in 100 mL of distilled water. Autoclave it.
6. First agar overlay: 0.6 mL of 2% agar and 2.4 mL of complete MEM.
7. Second agar overlay: 0.4 mL of 2% agar, 1.6 mL of complete MEM, and 120 μ L of 0.33% neutral red dye.
8. 0.45 μ m filter (Millipore).
9. Sharpie pen for demarcating plaques on bottom of plastic plates.

2.3 Equipment

1. Biosafety cabinet that is Class II, type A2 (air recirculates air after HEPA filtration; ThermoFisher).
2. CO₂ incubator MCO-18AC(UV) (Sanyo).
3. Speed pipettor (Eppendorf).
4. Water bath (ISOTEMP 210, Fisher).
5. Microwave oven.

3 Methods

3.1 Generation of the Bisegmented and Trisegmented PICV RG Systems

1. Seed 4×10^5 BSRT7-5 cells/well in 6-well plates at 24 h prior to transfection. (*see Note 1*).
2. Replace cell-culture supernatant with a fresh aliquot of the complete DMEM medium (without geneticin) prior to transfection (*see Note 2*).

3. (a) For bisegmented PICV system, mix 4 μg of the PICV L segment plasmid and 2 μg of the PICV S segment plasmid in 100 μL Opti-MEM (*see Note 3*).
 (b) For trisegmented PICV system, mix 2 μg of the PICV L segment plasmid and 1 μg of each of the PICV S1 and S2 segment plasmids in 100 μL Opti-MEM (*see Note 4*).
4. Add 9 μL of Lipofectamine 2000 in 100 μL Opti-MEM in a separate tube ($\mu\text{g DNA} \times 1.5 = \mu\text{L Lipofectamine 2000}$ needed).
5. Incubate the above two mixtures separately for 5 min at ambient temperature.
6. Mix the two mixtures (Opti-MEM–plasmid and Opti-MEM–Lipofectamine 2000), vortex the sample well and incubate the sample for 5 min at ambient temperature.
7. Dropwise add 200 μL of the sample onto the cells.
8. At 4 h post-transfection, replace the cell medium with a fresh aliquot of the complete DMEM medium (without geneticin).
9. Collect 1 mL of the cell-culture supernatant at 48 and 72 h post-transfection for plaque assay (below) and at each time add an equal fresh aliquot of DMEM medium (without any antibiotics) to the cells.

3.2 Plaque Assay and Plaque Purification of Recombinant Viruses

1. Seed 300,000 Vero cells/well in 6-well plates (using the complete MEM medium).
2. Prepare 10 \times serially diluted virus samples (above) in MEM media (without FBS and antibiotics; *see Note 5*).
3. Aspirate medium from cells and wash the cells once with PBS.
4. Add 500 μL of the diluted virus samples to the cells and incubate the cells at 37 $^{\circ}\text{C}$ for 60 min with intermittent gentle rocking of the plate to spread the virus uniformly.
5. After 60 min of virus adsorption, aspirate the virus from the cells and wash cells with PBS.
6. Slowly add the first agar overlay onto the cells (*see Notes 6–8*). (Calculate the volume of overlay needed and mix the medium and 2% agar in appropriate ratios as described in Subheading 2.)
7. Incubate the plates for 4 days at 37 $^{\circ}\text{C}$ with 5% CO_2 .
8. After 4 days of incubation, add the second agar overlay onto the cells and let it solidify for 5–10 min (*see Notes 6–8*).
9. Incubate the plates overnight at 37 $^{\circ}\text{C}$ and count the plaques the following day.
10. To pick a plaque for further virus amplification (below), choose a plaque that is not touching any others and mark it on the bottom of plate with a Sharpie pen.

11. Puncture the agar using the P1000 pipetman and insert the tip straight down to the plaque to aspirate a small volume of the medium that contains the virus. Dispense the virus sample into 1 mL of MEM, and pipet up and down to remove the agar from the pipet tip (*see Note 9*).

3.3 PICV Amplification

1. Seed 8×10^5 BHK-21 cells in a 10 cm dish at 24 h prior to infection.
2. Infect the cells by adding 1 mL of the plaque-purified virus to the cells for 60 min (*see Note 10*).
3. Remove the virus by aspiration and add 10 mL of complete DMEM medium to the cells.
4. After 48 h, collect the cell-culture supernatant, and filter it through a 0.45 μm filter.
5. Prepare small aliquots of the virus (0.5–1 mL) and store at $-80\text{ }^\circ\text{C}$ (*see Note 11*).
6. Determine the virus titer by plaque assay as described in Subheading 3.2 above.

4 Notes

1. Use low passaged BSRT7-5 cells for optimal transfection efficiency.
2. Maintain the BSRT7-5 cells in a medium free of any antibiotics for at least 24 h prior to transfection.
3. Using the bisegmented PICV RG system, recombinant viruses of two different strains (P2 and P18) are generated. Recombinant P2 viruses (rP2) produce smaller plaque sizes than the rP18 viruses, and grow slower with less viral titers than rP18 viruses in cell cultures (Fig. 2).
4. Using the trisegmented PICV RG system, recombinant viruses that carry three genomic segments are generated. Recombinant viruses with wild-type rP18 sequences replicated to a higher levels in cell cultures than rP18tri-GFP (Fig. 3).
5. Change the pipet tips at each dilution or use the speed pipettor to prepare the serial dilutions. This helps eliminate any human errors in pipetting.
6. Overlay media should be added immediately after the PBS wash in order to make sure that the cells do not get dried out.
7. In order to maintain the flowing consistency of the overlay medium for prolonged duration, keep the medium in $37\text{ }^\circ\text{C}$ water bath prior to mixing it with the 2% molten agar. Keep the molten agar in $65\text{ }^\circ\text{C}$ water bath.

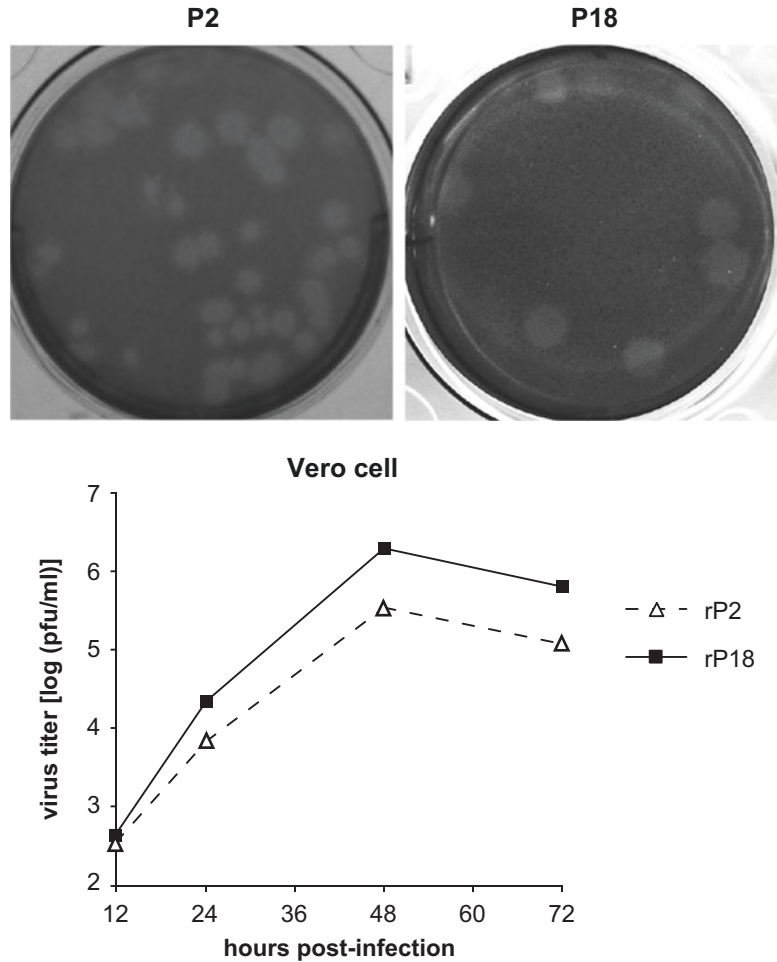


Fig. 2 Comparison of bisegmented PICV viruses: (a) Plaque sizes of the rP2 and rP18 wild-type viruses. (b) Growth kinetics of the rP2 and rP18 bisegmented Pichindé viruses

8. Do not immediately cover the plates after adding the overlay media in order to avoid accumulation of water condensations.
9. In order to pick up a purified plaque, cut the mouth of a 1000 μ L tip with a sterile razor. Broadened mouth tip can more easily aspirate a chunk of semisolidified agar.
10. Swirl the plate every 10 min to ensure uniform distribution of virus over the surface of the cell monolayer.
11. Make smaller aliquots in order to avoid repeated freeze-thawing of the virus stocks which may drastically impact the accuracy of the virus titers.

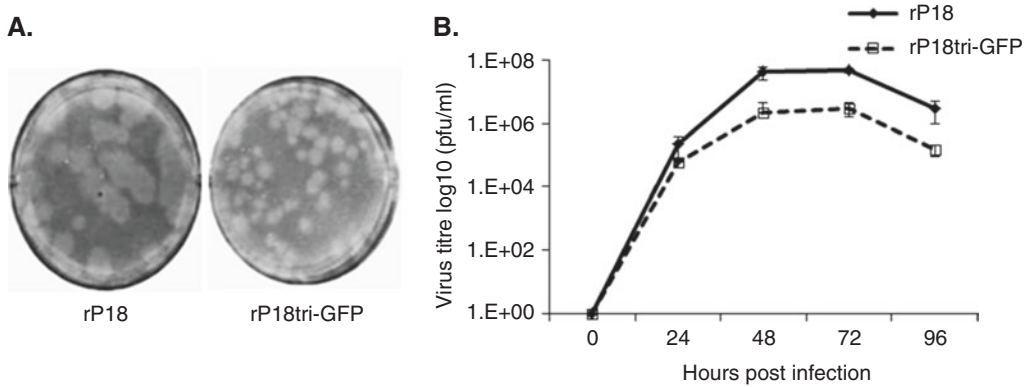


Fig. 3 Growth kinetics of bisegmented and trisegmented PICV: (a) Plaque sizes of rP18 (WT) and rP18tri-GFP PICV. (b) Analysis of growth kinetics of the rP18 and rP18tri-GFP in BHK-21 cells at MOI of 0.1

Acknowledgments

We thank Prof. Dr. K. Conzelmann (Ludwig-Maximilians-Universität, Germany) for providing the BSRT7-5 cells, and K. Curtis (USAMRIID, USA) for providing the pUC19-HDVT7t vector and Lassa genomic information. This work was supported in part by the NIAID/NIH through the new direction awards program of the SERCEB grant (U54-AI057157) to Y.L. and H.L., by the NIAID/NIH R01 AI083409 to Y.L., and R01 AI093580 and R56 AI091805 to H.L.

References

- Buchmeier MJ, Bowen MD, Peters CJ (2001) *Arenaviridae*: the viruses and their replication. In: Knipe DM, Howley PM (eds) *Fields virology*, vol 2, 4th edn. Lippincott-Raven Publisher, Philadelphia, PA, pp 1635–1668
- Flatz L, Bergthaler A, de la Torre JC, Pinschewer DD (2006) Recovery of an arenavirus entirely from RNA polymerase I/II-driven cDNA. *Proc Natl Acad Sci U S A* 103:4663–4668
- Sanchez AB, de la Torre JC (2006) Rescue of the prototypic arenavirus LCMV entirely from plasmid. *Virology* 350:370–380
- Emonet FS, Garidou L, McGavern DB, de la Torre JC (2009) Generation of recombinant lymphocytic choriomeningitis viruses with trisegmented genomes stably expressing two additional genes of interest. *Proc Natl Acad Sci U S A* 106:3473–3478
- Lan S, McLay Schelde L, Wang J, Kumar N, Ly H, Liang Y (2009) Development of infectious clones for virulent and avirulent pichindé viruses: a model virus to study arenavirus-induced hemorrhagic fevers. *J Virol* 83:6357–6362
- Liang Y, Lan S, Ly H (2009) Molecular determinants of Pichindé virus infection of guinea pigs – a small animal model system for arenaviral hemorrhagic fevers. *Ann N Y Acad Sci* 1171(Suppl 1):E65–E74
- Dhanwani R, Zhou Y, Huang Q, Verma V, Dileepan M, Ly H, Liang Y (2015) A novel live Pichindé virus-based vaccine vector induces enhanced humoral and cellular immunity after a booster dose. *J Virol* 90:2551–2560

Part III

***In Vivo* Models of Hemorrhagic Fever Virus Infection**

Murine Models for Viral Hemorrhagic Fever

Rosana Gonzalez-Quintial and Roberto Baccala

Abstract

Hemorrhagic fever (HF) viruses, such as Lassa, Ebola, and dengue viruses, represent major human health risks due to their highly contagious nature, the severity of the clinical manifestations induced, the lack of vaccines, and the very limited therapeutic options currently available. Appropriate animal models are obviously critical to study disease pathogenesis and develop efficient therapies. We recently reported that the clone 13 (Cl13) variant of the lymphocytic choriomeningitis virus (LCMV-Cl13), a prototype arenavirus closely related to Lassa virus, causes in some mouse strains endothelial damage, vascular leakage, platelet loss, and death, mimicking pathological aspects typically observed in Lassa and other HF syndromes. This model has the advantage that the mice used are fully immunocompetent, allowing studies on the contribution of the immune response to disease progression. Moreover, LCMV is very well characterized and exhibits limited pathogenicity in humans, allowing handling in convenient BSL-2 facilities. In this chapter we outline protocols for the induction and analysis of arenavirus-mediated pathogenesis in the NZB/LCMV model, including mouse infection, virus titer determination, platelet counting, phenotypic analysis of virus-specific T cells, and assessment of vascular permeability.

Key words Hemorrhagic fever virus, Arenavirus, Lassa virus, LCMV, Mouse model, NZB mouse, Virus titer, MHC tetramer, Platelet counting, Vascular leakage, Bronchoalveolar lavage

1 Introduction

Hemorrhagic fevers (HF) are caused by enveloped RNA viruses from seven families, i.e., *Arenaviridae* (including Lassa and Junín viruses), *Hantaviridae* (hantaviruses) *Nairoviridae* (Crimean-Congo hemorrhagic fever virus), *Peribunyaviridae* (orthobunyaviruses) *Phenuiviridae* (Rift Valley fever virus), *Filoviridae* (ebolaviruses and marburgviruses), and *Flaviviridae* (dengue and yellow fever viruses). Transmitted by exposure to infected reservoir animals (rodents, fruit bats), arthropod vectors (ticks, mosquitoes), or body fluids from infected animals or patients, these viruses are highly contagious, cause severe clinical manifestations with high case fatality rates, and are serious bioterrorism threats [1–3]. The main characteristics of HF include endothelial damage, platelet loss, and vascular leakage, leading to tissue edema, organ fail-

ure, and death in severe cases. How HF viruses cause life-threatening vascular disease in subsets of individuals remains unclear. These viruses efficiently infect endothelial cells but are generally considered non-cytopathic, suggesting that elevated vascular permeability may be more a consequence of an exaggerated immune response, leading to endothelial cell death or dysfunctions, than a direct effect of the virus [1–4]. However, studies that compare immune responses in mild versus fatal cases have been limited.

Availability of appropriate animal models is obviously critical for investigations of HF pathogenesis, susceptibility to lethal disease, and potential therapeutic interventions [5, 6]. The most relevant models use nonhuman primates including rhesus monkeys and cynomolgus macaques, African green monkeys, and marmosets. These animals, however, are difficult to manipulate genetically, and their inclusion in experimental protocols presents significant ethical, economic, and technical problems. Guinea pigs and hamsters have been used in multiple studies addressing HF pathogenesis and antiviral interventions, but these models are also limited by the paucity of reagents and genetic information.

A mouse model would be particularly useful for several reasons, including

- (a) Mice are cost-effective and reproduce quickly, and multiple inbred strains of genetically identical mice are available.
- (b) ~99% of human genes have a mouse homologue and ~80% a mouse orthologue [7, 8].
- (c) ~90% of the human and mouse genomes are constituted by segments that include sets of genes organized in the same order [7, 8].
- (d) The genome of the C57BL/6 mouse has been fully sequenced and annotated, and similar information for other strains is emerging from multiple studies, greatly facilitating forward genetic approaches [7–11].
- (e) Optimal reagents have been developed for *in vivo* and *in vitro* studies in mice, as well as to manipulate the mouse genome and generate transgenic, knock-out, knock-in, and conditionally mutant strains to interrogate gene function in physiological and pathological settings.

However, with a few exceptions such as the bunyavirus Rift Valley fever virus (RVFV) in BALB/c and C57BL/6 mice [12, 13], most HF viruses were found to be nonpathogenic in adult immunocompetent mice [6]. One approach to increase pathogenicity in mice has been the use of virus variants adapted to mouse hosts through serial passaging, as reported for the filoviruses Ebola (EBOV) and Marburg (MARV) viruses [14]. Alternatively, experiments have been performed using immunocompromised mice, including mice lacking the receptor for type I interferons (IFNAR^{-/-}), the receptors for both type I and type II interferons

(AG129), the signal transducer and activator of transcription 1 (STAT1^{-/-}), or class I MHC molecules (MHC-I^{-/-}) [6]. These models constitute important tools for studies evaluating aspects of HF pathogenesis and therapies. However, immunocompromised mice limit investigations of the contribution of the immune system to vascular and other pathologic alterations associated with severe HF virus infections.

We recently reported that the clone 13 (CI13) variant of lymphocytic choriomeningitis virus (LCMV-CI13), a prototype arenavirus closely related to Lassa virus, causes in NZB, PL/J, and SJL mice (but not in C57BL/6 and BALB/c mice), a lethal disease associated with endothelial damage, platelet loss, and vascular leakage, mimicking pathological aspects typically observed in Lassa and other HF syndromes [15]. In contrast, the variant Armstrong of this virus (LCMV-ARM) did not induce these symptoms in NZB mice [15]. Similar manifestations have been reported for FVB mice [16]. In addition to using immunocompetent mice, an important advantage of this model is that, compared to LASV and other HF viruses whose high virulence requires handling in highly restrictive BSL-4 facilities, LCMV is significantly less pathogenic in humans (causing disease only in immunocompromised individuals), and therefore *in vivo* and *in vitro* experiments can be carried out in more convenient BSL-2 facilities.

In this chapter we outline protocols for the induction and analysis of arenavirus-mediated pathogenesis in the NZB/LCMV mouse model, including mouse infection, virus titer determination, platelet counting, phenotypic analysis of virus-specific T cells identified by MHC tetramer staining, assessment of vascular permeability, and analysis of cytokines, chemokines, and other indicators of vascular dysfunctions in bronchoalveolar lavage fluid.

2 Materials

2.1 Mouse Infection and Anesthetization

1. Virus: LCMV-CI13 stock prepared by serial passage in BHK-21 cells is described [17, 18].
2. Mice: NZB and BALB/c mice, approximately 8 weeks of age (Jackson Laboratories).
3. Isoflurane anesthetic for murine inhalation.
4. 28-gauge (G) needles for inoculation of mice, and 18-G needles for bronchial lavage.
5. Microhematocrit EDTA-coated tubes for mouse eye bleeds.

2.2 Virus Titer Determination by Plaque-Forming Assay

1. Vero cells (ATCC #CRL-1587).
2. Vero medium: Dulbecco's modified eagle medium (DMEM) supplemented with 10% (v/v) heat-inactivated fetal bovine serum (FBS), 200 IU/ml penicillin, 200 mg/ml streptomycin.

3. 1% agarose: Dissolve 1% (w/v) ultra-pure agarose in sterile water, then autoclave.
4. 199 medium (2×): 100 ml of medium 199 (2×) with Earle's salts supplemented with 10 ml FBS, 2 ml 100× L-glutamine, 2 ml 100× penicillin/streptomycin.
5. Fixation solution: Dilute 37% formaldehyde stock with water to a final concentration of 25%.
6. Cell staining solution (10×): 1% crystal violet (w/v) in 20% ethanol. Dilute 1 volume with 9 volumes water before use.

2.3 Platelet Count

Hemavet 950FS hematology analyzer

2.4 T Cell Analysis

1. Flow cytometer.
2. 70 μm mesh cell strainers, 50 ml tubes, flow tubes.
3. 20× balanced salt solution (BSS).
4. ACK lysis buffer: 155 mM NH₄Cl, 10 mM KHCO₃, Na₂EDTA 0.1 mM, pH 7.5.
5. Flow buffer: BSS (1×) supplemented with 2% FBS and 0.1% w/v sodium azide.
6. Paraformaldehyde (PFA) 2% w/v in phosphate-buffered saline (PBS).
7. MHC-I tetramers: Biotinylated H-2L^d MHC-I molecules complexed with the LCMV NP_{118–126} peptide (NIH MHC tetramer core facility) and tetramerized with fluorescent streptavidin (*see Note 1*).
8. Antibodies against mouse CD4 and CD8 and/or other T cell surface markers, coupled to compatible fluorochromes (multiple vendors).

2.5 Vascular Leak Assessment

1. Evan's Blue Dye Solution: 0.5% dye powder in PBS.
2. PBS: 137 mM NaCl, 2.7 mM KCl, 10 mM Na₂HPO₄, 1.8 mM KH₂PO₄, pH 7.4.
3. Formamide.

2.6 Bronchoalveolar Lavage Fluid (BALF) Analysis

1. PBS (*see above*).
2. PBS supplemented with Complete Mini, EDTA-free protease inhibitor cocktail.
3. Protein content analysis: Pierce protein BCA assay kit.
4. LDH enzymatic activity: Cytotox 96 nonradioactive cytotoxicity assay.
5. IgM levels: IgM quantitation kit.
6. Cytokines and chemokines: DuoSet ELISA kit for CCL2 (MCP-1), CCL5 (RANTES), CXCL10 (IP-10), IL-6, TNF-α, and

IL-10; Quantikine kits for CCL3 and CXCL2; VeriKine Mouse IFN-Alpha Kit and IFN- β ELISA kit for type I interferons (can be obtained from R&D Systems or PBL InterferonSource).

3 Methods

3.1 Mouse Infection

1. Randomly assign individual mice of appropriate strain and genetic background to experimental groups. Based on previous experience, 6–8 mice per group are usually sufficient to ensure statistical significance. Use larger groups if necessary (*see Note 2*).
2. Thaw an aliquot of the LCMV-Cl13 stock and place on ice. Dilute to 20×10^6 PFU/ml in cold PBS. Preload 28-G needle syringes with 100 μ l, keep on ice until use (*see Note 3*).
3. To infect the mice intravenously (i.v.), carefully warm the mice with a heat lamp to promote vasodilation. Place one mouse in an appropriate restraint device with the tail exposed to locate the lateral vein. Clean the tail with 70% ethanol, insert the needle of a virus-loaded syringe superficially under the skin and parallel to the lateral vein, and advance 2–3 mm into vein lumen. Inject slowly, ensuring that the solution is entering i.v. and not subcutaneously (s.c.). Remove the needle and apply gentle pressure to the puncture site with a clean gauze to assist with wound closure. Return the mouse to the housing cage and proceed with the next mouse (*see Note 4*).
4. Observe the mice daily for disease symptoms, including reduced activity, ruffled fur, hunched posture, and labored breathing starting at day 4 post-infection (pi) and death between days 6 and 8 pi, as described [15] (*see Note 5*).

3.2 Virus Titer Determination (Plaque-Forming Assay)

1. At specific time-points post-infection, anesthetize mice by isoflurane inhalation and bleed by retro-orbital puncture using a microhematocrit EDTA-coated tube. Once sufficient blood has been obtained, remove the tube and apply pressure with a clean moist gauze until bleeding stops. Collect serum by centrifugation and store at -70 °C until use.
2. Plate Vero cells on 6-well plates (2×10^5 cells/ml in Vero medium, 2 ml/well). Incubate overnight to 50–60% confluence (*see Note 6*).
3. To prepare serial tenfold dilutions, add 60 μ l LCMV-infected mouse serum (or LCMV stock to be assessed) to a tube containing 540 μ l Vero medium and mix thoroughly (10^{-1} dilution). Then use a fresh pipet to transfer 60 μ l to the next tube, and repeat the procedure to generate a total of seven dilutions (10^{-1} to 10^{-7}).

4. Remove the medium from the wells containing Vero cells, add 500 μ l of diluted mouse serum (or media alone), and incubate 1 h at 37 °C. Rock every 10 min.
5. Microwave 1% agarose and cool the solution to ~50 °C in a water bath. Warm the 199 medium (2 \times) to 37 °C. Mix the two solutions (1:1) immediately before applying to the cells (**step 6**) (*see Note 7*).
6. After 1 h at 37 °C (**step 4**), aspirate the inoculum, and add 3 ml of the Agarose overlay mix (from **step 5**) to each well. Allow the Agarose to solidify (~10 min) before returning the plate into the incubator. Incubate 4 days.
7. To each well, add 800 μ l fixation solution and incubate for 2 h at room temperature. Aspirate the fixation solution with a pipette, then carefully remove the agarose plug using a spatula. Add 800 μ l of staining solution (1 \times) per well, and incubate 1 to 2 h at room temperature. Gently wash the plates with tap water, invert the plates on paper towels, and allow to dry.
8. Count plaques (1–2 mm holes in the cell monolayer) and calculate the original virus titers, correcting for the tenfold dilution and the twofold dilution resulting from transferring 0.5 ml of diluted virus to each well. Thus, if 12 plaques are counted in a well corresponding to a 10^{-6} dilution, the virus titer will be $12 \times 2 \times 10^6 = 24 \times 10^6$ plaque-forming units (PFU)/ml.

3.3 Platelet Counts

1. At specific time-points post-infection, bleed anesthetized mice by retro-orbital puncture using a microhematocrit EDTA-coated tube. Remove the tube once sufficient blood has been obtained (ca. 100 μ l) and apply pressure with a clean moist gauze until bleeding stops. Transfer the blood to a 0.5 ml tube, and gently flick the side of the capped tube to ensure that all blood mixes with the anticoagulant without formation of clots.
2. Analyze 20 μ l blood (for each replicate) using the Hemavet 950FS system, and calculate platelet counts in platelet number/ μ l blood.

3.4 T Cell Analysis, especially for Cell-Mediated-Immunity

1. At day 5 post-infection (before LCMV-Cl13-infected NZB mice die), sacrifice a group of infected and control mice, harvest the spleen, and crush each spleen through a 70 μ m mesh cell strainer into a 50 ml tube to generate a single cell suspension. Add 35 ml of BSS through the strainer to allow passage of the cells into the tube. Centrifuge (300 $\times g$, 5 min, 4 °C) and discard the supernatant.
2. Lyse red blood cells by adding 1.5 ml of ACK lysis buffer and incubating for 3 min at 4 °C. To wash the cells, add 40 ml BSS, centrifuge (300 $\times g$, 5 min, 4 °C), and discard the supernatant. Repeat this washing step as second time.

3. Resuspend the cells in 10 ml of flow buffer, count the cells, and adjust concentration to 20×10^6 cells/ml.
4. Transfer 2×10^6 cells to a FACS tube, add 3 ml flow buffer, centrifuge ($300 \times g$, 5 min, 4 °C), and discard the supernatant.
5. Add to the cells an appropriate amount of H-2L^d/NP₁₁₈₋₁₂₆ MHC-I/peptide tetramers and anti-CD16/anti-CD32 antibody in 70 µl of flow buffer, incubate 45 min at 4 °C (*see* **Notes 8** and **9**).
6. Prepare antibody mixes against CD8 and other surface molecules of interest (e.g., the negative regulatory molecules PD-1, LAG-3, TIM-3). Add 30 µl to the cells without washing away the tetramer stain, and incubate for an additional 30 min at 4 °C.
7. Add 3 ml of flow buffer/tube, centrifuge ($300 \times g$, 5 min, 4 °C), discard the supernatant. Repeat this washing step.
8. Resuspend the cells in 200 µl of flow buffer/tube, add 50 µl of 2% PFA to fix the cells, and vortex briefly. Keep the cells in the dark (covered by aluminum foil) at 4 °C until analysis. Analyze the cells on a flow cytometer.

3.5 Vascular Leak Assessment

1. Preload 28-G needle syringes with 200 µl Evan's Blue Dye Solution.
2. Carefully warm the mice with a heat lamp to promote vasodilation. Place the first mouse in a restraint device, clean the tail with 70% ethanol, insert the needle superficially under the skin, parallel to the lateral vein, and advance 2–3 mm into vein lumen. Inject slowly, ensuring that the solution is entering i.v., remove the needle, and apply gentle pressure to the puncture site with a clean gauze to assist with wound closure. Return the mouse to the housing cage. Wait for approximately 15–20 min (the time required for perfusion and lung harvest in one mouse, *see* **step 3**), and then proceed with the next mouse (*see* **Note 10**).
3. Exactly 20 min after Evan's Blue injection (**step 2**), sacrifice one mouse by lethal anesthesia. Place the mouse on its back by pinning the feet on a dissection board, open the abdominal and thoracic cavity to expose the heart, and perfuse the mouse by intracardial injection of 10 ml PBS. Harvest and transfer the lungs to a pre-weighted 5 ml tube. If necessary, follow the same procedure for other organs of interest, and then proceed with the next mouse. **Figure 1** illustrates the bright blue color of lungs that have taken up a great deal of Evan's Blue dye due to virus-mediated vascular permeability.
4. Place the tubes containing the organs (capped but not tightly closed to allow evaporation) in an oven at 56 °C to dry. After

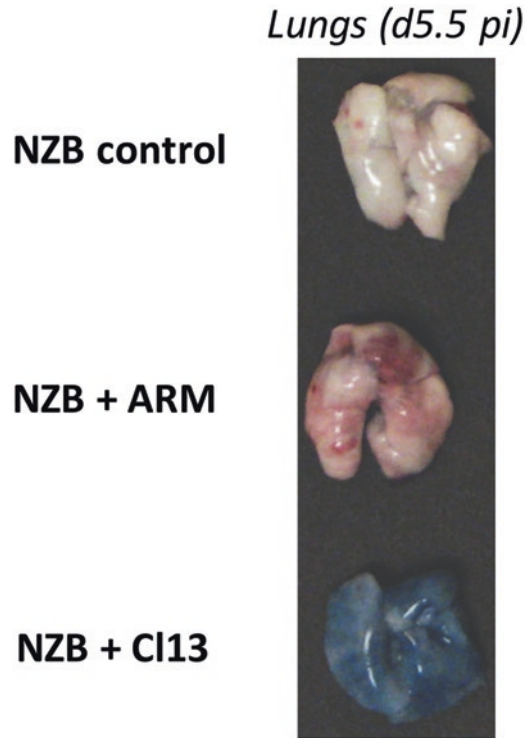


Fig. 1 Assessment of vascular leakage by the Evan's Blue Dye Method. NZB mice were either infected intravenously with LCMV-ARM or CI13 (2×10^6 PFU/mouse) or left untreated (controls). At day 5.5 post-infection (d5.5 pi), the mice were injected intravenously with Evan's Blue Dye Solution and, 20 min later, sacrificed by lethal anesthesia, perfused by intracardial PBS injection, and the lungs harvested. This analysis was performed as described [15], and this figure reproduces a portion of figure 4A in ref. [15]

48 h, weigh the tubes and calculate for each mouse the dry tissue weight. Add 0.5 ml of formamide, cap tightly, vortex, return the tubes to the oven at 56 °C, and incubate 24 h.

5. Prepare Evan's Blue twofold dilutions to use as standard curve (400, 200, 100, 50, 25, 12.5, 6.25, 3.12, 1.56, 0 µg/ml in PBS). Centrifuge the formamide/Evan's Blue mixture to pellet any remaining tissue fragments. Use 200 µl to measure absorbance at 620 nm. Calculate the amount of extravasated Evan's Blue in µg/g of dried tissue.

3.6 Bronchoalveolar Lavage Fluid (BALF) Analysis

1. At day 5 post-infection, euthanize a group of infected and control mice.
2. Open the abdominal and thoracic cavity. Transect and intubate the exposed trachea with an 18-G needle. Infuse 1 ml of PBS supplemented with protease inhibitors (Complete Mini, EDTA-free Protease Inhibitor Cocktail), recover and transfer

the solution (BALF) to a 15 ml tube, and repeat the lavage three additional times. Centrifuge the recovered BALF ($3000 \times g$, 3 min, 4 °C) and freeze at -80 °C until use.

3. Assess the BALF for total protein content (BCA kit), LDH enzymatic activity (Cytotox assay), and presence of IgM, cytokines, and chemokines (ELISA) using the commercially available kits according to manufacturer instructions.

4 Notes

1. MHC monomers can be flash-frozen in a dry ice/ethanol bath and stored at -80 °C, but after conjugation to fluorochromes, they should be kept at 4 °C in the dark like other fluorochrome-conjugated antibodies.
2. Mouse experimental protocols must be performed according to official Guide for the Care and Use of Laboratory Animals and approved by Institutional Animal Care and Use Committees.
3. Virus should be used as soon as possible. Unused stock virus should be discarded according to biosafety requirements, since secondary freezing and thawing would significantly reduce virus titer and infection characteristics.
4. There will be much less resistance when injecting i.v. than s.c; lightening of the usually dark-colored lateral vein is an additional confirmation of a successful i.v. injection.
5. Mice with severe symptoms should be sacrificed according to institutional guidelines.
6. Excessive Vero cell confluence will prevent formation of defined plaques.
7. The temperature of the melted agarose mix should be between 40 and 44 °C; higher temperature would kill Vero cells, whereas lower temperature would allow agarose solidification before transfer into the wells.
8. The appropriate amount of MHC tetramer to be used is determined in control experiments by staining spleen cells from infected and control mice with several dilutions of the specific tetramer and an irrelevant tetramer. The dilution resulting in maximal staining of infected cells and minimal staining of uninfected cells should be chosen.
9. Anti-CD16/anti-CD32 antibodies (clone 2.4G2) are used to block Fc receptors and avoid non-specific staining.
10. This procedure is better performed by two researchers, one injecting the mice and the other completing anesthesia, perfusion, and organ harvest.

References

- Chen JP, Cosgriff TM (2000) Hemorrhagic fever virus-induced changes in hemostasis and vascular biology. *Blood Coagul Fibrinolysis* 11(5):461–483
- Aleksandrowicz P, Wolf K, Falzarano D, Feldmann H, Seebach J, Schnittler H (2008) Viral haemorrhagic fever and vascular alterations. *Hamostaseologie* 28(1–2):77–84
- Paessler S, Walker DH (2013) Pathogenesis of the viral hemorrhagic fevers. *Annu Rev Pathol* 8:411–440. doi:[10.1146/annurev-pathol-020712-164041](https://doi.org/10.1146/annurev-pathol-020712-164041)
- Valbuena G, Walker DH (2006) The endothelium as a target for infections. *Annu Rev Pathol* 1:171–198. doi:[10.1146/annurev.pathol.1.110304.100031](https://doi.org/10.1146/annurev.pathol.1.110304.100031)
- Safronetz D, Geisbert TW, Feldmann H (2013) Animal models for highly pathogenic emerging viruses. *Curr Opin Virol* 3(2):205–209. doi:[10.1016/j.coviro.2013.01.001](https://doi.org/10.1016/j.coviro.2013.01.001)
- Smith DR, Holbrook MR, Gowen BB (2014) Animal models of viral hemorrhagic fever. *Antiviral Res* 112:59–79. doi:[10.1016/j.antiviral.2014.10.001](https://doi.org/10.1016/j.antiviral.2014.10.001)
- Waterston RH, Lindblad-Toh K, Birney E, Rogers J, Abril JF, Agarwal P, Agarwala R, Ainscough R, Alexandersson M, An P, Antonarakis SE, Attwood J, Baertsch R, Bailey J, Barlow K, Beck S, Berry E, Birren B, Bloom T, Bork P, Botcherby M, Bray N, Brent MR, Brown DG, Brown SD, Bult C, Burton J, Butler J, Campbell RD, Carninci P, Cawley S, Chiaromonte F, Chinwalla AT, Church DM, Clamp M, Clee C, Collins FS, Cook LL, Copley RR, Coulson A, Couronne O, Cuff J, Curwen V, Cutts T, Daly M, David R, Davies J, Delehaanty KD, Deri J, Dermitzakis ET, Dewey C, Dickens NJ, Diekhans M, Dodge S, Dubchak I, Dunn DM, Eddy SR, Elnitski L, Emes RD, Eswara P, Eyraas E, Felsenfeld A, Fewell GA, Flicek P, Foley K, Frankel WN, Fulton LA, Fulton RS, Furey TS, Gage D, Gibbs RA, Glusman G, Gnerre S, Goldman N, Goodstadt L, Grafham D, Graves TA, Green ED, Gregory S, Guigo R, Guyer M, Hardison RC, Haussler D, Hayashizaki Y, Hillier LW, Hinrichs A, Hlavina W, Holzer T, Hsu F, Hua A, Hubbard T, Hunt A, Jackson I, Jaffe DB, Johnson LS, Jones M, Jones TA, Joy A, Kamal M, Karlsson EK, Karolchik D, Kasprzyk A, Kawai J, Keibler E, Kells C, Kent WJ, Kirby A, Kolbe DL, Korf I, Kucherlapati RS, Kulbokas EJ, Kulp D, Landers T, Leger JP, Leonard S, Letunic I, Levine R, Li J, Li M, Lloyd C, Lucas S, Ma B, Maglott DR, Mardis ER, Matthews L, Mauceli E, Mayer JH, McCarthy M, McCombie WR, McLaren S, McLay K, McPherson JD, Meldrim J, Meredith B, Mesirov JP, Miller W, Miner TL, Mongin E, Montgomery KT, Morgan M, Mott R, Mullikin JC, Muzny DM, Nash WE, Nelson JO, Nhan MN, Nicol R, Ning Z, Nusbaum C, O'Connor MJ, Okazaki Y, Oliver K, Overton-Larty E, Pachter L, Parra G, Pepin KH, Peterson J, Pevzner P, Plumb R, Pohl CS, Poliakov A, Ponce TC, Ponting CP, Potter S, Quail M, Reymond A, Roe BA, Roskin KM, Rubin EM, Rust AG, Santos R, Sapojnikov V, Schultz B, Schultz J, Schwartz MS, Schwartz S, Scott C, Seaman S, Searle S, Sharpe T, Sheridan A, Shownkeen R, Sims S, Singer JB, Slater G, Smit A, Smith DR, Spencer B, Stabenau A, Stange-Thomann N, Sugnet C, Suyama M, Tesler G, Thompson J, Torrents D, Trevaskis E, Tromp J, Ucla C, Ureta-Vidal A, Vinson JP, Von Niederhausern AC, Wade CM, Wall M, Weber RJ, Weiss RB, Wendl MC, West AP, Wetterstrand K, Wheeler R, Whelan S, Wierzbowski J, Willey D, Williams S, Wilson RK, Winter E, Worley KC, Wyman D, Yang S, Yang SP, Zdobnov EM, Zody MC, Lander ES (2002) Initial sequencing and comparative analysis of the mouse genome. *Nature* 420(6915):520–562. doi:[10.1038/nature01262](https://doi.org/10.1038/nature01262)
- Church DM, Goodstadt L, Hillier LW, Zody MC, Goldstein S, She X, Bult CJ, Agarwala R, Cherry JL, DiCuccio M, Hlavina W, Kapustin Y, Meric P, Maglott D, Birtle Z, Marques AC, Graves T, Zhou S, Teague B, Potamousis K, Churas C, Place M, Herschleb J, Runnheim R, Forrest D, Amos-Landgraf J, Schwartz DC, Cheng Z, Lindblad-Toh K, Eichler EE, Ponting CP (2009) Lineage-specific biology revealed by a finished genome assembly of the mouse. *PLoS Biol* 7(5):e1000112. doi:[10.1371/journal.pbio.1000112](https://doi.org/10.1371/journal.pbio.1000112)
- Keane TM, Goodstadt L, Danecek P, White MA, Wong K, Yalcin B, Heger A, Agam A, Slater G, Goodson M, Furlotte NA, Eskin E, Nellaker C, Whitley H, Cleak J, Janowitz D, Hernandez-Pliego P, Edwards A, Belgard TG, Oliver PL, McIntyre RE, Bhomra A, Nicod J, Gan X, Yuan W, van der Weyden L, Steward CA, Bala S, Stalker J, Mott R, Durbin R, Jackson IJ, Czechanski A, Guerra-Assuncao JA, Donahue LR, Reinholdt LG, Payseur BA, Ponting CP, Birney E, Flint J, Adams DJ (2011) Mouse genomic variation and its effect on phenotypes and gene regulation. *Nature* 477(7364):289–294. doi:[10.1038/nature10413](https://doi.org/10.1038/nature10413)

10. Yalcin B, Wong K, Agam A, Goodson M, Keane TM, Gan X, Nellaker C, Goodstadt L, Nicod J, Bhomra A, Hernandez-Pliego P, Whitley H, Cleak J, Dutton R, Janowitz D, Mott R, Adams DJ, Flint J (2011) Sequence-based characterization of structural variation in the mouse genome. *Nature* 477(7364):326–329. doi:[10.1038/nature10432](https://doi.org/10.1038/nature10432)
11. Yalcin B, Adams DJ, Flint J, Keane TM (2012) Next-generation sequencing of experimental mouse strains. *Mamm Genome* 23(9–10):490–498. doi:[10.1007/s00335-012-9402-6](https://doi.org/10.1007/s00335-012-9402-6)
12. Gray KK, Worthy MN, Juelich TL, Agar SL, Poussard A, Ragland D, Freiberg AN, Holbrook MR (2012) Chemotactic and inflammatory responses in the liver and brain are associated with pathogenesis of Rift Valley fever virus infection in the mouse. *PLoS Negl Trop Dis* 6(2):e1529. doi:[10.1371/journal.pntd.0001529](https://doi.org/10.1371/journal.pntd.0001529)
13. Reed C, Lin K, Wilhelmsen C, Friedrich B, Nalca A, Keeney A, Donnelly G, Shamblin J, Hensley LE, Olinger G, Smith DR (2013) Aerosol exposure to Rift Valley fever virus causes earlier and more severe neuropathology in the murine model, which has important implications for therapeutic development. *PLoS Negl Trop Dis* 7(4):e2156. doi:[10.1371/journal.pntd.0002156](https://doi.org/10.1371/journal.pntd.0002156)
14. Bradfute SB, Warfield KL, Bray M (2012) Mouse models for filovirus infections. *Viruses* 4(9):1477–1508. doi:[10.3390/v4091477](https://doi.org/10.3390/v4091477)
15. Baccala R, Welch MJ, Gonzalez-Quintal R, Walsh KB, Tejjaro JR, Nguyen A, Ng CT, Sullivan BM, Zarpellon A, Ruggeri ZM, de la Torre JC, Theofilopoulos AN, Oldstone MB (2014) Type I interferon is a therapeutic target for virus-induced lethal vascular damage. *Proc Natl Acad Sci U S A* 111(24):8925–8930. doi:[10.1073/pnas.1408148111](https://doi.org/10.1073/pnas.1408148111)
16. Schnell FJ, Sundholm S, Crumley S, Iversen PL, Mourich DV (2012) Lymphocytic choriomeningitis virus infection in FVB mouse produces hemorrhagic disease. *PLoS Pathog* 8(12):e1003073. doi:[10.1371/journal.ppat.1003073](https://doi.org/10.1371/journal.ppat.1003073)
17. Salvato M, Borrow P, Shimomaye E, Oldstone MB (1991) Molecular basis of viral persistence: a single amino acid change in the glycoprotein of lymphocytic choriomeningitis virus is associated with suppression of the antiviral cytotoxic T-lymphocyte response and establishment of persistence. *J Virol* 65(4):1863–1869
18. Borrow P, Evans CF, Oldstone MB (1995) Virus-induced immunosuppression: immune system-mediated destruction of virus-infected dendritic cells results in generalized immune suppression. *J Virol* 69(2):1059–1070

Chapter 21

Testing Experimental Therapies in a Guinea Pig Model for Hemorrhagic Fever

Gary Wong, Yuhai Bi, Gary Kobinger, George F. Gao, and Xiangguo Qiu

Abstract

Hemorrhagic fever viruses are among the deadliest pathogens known to humans, and often, licensed medical countermeasures are unavailable to prevent or treat infections. Guinea pigs are a commonly used animal for the preclinical development of any experimental candidates, typically to confirm data generated in mice and as a way to validate and support further testing in nonhuman primates. In this chapter, we use Sudan virus (SUDV), a lethal filovirus closely related to Ebola virus, as an example of the steps required for generating a guinea pig-adapted isolate that is used to test a monoclonal antibody-based therapy against viral hemorrhagic fevers.

Key words Hemorrhagic fever, Sudan virus, Guinea pigs, Serial passaging, Monoclonal antibodies

1 Introduction

Viral hemorrhagic fevers (VHF) constitute a broad group of illnesses in which some infections cause mild disease in humans, but the majority can result in severe, life-threatening illness with high case fatality rates [1]. The initial onset of disease includes general symptoms such as fever, fatigue, dizziness, and muscle aches. As the disease progresses, due to damage to the vascular system, patients show signs of subcutaneous bleeding under the skin (rash), in internal organs, as well as various body orifices (hemorrhage) [2]. Death from VHF is typically a result of shock, seizure, and multiple organ failure [2]. VHF are known to be caused by member viruses from seven distinct families: *Arenaviridae* (Lassa virus, Lujó virus, Junín virus, Machupo virus, Sabiá virus, and Guanarito virus), *Hantaviridae* (hantaviruses) *Nairoviridae* (Crimean-Congo hemorrhagic fever virus), *Peribunyaviridae* (orthobunyaviruses) *Phenuiviridae* (Rift Valley fever virus), and *Flaviviridae* (dengue virus, yellow fever virus, Omsk hemorrhagic fever virus, and Kyasanur Forest disease virus) [3]. Many of these viruses need to be handled in biosafety level 4 (BSL-4) facilities due to their virulence in humans and due to the

fact that no approved vaccines or treatments exist for the majority of these pathogens. Patients typically receive supportive therapy, and ribavirin, an approved antiviral drug, has shown some efficacy in humans infected with Lassa [4] or hantaviruses [5]. Therefore, there is an urgent need for the development of prophylactics and/or therapeutics against VHF.

One considerable bottleneck for the development of medical countermeasures against VHF infections has been the lack of small animal models to screen potential experimental drugs for efficacy against a particular pathogen, before testing in nonhuman primates (NHP), which is a gold standard animal model for many VHF. With current technologies, it is simply not financially feasible in many instances to test candidate drugs directly in NHP without first confirming efficacy *in vitro* and *in vivo* in a smaller animal model. In the case of monoclonal antibodies (mAbs), production costs can rise in excess of US \$1000/g of mAbs [6], which make it prohibitively expensive to test mAbs in NHP without first acquiring supporting efficacy data in smaller animals.

An example of a success story with this developing and testing process for new drugs is ZMapp. ZMapp is a cocktail of three humanized mAbs targeting different regions of the glycoprotein on Ebola virus (EBOV) [7]. During the 2013–16 EBOV disease outbreak in Western Africa, ZMapp was initially used to treat two American health workers who had unfortunately contracted EBOV in Liberia [8]. Both workers survived, and ZMapp was fast-tracked for clinical trials and given to 36 more patients during the outbreak, of which 28 survived. While this is a resounding success considering that it was thought at one point that EBOV disease was a death sentence, these achievements would not have been possible had it not been for the prior development of small animal models for EBOV (mice [9] and guinea pigs [10]) that paved the way for the screening of experimental candidates, including the individual components of ZMapp [11, 12].

SUDV is a close relative of EBOV and is also deadly in humans (case fatality rate = 53%) [13]. SUDV is known to be endemic to eastern Africa, in the countries of South Sudan and the Republic of Uganda [13]. SUDV was the etiological agent behind the second largest filovirus outbreak in history, the 2000 outbreak in Gulu, Uganda [13]. The number of potential experimental candidates available for EBOV unfortunately does not exist for SUDV, in part due to the aforementioned lack of small animal models and in part due to the attention and resources spent on researching EBOV. A guinea pig animal model was recently developed by the Special Pathogens Program at the National Microbiology Laboratory in Winnipeg, Canada, in which serial passaging of SUDV in the livers and spleens of guinea pigs resulted in a virus variant that was uniformly lethal to these animals [14]. This animal model can now be used to test candidate vaccines and drugs against SUDV [15]. Experimental procedures involving the generation of the guinea

pig-adapted SUDV and the testing of a hypothetical mAb-based therapy in these animals will be presented in this chapter, to serve as a blueprint for the development of guinea pig models for other VHF and the testing of specific therapies.

2 Materials

2.1 *General Laboratory Supplies*

In addition to the specific materials required for the procedures below, the following general laboratory supplies should also be available:

1. Pipetman and Pipet-Aid.
2. Consumables including pipet tips, pipets, Eppendorf tubes, cryovials, T-150 tissue culture flasks, 48-well tissue culture plate, 50 ml Falcon tubes, and 60 × 15 mm petri dishes.
3. 37 °C incubator for tissue culture.
4. Tabletop centrifuge, benchtop centrifuge.
5. Vortex.
6. Optical (light) microscope.
7. Biosafety cabinet.
8. Weight scale.

2.2 *Serial Passaging in Guinea Pigs*

1. Guinea pigs (female, Hartley, 6–8 weeks old, two animals per passage).
2. Equipment needed for animal husbandry (cages, food, water, etc.).
3. Sudan virus progenitor (SUDV-p), isolate Boniface (GenBank accession no. FJ968794.1).
4. 27 gauge needles.
5. Dulbecco's Modified Eagle's Medium (DMEM).
6. Heat-inactivated fetal bovine serum (FBS).
7. Inhalational anesthetic (isoflurane – AErrane).
8. Small dissecting scissors.
9. Tweezers.
10. 40-mesh steel screen (40 mesh means 40 openings per square inch, allowing passage of a 350–400 µm particle).
11. Sterile plastic plunger.
12. Falcon nylon mesh cell strainers (accommodating a 40 µm particle size).
13. Phosphate buffered saline (PBS).
14. Tissue homogenizer.
15. 2 ml cryovials.

2.3 qRT-PCR Testing of Liver and Spleen Homogenates

1. RNA extraction kit (viral RNA mini kit, Qiagen). This kit contains a virus-lysing buffer called “Buffer AVL”, that is a mixture of guanidinium chloride and carrier (polyA) RNA. The kit contains Buffer AW1 and AW2 that are column wash buffers containing denaturing guanidinium chloride that helps stick nucleic acids to silica beads. Buffer AVE:10 mM Tris-Cl pH 8.3, 0.1 mM EDTA and 0.04% NaN₃ is used to remove nucleic acids from silica beads.
2. 96-well plates for qRT-PCR.
3. Lightcycler 480 RNA master hydrolysis probe kit.
4. ABI StepOnePlus real-time PCR instrument.
5. Primers (20 μM stock) and probes (10 μM stock) designed against SUDV:
 Forward: 5'-CAGAAGACAATGCAGCCAGA-3'
 Reverse: 5'-TTGAGGAATATCCCACAGGC-3'
 Probe: 5'-[FAM]-CTGCTAGCTTGGCCAAAGTCACAAG-[BHQ]-3'

2.4 Propagation and Titration of the Adapted Virus

1. CV-1 cells: *Cercopithecus aethiops* kidney cells (ATCC® CCL-70™).
2. Dulbecco’s Modified Eagle’s Medium (DMEM).
3. Heat-inactivated fetal bovine serum (FBS).
4. 0.05% Trypsin.

2.5 Determining the LD₅₀ of the Adapted Virus

1. Guinea pigs (Female, Hartley, 6–8 weeks old, 3 animals per dose to be tested).
2. Equipment needed for animal husbandry (cages, food, water, etc.).
3. Newly generated, guinea pig-adapted virus, known hereafter as SUDV-GA (GA for guinea pig-adapted).
4. Needles (27 gauge, 0.40 mm outer diameter).
5. Dulbecco’s Modified Eagle’s Medium (DMEM).
6. Heat-inactivated fetal bovine serum.

2.6 Testing of a Monoclonal Antibody Against SUDV in Guinea Pigs

1. Guinea pigs (Female, Hartley, 6–8 weeks old, 6 animals per mAb to test).
2. Equipment needed for animal husbandry (cages, food, water, etc.).
3. Monoclonal antibodies, enough for up to 20 mg per guinea pig.
4. 27 gauge needles.
5. SUDV-GA.

3 Methods

3.1 Serial Passaging in Guinea Pigs (See Note 1)

1. Inject two guinea pigs each intraperitoneally (IP) with $\sim 10^5$ TCID₅₀ of SUDV-p in 1 ml DMEM with 2% FBS.
2. If animals remain healthy for 7 days post-infection (dpi), euthanize them with an overdose of inhaled isoflurane.
3. Remove liver and spleen from euthanized animals using scissors and tweezers.
4. Pool and homogenize the organs by grinding them against a steel mesh (e.g., 40–60 mesh will suffice) with a sterile plastic plunger, until the majority of cells have been pushed through the mesh.
5. Suspend cells in 10 ml of PBS and aliquot to 2 ml cryovials.
6. Centrifuge cells on tabletop centrifuge at $400 \times g$ for 5 min.
7. Pass the supernatant through a 40 μ m nylon mesh Falcon cell strainer, and then homogenize the remaining cell pellets with a tissue homogenizer.
8. Centrifuge cells on tabletop centrifuge at $400 \times g$ for 5 min.
9. Pass the supernatant through the cell strainer.
10. Inject two new, naive guinea pigs IP with 1 ml of the filtered supernatant each. Also use some supernatant for viral RNA extractions such that it can be confirmed that SUDV is still present inside the guinea pig organs.
11. If still healthy for 7 dpi, repeat passaging process starting from **step 2** of this section.
12. If animals start to look sick, the investigator needs to judge whether they will live for 7 dpi. If so, repeat passaging process starting from **step 2** of this section.
13. If animals die before 7 dpi, harvest liver and spleen (i.e., repeat passaging process starting from **step 3** of this section, up until **step 10** and proceed to Subheadings [3.2](#) and [3.3](#)).

3.2 qRT-PCR Testing of Liver and Spleen Homogenates (See Note 2)

1. Take 140 μ l of supernatant from Subheading [3.1](#) and add 560 μ l of Buffer AVL in a 2 ml cryovial.
2. Mix well and incubate at room temperature for 10 min.
3. Briefly centrifuge the tubes to remove liquid from the lid.
4. Add 560 μ l of 100% ethanol to the sample, and mix well.
5. Briefly centrifuge the tubes to remove liquid from the lid.
6. Apply 630 μ l of the sample/AVL/ethanol mix to the column with a 2 ml collection tube.
7. Centrifuge on tabletop centrifuge at $6000 \times g$ for 1 min.
8. Discard waste liquid and reuse collection tube. Apply 630 μ l of the sample/AVL/ethanol mix to the column.

9. Centrifuge on tabletop centrifuge at $6000 \times g$ for 1 min.
10. Discard waste liquid and reuse collection tube.
11. Add 500 μl of Buffer AW1 to the column.
12. Centrifuge on tabletop centrifuge at $6000 \times g$ for 1 min.
13. Discard waste liquid and reuse collection tube.
14. Add 500 μl of Buffer AW2 to the column.
15. Centrifuge on tabletop centrifuge at $15,000 \times g$ for 3 min.
16. Discard waste liquid and reuse collection tube.
17. Centrifuge on tabletop centrifuge at $15,000 \times g$ for 1 min.
18. Discard waste liquid and use Eppendorf tube.
19. Add 50 μl of elution Buffer AVE to the column, let sit for 1 min.
20. Centrifuge on tabletop centrifuge at $6000 \times g$ for 1 min.
21. Set up qRT-PCR reaction as follows (using the Lightcycler 480 RNA master hydrolysis probe kit from Roche):

For 1 \times reaction:

Water	7.55 μl
Buffer	9.25 μl
Activator	1.60 μl
Enhancer	1.00 μl
Primer forward/reverse mix	0.30 μl
Probe	0.30 μl
RNA	5.00 μl
Total	25.00 μl

22. qRT-PCR cycling conditions:
 - 61 °C for 3 min (reverse transcription)
 - 95 °C for 30 s (initial denaturation)
 - 45 cycles (PCR): then, 95 °C for 15 s; then, 60 °C for 30 s
23. If results are positive for SUDV by qRT-PCR, there are two scenarios:
 - First, if this supernatant is from guinea pigs that succumbed to infection, proceed to Subheading 3.3. Second, if this supernatant is from healthy guinea pigs, use this supernatant to infect two more naïve guinea pigs (passaging).
24. If results are negative for SUDV by qRT-PCR, go back to the supernatant from the previous passage, inject guinea pigs IP with 1 ml of the supernatant, and repeat process starting from **step 2** of Subheading 3.1.

3.3 Propagation and Titration of the Adapted Virus (See Note 3)

1. Prepare T-150 flask(s) of CV-1 cells that are approximately 95% confluent on the day of infection.
2. Take 1 ml of supernatant, dilute in DMEM with 2% FBS to 5 ml, and apply to cells.
3. Incubate at 37 °C, 5% CO₂ for 1 h, rocking flask(s) gently every 15 min to ensure even spread of the virus.
4. Remove virus inoculum.
5. Add 30 ml of DMEM with 2% FBS, and incubate at 37 °C, 5% CO₂.
6. Observe cells daily until cytopathic effects occur.
7. When approximately 80% of cells show cytopathic effects, collect supernatant in 50 ml Falcon tubes.
8. Centrifuge on benchtop centrifuge at 400 × *g* for 5 min.
9. Making sure not to touch the cell pellet, aliquot the harvested SUDV-GA into 2 ml cryovials and store at -150 °C for future use.
10. Seed 48-well tissue culture plate of CV-1 for titering SUDV-GA.
11. Take one aliquot of SUDV-GA and prepare the virus dilutions in plain DMEM by tenfold serial dilution from 10⁻² to 10⁻⁸ (i.e., 100 µl virus +900 µl DMEM).
12. Remove media from CV-1 cells.
13. Add 100 µl of plain DMEM to the mock row.
14. Add 100 µl of the virus dilutions starting with the highest dilution to each well (6 wells per dilution).
15. Incubate at 37 °C, 5% CO₂ for 1 h, rocking flask(s) gently every 15 min to ensure even spread of the virus.
16. Remove virus inoculum.
17. Add 250 µl of DMEM with 2% FBS to cells, and incubate at 37 °C, 5% CO₂.
18. Observe cells daily until cytopathic effects occur.
19. Calculate titer in units of TCID₅₀/ml by the Reed and Muench method.
20. Proceed to Subheading 3.4.

3.4 Determining the LD₅₀ of the Adapted Virus (See Note 4)

1. Prepare the stock virus dilutions in plain DMEM by tenfold serial dilution, to get concentrations of ~10³ to 10⁻² TCID₅₀/ml (i.e., 500 µl virus +4500 µl DMEM)
2. Challenge guinea pigs (n = 3 per concentration) IP with SUDV-GA in a volume of 1 ml DMEM.
3. Monitor daily for clinical signs, weight loss, and survival.
4. Calculate LD₅₀ values using the method of Miller and Tainter (<http://ayubmed.edu.pk/JAMC/PAST/21-3/Randhawa.pdf>).
5. Proceed to Subheading 3.5.

**3.5 Testing
of a Monoclonal
Antibody
Against SUDV
in Guinea Pigs (See
Note 5)**

1. Prepare two doses of mAbs (5 or 10 mg mAbs per guinea pig diluted in 1 ml PBS).
2. Challenge guinea pigs (n = 6 or more per group) IP with SUDV-GA in a volume of 1 ml DMEM with 2% FBS.
3. One day later, treat guinea pigs IP with mAbs.
4. Monitor daily for clinical signs, weight loss, and survival.
5. Depending on survival results, adjust parameters of the experiment and try again: If animals survive, try lowering the dose and initiating treatment at later timepoints after infection. If animals do not survive, try increasing the dose, initiating treatment earlier, administering more injections, or combining with an adjuvant.

4 Notes

1. Serial Passaging in Guinea Pigs
 - (a) Reagents must be sterile to avoid cross contamination.
 - (b) Guinea pigs may or may not get sick and die, and if so, the timing (in terms of passage number) is generally unpredictable. It is up to the researcher to weigh and monitor these animals for signs of illness daily, and determine if the animal should be euthanized.
 - (c) This passaging process can be somewhat lengthy. For SUDV, it took 25 passages until the virus was able to cause death in guinea pigs.
2. qRT-PCR Testing of Liver and Spleen Homogenates
 - (a) The RNA extraction process is performed mostly following manufacturer instructions from the viral RNA mini kit (Qiagen).
 - (b) The qRT-PCR master mix was set up following manufacturer instructions from the Lightcycler 480 RNA master hydrolysis probe kit (Roche).
3. Propagation and Titration of the Adapted Virus
 - (a) The choice of cell line in which to grow the virus should be made carefully and based on past publications. CV-1 cells were used for SUDV but VeroE6 (VERO C1008; Vero 76, clone E6; ATCC® CRL-1586™) grows most filoviruses well.
 - (b) Under cell maintenance conditions, CV-1 cells should be grown in DMEM supplemented with 10% FBS.
 - (c) SUDV was not plaque purified (i.e., stock derived from a single clone) because the virus does not plaque well under normal plaque assay conditions.

- (d) Cytopathic effects from SUDV infection of CV-1 cells typically occur between 10 and 14 days after infection.
4. Determining the LD₅₀ of the Adapted Virus
 - (a) After infection, moribund animals tend to die quickly, typically within 7–10 dpi. However, the monitoring period should still be set for 28 days, as small numbers of animals do die later.
 - (b) Other experiments that can also be performed include investigating the mutations which allow SUDV-GA to kill its host, pathology studies, and clinical findings in animals infected with SUDV-GA and how the illness compares to that of human SUDV disease. This topic will not be covered here.
5. Testing of a Monoclonal Antibody against SUDV in Guinea Pigs
 - (a) Parameters associated with this experiment, i.e., dosing, timing of treatment, are flexible. Typically most researchers start with a single IP dose of 5 or 10 mg mAbs per guinea pig, and administer mAb 1 day before challenge, at the time of challenge, and 1 day after challenge.

Acknowledgments

G.W. is supported by the Banting Postdoctoral Fellowship from the Canadian Institutes of Health Research (CIHR) and the President's International Fellowship Initiative from the Chinese Academy of Sciences (CAS).

References

1. Falzarano D, Feldmann H (2013) Vaccines for viral hemorrhagic fevers—progress and shortcomings. *Curr Opin Virol* 3(3):343–351. doi:10.1016/j.coviro.2013.04.007
2. CDC.gov (2013) Viral Hemorrhagic Fevers. <http://www.cdc.gov/ncidod/dvrd/spb/mnpages/dispages/vhf.htm>. Accessed March 31 2016
3. Safronetz D, Rosenke K, Westover JB, Martellaro C, Okumura A, Furuta Y, Geisbert J, Saturday G, Komeno T, Geisbert TW, Feldmann H, Gowen BB (2015) The broad-spectrum antiviral favipiravir protects guinea pigs from lethal Lassa virus infection post-disease onset. *Sci Rep* 5:14775. doi:10.1038/srep14775
4. McCormick JB, King IJ, Webb PA, Scribner CL, Craven RB, Johnson KM, Elliott LH, Belmont-Williams R (1986) Lassa fever. Effective therapy with ribavirin. *N Engl J Med* 314(1):20–26. doi:10.1056/NEJM198601023140104
5. Huggins JW, Hsiang CM, Cosgriff TM, Guang MY, Smith JL, Wu ZO, LeDuc JW, Zheng ZM, Meehan JM, Wang QN et al (1991) Prospective, double-blind, concurrent, placebo-controlled clinical trial of intravenous ribavirin therapy of hemorrhagic fever with renal syndrome. *J Infect Dis* 164(6):1119–1127
6. Kelley B (2009) Industrialization of mAb production technology: the bioprocessing industry at a crossroads. *MAbs* 1(5):443–452
7. Qiu X, Wong G, Audet J, Bello A, Fernando L, Alimonti JB, Fausther-Bovendo H, Wei H, Aviles J, Hiatt E, Johnson A, Morton J, Swope K, Bohorov O, Bohorova N, Goodman C, Kim D, Pauly MH, Velasco J, Pettitt J, Olinger GG, Whaley K, Xu B, Strong JE, Zeitlin L, Kobinger GP (2014) Reversion of advanced Ebola virus

- disease in nonhuman primates with ZMapp. *Nature* 514(7520):47–53. doi:[10.1038/nature13777](https://doi.org/10.1038/nature13777)
8. Lyon GM, Mehta AK, Varkey JB, Brantly K, Plyler L, McElroy AK, Kraft CS, Towner JS, Spiropoulou C, Stroher U, Uyeke TM, Ribner BS (2014) Clinical care of two patients with Ebola virus disease in the United States. *N Engl J Med* 371(25):2402–2409. doi:[10.1056/NEJMoa1409838](https://doi.org/10.1056/NEJMoa1409838)
 9. Bray M, Davis K, Geisbert T, Schmaljohn C, Huggins J (1998) A mouse model for evaluation of prophylaxis and therapy of Ebola hemorrhagic fever. *J Infect Dis* 178(3):651–661
 10. Connolly BM, Steele KE, Davis KJ, Geisbert TW, Kell WM, Jaax NK, Jahrling PB (1999) Pathogenesis of experimental Ebola virus infection in guinea pigs. *J Infect Dis* 179(Suppl 1):S203–S217. doi:[10.1086/514305](https://doi.org/10.1086/514305)
 11. Qiu X, Alimonti JB, Melito PL, Fernando L, Stroher U, Jones SM (2011) Characterization of Zaire ebolavirus glycoprotein-specific monoclonal antibodies. *Clin Immunol* 141(2):218–227. doi:[10.1016/j.clim.2011.08.008](https://doi.org/10.1016/j.clim.2011.08.008)
 12. Zeitlin L, Pettitt J, Scully C, Bohorova N, Kim D, Pauly M, Hiatt A, Ngo L, Steinkellner H, Whaley KJ, Olinger GG (2011) Enhanced potency of a fucose-free monoclonal antibody being developed as an Ebola virus immunoprotectant. *Proc Natl Acad Sci USA* 108(51):20690–20694. doi:[10.1073/pnas.1108360108](https://doi.org/10.1073/pnas.1108360108)
 13. [CDC.gov](http://www.cdc.gov/vhf/ebola/outbreaks/history/chronology.html) (2016) Outbreaks chronology: Ebola virus disease. <http://www.cdc.gov/vhf/ebola/outbreaks/history/chronology.html>. Accessed March 31 2016
 14. Wong G, He S, Wei H, Kroeker A, Audet J, Leung A, Cutts T, Graham J, Kobasa D, Embury-Hyatt C, Kobinger GP, Qiu X (2015) Development and characterization of a guinea pig-adapted Sudan Virus. *J Virol* 90(1):392–399. doi:[10.1128/JVI.02331-15](https://doi.org/10.1128/JVI.02331-15)
 15. Howell KA, Qiu X, Brannan JM, Bryn C, Davidson E, Holsberg FW, Wec AZ, Shulenin S, Biggins JE, Douglas R, Turner HL, Pallesen J, Murin CD, He S, Kroeker A, Vu H, Herbert AS, Fusco ML, Nyakature EK, Lai JR, Saphire EO, Zeitlin L, Ward AB, Chandran K, Doranz BJ, Kobinger GP, Dye JM, Aman MJ (2016) Antibody treatment of Ebola and Sudan virus infection via a uniquely exposed epitope within the glycoprotein receptor-binding site. *Cell Rep* 15(7):1514–1526

A Primate Model for Viral Hemorrhagic Fever

**Maria S. Salvato, Igor S. Lukashevich, Yida Yang,
Sandra Medina-Moreno, Mahmoud Djavani, Joseph Bryant,
Juan David Rodas, and Juan Carlos Zapata**

Abstract

Lymphocytic choriomeningitis virus strain WE (LCMV-WE), a Risk Group 3 virus, causes a disease in rhesus monkeys that closely resembles human infection with Lassa fever virus, a Risk Group 4 agent. Three stages of disease progression have been defined and profiled in this model: pre-viremic, viremic, and terminal. The earliest or pre-viremic stage reveals changes in the blood profile predictive of the later stages of disease. In order to identify whether specific changes are pathognomonic, it was necessary to perform a parallel infection with an attenuated virus (LCMV-Armstrong). Here we review the use of nonhuman primates to model viral hemorrhagic fever and offer a step-by-step guide to using a rhesus macaque model for Lassa fever.

Key words Macaque model, LCMV-WE, Risk group 3, Lassa fever, Risk group 4, A-BSL-3

1 Introduction

Although rodents and other animal models are useful for preliminary studies, nonhuman primates (NHP) are needed to accurately model the systemic responses of infected human beings. Rodents account for 95% of the animal models for most in vivo research, and nonhuman primates account for only 0.5% of the models used [1]. NHP are generally more susceptible to viral hemorrhagic fevers (VHF) at lower inoculating doses than are rodents, and they develop signs and systemic responses similar to human beings, making them the best suited models to describe pathogenesis, test viral vaccines, and assess antiviral drugs.

Different kinds of NHP have been used as models for VHF, but the Indian rhesus macaque has been used most frequently, e.g., in studies of yellow fever [2], severe dengue [3], Lassa fever [4, 5], and filovirus disease [6]. *Cynomolgus* macaques have also been used for Lassa fever [5, 7] and Marburg and Ebola virus diseases [6]. Marmosets were found to accurately model Rift Valley fever

(RVF) [8], Argentinian hemorrhagic fever [9], and Lassa fever [10]; Crimean-Congo hemorrhagic fever virus (CCHFV) has been studied in livestock, but not yet in NHP [11].

A series of papers from the Salvato laboratory, based on observations from Czech scientists in the 1960s, describe a rhesus macaque model for Lassa fever using the Risk Group 3 agent, lymphocytic choriomeningitis virus WE (LCMV-WE) [12–17]. Rhesus monkeys inoculated with LCMV-WE follow a disease course of 10–14 days that resembles human infection with Lassa fever virus [13, 14, 17]. In these studies, viremia is detectable in plasma by day 4 and fever begins a day or two later. Viral loads are a prognostic disease marker and are directly proportional to virulence; e.g., $>10^4$ plaque-forming units (pfu)/ml plasma or $>10^{3.6}$ tissue culture infectious doses for 50% of the cultures (TCID₅₀)/ml are lethal in both human beings and in the monkey model [13, 18, 19]. The most consistent pathologic finding in Lassa fever infection in man and in the monkey model is hepatocellular necrosis [18, 20, 21]. Findings in the monkey model were similar to those for human beings in which liver enzymes that are $>$ fivefold over baseline levels (e.g., aspartate aminotransferase (AST) >150 IU/L) predict a lethal outcome. Levels of IL-6 in plasma were highly elevated as well, in conformation with results in NHP and human Lassa fever patients [14, 15]. The IL-6 titer was proposed as an additional marker of Lassa fever progression [7]. Coagulation defects are also a disease marker, such that prothrombin times (PT) greater than 13 s and activated partial thromboplastin times (APTT) greater than 40 s are signs of disease [18, 19]. Other signs of hemorrhagic fever include myocarditis and pulmonary edema, with late-stage hypovolemic shock due to vascular leakage [20, 21]. Transcriptome profiling of the LCMV-WE-infected macaques [22] defined three distinct stages of disease progression (Fig. 1): a pre-viremic stage in which CD14⁺ cells increased in the circulation; a viremic stage marked by abrupt onset of fever, malaise, and high liver enzymes; and a terminal stage with signs of vascular leakage at mucosal surfaces, bleeding at venipuncture sites, petechial rashes, listlessness, loss of appetite, dehydration, and respiratory distress.

The development of hemorrhagic fever depends on high viral titers that could best be achieved by intravenous delivery of a high-dose inoculum. Investigators at BSL-4 facilities in the USA have settled on intramuscular (i.m.) delivery to model the most frequent type of accidental infection of human beings [6]. A French group used subcutaneous (s.c.) inoculation of cynomolgus macaques to study Lassa fever [7], and, remarkably, one of three given 10^3 pfu died of VHF, and none of the three animals given 10^7 pfu died of VHF. The authors discovered higher viral RNA/pfu in survivors

Progression of Arenavirus Hemorrhagic Fever

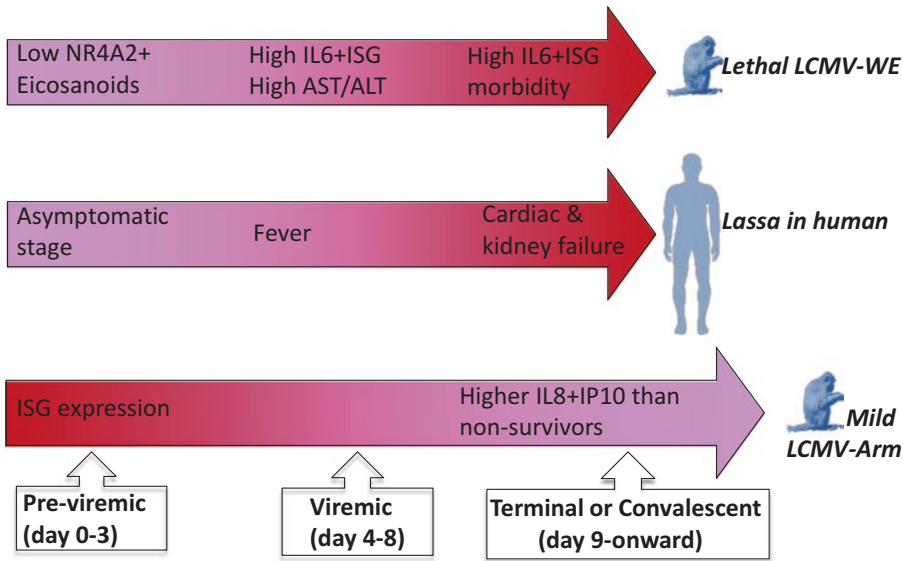


Fig. 1 Three stages of hemorrhagic fever disease progression. The pre-viremic stage has been called the “asymptomatic” stage in human subjects. The viremic stage is characterized by the onset of flu-like signs like fever and muscle aches. The terminal stage displays severe signs of vascular leakage, tissue edema, high liver enzymes, and coagulopathy. For profiles of NHP at these stages, *see* these refs. 22–24. For description of a medical doctor who received a high-dose “needle stick” and died 18 days later, *see* ref. 25

implying that there were more defective particles interfering with the replication of the virus and decreasing the severity of the disease. In our experience, i.m. and s.c. delivery are less reproducible than i.v. for achieving a rapid and systemic hemorrhagic fever. Oral delivery has not been very reproducible in our hands, but can result in severe disease and sometimes death [17]. The possibility that the gastrointestinal tract attenuates the viral infection conforms to observations in the field [26]. Aerosol Lassa infection using doses below 10^3 pfu per macaque resulted in four out of four animals acquiring disease [27]. A good example of i.v. infection is the study of dengue virus infection of rhesus monkeys: dengue fever was routinely observed at viral doses less than 10^6 pfu per animal; however, at an intravenous dose of 10^7 pfu, dengue hemorrhagic fever was observed in six out of six macaques [3] (Fig. 2).

In this chapter, we will describe the rhesus macaque model for Lassa fever: the Animal Biosafety Level 3 (ABSL-3) facilities, care, and sedation of NHP, the inoculation of macaques with infectious virus stocks, sampling macaques by blood draw and tissue biopsy, and the final harvesting of tissues during necropsy (*see Note 1*).

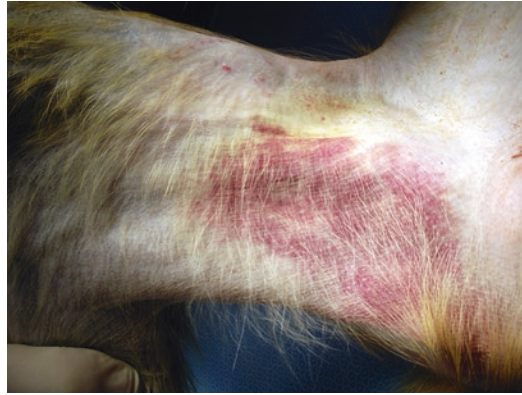


Fig. 2 Groin petechial rash of rhesus macaque with dengue hemorrhagic fever. Petechiae are due to blood leaking from capillaries under the skin. Macaques were infected intravenously with 10^7 pfu dengue 2 and experienced peak viremia by days 3–5. By day 7 investigators noted a slight drop in hematocrit, mild thrombocytopenia, neutropenia, and D-dimer elevation [3]. Photo by courtesy of Francois Villinger, Division of Microbiology and Immunology, Yerkes National Primate Research Center, Emory University, Atlanta, GA, USA; New Iberia Research Center, University of Louisiana at Lafayette, New Iberia, LA, USA

2 Materials

2.1 Facilities and Animals

1. A minimal ABSL-3 suite should have an anteroom for care staff to put on their personal protective equipment (PPE), a HEPA-filtered isolation room for housing animals in cages, and a HEPA-filtered room for examinations and necropsies.
2. The Indian rhesus macaque, *Macaca mulatta*, 3–10 years of age and 4–7 kg weight, is a frequent model for hemorrhagic fever virus infection. NHP should be prescreened for such pathogens as herpes B virus (lethal for human beings) and simian foamy virus (that prevents the immortalization of macaque B cells).
3. Personal protective equipment (PPE): lab coat, gloves, and safety glasses are minimal for BSL-2. Face shield, second pair of gloves, disposable shoe covers, disposable hair covers, disposable sleeves, and body suit are additional for BSL-3. For virus preparation or when expecting more than usual aerosols (as in bone cutting during necropsy), investigators will wear portable respiratory packs.
4. Anesthetic ketamine solution: 100 mg/ml in saline is frequently used at 15 mg/kg intramuscularly (i.m.) when anesthetizing a macaque (*see Note 2*).
5. Sterile gauze pads, used to apply pressure at sites of injection.
6. Biohazard bags for waste disposal and a sharps container for needle disposal, both suitable for autoclaving.

7. Measurement equipment: scale for weighing monkeys; calipers for measuring extremities, disease signs, organs, and tissues.

2.2 Inoculation and Infection of NHP

1. Virus stocks: LCMV-WE, a virulent virus strain, and LCMV-Armstrong 53B, a nonpathogenic virus strain in primates, are maintained at -80°C as stocks at 10^6 – 10^8 plaque-forming units (pfu)/ml in MEM medium. LCMV stocks can be inoculated at doses of 10^3 – 10^7 pfu by intravenous route or 10^5 – 10^8 pfu by intragastric routes (*see Note 3*).
2. Cannula (gastric tube) and syringe for intragastric (i.g.) gavage: virus in 1–4 ml of MEM is delivered by a 5 ml syringe attached to a flexible plastic cannula (no more than 4 mm diameter) with beveled leading edge. The length of the cannula is the distance from the animal's mouth to the bottom of its rib cage.
3. Alcohol wipes: gauze infused with 70% isopropanol to disinfect the skin and work surfaces.
4. Needles for intravenous (i.v.), intramuscular (i.m.), subcutaneous (s.c.) inoculations. Virus in 0.1–0.2 ml MEM is delivered i.v. by a syringe with a 23–25G needle via the saphenous vein or femoral vein of a NHP. The saphenous vein drains into the larger femoral vein and is sufficiently large to insure rapid delivery and dissemination of an infectious dose.
5. Sharps disposal bin (autoclavable). This is meant to accept used needles and to avoid having the investigator re-sheath the needle tips.

2.3 Tissue Sampling and NHP Hydration

1. Blood collection tubes for serum (~4 ml) or for un-clotted blood (~10 ml tubes containing anticoagulants EDTA, sodium citrate, or heparin) (*see Note 4*).
2. Blood collection tube holder attached to a needle and plastic “butterfly wings” to steady the procedure (e.g., the BD Vacutainer blood collection kits).
3. Biopsy needles to take liver or lymph node tissues before necropsy.
4. Evans blue dye solution: 0.5% dye powder in PBS. This is used to locate lymph nodes or to detect organ hemorrhage.
5. Saline: 9 g of NaCl per liter of water (0.9% NaCl). This is an isotonic solution for hydration of NHP. During sedation and during the course of an infection, macaques may need hydration by saline injection using 50 ml syringes with 20–25G needles.

2.4 Euthanasia and Necropsy

1. Sodium phenobarbital (0.25 ml/kg, by intracardiac injection) for euthanasia.
2. Liquid nitrogen and dry ice for cryopreservation of tissue samples.

3. Paraformaldehyde for embedding and histology of tissue samples.
4. Trizol for extraction of viral RNA from tissue samples.
5. Wire mesh sieves for isolating splenocytes or other dissociated tissue cells.
6. Enzyme cocktails for digesting lung or intestine or liver tissues.
7. A Drexel motor device for grinding, homogenizing, and extracting virus from tissue samples.
8. Bone saw for cutting through the cranium or other bone.
9. Optimal cutting temperature (OCT) tissue-freezing medium is composed of water-soluble glycols and resins for cryostat sectioning of tissues.

3 Methods

3.1 Facilities and NHP

1. Animals housed in BSL-2 facilities can be transferred to A-BSL-3. They should be allowed 2 weeks to acclimatize before infection.
2. On the day of a procedure in A-BSL-3, animal care staff should enter the anteroom and put on PPE.
3. Care staff should then enter the cage room, using squeeze-back cages to safely immobilize and anesthetize macaques.
4. Inoculate the anesthetic i.m. into the fleshy part of the macaque's arm or leg.
5. When the animal looks sleepy, weigh and examine him for disease signs, and after the procedure, return him safely to his cage and observe that he becomes fully awake.
6. All PPE should be removed and put in biohazard waste bags (destined for autoclave decontamination) before leaving the HEPA-filtered rooms.

3.2 Viral Infection

3.2.1 Intravenous Infection

1. To prepare an anesthetized macaque for i.v. inoculation with virus, first, place him faceup on an examination table within the ABSL-3 examination room.
2. Disinfect the groin area using an alcohol wipe.
3. Identify the femoral vein or the adjacent saphenous vein by placing a finger on the groin area to feel a pulse.
4. Using a 1 ml syringe with a 25G needle, inoculate the vein with a dose of virus (usually 10^3 – 10^7 pfu per animal).

3.2.2 Intra-gastric Infection

1. To prepare an anesthetized macaque for i.g. inoculation (gavage) with virus, place him faceup on an examination table within the ABSL-3 examination room.
2. Raise his head and torso with a pillow. Insert the gastric tube (attached to the syringe with virus) gently past the tongue and down the esophagus, never forcing it but withdrawing it and re-advancing when you come upon obstruction. The esophagus is dorsal to the trachea, so direct the tube along the back of the animal.
3. When the tube has gone as far as it will go this way, release the contents, by pushing the syringe plunger. This allows delivery of liquids just above the stomach sphincter which will cause the involuntary valve opening and ingestion of the gavage fluid (*see Note 5*).

3.3 Blood, Tissue Sampling, and Hydration

Samples are collected to study viral dissemination, gene expression and immune responses.

3.3.1 Blood Collection

1. To prepare an anesthetized macaque for blood sampling, first, place it faceup on an examination table within the ABSL-3 examination room (Fig. 3).

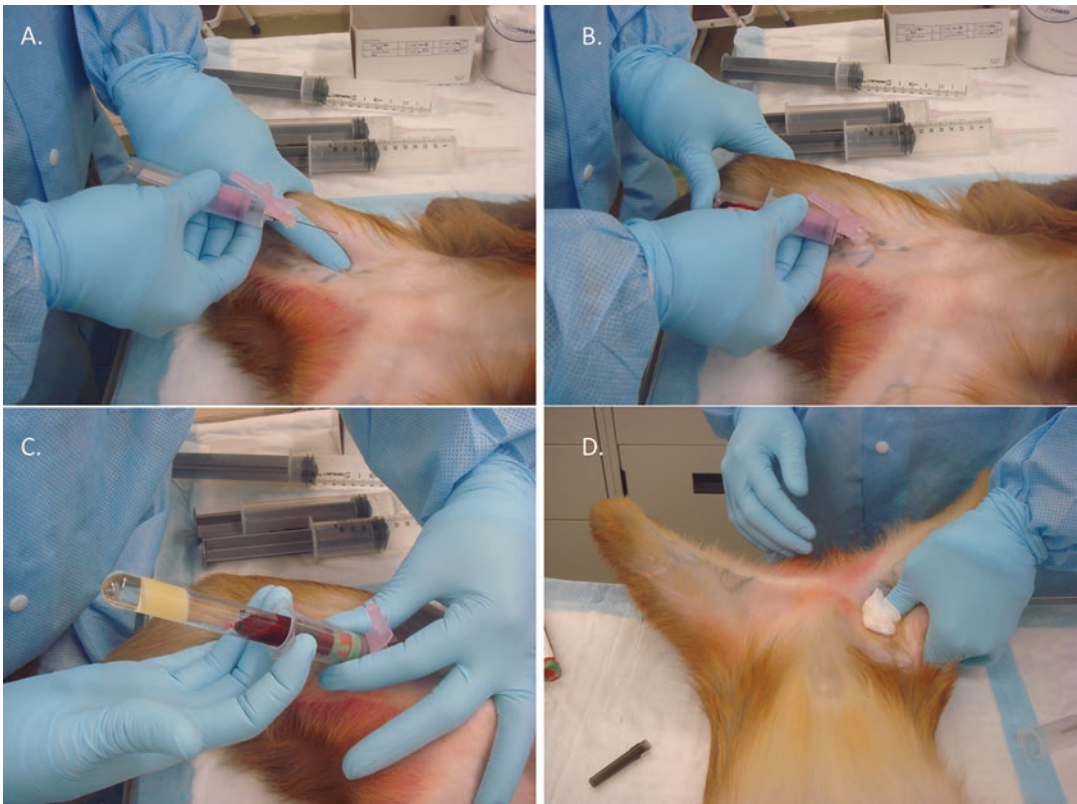


Fig. 3 Taking a blood sample from the saphenous vein. Palpating the vein (a). Injecting the Vacutainer holder (b). Inserting a (green cap in this case) blood collection tube into the holder (c). Applying pressure to the vein after removing the needle (d)

2. Disinfect the groin area using an alcohol wipe.
3. Identify the femoral vein or the adjacent saphenous vein by placing a finger on the groin area to feel a pulse.
4. Using a blood collection tube holder, fit it with a 21G needle plus stabilizing wings, threading the needle onto the holder before unsheathing it.
5. Enter the skin at the distal point of the vein chosen for infusion, with the needle directed proximally along the long axis of the vein.
6. Slowly advance the needle to find and penetrate the vein.
7. Apply vacuum or push the blood collection tube onto the needle of the holder.
8. Withdraw the desired amount of blood (*see Note 6*).
9. If multiple samples are to be collected, remove the tube and place a new tube into the holder.
10. If blood ceases to flow before collections are complete, remove the tube first and then the needle and repeat the procedure from **step 4**. Removing the tube first will avoid damaging the vein due to the vacuum in the tube.
11. Discard needle in a sharps device without re-sheafing it, and use a new tube and a new needle.
12. As each tube is filling, mix the previous tube gently by inversion. Do not shake tubes because that can cause hemolysis.
13. As soon as the last tube is collected and mixed, remove the needle and immediately apply pressure to the puncture site with dry sterile gauze until bleeding stops. Apply pressure for at least 1 min or longer if blood is not coagulating.
14. Label tubes with the animal identification number.
15. After collection, store tubes upright at room temperature until centrifugation. Blood samples should be centrifuged within 2 h of blood collection for best results.

3.3.2 Collecting Tissue Biopsies

1. While the macaque is still under sedation, it can also be subjected to tissue biopsy. As it lies faceup, palpate the tissue to be biopsied (liver is just under the sternum). In the absence of an expert liver doctor, one can be guided by sonogram. An expert can do this accurately and obtain a biopsy within a few seconds without accidentally damaging the gall bladder or surrounding structures (*see Note 7*).
2. Lymph nodes (LN) can be located by injecting Evans blue dye solution near the node, waiting 20 min, and then visualizing an intense blue nodule through the skin, since monocytes take up the dye and congregate in the closest LN.

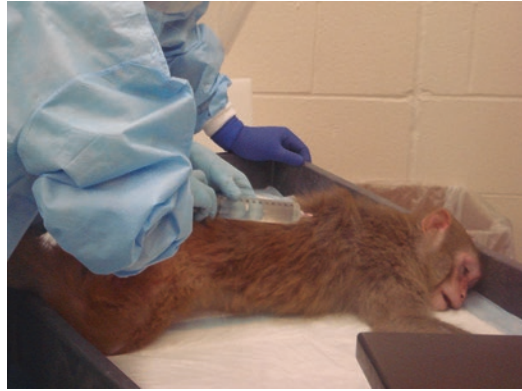


Fig. 4 Fluid replacement to hydrate a dehydrated macaque. The volume of fluid varies with the size of the animal. An anesthetized monkey can be given isotonic saline by subcutaneous injection. Inoculate 5–10 ml of fluid per kg body weight, but no more than 10 ml of fluid in any one injection. Pinch the skin and lift it, and then inject the solution between the skin and the muscle around the scruff of the neck and within folds of skin on the animal's back. This animal is receiving four subcutaneous injections with saline using a 25G needle on a 50 ml syringe

3. Insert the biopsy needle and pull back the plunger to get about 30 mg (about 10^6 cells) of tissue.
4. Eject tissue into paraformaldehyde or OCT if it is to be used for immunohistochemistry or into a chaotropic solution like guanidine isothiocyanate plus phenol if it is to be used for nucleic acid extraction.
5. During the course of infection and during sedation, macaques are subject to dehydration that can be prevented by subcutaneous saline injections using a 50 ml syringe with a 25G needle. (Fig. 4).

3.4 Euthanasia and Necropsy

Procedures should be consistent with the recommendations of the Panel on Euthanasia of a national Veterinary Medical Association and should be reviewed and approved by an institutional Office of Biological Safety.

4 Notes

1. All procedures like inoculation, sampling, and hydration must be done while the NHP is sedated. All procedures must be approved by an Institutional Animal Care and Use Committee (IACUC), and all animal care individuals must be trained and certified yearly (e.g., by a national agency like the US Department of Agriculture).
2. Anesthetic sedation of NHP must be performed by a licensed veterinarian and according to IACUC-recommended doses.

Ketamine alone can be used at doses of 5–15 mg/kg. A mixture of ketamine to xylazine (4:1, w:w) delivered i.m. was found to optimize the duration of anesthesia and recovery time [28]. 15 mg/kg ketamine without xylazine may result in less stressful recoveries. Recommendations for anesthesia can be found online [29].

3. Do not confuse infectious doses with drug doses. In dose-escalation studies, responses to drugs are linear over large ranges, whereas responses to infectious agents are modulated by infectious route, tissue tropism, replication rates in different tissues, the presence of other infectious agents, and the immune response. An inoculum (e.g., dose of 10^3 pfu delivered intravenously in 0.1 ml MEM) must have no more than 300–600 noninfectious virus particles per infectious particle, or it will induce inflammatory responses that will mute or prevent the infection (see references on high-dose immune suppression from the Zinkernagel laboratory [30]).
4. In blood sampling tubes, the type of anticoagulant is determined by the analyses to be performed with each blood sample. The EDTA tube (lavender top) is most frequently used for complete blood counts (CBC) and preferred for performing assays for cell-mediated immunity, to obtain peripheral blood mononuclear cells (PBMC) for culture or to extract nucleic acids. A citrate tube (pale blue top) is used if blood is to be subjected to coagulation studies like determining prothrombin times. Heparin (green top) tubes are used for plasma analyses.
5. Volumes of virus inoculum up to 10–20 ml/kg NHP can be administered by oral gavage.
6. Volumes of blood allowed for withdrawal are on the order of 1% body weight at a time, allowing at least 2 days for recovery (3 days for obviously sick animals). Blood collection can be as much as 10% body weight in a month. The minimum volume of blood that can be processed without significantly affecting the yield of PBMC is approximately 6 ml.
7. The animal care staff must be skilled in palpating the underlying organs in an NHP to do liver biopsy as described [14]. A good source for biopsy needles is Microvasive, Boston Scientific Co. One can use Evans dye to identify lymph nodes to be biopsied.

References

1. Haigwood N, Friedman HS, Van Rompay K, Golos T, Lisdberger S, Kordower J, Goldberg M, Newsome W, Allan AS, Shade R (2016) The critical role of NHP in medical research white paper 8-22-16. pp 1–2
2. Theiler M, Smith HH (1937) The use of yellow fever virus modified by in vitro cultivation for human immunization. *J Exp Med* 65:787–800
3. Onlamoon N, Noisakran S, Hsiao HM, Duncan A, Villinger F, Ansari AA, Perng GC (2010) Dengue virus-induced hemorrhage in a nonhuman primate model. *Blood* 115:1823–1834. doi:10.1182/blood-2009-09-242990

4. Fisher-Hoch SP, Mitchell SW, Sasso DR, Lange JV, Ramsey R, McCormick JB (1987) Physiological and immunologic disturbances associated with shock in a primate model of Lassa fever. *J Infect Dis* 155:465–474
5. Peters CJ, Jahrling PB, Liu CT, Kenyon RH, McKee KT Jr, Barrera Oro JG (1987) Experimental studies of arenaviral hemorrhagic fevers. *Curr Top Microbiol Immunol* 134:5–68
6. Geisbert TW, Strong JE, Feldmann H (2015) Considerations in the use of nonhuman primate models of Ebola virus and Marburg virus infection. *J Infect Dis* 212(Suppl. 2):S91–S97. doi:10.1093/infdis/jiv284
7. Baize S, Marianneau P, Loth P, Reynard S, Journeaux A, Chevallier M, Tordo N, Deubel V, Contamin H (2009) Early and strong immune responses are associated with control of viral replication and recovery in Lassa virus-infected cynomolgus monkeys. *J Virol* 83:5890–5903. doi:10.1128/JVI.01948-08. JVI.01948-08 [pii]
8. Smith DR, Bird BH, Lewis B, Johnston SC, McCarthy S, Keeney A, Botto M, Donnelly G, Shamblyn J, Albarino CG, Nichol ST, Hensley LE (2012) Development of a novel nonhuman primate model for Rift Valley fever. *J Virol* 86:2109–2120. doi:10.1128/JVI.06190-11
9. Samoilovich SR, Calello MA, Laguens RP, Weissenbacher MC (1988) Long-term protection against Argentine hemorrhagic fever in Tacaribe virus infected marmosets: virologic and histopathologic findings. *J Med Virol* 24:229–236
10. Carrion R Jr, Brasky K, Mansfield K, Johnson C, Gonzales M, Ticer A, Lukashevich I, Tardif S, Patterson J (2007) Lassa virus infection in experimentally infected marmosets: liver pathology and immunophenotypic alterations in target tissues. *J Virol* 81:6482–6490. doi:10.1128/JVI.02876-06. JVI.02876-06 [pii]
11. Spengler JR, Estrada-Pena A, Garrison AR, Schmaljohn C, Spiropoulou CF, Bergeron E, Bente DA (2016) A chronological review of experimental infection studies of the role of wild animals and livestock in the maintenance and transmission of Crimean-Congo hemorrhagic fever virus. *Antiviral Res* 135:31–47. doi:10.1016/j.antiviral.2016.09.013
12. Danes L, Benda R, Fuchsova M (1963) Experimental inhalation infection of monkeys of the macacus cynomolgus and macacus rhesus species with the virus of lymphocytic choriomeningitis (we). *Bratisl Lek Listy* 2:71–79
13. Lukashevich IS, Djavani M, Rodas JD, Zapata JC, Osborne A, Emerson C, Mitchen J, Jahrling PB, Salvato MS (2002) Hemorrhagic fever occurs after intravenous, but not after intragastric, inoculation of rhesus macaques with lymphocytic choriomeningitis virus. *J Med Virol* 67:171–186. doi:10.1002/jmv.2206
14. Lukashevich IS, Tikhonov I, Rodas JD, Zapata JC, Yang Y, Djavani M, Salvato MS (2003) Arenavirus-mediated liver pathology: acute lymphocytic choriomeningitis virus infection of rhesus macaques is characterized by high-level interleukin-6 expression and hepatocyte proliferation. *J Virol* 77:1727–1737
15. Lukashevich IS, Rodas JD, Tikhonov II, Zapata JC, Yang Y, Djavani M, Salvato MS (2004) LCMV-mediated hepatitis in rhesus macaques: WE but not ARM strain activates hepatocytes and induces liver regeneration. *Arch Virol* 149:2319–2336. doi:10.1007/s00705-004-0385-9
16. Lukashevich IS, Patterson J, Carrion R, Moshkoff D, Ticer A, Zapata J, Brasky K, Geiger R, Hubbard GB, Bryant J, Salvato MS (2005) A live attenuated vaccine for Lassa fever made by reassortment of Lassa and Mopeia viruses. *J Virol* 79:13934–13942. doi:10.1128/JVI.79.22.13934-13942.2005. 79/22/13934 [pii]
17. Rodas JD, Lukashevich IS, Zapata JC, Cairo C, Tikhonov I, Djavani M, Pauza CD, Salvato MS (2004) Mucosal arenavirus infection of primates can protect them from lethal hemorrhagic fever. *J Med Virol* 72:424–435. doi:10.1002/jmv.20000
18. Fisher-Hoch SP, McCormick JB (1987) Pathophysiology and treatment of Lassa fever. *Curr Top Microbiol Immunol* 134:231–239
19. Fisher-Hoch SP (1993) Arenavirus pathophysiology. Plenum Press, New York
20. McCormick JB, King IJ, Webb PA, Scribner CL, Craven RB, Johnson KM, Elliott LH, Belmont-Williams R (1986) Lassa fever. Effective therapy with ribavirin. *N Engl J Med* 314:20–26. doi:10.1056/NEJM198601023140104
21. McCormick JB, Walker DH, King IJ, Webb PA, Elliott LH, Whitfield SG, Johnson KM (1986) Lassa virus hepatitis: a study of fatal Lassa fever in humans. *Am J Trop Med Hyg* 35:401–407
22. Djavani MM, Crasta OR, Zapata JC, Fei Z, Folkerts O, Sobral B, Swindells M, Bryant J, Davis H, Pauza CD, Lukashevich IS, Hammamieh R, Jett M, Salvato MS (2007) Early blood profiles of virus infection in a monkey model for Lassa fever. *J Virol* 81:7960–7973. doi:10.1128/JVI.00536-07. JVI.00536-07 [pii]
23. Caballero IS, Yen JY, Hensley LE, Honko AN, Goff AJ, Connor JH (2014) Lassa and Marburg viruses elicit distinct host transcriptional responses

- early after infection. *BMC Genomics* 15:960. doi:[10.1186/1471-2164-15-960](https://doi.org/10.1186/1471-2164-15-960)
24. Zapata JC, Salvato MS (2015) Genomic profiling of host responses to Lassa virus: therapeutic potential from primate to man. *Future Virol* 10:233–256. doi:[10.2217/fvl.15.1](https://doi.org/10.2217/fvl.15.1)
 25. Bausch DG, Sesay SS, Oshin B (2004) On the front lines of Lassa fever. *Emerg Infect Dis* 10:1889–1890. doi:[10.3201/eid1010.IM1010](https://doi.org/10.3201/eid1010.IM1010)
 26. Ter Meulen J, Lukashevich I, Sidibe K, Inapogui A, Marx M, Dorlemann A, Yansane ML, Koulemou K, Chang-Claude J, Schmitz H (1996) Hunting of peridomestic rodents and consumption of their meat as possible risk factors for rodent-to-human transmission of Lassa virus in the Republic of Guinea. *Am J Trop Med Hyg* 55:661–666
 27. Malhotra S, Yen JY, Honko AN, Garamszegi S, Caballero IS, Johnson JC, Mucker EM, Trefry JC, Hensley LE, Connor JH (2013) Transcriptional profiling of the circulating immune response to Lassa virus in an aerosol model of exposure. *PLoS Negl Trop Dis* 7:e2171. doi:[10.1371/journal.pntd.0002171](https://doi.org/10.1371/journal.pntd.0002171)
 28. Naccarato EF, Hunter WS (1979) Anaesthetic effects of various ratios of ketamine and xylazine in rhesus monkeys (*Macaca mulatta*). *Lab Anim* 13:317–319
 29. <http://medschool.umaryland.edu/IACUC/guidelines.asp>. Observed 23 Oct 2016
 30. Althage A, Odermatt B, Moskophidis D, Kundig T, Hoffman-Rohrer U, Hengartner H, Zinkernagel RM (1992) Immunosuppression by lymphocytic choriomeningitis virus infection: competent effector T and B cells but impaired antigen presentation. *Eur J Immunol* 22:1803–1812. doi:[10.1002/eji.1830220720](https://doi.org/10.1002/eji.1830220720)

A Primary Human Liver Cell Culture Model for Hemorrhagic Fever Viruses

Mahmoud Djavani

Abstract

Viral hemorrhagic fevers affect liver functions such as important metabolic processes and the replacement of new blood cells, coagulation factors, and growth factors. Typically, multi-organ diseases such as viral hemorrhagic fevers are studied in an organism, but it is also possible to derive information about the molecular events involved in disease processes by focusing on liver cell culture. Here we describe a multi-cell culture system that is capable of replicating the arenavirus LCMV-WE, a virus that can cause hemorrhagic fever in primates, as a model for liver infection by a hemorrhagic fever virus.

Key words Human liver, Stem cells, Culture, LCMV-WE, Lassa model

1 Introduction

Arenaviruses such as Lassa fever virus (LASV) and virulent lymphocytic choriomeningitis virus WE strain (LCMV-WE) can cause severe viral hemorrhagic fever (VHF) in nonhuman primates and in human beings. Arenaviral hemorrhagic fever viruses cause multiple organ failure and have a major effect on the liver. Like LASV, virulent LCMV-WE targets the liver in experimental animals and replicates efficiently both in vivo and in vitro cell culture systems [1–4].

The human liver is composed of mainly parenchymal cells (hepatocytes), which constitute 80% of the cell population of the liver. Sinusoidal endothelial cells, perisinusoidal macrophages (Kupffer cells), liver-specific natural killer cells (pit cells), and stellate (Ito) cells represent the non-parenchymal cells [5]. Near the hepatic portal space, bile canaliculi transform into the canal of Hering, which is lined by both hepatocytes and cholangiocytes. The canal of Hering is thought to serve as a reservoir of liver progenitor cells [5, 6]. The epithelial cells of the canal are oval in shape, called “oval cells,” and can differentiate into both hepatocytes and cholangiocytes [6]. Several studies described the role of

cultured oval/epithelial cells as progenitors of hepatocytes and/or bile duct cells [7–11].

Liver stem/progenitor cells or hepatic progenitor cells in humans emerge when hepatocyte proliferation is overwhelmed by severe liver injury [12]. These cells can be activated to proliferate after viral infection or hepatic injury. Hepatic stem/progenitor cells can be isolated from fetal, neonatal, pediatric, and adult human livers with identical characteristics as described [13, 14]. An overview about human hepatic progenitors that have been isolated and characterized is given in Table 1.

The use of a purified population of freshly isolated liver precursor cells may be preferable for cell maturation studies. The whole liver cell population can be prepared by mechanical or enzymatic methods. To date, a two-step collagenase perfusion protocol is the most robust procedure that can be used for isolation of hepatocytes with high viability [19–21]. The donated human liver pieces used in this study were from federally (USA) designated organ procurement organizations. Liver cells were isolated from intact donor livers by using the two-step collagenase perfusion protocol. Subsequently, the liver cells were further separated into mature human hepatocytes and immunoselected into small immature hepatocytes, non-parenchymal cells, and human hepatic stem/progenitor cells (hHSPCs) [21].

In our studies, we investigated the effect of virus infection on maturation of liver stem/progenitor cells in order to identify an

Table 1
An overview of isolated and characterized adult human hepatic progenitors cells

Term used by authors	Phenotype	Isolation method	References
Human liver stem cells (HLSCs)	Positive Albumin, AFP, CD29, CD44, CD73, CD90, vimentin, nestin	Negative CD34, CD45, CD117, CD133, CK19	Culture Herrera et al. 2006 [15]
Human liver stem/progenitor cells (HLSCs)	Positive CD13, CD29, CD44, CD90, CD73, HLA-class I	Negative CD34, CD45, CD105, CD117, CD133, HLA-DR	Culture Najimi et al. 2007 [16] Khuu et al. 2011 [17]
Human hepatic stem/progenitor cells (hHpSCs)	Positive EpCAM, NCAM, CK19	Negative AFP	Culture Livers of all donor ages Zhang et al. 2008 [18]

Abbreviations: *AFP* a-fetoprotein, *CD* cluster of differentiation, *CK* cytokeratin, *HLSC* human liver stem cell, *NCAM* neural cell adhesion molecule, *EpCAM* epithelial cell adhesion molecule

effective method to induce maturation of hHSPCs in culture. A hormonally defined medium (HDM) was used to differentiate hHSPCs to hepatocytes at different times of LCMV infection (Fig. 1). Freshly isolated human cell populations and hepatic cell lines, HepG2 cells (Fig. 2), were cultured and infected with LCMV-WE for the times indicated. The highest virus yield in hHSPCs was obtained at 72 h after infection, whereas the highest virus yield in HepG2 cells was obtained at 48 h after infection (data not shown). At 72 h after infection, the hHSPCs had a differentiated morphology similar to that of uninfected hepatocytes (Fig. 1i). Cell growth rates (not shown) and hHSPCs maturations slowed

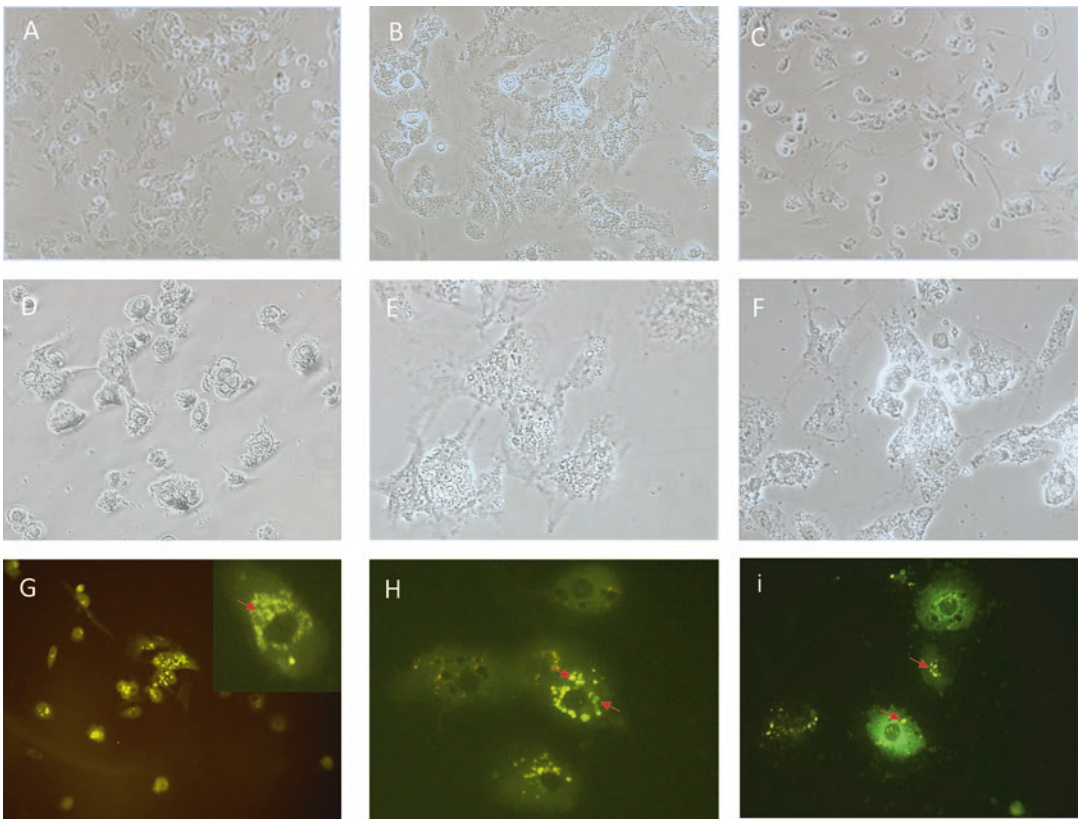


Fig. 1 Isolation and maturation of human hepatic stem/progenitor cells (hHSPCs) into hepatocytes. (a) Whole liver cell population [LV-1], (b) mature human hepatocytes [LV2], and (c) hHSPCs [LV-3] were cultured in a hormonally defined medium containing 0.2% AlbuMax (representative images (a–c) and (d–f) are shown at $\times 200$ and $\times 400$ magnification, respectively). For assessment of hHSPC maturation to hepatocytes, cells were grown on coverslips and infected with LCMV-WE at an MOI of 1 PFU per cell for various time points, stained with anti-LCMV antibody and examined by immunofluorescence microscopy. Representative images at 72 h after infection are displayed. Immunofluorescence images of LCMV-WE-infected (g) whole human liver cells, magnification $\times 200$ with an inset shown at 1000 magnification, and (h) mature hepatocytes and (i) human liver stem/progenitor cells are shown at 1000 magnification. Cell growth rates (*not shown*) slowed down upon infection by LCMV-WE, and yet their cultures were morphologically indistinguishable when compared to uninfected control cells (a–f)

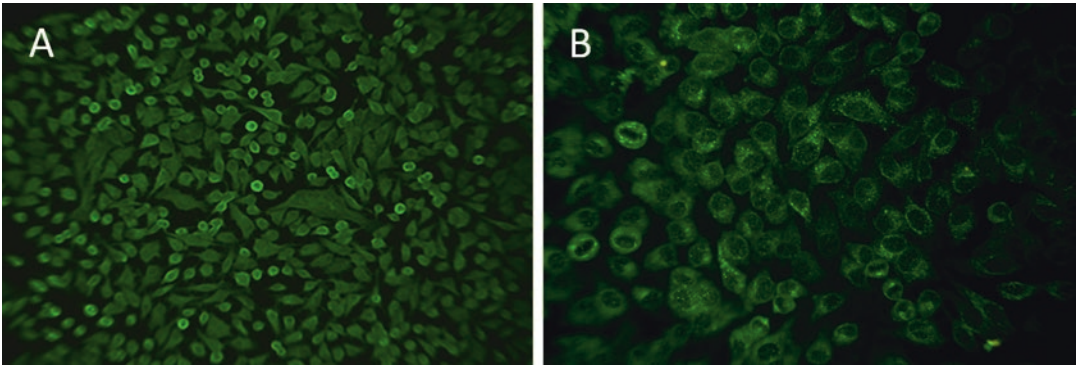


Fig. 2 Immunofluorescence images of HepG2 cells infected with LCMV-WE. HepG2 cells were grown on coverslips and infected with LCMV as described in Subheadings 2 and 3. Infected HepG2 cells served as positive control (**a** and **b** are representative images at $\times 200$ and $\times 400$ magnification, respectively)

down upon infection by LCMV-WE, and yet their cultures were morphologically indistinguishable when compared to uninfected control cells (Fig. 1a–f). We report here the LCMV infected hHSPCs were able to differentiate into hepatocytes in vitro at a significantly slower rate than uninfected cells. The study of virus infection on hHSPCs maturation will open new perspective on disease mechanisms in VHF-infected livers.

We describe here the isolation, maturation, and infection of human liver stem/progenitor cells from liver tissue. Some of these are able to differentiate into hepatocytes after virus infection, but in general, arenavirus infection slows down the process of normal maturation.

2 Materials

2.1 Isolating Liver Stem Cells

1. Fresh human livers were obtained from federally designated organ procurement organizations.
2. *Perfusion buffers Solution 1*: 154 mM sodium chloride, 20 mM HEPES, 5.6 mM potassium chloride, 5 mM glucose, 25 mM sodium hydrogen carbonate. *Solution 2*: 10 mL of 100 mM EGTA to 990 mL of Solution 1. *Solution 3*: Add 10 mL of 0.5 M calcium chloride dihydrate to 990 mL of Solution 1.
3. Liberase TL Research Grade (Roche) contains highly purified collagenase I and collagenase II.
4. Collagenase buffer: Add 10 U/mL collagenase (Liberase) per gram of the liver to Solution 3.
5. Isolation buffer: 120 mM sodium chloride, 10 mM HEPES, 0.9 mM calcium chloride dihydrate, 6.2 mM potassium chloride, 0.1% (w/v) albumin.

6. Hanks' calcium- and magnesium-free buffer: 53 mM potassium chloride, 4.4 mM potassium phosphate monobasic, 1379 mM sodium chloride, 3.4 mM sodium phosphate dibasic, 56 mM D-glucose or dextrose.
7. Phosphate-buffered saline stock (10× PBS): 10.6 mM potassium phosphate, 1551.7 mM sodium chloride, 29.7 mM sodium phosphate, pH 7.4.
8. Antihuman red blood cell antibodies (1:5000 dilution).
9. Peristaltic pump and tubing, forceps, scalpel, conical flasks, Buchner funnel, crystallizing dish, nylon meshes 70 μm and 210 μm, microvascular clamps, refrigerated centrifuges, water baths.
10. Tools to tease tissues to free the cells and 1000, 500, and 150 μm pore filters to filter whole cells from debris.
11. Stock isotonic Percoll solution: Percoll density gradients are used to isolate healthy or infected liver cells. Percoll® is colloidal silica coated with polyvinylpyrrolidone (PVP). Isotonic Percoll is made by mixing nine volumes of Percoll® with one volume 10× phosphate-buffered saline, resulting in a final Percoll concentration of 90% at pH 7.4. Keep the Percoll solution at 4 °C.
12. Magnetic cell selection can be carried out using the CliniMACS apparatus (Miltenyi Biotec). For example, magnetic beads selecting EpCAM (Miltenyi), a cell-surface marker for immature epithelial cells, are employed.
13. Several types of centrifuge tubes, storage tubes, or culture dishes: 2 mL sterile cryogenic storage vials; 1.5 mL tubes; 10 and 50 mL conical tubes; 500 mL bottles; 1 L bottles; sterile Pasteur pipettes.

2.2 Liver Cell Culture

1. 6-well plates with covers.
2. 100× SPITE medium hormonal supplement (Gibco): 2.5 g/mL bovine insulin, 2.5 g/mL human transferrin, 2.5 ng/mL sodium selenite, 55 mM 2-mercaptoethanol, 10,000 U/mL penicillin, 10,000 g/mL streptomycin, 50 g/mL gentamycin, 600 mg/L niacinamide as described [21].
3. Liver Cell Culture Medium (a hormonally defined medium, HDM): RPMI 1640 plus 2 mM glutamate, 0.2% AlbuMax-I (a replacement for serum supplementation, Gibco), and the medium is made 1× in SPITE medium.
4. Minimal essential medium (MEM) was supplemented with 100 U/mL penicillin/streptomycin (pen/strep), 2 mM glutamine, and 10% heat-inactivated fetal bovine serum (FBS).
5. Liver suspension wash buffer (PBS-EDTA buffer): Phosphate-buffered saline (PBS) containing 5 mM EDTA and 0.5% bovine serum albumin. Make it fresh.

6. Coverslips coated with collagen type I.
7. Cold storage medium: Minimum essential medium (MEM) containing 10 µg/mL bovine insulin, 0.1% bovine serum albumin (BSA), 10% fetal calf serum (FCS), 10 IU penicillin/mL, and 50 µg streptomycin/mL. pH is adjusted to 7.4. Isolated hepatocytes are stored at 4 °C in this prior to immunoselection.
8. Cryopreservation medium: Dulbecco's modified Eagle's medium (DMEM) supplemented with 70% FCS and 10% dimethyl sulfoxide (DMSO). Cold DMSO should be added when cells are at 4 °C.

2.3 Cell Lines and Virus Stocks

1. LCMV-ARM (Armstrong 53b strain) and LCMV-WE were plaque purified and stored at 1×10^8 and 2×10^7 plaque-forming units (PFU)/mL, respectively.
2. T25 and T75 tissue culture flasks.
3. Dulbecco's modified Eagle's medium (DMEM) is supplemented with 10% FBS, 100 U/mL penicillin/streptomycin (pen/strep), and 2 mM L-glutamine.
4. Baby hamster kidney (BHK) cells can be propagated in DMEM supplemented with FBS, pen/strep, and glutamine.
5. Virus plaque assays use serum-free Eagle's minimal essential medium (EMEM).
6. Vero E6 cells are cultivated in supplemented DMEM.
7. Normal human primary hepatocytes (hNHep cells, Clonetics) can be maintained in Hepatocyte Maintenance Medium (HMM™).
8. The HepG2 liver cell line (ATCC) is best maintained in EMEM supplemented with 10% FCS, 100 U/mL pen/strep, 0.45% glucose, and 2 mM L-glutamine.

2.4 Supplies for Analyzing Results

1. Microscopy reagents. Sterilized coverslips, fine tweezers. 1× PBS buffer, Wash buffer: 0.1% BSA in 1× PBS, primary antibodies, fluorochrome-labeled secondary antibody, antibody controls. Blocking buffer: 10% normal donkey serum, 0.3% Triton® X-100. DAPI (4',6-diamidino-2-phenylindole) solution (*see Note 1*).

Dilution buffer: 1× PBS, 1% bovine serum albumin (BSA), 1% normal donkey serum, 0.3% Triton X-100, and 0.01% sodium azide. Anti-fade mounting medium. Paraformaldehyde-methanol fixation solution. 95% and 100% ethanol.

2. Flow cytometry. FACS tubes (5 mL round-bottom polystyrene tubes), pipette tips and pipettes, centrifuge, vortexer. Monoclonal antibody directly conjugated with fluorescein (FITC) or phycoerythrin (PE). Fixative solution: 2% paraformaldehyde in PBS for 10 min at room temperature.

Permeabilization/blocking buffer (2% Triton X-100, 10% goat serum, and 2% teleostean fish gel in PBS), fluorescent-labeled secondary antibody. Isotype control antibodies.

3 Methods

3.1 Isolation of Total Cell Population from Fresh Human Liver

Human hepatocyte isolation was performed using a two-step collagenase perfusion procedure as previously described [20].

1. A 15 g piece of the liver, which has intact Glisson's capsule on all surfaces except for one cut surface, was used for perfusion.
2. All buffers were warmed up to 37 °C during perfusion in a water bath.
3. Perfusion was set up with a peristaltic pump at flow rate between 110 and 460 mL/min. The perfusion system should be primed with Solution 1.
4. The organ was placed on a Buchner funnel, and the portal vein and/or the hepatic artery were cannulated and washed with Hanks' calcium- and magnesium-free buffer for 5 min to flush out blood in the liver piece.
5. After the liver was free of blood, the liver was perfused twice with glucose and EGTA-containing solution buffer 2 for 10 min.
6. Switch the perfusion fluid to Solution 3 and perfuse with 0.5 L.
7. Change the perfusion fluid to collagenase buffer.
8. Allow collagenase digestion for 15 min. A perfusion rate of 40 mL/min per cannula and temperature at 37 °C were maintained during the entire procedure. After the perfusion was terminated, the liver tissue appeared to break apart and soften.
9. Turn off the peristaltic pump and place the liver piece in a crystallizing dish containing 100–200 mL of isolation buffer.
10. Serrate the Glisson's capsule and separate the cells mechanically from the vascular tree, and add more isolation buffer as needed during process.
11. Add more isolation buffer up to a final volume of 500 mL.
12. Eliminate red blood cells from pellets of parenchymal cells by low-speed centrifugation or by treating suspensions with anti-human red blood cell antibodies (1:5000 dilution; Rockland) for 15 min.
13. Pass the resulting cell suspension through filters of pore size 1000 µm, 500 µm, and 150 µm and collect cells. Pour the cell suspension into 200 mL centrifuge tubes.

14. Centrifuge the cell suspension at $50 \times g$ for 5 min at 4°C . Aspirate supernatant and gently resuspend cell pellet in 200 mL of the isolation buffer.
15. Repeat the washing **steps 13** and **14** three times. Resuspend cells in cold storage medium.
16. Fractionate live cells from dead cells and debris using density gradient centrifugation at $500 \times g$ for 15 min at room temperature. Collect the resulting hepatic cell band at the interface.
17. Estimate cell viability by trypan blue exclusion assay.
18. Alternatively to **step 16**, cells could be isolated on Percoll density gradients as follows: Three volumes of hepatic cell suspension (cell concentration not to exceed 5×10^6 cell/mL) is mixed with one volume cold isotonic Percoll, resulting in a final Percoll concentration of 40% [4 part 100% percoll + 6 parts cell suspension].
19. This mixture is then placed into a conical centrifuge bottle and centrifuged at $50 \times g$ for 5 min at 4°C . [After this step, viable hepatocytes are at the bottom of the tubes.]
20. Wash cells two times with wash solution and centrifuge at $50 \times g$ for 5 min at 4°C .
21. The supernatant and pellet are collected separately. The pelleted cells are typically used for subsequent studies. The hepatic stem/progenitor cells are isolated far more efficiently by immunoselection technologies.
22. Cells which do not pellet from the Percoll gradient, in the collected supernatant, are diluted fivefold with ice-cold RPMI 1640 without phenol red, placed into conical centrifuge bottles, and centrifuged at $300 \times g$ for 5 min at 4°C . These are small, low-density cells.
23. Assess cell viability by trypan blue exclusion. The purity of isolated liver cells was consistently $>90\%$ as determined by positively staining for albumin content and morphology. The yield of isolated hepatocytes could be around 12×10^6 cells per gram of the liver.

3.2 Isolation of Human Hepatic Stem/Progenitor Cells (hHSPCs)

Liver cell suspensions are prepared as in Subheading 3.1 and further immunoselected into small immature hepatocytes, non-parenchymal cells, and human hepatic stem/progenitor cells (hHSPCs) using magnetic beads conjugated with antibodies to cell-surface antigens. Cells obtained in this way are highly viable and expand well in culture.

1. Size- and density-selected cells are washed once with cold PBS-EDTA buffer at 4°C .

Table 2
Cell-surface receptor and cell markers for human liver cells

Cell type	Antigen	Antibody
Hepatocellular progenitor/ stem cells	Epithelial cell adhesion molecule (EpCAM)	Antihuman CD326 [Biocompare]
Differentiated cells	Albumin	Antihuman albumin [Dakoppats, DK]
	CK19	Antihuman CK19 [Bio-Rad, USA]
Liver Kupffer cells	CD68	Antihuman CD68 [Dako, USA]
Parenchymal cell markers	Albumin, AFP, EpCAM, CK19, CK8, CK18	

Abbreviations: *AFP* a-fetoprotein, *CD* cluster of differentiation, *CK* cytokeratin, *EpCAM* epithelial cell adhesion molecule

2. Resuspend 2×10^7 cells in 200 μL cold RPMI medium without phenol red containing 2% FBS, and add sample into 5 mL polystyrene round-bottom tube (*see Note 2*).
3. Add 100 μL of monoclonal antibody in PBS, mix, and incubate on ice for 20 min (*see Table 2*).
4. Mix magnetic microbeads and add 50 μL microbeads/mL of sample, pipette up and down five times, and incubate on ice for 15 min.
5. Add cold medium to bring the sample up to 2.5 mL, and mix it twice.
6. Incubate the bead and cell suspension at room temperature for 15 min (*see Note 3*).
7. Wash cells with PBS-EDTA buffer and then attach to the CliniMACS Tubing Set for magnetic cell selection.
8. Invert the magnet and tube, and pour off the supernatant. The tube contains the isolated cells. Resuspend cells in cold storage medium.
9. All manipulations should be performed in a laminar flow hood under sterile conditions.
10. Liver cells are now separated into three different cell populations and labeled as follows: [LV1] is the whole liver cell population as prepared above, [LV2] is mature human hepatocytes, and [LV3] is a mixture of small immature hepatocytes, non-parenchymal cells, and hepatic stem/progenitor cells (HSPCs).
11. Cryopreservation procedure: Resuspend each of the isolated cell populations in cryopreservation medium in cryovials and quickly place them into a $-80\text{ }^\circ\text{C}$ freezer. After 1 day, the fro-

zen tubes should be transferred to a liquid nitrogen tank for storage.

3.3 Liver Cell Culture

1. Suspend each isolated cell population in Liver Cell Culture Medium, and plate them out at 3×10^5 cells per well on collagen-coated 6-well plates (or on collagen-coated glass coverslips) for 2–3 h at 37 °C in a humidified atmosphere of 5% CO₂ to ensure hepatocyte adherence to plates.
2. Wash once to remove dead cells and add fresh Liver Cell Culture Medium.
3. Maintain hepatocytes in this medium for 24 h prior to virus infection.
4. As controls, plate hNHep cells in HMM, and HepG2 cells in MEM on glass coverslips and at 37 °C in a humidified atmosphere of 5% CO₂.
5. Once cells have adhered, initiate virus infection of cultures.

3.4 Virus Titration

1. Isolates of the arenaviruses LCMV-ARM and LCMV-WE are titrated by plaque assays on Vero E6 cells as described previously [22].
2. To assess virus production in hepatic cells, and effect of virus on hHSPCs maturation, cells are plated at 2×10^5 /well in 6-well plates, with coverslips on the bottom, for 24 h at 37 °C, and then are infected with virus at a multiplicity of infection (MOI) of 1 PFU per cell.
3. At various times, collect the culture medium and spin at low speed to remove cell debris. The supernatants are serially diluted, and virus titers are determined by a plaque assay on Vero E6 cells and are expressed as PFU/mL of supernatant.

3.5 Analyzing Results by Microscopy and Flow Cytometry

1. For microscopy, fix cells on coverslips in 4% paraformaldehyde for 10–20 min at room temperature. Rinse briefly with PBS. Permeabilize with cooled methanol for 5–10 min at –20 °C.
2. Incubate cells with antibody to cell-surface marker for 30 min at room temperature, and then rinse twice in Tris buffer. Then incubate with secondary antibody for fluorescence. As controls use antibody of the same isotype as the first but not expecting to bind to the target cells.
3. Examine samples by a light microscope.
4. For flow cytometry, wash the cells twice in PBS buffer without calcium and magnesium, and then stain cells with FITC alone or with fluorescein-conjugated monoclonal antibodies.

4 Notes

1. For microscopy it is useful to identify nuclei using 4',6-diamidino-2-phenylindole (DAPI) solution: Add 1 μ L of 14.3 mM DAPI stock for every 5 mL of PBS. Store any unused DAPI at 2–8 °C, wrapped in aluminum foil.
2. To minimize cell clumping, use cold buffers and keep cells on ice as much as possible. If sample begins to clump, add DNase 1 solution at 1 mg/mL.
3. Cells expressing EpCAM (CD326) from human liver cell suspensions are pulled out of suspension using the monoclonal antibody HEA-125 coupled to magnetic microbeads and are separated using a miniMACS, a MidiMACS, an AutoMACS, or a CliniMACS magnetic column separation system from Miltenyi Biotec, following the manufacturer's recommended procedures.

References

1. Carrion R, Brasky K, Mansfield K, Johnson C, Gonzales M et al (2007) Lassa virus infection in experimentally infected marmosets: liver pathology and immunophenotypic alterations in target tissues. *J Virol* 81(12):6482–6490. doi:10.1128/JVI.02876-06
2. Lukashovich IS, Rodas JD, Tikhonov II, Zapata JC, Yang Y, Djavani M, Salvato MS (2003) LCMV-mediated hepatitis in rhesus macaques: WE but not ARM strain activates hepatocytes and induces liver regeneration. *Arch Virol* 149(12):2319–2336
3. Djavani M, Topisirovic I, Zapata JC, Sadowska M, Yang Y, Rodas J et al (2005) The proline-rich homeodomain (PRH/HEX) protein is down-regulated in liver during infection with lymphocytic choriomeningitis virus. *J Virol* 79:2461–2473
4. Djavani M, Crasta OR, Zhang Y, Zapata JC, Sobral B, Lechner MG, Bryant J, Davis H, Salvato MS (2009) Gene expression in primate liver during viral hemorrhagic fever. *Virology* 393(1):6–20. doi:10.1016/j.virus.2009.06.020
5. Esrefoglu M (2013) Role of stem cells in repair of liver injury: experimental and clinical benefit of transferred stem cells on liver failure. *World J Gastroenterol* 19(40):6757–6773. doi:10.3748/wjg.v19.i40.6757. Available from <http://www.wjgnet.com/1007-9327/full/v19/i40/6757.htm>
6. Roskams TA, Theise ND, Balabaud C, Bhagat G, Bhathal PS, Bioulac-Sage P et al (2004) Nomenclature of the finer branches of the biliary tree: canals, ductules, and ductular reactions in human livers. *Hepatology* 39:1739–1745
7. Roskams T, DeVos R, VanEyken P, Myazaki H, VanDamme B, Desmet V (1998) Hepatic OV-6 expression in human liver disease and rat experiments: evidence for hepatic progenitor cells in man. *J Hepatol* 29:455–463
8. Baumann U, Crosby HA, Ramani P, Kelly DA, Strain AJ (1999) Expression of the stem cell factor receptor c-kit in normal and diseased pediatric liver: identification of a human hepatic progenitor cell? *Hepatology* 30:112–117
9. Petersen BE, Goff JP, Greenberger JS, Michalopoulos GK (1998) Hepatic Oval Cells Express the Hematopoietic Stem Cell Marker Thy-1 in the Rat. *Hepatology* 27:433–445
10. Fausto N, Campbell JS (2003) The role of hepatocytes and oval cells in liver regeneration and repopulation. *Mech Dev* 120(1):117–130. doi:10.1016/S0925-4773(02)00338-6
11. Kuwahara R, Kofman AV, Landis CS, Swenson ES, Barendsward E, Theise ND (2008) The hepatic stem cell niche: identification by label-retaining cell assay. *Hepatology* 47(6):1994–2002
12. De Vos R, Desmet V (1992) Ultrastructural characteristics of novel epithelial cell types identified in human pathologic liver specimens with chronic ductular reaction. *Am J Pathol* 140(6):1441–1450

13. Schmelzer E, Wauthier E, Reid LM (2006) The phenotypes of pluripotent human hepatic progenitors. *Stem Cells* 24(8):1852–1858
14. Schmelzer E, Zhang L, Bruce A et al (2007) Human hepatic stem cells from fetal and post-natal donors. *J Exp Med* 204(8):1973–1987. doi:[10.1084/jem.20061603](https://doi.org/10.1084/jem.20061603)
15. Herrera MB, Bruno S, Buttiglieri S et al (2006) Isolation and characterization of a stem cell population from adult human liver. *Stem Cells* 24:2840–2850
16. Najimi M, Khuu DN, Lysy PA, Jazouli N, Abarca J, Sempoux C et al (2007) Adult-derived human liver mesenchymal-like cells as a potential progenitor reservoir of hepatocytes? *Cell Transplant* 16(7):717–728
17. Khuu DN, Scheers I, Ehnert S, Jazouli N, Nyabi O, Buc-Calderon P et al (2011) In vitro differentiated adult human liver progenitor cells display mature hepatic metabolic functions: a potential tool for in vitro pharmacotoxicological testing. *Cell Transplant* 20(2):287–302
18. Zhang L, Theise N, Chua M, Reid LM (2008) The stem cell niche of human livers: symmetry between development and regeneration. *Hepatology* 48:1598–1607. doi:[10.1002/hep.22516](https://doi.org/10.1002/hep.22516)
19. Seglen PO (1976) Preparation of isolated rat liver cells: the enzymatic preparation of isolated intact parenchymal cells from rat liver. *Methods Cell Biol* 13:29–83
20. Lee SML, Schelcher C, Demmel M, Hauner M, Thasler WE (2013) Isolation of human hepatocytes by a two-step collagenase perfusion procedure. *J Vis Exp* 79:e50615. doi:[10.3791/50615](https://doi.org/10.3791/50615)
21. Kubota H, Reid LM (2000) Clonogenic hepatoblasts, common precursors for hepatocytic and biliary lineages, are lacking classical major histocompatibility complex class I antigen. *Proc Natl Acad Sci U S A* 97:12132–12137
22. Doyle MV, Oldstone MBA (1987) Interactions between viruses and lymphocytes. I. In vivo replication of lymphocytic choriomeningitis virus in mononuclear cells during both chronic and acute viral infections. *J Immunol* 121:1262–1269

Part IV

Immune Assays and Vaccine Production for Hemorrhagic Fever Viruses

Protocol for the Production of a Vaccine Against Argentinian Hemorrhagic Fever

Ana María Ambrosio, Mauricio Andrés Mariani, Andrea Soledad Maiza, Graciela Susana Gamboa, Sebastián Edgardo Fossa, and Alejandro Javier Bottale

Abstract

Argentinian hemorrhagic fever (AHF) is a febrile, acute disease caused by Junín virus (JUNV), a member of the *Arenaviridae*. Different approaches to obtain an effective antigen to prevent AHF using complete live or inactivated virus, as well as molecular constructs, have reached diverse development stages. This chapter refers to JUNV live attenuated vaccine strain Candid #1, currently used in Argentina to prevent AHF. A general standardized protocol used at Instituto Nacional de Enfermedades Virales Humanas (Pergamino, Pcia. Buenos Aires, Argentina) to manufacture the tissue culture derived Candid #1 vaccine is described. Intermediate stages like viral seeds and cell culture bank management, bulk vaccine manufacture, and finished product processing are also separately presented in terms of Production and Quality Control/Quality Assurance requirements, under the Administracion Nacional de Medicamentos, Alimentos y Tecnología Medica (ANMAT), the Argentine national regulatory authority.

Key words Argentinian hemorrhagic fever, Junin virus, *Arenaviridae*, Attenuated viral vaccines, Arenavirus vaccines

1 Introduction

Argentinian hemorrhagic fever (AHF) is a febrile, acute disease caused by Junín virus (JUNV), a member of the *Arenaviridae*. First described by Arribalzaga in 1955 [1], this disease has been the focus of extensive research, the results of which greatly contributed to our actual knowledge of arenaviruses and the diseases they cause [2–7]. The historic progressive expansion of the AHF endemic area and the growing number of people exposed to this severe disease, led to the consensus that immunization of the at-risk population would be a feasible way to control the epidemics [8].

Different approaches to obtain an effective antigen to prevent AHF using live or inactivated virus, as well as molecular constructs, have reached diverse stages of development [9, 10]. This chapter

will refer to JUNV live-attenuated vaccine strain Candid #1, currently used in Argentina to prevent AHF. This vaccine was developed through a joint international effort that envisioned it as an orphan drug [11, 12]. With transferred technology, the Argentine government committed itself to be the Candid #1 (C#1) manufacturer and to register this vaccine as a novel medical product under the Argentine Regulatory Authority [13–15]. For this purpose, Master and Working Viral Seeds of C#1 (received in Argentina as originally established by international cooperation) were used to set up the manufacturing process in Argentina. This chapter describes the standardized protocol, used since 2003, at Instituto Nacional de Enfermedades Virales Humanas (Pergamino, Pcia. Buenos Aires, Argentina) to manufacture Candid #1 vaccine to prevent AHF. Before starting the manufacturing process it was mandatory to establish facilities, installations, and materials under a Good Manufacturing Practice (GMP) system [16–18] (*see Note 1*).

2 Materials

1. *Physical plant*: Four independent biosafety level 2–3 units (a specific pathogen-free breeding mouse colony, tissue culture banking area, vaccine production, and vaccine quality control/quality assurance areas) are contained in a 3267 square meter plant. The four units have independent ventilation systems and restricted unidirectional circulation for operators, materials, and waste. Figure 1 shows an external view of the facility inspected and approved by ANMAT, the Argentine



Fig. 1 Front view of the plant dedicated to manufacture of Candid #1 vaccine

regulatory authority, as a plant to manufacture live-attenuated vaccines for human use (ANMAT Disposition N° 3775/01).

2. *Installations:* Systems for air treatment, water treatment, water and steam for heaters, autoclaves and other connections, freeze dryer installation and qualification, and Class 100 clean room areas for sterile processing were put in place previous to starting production activities. In Figs. 2, 3, and 4 are shown the stages of deionization, reverse osmosis treatment, and four-effect (or four-stage) distillation to obtain water of injection quality [19], which is a central ingredient in making Candid #1 vaccine.



Fig. 2 Photograph of the skid holding the water deionization equipment



Fig. 3 View of the reverse osmosis device to treat deionized water to obtain purified water



Fig. 4 Multiple effect distillation equipment to process pure water to collect water “for injection” quality

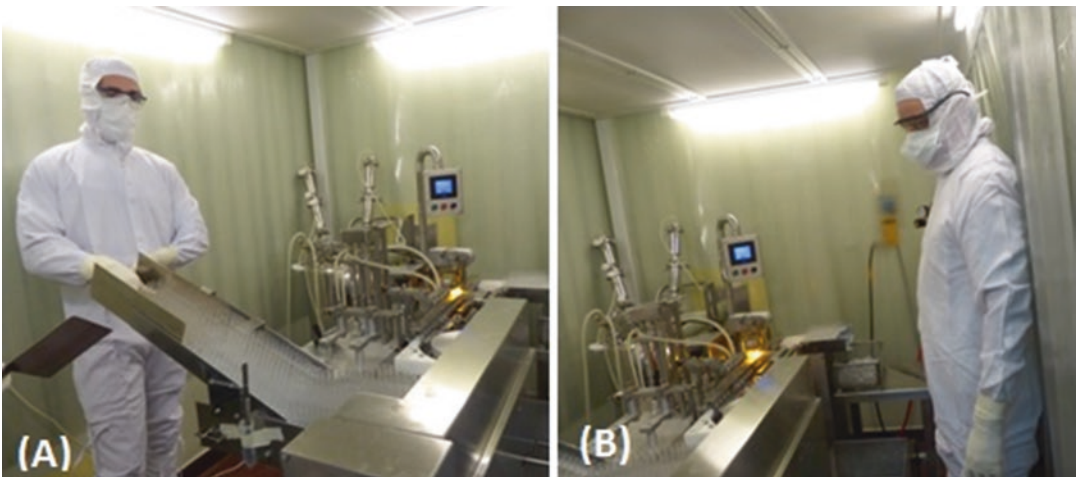


Fig. 5 View of the filling process of water for injection: (a) charge of glass ampoules to feed the filling machine; (b) filling and sealing of 5.5 mL ampoules to be used as Candid #1 vaccine diluent

Water for Injection is also the diluent to reconstitute the vaccine, and in Fig. 5, views of the Water for Injection filling of ampoules are presented. These diluent ampoules, registered under ANMAT as a pharmaceutical product, are distributed with Candid #1 vials.

3. *Specific pathogen-free (SPF) breeding mouse colony.* In 1994, from an imported nucleus from Charles Rivers Laboratories (Wilmington, MA, USA) an outbred CD-1 strain of Swiss mice was started in our facility. Animals are bred under barrier conditions, with continuous quality monitoring of air, water,



Fig. 6 Automatic washing of cages in the ancillary area of the SPF mouse breeding colony



Fig. 7 View of the foremost autoclave to treat food, beverage, and bedding before entering the SPF area of the mouse-breeding colony

food, and environmental conditions. Figures 6, 7, and 8 show activities performed in ancillary and sterile areas of the breeding colony. Tests performed on samples from this colony certify its SPF condition [20].

4. *A colony of Hartley guinea pigs* is also maintained outside this central building. Both mice and guinea pigs are used in quality control in vivo tests for Candid #1 vaccine.
5. *Certified cell bank laboratory*. Candid #1 vaccine is a cell culture-derived product, and in vitro quality control tests are done on different diploid, heteroploid, and primary tissue cul-



Fig. 8 Activities at the sterile SPF area of breeding premises: (a) selection for mating in out breeding Poiley system; (b) sex segregation of SPF mice

Table 1
Composition of cell culture media used in Candid #1 manufacturing process

Medium	Components				
	MEM-NEAA (Gibco)	Protein source	Antibiotic	DMSO	L-Glutamine (2 mM)
Growth medium	✓	FBS 10%	Neomycine 1 mg/L		✓
Cell freezing medium	✓	FBS 25%	Neomycine 1 mg/L	7.5%	✓
Thawing cell medium	✓	FBS 25%	Neomycine 1 mg/L		✓
Candid #1 growth medium	✓	HSA 0.25 gr%	Neomycine 1 mg/L		✓

DMSO dimethylsulphoxide, FBS fetal bovine serum, HSA human serum albumin final concentration in the medium

tures. All cell lines are obtained from ATCC, Rockville, MD and are maintained as Master Cell Seeds (MCS) or Working Cell Seeds (WCS). MRC-5 (ATCC CCL 171) RK-13 (ATCC CCL 37), Vero C76 (ATCC CCL 81) are commonly used. Cell Washing Media is Hanks BSS (Sigma). Growth media, Freezing, and Thawing media are described in Table 1.

A macaque lung cell line (certified and diploid) DBS-FRHL2 (ATCC CL-160) is used to replicate Candid #1. Figures 9, 10, and 11 show cell harvest, freezing, and thawing procedures in the cell bank premises [21–26].

6. *JUNV Candid #1 strain* was derived from JUNV XJ #44 parental strain, so designated to define the XJ prototype strain



Fig. 9 Harvest of cells for a new lot of frozen FRhL-2 cells



Fig. 10 Freezing of cell ampoules using a progressive cooling rate equipment to end in storage at -196°C

of JUNV after two passages in guinea pig and 44 passages in mouse brain. Viral Master Seed (VMS) is the starting stock, and Viral Working Seed (VWS) is the working stock.

7. *Unformulated Candid #1 Bulk Vaccine* is viral fluid containing 7% (v/v) human serum albumin (HSA). It is homogenized and dispensed to 500 mL bottles and stored at -70°C .
8. *Components of final vaccine formulation*: human serum albumin, hydrolyzed gelatin, sorbitol, monosodium glutamic acid, and 0.5% phenol red solution.
9. *The AuthentiKit™ System* from Innovative Chemistry, Inc., Marshfield, MA, USA.



Fig. 11 Extraction of frozen cell ampoules from liquid nitrogen for thawing and establishing new cultures

10. *Bacterial reference strains for contamination tests: Escherichia coli* (ATCC 4157), *Pseudomonas aeruginosa* (ATCC 14502), *Micrococcus salivarius* (ATCC 14344), *Bacteroides distasonis* (ATCC8503), *Penicilium notatum* (ATCC 9478), *Aspergillus niger* (ATCC34467), *Candida albicans* (ATCC 10231).
11. *Mycoplasma reference strains: Acholeplasma laidlawii* (ATCC23206), *Mycoplasma pneumoniae* (ATCC 15535), and *Mycoplasma arginini* (ATCC 23838).
12. *The BCG strain of Mycobacterium* (from BCG vaccine) is used as positive control for a contamination test.
13. *Chick primary embryonic fibroblasts* and *Chick red blood cells* are used in the QC/QA tests for adventitious agents and in testing for heme-adsorbing viruses, respectively.
14. *Endotoxin test* uses the blood of the Blue Horseshoe Crab, *Limulus polyphemus*, which forms a gel-like clot when incubated in the presence of endotoxins. Sample vials of Candid #1 vaccine are endotoxin-tested alongside vials of Control Standard Endotoxin (CSE) standards.

3 Methods

3.1 Preparation for Vaccine Production

The manufacture of Candid #1 vaccine is a complex, multistep procedure, in which quality of raw materials, laboratory practice, and environmental conditions must be certified before, during, and after lab procedures according to Good Manufacturing Practices (GMP) [16–18]. Steps to obtain Candid #1 vaccine are schematized in Fig. 12.

1. The general procedure consists of the inoculation of FRhL2 diploid cells with Candid #1 VWS.
2. After 4 days incubation at 35–36 °C in a 5% CO₂ atmosphere, supernatants of infected cell cultures are collected, pooled, and frozen at –70 °C as Unformulated Candid #1 Bulk Vaccine.
3. To obtain final vaccine fluid, several bottles of “Unformulated Candid #1 Bulk Vaccine” from different lots are thawed, pooled, formulated, sampled, and dispensed in ten-dose vials to be freeze-dried through a cycle that can take 3–3.5 days.
4. After Quality Control testing, vials containing final product are labeled and kept at –20 °C. Stability studies demonstrated that dried vaccine vials can be kept in this condition up to 9 years to be reconstituted to immunize people.

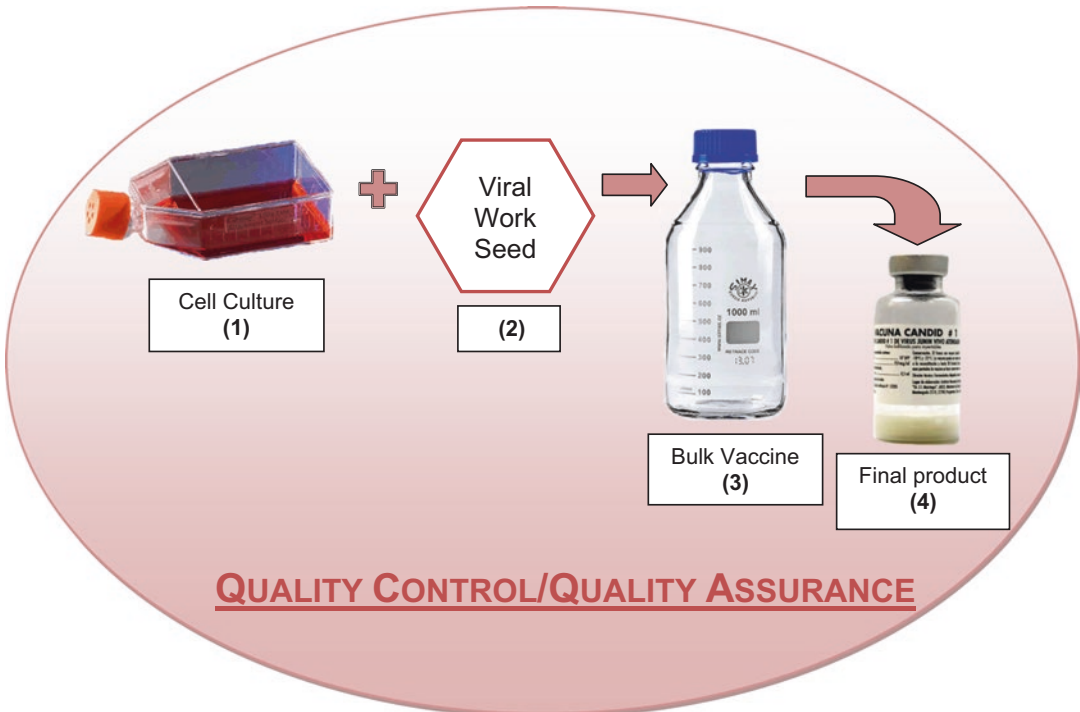
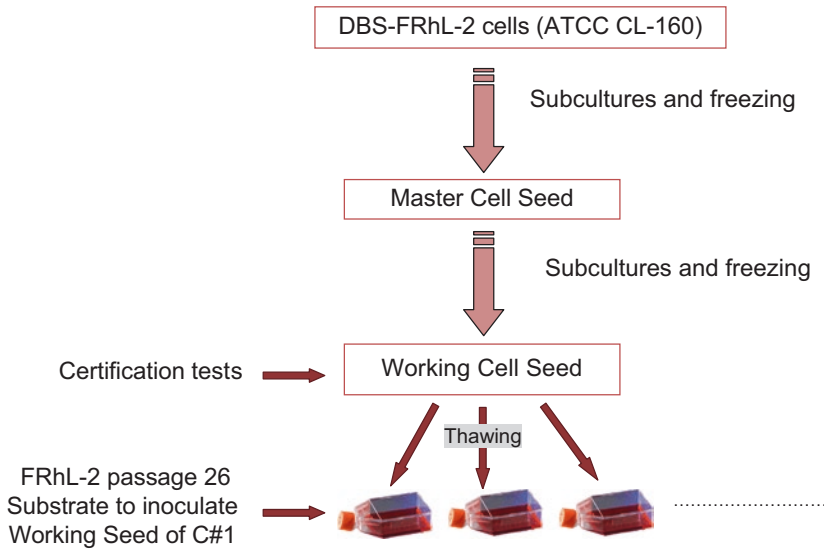


Fig. 12 Schematic procedures to manufacture Candid #1 vaccine



Notice: Certification tests are repeated one passage after that of the viral inoculation

Fig. 13 Schematic representation of steps to obtain FRhL-2 cell cultures to inoculate the viral strain C#1 (step 1 in Fig. 12)

3.2 Quality Control of Cell Lines Used in Quality Control Testing

Tissue culture cells are used in production and/or quality control procedures. As depicted in Fig. 13, cells are cultivated with Growth Medium, frozen in Cell Freezing Medium (Table 1) and cryopreserved in liquid nitrogen as Master Cell Seed (MCS). Cell ampoules are thawed, using Thawing Cell Medium, and stored as Working Cell Seed (WCS). From WCS, cells are sampled and submitted to certification tests to ensure their quality. Following release by Q.C., the cell lines go through different rates of subculture and retesting depending on the cell line karyotype (diploid or heteroploid) and their use in the manufacturing protocol:

1. Cells are grown in T150 flasks as monolayers fed with Growth Medium.
2. After 4 days incubation at 37 °C cells should be about 98% confluent and be sub-passaged at a 1:5 ratio.
3. Resuspend cells in Cell Freezing Medium and cryopreserve them in vials immersed in liquid nitrogen. FRhL2 cells are inoculated at passage 26 with C#1, therefore called End of Production Passage (EOPP). Certification tests are performed on passages 25 (WCS) and 27.
4. Cell lines used in quality control at different stages of vaccine production (MRC-5, FRhL-2, RK-14, Vero C76) are cultivated as shown in Fig. 13, except that they are used up to ten passages after WCS certification.

5. Cell lines are subjected to several certification tests [25, 26]. We perform these at the WCS level to insure that cells resemble the certified MCS through to their End of Production Passage (EOPP). Tests to characterize and qualify cells assure the identity and absence of contaminants in the cell line. These assays test cell properties like morphology and growth kinetics, modal number of chromosomes, cell species identity, and tumorigenicity. They also test for bacteria, fungi, mycoplasma, and mycobacterium contaminations, as well as for viral contaminants [26–30]. At our facility, certification for viral contamination at WCB level is accomplished by means of in vivo and in vitro assays as described in Subheading 3.6 QC/QA and summarized as follows: In vivo tests in suckling and adult mice, in guinea pigs, in rabbits, and in embryonated chicken eggs; in vitro safety tests by inoculation of different certified cell cultures.

3.3 Manufacture of Candid #1 Working Viral Seed (WVS) from Master Viral Seed (MVS)

An aliquot of C#1 MVS, received in Argentina at the end of an international cooperative project [10, 11], is used, and the protocol presented herein describes the expansion of this MVS in FRhL2 cells to obtain C #1 WVS.

1. The necessary number of FRhL-2 frozen cell ampoules are thawed, suspended in Cell Thawing Medium, and pooled to seed approximately 2.6×10^6 cells/T150 flask.
2. Cultures are incubated at 37 °C in 5% CO₂ atmosphere for 3–4 days.
3. Following the first day of incubation, a sample of cultures randomly selected is microscopically observed for growth kinetics, and the medium is replaced by growth medium in all cultures.
4. On the third or fourth day of incubation 100% of the cultures are examined under the microscope. They are acceptable for use if at least 95% of the flasks show an expected morphology and growth pattern, as well as 85–95% confluence.
5. Flasks are numbered and distributed as follows: five flasks are taken at random and kept at 35 °C as control cultures for 14 days, at the end of which monolayers will be used in a heme-adsorption test as part of the safety testing; 20 flasks are devoted to medium (diluent) inoculation and the remaining flasks are inoculated with MVS.
6. The inocula, working dilutions (virus and diluents), are prepared and kept on ice until needed.
7. Media are decanted from tissue culture flasks and every culture is washed three times with Hanks BSS, starting the process with medium control flasks.

8. Hanks solution from the third wash is decanted and control cultures are inoculated with 2 mL/flask of diluents.
9. The same is done with the remaining cultures that are inoculated with 2 mL/flask of the dilution of MVS as to arrive to an approximate MOI of 0.0002.
10. To allow adsorption, control and virus-inoculated cultures are incubated at 35 °C for 90 min with agitation every 15 min.
11. At the end of the adsorption step all cultures are fed Growth Medium and incubated at 35 °C in 5% CO₂ for 4 days.
12. At the end of this incubation and after every culture is observed under the microscope to check for morphology of monolayers, supernatants of cultures are decanted, pooled, and conditioned by the addition of 7% (v/v) of Human Serum Albumin (HSA). From this pool, that constitutes the Working Viral Seed (WVS) samples are separated to be used in quality control tests.
13. The remaining volume is aliquoted to labeled vials that are stored at -70 °C until the lot passes quality requirements, *see* Subheading 3.6 QC/QA, and is used in vaccine elaboration. The same is done with control cultures except that this lot is aliquoted to a small number of bottles (*see* Note 2).
14. Tests that apply to quality control for WVS are described in Subheading 3.6 QC/QA and are summarized in Table 2.

3.4 Manufacture of CANDID #1 Bulk Vaccine

1. To obtain Candid #1 bulk vaccine (step 3 in Fig. 12), the necessary number of frozen FRhL-2 cell ampoules is thawed by immersion in a water bath at 37 °C.
2. Ampoules are cleaned with alcohol and opened to collect the cell suspensions and pool them into an adequate glass bottle by adding Cell Thawing Medium (Table 1).
3. In a sample from the cell suspension, viable cells are counted by Trypan Blue dye exclusion and cell concentration is adjusted to seed 2.6×10^6 cells/T150 flask containing 45 mL of thawing growth medium.
4. Cells are incubated at 37 °C with 5% CO₂ for 24 h.
5. At 24 h, media is decanted from all cultures and replaced by growth medium. Incubation is continued under the described conditions for 72 h.
6. On the fourth day of incubation 100% of the cultures are microscopically inspected and cells are expected to be 85–90% confluent, with good morphology and clean supernatants to be incorporated into the process of obtaining Candid #1 Bulk Vaccine.
7. Numbers of accepted and rejected cultures are to be recorded.
8. Preapproved 4 days old FRhL-2 cells are sent from “Tissue Culture” facility to “Vaccine” facility. There, cultures are

Table 2
Summary of testing scheme for manufacturing of Candid #1 vaccine

N°	Test	Cell substrate testing		Testing of intermediates and final product		
		WCB	EOP (ONLY for FRhL-2)	Work virus seed	Bulk vaccine	Final filled
1	Morphology and growth kinetic	✓	✓			
2	Modal number of chromosome	✓	✓			
3	Identity	✓	✓			
4	Tumorigenicity	✓	✓			
5	Bacterial and fungal sterility	✓	✓	✓	✓	✓
6	<i>Mycoplasma</i>	✓	✓	✓	✓	
7	<i>Mycobacterium</i>	✓	✓	✓	✓	
8	Safety in suckling mice	✓	✓	✓	✓	✓
9	Safety in adult mice	✓	✓	✓	✓	✓
10	Safety in embryonated eggs	✓	✓	✓	✓	
11	Safety in guinea pig	✓	✓	✓	✓	✓
12	Safety in rabbits			✓	✓	
13	Safety in tissue culture	✓	✓	✓	✓	
14	Hemadsorbing virus	✓	✓	✓	✓	
15	General safety					✓
16	Potency (viral titer)			✓	✓	✓
17	Viral identity			✓	✓	✓
18	Osmolality					✓
19	Residual moisture					✓
20	Endotoxin					✓
21	PH					✓

numbered and labeled as “Unopened” (ten T150), and the remaining T150 as “JUNV.”

9. From this point, the procedure to obtain Candid #1 Bulk Vaccine is identical to that described in Subheading 3.3 above, except that the viral inoculum is WVS. Procedures of cell culture washing and posterior viral inoculation are shown in Fig. 14.
10. Tests that apply to quality control for C#1 Bulk Vaccine are described in Subheading 3.6 *QC/QA* and summarized in Table 2.



Fig. 14 Cell culture washing and viral inoculation during the manufacture of Candid #1 bulk vaccine

3.5 Manufacture of CANDID #1 Filled Product

1. Candid #1 as final or filled product is a vial containing ten doses of lyophilized Candid #1 vaccine. One week before the vaccine filling is started an integrity test is performed to certify that the freeze dryer is ready to be vapor sterilized and to perform the operations involved in the freeze drying of the final product. Cleaning and disinfection, as well as air quality and sterility procedures before and during filling process, are certified by Quality Control/Quality Assurance, as briefly described in Subheading 3.6 QC/QA.
2. Filling starts by selecting the necessary number of Candid #1 Bulk Vaccine bottles and by placing them in a 37 °C water bath, with agitation to speed thawing. Bottles of Bulk Vaccine proceed from different approved lots. The volume of thawed bulk is determined and pooled in a sterile stainless-steel tank. From this pool, samples are taken for “pre-filtration viral titration” and stored at -70 °C.
3. By applying nitrogen gas, the content of this tank is forced through 0.45 µm filters and collected in 2 L apyrogenic glass cylinders to record exact volumes for latter formulation (Fig. 15a).
4. The filtered pool is transferred into a stainless-steel refrigerated (4 °C) tank with constant agitation (Fig. 15b).
5. New samples are taken for “post-filtration viral titration” and stored at -70 °C.

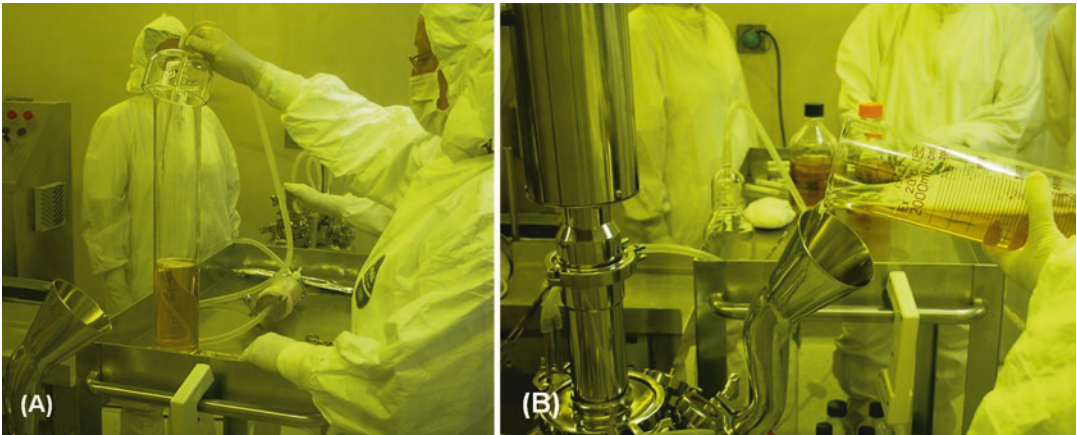


Fig. 15 Formulation of Candid #1 pre-filling: (a) filtration of thawed and pooled bulk lots; (b) volume-determination for components mixture in the filling tank

6. Components of final vaccine formulation (human serum albumin, hydrolyzed gelatin, sorbitol, monosodium glutamic acid, and 0.5% phenol red solution) are added to the measured volume of bulk and completed to final volume of formulated product by adding necessary quantities of sterile water for injection.
7. Samples are taken from this mix for pH determination, and the final value is adjusted to 6.8 with sterile hydrochloric acid.
8. New samples are taken for “pre-filling viral titration” and stored at $-70\text{ }^{\circ}\text{C}$.
9. The agitated content of this mixing tank is connected to the filling machine pre-calibrated to dispense a volume equivalent to ten doses of rehydrated vaccine (Fig. 16).
10. Pre-stoppered vials are collected in annealed pans that allow the direct deposit of vials on the freeze-dryer cold ($-40\text{ }^{\circ}\text{C}$) shelves (Fig. 17).
11. Calibration of the filling pumps is verified several times during the filling procedures, and corrected when necessary.
12. After completing the freeze-dryer charge and the product has remained 4 h at $-40\text{ }^{\circ}\text{C}$, primary drying is started at $100\text{ }\mu$ vacuum.
13. Secondary drying is accomplished at $20\text{ }^{\circ}\text{C}$ shelf temperature and $50\text{ }\mu\text{m}$ vacuum. Depending on the amount of in-process vials, the whole freeze-drying takes 48–72 h. When the operation is finished, commands are activated in the machine to allow stoppers to be placed on each freeze dried vial and the freeze-dryer door is opened.
14. Aluminum seals are applied on those vials selected after visual inspection of 100% of the lot.



Fig. 16 Filling and stopping of Candid #1 vaccine in ten-dose vials



Fig. 17 Translation of pre-stoppered vials into the freeze dryer chamber before the freeze dry process

15. Pans containing closed vials of vaccine are transferred to the labeling room, where labels and expiration date are applied to each vial (Fig. 18).
16. Sample vials are separated for sterility, residual moisture, osmolality, pH, potency, identity, general safety, and endotoxin testing (Subheading 3.6 QC/QA and Table 2).

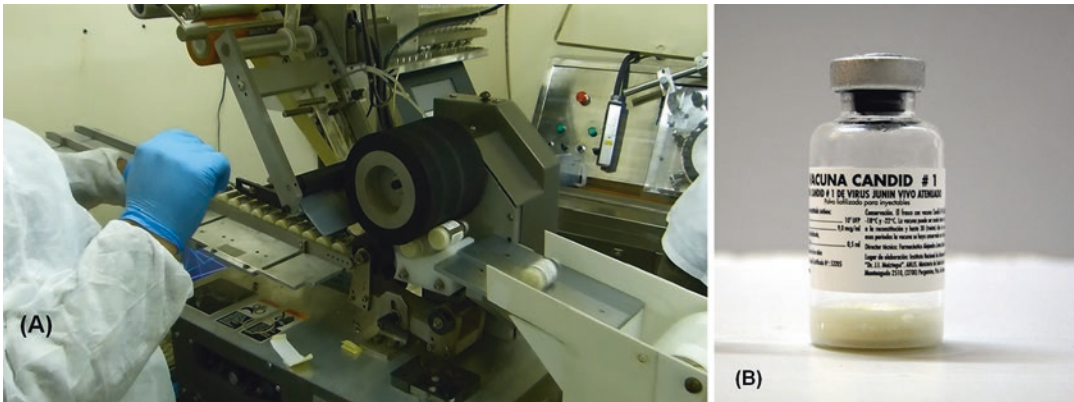


Fig. 18 Labeling of finished product: (a) view of labels and expiration date application to Candid #1 vials; (b) Candid #1 vaccine finished product

17. The remaining vials of the lot are placed on boxes, labeled with all data required for “on hold product,” and kept at -20°C in a dedicated freezer until the lot approval by QC/QA.
18. The moment in which the lot is transferred to another -20°C freezer, it is designated as “released product.” From there the vaccine leaves the production plant for distribution to another area at INEVH.

3.6 Quality Control/ Quality Assurance (QC/QA) Tests

QC/QA procedures ensure that Candid #1 vaccine meets the quality level established by the developers. They are also applied to initial raw materials (water, fetal bovine serum, trypsin, cell growth media, antibiotics, human serum albumin, and the remaining vaccine formulation components), and packaging materials (vials, stoppers, aluminum seals). Every method involved in the production of C#1 is performed following written procedures (as part of a whole documentation system), in a controlled environment, using validated procedures, and calibrated instruments [31, 32]. For example, Fig. 19 shows the verification of gowning and laboratory disinfection procedure.

1. *Morphology and growth kinetics of the cells.* We determine whether the basic morphology of the cultured cells (fibroblastic, epithelial, muscle, lymphocytic, etc.) remains as described by the developer, and that growth rate is that expected from previous subcultures.
2. *Modal number of chromosome.* On selected cultures in Log phase (full active growth), metaphases are synchronized by using colchicine. Cells are then detached and seeded on glass for fixation and Giemsa stain. One hundred selected metaphases are chromosome-counted. The calculated modal



Fig. 19 Verifications of (a) sterile gowning; (b) efficacy of laboratory-surface disinfection by Quality Assurance

number should be coincident with that reported by the developer in the original presentation document of the cell line under study.

3. *Identity*. Cell line species of origin is determined by using The AuthentiKit™ System. In this test, the migration distances of several enzymes obtained from a cell concentrate under identification are measured and compared to migration distances in tables of Standardized Migration Distances for a variety of species. Species of origin described in the original publication for a cell line has to be corroborated by results from the corresponding isoenzymes.
4. *Tumorigenicity*. This test is done to determine whether a cell substrate is capable of forming tumors after inoculation into animals. For this assay, detailed elsewhere [26] 24 adult nude (Nu/Nu) mice are used, distributed as follows: ten mice are inoculated for the cell line under test; ten for HeLa cells as positive control; and four for negative control (serum-free growth medium). Animals are observed for tumor development for 21 days. At the end of the test all animals are sacrificed and submitted to histopathological examination. The test is considered valid if at least 90% of positive control animals develop tumors.
5. *Bacteria and fungi*. Procedures for detection of bacterial and fungal contaminants have been extensively described elsewhere [25–27]. Media used in these tests must have undergone a growth promotion proof, which demonstrates the capacity of each to grow less than 100 CFU inocula of the following refer-

ence strains: *Escherichia coli*, *Pseudomonas aeruginosa*, *Micrococcus salivarius*, *Bacteroides distasonis*, *Penicillium notatum*, *Aspergillus niger*, *Candida albicans*.

6. *Mycoplasma*. Testing for Mycoplasma contamination is done using two approaches: (a) the broth and agar cultivation procedure; (b) the indicator cell culture method staining cells with a DNA-specific fluoro-chrome such as bisbenzimidazole (or Hoechst 33258) plus DAPI [28, 29].

The culture test system should be carried out using solid and liquid media that are known to promote the growth of low inocula of the following reference strains: *Acholeplasma laidlawii* (ATCC23206), *Mycoplasma pneumoniae* (ATCC 15535), and *Mycoplasma arginini* (ATCC 23838).

7. *Mycobacterium*. Supernatants of the tissue culture under test are inoculated on specific solid media Lowenstein-Jensen and Middlebrook 7H10. The strain BCG of *Mycobacterium* is inoculated as a positive control.
8. *In vivo tests using suckling mice*.

Testing cell culture supernatants for adventitious agents: 20 suckling mice less than 24 h old are inoculated intraperitoneally with 0.1 mL and intracerebrally with 0.01 mL of the supernatant of the cell line under test [26, 30]. Ten additional uninoculated mice are kept as normal controls. The cell line passes this test if at least 80% of the inoculated mice remain healthy and survive the entire observation period and if none of the mice show evidence of disease.

Testing viral fluids (WVS and Bulk Vaccine) for adventitious agents: 20 suckling mice less than 24 h old are inoculated intraperitoneally with 0.2 mL and intracerebrally with 0.02 mL of viral fluid in which JUNV has been neutralized with a specific anti-JUNV rabbit serum.

Twenty suckling mice less than 24 h old are inoculated intraperitoneally with 0.2 mL and intracerebrally with 0.02 mL of non-neutralized viral fluid.

Ten extra suckling mice are inoculated intraperitoneally with 0.1 mL and intracerebrally with 0.01 mL of rabbit anti-JUNV serum used in the viral neutralization of inocula (anti-serum control).

Ten extra non-inoculated suckling mice are kept as animal controls.

The mice are observed daily for at least 14 days. Each mouse that dies after the first 24 h of the test, or is sacrificed because of illness, is necropsied (or frozen at -70°C) and examined for evidence of viral infection by gross observation and intraperitoneal and intracerebral inoculation of appropriate tissue into at least five additional mice, which are observed daily for 14 days. In addition, a blind passage (via intraperitoneal and

intracerebral inoculation into at least five additional mice) is made of a single pool of the emulsified tissue (minus skin and viscera) of all mice surviving the original 14-day test. The viral fluids under study pass the test only if at least 80% of the originally inoculated mice and at least 80% of each group of subsequently inoculated mice remain healthy and survive the entire observation period and if none of the mice show evidence of a transmissible agent or other viral infection, other than agents known to be a component of the tested material (i.e., vaccine strains of virus, when relevant) [30]. This test detects adventitious agents including many human viruses, such as coxsackievirus types A and B and other picornaviruses, alphaviruses, bunyaviruses, arenaviruses, flaviviruses, rabies, and herpesviruses. This test can also detect many murine agents.

9. *In vivo tests using adult mice.*

Testing cell culture supernatants for adventitious agents: 20 adult mice weighing 15–20 g are inoculated intraperitoneally with 0.5 mL and intracerebrally with 0.03 mL of supernatants of the cell line under test. The mice should be observed daily for 21 days. Four additional uninoculated mice are kept as normal controls. The cell line will pass this test if at least 80% of the originally inoculated mice remain healthy and survive the observation period, and if none of the mice show evidence of any disease.

Testing viral fluids (WVS and Bulk Vaccine) for adventitious agents: The same number of animals and inoculation sites apply to this test for viral fluids. This test detects adventitious viruses including lymphocytic choriomeningitis virus (LCMV), coxsackieviruses, flaviviruses, and rabies virus.

10. *In vivo tests using guinea pigs.*

Testing cell culture supernatants for adventitious agents: five guinea pigs each weighing 350–450 g are inoculated intraperitoneally with 5 mL and intracerebrally with 0.1 mL of supernatants of the cell line under test. The animals are observed daily for at least 42 days. Two additional non-inoculated guinea pigs are kept as normal controls.

Testing viral fluids (WVS and Bulk Vaccine) for adventitious agents: the same protocol as above is followed with inoculation of viral fluid. This test detects *Mycobacterium tuberculosis* and adventitious viruses like paramyxoviruses (including Sendai virus), reoviruses, and filoviruses.

11. *In vivo tests of culture supernatants using rabbits.* Ten healthy rabbits each weighing 1500–2500 g are inoculated intradermally in multiple sites with a total of 1.0 mL, and subcutaneously with 2.0 mL of the material to be tested. The animals should be observed daily for at least 30 days. Two additional non-inoculated rabbits are kept as normal controls. This test detects simian herpes B virus.

12. *In vivo tests using embryonated chicken egg to detect adventitious agents.* A sample volume, equivalent to at least 10^6 cells suspended in 0.5 mL, is used in egg testing. At least ten embryonated eggs, 10–11 days old, should be inoculated by the allantoic route using 0.5 mL per egg. At least ten additional embryonated eggs, 6–7 days old, should be inoculated by the yolk sac route using 0.5 mL per egg. Following incubation at 37.5 ± 0.5 °C with 60/70% humidity for 5 days, the allantoic fluids are harvested, pooled, and tested for the presence of hemagglutinating agents with chicken red cells. A cell culture sample passes the test if at least 80% of the embryos appear normal and there is no evidence of viral or hemagglutinating agents. By the allantoic route, this test detects adventitious viruses like orthomyxoviruses (influenza virus) and paramyxoviruses (mumps, measles, parainfluenza viruses), alphaviruses, and vesiculoviruses; and by the yolk sac route it screens for herpesviruses, poxviruses, rhabdoviruses, as well as rickettsiae, mycoplasmas, and bacteria.
13. *Testing general safety of final vaccine product in guinea pigs and mice.* Two guinea pigs weighing less than 400 g and two adult mice are intraperitoneally inoculated (in multiple sites) with 5 and 0.5 mL respectively of reconstituted vaccine from the lot in test [33]. Animals are observed for health parameters for 7 days. This test, performed only with filled product, is to determine any level of toxicity in the final vaccine product.
14. *In vitro safety tests.* In vitro tests are carried out by the inoculation of cells and/or supernatants into various susceptible indicator cell cultures capable of detecting a wide range of possible contaminating viruses. The choice of cells used in the test is related to the species of origin of the cell bank to be tested, but should include a human and/or a nonhuman primate cell line susceptible to human viruses [26, 30]. In the present protocol, the in vitro tests to search for viral contaminants are as follows: 12 T75 flasks are seeded with: MRC-5, DBS FRhL-2, RK-13, Vero C76 (*the ATCC numbers were placed in Subheading 2*), and primary chick embryo cells. For each type of culture, two flasks are kept unopened as cell control; five flasks are used as growth medium control, and in the remaining five flasks, growth medium is replaced by supernatant of the cell line under test, diluted 1:3 (v/v) with the growth medium. All the cultures are kept at 37 °C, in a 5% CO₂ incubator. At day 7 cultures are observed for the presence of cytopathic effects (CPE), recorded and refed with fresh medium. Incubation is continued until day 14, when microscopic observation is repeated and recorded. The inoculated cultures of each type plus two growth medium controls are

subjected to a heme-adsorption test using chick red blood cells to detect the presence of heme-adsorbing viruses. This whole procedure is repeated on Vero cells in which media collected from initially inoculated Vero cells is sub-passaged into fresh Vero cultures, ending with a heme-adsorption test. This test is considered satisfactory only if there is no evidence of adventitious agents and at least 80% of the cultures are available for observation at the end of the observation period.

15. *Testing viral infectivity (vaccine potency)*. Viral titration to determine infectivity or potency in WVS or Bulk Vaccine, respectively, is done on Vero C76 cell monolayers that are 80–90% confluent, by counting of plaque-forming units (PFU) under agarose [34]. A Candid #1 internal viral standard and cell culture controls are incorporated into every test. End points are calculated by Reed and Muench method [35] and expressed as the number of PFU/mL. Requirements for the different stages are:

WVS and Bulk Vaccine: $\geq 1 \times 10^5$ PFU/mL.

Filled Vaccine: $\geq 1 \times 10^4$ PFU/mL.

16. *Testing vaccine viral identity*. JUNV Candid #1 identity is assessed by confronting Candid #1 internal viral standard and the material under test (WVS, Bulk vaccine, or filled product) with an anti-JUNV rabbit serum [34, 36]. The virus-serum mixtures are incubated 1 h at 37 °C and then inoculated into Vero C76 cells seeded in 6-well plates. Standard non-neutralized Candid #1 virus and rabbit antiserum controls are incorporated in each test. Viral adsorption is allowed for 90 min at 36 °C, and cell monolayers are coated with 3 mL/well of agarose medium [36]. Incubation is done for 5 days at 37 °C in 5% CO₂ atmosphere, at this time a second overlay containing 2.3% Neutral Red is added to each monolayer. Incubation is continued for an extra day and the PFU are counted. The acceptable result of this test is as follows: No PFU are to be observed in the cells inoculated with neutralized virus and in serum and cell controls, while viral titer of standard and non-neutralized viral fluid under test should render the known expected titers.
17. *Osmolality*. The determination of osmolality (concentration of a solution expressed in osmoles of solute particles per kilogram of solvent) is done on a sample of four reconstituted freeze-dried vaccine vials by means of a freezing point osmometer, with valid calibration certificate. The accepted osmolality value for Candid #1 filled product is between 260 and 330 mOsm/kg.

18. *Residual Moisture*. This parameter is determined on a sample of three vials of Candid #1 filled product by using a device that titrates moisture through a coulombimetric measurement (Karl Fisher) using Karl Fisher Reagent TU (with methoxyethanol, without pyridine), Solvent S, and dihydrated sodium tartrate (5 ± 0.5 mg water/mL) as solid water standard. Residual moisture in the Candid #1 filled product should be <3%.
19. *Endotoxin*. Presence of bacterial endotoxin is tested in filled product as well as in diverse intermediate and/or raw materials by the Horseshoe Crab (*Limulus*) gel clot method. Sample vials of reconstituted lyophilized Candid #1 vaccine are incubated along with CSE standards as positive controls and the unexposed extract fluid as a negative control. After the incubation period, the tubes containing the controls and the extract are observed for the presence of the gel clot. If it clots, endotoxin is present. If no clot is observed, product is free of endotoxin. The endotoxin limit value for Candid #1 vaccine is <0.3 EU/mL [31, 37].
20. *pH determination*. These data are obtained by a potentiometric determination using a pH meter with valid calibration. The pH value required for Candid #1 filled product is from 6.5 to 7.5.

4 Notes

1. GMP procedures from one facility cannot be easily transplanted to another facility because the instructions are so specific that they account for the distances between one operation and another. For example, when clarifying a viral supernatant, the instructions may say: “Collect viral supernatants into an even number of 50 mL conical tubes in Biosafety Cabinet #3 and walk three steps to low speed centrifuge #6 to clarify the supernatant at $400 \times g$ for 5 min at 4 °C.”
2. Control cultures are handled in a separate room from those cultures inoculated with the MVS. Air quality and other requirements for safe performance of these procedures are mentioned in Subheading 3.6 QC/QA.

Acknowledgments

The authors wish to specially acknowledge the collaboration of: Enria DAM, Saavedra MC, Banuera GR, Bilos PG, Brun HL, Cantore MF, Cascardo EA, Chiarito LI, Ciganda MI, Cogo GN, Diaz CI, Escallier AL, Fassio R M, Fazzi CJ, Fernandez MF, Galante MD, Gazza PO, Giovannoni NP, Grosso FL, Jesus EF, Lazzari GE, Ludueña SD, Margall AI, Martinez NE, Marzano ME, Medina MJ, Olivera DG, Paz C, Pellegrino IA, Raggio A, Riera LMC, Taborda LR, Vidal JA, Zain EJ.

References

1. Arribalzaga RA (1955) Una nueva enfermedad epidémica a germen desconocido: hipertermia nefrotóxica, leucopenia, y enantémica. *Dia Medico* 27
2. Maiztegui JI (1975) Clinical and epidemiological patterns of Argentine hemorrhagic fever. *Bull WHO* 52:567–575
3. Sabattini MS, Gonzalez LE, Díaz G, Vega VR (1977) Infección natural y experimental de roedores con virus Junín. *Medicina (Buenos Aires)* 37:149–161
4. Maiztegui J, Feuillade M, Briggiler A (1986) Progressive extension of the endemic area and changing incidence of Argentine hemorrhagic fever. *Med Microbiol Immunol* 175:149–152
5. Weissenbacher MC, Laguens RP, Coto CE (1987) Argentine hemorrhagic fever. *Curr Top Microbiol Immunol* 134:79–116
6. Peters CJ, Jahrling PB, Liu CT, Kenyon RH, McKee KT Jr, Barrera Oro JG (1987) Experimental studies of arenaviral hemorrhagic fevers. *Curr Top Microbiol Immunol* 134:5–68
7. Mills JN, Ellis BA, Childs JE, McKee KT Jr, Maiztegui JI, Peters CJ et al (1994) Prevalence of infection with Junin virus in rodent populations in the epidemic area of Argentine hemorrhagic fever. *Am J Trop Med Hyg* 51:554–562
8. Barrera Oro JG, Eddy G (1977) Seminario Internacional sobre Fiebres Hemorrágicas Producidas por Arenavirus Discusión General. *Medicina (Buenos Aires)* 32:257–259
9. Barrera Oro JG, Eddy GA (1982) Characteristics of candidate live attenuated Junin virus vaccine. Paper presented at the international conference on comparative virology, Banff, AB
10. Barrera Oro JG, McKee KT (1991) Toward a vaccine against Argentine hemorrhagic fever. *Bull PAHO* 25:118–126
11. Enría DA, Barrera Oro JG (2002) Junin virus-vaccines. *Curr Top Microbiol Immunol* 263:239–264
12. Maiztegui JI, McKee KT Jr, Barrera Oro JG, Harrison LH, Gibbs PH, Feuillade MR et al (1998) Protective efficacy of a live attenuated vaccine against Argentine hemorrhagic fever. *J Infect Dis* 177:277–283
13. Ambrosio AM, Riera LM, Saavedra MC, Sottosanti MJ (2005) Ensayo preclínico de la vacuna candid #1 (fiebre hemorrágica Argentina) producida en Argentina. *Medicina (Buenos Aires)* 65:329–332
14. Ambrosio AM, Saavedra MC, Riera LM, Fassio RM (2006) La producción nacional de vacuna a virus Junín vivo atenuado (candid # 1) anti-fiebre hemorrágica Argentina. *Acta Bioquím Clín Latinoam* 40:5–17
15. Enría DA, Ambrosio AM, Briggiler AM, Feuillade MR, Crivelli E, y Grupo de Estudio de la vacuna contra la fiebre hemorrágica argentina (2010) Vacuna contra la fiebre hemorrágica Argentina candid #1 producida en La Argentina. *Inmunogenicidad y seguridad Medicina (Buenos Aires)* 70:215–222
16. WHO Expert Committee on Specifications for Pharmaceutical Preparations (2014) WHO technical report series N° 986, p. 402
17. Disposición 2819/04. Buenas Prácticas de Fabricación para Elaboradores, Importadores/Exportadores de Medicamentos (2004) Administración nacional de Medicamentos, Alimentos y Tecnología Médica. Instituto Nacional de Medicamentos.
18. Disposición 705/2005. Administración Nacional de Medicamentos, Alimentos y Tecnología Médica (2005) Especialidades medicinales. Requisitos para la inscripción de vacunas. Presentación de la documentación técnica. Establecimientos elaboradores. Información Preclínica-Clinica. Formularios.
19. US Pharmacopeia (1231) Water for pharmaceutical purposes. Expert Committee: (PW05) *Pharmaceutical Waters* 05
20. Baker DG (1998) Natural pathogens of laboratory mice, rats, and rabbits and their effects on research. *Microbiol Rev* 11(2):231–266
21. Hay RJ (1998) The seed stock concept and quality control for cell lines. *Anal Biochem* 171:225–237
22. Coecke, S. et al. (2005) Guidance on good cell culture practice. *ATLA* 33:261–287. Available in the best practices (GCCP) on the ESACT-UK The UK Society for Cell Culture Biotechnology. <http://www.esactuk.org.uk/>
23. World Health Organization (2010) Recommendations for the evaluation of animal cell cultures as substrates for the manufacture of biological medicinal products and for the characterization of cell banks. Proposed replacement of TRS 878, Annex 1
24. Wallace RE et al (1973) Development of a diploid cell line from fetal rhesus monkey lung for virus vaccine production. *In Vitro* 8:323–332
25. Hay RJ, Caputo J, Macy ML (eds) (1992) *ATCC Quality control methods for cell lines*, 2nd edn. ATCC, Rockville, MD, p 132
26. Guidance for Industry. Characterization and Qualification of Cell Substrates and Other Biological Materials Used in the Production of Viral Vaccines for Infectious Disease Indications (2010) U.S. Department of Health and

- Human Services Food and Drug Administration Center for Biologics Evaluation and Research. View at <http://www.fda.gov/BiologicsBloodVaccines/GuidanceComplianceRegulatoryInformation/Guidances/default.htm>
27. Office of the Federal Register, Code of Federal Regulations (2016) 21 CFR part 610.12 (a) to (e).eCFR, 29 Mar 2016
 28. FDA, CFR-Code of Federal Regulations (1998) Title 21, Part 610 – General Biological Products Standards, Subpart D – Mycoplasma, Section 610.30, Test for Mycoplasma
 29. VICH GL34: biologicals: testing for the detection of mycoplasma contamination. EMA/CVMP/VICH/463/2002. Committee for Medicinal Products for Veterinary Use (CVMP), Mar 2013
 30. International conference on harmonization of technical requirements for registration of pharmaceuticals for human use. ICH harmonized tripartite guideline. Viral safety evaluation of biotechnology products derived from cell lines of human or animal origin q5a(r1). Sept 1999
 31. Administración Nacional de Medicamentos, Alimentos y Tecnología Médica. Farmacopea argentina (2013) 7° edn, Buenos Aires
 32. FDA, draft guidance for industry: process validation: general principles and practices (Nov 2008). <http://www.fda.gov/downloads/Drugs/GuidanceComplianceRegulatoryInformation/Guidances/UCM070336.pdf>. Accessed 29 Apr 2016
 33. FDA, CFR-Code of Federal Regulations (1998) Title 21, part 610 – general biological products standards, Section 610.11
 34. Webb P, Johnson K, Mackenzie R (1969) The measurement of specific antibodies in Bolivian hemorrhagic fever by neutralization of virus plaques. Proc Soc Exp Biol Med 130: 1013–1019
 35. Reed LJ, Muench HA (1938) A simple method of estimating fifty per cent endpoints. Am J Hyg 27:493–497
 36. Barrera Oro J G, McKee KT Jr, Spisso J, Mahlandt BG, Maiztegui JI (1990) A refined complement-enhanced neutralization test for detecting antibodies to Junin virus. J Virol Methods 29:71–80
 37. Case MJ, Ryther SS, Novitsky TJ (1983) Detection of endotoxin in antibiotic solutions with *Limulus* amoebocyte lysate. Antimicrob Agents Chemother 23:649–652

Detection of Virus-Antibody Immune Complexes in Secondary Dengue Virus Infection

Meng Ling Moi, Tomohiko Takasaki, and Ichiro Kurane

Abstract

It has been reported that virus-antibody immune complexes formed during secondary dengue virus infection are associated with increased disease severity. Here, we describe the details of a plaque titration method that uses FcγR-expressing BHK cells to detect and quantify infectious virus-immune complexes and a quantitative real-time PCR method for the quantification of virus genome in patients with secondary dengue infection. These methods detect both viruses in free-form and in immune complexes in patients with dengue infection, and are useful for determining viremia levels and patterns that better reflect in vivo conditions.

Key words Dengue, Secondary infection, Plaque assay, Antibody, Immune complex

1 Introduction

Dengue is a major public health threat in the tropics and temperate regions. It is estimated that approximately half of the global population is at risk of dengue infection and 400 million cases occur annually worldwide [1]. Common symptoms of dengue include fever, headache, myalgia, and thrombocytopenia. Infection with any of the four dengue virus (DENV1–4) serotypes confers life-long immunity to infection with the same serotype but protective immunity to other serotypes is short-lived [2]. During primary infection, cross-reactive antibodies to other serotypes are induced, and these antibodies, when present at non-neutralizing levels, are hypothesized to play a major role in the development of severe dengue [2]. In severe dengue, life-threatening symptoms include severe bleeding and multiple organ failures. It is speculated that those with secondary dengue virus infection are at higher risk of developing severe dengue [3]. During secondary infection, these non-neutralizing cross-reactive antibodies form virus-antibody immune complexes with the infecting virus and circulate as virus-immune complexes during the acute phase [4]. These infectious

virus-antibody immune complexes in turn facilitate infection of Fc γ R-bearing monocyte lineage cells, leading to the production of higher titers of virus progeny and an aberrant immune response that ultimately results in severe dengue [5, 6].

Understanding the relationship between viremia and these virus-antibody immune complexes during infection would contribute to a better understanding of the pathogenesis of dengue. Currently, the gold-standard for the detection of infectious DENV particles is by the plaque titration method [7]. Other virus detection tools include reverse-transcriptase PCR (RT-PCR) for the detection of virus genome and detection of viral antigen by immunofluorescence and flow cytometry. The RT-PCR and antigen detection methods are rapid, sensitive, and relatively simple to perform. However, the plaque titration method is the most specific method for providing information on virus infectivity.

In this chapter, we will describe the detection and quantification of virus-antibody immune complex in patients with secondary dengue virus infection using Fc γ R-expressing BHK cells. Infectious virus particles are quantitated using a conventional plaque titration method [7] and virus genomes are quantitated using a fluorogenic real-time RT-PCR method [8]. The Fc γ R-expressing BHK cells have been proved useful in the titration of DENV in both free virus and immune complex forms in both dengue patients and an animal model [9–11]. Thus, the described method could give a better approximation of dengue viremia under *in vivo* conditions.

2 Materials

All materials and reagents are prepared on a clean bench, sterilized and stored at 4 °C until use. Procedures are done according to institutional biosafety regulations. Fetal bovine serum (FBS) used in these procedures are heat-inactivated at 56 °C for 30 min prior to use.

2.1 Plaque Titration Assay

1. DENV stock: virus collected from cell culture supernatants are stored at –80 °C prior to use. All virus stocks are aliquoted to avoid freeze-thawing of samples.
2. Cell lines: Baby hamster kidney-derived cell lines (BHK cells) and Fc γ R-expressing BHK cells are used.
3. Growth and maintenance medium: Eagle's Minimum Essential Medium (EMEM) is supplemented with 10% FBS. For Fc γ R-expressing BHK cells, 0.5 mg/ml neomycin (G418, Roche) is added to the growth and maintenance medium to maintain plasmid expression.
4. 1 \times Trypsin-EDTA solution: 0.05% Trypsin-EDTA solution (v/v).

5. 1× Dulbecco's Phosphate Buffered Saline (DPBS), calcium and magnesium-free.
6. Maintenance medium for plaque assay: 1% Methylcellulose-4000 (Wako) supplemented with 0.94% EMEM containing kanamycin (Nissui), with 2% FBS, 2 mM L-Glutamine, and 7.5% (w/v) sodium bicarbonate solution. For 1 L of maintenance medium, prepare two solutions, "Solution A" and "Solution B" separately. In "Solution A," add 9.4 g of EMEM containing kanamycin and top-up with 1 L of ultrapure water (MilliQ water). Allow the EMEM powder to dissolve thoroughly in the solution. In "Solution B," add 10 g of methylcellulose and a stir-bar. Autoclave both reagents. Cool both reagents to 60 °C and add "Solution A" to "Solution B." Mix the solution with the magnetic stirrer and allow the solution to cool to room temperature. Next, place the solution on ice, and mix the solution with the magnetic stirrer until the solution turns clear yellow. Add 31.5 ml 7.5% (w/v) sodium bicarbonate, 20 ml of FBS, and 10 ml of 200 mM L-Glutamine and mix until all components are dissolved in the reagent. Store the methyl-cellulose solution at 4 °C until use.
7. Fixation solution: 10% (v/v) formaldehyde. Dilute formaldehyde solution (Wako) with tap-water. Store reagent at room temperature.
8. Staining solution: Methylene blue dye, 30× solution. Add 11.25 g of methylene blue tetrahydrate (Wako) to 500 ml of distilled water. To dissolve the methylene blue, add 1.9 ml of 1 N sodium hydroxide solution (*see Note 1*). Store the reagent at room temperature.
9. Maintenance medium for RT-PCR: EMEM supplemented with 2% FBS.
10. Patient serum samples: Samples collected from patients are stored at -80 °C prior to use. Avoid freeze-thaw cycles. All samples should be treated as biohazard materials according to institutional regulations.
11. Class II Biosafety Cabinet.
12. For plaque enumeration: Light-box and colony counter.

2.2 Quantitative Real-Time PCR

1. RNA isolation: High Pure RNA Isolation kit (Roche).
2. Real-time PCR uses Fast virus 1-step master mix (Applied Biosystems), DENV primers and probe sets (TaqMan), RNase, DNase-free water [8]. The PCR Reaction Mix is typically 15 µl: 5 µl of TaqMan Master Mix, 9 µl water, 0.25 µl of 100 µM forward primer, 0.25 µl of 100 µM reverse primer, 0.5 µl of fluorogenic probe (final 250 nM). To this Reaction Mix, 5 µl of RNA (approximately 0.1 µg) will be added before the thermocycling.

3. Optical tube and cap strips, 96-well plate, and adhesive cover.
4. Real-time PCR system.

3 Methods

3.1 Plaque

Titration Assay

1. Prepare a monolayer of BHK and FcγR-expressing BHK cells at a confluency of 70–80% using 12-well plates. Seed cells at the concentration of 1×10^5 to 5×10^5 cells per well (*see Note 2*). Incubate the plates overnight in a CO₂ incubator at 37 °C overnight.
2. Discard the old cell culture supernatant and infect the cells at a 1:10 serial dilution of the serum samples (10^1 – 10^6 dilution).
3. Prepare 50 μl of the immune-complex virus mixture and incubate the mixture at 37 °C for 30 min to allow formation (re-formation) of virus-antibody immune complexes.
4. Add 50 μl of virus-immune complex mixture to the cells. After inoculation, tilt the plates gently every 10 min for a total of six times (total of 60 min) (*see Notes 3 and 4*).
5. Add 1.5 ml of growth and maintenance medium for plaque assay. Incubate the cells in a humidified incubator (5% CO₂) at 37 °C for 5–7 days (*see Note 5*).
6. At 3–4 days after incubation, examine for the presence of cytopathic effect (CPE) under the microscope. Also examine for the appearance of plaques under fluorescent light by naked eye. DENV plaque typically appears 5–7 days after incubation; however, some virus strains isolated directly from clinical samples do not form clear plaques (*see Note 6*). Incubation periods are also dependent on cell culture conditions (*see Note 7*).
7. Upon confirmation of plaques by naked eye, fix the cells with fixation solution for 60 min (*see Note 8*). Rinse the plates with tap water and stain the cells with staining solution for 60 min. Rinse the plate to remove the staining solution.
8. Dry the plates and count the number of plaques.
9. Stained plates can be stored long-term at room temperature.
10. Virus titers are expressed as plaque forming units per milliliter (PFU/ml). The calculations are performed using the formula: (average number of plaques) × (dilution rate)/(volume added).

3.2 Quantitative

RT-PCR

1. Prepare cells and perform the infection assay as in Subheading 3.1, steps 1–4.
2. Add 1.0 ml of maintenance medium for RT-PCR. Incubate the cells in a humidified incubator (5% CO₂) at 37 °C for 5 days (*see Note 9*).

3. Remove 200 μ l of cell culture supernatant fluids.
4. Mix the supernatant (200 μ l) with 400 μ l of viral-binding buffer (Roche) and incubate at room temperature for 10 min.
5. Further steps of removal of binding buffer, washing, and elution of RNA are performed according to manufacturer's protocol (https://lifescience.roche.com/wcsstore/RASCatalogAssetStore/Articles/05204909001_03.08.pdf). The volume of RNA elution is 50 μ l.
6. Prepare and mix the PCR Reaction Mix of 15 μ l.
7. Add in 5 μ l of isolated virus RNA to make up a volume of 20 μ l. Perform the assay in duplicates or triplicates.
8. Perform the RT-PCR reaction with the following cycle conditions:
 - (a) *RT step* (1 cycle).
50 °C for 5 min.
95 °C for 20 s.
 - (b) *Amplification step* (40 cycles data collection at the end of each cycle).
95 °C for 3 s.
60 °C for 30 s.
9. Analyze the real-time PCR results. Confirm the amplification plots and exclude data with abnormal amplification plots. Adjust threshold and baseline accordingly (*see Note 10*).

4 Notes

1. The staining solution is typically made as a 30 \times concentrated solution. However, higher concentration of staining solution (5 \times –10 \times) could be used for rapid staining of cells or with cells that do not stain well at lower concentration. As these reagents stain live cells, use appropriate gloves and other personal protective equipment.
2. Confluency depends on the ability of cells to attach within the wells and multiply. Thus, depending on the cell condition, the cells may not reach 70% confluency after an overnight incubation. In the event that the cells do not reach the optimal confluency, incubate the plates for another 24 h.
3. Ensure that the medium covers the cells during tilting to avoid cell death by drying.
4. Alternatively, to avoid drying, switch off the clean-bench fan during the infection step. After the infection step, immediately replace the plate cover and tilt the plates to avoid drying.

5. DENV plaques typically form at days 5–7 after infection. In the event of no plaque formation, the plates can be further incubated up to 8 days, with the addition of 1 ml of fresh maintenance medium to the old medium.
6. As some clinical DENV strains do not form well-defined plaques, DENV-immune complex could be detected and titered by staining the plaques using antibodies (focus forming assay and immunofluorescence assay).
7. Note the number of cell passages, incubation periods, and other incubation conditions. Some laboratory-established BHK and Vero cell lines lose the ability to form plaques after repeated passages.
8. Directly add the fixation solution to the cells in maintenance medium. The cells could be left in fixation solution up to 24 h. Longer incubation will result in drying of fixation solution.
9. To perform growth curve analyses, cell culture supernatant could be removed daily or other fixed periods for RT-PCR analysis. Day 5 is chosen in this example because DENV growth generally reaches a plateau at this stage.
10. A Ct value of 35 and above the presence of DENV nucleic acid is considered equivocal and values above 40 are considered negative.

Acknowledgment

We thank Dr. Jeffrey V. Ravetch, Rockefeller University, New York for generously providing the Fc γ RIIA cDNA and Dr. Susheela Tridandapani, Ohio State University College of Medicine, Columbus, Ohio for assistance in obtaining the Fc γ RIIA cDNA used in this work. This work was supported in part by the research grant, Research on Emerging and Re-emerging Infectious Diseases (H26-shinkou-jitsuyouka-007), and a Grant-in-Aid for Young Scientists (B) from JSPS (26870872).

References

1. Bhatt S, Gething PW, Brady OJ, Messina JP, Farlow AW, Moyes CL et al (2013) The global distribution and burden of dengue. *Nature* 496(7446):504–507
2. World Health Organization (2009) Dengue: guidelines for diagnosis, treatment, prevention and control, New edn. World Health Organization, Geneva
3. Guzman MG, Alvarez M, Halstead SB (2013) Secondary infection as a risk factor for dengue hemorrhagic fever/dengue shock syndrome: an historical perspective and role of antibody-dependent enhancement of infection. *Arch Virol* 158(7):1445–1459
4. Wang WK, Chen HL, Yang CF, Hsieh SC, Juan CC, Chang SM et al (2006) Slower rates of clearance of viral load and virus-containing immune complexes in patients with dengue hemorrhagic fever. *Clin Infect Dis* 43(8): 1023–1030
5. Modhiran N, Kalayanarooj S, Ubol S (2010) Subversion of innate defenses by the interplay

- between DENV and pre-existing enhancing antibodies: TLRs signaling collapse. PLoS Negl Trop Dis 4(12):e924
6. Ubol S, Phuklia W, Kalayanaroj S, Modhiran N (2010) Mechanisms of immune evasion induced by a complex of dengue virus and preexisting enhancing antibodies. J Infect Dis 201(6):923–935
 7. World Health Organization (2007) Guidelines for plaque-reduction neutralization testing of human antibodies to dengue viruses <http://www.who.int/immunization/documents/date/en/index.html>
 8. Ito M, Takasaki T, Yamada K, Nerome R, Tajima S, Kurane I (2004) Development and evaluation of fluorogenic TaqMan reverse transcriptase PCR assays for detection of dengue virus types 1 to 4. J Clin Microbiol 42(12):5935–5937
 9. Moi ML, Lim CK, Kotaki A, Takasaki T, Kurane I (2010) Development of an antibody-dependent enhancement assay for dengue virus using stable BHK-21 cell lines expressing Fc gammaRIIA. J Virol Methods 163(2):205–209
 10. Moi ML, Lim CK, Kotaki A, Takasaki T, Kurane I (2011) Detection of higher levels of dengue viremia using FcγR-expressing BHK-21 cells than FcγR-negative cells in secondary infection but not in primary infection. J Infect Dis 203(10):1405–1414
 11. Moi ML, Ami Y, Shirai K, Lim CK, Suzuki Y, Saito Y et al (2015) Formation of infectious dengue virus-antibody immune complex in vivo in marmosets (*Callithrix jacchus*) after passive transfer of anti-dengue virus monoclonal antibodies and infection with dengue virus. AmJTrop Med Hyg 92(2):370–376

Future Approaches to DNA Vaccination Against Hemorrhagic Fever Viruses

John J. Suschak and Connie S. Schmaljohn

Abstract

To date, there is no protective vaccine for Ebola virus infection. Safety concerns have prevented the use of live-attenuated vaccines, and forced researchers to examine new vaccine formulations. DNA vaccination is an attractive method for inducing protective immunity to a variety of pathogens, but the low immunogenicity seen in larger animals and humans has hindered its usage. Various approaches have been used to improve the immunogenicity of DNA vaccines, but the most successful, and widespread, is electroporation. Of increasing interest is the use of molecular adjuvants to produce immunomodulatory signals that can both amplify and direct the immune response. When combined, these approaches have the possibility to push DNA vaccination into the forefront of medicine.

Key words DNA vaccination, Delivery methods, Electroporation, Molecular adjuvants, Intramuscular, Intradermal

1 Introduction

The *Filoviridae* family of viruses is composed of enveloped RNA viruses with non-segmented, negative-sense genomes. Filoviruses are divided into three genera: *Ebolavirus*, *Marburgvirus*, and *Cuevavirus* [1]. The *Ebolavirus* genus includes five species including *Zaire ebolavirus* (Ebola virus, EBOV), *Sudan ebolavirus* (Sudan virus, SUDV), *Tai Forest ebolavirus* (Tai Forest virus, TAFV), *Reston ebolavirus* (Reston virus, RESTV), and *Bundibugyo ebolavirus* (Bundibugyo virus, BDBV), all of which cause disease except RESTV. EBOV is considered the most lethal species with a case-fatality or lethality range of 40–90% in human outbreaks [2]. The *Marburgvirus* genus currently includes a single viral species, *Marburg marburgvirus*, the members of which are lethal in 70–85% of cases. These two members are Marburg virus (MARV) and Ravn virus (RAVV). *Cuevavirus* genus includes a single viral species, *Lloviu cuevavirus*, for one virus, Lloviu virus (LLOV). Due to the

high case-fatality rate, person-to-person transmissibility, and potential to instill panic within the public, a concerted effort has been made to develop an effective filovirus vaccine.

Early efforts to design a protective EBOV vaccine were not completely successful due to a lack of knowledge surrounding the correlates of protective immunity, but progress has recently been made. The viral envelope glycoprotein, GP, is the main target of antibody responses [1]. Numerous studies have demonstrated that humoral immunity confers protection against filovirus challenge in both rodent and nonhuman primate (NHP) models [3–8]. Conversely, recent studies utilizing knockout murine models have suggested that cell-mediated immune responses are critical in controlling filovirus infections [9, 10]. Therefore, it is believed that truly protective filovirus vaccines must elicit both arms of the adaptive immune response. The ability of plasmid DNA vaccination to induce both humoral and cell-mediated immune responses has made DNA vaccines an attractive platform for generating protective immunity against filovirus infection [11].

The demonstration of effective DNA vaccination in small animal models changed the paradigm for vaccine technology. For the first time, genes encoding antigens, instead of antigens themselves, were shown to elicit broad immunity against a variety of pathogens. DNA vaccination has many advantages over other established vaccination platforms. Foremost is the endogenous production and presentation of antigen without danger of toxicity or infection, a common concern with live-attenuated and, sometimes, with inactivated viral vaccines. As antigen is produced *in vivo*, antigen presentation occurs on both Class I and Class II major histocompatibility complex (MHC) molecules, yielding both CD4⁺ and CD8⁺ T cell responses. Therefore, DNA vaccination may yield a balanced, protective immune response that is similar to that of authentic viral infection.

Whereas small animal studies have proven the utility of DNA vaccines delivered by intramuscular injection, similar studies in larger animals and humans have been less successful. This has led to the investigation of alternative approaches capable of increasing both the strength and duration of vaccine-induced immune responses (*see Note 1*). The most promising methods of DNA vaccination are intramuscular (IM) injection or intradermal (ID) injection of DNA, diluted in saline buffer, followed by electroporation, the brief delivery of an electrical pulse to cells. Electroporation transiently opens pores in the lipid bilayer, allowing DNA to travel down the concentration gradient and cross the cellular membrane. Electroporation increases gene expression up to 1000-fold when compared to animals receiving only intramuscular injections of DNA. Furthermore, electroporation has the added benefit of increasing DNA distribution throughout the tissue and initiating a pro-inflammatory reaction at the site of injection, thereby propagating the immune response [12–15].

Another approach that has been effective in increasing DNA vaccine immunogenicity is the use of “vaccine cocktails” containing the DNA vaccine as well as plasmids encoding immunomodulatory proteins. Molecular adjuvant plasmids expressing cytokines, chemokines, or co-stimulatory molecules may be co-administered with the antigenic DNA vaccine plasmid (*see Note 2*). Cells transfected by molecular adjuvant plasmids secrete the adjuvant into the surrounding region, stimulating both local antigen presenting cells and cells in the draining lymph node. This results in sustained, low-level production of immune modulating cytokines that can tailor the immune response toward a more desirable outcome. A wide range of inflammatory and helper T cell cytokines have been studied in small animal models in conjunction with DNA vaccination [16, 17], however, a few in particular stand out for their potential in human vaccination [18]. In addition to electroporation, there are several other DNA vaccine delivery methods that have been experimented with to varying degrees of success. Needle-free injection systems such as bio-injectors deliver vaccine plasmid by forcing a liquid stream through the skin, resulting in either intradermal or intramuscular delivery. These systems yield wider distribution of the vaccine, and increased antigen production than does straight IM or ID injection [19, 20]. Delivery systems such as nanoparticles and liposomes have shown promise, but have certain drawbacks related to difficulty of formulation and delivery, particularly when it comes to vaccination in the field [21–30]. Another method that is gaining interest is the formulation of DNA-launched virus-like particles (VLP). In this case, the antigen is encoded in one DNA plasmid, while structural proteins are encoded in a second plasmid. Transfection of a cell by both plasmids allows for expression of endogenously produced VLPs. This allows for increased extracellular bioavailability of the antigen and therefore increased immunogenicity [31].

Here, we present a detailed method for delivering an antigen/adjuvant DNA vaccine cocktail in conjunction with electroporation. Importantly, this protocol may be used with a wide range of antigens, providing a strong foundation for future vaccine research.

2 Materials

2.1 DNA Vaccine

1. Endotoxin free, calcium and magnesium free phosphate-buffered saline.
2. DNA plasmid coding for the antigenic transgene dissolved in endotoxin-free phosphate-buffered saline to appropriate concentration (*see Note 3*).
3. DNA plasmid coding for the molecular adjuvant transgene dissolved in endotoxin-free phosphate-buffered saline to appropriate concentration (*see Note 3*).

2.2 Electroporation

1. Appropriate anesthesia or tranquilizer for animal (e.g., ketamine or isoflurane gas).
2. Electric razor to shave skin at the site of injection (*see Note 4*).
3. U-100 insulin syringe with 29G1/2 needle or tuberculin syringe with 28G needle.
4. Electropulse generator.
5. Electrode needle array (different arrays for intramuscular and intradermal injection).

3 Methods for DNA Vaccine Delivery
3.1 Intramuscular Electroporation of Mice

1. Mix the appropriate amount of antigen encoding DNA plasmid and molecular adjuvant encoding plasmid to obtain the desired ratio of antigen to adjuvant. For bilateral vaccination, you will need a maximum of 100 μL for each mouse (*see Note 5*).
2. Adjust the electroporation parameters according to the manufacturer's suggested values (*see Note 6*).
3. Draw DNA solution into syringe (*see Note 7*).
4. Anesthetize the animal with the appropriate anesthesia or tranquilizer (*see Note 8*).
5. Shave the fur over the anterior, lateral, and medial surfaces of the leg.
6. Position the animal on its back or side. Extend the leg to provide increased access to the tibialis muscle. A bent or crooked leg will limit the success of the injection and subsequent electroporation.
7. Insert the needle and syringe into the center of the electrode array (integrated array). Alternatively, some electroporation systems may lack space for the needle and syringe in between the microarray. In this case, the injection must be delivered first, and then the electrode microarray is positioned around the site of injection and the electropulse is delivered. It is useful to mark the site with a dark-colored marker.
8. Align the needle/electrode array along the middle of the tibialis muscle. Insert both the needle and electrodes into the muscle. Needle should be inserted between 2 and 3 mm into the muscle.
9. Slowly inject the DNA solution (i.e., between 5 and 10 s) without changing the pressure exerted on the syringe plunger.
10. Administer the electrical pulse. The number of pulses, pulse length, magnitude, and interval are dependent on both the animal and the manufacturer of the electroporation device (*see Note 9*).

11. Retain the needle and electrode array in place for a few additional seconds upon completion of injection/pulse delivery to prevent the seepage of vaccine from the site of injection.

3.2 Intramuscular Electroporation of Nonhuman Primates

1. Mix the appropriate amount of antigen encoding DNA plasmid and molecular adjuvant encoding plasmid to obtain the desired ratio of antigen to adjuvant. Usually, between 200 μ L and 1 mL is delivered.
2. Adjust the electroporation parameters according to the manufacturer's suggested values (*see Note 6*).
3. Draw DNA solution into syringe (*see Note 7*).
4. Anesthetize the animal with the appropriate anesthesia or tranquilizer (*see Note 8*).
5. Shave the area over the injection site. The deltoid, biceps, and quadriceps are the most common regions and have been shown to successfully result in immune responses.
6. Position the animal on its back or side. Extend the limb to provide increased access to the muscle. A bent or crooked limb will limit the success of the injection and subsequent electroporation.
7. Insert the needle and syringe into the center of the electrode array (integrated array). Alternatively, some electroporation systems may lack space for the needle and syringe in between the microarray. In this case, the injection must be delivered first, and then the electrode microarray is positioned around the site of injection and the electropulse is delivered. It is useful to mark the site with a dark-colored marker.
8. Align the needle/electrode array along the middle of the muscle. Insert both the needle and electrodes into the muscle.
9. Slowly inject the DNA solution (i.e., between 5 and 10 s) without changing the pressure exerted on the syringe plunger.
10. Administer the electrical pulse. The number of pulses, pulse length, magnitude, and interval are dependent on both the animal and the manufacturer of the electroporation device (*see Note 9*).
11. Retain the needle and electrode array in place for a few additional seconds upon completion of injection/pulse delivery to prevent the seepage of vaccine from the site of injection.

3.3 Intradermal Electroporation of Mice

1. Mix the appropriate amount of antigen encoding DNA plasmid and molecular adjuvant encoding plasmid to obtain the desired ratio of antigen to adjuvant. The maximum volume recommended for intradermal vaccination of mice is 20–25 μ L per mouse (*see Note 5*).

2. Adjust the electroporation parameters according to the manufacturer's suggested values (*see Note 6*).
3. Draw DNA solution into syringe (*see Note 7*).
4. Anesthetize the mouse with the appropriate anesthesia or tranquilizer (*see Note 8*).
5. Position the mouse on its stomach and shave the fur over the lower back (*see Note 10*).
6. Insert the needle and syringe into the center of the electrode array (integrated array). Alternatively, some electroporation systems may lack space for the needle and syringe in between the microarray. In this case, the injection must be delivered first, and then the electrode microarray is positioned around the bleb and the electropulse is delivered.
7. Stretch the skin taut between the thumb and index finger.
8. Align the needle/electrode array along the middle of the shaved patch. Insert both the needle and electrodes into the epidermal region of the skin. Needle should be inserted between 2 and 3 mm into the skin. The needle should be inserted bevel up, parallel to the skin, and then rotated 90°. This results in a shallow delivery of drug to the epidermal layer of the skin. To assist in positioning, a pair of forceps may be used to pinch the skin.
9. Slowly inject the DNA solution (i.e., between 5 and 10 s) without changing the pressure exerted on the syringe plunger (*see Note 11*).
10. Administer the electrical pulse. The number of pulses, pulse length, magnitude, and interval are dependent on both the animal and the manufacturer of the electroporation device (*see Note 9*).
11. Retain the needle and electrode array in place for a few additional seconds upon completion of injection/pulse delivery to prevent the seepage of vaccine from the site of injection.

3.4 Intradermal Injection of Nonhuman Primates

1. Mix the appropriate amount of antigen encoding DNA plasmid and molecular adjuvant encoding plasmid to obtain the desired ratio of antigen to adjuvant. The maximum volume for intradermal injection of nonhuman primates is 100 μ L.
2. Adjust the electroporation parameters according to the manufacturer's suggested values (*see Note 6*).
3. Draw DNA solution into syringe (*see Note 7*).
4. Anesthetize the animal with the appropriate anesthesia or tranquilizer (*see Note 8*).
5. Shave the area over the injection site. For nonhuman primates, the skin covering the back and limbs is considered the optimal site of injection.

6. Insert the needle and syringe into the center of the electrode array (integrated array). Alternatively, some electroporation systems may lack space for the needle and syringe in between the microarray. In this case, the injection must be delivered first, and then the electrode microarray is positioned around the bleb and the electropulse is delivered.
7. Stretch the skin taut between the thumb and the index finger.
8. Align the needle/electrode array along the middle of the shaved patch. Insert both the needle and electrodes into the epidermal region of the skin. The needle should be inserted between 2 and 3 mm into the skin. The needle should be inserted bevel up, parallel to the skin, and then rotated 90°. This results in a shallow delivery of drug to the epidermal layer of the skin. To assist in positioning, a pair of forceps may be used to pinch the skin.
9. Slowly inject the DNA solution (i.e., between 5 and 10 s) without changing the pressure exerted on the syringe plunger (*see Note 11*).
10. Administer the electrical pulse. The number of pulses, pulse length, magnitude, and interval are dependent on both the animal and the manufacturer of the electroporation device (*see Note 9*).
11. Retain the needle and electrode array in place for a few additional seconds upon completion of injection/pulse delivery to prevent the seepage of vaccine from the site of injection.

4 Notes

1. There are several methods for increasing DNA plasmid protein production. Inclusion of Kozak sequences upstream of the start site, or removal of any ATG codon sites in the 5' untranslated region may increase the rate of transcription. Likewise, codon optimization has proven extremely successful in increasing the rate of protein synthesis. Conversely, commercial expression vectors are available. These do not generally require much optimization, although depending on the antigen and model used, they may not be the ideal choice. Careful thought should be given to developing the vaccine plasmid, and it may be necessary to perform preliminary studies to confirm the overall expression and immunogenicity of the DNA vaccine.
2. Incorporation of molecular adjuvants (i.e., cytokines) is not always straightforward. It is important to remember that cytokines are species specific and must often times be designed to

account for this. For cloning purposes, PCR primers should be designed to recognize the most conserved sequences across multiple species.

3. Phosphate-buffered saline is preferable to water, as water can relax the super-coiled state of the DNA plasmid.
4. Shaving of the fur is essential for proper visualization of the injection site. The best electric razors for mice are those with closely spaced teeth. Regular veterinary or dog grooming razors are suitable for larger animals as they do not get tangled in long hair as easily.
5. Allow for dead space within the syringe by preparing enough DNA for $n + 3$ doses. Insulin syringes are preferable because they have little dead space. Tuberculin syringes have about 100 μL of dead space and often develop air bubbles, making it difficult to accurately deliver the appropriate amount of DNA. A volume of 50 $\mu\text{L}/\text{site}$ is the most optimal, as this allows for proper distribution of the vaccine plasmid within the muscle without causing damage to the tissue itself. Additionally, larger volumes may cause the DNA vaccine to leak out of the muscle, limiting the immune response.
6. It may be necessary to perform preliminary studies to determine the optimal electroporation settings, depending on the type of machine and antigen used.
7. Ensure there are no air bubbles present by tapping on the side of the syringe with thumb and expelling air bubble by slowly depressing plunger until only DNA/saline solution is present in syringe.
8. Animals should be anesthetized prior to vaccination, as when awake, they may contract their muscles, thereby squeezing the DNA vaccine out. This also limits the possibility of animals struggling or biting during injection.
9. Good contact is required for the electroporation procedure to work properly. Ensure that electrodes are properly inserted and that a consistent current/resistance is being registered before delivering the pulse. It may be necessary to recruit a helper to work the electropulse generator depending on the model used. Some generators have an available foot pedal that allows a single operator to both align the electrode array and trigger the machine. However, many generators lack this accessory. In this case, it may be too cumbersome for a single person to hold the electrode array in place and work the controls.
10. The thickness of the skin can directly impact the level of plasmid gene expression. Ensure that vaccination sites are of consistent thickness by using a central location and keeping away from the belly of the animal.

11. Intradermal injection should result in a bleb in the skin that persists for several minutes. If this does not appear, or quickly dissipates, the injection has most likely been given subcutaneously. This will result in poor immune responses.

Disclaimer

Opinions, interpretations, conclusions, and recommendations are those of the author and are not necessarily endorsed by the U.S. Army.

References

1. Kuhn JH, Becker S, Ebihara H, Geisbert TW, Johnson KM, Kawaoka Y, Lipkin WI, Negredo AI, Netesov SV, Nichol ST, Palacios G, Peters CJ, Tenorio A, Volchkov VE, Jahrling PB (2010) Proposal for a revised taxonomy of the family *Filoviridae*: classification, names of taxa and viruses, and virus abbreviations. *Arch Virol* 155:2083–2103
2. Feldmann H, Geisbert TW (2011) Ebola haemorrhagic fever. *Lancet* 377:849–862
3. Hart MK (2003) Vaccine research efforts for filoviruses. *Int J Parasitol* 33:583–595
4. Hevey M, Negley D, VanderZanden L, Tammariello RF, Geisbert J, Schmaljohn C, Smith JF, Jahrling PB, Schmaljohn AL (2001) Marburg virus vaccines: comparing classical and new approaches. *Vaccine* 20:586–593
5. Wilson JA, Hevey M, Bakken R, Guest S, Bray M, Schmaljohn AL, Hart MK (2000) Epitopes involved in antibody-mediated protection from Ebola virus. *Science* 287:1664–1666
6. Dye JM, Herbert AS, Kuehne AI, Barth JF, Muhammad MA, Zak SE, Ortiz RA, Prugar LI, Pratt WD (2012) Postexposure antibody prophylaxis protects nonhuman primates from filovirus disease. *Proc Natl Acad Sci U S A* 109:5034–5039
7. Marzi A, Yoshida R, Miyamoto H, Ishijima M, Suzuki Y, Higuchi M, Matsuyama Y, Igarashi M, Nakayama E, Kuroda M, Saijo M, Feldmann F, Brining D, Feldmann H, Takada A (2012) Protective efficacy of neutralizing monoclonal antibodies in a nonhuman primate model of Ebola hemorrhagic fever. *PLoS One* 7:e36192
8. Qiu X, Audet J, Wong G, Pillet S, Bello A, Cabral T, Strong JE, Plummer F, Corbett CR, Alimonti JB, Kobinger GP (2012) Successful treatment of Ebola virus-infected cynomolgus macaques with monoclonal antibodies. *Sci Transl Med* 4:138ra81. doi:[10.1126/scitranslmed.3003876](https://doi.org/10.1126/scitranslmed.3003876)
9. Warfield KL, Olinger G, Deal EM, Swenson DL, Bailey M, Negley DL, Hart MK, Bavari S (2005) Induction of humoral and CD8+ T cell responses are required for protection against lethal Ebola virus infection. *J Immunol* 175:1184–1191
10. Raymond J, Bradfute S, Bray M (2011) Filovirus infection of STAT-1 knockout mice. *J Infect Dis* 204(Suppl 3):S986–S990
11. Roy MJ, Wu MS, Barr LJ, Fuller JT, Tussey LG, Speller S, Culp J, Burkholder JK, Swain WF, Dixon RM, Widera G, Vessey R, King A, Ogg G, Gallimore A, Haynes JR, Heydenburg Fuller D (2000) Induction of antigen-specific CD8+ T cells, T helper cells, and protective levels of antibody in humans by particle-mediated administration of a hepatitis B virus DNA vaccine. *Vaccine* 19:764–778
12. Condon C, Watkins SC, Celluzzi CM, Thompson K, Falo LD Jr (1996) DNA-based immunization by in vivo transfection of dendritic cells. *Nat Med* 2:1122–1128
13. Ledgerwood JE, Hu Z, Gordon IJ, Yamshchikov G, Enama ME, Plummer S, Bailer R, Pearce MB, Tumpey TM, Koup RA, Mascola JR, Nabel GJ, Graham BS, Vrc and Teams VRCS (2012) Influenza virus h5 DNA vaccination is immunogenic by intramuscular and intradermal routes in humans. *Clin Vaccine Immunol* 19:1792–1797
14. Porgador A, Irvine KR, Iwasaki A, Barber BH, Restifo NP, Germain RN (1998) Predominant role for directly transfected dendritic cells in antigen presentation to CD8+ T cells after gene gun immunization. *J Exp Med* 188:1075–1082
15. Rols MP, Delteil C, Golzio M, Dumond P, Cros S, Teissie J (1998) In vivo electrically mediated protein and gene transfer in murine melanoma. *Nat Biotechnol* 16:168–171. doi:[10.1038/nbt0298-168](https://doi.org/10.1038/nbt0298-168)

16. Abdulhaqq SA, Weiner DB (2008) DNA vaccines: developing new strategies to enhance immune responses. *Immunol Res* 42:219–232
17. Laddy DJ, Weiner DB (2006) From plasmids to protection: a review of DNA vaccines against infectious diseases. *Int Rev Immunol* 25:99–123
18. Flingai S, Czerwonko M, Goodman J, Kudchodkar SB, Muthumani K, Weiner DB (2013) Synthetic DNA vaccines: improved vaccine potency by electroporation and co-delivered genetic adjuvants. *Front Immunol* 4:354
19. Aguiar JC, Hedstrom RC, Rogers WO, Charoenvit Y, Sacci JB Jr, Lanar DE, Majam VF, Stout RR, Hoffman SL (2001) Enhancement of the immune response in rabbits to a malaria DNA vaccine by immunization with a needle-free jet device. *Vaccine* 20:275–280
20. Choi AH, Smiley K, Basu M, McNeal MM, Shao M, Bean JA, Clements JD, Stout RR, Ward RL (2007) Protection of mice against rotavirus challenge following intradermal DNA immunization by Biojector needle-free injection. *Vaccine* 25:3215–3218
21. Hartikka J, Bozoukova V, Ferrari M, Sukhu L, Enas J, Sawdey M, Wloch MK, Tonsky K, Norman J, Manthorpe M, Wheeler CJ (2001) Vaxfectin enhances the humoral immune response to plasmid DNA-encoded antigens. *Vaccine* 19:1911–1923
22. Reyes L, Hartikka J, Bozoukova V, Sukhu L, Nishioka W, Singh G, Ferrari M, Enas J, Wheeler CJ, Manthorpe M, Wloch MK (2001) Vaxfectin enhances antigen specific antibody titers and maintains Th1 type immune responses to plasmid DNA immunization. *Vaccine* 19:3778–3786
23. Sedegah M, Rogers WO, Belmonte M, Belmonte A, Banania G, Patterson NB, Rusalov D, Ferrari M, Richie TL, Doolan DL (2010) Vaxfectin enhances both antibody and in vitro T cell responses to each component of a 5-gene *Plasmodium falciparum* plasmid DNA vaccine mixture administered at low doses. *Vaccine* 28:3055–3065
24. Smith LR, Wloch MK, Ye M, Reyes LR, Boutsaboualoy S, Dunne CE, Chaplin JA, Rusalov D, Rolland AP, Fisher CL, Al-Ibrahim MS, Kabongo ML, Steigbigel R, Belshe RB, Kitt ER, Chu AH, Moss RB (2010) Phase I clinical trials of the safety and immunogenicity of adjuvanted plasmid DNA vaccines encoding influenza A virus H5 hemagglutinin. *Vaccine* 28:2565–2572
25. Alexakis T, Boadi DK, Quong D, Groboillot A, O'Neill I, Poncelet D, Neufeld RJ (1995) Microencapsulation of DNA within alginate microspheres and crosslinked chitosan membranes for in vivo application. *Appl Biochem Biotechnol* 50:93–106
26. Herrmann JE, Chen SC, Jones DH, Tinsley-Bown A, Fynan EF, Greenberg HB, Farrar GH (1999) Immune responses and protection obtained by oral immunization with rotavirus VP4 and VP7 DNA vaccines encapsulated in microparticles. *Virology* 259:148–153
27. Kaur R, Rauthan M, Vrati S (2004) Immunogenicity in mice of a cationic microparticle-adsorbed plasmid DNA encoding Japanese encephalitis virus envelope protein. *Vaccine* 22:2776–2782
28. Otten GR, Schaefer M, Doe B, Liu H, Srivastava I, Megede J, Kazzaz J, Lian Y, Singh M, Ugozzoli M, Montefiori D, Lewis M, Driver DA, Dubensky T, Polo JM, Donnelly J, O'Hagan DT, Barnett S, Ulmer JB (2005) Enhanced potency of plasmid DNA microparticle human immunodeficiency virus vaccines in rhesus macaques by using a priming-boosting regimen with recombinant proteins. *J Virol* 79:8189–8200
29. Wang F, He XW, Jiang L, Ren D, He Y, Li DA, Sun SH (2006) Enhanced immunogenicity of microencapsulated multi-epitope DNA vaccine encoding T and B cell epitopes of foot-and-mouth disease virus in mice. *Vaccine* 24:2017–2026
30. Minigo G, Scholzen A, Tang CK, Hanley JC, Kalkanidis M, Pietersz GA, Apostolopoulos V, Plebanski M (2007) Poly-L-lysine-coated nanoparticles: a potent delivery system to enhance DNA vaccine efficacy. *Vaccine* 25:1316–1327
31. Szecsi J, Gabriel G, Edfeldt G, Michelet M, Klenk HD, Cosset FL (2009) DNA vaccination with a single-plasmid construct coding for viruslike particles protects mice against infection with a highly pathogenic avian influenza A virus. *J Infect Dis* 200:181–190

Part V

Host Responses to Viral Hemorrhagic Fever

Chapter 27

Identifying Restriction Factors for Hemorrhagic Fever Viruses: Dengue and Junín

Federico Giovannoni, Jose Rafael Peña Cárcamo, María Laura Morell, Sandra Myriam Cordo, and Cybele C. García

Abstract

Host restriction factors are cellular components that interfere with viral multiplication. They are up-regulated and expressed upon viral infection and in consequence their activity is specific. So far several important restriction factors have been described against diverse viruses. The cellular antiviral mechanisms defined include proteins with the ability to interfere with early steps of viral replication and others that have been shown to block viral morphogenesis. However, other strategies by which the antiviral action is exerted still remain elusive. An additional interesting matter is how viruses also developed ways to by-pass these host-specific obstacles. Thus, unusual cell localization or re-localization represents a frequent virus choice to evade the cellular surveillance. In the present chapter, we summarize methods to identify cell restriction factors, their antiviral activity, and possible subcellular locations where their activity can take place.

Key words Viral restriction, Dengue, Junín, siRNA, Lipid droplets, Antiviral proteins, Microscopy

1 Introduction

The identification and characterization of antiviral genes with the ability to interfere with virus replication has established innate immunity as the first line of antiviral defense. Innate immunity includes host molecules that directly bind viral molecules, such as the cell-intrinsic restriction factors, and host molecules that indirectly induce antiviral responses [1]. This latter “classical” innate immunity includes the induction of cytokines, interferon-stimulated genes (ISG; some of which are also restriction factors), and inflammatory responses that result in virus-specific acquired immune responses [1].

In the beginning, comparative transcriptomics were used to identify genes that were preferentially expressed in restrictive cells relative to susceptible cells [2–4]. Currently, the experimental approach to elucidate the function of a gene *in vivo* is the selective blockage of its expression or activity. This can be achieved by several loss-of-function approaches. Due to their high efficiency

and efficacy and low cost compared with other techniques, high-throughput genome-wide RNAi screening approaches are the most powerful tools for the identification of host factors and pathways involved in any step of a viral replication cycle [5–7]. Upon depletion of a particular host cell factor, virus multiplication can be either reduced or increased. Thus, according to the loss-of-function phenotype, host factors are classified as host dependency factors or host restriction factors. Well-established host restriction factors have been shown to interfere with viral entry, early post-entry steps, viral budding and even to reduce the infectious quality of extracellular released particles [8–9]. On the other hand, viruses have evolved in extraordinary ways to counteract these cell antiviral responses through host-viral interactions and mechanisms involving cellular components such as lipid droplets to evade intrinsic innate immune pathways [10–11]. In immunity, new roles for lipid droplets, not directly linked to lipid metabolism, have been uncovered, showing they act as assembly platforms for specific viruses and as reservoirs for host restriction factors [12–13]. A better understanding of these cellular antiviral mechanisms may open new avenues toward the design of antiviral drugs.

Here, we summarize the methods to identify cell restriction factors for dengue and Junín viruses (DENV and JUNV), evaluating their impact on viral gene expression, virus production, and viral infectivity. Experimental approaches that reveal their subcellular localization and possible interaction with lipid droplets and viral proteins are also included. By means of these approaches it has been possible to characterize cellular proteins with significant antiviral activity against dissimilar viruses. Most of the characterized restriction factors have been first identified in the context of the HIV-1 life cycle [14–16]. However, in the last years, these studies have been expanded to other viruses that have a meaningful impact on human health such as influenza, human cytomegalovirus, West Nile virus, and hepatitis C virus [17–20], and also many studies include hemorrhagic fever viruses [21–24]. From these valuable results the scientific community learned how viral genome replication and expression, together with particle release, could be endogenously restricted by the host cell. Thus, restriction factors have emerged as important topics to address. This productive field of research will help to better understand how these cellular factors may facilitate the design of new drugs and strategies to repress virus infection and spread.

2 Materials

2.1 Cell Cultures and Media

1. Vero cells (ATCC CCL81) cultured at 37 °C in Modified Eagle's Medium (MEM) containing 5% fetal bovine serum (FBS), 100 U penicillin/ml, and 100 µg streptomycin/ml.

2. A549 cells (ATCC CCL-185) cultured at 37 °C in MEM containing 10% fetal bovine serum (FBS), 100 U penicillin/ml, and 100 µg streptomycin/ml.

2.2 Host Factor siRNA-Mediated Knockdown and Plasmid-Mediated Overexpression

1. Lipofectamine 2000 Transfection Reagent (Thermo Scientific).
2. Opti-MEM I Reduced Serum Media (Thermo Scientific).
3. Host-factor-specific siRNA.
4. Scrambled-siRNA.
5. Host-factor cDNA cloned into expression vector.

2.3 Plaque Assay

1. Vero cell cultures.
2. 24-well microplate.
3. 10× Phosphate-buffered saline (PBS): 80 g NaCl; 2 g KCl; 2 g KH₂PO₄; 29 g Na₂HPO₄·12H₂O; bring to 1000 ml with room temperature, deionized water. Working solution: 1:10 dilution in deionized water.
4. MEM is supplemented with 1.5% inactivated calf serum and 50 µg/ml gentamycin.
5. Plaquing medium (PM): MEM with 2% inactivated calf serum containing 50 µg/ml gentamycin, 0.7% methylcellulose.
6. 10% formaldehyde.
7. Crystal violet stain for viral plaques: 0.05% crystal violet in 10% ethanol in water.

2.4 Indirect Immunofluorescence Assays

1. 12 mm diameter cover slips (0.17 mm thickness).
2. Cold methanol (−20 °C), 4% paraformaldehyde (PFA) or 2% PFA and 0.1% Triton X-100 (depending on fixation method).
3. PBS and 5% serum-PBS.
4. Primary antibodies.
5. Fluorescently labeled secondary antibodies.
6. Serum from animals of the same species as the secondary antibody.
7. 4',6-diamidino-2-phenylindole (DAPI) stain that binds DNA in microscopy.
8. Mounting medium: 90% glycerin, 10% 10× PBS pH 9. Add 2.5% 1,4-diazabicyclo[2.2.2]octane (DABCO).
9. Microscope slides.
10. Nail polish.

2.5 Real-Time PCR (RT-PCR)

2.5.1 RNA Extraction

1. TRIzol Reagent (Thermo Scientific).
2. Chloroform.
3. Isopropyl alcohol.

4. 75% ethanol.
5. RNase-free water.
6. Microcentrifuge.
7. UV-Vis spectrophotometer (e.g., NanoDrop, Thermo Scientific) for nucleic acid quantification.
8. 1.5 ml tubes and Ultra-Clear tubes.

2.5.2 *cDNA Synthesis*

1. Random primers (Promega).
2. Nuclease-free water.
3. M-MLV Reverse Transcriptase (Promega).
4. 10 mM dNTP Mix (Promega).

2.5.3 *Quantitative Polymerase Chain Reaction (qPCR)*

1. qPCR mix: 12.5 μ l SYBR Green qPCR master mix (e.g., Roche SYBR Green Master), 0.4 μ l Forward primer (stock solution 50 μ M), 0.4 μ l Reverse primer (stock solution 50 μ M), 9.7 μ l nuclease-free water, 2 μ l cDNA.
2. Primers for amplifying host-factors, viral and housekeeping genes (50 μ M).
3. PCR tubes, plates, and caps or strips depending on the qPCR instrument.

2.6 *Cellular Fractionation*

1. T75 cm² flasks.
2. 15 ml Falcon tubes.
3. 20 μ M cytochalasin B.
4. Protease inhibitor mix (100 \times): 2 μ g/ml leupeptin, 2 μ g/ml pepstatin A, 0.5% aprotinin.
5. Buffer A: 110 mM potassium acetate, 2 mM magnesium, 2 mM dithiothreitol (DTT), 10 mM HEPES pH 7.3.
6. Buffer B: 10 mM potassium acetate, 2 mM magnesium acetate, 2 mM DTT, 5 mM HEPES pH 7.3.
7. 1 M KCl stock solution.
8. 18-, 21-, and 23-G needles.

2.7 *Western Blot*

1. Laemmli Sample Buffer (Bio-Rad).
2. Bis-Tris Pre-Cast gels (Thermo).
3. Molecular weight markers.
4. Polyvinylidene difluoride (PVDF) membrane (Thermo).
5. Semi-Dry Transfer Cell (Bio-Rad).
6. Blotting filter paper (Bio-Rad).
7. Blocking buffer: 5% skimmed milk in Western Blot Wash Buffer.
8. Western blot Wash Buffer: 0.05% Tween-100 in PBS.

9. Peroxidase-conjugated secondary antibodies.
10. Signal development kit (ECL, Bio-Rad).

2.8 Lipid Droplet Staining

1. Distilled water.
2. 4% paraformaldehyde (PFA).
3. 0.1% Triton X-100.
4. Bodipy 493/503 (Thermo).
5. 0.1 M cacodylate buffer.
6. 1.5% OsO₄.
7. 1% thiocarbohydrazide.
8. 1,4-diazabicyclo [2] octane (DABCO).

2.9 Lipid Droplet Isolation

1. T150 cm² flasks.
2. 20 mM Tris.
3. 1 mM EDTA.
4. 1 mM EGTA.
5. 100 mM KCl buffer.
6. Protease inhibitors: 10 µg/ml leupeptin, 10 µg/ml benzamidine, 0.7 µg/ml pepstatin, and 0.1 mmol/l phenylmethylsulfonylfluoride.
7. Sucrose isotonic buffer.
8. Isotonic buffer containing either 1.08 M, 0.27 M, or 0.13 M sucrose.
9. Top buffer: 25 mM Tris HCl, 1 mM EDTA, and 1 mM EGTA.
10. Trichloroacetic acid (TCA).

2.10 Immuno-precipitation Assay

1. Co-immunoprecipitation buffer: 100 mM KCl, 5 mM EDTA, 1 mM DTT, 10 mM HEPES (pH 7.3), 2 µg/ml leupeptin, 2 µg/ml pepstatin A, 0.5% aprotinin.
2. Primary antibody.
3. Protein A or G agarose beads (Sigma-Aldrich).
4. 0.5% Triton X-100.
5. SDS sample buffer.

3 Methods

3.1 Detecting Host Restriction Factors by siRNA-Mediated Knockdown

This protocol should be used to transfect host factor-siRNA into A549 cells using Lipofectamine 2000 in a single well of a 24-well microplate. Add replicates and appropriate controls, including a siRNA-negative control (using siRNA with a scrambled sequence).

1. Plate $4\text{--}5 \times 10^4$ A549 cells per well in 400 μl of complete growth medium. Cell density should be 60% at the time of transfection.
2. Dilute 50 pmol of siRNA in 50 μl of Opti-MEM Medium. Mix gently and incubate for 5 min.
3. Mix Lipofectamine 2000 before use and then dilute 1 μl in 50 μl of Opti-MEM. Mix gently and incubate for 5 min at room temperature.
4. Combine the diluted siRNA and the diluted Lipofectamine 2000 (the total volume should be 100 μl). Mix and incubate for 15–20 min at room temperature.
5. Add the siRNA-Lipofectamine 2000 complexes (100 μl) to the 400 μl of growth medium of the well containing the cells to be transfected.
6. Incubate the cells at 37 °C in a humidified CO₂ incubator for 48 h.
7. Infect cells with DENV or JUNV at a MOI of 0.1.
8. Harvest supernatants or cell monolayers and perform viral quantification assays (*see* Subheadings 3.3–3.5).
9. Compare viral quantification results obtained from host factor-silenced cells and scrambled siRNA-transfected cells.

3.2 Detecting Host Restriction Factors by Plasmid-Mediated Overexpression

This protocol requires having the gene for the protein-of-interest cloned into a mammalian expression vector, such as pcDNA3.1. It should be used to transfect the expression vector into A549 cells using Lipofectamine 2000 in a single well of a 24-well microplate. Add replicates and appropriate controls, including an empty-vector negative control.

1. Plate $6\text{--}8 \times 10^4$ A549 cells per well in 400 μl of complete growth medium. Cell density should be at least 70–80% at the time of transfection.
2. Dilute 0.5 μg of DNA into 50 μl of Opti-MEM. Mix gently and incubate for 5 min.
3. Mix Lipofectamine 2000 before use and then dilute 2 μl in 50 μl of Opti-MEM. Mix gently and incubate for 5 min at room temperature.
4. Combine the diluted DNA and the diluted Lipofectamine 2000 (total volume should be 100 μl). Mix gently and incubate for 15–20 min at room temperature.
5. Add the DNA-Lipofectamine 2000 complexes (100 μl) to the 400 μl of growth medium of the well containing the cells to be transfected.
6. Incubate cells at 37 °C in a humidified CO₂ incubator for 48 h.

7. Infect cells with DENV or JUNV at a MOI of 0.1.
8. Harvest supernatants or cell monolayers and perform viral quantification assays (*see* Subheadings 3.3–3.5).
9. Compare viral quantification results obtained from host factor-overexpressing cells and empty vector-transfected cells.

3.3 Assessing Viral Restriction by Plaque Assay

1. Harvest supernatants from infected cells at 24, 48, and 72 h post infection (p.i.) and freeze them at -80°C until ready to perform plaque assay.
2. Plate $5\text{--}8 \times 10^4$ Vero cells per well in a 24-well microplate. Cell density should be 70–80% on the day of infection.
3. Perform serial tenfold dilutions ($10^{-1}\text{--}10^{-4}$) of the supernatants in MEM (with 1.5% serum).
4. Infect Vero cells with 100 μl of each dilution. Incubate for 1 h at 37°C .
5. Remove the inoculum and wash three times with PBS.
6. Add 1 ml of PM to each well.
7. Incubate cells at 37°C for 6–7 days, until PFU are clearly visible.
8. Fix cells by adding 1 ml of 10% formaldehyde per well.
9. Stain the microplate with crystal violet solution.
10. Count plaque-forming units (PFU) and determine the virus titer (PFU/ml) as $\text{PFU}/(\text{inoculum volume} \times \text{dilution})$.

3.4 Assessing Viral Restriction by Indirect Immunofluorescent Staining of Virus

1. Grow cells on coverslips in a 24-well microplate. Proceed with Subheading 3.1 or 3.2, steps 1–7.
2. At 24, 48, and 72 h p.i., remove growth medium and wash cells three times with PBS.
3. Fix cells with methanol for 10 min at -20°C . Wash three times with PBS and dry for 10 min.
4. Block with 5% serum-PBS from animals of the same species the secondary antibody was raised and incubate for 30 min.
5. Incubate with the primary antibody against a major viral protein. Refer to the antibody datasheet for details about incubation time and concentration.
6. Wash three times with PBS.
7. Incubate with secondary antibody. Refer to the antibody datasheet for details about incubation time and concentration.
8. Wash three times with PBS.
9. Stain cell nuclei with DAPI for 5 min at room temperature.
10. Wash three times with PBS.
11. Wash with water to remove residual salts of PBS.

12. Mount coverslips with a drop of mounting medium on a microscope slide.
13. Seal coverslips with nail polish.
14. Acquire images following microscope manufacturer's recommendations.
15. Count fluorescent cells using FIJI.
16. Download FIJI software from <http://FIJI.sc/>; FIJI is a software based on Image J plus different plugins. FIJI was developed and it is supported by the US NIH.
17. Download and install Cell Counter Plugin for FIJI (<http://rsbweb.nih.gov/ij/plugins/cell-counter.html>).
18. Open the image to be analyzed in FIJI.
19. If the images acquired using the microscope are 8-bit grayscale, then an overlay should be created. If the images acquired are colored, proceed to **step 21**.
20. Select Image → Color → Merge Channels. In the Merge Channels box, select the appropriate fluorescent images in the Blue channel (DAPI) and the Red or Green channels (viral antigen). Select "Create Composite" and click "OK."
21. Select Image → Type → RGB Color.
22. Run the Cell Counter Plugin. Go to Plugins → Cell counter.
23. In the cell counter window, click Initialize and select "Type 1."
24. Count every single DAPI-stained nucleus in the image by clicking over it.
25. Select "Type 2," and count every single antigen-expressing cell by clicking over it.
26. The total number of cells counted for "Type-1" (DAPI) and "Type-2" (viral antigen) will be shown in the cell counter Window. With this information, calculate the percentage of viral antigen-expressing cells.

3.5 Assessing Viral Restriction by Real-Time PCR of Viral RNA

3.5.1 RNA Extraction

1. Proceed with Subheading **3.1** or **3.2**, **steps 1–7**.
2. At 24, 48, and 72 h p.i., remove growth medium and wash the cells three times with PBS.
3. Lyse cell monolayers directly in the culture dish by adding of TRIzol Reagent. 1 ml of TRIzol should be used per 10 cm² of culture dish area. Tissues or suspension cells may require additional steps.
4. Pipette up and down several times and transfer samples to 1.5 ml tubes.
5. Incubate the samples for 5 min at room temperature.

6. Add 0.2 ml of chloroform per 1 ml of TRIzol, cap tubes, and shake by hand for 15 s.
7. Incubate at room temperature for 3 min.
8. Centrifuge at $14,000 \times g$ for 2 min at 2–8 °C.
9. Transfer the aqueous phase to new 1.5 ml tubes. Ultra-Clear 1.5 ml tubes are best. Avoid transferring the interphase or the phenol-chloroform (red) phase.
10. Add 0.5 ml of 100% isopropyl alcohol per 1 ml of TRIzol.
11. Incubate samples at room temperature for 10 min.
12. Centrifuge at $14,000 \times g$ for 15 min at 2–8 °C.
13. A gel-like pellet should be visible. Remove the supernatant and wash the RNA with 1 ml of 75% ethanol per 1 ml of TRIzol.
14. Vortex for 3 s.
15. Centrifuge at $10,000 \times g$ for 5 min at 2–8 °C.
16. Air-dry the pellet for 10 min.
17. Dissolve RNA in 50 μ l of RNase-free water.
18. Determine RNA yield by using spectrophotometer readings at 260/280 nm.
19. Store at –70 °C.

3.5.2 cDNA Synthesis

1. In a sterile RNase-free 1.5 ml tube add: 1 μ g RNA, 1 μ g of random primers and nuclease-free water to the final volume of 10 μ l.
2. Incubate for 5 min at 70 °C.
3. Cool on ice for 5 min.
4. Add the following components: 5 μ l RT-Buffer 5 \times , 2.5 μ l dNTPs 10 mM, 1 μ l M-MLV Reverse Transcriptase (200 units), 6.5 μ l nuclease-free water.
5. Mix by pipetting up and down a few times.
6. Incubate for 1–2 h at 42 °C.

3.5.3 Quantitative Real-Time PCR (qRT-PCR)

1. In addition to assessing viral restriction by noting changes in amounts of viral RNA, this protocol can also be used to quantify the expression of a host factor by using specific primers. It could be useful for studying host factor expression in virus-infected cells or to validate gene silencing and overexpression experiments (*see* Subheadings 3.1 and 3.2). Whether designing a new pair of primers or obtaining their sequence from the literature, always check specificity using Primer-Blast (<http://www.ncbi.nlm.nih.gov/tools/primer-blast/>)
2. For each sample to be analyzed, two reactions should be prepared: one of them including the gene-of-interest-specific

primers and the other one including housekeeping-gene-specific primers.

3. Run the qPCR according to the instrument's manufacturer's instructions.
4. Determine the PCR cycle at which double-stranded nucleic acids begin to increase in fluorescence above baseline; this is called the Threshold Cycle or C_T . $\Delta C_T = C_T$ of host-factor gene $- C_T$ housekeeping gene. To determine the relative expression of a restriction factor in infected cells versus its expression in uninfected cells: $\Delta\Delta C_T = \Delta C_T$ of infected cells $- \Delta C_T$ of uninfected cells. The relative change in expression or Fold Change of Expression = $2^{\Delta\Delta C_T}$.

**3.6 Subcellular
Localization of Viral
Restriction Factor
by Indirect
Immunofluorescence
of Nuclei and Cytoplasm**

1. Plate $5-8 \times 10^4$ cells on coverslips per well in a 24-well microplate. Cell density should be 70–80% on the day of infection.
2. Infect cells with DENV or JUNV at a MOI of 0.1. Include noninfected controls.
3. At 24 or 48 h p.i., remove growth medium and wash cells with PBS.
4. Fix cells with 4% PFA for 10 min and wash three times with PBS. Cell confluence should not be higher than 80–90% on the day of fixation.
5. Permeabilize cells with 0.1% TX-100/PBS for 15 min.
6. Wash three times with PBS.
7. Block with 5% serum-PBS from animals of the same species used to raise the secondary antibody and incubate for 30 min.
8. Incubate with the primary antibody against the host-factor. Refer to the antibody datasheet for details about incubation time and concentration.
9. Wash three times with PBS.
10. Incubate with the secondary antibody. Refer to the antibody datasheet for details about incubation time and concentration.
11. Repeat **steps 8–10** with the primary antibody against a viral component and the appropriate secondary antibody.
12. Wash three times with PBS.
13. Stain cell nuclei with DAPI for 5 min at room temperature.
14. Wash three times with PBS.
15. Wash with water to remove residual salts of PBS.
16. Mount coverslips with a drop of mounting medium on a microscope slide.
17. Seal coverslips with nail polish.
18. Acquire images following microscope manufacturer's recommendations.

19. Compare expression pattern of host factor between noninfected and virus-infected cells. Host factor expression pattern may be affected immediately after infection. Therefore, a time-course study is usually needed that covers different time-points p.i.

3.7 Localization of Virus Restriction Factor by Indirect Immunofluorescent Surface Staining

1. Plate $5-8 \times 10^4$ cells on coverslips per well in a 24-well microplate. Cell density should be 70–80% on the day of infection.
2. Infect cells with DENV or JUNV at a MOI of 0.1.
3. At 24 or 48 h p.i., remove growth medium and wash cells with PBS.
4. Block with 5% serum-PBS from animals of the same species used to raise the secondary antibody, and incubate for 30 min.
5. Incubate with the primary antibody against the host-factor. Refer to the antibody datasheet for details about incubation times and concentration.
6. Wash three times with PBS.
7. Fix cells with 2% formaldehyde for 5–10 min and wash three times with PBS.
8. Continue with protocol in Subheading 3.6, steps 10–19.

3.8 Obtaining Cytoplasmic and Nuclear Cell Fractions

1. Trypsinize cells (1×10^7 cells grown in a T75 flask).
2. Wash cells with cold PBS and transfer them to 15 ml Falcon tubes.
3. Centrifuge for 5 min at $1500 \times g$.
4. Resuspend cells in 5 ml of buffer A.
5. Centrifuge for 5 min at $1500 \times g$ and resuspend cells with 20 μ M cytochalasin B in 5 ml of buffer B. Add protease inhibitor mix so that it is 1% of the suspended volume.
6. Incubate cells on ice for 10 min.
7. Passage cells through 18-, 21-, and 23-G needles. Add KCl to a final concentration of 100 mM.
8. Centrifuge the lysate at $1500 \times g$ for 15 min at 4 °C. The resulting supernatant and pellet are the cytoplasmic and nuclear fractions, respectively.
9. Further fraction analysis can be performed through Western Blot (Subheading 3.9).

3.9 Western Blot Identification of Restriction Factors

1. Prepare cytoplasmic fraction samples for Western blot by mixing 3 volumes of supernatant obtained in Subheading 3.8, step 8 and 1 volume of 4 \times Laemmli sample buffer. Boil for 5 min.
2. Prepare nuclear fraction samples for Western Blot by resuspending the pellet from Subheading 3.8, step 8 in 50 μ l 1 \times Laemmli sample buffer. Boil for 5 min.

3. Prepare an acrylamide gel for electrophoresis, transfer, and antibody staining. Select the gel percentage according to the size of the protein of interest. SDS-Page precast gels can be used.
4. Load equal amounts of protein into the wells of an SDS-PAGE gel along with a molecular weight marker.
5. Run the gel for 1–2 h at 100 V.
6. Cut a PVDF membrane to the appropriate size of the gel.
7. Activate PVDF membrane with methanol for 1 min and rinse with transfer buffer.
8. Transfer proteins from the gel to a PVDF membrane using available equipment and the manufacturer's instructions.
9. Place a pre-wetted sheet of thick filter paper onto the anode of a semi-dry electrophoretic transfer cell. Remove all air bubbles.
10. Place the pre-wetted PVDF membrane on the top of the filter paper and remove bubbles.
11. Place the gel on the top of the PVDF membrane and remove any bubbles.
12. Place a pre-wetted sheet of thick filter paper on the top of the gel and remove any bubbles.
13. Place the cathode onto the stack and plug the unit to a power supply.
14. Turn on the power supply. Transfer is usually performed for 30–60 min at 15–25 V.
15. Block the membranes with blocking buffer for 1 h at 37 °C.
16. Incubate overnight at 4 °C with appropriate dilutions of primary antibody in blocking buffer. Check the antibody data-sheet for detailed information.
17. Wash three times, 5 min each time, with Western Blot Wash Buffer.
18. Incubate for 1 h at 37 °C with the appropriate dilution of peroxidase-conjugated secondary antibody.
19. For signal development, follow the kit manufacturer's recommendations (ECL, Bio-Rad).

3.10 Lipid Droplets (LDs) Staining

1. Grow cells on coverslips in a 24-well microplate.
2. Infect cells with DENV or JUNV at a multiplicity of infection (MOI) of 0.1.
3. At 24 and 48 h p.i., remove growth medium.
4. Wash the cells three times with PBS.
5. For cell fixing, 4% PFA is recommended instead of methanol because the latter disrupts LDs.

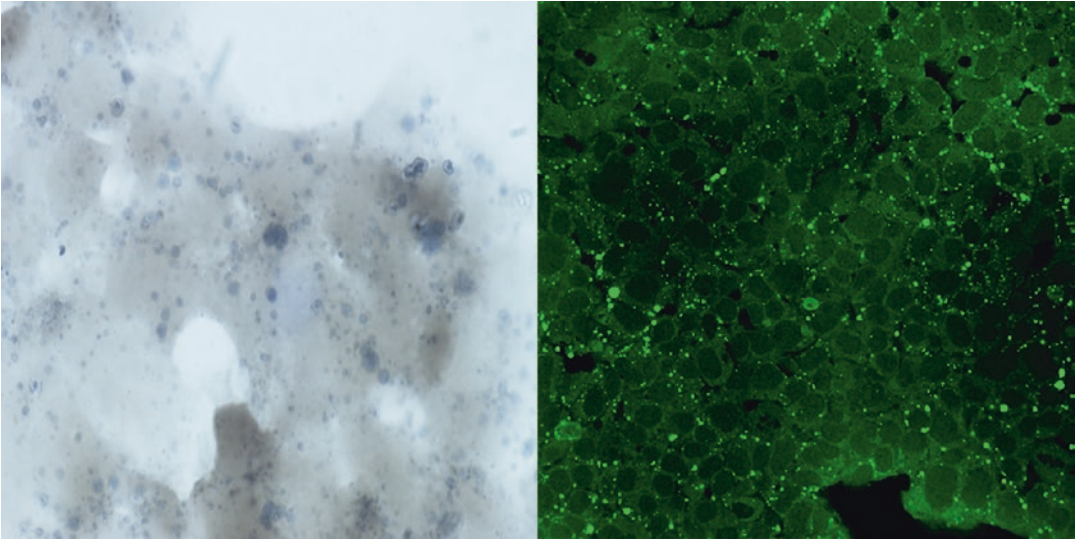


Fig. 1 Lipid Droplets staining with OsO_4 (*left*) and Bodipy (*right*) seen with bright-field and confocal microscopy, respectively. Magnification: 1000 \times and 600 \times respectively

6. Wash three times with PBS.
7. Permeabilize cells with 0.1% Triton X-100 for 10 min at room temperature.
8. Wash three times with PBS and proceed to stain (Subheading [3.10.1](#) or [3.10.2](#)).

3.10.1 Bodipy Staining

Bodipy consists of a fluorescent probe that is observed by exciting it with a red laser, so LDs are seen like green particles (Fig. 1).

1. Stain samples with 1 μM Bodipy 493/503 for 15 min.
2. Wash three times for 5 min with PBS.
3. Mount samples in a glycerol solution containing DABCO for further analyses (Subheading [3.10.3](#)).

3.10.2 OsO_4 Staining

OsO_4 is a crystal oxide that reacts with lipids; LDs are seen like dark dots, darker than cells (Fig. 1).

1. Rinse in 0.1 M cacodylate buffer.
2. Incubate with 1.5% OsO_4 for 40 min.
3. Rinse in water and immerse in 1% thiocarbohydrazide for 5 min.
4. Rinse in 0.1 M cacodylate buffer.
5. Incubate in 1.5% OsO_4 for 5 min.
6. Rinse in distilled water, allow drying and mount samples for further analyses (Subheadings [3.10.3](#) and [3.10.4](#)).

3.10.3 Image Acquisition and Calibration for LDs Quantification

1. Load sample slide onto the stage of the microscope.
2. Place highest power objective and observe sample slide.
3. Select red laser from confocal microscope for Bodipy staining or use bright-field for OsO₄ staining.
4. Acquire images of 20 different fields selected randomly.
5. Set the scale. Go to Image → Show Info. Search for inches-pixels (value between parentheses) equivalency under “Width” or “Height.”
6. Transform inches value to a more suitable unit of length (μm, nm, pm, etc.).
7. Go to Analyze → Set scale. Complete “Distance in pixels” with the number of pixels equivalent to the reference unit of length chosen.
8. Complete “Known Distance” with 1.00, so the number of pixels set on **step 7** equals 1.00 of the reference unit length and be coherent when completing other fields. Click Ok.
9. Set the scale bar. Go to Analyze → Tools → Scale Bar.
10. Complete “Width” with the length you want the scale bar to show. Complete remaining fields as preferable (*see Note 1*). Click Ok.
11. Go to Image → Overlay → Flatten. It will open another window with the same picture (*see Note 2*).
12. Go to File → Save as → Tiff.

3.10.4 Image Analysis: LDs Quantification by Use of Fiji Software

A binary image, meaning a black and white one, is required to do an automatic particle analysis. A threshold is set to differentiate the background from the objects suitable for analysis, then create a mask and subtract it from the original image (Fig. 2).

1. Go to File → Open. Open the image to be quantified. For grayscale images go to Image → Type → RGB to 8-bit.
2. Duplicate the image to keep the original. Go to Image → Duplicate.
3. Select the duplicated image by clicking on it. Go to Image → Color → Split Channels for color images and select the one correspondent to the fluorophore used.
4. Go to Image → Adjust → Threshold.
5. Select on “Method”: Default.
6. Select red as the color LDs will be marked.
7. Adjust minimum and maximum values with top and down sliders respectively, to select or deselect LDs based on their size. Uncheck “Dark background” box for grayscale images. Apply (*see Note 3*).
8. Improve the quality of the mask. Go to Process → Binary → Dilate.

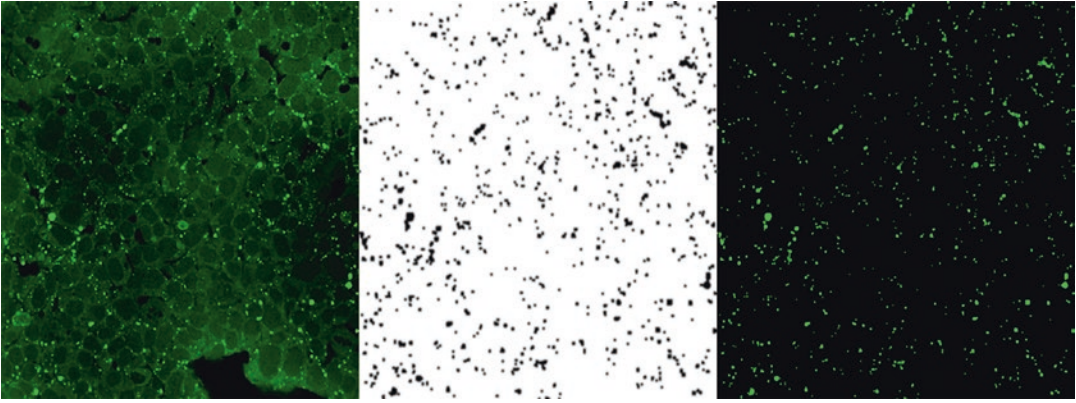


Fig. 2 Background subtraction between Bodipy staining (*left*) and a Mask (*center*) through use of FIJI software. Image of Lipid Droplets without background (*right*) allows an accurate quantification

9. Go to Process → Smooth.
10. Go to Process → Image Calculator.
11. Select on “Image 1,” original image from **step 1**.
12. Select on “Operation,” subtract.
13. Select on “Image 2,” binary mask (black and white image you obtained from **step 9**). Images from **steps 1** and **9** must be opened simultaneously, otherwise subtraction cannot be done. Invert order for grayscale images (*see Note 4*).
14. Go to Image → Color → Split Channels for color images and select the one correspondent to the fluorophore used.
15. Set a new threshold. Go to Image → Adjust → Threshold.
16. Repeat **steps 5** and **6**.
17. Repeat adjustment made on **step 7** (*see Note 5*).
18. Check “Dark background” box for color images.
19. Go to Process → Binary → Fill holes. It stains big particles completely red when they were only marked with a dot.
20. Go to Process → Binary → Watershed. Make a physical division between two particles that are too close together and separate them to be counted as two independent LDs.
21. Set the measurements to analyze. Go to Analyze → Set measurements.
22. Check the following boxes: Area, Min & Max gray value, Integrated density, Area fraction, Mean gray value, Perimeter, Limit to threshold.
23. Do the automatic analysis. Go to Analyze → Analyze Particles.
24. Complete on “Size,” range of sizes of LDs you want to count. Notice that the image is calibrated, so it measures area in the unit length you set in Subheadings [3.10.3](#) and [3.10.4](#).

25. Set in “Circularity” values from 0.50 to 1.00. Choose values closer to 1.00 to be stricter and consider particles that are a perfect circle (*see Note 6*).
26. Check the following boxes: Display Results, Exclude on edges, and Summarize.
27. Extract the total number of LDs. Look in Summary for the “Count” column.
28. Obtain the average area of LDs. Look in Summary for the “Average size” column.

3.11 LDs Isolation

Lipid droplets can be isolated by subcellular fractionation based on the buoyancy property of these lipid-rich organelles in sucrose gradients. Isolation and purification of LDs is a useful method to measure the association of viral and cellular factors with LDs.

1. Grow cells at 90% confluence in a T150 cm² flask.
2. Infect cells with DENV or JUNV at a MOI of 0.1.
3. At 24 and 48 h p.i. scrape cell monolayers in 3 ml of disruption buffer containing a protease inhibitor mix.
4. Disrupt cell suspension by nitrogen cavitation at 700 ψ for 5 min at 4 °C.
5. Collect in an equal volume of buffer containing 1.08 M sucrose.
6. Centrifuge the homogenates at 1500 $\times g$ for 10 min to remove nuclei.
7. Transfer the supernatant to a 12 ml ultracentrifugation tube.
8. Overlay sequentially 2 ml each of 0.27 M sucrose buffer, 0.13 M sucrose buffer, and top buffer (25 mM Tris-HCl, 1 mM EDTA, and 1 mM EGTA).
9. Centrifuge gradient at 250,000 $\times g$ for 1 h at 4 °C.
10. Collect fractions from the top containing: LD, cytosol, microsomal fraction, and pellet.
11. Precipitate proteins from these fractions overnight with TCA.
12. Wash with cold acetone, and analyze precipitated proteins by Western blot (Subheading 3.9) to detect LD-associated proteins (e.g., adipose differentiation-related protein) or cytosolic-associated proteins (e.g., transferrin).

3.12 Host Factor-Viral Protein Interactions

3.12.1 Assessing Host Factor-Viral Protein Interactions by Confocal Imaging

Two antigens should be stained: the host restriction factor and a virus component whose colocalization you would like to analyze. Therefore, two primary antibodies from animals of different host species are required (e.g., mouse and rabbit). Fluorescently labeled secondary antibodies should be chosen taking into account available microscope filter sets. Alexa Fluor 488 and Alexa Fluor 568 labeled antibodies are commonly used in imaging applications.

1. Grow cells on coverslips in a 24-well microplate. Cell confluence should not be higher than 80–90% on the day of fixation, so the number of cells to be seeded will have to be adjusted depending on the different time points post infection to be analyzed.
2. The next day, infect cells with DENV or JUNV at a MOI of 1.
3. At different time points (12, 24, 48, and 72 h p.i.), remove growth medium and wash cells with PBS.
4. Fix cells with 4% PFA for 10 min and wash three times with PBS.
5. Permeabilize with 0.1% TX-100/PBS for 15 min.
6. Wash three times with PBS.
7. Block with 5% serum-PBS from animals of the same species the secondary antibody was raised and incubate for 30 min.
8. Incubate with a mix of the primary antibody against the host factor and primary antibody against a viral component. Refer to the antibodies datasheets for details about incubation time and concentration.
9. Wash three times with PBS.
10. Incubate with the appropriate mix of secondary antibodies. Refer to the antibodies datasheets for details about incubation time and concentration.
11. Wash three times with PBS.
12. Stain cell nuclei with DAPI for 5 min at room temperature.
13. Wash three times with PBS.
14. Wash with water to remove residual salts of PBS.
15. Mount coverslips with a drop of mounting medium on a microscope slide.
16. Seal coverslips with nail polish.
17. Collecting images will largely depend on available instrument and software. For basic and general details regarding image acquisition, *see* [25].

3.12.2 Analysis of Confocal Images

1. Open the images to be analyzed in FIJI.
2. If the image has more than two channels, split them into separate images. Go to Image → Color → Split Channels. Keep open only the two windows corresponding to the channels on which the analysis will be performed (e.g., red and green).
3. Select the region of interest (ROI) in one of the images with any of the FIJI selection tools (rectangular, oval, freehand, etc.).

4. Run the Coloc 2 plugin. Go to Analyze → Colocalization → Coloc 2.
5. In the plugin's menu, assign one of the images to be analyzed to the channel 1 and the other one to the channel 2 using the first two drop down lists.
6. In the third drop down list ("ROI or Mask"), choose the image in which the ROI was selected on **step 3**.
7. Choose the algorithms to be run and the statistics to be calculated. For beginners, we suggest running default options.
8. Click OK and wait for the analysis to be completed. The results window will open showing statistics and images.
9. Look for Pearson's *R* value. This value describes correlation between the pattern overlap in the two channels. Pearson's *R* values range from -1 (two images whose overlap is perfectly inversed) to 1 (two images whose overlap is perfectly correlated). Values near zero correspond to an uncorrelated overlap pattern.

*3.12.3 Assessing Host
Factor-Viral Protein
Interaction
by Immunoprecipitation
Assay*

1. Proceed with cell fractionation as described in Subheading [3.8](#) to obtain cell lysates.
2. Resuspend the nuclear pellet in 1 ml of coimmunoprecipitation buffer.
3. Add primary antibody to 200 μ l of the cell lysates. Refer to the antibody datasheet to find out the recommended concentration.
4. Incubate overnight with gentle agitation at 4 °C.
5. Add protein A or G agarose beads (20 μ l of 50% bead slurry).
6. Incubate with rotary agitation for 2 h at 4 °C.
7. Centrifuge for 30 s at 4 °C.
8. Wash pellet three times with 500 μ l of coimmunoprecipitation buffer and 0.5% Triton X-100.
9. Resuspend pellet with 20 μ l 3 \times SDS sample buffer.
10. Centrifuge for 30 s.
11. Boil samples for 5 min and centrifuge for 1 min at 14,000 $\times g$.
12. Load samples (20 μ l) on a SDS-PAGE gel and analyze by Western blotting (Subheading [3.9](#)).

4 Notes

1. Check the Overlay box. It adds the scale bar to the image without altering the quality of the pixels around it.
2. Flatten, incorporates the scale bar into the image in one single file so that when you save it, you save the picture along with it.

Also, if you are doing the quantification on various images taken under the same magnification you can set the same scale for all by checking the “Global” box.

3. Selecting LDs for OsO₄ staining is more complicated than for Bodipy but it is preferable to choose bigger particles and not lose the smallest ones in this step and be more selective on particle analysis and restrict size after the second setting of thresholding.
4. When doing the subtraction operation follow the steps in order and choose the original image first and the binary mask second for color images. Follow inverse order for grayscale images. This way the background is removed and the chosen particles remained in the new image.
5. Setting of the second threshold is critical because these values determine which particles are marked in red and hence considered LDs. This step is crucial since it differentiates very small particles (dots almost) that could be considered background from real LDs. Make sure to set the right values since the particle analysis will be based on this.
6. Circularity is a parameter that measures ratio between area and perimeter of the particle. So, the closer the value to 1.00, the rounder the particle is. Considering that LDs are round, a minimal value between 0.50 and 0.80 shall work fine. $\text{Circularity} = 4\pi \times \text{Area} / \text{Perimeter}^2$.

References

1. Yan N, Chen ZJ (2012) Intrinsic antiviral immunity. *Nat Immunol* 13(3):214–222
2. Bowick GC, Fennewald SM, Elsom BL, Aronson JF, Luxon BA, Gorenstein DG, Herzog NK (2006) Differential signaling networks induced by mild and lethal hemorrhagic fever virus infections. *J Virol* 80:10248–10252
3. Müller S, Geffers R, Günther S (2007) Analysis of gene expression in Lassa virus-infected HuH-7 cells. *J Gen Virol* 88:1568–1575
4. Djavani M, Crasta OR, Zhang Y, Zapata JC, Sobral B, Lechner MG, Bryant J, Davis H, Salvato MS (2009) Gene expression in primate liver during viral hemorrhagic fever. *Virology* 6(20):1–20
5. Panda D, Das A, Dinh PX, Subramaniam S, Nayak D, Barrows NJ, Pearson JL, Thompson J, Kelly DL, Ladunga I, Pattnaik AK (2011) RNAi screening reveals requirement for host cell secretory pathway in infection by diverse families of negative-strand RNA viruses. *Proc Natl Acad Sci U S A* 108(47):19036–19041
6. Panda D, Cherry S (2015) A genome-wide RNAi screening method to discover novel genes involved in virus infection. *Methods* 91:75–81
7. Lavanya M, Cuevas CD, Thomas M, Cherry S, Ross SR (2013) siRNA screen for genes that affect Junin virus entry uncovers voltage-gated calcium channels as a therapeutic target. *Sci Transl Med* 5(204):204ra131
8. Perez-Caballero D, Zang T, Ebrahimi A, Mcnatt MW, Gregory DA, Johnson MC, Bieniasz PD (2009) Tetherin inhibits HIV-1 release by directly tethering virions to cells. *Cell* 139:499–511
9. Tartour K, Appourchaux R, Gaillard J, Nguyen XN, Durand S, Turpin J, Beaumont E, Roch E, Berger G, Mahieux R, Brand D, Roingard P, Cimarelli A (2014) IFITM proteins are incorporated onto HIV-1 virion particles and negatively imprint their infectivity. *Retrovirology* 11:103
10. Hinson ER, Cresswell P (2009) The antiviral protein, viperin, localizes to lipid droplets via its N-terminal amphipathic alpha-helix. *Proc Natl Acad Sci U S A* 106(48):20452–20457
11. Helbig KJ, Carr JM, Calvert JK, Wati S, Clarke JN et al (2013) Viperin is induced following

- dengue virus type-2 (DENV-2) infection and has anti-viral actions requiring the C-terminal end of viperin. *PLoS Negl Trop Dis* 7:e2178
12. Jiang X, Chen ZJ (2011) Viperin links lipid bodies to immune defense. *Immunity* 34(3):285–287. doi:[10.1016/j.immuni.2011.03.012](https://doi.org/10.1016/j.immuni.2011.03.012)
 13. Saka HA, Valdivia R (2012) Emerging roles for lipid droplets in immunity and host-pathogen interactions. *Annu Rev Cell Dev Biol* 28:411–437. doi:[10.1146/annurev-cellbio-092910-153958](https://doi.org/10.1146/annurev-cellbio-092910-153958)
 14. Bieniasz PD (2003) Restriction factors: a defense against retroviral infection. *Trends Microbiol* 11(6):286–291
 15. Harris RS, Hultquist JF, Evans DT (2012) The restriction factors of human immunodeficiency virus. *J Biol Chem* 287:40875–40883
 16. Simon V, Bloch N, Landau NR (2015) Intrinsic host restrictions to HIV-1 and mechanisms of viral escape. *Nat Immunol* 16(6):546–553
 17. Wang X, Hinson ER, Cresswell P (2007) The interferon-inducible protein viperin inhibits influenza virus release by perturbing lipid rafts. *Cell Host Microbe* 2:96–105
 18. Seo JY, Yaneva R, Hinson ER, Cresswell P (2011) Human cytomegalovirus directly induces the antiviral protein viperin to enhance infectivity. *Science* 332:1093–1097
 19. Lazear HM, Diamond MS (2015) New insights into innate immune restriction of West Nile virus infection. *Curr Opin Virol* 11:1–6
 20. Zhou LY, Zhang LL (2016) Host restriction factors for hepatitis C virus. *World J Gastroenterol* 22(4):1477–1486
 21. Jouvenet N, Neil SJD, Zhadina M, Zang T, Kratovac Z, Lee Y, McNatt M, Hatzioannou T, Bieniasz PD (2009) Broad-spectrum inhibition of retroviral and filoviral particle release by tetherin. *J Virol* 83:1837–1844
 22. Sakuma T, Noda T, Urata S, Kawaoka Y, Yasuda J (2009) Inhibition of Lassa and Marburg virus production by tetherin. *J Virol* 83:2382–2385
 23. Pan XB, Han JC, Cong X, Wei L (2012) BST2/tetherin inhibits dengue virus release from human hepatoma cells. *PLoS One* 7(12):e51033
 24. Giovanni F, Damonte E, García C (2015) Cellular promyelocytic leukemia protein is an important dengue virus restriction factor. *PLoS One* 10(5):e0125690
 25. North AJ (2006) Seeing is believing? A beginners' guide to practical pitfalls in image acquisition. *J Cell Biol* 172(1):9–18

Determining the Virus Life-Cycle Stage Blocked by an Antiviral

Claudia S. Sepúlveda, Cybele C. García, and Elsa B. Damonte

Abstract

Among the members of the *Arenaviridae* family, Junín virus and Lassa virus represent important human health threats generating annual outbreaks of severe human hemorrhagic fever (HF) in endemic areas of Argentina and Western Africa, respectively. Given the lack of a specific and safe chemotherapy, the search for effective antiviral compounds is a continuous demanding effort. During the last two decades, academic research studies originated important results identifying novel molecules to be considered for further in vivo characterization. This chapter summarizes experimental in vitro approaches used to determine the possible mechanism of action of these antiviral agents.

Key words Arenaviruses, Antiviral compound, Antiviral mechanism

1 Introduction

Current anti-arenaviral therapies are limited to the use of immune convalescent plasma with defined doses of JUNV-neutralizing antibodies for Argentinian hemorrhagic fever patients [1], or the guanosine analog ribavirin (1- β -D-ribofuranosyl-1,2,4-triazole-3-carboxamide) (RIB), effective by intravenous administration against Lassa fever in Western Africa [2]. However, several drawbacks are associated with both treatments: plasma transfusion is not effective in advanced cases and 10% of JUNV infected treated patients develop late neurological complications [1]. Furthermore, RIB is not efficient in advanced LASV infections and it can also induce adverse side effects such as thrombocytopenia, anemia, and birth defects [2–4].

Arenaviral therapies have been historically ignored by pharmaceutical companies due to their limited profitability; thus, mainly academic research efforts have progressed in this area (Table 1). Several groups have been focused on arenaviral antivirals during the last few years, targeting the viral entry or a specific viral protein [5–8]. Antivirals against specific viral proteins have limited utility

Table 1
Main anti-arenaviral agents assessed in the last two decades

Agent	Virus	References
ST-193, ST-194	GTOV, JUNV, LASV, MACV, TCRV	[5, 20–23]
Iminodiacetic acid- and pyrrolidine-based peptidomimetics	GTOV, JUNV, LASV, MACV	[6, 24]
Amphipathic DNA polymers (APs)	LCMV	[25]
Aryl methyldiene rhodanine derivative	JUNV	[26]
mAb	JUNV	[27]
Azoic compounds, hydrazide derivatives	JUNV, LCMV, TCRV	[28, 29]
Thiuram and aromatic disulfides	JUNV, LCMV, TCRV	[28, 30–34]
Acridones	JUNV, LCMV, TCRV	[9, 10]
Mycophenolic acid (MPA)	JUNV	[10]
A3	JUNV, LCMV	[35]
Brassinosteroids	JUNV	[36, 37]
Dehydroepiandrosterone, epiandrosterone	JUNV	[38]
Azoles	JUNV, TCRV	[39, 40]
Favipiravir	JUNV, PICV, TCRV	[41, 42]
siRNA	JUNV, LASV	[43, 44]
PTAP Inhibitors	JUNV	[45]
Peptide-conjugated morpholino oligomers	JUNV, LCMV, PICV, TCRV	[46]
Oxime, piperazyl and quinoline derivatives, tetrandrine,	Broad-spectrum	[47]
Valproic acid	LCMV	[48]
SKI-1/S1P protease inhibitor	LCMV, JUNV	[49]

Our lab findings are highlighted in bold

GTOV Guanarito virus, JUNV Junín virus, LASV Lassa virus, LCMV lymphocytic Choriomeningitis virus, MACV Machupo virus, PICV Pichindé virus, TCRV Tacaribe virus

for specific viral infections and are subject to viral escape. More recently, efforts have been concentrated on characterizing broad-spectrum antivirals, most of them targeting cellular proteins. Our finding and characterization of molecules with broad-spectrum inhibitory action and minor cellular toxicity, such as mycophenolic acid and acridones, represent novel and promising alternatives for chemotherapy [9–11], although further in vivo evaluation is necessary to renew the consideration of this class of metabolic inhibitors against arenaviruses. Another approach to be considered is the

modulation of survival signaling pathways as a critical event in the viral replication cycle [12]. Given that these pathways are highly involved in the cellular deregulation that occurs during cancer, much progress has been obtained in re-purposing such drugs as antivirals. Hopefully, advances in understanding the detailed molecular biology of hemorrhagic fever virus replication, coupled with determination of three-dimensional structures of viral molecules, could lead to the development of highly effective antiviral drugs against arenaviruses in a near future.

In the beginning, antivirals were found using a “trial-and-error” drug discovery strategy, which is a time and resource-consuming task. Then, the era of large-scale screening made possible the random exploration of a broader number of compounds which brought the discovery of some interesting active molecules (e.g., antiretroviral inhibitors). A further step was taken with the involvement of computer-aided structure activity relationship (SAR) studies that, in conjunction with available high-throughput screening (HTS) techniques, allow a targeted analysis of millions of compounds. Once an active antiviral compound is identified, the next step is to characterize its mechanism of action by determining the virus cycle stage that is being altered. The process is not very complex, and relies on the availability of a cell culture system able to support the specific virus growth. In particular, for some hemorrhagic fever viruses, there is also a requirement for BSL-4 facilities, which has been an important limitation for the evaluation of antiviral agents. This biosafety restriction can be overcome by the use of attenuated strains [13–15] or viral subunits like virus-like-particles (VLP) generated by reverse genetic systems that are in place for JUNV [16, 17] and LASV [18]. These strategies are currently used in our lab for the characterization of JUNV antiviral molecules and have enabled the identification of several interesting candidates. Here, we describe assays to determine the cytotoxic and cytostatic effects of antivirals as well as their specific stage of action: virus attachment to the cell surface, virus entry, virus uncoating, virus transcription/replication, expression of viral proteins, virus assembly, virus budding, as well as direct antiviral effects on virus particles.

2 Materials

2.1 Virus and Cell Propagation

1. Opti-MEM I Reduced Serum Media (Thermo Scientific).
2. 10× Phosphate-buffered saline (PBS): 80 g NaCl, 2 g KCl, 2 g KH_2PO_4 , 29 g $\text{Na}_2\text{HPO}_4 \cdot 12\text{H}_2\text{O}$; add deionized water to a final volume of 1000 ml at room temperature. Working solution: 1:10 dilution in deionized water.

3. Maintenance medium (MM): Minimum essential medium (MEM) supplemented with 1.5% inactivated calf serum and 50 µg/ml gentamicyn.
4. Plaquing medium (PM): MM containing 0.7% methylcellulose.
5. 10% formaldehyde to fix the plaques before staining.

2.2 Cytotoxicity and Cytostatic Assays

1. MTT: (3-(4,5-dimethylthiazol-2-yl)-2,5-diphenyltetrazolium bromide) 0.5 mg/ml in water (*see Note 1*).
2. MTS(3-(4,5-dimethylthiazol-2-yl)-5-(3-carboxymethoxyphenyl)-2-(4-sulfophenyl)-2H-tetrazolium) stock solution: 2 mg/ml DPBS and 0.92 mg/ml PMS (phenazine methosulfate) in DPBS. Filter-sterilize through a 0.2 µm filter into a sterile, light-protected container. Store at -20 °C. For working solution, mix 20 ml of MTS stock solution and 1 ml of PMS (*see Note 1*).
3. DPBS (Dulbecco's phosphate-buffered saline) 0.2 g KCl; 8.0 g NaCl; 0.2 g KH₂PO₄; 1.15 g Na₂HPO₄; 100 mg MgCl₂-6H₂O; 133 mg CaCl₂-2H₂O. At room temperature add deionized water to the KCl, NaCl, KH₂PO₄, and Na₂HPO₄ to a 1 l final volume. Adjust pH to 7.35 using 1 N HCl or 1 N NaOH. Add the MgCl₂-6H₂O; mix thoroughly; then add the CaCl₂-2H₂O and mix thoroughly.
4. Crystal violet: 0.05% crystal violet in 10% ethanol in water. The dye, crystal violet, helps detect plaques and accentuates cytopathicity.
5. Crystal violet bleaching solution: 50% ethanol, 0.1% acetic acid in water.

2.3 Virus Entry Assays

1. 50 µCi/ml of ³⁵S-methionine.
2. Citrate buffer: 40 mM citric acid, 10 mM KCl, 135 mM NaCl, pH 3.
3. Scintillation liquid: dissolve 10 g of PPO (2,5-diphenyloxazole) and 150 mg of POPOP 1,4-bis[-2(5-phenyloxazole)-benzene] in 237 ml of Triton X-100. Bring to 1 l with toluene. Filter the scintillation solution to remove any particles and store in a brown bottle to prevent deterioration by light.

2.4 Electron Microscopy

1. Fixatives: 1.5% (for cells) or 2.5% (for virus) glutaraldehyde in PBS.
2. Formvar- and carbon-coated nickel grids.
3. 5% uranyl acetate.
4. 0.32 M sucrose in PBS.
5. 1.5% OsO₄.
6. Graded ethanol.
7. Epon 812 resin (TAAB) for embedding cell samples).

2.5 Assessing Virus Protein and RNA Production

1. TRIzol® Reagent (Invitrogen-Thermo Fisher Scientific Inc.).
2. RIPA buffer: 10 mM Tris/ClH (pH 7.4), 0.15 M NaCl, 0.1% SDS, 1% Triton X-100, 1% sodium deoxycholate, and 0.4 mM PMSF (phenylmethylsulfonyl fluoride). Two milliliter 0.5 M Tris/ClH (pH 7.4), 5 ml 3 M NaCl, 1 ml 10% SDS, 1 ml Triton X-100, 10 ml sodium deoxycholate 10%, 1 ml 40 mM PMSF in ethanol, deionized 80 ml water.
3. Laemmli sample buffer: (4×) 5% SDS, 10% glycerol, 0.0625 M Tris/ClH (pH 6.8), 2% β-mercaptoethanol, 2% bromophenol blue. 2 g SDS, 4.6 ml 87% glycerol, 1.7 ml Tris/ClH 1.5 M (pH 8.8), 0.8 ml β-mercaptoethanol, 2 ml 0.1% bromophenol blue, deionized water to 10 ml.
4. Transfer buffer: 39 mM glycine, 48 mM Tris, 0.0375 w/v SDS, 20% methanol. 2.930 g glycine, 5.810 g Tris, 0.375 g SDS, 200 ml methanol; add deionized water to 1000 ml.
5. Blocking buffer: 5% skimmed milk in 0.05% Tween 20-PBS buffer.
6. Buffered glycerin: 90% glycerine, 10% PBS 10× pH 9. Add 2.5% 1,4-diazabicyclo[2.2.2]octane (DABCO).

2.6 Assessing Virus Budding

1. Phosphate buffer 0.2 M: 77 ml of Na₂HPO₄-2H₂O 0.5 M in water plus 33 ml of 0.5 M NaH₂PO₄-H₂O in water.
2. Lipofectamine 2000 Transfection Reagent (Thermo Scientific).

3 Methods

3.1 Cytotoxicity Assays

3.1.1 MTT/MTS-Based Cytotoxicity Assay

1. Grow virus-susceptible infected cells in a 96-well microplate (90% confluence).
2. Make serial twofold dilutions of the antiviral compound to test in MM. Make a nontreated cell control with MM and the compound dissolvent.
3. Wash the cells three times with PBS.
4. Cover cells with 200 μl of each antiviral dilution in triplicate.
5. Incubate cells at 37 °C during the same time required to obtain infectious virus in the supernatant.
6. After this time, replace the supernatant per 100 μl of MEM and add 10 μl of fresh MTT stock solution or 20 μl of MTS stock solution to each well. (*see Note 1*). Incubate the MTT solution with cells for 2 h, discard the supernatant, and dissolve the formazan crystals in 200 μl of ethanol 96°. If you are using the MTS method, incubate the MTS solution with cells at 37° for 1–4 h until color development.

7. Read the absorbance at 490 nm on a microplate reader.
8. Calculate the cytotoxic concentration required to reduce cell viability by 50% (CC₅₀) (Subheading 3.7.1).

3.1.2 Crystal Violet-Based Cytotoxicity Assay

1. Do the same protocol as detailed in Subheading 3.1.1, steps 1–5.
2. After this time, fix the cells to the microplate with formaldehyde 10%.
3. Wash the cells with tap water.
4. Dry the monolayers.
5. Stain with crystal violet solution for 30 min.
6. Remove the excess and wash three times with tap water and dry.
7. Redissolve the violet dye with 200 µl bleaching solution per well.
8. Read the absorbance at 590 nm on a microplate reader.
9. Calculate the CC₅₀ (Subheading 3.7.1).

3.2 Cytostatic Assay

1. Grow susceptible cells in a 96-well microplate (90% confluence).
2. Incubate for 2.5 h at 37 °C to allow cell adhesion to the surface.
3. Make serial twofold dilutions of the compound to test in MM.
4. Wash the cells three times with PBS.
5. Cover cells with 200 µl of each dilution in triplicate.
6. Continue with protocols detailed in Subheading 3.1.1, steps 5–7 or Subheading 3.1.2, steps 2–8.
7. Calculate the anti-proliferative concentration 50% (AC₅₀), concentration required to inhibit cell proliferation by 50% (Subheading 3.7.1).

3.3 Viral Stock Production

3.3.1 Viral Stock Production (Non-radiolabeled)

1. Infect cells in a T150 flask at a MOI (multiplicity of infection: rate between infective viral particles in the inocula and total number of cells to be infected) of 0.1 for 1 h at 37 °C.
2. Remove the inoculum and wash three times with PBS.
3. Refeed the cells with MM.
4. Harvest the supernatant at the time where the viral peak production occurs (*see Note 2*).
5. Clarify the stock by low-speed centrifugation and concentrate by ultracentrifugation at 100,000 × *g* for 2 h.
6. Titer the stock (Subheadings 3.4.1 or 3.4.2).

3.3.2 Radiolabeled Viral Stock Production

1. Infect the cells at a MOI of 1 during 1 h at 37 °C in a T150 flask.

2. Remove the inoculum and wash three times with PBS.
3. Refeed the cells with methionine-free MM containing 50 $\mu\text{Ci}/\text{ml}$ of ^{35}S -methionine.
7. Harvest the supernatant at the time where the viral peak production occurs (*see Note 2*).
4. Clarify the stock by low-speed centrifugation and concentrate by ultracentrifugation at $100,000 \times g$ for 2 h.
5. Titer the stock (Subheading 3.4.2 or 3.4.3).
6. Quantify the radioactivity using a liquid scintillation counter.

3.4 Viral Quantification

3.4.1 Cytopathic Effect Assay

1. Grow susceptible cells in a 96-well microplate (100% confluence).
2. Wash three times with PBS.
3. Make serial tenfold dilutions of the virus to titer in 1 ml of PBS.
4. Infect the cells with 10 μl of each dilution per quintupled during 1 h at 37 °C.
5. Remove the inoculum and wash three times with PBS.
6. Cover cells with 200 μl of MM.
7. Incubate cells at 37 °C until time to observe under an inverted microscope the virus cytopathic effect (rounding, detachment, monolayer destruction, syncytia formation, development of inclusion bodies, etc.). Evaluation of cytopathic effects can be also performed by viability assays (protocols in Subheadings 3.1.1 and 3.1.2).
8. Calculate the tissue culture infectious dose 50% (TCID₅₀) as the dilution that produces 50% positive responses and represents the viral amount necessary to infect 50% of cell culture (Subheading 3.7.2).

3.4.2 Plaque Assay

1. Grow susceptible cells in a 24-well microplate (80% confluence).
2. Make serial tenfold dilutions of the virus to titer in 1 ml of PBS.
3. Infect the cells with 100 μl of each dilution per triplicate during 1 h at 37 °C.
4. Remove the inoculum and wash three times with PBS.
5. Cover cells with 1 ml of PM.
6. Incubate the cells at 37 °C for the necessary days to obtain lysis plaques (~5–7 days).
7. Fix the cells to the microplate with 1 ml of formaldehyde 10% per well for 10 min.

8. Wash three times with tap water.
9. Stain fixed cells with crystal violet for 10 min.
10. Wash three times with tap water.
11. Count the lysis plaques in the dilution with about 50–100 plaques and calculate the viral titer as plaque forming units (PFU)/ml (Subheading 3.7.3).

**3.4.3 Indirect
Immunofluorescence
Staining (IF)**

1. Grow susceptible cells in a 24-well microplate on coverslips (60% confluence).
2. Make serial tenfold dilutions of the virus to titer in 1 ml of PBS.
3. Infect the cells with 100 µl of each dilution per triplicate during 1 h at 37 °C.
4. Remove the inoculum and wash three times with PBS.
5. Cover cells with 1 ml of MM.
6. Incubate the cells at 37 °C for 24–48 h.
7. Fix the cells with 4% paraformaldehyde for 10 min at 37 °C.
8. Wash three times with PBS.
9. Incubate with 20 mM NH₄Cl for 10 min at 37 °C.
10. Wash three times with PBS.
11. For total immunofluorescence permeabilize cells with PBS-0.3% Triton X-100 for 10 min at 37 °C, for surface immunofluorescence omit this step.
12. Incubate with the first antibody. Recommended antibodies for JUNV are reported by Sanchez et al. [19].
13. Wash three times with PBS.
14. Incubate with the second labeled antibody according to the manufacturer's instructions.
15. Wash three times with PBS.
16. Stain the cell nuclei with DAPI for 10 min at room temperature.
17. Wash with water and mount in buffered glycerine 2.5% DABCO.
18. Calculate the percentage of fluorescent cells in each preparation from 20 randomly selected microscope fields (Subheading 3.7.4).

**3.4.4 Quantitative
Real-Time PCR (qRT-PCR)**

RNA Extraction

Antiviral assays can be quantified by qRT-PCR. It should be considered that the values obtained correspond to relative fold-change between treated and untreated samples.

1. Lyse cells directly in a culture dish by adding TRIzol® and passing the cell lysate several times through a 1 ml pipette.

2. Incubate the homogenized samples for 5 min at 15–30 °C.
3. Add 0.2 ml of chloroform per 1 ml of TRIzol[®], cap samples tubes and shake vigorously by hand for 15 s.
4. Centrifuge at not more than 12,000 × *g* for 2 min at 2–8 °C.
5. Transfer the aqueous phase to a fresh tube.
6. Add 0.5 ml of isopropyl alcohol per 1 ml of TRIzol[®].
7. Incubate samples at 15–30 °C for 10 min.
8. Centrifuge at not more than 12,000 × *g* for 15 min at 2–8 °C.
9. Remove the supernatant and wash the RNA precipitate with 1 ml of 75% ethanol.
10. Mix by vortexing.
11. Centrifuge at not more than 7500 × *g* for 5 min at 2–8 °C.
12. Briefly dry the RNA pellet, air-dry or vacuum-dry for 5–10 min.
13. Dissolve RNA in RNase-free water or 0.5% sodium dodecyl sulfate (SDS) solution by passing the solution a few times through a pipette tip.
14. Incubate for 10 min at 55–60 °C.
15. Store at –70 °C.

cDNA Synthesis

1. Combine the Premix for each reaction: 3 µg RNA, 1 µg of random primers, and nuclease-free water necessary volume to complete 10 µl per reaction.
2. Incubate the Premix for 5 min at 65 °C, and then for 5 min at room temperature.
3. Combine cDNA synthesis reagents for each reaction: 1 µl RT (200 units reverse transcriptase per reaction), 4 µl 5× RT-Buffer, 1 µl 10 mM dNTPs, 4 µl nuclease-free water.
4. Bind the premix with the cDNA synthesis mix, vortex, centrifuge for a spin, and incubate for 2 h at 42 °C.
5. Quantify the cDNA (µg/µl) in each sample with UV/VIS nanospectrophotometer (Thermo Scientific NanoDrop[™]).
6. Determinate the cDNA quality by the rate A_{260}/A_{280} , it must be 1.8–2.0 to be accepted as “pure.”

qRT-PCR

1. Amplify the viral cDNA using specific viral gene primers.
2. Amplify housekeeping cDNA using gene-specific primers.
3. Combine these components for each qRT-PCR reaction: 12.5 µl of 2× Master mix (containing 5× Taq-Buffer, 25 mM MgCl, 25 mM dNTPs, SybrGreen dye and Taq polymerase), 0.25 µl 50 µM Forward primer, 0.25 µl 50 µM Reverse primer, 10 µl nuclease-free water, 2 µl cDNA sample.

4. Run settings: 5 min at 95 °C; 45 cycles of 30 s at 95 °C, 45 s at 60 °C, and 30 s at 72 °C; finally 5 min at 72 °C.
5. Normalize average viral RNA Ct values to the average Ct values of housekeeping gene amplification and set $\Delta\Delta\text{Ct}$ -based fold-change calculations relative to untreated virus-infected cells using some specific software (Subheading 3.7.5).

3.4.5 Radiolabeled Virus Quantification

1. Lyse the radiolabeled virus-infected cells with 0.1 M NaOH solution containing 1% SDS.
2. Complete the sample vial volume with scintillator liquid according to the scintillation counter specifications.
3. Quantify the radioactivity using a liquid scintillation counter.

3.5 Antiviral Assays

3.5.1 Cytopathic Effect Reduction Assay

1. Grow susceptible cells in a 96-well microplate (100% confluence).
2. Wash three times with PBS.
3. Infect with the adequate dose of virus during 1 h at 37 °C in quintuplet.
4. Make serial twofold dilutions of the compound to test in MM.
5. Include cell controls and virus controls (non-infected and non-compound-treated infected cells).
6. Remove the inoculum and wash three times with PBS.
7. Cover cells with 200 μl of each compound dilution or with MM for controls.
8. Incubate cells at 37 °C by the necessary time to observe under an inverted microscope the virus cytopathic effect. Evaluation can be also made by viability assays (Subheadings 3.1.1 and 3.1.2).
9. Calculate the effective concentration 50% (EC_{50}), concentration required to reduce cytopathic effect by 50% (Subheading 3.7.6).

3.5.2 Virus Plaque-Reduction Assay

1. Grow susceptible cells in a 24-well microplate (80% confluence).
2. Wash three times with PBS.
3. Infect with about 50 PFU of virus per well during 1 h at 37 °C in absence or presence of serial twofold concentrations of the compound in triplicate.
4. Remove the inoculum and wash three times with PBS.
5. Cover cells with 1 ml of each compound dilution in triplicate in PM or PM without compound for a viral control.
6. Follow steps 6–10 of protocol in Subheading 3.4.2.

- Count the lysis plaques and calculate the effective concentration 50% (EC_{50}), or the concentration required to reduce plaque number by 50% (Subheading 3.7.6).

3.5.3 Virus Yield Inhibition Assay

- Grow susceptible cells in a 24-well microplate (90% confluence).
- Wash three times with PBS.
- Infect with virus at a MOI of 0.1 during 1 h at 37 °C.
- Make serial twofold dilutions of the compound to test in MM.
- Remove the inoculum and wash three times with PBS.
- Cover cells with 500 μ l of each dilution in triplicate or with MM without compound for a control.
- Incubate cells at 37 °C for the necessary time to obtain infectious virus in the supernatant.
- Harvest supernatant cell cultures or process cell culture monolayers for viral quantification (*see* Subheading 3.4).
- Calculate the effective concentration 50% (EC_{50}), concentration required to reduce virus yield by 50% (Subheading 3.7.6).

3.6 Determining Mechanism of Antiviral Action

3.6.1 Cellular Pretreatment with Antiviral Compounds

- Grow susceptible cells in a 24-well microplate (80% confluence).
- Wash three times with PBS.
- Treat triplicate wells with the compound dilutions at different times before infection; simultaneously, perform a control culture without drug treatment at each time point.
- Then, discard cell supernatants, wash the cell monolayers.
- Evaluate the antiviral effect by a virus plaque reduction assay: Infect with about 50 PFU of virus per well during 1 h at 37 °C. Follow steps 4–10 of protocol in Subheading 3.4.2 and then count lysis plaques.
- Alternatively, evaluate the antiviral effect by a virus yield inhibition assay: Infect with the virus at a MOI of 0.1 during 1 h at 37 °C in PBS. After adsorption, remove the inoculum and wash three times with PBS. Add compound-free MM. Incubate cells at 37 °C by the necessary time to perform viral quantification of cell supernatants (*see* Subheading 3.4).

3.6.2 Time of Addition Assay to Determine How late in the Virus Life Cycle Antivirals Can Be Added

- Grow susceptible cells in a 24-well microplate.
- Wash three times with PBS.
- Infect with the virus at a MOI of 0.1 during 1 h at 4 °C.
- Remove the inoculum and wash three times with PBS.
- Refeed with MM and incubate at 37 °C.

6. Treat duplicate wells with the adequate compound concentration at various times after infection, simultaneously perform a control-infected culture without drug treatment at each time point.
7. Incubate for 24 h at 37 °C and perform viral quantification (*see* Subheading 3.4).

**3.6.3 Time of Removal
Assay to Determine
whether Antiviral
Compound must
Be Sustained**

1. Do the same protocol as detailed in Subheading 3.6.2, **steps 1–4**.
2. Refeed with MM containing the indicated compound concentration and incubate at 37 °C per duplicate, simultaneously perform a control-infected culture without drug treatment at each time point.
3. At different time points, remove the MM with compound and refeed with MM.
4. Incubate for 24 h at 37 °C and perform viral quantification (*see* Subheading 3.4).

**3.6.4 Prevention of Viral
Attachment by an Antiviral**

**Assessing Prevention of
Viral Attachment by Virus
Plaque-Reduction Assay**

1. Grow susceptible cells in a 24-well microplate (90% confluence).
2. Wash three times with PBS.
3. Infect with about 500 PFU of virus per well (*see* **Note 3**) during 1 h at 4 °C in MM containing the indicated compound concentration or serial twofold compound concentrations. Simultaneously perform a control-infected culture without drug treatment.
4. Follow **steps 4–10** of protocol in Subheading 3.4.2 and then count lysis plaques.

**Assessing Prevention
of Attachment by Virus
Yield-Inhibition Assay**

1. Grow susceptible cells in a 24-well microplate (90% confluence).
2. Wash three times with PBS.
3. Infect with the virus at a MOI of 1–2 during 1 h at 4 °C in MM containing the indicated compound concentration or twofold serial concentrations of the compound to test. Simultaneously perform a control-infected culture without drug treatment.
4. After adsorption, remove the inoculum with the compound and wash three times with cold PBS at 4 °C.
5. Add compound-free MM.
6. Incubate cells at 37 °C by the necessary time to obtain infectious virus production and perform viral quantification assay of cell supernatants (*see* Subheading 3.4).

Assessing Prevention
of Attachment by
Determining Infectious
Virus Binding

1. Grow susceptible cells in a 24-well microplate (100% confluence).
2. Wash three times with PBS.
3. Infect with the virus or radiolabeled virus at a MOI of 1–2 during 1 h at 4 °C in MM containing the indicated compound concentration, or twofold concentrations of the compound to test. Simultaneously, perform a control-infected culture without drug treatment.
4. After adsorption, remove the inoculum and wash three times with cold PBS at 4 °C.
5. Disrupt cells by three cycles of freezing and thawing.
6. Centrifuge at low velocity for 2 min.
7. Determine infectious virus bound by viral quantification assay (*see* Subheadings 3.4.1 and 3.4.2).
 - If you used radiolabeled virus, after **step 4**, continue with Subheading 3.4.5.
 - If you quantify by qRT-PCR after **step 4**, continue with Subheading 3.4.4.

3.6.5 Antiviral Prevention
of Viral Internalization

1. Grow susceptible cells in a 24-well microplate (100% confluence).
2. Wash three times with PBS.
3. Infect with about 500 PFU or radiolabeled PFU per well during 1 h at 4 °C in MM.
4. After adsorption, remove the inoculum and wash three times with cold PBS at 4 °C.
5. Treat the cells with MM containing the indicated compound concentration, or twofold dilutions of the compound to test; simultaneously, perform a control-infected culture without drug treatment.
6. Incubate 1 h at 37 °C to permit the viral entry.
7. Remove the medium and wash the cells three times with PBS.
8. Treat with 0.1 ml of citrate buffer for 1 min to inactivate adsorbed but not internalized virus (*see* **Note 4**).
9. Wash the cells with PBS and treat with trypsin for 5 min at 37 °C.
10. Inactivate trypsin with MEM 5% inactivated fetal bovine serum.
11. Wash the cells with PBS by low-speed centrifugation.
12. Resuspend the cellular pellet in MM.
13. Make serial tenfold dilutions of the cellular suspension in MM and plaque onto a new 24-well microplate with susceptible cellular monolayer (80% confluence).

14. Incubate for 2 h at 37 °C.
15. Cover cells with 1 ml of PM and incubate the cells at 37 °C for the necessary days to obtain lysis plaques.
16. If you used radiolabeled virus after **step 11**, continue with Subheading 3.4.5. If you quantify by qRT-PCR after **step 11**, continue with Subheading 3.4.4.

3.6.6 Prevention of Viral Uncoating

1. Grow susceptible cells in a 24-well microplate (100% confluence).
2. Wash three times with PBS.
3. Infect with the virus at a MOI of 1–2 during 1 h at 4 °C.
4. Remove the inoculum and wash three times with PBS.
5. Refeed with MM containing the indicated compound concentration and incubate at 37 °C per duplicate for different post-adsorption times; simultaneously perform control-infected cultures without drug treatment and include concanamycin A 5 nM-treated cultures in the same conditions as uncoating blockade positive control.
6. Continue as detailed in Subheading 3.6.5, **steps 8–12**.
7. Disrupt the cells by three cycles of freezing and thawing.
8. Clarify the supernatant by low-speed centrifugation or 2 min.
9. Determinate the intracellular infectivity by viral quantification assays (Subheadings 3.4.1 and 3.4.2).

3.6.7 Antiviral Prevention of Transcription/Replication

1. Grow susceptible cells in a 24-well microplate (100% confluence).
2. Wash three times with PBS.
3. Infect with the virus at a MOI of 1–2 during 1 h at 37 °C.
4. Remove the inoculum and wash three times with PBS.
5. Refeed with MM containing the indicated compound concentration and incubate at 37 °C for different times (1, 3, 5, 7, 9, and 12 h), simultaneously perform the corresponding control-infected cultures.
6. At each time point, discard the supernatant, wash the monolayer, and extract the total RNA to measure the RNA synthesis by qRT-PCR (*see* Subheading 3.4.4).

3.6.8 Antiviral Prevention of Synthesis of Specific Viral Protein(S)

Western Blot to Assess Antiviral Effects on Expression of Viral Proteins

1. Grow susceptible cells in a 24-well microplate (90% confluence).
2. Wash three times with PBS.
3. Infect with the virus at a MOI of 0.1 during 1 h at 37 °C.
4. Remove the inoculum and wash three times with PBS.

5. Refeed with MM containing the indicated compound concentration and incubate at 37 °C per duplicate, simultaneously perform a control-infected culture without drug treatment. Include a noninfected cellular control.
6. At 48 h p.i. lyse the cells in RIPA buffer.
7. Clarify cell lysates by low-speed centrifugation for 2 min.
8. Separate the polypeptides by electrophoresis on SDS-PAGE gels.
9. Mix 3 volumes of sample and 1 volume of 4× Laemmli sample buffer.
10. Boil for 5 min.
11. Select the percentage acrylamide gel according to the size of the protein of interest.
12. Load equal amounts of protein into the wells of an SDS-PAGE gel. Include a MW marker.
13. Run the gel for 1–2 h at 100 V.
14. Cut a polyvinylidene difluoride (PVDF) membrane to the appropriate size of the gel.
15. Activate PVDF membrane with methanol for 1 min and rinse with transfer buffer (*see Note 5*).
16. Transfer proteins from the gel to a PVDF membrane using available equipment and the manufacturer's instructions.
17. Place a pre-wetted sheet of thick filter paper onto the anode of a semidry electrophoretic transfer cell. Remove all air bubbles.
18. Place the pre-wetted PVDF membrane on the top of the filter paper and remove bubbles.
19. Place the gel on the top of the PVDF membrane and remove any bubbles.
20. Place a pre-wetted sheet of thick filter paper on the top of the gel and remove any bubbles.
21. Place the cathode onto the stack and plug the unit to a power supply.
22. Turn on the power supply. Transfer is usually performed for 30–60 min at 15–25 V.
23. Block the membranes with blocking buffer for 1 h at 37 °C.
24. Incubate overnight at 4 °C with appropriate dilutions of primary antibody in blocking buffer. Check the antibody data-sheet for detailed information.
25. Wash three times with 0.05% PBS-Tween 20 for 5 min.
26. Incubate for 1 h at 37 °C with the appropriate dilution of peroxidase-conjugated secondary antibody.

27. For signal development, follow the kit manufacturer's recommendations (ECL, Bio-Rad).
28. Quantify the protein bands by densitometry using some specific software.
29. To normalize the amount of interest protein to the amount of a constitutive cellular protein, like actin, in cellular extracts, strip the blots and then reprobe with an anti-actin primary antibody followed by chemiluminescence and quantification by densitometry, as above.

Immunofluorescence
to Assess Antiviral
Blockage of Specific Viral
Protein Expression

1. Grow susceptible cells in a 24-well microplate on coverslips (60% confluence).
2. Continue as detailed in Subheading 3.6.1, steps 2–5.
3. At convenient time p.i., follow steps 7–18 of protocol in Subheading 3.4.3.

3.6.9 Prevention
of Assembly or Release
of New Infectious Virions

By Electron Microscopy

1. Grow susceptible cells in a 6-well microplate (100% confluence).
2. Wash three times with PBS.
3. Infect with the virus at a high MOI during 1 h at 37 °C.
4. Remove the inoculum and wash three times with PBS.
5. Refeed with MM and incubate at 37 °C.
6. Treat duplicate wells with the presumptive-antiviral-compound for 16 h p.i., and simultaneously perform a control-infected culture without drug treatment.
7. Harvest the supernatant (viral suspension) and fix it overnight in 2.5% glutaraldehyde.
8. Fix the cells with 1.5% glutaraldehyde for 4 h at 4 °C.
9. For viral suspensions: deposit a 10 µl drop of the suspension on Formvar-carbon-coated nickel grids for 1 min, blot away the excess fluid with Whatman filter paper, and stain the samples negatively for 1 min in 0.5% uranyl acetate before observing with transmission electron microscopy.
10. For cellular monolayers: harvest the fixed cells mechanically with scrapers and incubate in 0.32 M sucrose for 12 h at 4 °C, spin the cells 10 min at 2000 × *g*, resuspend the pellet in 1.5% OsO₄ in 0.32 M sucrose, and then incubate 2 h at 4 °C.
11. Centrifuge the cells and wash with bidistilled water.
12. Incubate for 12 h in 2% uranyl acetate in water.
13. Subject the cells to dehydration through an ethanol gradient followed by propylene oxide.
14. Embed in Epon 812 resin mixture (TAAB), and polymerize at 70 °C for 2 days.

15. Restain the ultrathin sections with 2% uranyl acetate in water.
16. Observe the specimens with a transmission electron microscope.

Virus-Like Particles (VLP)
Budding Assay

This protocol requires the previous cloning of the arenavirus matrix Z protein or the corresponding viral protein responsible for viral budding into a mammalian expression vector, such as pcDNA3.1. It should be used for cell transfection with appropriate controls, including an empty-vector negative control.

1. Grow susceptible cells in a 24-well microplate (70–80% confluence).
2. Dilute 0.5 µg of DNA into 50 µl of Opti-MEM. Mix gently and incubate for 5 min.
3. Mix Lipofectamine 2000 before use and then dilute 2 µl in 50 µl of Opti-MEM. Mix gently and incubate for 5 min at room temperature.
4. Combine the diluted DNA and the diluted Lipofectamine 2000 (total volume should be 100 µl). Mix gently and incubate for 15–20 min at room temperature.
5. Add the DNA-Lipofectamine 2000 complexes (100 µl) to the 400 µl of growth medium of the well containing the cells to be transfected.
6. Incubate cells at 37 °C for 4 h.
7. Discard the transfection mix and wash three times with PBS.
8. Treat the cells with MM containing the indicated compound concentration, or twofold dilutions of the compound to test; simultaneously, perform a control-infected culture without drug treatment.
9. Incubate for 48 h at 37 °C.
10. Harvest the culture supernatants and lyse the cell monolayers in 2× Laemmli sample buffer.
11. Purify the VLPs from the culture supernatants by ultracentrifugation through 20% (w/v) sucrose cushions at 34,000 rpm for 2 h at 4 °C in a Beckman SW 50.1 rotor.
12. Resuspend the purified VLPs in 2× Laemmli sample buffer.
13. Boil for VLPs and cell lysates aliquots.
14. Separate the polypeptides by electrophoresis on SDS-PAGE gels. (Subheading 3.6.8, steps 11–29).

3.6.10 *Inactivation
of Extracellular Virus
Particles (Virucidal Assay)*

1. Make serial twofold dilutions of the compound to test in MM.
2. Mix an aliquot of a viral suspension containing approximately 1×10^6 PFU with the same volume of the compound dilutions.

3. Incubate the mixtures at the temperature and times indicated.
4. As control, incubate an equivalent aliquot of the virus suspension in parallel with MM under the same conditions.
5. Dilute the chilled samples at least 100-fold in PBS (*see* Subheading **Note 6**) and determine the remaining viral titer (*see* Subheadings **3.4.1** and **3.4.2**).
6. Calculate the inactivating concentration required to inactivate 50% of infective viral particles (IC₅₀).

3.7 Calculations

3.7.1 CC₅₀/AC₅₀

1. Calculate the mean of absorbance of each treatment and determine the percentage of viability with respect to the non-treated cells.
2. Graph viability vs. compound concentration and make a linear regression.
3. Determine the compound concentration for 50% viability by extrapolation (*see* **Note 7**).

3.7.2 Viral Titer by Quantal or End Point Method

Use the statistical method of Reed and Muench to determine the 50% end point.

1. Calculate the percentage of positive responses for each virus dilution.
2. Calculate the Reed and Muench index:

$$\text{Index} = \frac{\% \text{infected at dilution immediately above } 50\% - 50\%}{\% \text{infected at dilution immediately above } 50\% - 50\% \text{infected dilution immediately below } 50\%}$$

3. Apply the index to the dilution with an infection rate immediately above 50%

$$(X) = 10^{-(X + \text{index})}$$

4. This dilution of the virus suspension contains a TCID₅₀ unit of virus in 0.1 ml.
5. Titer (TCID₅₀/ml) = 10 × 1/(×)

3.7.3 Viral Titer by PFU/ml

1. Calculate the mean of lysis plaques among the replicates (PFU).
2. Titer (PFU/ml) = PFU/(inoculum volume × dilution)

3.7.4 Fluorescent Cell Percentage

1. Select 20 random microscope fields.
2. Count all the cells present in the fields and discriminate the positive fluorescent cells (positive for the viral epitope).

3. Calculate the fluorescent cell percentage as:

Number of fluorescent positive cells / Number of total cells.

3.7.5 Fold Change of Expression Method

1. $\Delta\text{Ct} = \text{Ct gene of interest} - \text{Ct gene housekeeping}$.
2. $\Delta\Delta\text{Ct} = \Delta\text{Ct treated} - \Delta\text{Ct untreated}$.
3. Fold Change of Expression = $2^{-\Delta\Delta\text{Ct}}$.

3.7.6 EC_{50}

1. Calculate the viral inhibition percentage for each compound concentration as percentage of positive responses (cytopathic effect assay) or percentage of PFU (plaque assay) in treated samples in comparison to control virus.
2. Graphic % inhibition vs. compound concentration and make a lineal regression.
3. Determinate the compound concentration for the 50% of virus inhibition (*see Note 7*).

4 Notes

1. MTT stock solution should be prepared 5 mg/ml in culture medium or in sterile double distilled water. Please note that the solution must be fresh and protected from light, it can be stored at 4 °C until use. MTS stock solution can be stored at -20 °C protected from light for 18 months.
2. Usually, the supernatants for the day of peak viral production and the two subsequent days are harvested. The culture should be observed under the microscope and ensure that the cell monolayer remains in good condition.
3. In virus attachment assays adsorption is performed for 1 h at 4 °C. Consequently, virus inoculum must be increased in comparison with a standard plaque assay with 1 h adsorption at 37 °C (500 PFU vs 50 PFU) to assess binding of a significant amount of virions at low temperature.
4. Instead of citrate, treat the cells with a solution of 1 mg/ml proteinase K for 45 min at 4 °C. Inactivate the proteinase K with 0.2% bovine serum albumin (BSA) in PBS, containing 2 mM PMSF. Then follow with **steps 11–16** of Subheading **3.6.5**.
5. Take special care that membrane never dries, for optimum transfer.
6. Samples must be adequately diluted before titration of virus infectivity to assess that, when the compound-virus mixtures are incubated on the cell monolayers, the compound concentration is below the antiviral EC_{50} value and infectivity reduction is only due to virion inactivation.

7. The effectiveness of an antiviral compound is evaluated by the selectivity index (SI): ratio CC_{50}/EC_{50} . A good antiviral should have at least a $SI > 10$, and hopefully be in the hundreds to be safe and effective.

References

- Enria DA, Briggiler AM, Sánchez Z (2008) Treatment of Argentine hemorrhagic fever. *Antivir Res* 78:132–139. doi:[10.1016/j.antiviral.2007.10.010](https://doi.org/10.1016/j.antiviral.2007.10.010)
- McCormick JB, King IJ, Webb PA, Scribner CL, Craven RB et al (1986) Lassa fever. Effective therapy with ribavirin. *N Engl J Med* 314:20–26
- Peters CJ (2002) Human infection with arenaviruses in the Americas. *Curr Top Microbiol Immunol* 262:65–74. doi:[10.1007/978-3-642-56029-3_3](https://doi.org/10.1007/978-3-642-56029-3_3)
- Fisher-Hoch SP, Ghorie S, Parker L, Huggins J (1992) Unexpected adverse reactions during a clinical trial in rural West Africa. *Antivir Res* 19:139–147. doi:[10.1016/0166-3542\(92\)90073-E](https://doi.org/10.1016/0166-3542(92)90073-E)
- Larson RA, Dai D, Hosack VT, Tan Y, Bolken TC et al (2008) Identification of a broad-spectrum arenavirus entry inhibitor. *J Virol* 82:10768–10775. doi:[10.1128/JVI.00941-08](https://doi.org/10.1128/JVI.00941-08)
- Lee AM, Rojek JM, Spiropoulou CF, Gundersen AT, Jin W et al (2008) Unique small molecule entry inhibitors of hemorrhagic fever arenaviruses. *J Biol Chem* 283:18734–18742. doi:[10.1074/jbc.M802089200](https://doi.org/10.1074/jbc.M802089200)
- Capul AA, de la Torre JC (2008) A cell-based luciferase assay amenable to high-throughput screening of arenavirus budding. *Virology* 382:107–114. doi:[10.1016/j.virol.2008.09.008](https://doi.org/10.1016/j.virol.2008.09.008)
- Lee AM, Pasquato A, Kunz S (2011) Novel approaches in anti-arenaviral drug development. *Virology* 411:163–169. doi:[10.1016/j.virol.2010.11.022](https://doi.org/10.1016/j.virol.2010.11.022)
- Sepúlveda CS, Fascio ML, Mazzucco MB, Palacios ML, Pellón RF et al (2008) Synthesis and evaluation of N-substituted acridones as antiviral agents against hemorrhagic fever viruses. *Antivir Chem Chemother* 19:41–47. doi:[10.1016/j.antiviral.2011.10.007](https://doi.org/10.1016/j.antiviral.2011.10.007)
- Sepúlveda CS, García CC, Fascio ML, D'Accorso NB, Docampo Palacios ML et al (2012) Inhibition of Junín virus RNA synthesis by an antiviral acridone derivative. *Antivir Res* 96:16–22. doi:[10.1016/j.antiviral.2011.10.007](https://doi.org/10.1016/j.antiviral.2011.10.007)
- García CC, Sepúlveda CS, Damonte EB (2011) Novel therapeutic targets for arenavirus hemorrhagic fevers. *Future Virol* 6:27–44
- Linero FN, Scolaro LA (2009) Participation of the phosphatidylinositol 3-kinase/Akt pathway in Junín virus replication in vitro. *Virus Res* 145:166–170. doi:[10.1016/j.virusres.2009.07.004](https://doi.org/10.1016/j.virusres.2009.07.004)
- de Guerrero LB, Weissenbacher MC, Parodi AS (1969) Inmunización contra la fiebre hemorrágica Argentina con una cepa atenuada de virus Junín. *Medicina (Buenos Aires)* 29:1–5
- Maiztegui JI, McKee KT, Barrera Oro JG, Harrison LH, Gibbs PH et al (1998) Protective efficacy of a live attenuated vaccine against Argentina hemorrhagic fever. *J Infect Dis* 177:277–283. doi:[10.1086/514211](https://doi.org/10.1086/514211)
- Contigiani MS, Sabbatini MS (1977) Virulencia diferencial de cepas de virus Junín por marcadores biológicos en ratones y cobayos. *Medicina (Buenos Aires)* 37:244–251
- Albariño CG, Bergeron E, Erickson BR, Khristova ML, Rollin PE, Nichol ST (2009) Efficient reverse genetics generation of infectious Junin viruses differing in glycoprotein processing. *J Virol* 83:5606–5614. doi:[10.1128/JVI.00276-09](https://doi.org/10.1128/JVI.00276-09)
- Emonet SF, Seregin AV, Yun NE, Poussard AL, Walker AG et al (2011) Rescue from cloned cDNAs and in vivo characterization of recombinant pathogenic Romero and live-attenuated candid #1 strains of Junin virus, the causative agent of Argentine hemorrhagic fever disease. *J Virol* 85:1473–1483. doi:[10.1128/JVI.02102-10](https://doi.org/10.1128/JVI.02102-10)
- Carnec X, Baize S, Reynard S, Diancourt L, Caro V et al (2011) Lassa virus nucleoprotein mutants generated by reverse genetics induce a robust type I interferon response in human dendritic cells and macrophages. *J Virol* 85:12093–12097. doi:[10.1128/JVI.00429-11](https://doi.org/10.1128/JVI.00429-11)
- Sanchez A, Pifat DY, Kenyon RH, Peters CJ, McCormick JB, Kiley MP (1989) Junin virus monoclonal antibodies: characterization and cross-reactivity with other arenaviruses. *J Gen Virol* 70:1125–1132. doi:[10.1099/0022-1317-70-5-1125](https://doi.org/10.1099/0022-1317-70-5-1125)
- Bolken TC, Laquerre S, Zhang Y, Bailey TR, Pevear DC et al (2006) Identification and characterization of potent small molecule inhibitor of hemorrhagic fever new world arenavirus. *Antivir Res* 69:86–97. doi:[10.1016/j.antiviral.2005.10.008](https://doi.org/10.1016/j.antiviral.2005.10.008)

21. York J, Dai D, Amberg S, Nunberg JH (2008) pH-induced activation of arenavirus membrane fusion is antagonized by small-molecule inhibitors. *J Virol* 82:10932–10939. doi:10.1128/JVI.01140-08
22. Cashman KA, Smith MA, Twenhafel NA, Larson RA, Jones KF, Allen RD III et al (2011) Evaluation of Lassa antiviral compound ST-193 in a Guinea pig model. *Antivir Res* 90:70–79. doi:10.1016/j.antiviral.2011.02.012
23. Thomas CJ, Casquilho-Gray HE, York J, DeCamp DL, Dai D (2011) A specific interaction of small molecule entry inhibitors with the envelope glycoprotein complex of the Junín hemorrhagic fever arenavirus. *J Biol Chem* 286:6192–6200. doi:10.1074/jbc.M110.196428
24. Whitby LR, Lee AM, Kunz S, Oldstone MBA, Boger DL (2009) Characterization of Lassa virus cell entry inhibitors: determination of the active enantiomer by asymmetric synthesis. *Bioorg Med Chem Lett* 19:3771–3774. doi:10.1016/j.bmcl.2009.04.098
25. Lee AM, Rojek JM, Gundersen AT, Ströher U, Juteau JM et al (2008) Inhibition of cellular entry of lymphocytic choriomeningitis virus by amphipathic DNA polymers. *Virology* 372:107–117. doi:10.1016/j.virol.2007.10.016
26. Wolf MC, Freiberg AN, Zhang T, Akyol-Ataman Z, Grock A (2010) A broad-spectrum antiviral targeting entry of enveloped viruses. *Proc Natl Acad Sci U S A* 107:3157–3162. doi:10.1073/pnas.0909587107
27. York J, Berry JD, Ströher U, Li Q, Feldmann H (2010) An antibody directed against the fusion peptide of Junín virus envelope glycoprotein GPC inhibits pH-induced membrane fusion. *J Virol* 84:6119–6129. doi:10.1128/JVI.02700-09
28. García CC, Candurra NA, Damonte EB (2000) Antiviral and virucidal activities against arenaviruses of zinc-finger active compounds. *Antivir Chem Chemother* 11:231–237. doi:10.1177/095632020001100306
29. García CC, Candurra NA, Damonte EB (2003) Differential inhibitory action of two azoic compounds against arenaviruses. *Int J Antimicrob Agents* 21:319–324. doi:10.1016/S0924-8579(02)00390-4
30. García CC, Candurra NA, Damonte EB (2002) Mode of inactivation of arenaviruses by disulfide based compounds. *Antivir Res* 55:437–446. doi:10.1016/S0166-3542(02)00076-1
31. García CC, Ellenberg PC, Artuso MC, Scolaro LA, Damonte EB (2009) Characterization of Junín virus particles inactivated by a zinc finger-reactive compound. *Virus Res* 143:106–113. doi:10.1016/j.virusres.2009.03.010
32. García CC, Djavani M, Topisirovic I, Borden KL, Salvato MS, Damonte EB (2006) Arenavirus Z protein as an antiviral target: virus inactivation and protein oligomerization by zinc finger reactive compounds. *J Gen Virol* 87:1217–1228. doi:10.1099/vir.0.81667-0
33. Sepúlveda CS, García CC, Damonte EB (2010) Inhibition of arenavirus infection by thiuram and aromatic disulfides. *Antivir Res* 87:329–337. doi:10.1016/j.antiviral.2010.06.005
34. Sepúlveda CS, García CC, Livingston Macleod JM, López N, Damonte EB (2013) Targeting of arenavirus RNA synthesis by a carboxamide-derivatized aromatic disulfide with virucidal activity. *PLoS One* 8:e81251. doi:10.1371/journal.pone.0081251
35. Ortiz-Riaño E, Ngo N, Devito S, Eggink D, Munger J et al (2014) Inhibition of arenavirus by A3, a pyrimidine biosynthesis inhibitor. *J Virol* 88:878–889. doi:10.1128/JVI.02275-13
36. Wachsman MB, López EMF, Ramírez JA, Galagovsky LR, Coto CE (2000) Antiviral effect of brassinosteroids against herpes virus and arenavirus. *Antivir Chem Chemother* 11:71–77. doi:10.1177/095632020001100107
37. Castilla V, Larzábal M, Aguirre Sgalippa N, Wachsman MB, Coto CE (2005) Antiviral mode of action of a synthetic brassinosteroid against Junín virus replication. *Antivir Res* 68:88–95. doi:10.1016/j.antiviral.2005.07.007
38. Acosta EG, Bruttomesso AC, Bisceglia JA, Wachsman MB, Galagovsky LR, Castilla V (2008) Dehydroepiandrosterone, epiandrosterone and synthetic derivatives inhibit Junín virus replication in vitro. *Virus Res* 135:203–212. doi:10.1016/j.virusres.2008.03.014
39. Barradas JS, Errea MI, D'Accorso NB, Sepúlveda CS, Talarico LB, Damonte EB (2008) Synthesis and antiviral activity of azoles obtained from carbohydrates. *Carbohydr Res* 343:2468–2474. doi:10.1016/j.ejmech.2010.11.012
40. Barradas JS, Errea MI, D'Accorso NB, Sepúlveda CS, Damonte EB (2011) Imidazo[2,1-b]thiazole carbohydrate derivatives: synthesis and antiviral activity against Junin virus, agent of Argentine hemorrhagic fever. *Eur J Med Chem* 46:259–264. doi:10.1016/j.ejmech.2010.11.012
41. Gowen BB, Wong MH, Jung KH, Sanders AB, Mendenhall M et al (2007) In vitro and in vivo activities of T-705 against arenavirus and bunyavirus infections. *Antimicrob Agents Chemother* 51:3168–3176. doi:10.1128/AAC.00356-07

42. Gowen BB, Smee DF, Wong M-H, Hall JO, Jung KH et al (2008) Treatment of late stage disease in a model of arenaviral hemorrhagic fever: T-705 efficacy and reduced toxicity suggests an alternative to ribavirin. *PLoS One* 3:e3725. doi:[10.1371/journal.pone.0003725](https://doi.org/10.1371/journal.pone.0003725)
43. Müller S, Günther S (2007) Broad-spectrum antiviral activity of small interfering RNA targeting the conserved RNA termini of Lassa virus. *Antimicrob Agents Chemother* 51:2215–2218. doi:[10.1128/AAC.01368-06](https://doi.org/10.1128/AAC.01368-06)
44. Artuso MC, Ellenberg PC, Scolaro LA, Damonte EB, García CC (2009) Inhibition of Junín virus replication by small interfering RNAs. *Antivir Res* 84:31–37. doi:[10.1016/j.antiviral.2009.07.001](https://doi.org/10.1016/j.antiviral.2009.07.001)
45. Lu J, Han Z, Liu Y, Liu W, Lee MS et al (2014) A host-oriented inhibitor of Junin Argentine hemorrhagic fever virus egress. *J Virol* 88:4736–4743. doi:[10.1128/JVI.03757-13](https://doi.org/10.1128/JVI.03757-13)
46. Neumann BW, Bederka LH, Stein DA, Ting JPC, Moulton HM, Buchmeier MJ (2011) Development of peptide-conjugated morpholino oligomers as pan-arenavirus inhibitors. *Antimicrob Agents Chemother* 55:4631–4638. doi:[10.1128/AAC.00650-11](https://doi.org/10.1128/AAC.00650-11)
47. Rathbun J, Droniou ME, Damoiseaux R, Haworth KG, Henley JE et al (2015) Novel arenavirus entry inhibitors discovered by using a minigenome rescue system for high-throughput drug screening. *J Virol* 89:8428–8443. doi:[10.1128/JVI.00997-15](https://doi.org/10.1128/JVI.00997-15)
48. Vázquez-Calvo A, Martín-Acebes MA, Sáiz JC, Ngo N, Sobrino F, de la Torre JC (2013) Inhibition of the multiplication of the prototypic arenavirus LCMV by valproic acid. *Antivir Res* 99:172–179. doi:[10.1016/j.antiviral.2013.05.012](https://doi.org/10.1016/j.antiviral.2013.05.012)
49. Pasquato A, Rochat C, Burri DJ, Pasqual G, de la Torre JC, Kunz S (2012) Evaluation of the anti-arenaviral activity of the subtilisin kexin isozyme-1/site-1 protease inhibitor PF-429242. *Virology* 423:14–22. doi:[10.1016/j.virol.2011.11.008](https://doi.org/10.1016/j.virol.2011.11.008)

Retrovirus-Based Surrogate Systems for BSL-2 High-Throughput Screening of Antivirals Targeting BSL-3/4 Hemorrhagic Fever-Causing Viruses

Sheli R. Radoshitzky, Veronica Soloveva, Dima Gharaibeh, Jens H. Kuhn, and Sina Bavari

Abstract

The majority of viruses causing hemorrhagic fever in humans are Risk Group 3 or 4 pathogens and, therefore, can only be handled in biosafety level 3 or 4 (BSL-3/4) containment laboratories. The restricted number of such laboratories, the substantial financial requirements to maintain them, and safety concerns for the laboratory workers pose formidable challenges for rapid medical countermeasure discovery and evaluation. BSL-2 surrogate systems are a less challenging, cheap, and fast alternative to the use of live high-consequence viruses for dissecting and targeting individual steps of viral lifecycles with a diminished threat to the laboratory worker. Typical surrogate systems are virion-like particles (VLPs), transcriptionally active (“infectious”) VLPs, minigenome systems, recombinant heterotypic viruses encoding proteins of target viruses, and vesiculoviral or retroviral pseudotype systems. Here, we outline the use of retroviral pseudotypes for identification of antivirals against BSL-4 pathogens.

Key words Antiviral, Biosafety level 4, BSL-4, High-throughput screening, Pseudotypes, Viral hemorrhagic fever, Virus entry

1 Introduction

Single-stranded RNA viruses from at least seven different families (*Arenaviridae*, *Hantaviridae*, *Nairoviridae*, *Peribunyaviridae*, *Phenuiviridae*, *Filoviridae*, *Flaviviridae*) can cause severe clinical syndromes termed “viral hemorrhagic fevers” (VHFs) in humans [1]. Because of their high virulence, experimental work with most of these viruses is restricted to BSL-3 or maximum containment (BSL-4) laboratories. To screen for or study antivirals that inhibit specific lifecycle stages of these viruses under standard BSL-2 conditions, several virus surrogate systems have been developed. These systems include virion-like particles (VLPs), transcriptionally active

(“infectious”) VLPs, minigenome systems, recombinant heterotypic viruses encoding proteins of target viruses, and vesiculoviral or retroviral pseudotype systems [2–16].

This chapter will focus on a surrogate system to screen and investigate potential cell-entry inhibitors of human hemorrhagic fever-causing viruses. This system makes use of capsid-encoding vectors derived from retroviruses (most commonly Moloney murine leukemia virus [MoMLV], human immunodeficiency virus 1, or simian immunodeficiency virus) or vesiculoviruses (most commonly vesicular stomatitis Indiana virus, sometimes rabies virus). Typically, two additional vectors are transfected into cells to create retrovirion-like particles. The first vector encodes the envelope spike glycoprotein of the hemorrhagic fever-causing virus of interest; the second vector encodes a reporter gene, such as enhanced green fluorescent protein (eGFP) or luciferase, flanked by packaging signals. Upon co-transfection, retrovirion-like capsids are produced that package the reporter gene-encoding nucleic acid, and the resulting ribonucleocapsid particles bud from host cell membranes, thereby incorporating the glycoprotein of interest. Traditionally, such particles are called pseudotypes because they acquire the serological and receptor specificities from their origin, i.e., those of the hemorrhagic fever-causing virion from which the heterotypic spike protein is derived. Such pseudotypes can then be used to transduce cells expressing the target virus receptor with the reporter gene-encoding nucleic acid: expression of the reporter signifies successful cell entry of the pseudotypes. To date, such pseudotypes have been described for mammarenaviruses, bunyaviruses, filoviruses, and flaviviruses [17–27], allowing rapid and reliable screening of small-molecule libraries targeting virus entry in a high-throughput format.

Below, we outline the experimental setup for creating and using retroviral pseudotypes using MoMLV capsids.

2 Materials

2.1 Reagents and Plastic Ware

1. 1–10 ml plastic disposable pipettes and electronic tissue-culture pipettors.
2. Dulbecco’s modified Eagle medium (DMEM)/High Glucose without sodium pyruvate (HyClone).
3. Fetal bovine serum (FBS) (HyClone). FBS is heat-inactivated for 1 h in a 56 °C water bath, and then stored at 4 °C.
4. 100× Penicillin–streptomycin solution (PenStrep).
5. Trypsin- EDTA: 0.25% trypsin in 0.53 mM EDTA.
6. Dulbecco’s phosphate-buffered saline (DPBS) containing calcium and magnesium.

7. 2.5 M CaCl₂ solution (50 ml): bring 27.38 g calcium chloride (CaCl₂) to 50 ml with H₂O, filter through a 0.22- μ m filter, and store at 4 °C.
8. 0.15 M Na₂HPO₄ solution (50 ml): dissolve 2.01 g of Na₂HPO₄ in 50 ml of H₂O.
9. 2 \times Hepes-buffered saline (HBS) solution (100 ml): mix 5.6 ml of 5 M NaCl, 5 ml of 1 M 4-(2-hydroxyethyl)-1-piperazine-ethanesulfonic acid (HEPES), 1 ml of 0.15 M Na₂HPO₄, and 88.4 ml of H₂O. Adjust solution to pH 7.1 with a few drops of 1 N NaOH, filter through a 0.22- μ m filter, aliquot, and freeze at -20 °C.
10. 50-ml conical styrene centrifuge tubes.
11. 20% sucrose solution (100 ml): dissolve 20 g of UltraPure sucrose, 100 mM NaCl, 20 mM HEPES (pH 7.4), and 1 mM EDTA. Adjust the volume to 100 ml by adding H₂O, filter, and then sterilize. This solution can be stored at 4 °C for at least 6 months.
12. 1 \times PBS, without calcium chloride and magnesium.
13. 0.45 or 0.22 μ m, 250-ml Stericup filter units, polyvinylidene fluoride membrane (Durapore).
14. 38.5 ml, Ultra-Clear SW 32 Ti Beckman ultracentrifuge tubes.
15. 10% buffered formalin.
16. Hoechst nucleic acid stain 33342.
17. 175 cm² vented tissue-culture flasks (T175).
18. DRAQ5 fluorescent probe solution (a far-red fluorescent DNA stain).

2.2 Cells and Medium

1. Human embryonic kidney (HEK) 293T cells (ATCC, #CRL-11268) or HeLa cells (ATCC, #CCL-2).
2. Growth media: DMEM/High Glucose for HEK-293T cells contains 1% penicillin–streptomycin and 10% FBS. Minimum essential medium (MEM) for HeLa cells contains 1% penicillin–streptomycin, 10% FBS, 1% L-glutamine, 10 mM HEPES, 1% nonessential amino acids.

2.3 Plasmids

1. Maxi-prep- or midi-prep-quality plasmid DNA encoding MoMLV LTR-eGFP-LTR (*see Note 1*) and MoMLV gag/pol (retroviral capsid/polymerase proteins).
2. Maxi-prep- or midi-prep-quality plasmid DNA encoding viral spike glycoprotein of choice.

2.4 High-Throughput Screening

1. Antiviral library of choice.
2. Opera screening system (Perkin Elmer) for high-throughput screening of confocal images.

3. VIAFILL reagent dispenser with a touch-screen graphic interface to program repeat dispenses.
4. Multidrop Combi reagent dispenser for dispensing liquid to 96-well plates.
5. Greiner black 96-well microplates for fluorescence assays.

3 Methods

3.1 Seeding of Cells

1. Use healthy cells that have not been passaged more than 20 times. This is critical for pseudotype quality and titer.
2. Start with two T175 flasks of confluent HEK 293T cells in DMEM growth medium.
3. Detach cells using trypsin 1 day (18–24 h) before transfection. Split cells at 1:6 dilution into 12 new T175 flasks in 25 ml of growth medium per flask. Empirically, best results are achieved using this ratio.

3.2 Transfection of HEK 293T Cells

1. Inspect the cells under a microscope for attachment to flask (no clumping) and even distribution at around 30–40% confluence.
2. Mix 228 µg of MoMLV LTR-eGFP-LTR plasmid, 228 µg of MoMLV gag-pol plasmid, and 228 µg of spike protein-encoding plasmid in a sterile 50 ml polystyrene tube (labeled 1) (19 µg of each plasmid at 1:1:1 ratio per flask; *see Note 2*). Fill tube up to 10.8 ml (900 µl per flask) with sterile H₂O and mix. Then add 1200 µl (100 µl per flask) of 2.5 M CaCl₂ to tube and vortex briefly.
3. Add 12 ml (1000 µl per flask) of 2× HBS to a sterile 50-ml polystyrene tube (labeled 2).
4. Slowly add contents of tube 1 one drop at a time to tube 2 while vortexing lightly.
5. Incubate tube at room temperature for 10–20 min. The solution should turn slightly milky.
6. Place T175 flasks in upright position and evenly distribute 2 ml of mixed content of tube 2 one drop at a time to the medium of each flask. The medium should turn slightly yellow when the drops hit. Be sure to work swiftly so that cells do not dry out.
7. Gently turn the flask into the horizontal position and incubate at 37 °C in a 5% CO₂ atmosphere for 6 h.

3.3 Changing the Media

1. Carefully examine flasks under a light microscope to detect numerous visible calcium phosphate crystals (reminiscent of small debris among the cells).

2. Remove medium by aspiration and wash cells with 10 ml of warm DPBS via gentle immersion. Some cells will detach during this process.
3. Add 17 ml of warm DMEM growth medium.
4. Monitor the transfected cells under a microscope for the development of fluorescent signal. If the eGFP reporter gene is used, more than 95% of the cells should fluoresce green.

3.4 Harvesting Pseudotype-Containing Cell Supernatant

1. Transfer media into 50-ml conical tubes. Some cells will detach, which is normal.
2. Spin the tubes in a tabletop centrifuge at 4 °C for 10 min. at 2000 rpm ($631 \times g$) to pellet cells and large cell debris.
3. Pour supernatant through a 0.45- μ m filter unit. Replace the filter unit if the filter starts to clog.
4. Aliquot and store at 4 °C if use is planned within the next 3–4 days or freeze at –80 °C for long-term storage. Alternatively, cleared supernatant can be concentrated as outlined below (*see Note 3*).

3.5 Concentrating Pseudotypes

1. Sterilize six SW 32 Ti centrifuge tubes by placing the tubes into a laminar flow hood under UV light for 30 min.
2. Transfer 25-ml aliquots of filtered cell-culture supernatant into each of the six UV-sterilized SW 32 Ti tubes.
3. Fill a 10-ml pipette to the 12-ml mark with a 20% sucrose solution. Insert the pipette all the way to the bottom of a SW 32 Ti tube filled with the filtered supernatant and gently underlay it by slowly expelling 4 ml of the sucrose solution. Repeat this step for two more of the SW 32 Ti tubes using the remaining 8 ml (4 ml/tube) of the 20% sucrose solution from the same 10-ml pipette. Use a new 10-ml pipette filled with 12 ml of a 20% sucrose solution and expel 4 ml of the sucrose solution at the bottom of the remaining three tubes.
4. Gently add additional 9 ml of filtered cell-culture supernatant into each of the six SW 32 Ti tubes.
5. Adjust the weight of each tube by adding DMEM until they are within 0.1 g of each other.
6. Place all the six tubes into a Beckman SW 32 Ti ultracentrifuge rotor and spin for 2 h at 28,000 rpm ($133,907 \times g$) at 4 °C.
7. Carefully remove tubes from the rotor, pour off supernatant, and leave tubes on a paper towel in an inverted position for 10 min to allow residual liquid to drip away from the pellet.
8. Add 0.5 ml of PBS (without calcium/magnesium) to each pellet.
9. Place the ultracentrifuge tubes into 50-ml conical tubes and cap tubes with their lids.

10. Incubate the tubes at 4 °C for 2 h. Vortex very gently every 20 min.
11. Spin the tubes at 500 × *g* for 1 min at room temperature to collect the pseudotype-containing liquid.
12. Resuspend the pellet by gently pipetting the liquid up and down with a 1-ml pipette. Avoid forming bubbles. Combine liquid from all resuspended pellets in a single ultracentrifuge tube.
13. Aliquot in screw-cap microcentrifuge tubes in 100–500 µl portions, and store at -80 °C.

3.6 Titration of Pseudotypes in 96-well Plates

1. Plate HeLa cells (or other cell type of choice) using a Multidrop Combi reagent dispenser at a density of 7000 cells per well in 100 µl of culture media in a 96-well plate 1 day before transduction.
2. Add twofold serial dilutions of pseudotypes 24 h after seeding in a total volume of 100 µl per well using 3–6 wells per each dilution. Use 5–50 µl of unconcentrated stocks and 1–50 µl of concentrated stocks of pseudotypes for dilutions.
3. Add media only to at least 6–8 wells for use as non-transduced controls.
4. Incubate the cells at 37 °C for 2 h (for arenavirus pseudotypes) to 6 h (for filovirus pseudotypes) (*see Note 4*).
5. Remove media with unattached pseudotypes and replace with 100 µl fresh growth medium per well.
6. Incubate the cells at 37 °C for an additional 48 h (*see Note 5*).
7. Observe/analyze the transduced cells (e.g., eGFP-positive cells under a fluorescent microscope) to determine the assay end point.
8. Remove media from cells and fix with 10% buffered formalin for 15 min at room temperature.
9. Wash cells three times with PBS (100 µl per well).
10. Dilute Draq5 fluorescent probe solution (made fresh on demand) 1:2500 in PBS. Stain cell nuclei with Draq5 fluorescent probe solution by adding 100 µl of solution per well.
11. If an eGFP reporter is used: image cells using fluorescence microscopy and determine the percentage of positive fluorescent cells (% transduced cells).
12. Acquire images of the cells in 96-well plates with an Opera Confocal plate reader using a 10× air objective.
13. Specify acquisition channels for measuring signal from eGFP reporter and from stained cell nuclei. Detect the signal from the eGFP reporter from the 488-nm channel. Detect the signal

from the stained cell nuclei (using Draq5) from the 640-nm channel.

14. Perform image analysis using Acapella algorithms (PerkinElmer). Generate a cellular mask showing cell boundaries using Acapella algorithm.
15. Measure output parameter, *Number of Objects*, based on the nuclei count in the 640-nm channel.
16. Measure *Positive Pseudotyped Number of Objects* using number of objects (nuclei) with cellular mask containing pseudotype specific signal/reporter at 488-nm channel. Use threshold value at the beginning of the dynamic range for the eGFP signal to differentiate positive eGFP-containing cells.
17. Calculate, using Acapella, the percentage of transduced cells directly for each image by the equation:

$$\%transduced\ cells = \frac{Positive\ Pseudotyped\ Number\ of\ Objects\ (s)}{Number\ of\ objects\ (s)} * 100$$

Use 3–6 wells for collecting statistically significant results.

18. Calculate titer (transducing units [TU] ml⁻¹) according to the following formula: TU ml⁻¹ = (P × N × D × 1000) / V, with P = percentage of transduced cells, N = number of cells (objects), D = fold dilution of sample used for transduction, and V = volume (μl) of diluted sample added into each well for transduction.
19. Calculate an average titer from cells transduced with different amounts of pseudotypes (*see Note 6*).
20. Select the amount of pseudotypes to be used for the screen (optimal transduction rates are in a range in which a linear relationship is observed between the percentage of fluorescence-positive cells and the amount of pseudotypes added).

3.7 Screening

1. Plate HeLa cells (or other cell type of choice) using the Multidrop Combi reagent dispenser at a density of 7000 cells per well in 100 μl of culture media in a 96-well plate 1 day before transduction.
2. Treat wells containing cells with test and control compounds of choice (50 μl per well) at least 2 h prior to addition of pseudotypes (*see Note 7*). Treat at least 6–8 wells with DMSO only as a control for transduction (high-signal control, HC). Leave 6–8 wells uninfected for the low-signal control (LC). Use three replicates (*n* = 3) of each compound.
3. Add pseudotypes using VIAFILL touch screen rapid reagent dispenser, in a volume of 50 μl per well. Make sure to include non-transduced control wells (*see Note 8*).

4. Incubate the plates at 37 °C for 2–6 h (*see Note 4*).
5. Replace the media with 100 of µl fresh growth medium per well.
6. Incubate the cells at 37 °C for 48 h (*see Note 5*).
7. Remove media and submerge plates in 10% buffered formalin for 15 min.
8. Wash cells three times with PBS (100 µl per well) and stain with Draq5 for nuclei and cytoplasm detection (dilute Draq5 1:2500 in PBS, add 100 µl per well).
9. Determine the rate of positive fluorescent cells (% transduced cells) as well as cell number as described above.
10. Use clear criteria for quality of transduction. Use the Z' (Z -prime, do not confuse with Z -score) factor (*see Note 9*) to assess quality of the assay performed using multi-well plates and multiple plates:

$$Z' = 1 - \frac{3(SD(LC) + SD(HC))}{Mean(HC) - Mean(LC)}$$

11. Normalize the change in transduction rates for each plate by using control wells on the same plate: HC, transduced but treated with DMSO only, used as 0% inhibition of transduction; and LC, non-transduced control, used as 100% inhibition of transduction (*see Note 10*).

4 Notes

1. Retroviral packaging signals, i.e., long-terminal repeats (LTRs), flanking eGFP, or any other reporter gene of choice.
2. Depending on spike protein, further optimization of the ratio between spike and MoMLV plasmids may be needed if results are unsatisfactory.
3. Concentration is typically recommended if the rate of transduction is less than 10% (depending on statistical significance).
4. Optimal incubation time with each pseudotype depends on viral glycoprotein-mediated entry kinetics. For best results, determine the optimal incubation time with the pseudotypes of choice.
5. Incubation time following pseudotype transduction will depend on chosen cell type. If using a cell line other than HeLa, optimization is recommended.
6. For accurate titer determination, the amount of pseudotypes used should fall in a range in which linear relationship is

observed between the percentage of fluorescence-positive cells and the amount of pseudotypes added.

7. If the compounds in the library are dissolved in DMSO, dilute the compounds to achieve a final DMSO concentration of not more than 1%.
8. Compounds are diluted two-fold after addition of pseudotypes.
9. The acceptable range for Z' is 0.5–1 [28].
10. Plate-based normalization is necessary for data comparison between different plates. Normalization should be used with caution if the transduction rate is too variable between plates.

Acknowledgment/Disclaimer

This work was supported by the Joint Science and Technology Office for Chemical and Biological Defense (JSTO-CBD) of the Defense Threat Reduction Agency (DTRA) (proposal # 1323839 and CCAR# CB3849) to SB and in part through Battelle Memorial Institute's prime contract with the US National Institute of Allergy and Infectious Diseases (NIAID) under Contract No. HHSN272200700016I. A subcontractor to Battelle Memorial Institute who performed this work is: J.H.K., an employee of Tunnell Government Services, Inc. The content of this publication does not necessarily reflect the views or policies of the US Department of the Army, the US Department of Defense, the US Department of Health and Human Services, or the institutions and companies affiliated with the authors.

References

1. Kuhn JH, Clawson AN, Radoshitzky SR, Wahl-Jensen V, Bavari S, Jahrling PB (2013) Viral hemorrhagic fevers: history and definitions. *Viral hemorrhagic fevers*. Taylor & Francis/CRC Press, Boca Raton, Florida, USA
2. Suomalainen M, Garoff H (1994) Incorporation of homologous and heterologous proteins into the envelope of Moloney murine leukemia virus. *J Virol* 68(8):4879–4889
3. Capul AA, de la Torre JC (2008) A cell-based luciferase assay amenable to high-throughput screening of inhibitors of arenavirus budding. *Virology* 382(1):107–114. doi:10.1016/j.virol.2008.09.008
4. Bouloy M, Flick R (2009) Reverse genetics technology for Rift Valley fever virus: current and future applications for the development of therapeutics and vaccines. *Antivir Res* 84(2):101–118. doi:10.1016/j.antiviral.2009.08.002
5. Devignot S, Bergeron E, Nichol S, Mirazimi A, Weber F (2015) A virus-like particle system identifies the endonuclease domain of Crimean-Congo hemorrhagic fever virus. *J Virol* 89(11):5957–5967. doi:10.1128/JVI.03691-14
6. Hoenen T, Feldmann H (2014) Reverse genetics systems as tools for the development of novel therapies against filoviruses. *Expert Rev Anti-Infect Ther* 12(10):1253–1263. doi:10.1586/14787210.2014.948848
7. Ikegami T, Peters CJ, Makino S (2005) Rift Valley fever virus nonstructural protein NSs promotes viral RNA replication and transcription in a minigenome system. *J Virol* 79(9):5606–5615. doi:10.1128/JVI.79.9.5606-5615.2005
8. Masse N, Davidson A, Ferron F, Alvarez K, Jacobs M, Romette JL, Canard B, Guillemot JC (2010) Dengue virus replicons: production of an interserotypic chimera and cell lines from

- different species, and establishment of a cell-based fluorescent assay to screen inhibitors, validated by the evaluation of ribavirin's activity. *Antivir Res* 86(3):296–305. doi:[10.1016/j.antiviral.2010.03.010](https://doi.org/10.1016/j.antiviral.2010.03.010)
9. Mühlberger E, Lötfering B, Klenk HD, Becker S (1998) Three of the four nucleocapsid proteins of Marburg virus, NP, VP35, and L, are sufficient to mediate replication and transcription of Marburg virus-specific monocistronic minigenomes. *J Virol* 72(11):8756–8764
 10. Mühlberger E, Weik M, Volchkov VE, Klenk HD, Becker S (1999) Comparison of the transcription and replication strategies of Marburg virus and Ebola virus by using artificial replication systems. *J Virol* 73(3):2333–2342
 11. Ng CY, Gu F, Phong WY, Chen YL, Lim SP, Davidson A, Vasudevan SG (2007) Construction and characterization of a stable subgenomic dengue virus type 2 replicon system for antiviral compound and siRNA testing. *Antivir Res* 76(3):222–231. doi:[10.1016/j.antiviral.2007.06.007](https://doi.org/10.1016/j.antiviral.2007.06.007)
 12. Weber F, Dunn EF, Bridgen A, Elliott RM (2001) The Bunyamwera virus nonstructural protein NSs inhibits viral RNA synthesis in a minireplicon system. *Virology* 281(1):67–74. doi:[10.1006/viro.2000.0774](https://doi.org/10.1006/viro.2000.0774)
 13. Yang CC, Tsai MH, Hu HS, Pu SY, Wu RH, Wu SH, Lin HM, Song JS, Chao YS, Yueh A (2013) Characterization of an efficient dengue virus replicon for development of assays of discovery of small molecules against dengue virus. *Antivir Res* 98(2):228–241. doi:[10.1016/j.antiviral.2013.03.001](https://doi.org/10.1016/j.antiviral.2013.03.001)
 14. Kranzusch PJ, Schenk AD, Rahmeh AA, Radoshitzky SR, Bavari S, Walz T, Whelan SP (2010) Assembly of a functional Machupo virus polymerase complex. *Proc Natl Acad Sci U S A* 107(46):20069–20074. doi:[10.1073/pnas.1007152107](https://doi.org/10.1073/pnas.1007152107). 1007152107 [pii]
 15. Hass M, Gölnitz U, Müller S, Becker-Ziaja B, Günther S (2004) Replicon system for Lassa virus. *J Virol* 78(24):13793–13803. doi:[10.1128/JVI.78.24.13793-13803.2004](https://doi.org/10.1128/JVI.78.24.13793-13803.2004). 78/24/13793 [pii]
 16. Albariño CG, Bird BH, Chakrabarti AK, Dodd KA, White DM, Bergeron E, Shrivastava-Ranjan P, Nichol ST (2011) Reverse genetics generation of chimeric infectious Junin/Lassa virus is dependent on interaction of homologous glycoprotein stable signal peptide and G2 cytoplasmic domains. *J Virol* 85(1):112–122. doi:[10.1128/jvi.01837-10](https://doi.org/10.1128/jvi.01837-10)
 17. Radoshitzky SR, Abraham J, Spiropoulou CF, Kuhn JH, Nguyen D, Li W, Nagel J, Schmidt PJ, Nunberg JH, Andrews NC, Farzan M, Choe H (2007) Transferrin receptor 1 is a cellular receptor for New World haemorrhagic fever arenaviruses. *Nature* 446(7131):92–96. doi:[10.1038/nature05539](https://doi.org/10.1038/nature05539)
 18. Radoshitzky SR, Kuhn JH, Spiropoulou CF, Albariño CG, Nguyen DP, Salazar-Bravo J, Dorfman T, Lee AS, Wang E, Ross SR, Choe H, Farzan M (2008) Receptor determinants of zoonotic transmission of New World hemorrhagic fever arenaviruses. *Proc Natl Acad Sci U S A* 105(7):2664–2669. doi:[10.1073/pnas.0709254105](https://doi.org/10.1073/pnas.0709254105)
 19. Reignier T, Oldenburg J, Noble B, Lamb E, Romanowski V, Buchmeier MJ, Cannon PM (2006) Receptor use by pathogenic arenaviruses. *Virology* 353(1):111–120. doi:[10.1016/j.viro.2006.05.018](https://doi.org/10.1016/j.viro.2006.05.018)
 20. Rojek JM, Spiropoulou CF, Kunz S (2006) Characterization of the cellular receptors for the South American hemorrhagic fever viruses Junin, Guanarito, and Machupo. *Virology* 349(2):476–491. doi:[10.1016/j.viro.2006.02.033](https://doi.org/10.1016/j.viro.2006.02.033)
 21. Hu HP, Hsieh SC, King CC, Wang WK (2007) Characterization of retrovirus-based reporter viruses pseudotyped with the precursor membrane and envelope glycoproteins of four serotypes of dengue viruses. *Virology* 368(2):376–387. doi:[10.1016/j.viro.2007.06.026](https://doi.org/10.1016/j.viro.2007.06.026)
 22. Ma M, Kersten DB, Kamrud KI, Wool-Lewis RJ, Schmaljohn C, Gonzalez-Scarano F (1999) Murine leukemia virus pseudotypes of La Crosse and Hantaan bunyaviruses: a system for analysis of cell tropism. *Virus Res* 64(1):23–32
 23. Oginio M, Ebihara H, Lee BH, Araki K, Lundkvist Å, Kawaoka Y, Yoshimatsu K, Arikawa J (2003) Use of vesicular stomatitis virus pseudotypes bearing Hantaan or Seoul virus envelope proteins in a rapid and safe neutralization test. *Clin Diagn Lab Immunol* 10(1):154–160
 24. Shtanko O, Nikitina RA, Altuntas CZ, Chepurinov AA, Davey RA (2014) Crimean-Congo hemorrhagic fever virus entry into host cells occurs through the multivesicular body and requires ESCRT regulators. *PLoS Pathog* 10(9):e1004390. doi:[10.1371/journal.ppat.1004390](https://doi.org/10.1371/journal.ppat.1004390)
 25. Sinn PL, Hickey MA, Staber PD, Dylla DE, Jeffers SA, Davidson BL, Sanders DA, McCray PB Jr (2003) Lentivirus vectors pseudotyped with filoviral envelope glycoproteins transduce airway epithelia from the apical surface independently of folate receptor alpha. *J Virol* 77(10):5902–5910
 26. Takada A, Robison C, Goto H, Sanchez A, Murti KG, Whitt MA, Kawaoka Y (1997) A system for functional analysis of Ebola virus glycoprotein. *Proc Natl Acad Sci U S A* 94(26):14764–14769

27. Wool-Lewis RJ, Bates P (1998) Characterization of Ebola virus entry by using pseudotyped viruses: identification of receptor-deficient cell lines. *J Virol* 72(4):3155–3160
28. Zhang JH, Chung TD, Oldenburg KR (1999) A simple statistical parameter for use in evaluation and validation of high throughput screening assays. *J Biomol Screen* 4(2):67–73

Protocols to Assess Coagulation Following In Vitro Infection with Hemorrhagic Fever Viruses

Melissa L. Tursiella, Shannon L. Taylor, and Connie S. Schmaljohn

Abstract

During the course of infection with a hemorrhagic fever virus (HFV), the checks and balances associated with normal coagulation are perturbed resulting in hemorrhage in severe cases and, in some patients, disseminated intravascular coagulopathy (DIC). While many HFVs have animal models that permit the analyses of systemic coagulopathy, animal infection models do not exist for all HFVs and moreover do not always recapitulate the pathology observed in human tissues. Furthermore, molecular analyses of how coagulation is affected are not always straightforward or practical when using ex-vivo animal-derived samples, thus reinforcing the importance of cell culture studies. This chapter highlights procedures utilizing human umbilical vein endothelial cells (HUVECs) as a model system to evaluate components of the intrinsic (prekallikrein (PK), factor XII (FXII), kininogen, and bradykinin (BK)) and extrinsic (Tissue Factor (TF)) systems. Specifically, protocols are included for the generation of a coculture blood vessel model, plating and infection of HUVEC monolayers and assays designed to measure activation of PK and FXII, cleavage of kininogen, and to measure the expression of TF mRNA and protein.

Key words Coagulation, Tissue factor, Factor XII, FXIIa, HUVEC, Bradykinin, Kininogen, Prekallikrein

1 Introduction

Viral hemorrhagic fever (VHF) results from infection with RNA viruses of the *Arenaviridae*, *Bunyavirales*, *Filoviridae*, and *Flaviviridae*, and is characterized by coagulation abnormalities, including hemorrhage (reviewed in [1, 2]). Hemostasis, or the balance between coagulation and fibrinolysis, is critical for maintaining the equilibrium between blood clot formation and wound healing and the inhibition of continued clot growth and dissolution of fibrin clots (reviewed in [3]). Coagulation is divided into two pathways, the intrinsic and extrinsic pathways that converge at the common pathway, encompassing fibrin generation, crosslinking, and fibrinolysis (reviewed in [3]).

There have been numerous studies evaluating the effects of HFVs on components of coagulation and it has become increasingly clear that expression and/or activity of coagulation proteins are influenced by infection. For example, tissue factor (TF), the initiator of the extrinsic coagulation cascade, is upregulated in macrophages following infection of nonhuman primates with the filovirus Ebola virus. Likewise, patients infected with the flavivirus dengue virus who develop severe dengue have increased levels of TF in their sera/plasma [4–6]. DHF patients also exhibit upregulated, von Willebrand factor antigen (vW: Ag), which facilitates platelet attachment and transports factor VIII [7], and plasminogen-activating factor (PAI-1), an inhibitor of fibrinolysis [4]. Following infection with the arenavirus Junín virus, Argentine hemorrhagic fever patients display increased PAI-1, and tissue plasminogen activator (tPA), a serine protease involved in the dissolution of clots (reviewed [8, 10]). Furthermore, research from our laboratory demonstrates that infection with either Hantaan or Andes viruses results in the liberation of bradykinin and increased FXII activity and binding [9], all of which are involved in the intrinsic pathway.

Numerous studies have evaluated coagulation in the course of *in vivo* experiments, or through analysis of clinical samples. While these studies are extremely valuable, they can also be expensive, and are limited by sample availability and existing reagents for assessing various coagulation markers in nonhuman samples. Therefore, we have studied the effects of HFV infection on coagulation following endothelial cell infection. This chapter will highlight methods to assess select components of the intrinsic and extrinsic pathways and some of the challenges associated with inactivating samples following HFV infection.

2 Materials

2.1 *Cells for Infection and Viral Stocks*

1. Pooled human umbilical vein endothelial cells (HUVECs); no greater than passage 7 and cultured with manufacturer's recommendation (Lonza).
2. HEPES-buffered saline (HBSS) (Lonza).
3. Phosphate-buffered saline (PBS).
4. TrypLE Express, a mix of enzymes meant to replace trypsin (Life Technologies).
5. 0.1% gelatin (Millipore).
6. Endothelial growth medium (EGM-2) bullet kit (Lonza).
7. Phorbol 12-myristate 13-acetate (PMA) (Sigma). PMA is a strong inducer of tissue factor. Since it is a plant-derived compound sold as a crude powder, the optimal inducing concen-

tration must be determined for each batch. It is generally used at 25–50 nM PMA in culture media.

8. Viral stocks: HFVs and respective media for mock samples.

2.2 mRNA Isolation and Quantitative Real-Time Polymerase Chain Reaction (qRT-PCR)

1. RNA isolation and purification: TRizol-LS and Purelink RNA Mini Kit (Thermo Fischer/Life Technologies).
2. 1.5 mL microfuge tubes with O-ring to prevent spills and generation of aerosol (Sarstedt).
3. NanoDrop spectrophotometer (Thermo/Fisher).
4. MicroChem, a detergent disinfectant (National Chemical Laboratories Inc.).
5. qRT-PCR 1-Step Master Mix (Brilliant II, Agilent).
6. qRT-PCR assays for tissue factor (TF) and TATA-box binding protein (TBP, a housekeeping gene) (Life Technologies assays Hs01076032_m1 and Hs00427621_m1, respectively). In the described assays, the TF probe is labeled with a FAM™ dye while the TBP probe is labeled with a HEX™ dye for detection by the PCR machine.
7. 0.2 mL PCR strip cap tubes (Bio-Rad).
8. CFX96 qRT-PCR machine and CFX Manager software (Bio-Rad).

2.3 Flow Cytometry

1. Infected and/or PMA-treated HUVECs.
2. MicroChem, a detergent disinfectant (National Chemical Laboratories Inc.).
3. PBS (Hyclone; Thermo Fischer Scientific).
4. 10% neutral buffered formalin (PROTOCOL™).
5. Permeabilization buffer: 0.1% Triton X-100 in PBS.
6. Blocking buffer: PBS with 5.0% fetal bovine serum.
7. Tissue factor antibody (Abcam ab48647).
8. Isotype control antibody (KPL affinity purified goat x rabbit IgG heavy and light).

2.4 On-Cell ELISA, for Analysis of Antigens on the Surface of Cells

1. Infected and/or PMA-treated HUVECs.
2. MicroChem, a detergent disinfectant (National Chemical Laboratories Inc.).
3. HEPES-buffered saline (HBSS) (Lonza).
4. 10% neutral buffered formalin (PROTOCOL™).
5. PBS (Hyclone).
6. 5% and 1% final concentrations (in PBS) Carnation powdered skim milk.
7. Tissue Factor antibody (Abcam ab48647).

8. Secondary antibody GtxRb Poly-HRP (Pierce).
9. SureBlue TMB Solution and TMB Stop Solution (KPL).
10. Crystal Violet (CV) solution, 1:10 dilution (Sigma): 0.2% CV and 2% ethanol (final concentration).
11. Cell culture grade water (Hyclone).
12. 1% Sodium dodecyl sulfate (SDS).

2.5 Vascular Coculture Model

1. Pooled HUVECs.
2. Human pulmonary artery smooth muscle cells (PaSMCs).
3. EGM-2 bullet kit (Lonza).
4. Smooth muscle growth medium (SmGM-2) bullet kit (Lonza).
5. Trypsin and Trypsin neutralizing solution (TNS) (Lonza).
6. HEPES buffer (Lonza).
7. 0.1% gelatin (Millipore).
8. Cell culture plates.

2.6 Analysis of Kininogen Cleavage

1. Pooled HUVECs.
2. EGM-2 Bullet Kit (Lonza).
3. Trypsin and Trypsin neutralizing solution (TNS) (Lonza).
4. HEPES buffer (Lonza).
5. Purified prekallikrein (PK), single chain high molecular weight kininogen (HK), and FXII (Enzyme Research Labs).
6. HEPES-Tyrode's Buffer without and with zinc: 0, 1 or 8 μ M Zinc-HEPES Tyrode's buffers.
7. 10 mM stock zinc chloride solution in water (Sigma).
8. Lysis buffer: 150 mM NaCl, 50 mM Tris-HCl pH 8.0, 1% NP-40, and protease inhibitors.
9. Rabbit anti-HK (Abnova Catalog # H00003827).

2.7 Measurement of Plasma Prekallikrein and FXII Activation

1. Pooled HUVECs.
2. EGM-2 Bullet Kit (Lonza).
3. Trypsin and Trypsin neutralizing solution (TNS) (Lonza).
4. HEPES buffer (Lonza).
5. Purified prekallikrein (PK), kininogen (HK), and FXII (Enzyme Research Labs).
6. HEPES-Tyrode's Buffer without and with zinc: 0, 1, or 8 μ M Zinc-HEPES Tyrode's Buffer.
7. 10 mM stock zinc chloride solution in water (Sigma).
8. Chromozym PK (Sigma Aldrich).

2.8 Quantitative Analysis of Bradykinin Formation

1. Pooled HUVECs.
2. Trypsin and Trypsin neutralizing solution (TNS) (Lonza).
3. HEPES buffer (Lonza).
4. Bradykinin (BK) EIA kit (Enzo Life Sciences).
5. Purified prekallikrein (PK), kininogen (HK), and FXII (Enzyme Research Labs).
6. HEPES-Tyrode's Buffer without and with zinc: 0, 1, or 8 μM Zinc-HEPES Tyrode's Buffer.
7. 10 mM stock zinc chloride solution in water (Sigma).
8. HOE 140, a bradykinin antagonist, and Trandolapril, an ACE-inhibitor used to treat high blood pressure (both from Sigma Aldrich), are used to prevent BK degradation and receptor binding.

3 Methods

3.1 Tissue Factor (TF) mRNA Analyses

3.1.1 Infection and Trizol-LS Inactivation

1. Coat T25 tissue culture-treated flasks with 0.1% gelatin for at least 30 min and then rinse with water.
2. The number of cells plated is dependent on the length of the infection. For a 5 day infection, plate 5×10^4 HUVEC cells per T25 in 5 mL EGM-2, 24 h prior to infection.
3. On the day of infection, remove media and add 1.5 mL EGM-2 to each T25 flask so that infections are allowed to proceed in low volume.
4. Infect cells at an appropriate MOI for 1 h with rocking every 15 min to allow for adsorption. After 1 h, the viral inoculum can be removed and cells can be rinsed with 2 mL of HBSS. Then, 5 mL of new EGM-2 can be added. Alternatively, viral inoculum can be left on the cells and the total volume of media can be brought to 5 mL (*see Note 4.1.1*).
5. After the desired length of infection, remove supernatant (*see Note 4.1.2*) and rinse cells once gently with 2–3 mL of PBS.
6. For Trizol-LS, 0.4 mL is required for inactivation of a 10 cm² cell culture plate (*see Note 4.1.3*). However, to effectively cover the T25 surface, 1.0 mL of Trizol-LS is added to the flask and rocked periodically. Following a 10 min inactivation, the Trizol-LS sample is transferred to a microfuge tube containing an O-ring. Additionally, pipette a small amount of Trizol-LS around the O-ring gasket before closing tubes.

3.1.2 RNA Isolation

1. Following the manufacturer's instructions for compatibility with Trizol, isolate the RNA using the Pure Link RNA Mini Kit.
2. Elute RNA in 30 μL of the RNase-free water provided with kit and analyze concentration and purity using the NanoDrop spectrophotometer.

3.1.3 qRT-PCR

1. For analysis by qRT-PCR, multiplexing the TF and TBP master mixes may result in a reduction in signal. Therefore, separate reactions may need to be run with each master mix. To set up individual reactions, *see* Table 1 (*see* 4.1.4 and 4.1.5).
2. qRT-PCR reaction conditions are as follows: 50 °C—30 min, 95 °C—10 min, 95 °C—15 s, 60 °C—1 min, repeat **steps 3** and **4** for 39 cycles.
3. Adjust threshold cutoff values where appropriate and ensure appropriate parameters for HEX and FAM dye signal standard curves (Fig. 1).
4. Analyze qRT-PCR by normalizing TF Ct values to those of TBP, a housekeeping gene (*see* Note 4.1.6).

3.2 Analysis of Tissue Factor (TF) Protein Expression

3.2.1 Infection and Cell Staining for Flow Cytometric Analysis of Tissue Factor

1. Coat T75 flasks with 0.1% gelatin as described above.
2. For a 5 day infection, plate 2×10^5 HUVEC cells per T75 in 10 mL EGM-2, 24 h prior to infection.
3. On the day of infection, remove media and add 5 mL of media to each T75.
4. Infect cells as described previously in **step 4** of Subheading 3.1.1.
5. Cells can be treated with PMA as a positive control for TF induction. 2–4 h prior to harvest, add 25–50 nM PMA to the culture media (Fig. 2).

Table 1
Reaction volumes for TBP and TF qRT-PCR

	Volume in μL
TBP reaction	
H ₂ O	6.25
2× Brilliant II qRT-PCR 1-step Master Mix	12.5
20× TBP primer/probe set (final of 0.2×)	0.25
RNA (50 ng/ μL)	5.00
Reverse transcriptase/RNase	1.00
TF reaction	
H ₂ O	5.25
2× Brilliant II qRT-PCR 1-step Master Mix	12.5
20× TBP primer/probe set (final of 1×)	1.25
RNA (50 ng/ μL)	5.00
Reverse transcriptase/RNase	1.00

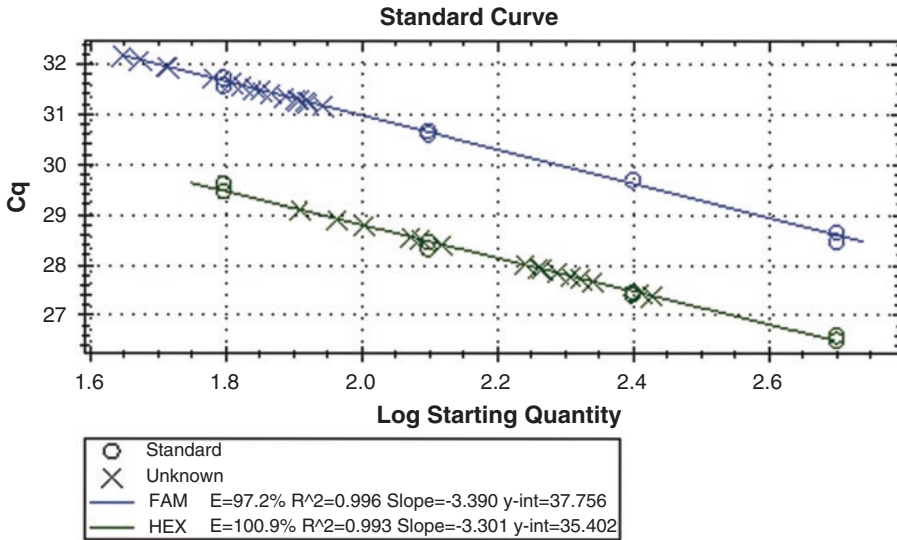


Fig. 1 Standard curves for HEX (the dye labeling TBP) and FAM (the dye labeling TF) signals using HUVEC RNA. Data analyzed using Bio-Rad CFX Manager

6. Remove media and inactivate in Microchem. Put PMA-containing media in appropriate waste container with Microchem.
7. Rinse cells 1× with 10 mL HBSS and add 2 mL of trypsin to each flask. Allow cells to detach at 37 °C for 3–5 min.
8. Neutralize trypsin with 8 mL of EGM-2 and centrifuge at 150 × *g* for 5 min (*see Note 4.2.1*).
9. Remove supernatant and discard. Add 3–5 mL of PBS to each cell pellet and centrifuge as described above.
10. Remove supernatant and resuspend cell pellet in 1.0 mL of 10% neutral buffered formalin. Incubate for 10 min at room temperature (*see 4.2.2–4.2.3*).
11. Centrifuge cells and discard formalin in appropriate waste container. Wash cells 1× with 1-2 mL of PBS.
12. Remove PBS wash and add 100 μL of permeabilization buffer to each pellet and pipette up and down with p1000 tip. Allow cells to permeabilize for 10 min (*see Note 4.2.4*).
13. Add 1 mL of PBS to wash and centrifuge.
14. Remove supernatant and add 200 μL of blocking buffer. Allow cells to block for 10 min (can incubate longer if desired) (*see Note 4.2.5*).
15. Separate cells in blocking buffer into two Sarstedt tubes containing 100 μL each. One tube will be for the isotype control while the other is for TF antibody.

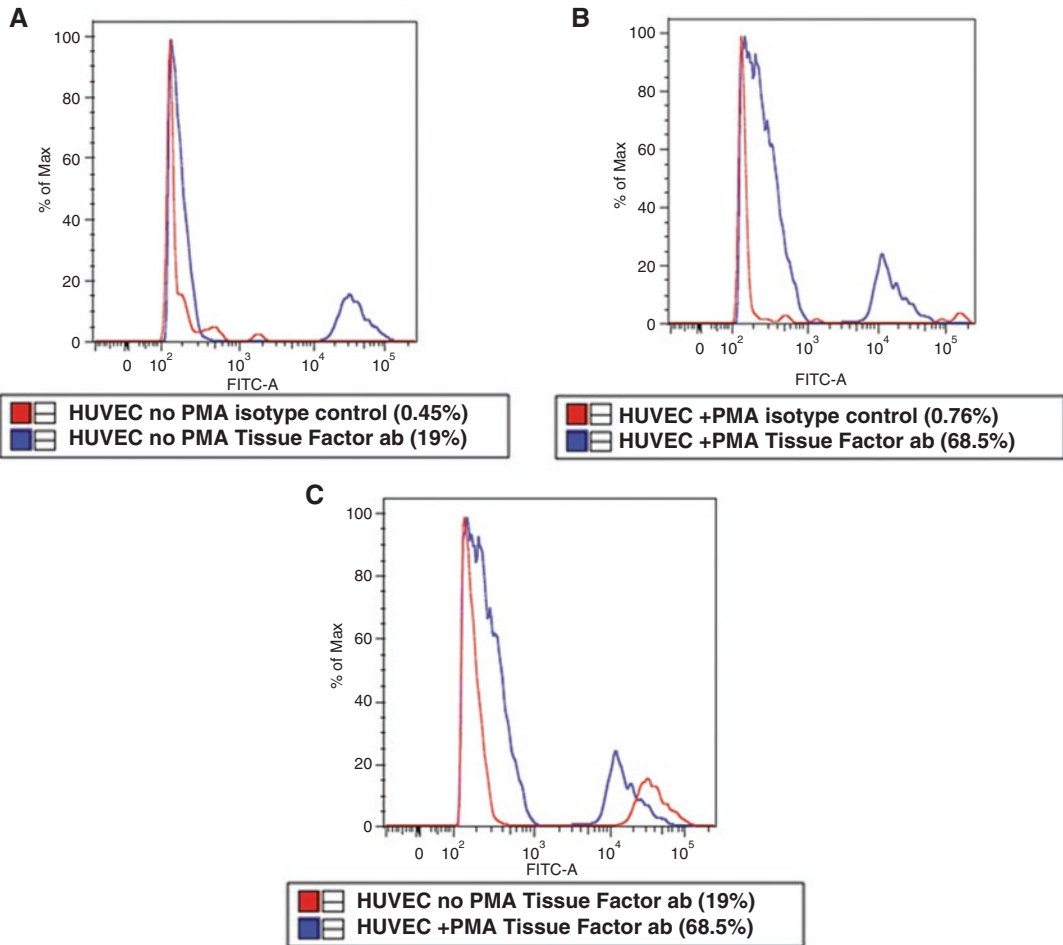


Fig. 2 Analysis of TF expression in PMA-treated and untreated HUVECs. HUVECs were treated (**a** and **c**) with 25 nM PMA for 4 h or left untreated (**b** and **c**). Cells were harvested, fixed (for 10 min), permeabilized, and stained as described in methods with the exception of the 24 h fixation that was not necessary in this experiment since no infectious agents were present. 10,000 cells were collected on BD FACS Canto II using FACSDIVA software and then analyzed in FlowJo

16. Add 100 μ L of primary antibody (diluted at 1:50 in blocking buffer for a final concentration of 1:100) or isotype control (containing the same concentration of antibody as the TF primary) to the respective tubes. Allow staining to proceed for 1 h.
17. Wash cells with 1 mL of PBS, centrifuge and remove supernatant.
18. Resuspend pellet in 100 μ L of secondary antibody (1:1000) diluted in blocking buffer and incubate for 1 h.
19. Wash with 1 mL of PBS, centrifuge and remove the supernatant.
20. Resuspend pellet in 1 mL of 10% formalin and inactivate for 24 h at room temperature (*see* 4.2.6–4.2.7).

3.2.2 Tissue Factor On-Cell ELISA

1. Plate 2.0×10^4 cells per well (for 3 day infection) in a 0.1% gelatin-coated 96-well plate in 100 μL final volume EGM-2.
2. Remove media and replace with 80 μL EGM-2 24 h after plating.
3. Infect wells with HFV of choice.
4. On the day of harvest, add 25 nM PMA for 2–4 h.
5. Remove media from wells with PMA and place in an appropriate waste container with 5% Microchem if infectious agent is used on the same plate. Then remove media from infected wells and inactivate in 5% Microchem.
6. Rinse wells 1 \times with 100 μL of PBS (*see Note 4.3.1*).
7. Fill all wells with 200 μL of 10% formalin and submerge plate and lid in seal bags containing formalin. Then seal in a secondary bag to prevent leaks. Inactivate for 24 h.
8. Remove formalin from bags and plate and discard in a waste container.
9. Rinse wells 1 \times with 100 μL HBSS or PBS.
10. Add 50 μL of anti-TF antibody (1:100 made in 1% milk) and incubate for 1 h.
11. Gently wash cells 5–7 \times with 200 μL HBSS or PBS.
12. Add secondary antibody (GtxRb 1:500 in 1% milk) and incubate for 1 h.
13. Repeat wash as described in **step 11**.
14. Add 100 μL of room temperature SureBlue TMB solution and incubate for 30 min (*see Note 4.3.2*).
15. Add 100 μL of TMB Stop Solution and read at 405 nm.
16. After reading remove substrate and stop solution and rinse 2 \times with 100 μL PBS.
17. Add 100 μL of CV solution and allow cells to stain for 10–20 min at room temperature.
18. Remove CV solution and gently wash several times with water. Continue washing until water removed is clear.
19. Add 100 μL 1% SDS to each well and rock/swirl plate at room temperature to solubilize CV.
20. Read at 590 nm.
21. Normalize each well using the following formula: OD_{405}/OD_{590} . The values of blank wells can then be subtracted from experimental well values (*see Note 4.3.3*).

3.3 Vascular Coculture Model

1. Wash cells grown in flasks three times with HBSS, add trypsin for 5 min and then inactivate the trypsin by adding TNS.
2. Place HUVEC and PaSMC in separate conical tubes and centrifuge at $200 \times g$ for 5 min.

3. Remove supernatant, resuspend cell pellets in their respective media, and count the number of cells.
4. To form capillary blood vessels in a 0.5 cm² well, mix 5×10^4 PaSMC cells with 1×10^4 HUVEC cells (*see Notes 4.4.1–4.4.2*).
5. Add 200 μ L of combined cells to gelatin-coated wells.
6. After 24 h, replace the media with 200 μ L of EGM-2 and culture for an additional 48 h.
7. For longer culturing conditions, change the media every 48 h.
8. Infect cells with the appropriate multiplicity of infection.

3.4 Analysis of Kininogen Cleavage

1. Plate HUVEC on gelatin-coated plates and infect at the desired MOI and length of infection.
2. Remove media and wash cells with HEPES-Tyrode's buffer.
3. Dilute HK to 50 nM in the presence of 1 μ M Zn²⁺ HEPES-Tyrode's buffer, add to cells, and incubate at 37 °C for 1 h.
4. Wash cells and incubate with 50 nM of PK and FXII diluted in 8 μ M Zn²⁺ HEPES-Tyrode's buffer (*see Note 4.5*).
5. After the 1 h incubation at 37 °C, wash cells and lyse in NP-40 lysis buffer. Examine HK cleavage by western blotting.

3.5 Measurement of Plasma Prekallikrein and FXII Activation

1. Plate HUVEC on gelatin-coated plates and infect at the desired MOI and length of infection.
2. Remove media and wash cells with HEPES-Tyrode's buffer.
3. Dilute HK to 20 nM in the presence of 1 μ M Zn²⁺ HEPES-Tyrode's buffer, add to cells, and incubate for 1 h at 37 °C.
4. Wash cells and incubate with 20 nM of PK and FXII and 0.6 mM of Chromozym PK in the presence of 8 μ M Zn²⁺ HEPES-Tyrode's buffer for 1 h at 37 °C (*see Note 4.6*).
5. Determine the hydrolysis of the chromogenic substrate Chromozyme PK by taking absorbance readings at 405 nm.

3.6 Quantitative Analysis of Bradykinin Formation

1. Plate HUVEC on gelatin-coated plates and infect at the desired MOI and length of infection.
2. Pretreat cells with 1 μ M HOE 140 and 5 μ M Trandolapril for 30 min and throughout the experiment (*see Note 4.7.1*).
3. Dilute PK, HK, and FXII to 50 nM in HEPES-Tyrode's buffer containing 8 μ M Zn²⁺ for 1 h at 37 °C (*see Note 4.7.2*).
4. Remove supernatants and perform BK EIA according to the manufacturer's instructions.

4 Notes

4.1 qRT-PCR

1. If a T0 time point is desired, one may choose to harvest a T25 flask immediately following the addition of input virus or after the 1 h incubation.
2. Ensure that all inocula and supernatants generated post infection are inactivated with 5.0% Microchem or approved disinfectant to inactivate all infectious agents.
3. For HFVs, check with institutional policies on inactivation of *Flaviviridae*, since they are positive-sense RNA and pose additional risks. Therefore, RNA isolation and qRT-PCR may have to be performed in containment. However, for negative-sense viruses this method of inactivation is likely acceptable.
4. All samples, including standard curve samples, should be run in at least duplicate.
5. To avoid cross contamination between PCR strip tubes, use filter tips, clean all surfaces and pipettes, and cap each row before moving to next.
6. TF mRNA expression is highly induced following PMA treatment (as described in Subheading 2.3 section). Therefore, the addition of PMA can be used to ensure induction within the given pool of cells and as a positive control.

4.2 Flow Cytometry

1. Use rotors with sealed gaskets and only open rotors post centrifugation in a biosafety cabinet to avoid potentially aerosolizing virus.
2. For this step, it is critical to use a wide pipette tip (such as p1000) to avoid shearing cells. Formalin should also be added to each pellet individually and resuspend immediately to avoid clumping.
3. If using infected cells, or performing the assay in a containment laboratory, cells can be inactivated for 24 h in formalin and then stained following removal from containment. With this option, prolonged fixation may affect signal. Alternatively, cells can be stained in the containment laboratory and then fixed as described in the current protocol.
4. This protocol will measure total TF expression. If cell-surface-only expression is desired, one can omit the permeabilization step; however, this may require re-optimization of the antibody conditions.
5. Standard blocking/FACs buffer can be replaced with a species-specific serum, which should be from animals of the same species as the primary antibody.

6. The 24 h fixation protocol has been performed on cells prior to staining, with some reduction of signal in the basal population. While fixation after TF staining has not yet been performed, it is likely to result in better staining. However, if this approach is desired, it should be optimized with this antigen-antibody prior to infection.
7. As described in the legend of Fig. 2, the 24 h formalin inactivation can be omitted if no infectious agents are involved (and experiment is not conducted in containment). However, the 10 min fixation should be maintained.

4.3 On-Cell ELISA

1. When washing, buffer must be added slowly down the side of the well rather than applied directly to cells as cells can be easily sloughed off. Removing reagents from wells must also be done by pipetting to remove and not by tapping/flicking plate or using a plate washer.
2. Incubation time may vary depending on level of induction in positive control (PMA-treated) samples. However, the 30 min suggested in the protocol is recommended for the detection of basal HUVEC TF levels.
3. The purpose of the CV stain is to account for the number of cells in each well so that the OD405 (TF values) are normalized between wells.

4.4 Vascular Coculture Model

1. To form capillary blood vessels in larger wells, scale up the cell number according to well size while maintaining the ratio of PaSMC to HUVEC.
2. Human mesenchymal stem cells can also be cocultured with HUVEC to form in vitro capillary blood vessels.

4.5 Analysis of Kininogen Cleavage

To examine HK cleavage independently of activated FXII, incubate cells with only PK and HK.

4.6 Measurement of Plasma Prekallikrein and FXII Activation

To examine activation of PK independently of activated FXII, incubate cells with only PK and HK.

4.7 Quantitative Analysis of Bradykinin Formation

1. Inhibitor treatment is required to prevent degradation of BK and prevent binding of BK to its respective receptor. Failure to treat cells will result in inaccurate measurements of BK levels.
2. To measure BK formation independently of FXIIa, incubate cells with only PK and HK.

Disclaimer

Opinions, interpretations, conclusions, and recommendations are those of the author and are not necessarily endorsed by the U.S. Army.

References

1. Paessler S, Walker DH (2013) Pathogenesis of the viral hemorrhagic fevers. *Annu Rev Pathol* 8:411–440. doi:10.1146/annurev-pathol-020712-164041
2. Centers for Disease Control and Prevention. Special Pathogens Branch. (2013) Viral hemorrhagic fevers. <http://www.cdc.gov/ncidod/dvrd/spb/mnpages/dispages/vhf.htm>
3. Versteeg HH, Heemskerk JW, Levi M, Reitsma PH (2013) New fundamentals in hemostasis. *Physiol Rev* 93:327–358. doi:10.1152/physrev.00016.2011
4. Soothikul D, Seksarn P, Pongsewalak S, Thisyakorn U, Lusher J (2007) Activation of endothelial cells, coagulation and fibrinolysis in children with dengue virus infection. *Thromb Haemost* 97:627–634
5. Geisbert TW, Hensley LE, Jahrling PB, Larsen T, Geisbert JB, Paragas J, Young HA, Fredeking TM, Rote WE, Vlasuk GP (2003) Treatment of Ebola virus infection with a recombinant inhibitor of factor VIIa/tissue factor: a study in rhesus monkeys. *Lancet* 362:1953–1958 . doi:10.1016/S0140-6736(03)15012-XS0140-6736(03)15012-X [pii]
6. Geisbert TW, Young HA, Jahrling PB, Davis KJ, Kagan E, Hensley LE (2003) Mechanisms underlying coagulation abnormalities in Ebola hemorrhagic fever: overexpression of tissue factor in primate monocytes/macrophages is a key event. *J Infect Dis* 188:1618–1629 . doi:10.1086/379724JID30697 [pii]
7. National Library of Medicine (2012) vWF Genetics Home Reference U.S. National Library of Medicine. <http://ghr.nlm.nih.gov/gene/VWF>
8. Adams RL, Bird RJ (2009) Review article: coagulation cascade and therapeutics update: relevance to nephrology. Part 1: overview of coagulation, thrombophilias and history of anticoagulants. *Nephrology (Carlton)* 14:462–470. doi: NEP1128 [pii] 1111/j.1440-1797.2009.01128.x]
9. Schattner M, Rivadeneira L, Pozner RG, Gomez RM (2013) Pathogenic mechanisms involved in the hematological alterations of arenavirus-induced hemorrhagic fevers. *Viruses* 5:340–351. doi:10.3390/v5010340
10. Taylor SL, Wahl-Jensen V, Copeland AM, Jahrling PB, Schmaljohn CS (2013) Endothelial cell permeability during hantavirus infection involves factor XII-dependent increased activation of the Kallikrein-Kinin system. *PLoS Pathog* 9:e1003470. doi:10.1371/journal.ppat.1003470. PPATHOGENS-D-13-00307 [pii]

INDEX

A

- A549 cells139, 146, 353, 355, 356
- AC₅₀ 376, 388
- Activated partial thromboplastin times (APTT).....280
- Adaptive immune response
 - cell-mediated immune response340
- Aadjuvant 276, 341
- Administracion Nacional de Medicamentos, Alimentos y
Tecnología Medica (ANMAT).....306–308
- Adventitious agents 312, 323–326
- Aedes*
 - egypti*..... 10, 15
 - albopictus* 15
- Agarose gels..... 60, 67, 200
- Alignment34, 36, 38, 39, 44, 73
- Ammonium chloride138, 139, 147, 149, 151–153
- Amplicons 66, 67, 73
- Amylose resin 181–183, 190, 193
- Animal Biosafety Level 3 (A-BSL-3) 281, 282,
284, 285
- Antibody QC03-BF11160
- Anti-CD16/anti-CD32 antibodies263, 265
- Antiviral
 - compound.....373, 375, 381, 382, 386, 390
 - drugs.....158, 270, 279, 352, 373
 - mechanism.....352
- Arboviruses..... 4, 10–12
 - collection methods.....91, 93
 - vector surveillance.....89–91
- Arenaviridae* 4, 5, 7, 13, 17, 34, 45, 46, 48, 179,
190, 209, 247, 248, 257, 269, 305, 393, 405
- Arenaviruses 12, 34, 57, 58, 73, 101, 103,
113–132, 157, 169, 175, 179, 189, 209, 259, 291, 294,
300, 305, 324, 372, 373, 387, 398, 406
- Arenavirus Z Protein
 - genome218
 - IFN- β promoter-driven luciferase
reporter assay221–222
 - LUJV217
 - materials219
 - NP-Z budding assay.....220–221
 - type I interferon-induction pathway.....218
 - Z self-budding assay220
 - Z-Mediated viral minigenome (MG) replication
and transcription assay.....223–225

- Argentine hemorrhagic fever (AHF)..... 12, 14, 57,
114, 280, 305–327, 371, 406
- Aspartate aminotransferase (AST).....280
- Assessment of vascular permeability.....259

B

- Baby hamster kidney (BHK) cells 140, 141, 296,
332, 334
 - BALB/c mice259
 - Barrier conditions.....308
 - Basic Local Alignment Search Tool (BLAST)
 - alignment method..... 35, 39, 44, 46
 - Bicistronic minigenomes239
 - Bioinformatics 34, 35, 39
 - Biosafety cabinet (BSC)
 - Type II.....63
 - Biosafety level 2-3 (BSL 2-3).....306
 - Biosafety level-2 (BSL-2).....66, 67, 136, 137,
141–144, 152, 209, 259, 282, 284, 393–401
 - Biosafety level-3 (BSL-3).....282, 393
 - Biosafety level-4 (BSL-4).....81, 179, 209, 259,
269, 280, 393
 - Blood collection..... 283, 285, 286, 288
 - Blue Horseshoe Crab312
 - Bradykinin (BK).....406, 409, 414, 416, 417
 - Bronchoalveolar lavage 259–261, 264, 265
 - Bronchoalveolar Lavage Fluid (BALF)
 - Analysis 260, 261, 264, 265
 - BSRT7-5 cells170
 - Budding 213, 352, 373, 375
 - Bulk Vaccine 310, 313, 316–318, 323, 324, 326
 - Bundibugyo ebolavirus*..... 339
 - Bunyaviridae*..... 4, 5, 13, 34, 46, 48, 101, 393, 405
- ## C
- C57BL/6 mice.....258
 - Canal of Hering291
 - Candid #1 (C#1)
 - Candid #1 Bulk Vaccine 306–313, 315–321,
326, 327
 - Candid #1 Filled Product 318–321, 327
 - Category A agent179
 - CC₅₀ 376, 388, 390
 - CD-1 strain308
 - Cell entry..... 135, 394

Cell lines.....248–249
 Cell seeds
 Master Cell Seed (MCS).....310, 314
 Working Cell Seed (WCS)310, 314
 Cell viability120, 126, 140, 150, 298
 Cell-cell fusion157–166, 176
 Cell-entry inhibitors.....394
 Cell-mediated immune response340
 Chikungunya12, 20
 Chloramphenicol acetyltransferase (CAT)239
 Choclo virus101
 Clathrin
 coated pits.....114, 115
 mediated endocytosis.....114, 132, 136, 157
 Clinical samples.....55, 56, 58, 59, 334, 406
 Clone 13 (Cl13)137, 259
 Coagulation14, 280, 288, 405–416
 Colchicine321
 Cold chain57, 65
 Complete blood counts (CBC)288
 Correlates of protective immunity.....340
 Crimean-Congo hemorrhagic fever virus
 (CCHFV).....4, 18, 34, 57, 280
 cell lysis buffer230
 minigenomes231–232
 qRT-PCR.....230–231
 qRT-PCR primers.....233
 RNA extraction233
 tecVLP233
 Ct values125, 336, 380, 410
 CT, ΔCT131, 360, 380, 389
Cuevavirus.....339
 CV-1 cells.....272, 275–277
 Cynomolgus macaques258, 279, 280
 Cytopathic effect (CPE).....65, 69, 72, 82, 162,
 165, 275, 277, 325, 334, 377, 380, 389
 Cytotoxicity213, 260, 374–376

D

Databases
 European sequence database (EMBL)34
 Japanese sequence database (DDBJ).....34
 US sequence database (GenBank).....35
 Virus Pathogen Resource (ViPR).....34
 DBS-FRhl2310
 DC-specific ICAM-3 grabbing nonintegrin
 (DC-SIGN)136
 Delivery methods341
 Dengue virus (DENV).....5, 10, 12, 15, 51,
 59, 61, 70, 281, 331–334, 336, 352, 356, 357,
 360–362, 366, 367, 406
 4',6-diamidino-2-phenylindole (DAPI)
 solution122, 130, 131, 140, 203, 206,
 296, 301, 323, 353, 357, 358, 360, 367, 378

Double-stranded RNA (dsRNA)194, 195
 Dystroglycan (DG)135, 136, 152, 170

E

Ebola virus (EBOV).....237, 239, 240
 virus disease (EVD).....10, 13, 16, 21
 Electron microscopy (EM)114, 119, 120,
 122, 125, 126, 374, 386, 387
 Electroporation.....340–346
 Eliminate red blood cells297
 Emerging.....13, 17, 18, 20, 21, 24,
 27, 158, 160, 258
 End of Production Passage (EOPP).....314, 315
 Endocytosis pathways
 Rab5 early endosomes114, 121
 Rab7 late endosomes114
 Endosomal sorting complex required for
 transport (ESCRT)136
 Endosomes114, 129, 136, 138, 139,
 151–153, 157, 170
 Endotoxin test312
 Enhanced green fluorescent protein
 (EGFP)137, 144–147, 149, 151,
 152, 170, 173, 174, 176–178, 394, 397–400
 Envelope glycoprotein115, 130, 157, 169, 340
 Zoonotic diseases12
 EpCAM (CD326).....301
 Epidemic
 predicting risk of.....21
 Epidemiological
 linkage criteria57
 Evan's Blue dye.....260, 263, 264, 283
 eVP40.....210, 211, 213
 3'-5'exoribonuclease (RNase)180, 190
 Extracellular matrix (ECM)135, 136

F

Factor XII (FXII)406, 408, 409, 414, 416
 Factor XIIa (FXIIa).....416
 FcγR.....332, 334
 Femoral vein283, 284, 286
 FIJI software for microscope images364–366
 Filoviridae
 Ebola virus (EBOV).....16, 210, 258, 270, 340
 Marburg virus (MARV).....339
 Filoviruses.....34, 57, 58, 103, 209, 258, 270,
 276, 279, 324, 339, 340, 394, 398, 406
 Firefly luciferase assay.....171, 174, 198
Flaviviridae.....4, 5, 7, 13, 34, 48, 50–52,
 257, 269, 393, 405, 415
 Freeze-drying319
 FRhl-2311, 314–317, 325
 Fruit bat (*Rousettus* spp.)16
 Fusion.....157, 158, 162–166

- Fusion inhibitors.....158, 165
FVB mice259
- G**
- GenBank34, 35, 39, 43, 45–49,
51, 123, 206, 271
- Genetic trees
bootstrap.....37, 40
maximum likelihood.....40
maximum parsimony.....40
- Geographic information system (GIS)
ArcGis104
design surveillance.....94–95
mosquitoes trap94
QGIS.....104
surveillance design.....93–94
vector surveillance.....89–91
- Global expansion of diseases
dengue fever.....4, 8, 79, 281
Ebola virus disease.....9, 13, 16
West Nile Virus.....352
yellow fever.....4, 34, 57, 60, 61, 64, 65
- Glycoprotein precursor complex (GPC).....114, 123,
137, 158, 160–166, 169–177/180
- Good Manufacturing Practice (GMP).....306, 313, 327
- Guanarito virus.....101, 269
- Guinea pig-adapted isolate.....270, 272
- Guinea pigs10, 69, 171, 172, 258, 277,
309, 311, 315, 317, 324, 325
- H**
- Hantaan virus101
- Hantavirus
hyperimmune mouse ascitic fluid (HMAF)63
primary immune serum69
Sin Nombre virus.....101
- Hantavirus Pulmonary Syndrome (HPS).....101
- Hartley guinea pigs.....309
- Heme-adsorption test.....315, 326
- Hemorrhagic fever (HF)4–28, 33–40, 43, 55,
81, 101, 114, 157, 202, 213, 269–277, 288, 301, 305,
369, 373, 401, 416
- Hemorrhagic fever virus (HFV).....4, 33, 43–52,
81, 157, 202, 209–213, 288, 301, 369, 373, 416
- Hemorrhagic fever with renal syndrome
(HFRS).....17, 101
- HEPA-filtered isolation room.....282
- HEPA-filtered rooms.....284
- Hepatic stem/progenitor cells (hHSPCs).....292, 293,
298–300
- HepG2 cells.....293, 294, 300
- Herd immunity.....10
- High throughput screening (HTS)373, 395, 396
- Hormonally defined medium (HDM)293, 295
- Human liver291–301
- Human liver stem cells (HLSCs).....292
- Human umbilical vein endothelial cell
(HUVEC)406–414, 416
- Humoral immunity340
- I**
- IC₅₀.....388
- IFN- β promoter-driven luciferase
reporter assay221–222
- Immunocompetent mice258, 259
- Immunocompromised mice.....258, 259
(mice lacking) class I MHC molecules
(MHC-I $^{-/-}$).....259
(mice lacking) receptors for both type I and type II
interferons (AG129)258
mice lacking the receptor for type I interferons
(IFNAR $^{-/-}$)258
(mice lacking) the signal transducer and activator of
transcription 1 (STAT1 $^{-/-}$).....259
- Immunofluorescence (IF) microscopy63, 68, 69,
122, 130, 293
- Incubation period10, 11, 70, 83
21 d standard10
- Incubation periods.....334, 336
- Inhibitors126–129, 138, 139, 141,
150–153, 158, 160, 163, 165, 181, 190, 191, 211, 212,
260, 264, 354, 355, 361, 366, 372, 373, 406, 408,
409, 416
- Inhibitory121, 372
- Institutional Animal Care and Use Committee
(IACUC)265, 287
- Instituto Nacional de Enfermedades Virales
Humanas (INEVH)306, 321
- Intergenic regions (IGR)248
- Interleukin-6 (IL-6)260, 280
- International Committee on Taxonomy of
Viruses (ICTV)43, 44, 46–48, 51
- Intradermal (ID)106, 324, 340, 342–345
- Intragastric (i.g.)283, 285
- Intramuscular (i.m.).....280, 282–284, 288,
340, 342, 343, 347
- Intraperitoneally (IP).....273, 323–325
- Intravenous (i.v.).....261, 264, 280,
282–284, 288, 371
- J**
- Juin \acute{a} n virus (JUNV).....101, 114, 115, 123,
169, 257, 269, 305, 306, 310, 311, 317, 323, 326, 406
- K**
- Kininogen (HK)408, 414, 416
- Kupffer cells.....291, 299
- Kyasatur Forest disease virus.....269

L

LAG-3263
 LARGE gene135
 Lassa virus (LASV).....80–83, 135–153, 163,
 166, 169, 170, 179, 180, 184, 185, 189, 190, 195, 199,
 259, 269, 291, 371, 372
 Lassa virus and Lujo virus (LUJV).....217
 LCMV-Armstrong 53b strain
 (LCMV-ARM)283, 296
 LCMV-WE 280, 283, 291, 293, 294, 296, 300
 LD₅₀ values275
 Lectins.....136
 human C-type lectins (hDC- and hL-SIGN).....114
 Life cycle modeling system.....237
 Like virus-like-particles (VLP)373
 Lipid droplets (LD).....352, 355, 362–366, 369
 Lithium-Polyethylene glycol (Li-PEG).....182, 185
 Lloviu virus (LLOV)339
 LSECTin, a C-type lectin136
 Luciferase reporter.....137, 170, 190, 192, 197–199
 Luciferase reporter gene198
 Lujo virus269
 Lymphocytic choriomeningitis virus (LCMV)248
 LCMV-Armstrong (LCMV-ARM) 259, 264,
 283, 296, 300
 LCMV-clone 13 (LCMV-C113)..... 259, 261, 262
 LCMV-WE 280, 283, 291, 293, 294, 296, 300

M

Machupo virus (MACV)101, 269
 MagMax RNA extraction kit230
 Magnetic cell selection295, 299
 Maltose binding protein (MBP)
 MBP-NP fusion protein.....183, 187, 199
 Marburgvirus.....237
 Marburg virus (MARV).....15, 16, 57, 258, 339
 Ravn virus (RAVV)339
 Marmosets.....258, 279
 Master Cell Seed (MCS).....310, 314, 315
 Matrix protein135, 218, 387
 Membrane fusion157, 169, 170, 175, 176
 Methylene blue dye333
 MG assay.....190, 192, 195–197
 MGLF7-5Rluc3 plasmid192, 195
 MHC tetramer259, 260, 265
 Microscopy116–120, 122, 124–126, 130,
 173, 175, 177, 178, 203, 204, 210, 293, 296, 300, 301,
 353, 363, 374, 386, 387, 398
 Minigenome (MG) system.....190, 195, 197, 198, 394
 cRNA antigenomes239
 ebolaviruses.....237, 240
 filovirus minigenome systems237
 materials240
 miniature versions.....238

polycistronic.....239
 replication-competent and
 replication-deficient.....238
 reporter activity.....241–242
 vRNA239
 6-well format240–241
 96-well format241–242
 Modal number of chromosome315, 317, 321
 Molecular adjuvants.....341–345
 Molecular Evolutionary Genetic Analysis
 (MEGA) software35, 36, 39, 40
 Monoclonal antibodies (mABs)140, 143,
 148, 149, 153, 160, 162, 165, 270–272, 276, 277, 296,
 299, 300, 372
 Monoclonal antibody HEA-125301
 Mopeia/Lassa reassortant virus (ML29)82–84
 as attenuated Lassa vaccine.....82
 as ELISA antigen82
 Mosquitoes
 field trapping96–97
 trapping94
 Mouse eye bleeds.....259
 Mouse model.....258, 259
 MRC-5.....310, 314, 325
 mRNA Isolation407
 MTS374–376, 389
 Multiplexed probe detection.....204
 Multiplicity of infection (MOI)123–126, 128,
 129, 141, 144, 146, 148, 149, 151, 161, 204, 293, 300,
 316, 356, 357, 360–362, 366, 367, 376, 381, 382, 384,
 386, 409, 414
Mycobacterium312, 315, 317, 323, 324
Mycoplasma.....312, 315, 317, 323

N

National Center for Biotechnology
 Information (NCBI).....34, 35, 39, 43, 44, 47, 50, 51
 Neutralization test (NT).....69–71, 74, 82, 131
 N-linked glycosylation.....175
 Nonhuman primates (NHP)81, 258, 270,
 279–284, 287, 288, 291, 343–345, 406
 Normal human primary hepatocytes
 (hNHep) cells296, 300
 Nosocomial infections11
 Nosology13
 NP-Z budding assay.....220–221
 Nucleoprotein (NP).....187, 189–200
 NZB mice.....264
 NZB mouse.....259, 262

O

Optimal cutting temperature (OCT)
 tissue-freezing medium.....284, 287
 Osmolality320, 326

Outbreak
 2000 outbreak in Gulu, Uganda270
 2014-16 EBOV disease outbreak in West Africa270
 Oval cells291

P

Pairwise sequence comparison (PASC) analysis43
 Pandemic
 AIDS7, 8
 influenza6, 25
 Parenchymal cells291, 297, 299
 pCAGGS192, 210
 pCAGGS-GPC plasmid170, 172, 173
 pCMV-EGFP173
 PD-1263
 Perfusion263, 265, 292, 294, 297
 Peripheral blood mononuclear cells
 (PBMC)64, 288
 Personal protective equipment (PPE)282, 284, 335
 Petechial rash79, 80, 280, 282
 pH determination319, 327
 pHR'-eGFP174
 Phylogenetics. *See . See* Genetic trees
 Pichindé virus (PICV)218-225
 amplification251
 bisegmented/trisegmented249, 250, 252, 253
 cell lines248-249
 cis-acting elements247
 equipment249
 media248-249
 P18197, 198
 P2197, 198
 plasmids248-249
 reagents and buffers249
 RNA virus247
 Z protein247
 Pit cells291
 PL/J mice259
 Plaque assays107, 127, 128, 250, 251,
 276, 296, 300, 333, 334, 353, 357, 377, 378, 389
 Plaque-forming units (PFU)70, 83, 115,
 116, 122-124, 128, 129, 140, 144-149, 151, 261,
 262, 264, 280, 283, 293, 296, 300, 326, 334, 357, 378,
 380-383, 387-389
 Plaque Titration Assay332-333
 Plasmids248-249
 Platelet counting259, 260, 262
 pLOU3 vector180, 190
 Polyethylene glycol (PEG)59, 65, 73, 103,
 140, 142, 182
 Polyvinylidene difluoride (PVDF) membrane354, 385
 Powder air-purifying respirator (PAPR)102, 105
 Prekallikrein (PK)408, 409, 414, 416
 Primary infection331

Primary tissue cultures309-310
 Primer-Blast359
 Prognostic disease marker280
 Prothrombin times (PT)280, 288
 Pseudotypes114-116, 123, 127, 130,
 137, 144-147, 149, 151-153, 394, 396-401
 pT7-Fluc170, 173
 PVDF membrane171, 172, 362, 385

Q

Quality Control/ Quality Assurance
 (QC/QA)306, 312, 315-318, 320-327
 Quantitative Polymerase Chain Reaction
 (qPCR)108, 354, 360
 Quantitative real time PCR (qRT-PCR)125, 272-274,
 276, 333, 334, 359, 360, 378-380, 383, 384, 407,
 410, 415

R

Receptor recognition136
 Receptors113, 114, 120, 126, 127, 131,
 135-138, 146, 147, 152, 157, 158, 169, 299, 394,
 409, 416
 Reed and Muench method275, 326, 388
 Renilla Luciferase Assay225
 Reproductive ratio or *R*₀9
 Residual moisture317, 320, 327
Reston ebolavirus (REBOV),339
 Restriction factors351-369
 Retro-orbital puncture261, 262
 Retroviral vectors152
 Reverse genetics (RG) system237, 248
 Reverse-transcriptase polymerase chain reaction
 (RT-PCR)38, 56, 57, 59, 60, 66, 67,
 73, 81, 332-336, 353, 354
*R*_{factor} and *R*_{free}187
Rhabdoviridae4, 5, 13, 46-49
 Rhesus macaque model279-282
 Rhesus macaques81, 280
 Ribavirin (RIB)14, 270, 371
 Ribonucleoprotein (RNP)136, 180
 Rift Valley fever virus (RVFV)258
 Risk factors (epidemiological linkage criteria)21, 23,
 24, 27, 56, 57
 Risk-group
 risk-group 357
 risk-group 457
 RK-13310, 325
 RNA fluorescence in situ hybridization
 (FISH)201-207
 RNA interference (RNAi)136, 352
 RNA isolation59, 73, 333, 409, 415
 RNA localization203
 Roboviruses101-108

S

Sabiá virus 34, 57, 269
 Saline injections 283, 287
 Sampling 58, 71, 102, 281, 283, 285–288
 Saphenous vein 283–286
 SDS-PAGE 63, 64, 71, 72, 75, 149, 172, 181, 184, 185, 193, 211, 212, 362, 368, 385, 387
 Secondary infection 331
 Select Agents 13, 16
 Selectivity index (SI) 390
 Sendai virus (SeV) 192, 198, 199
 Serial passaging 258, 270, 271, 273, 276
 Serotypes 15, 61, 69, 70, 73, 331
 Sherman live traps 102, 108
 Sin Nombre virus (SNV) 63, 68, 101
 Single-stranded RNA (ssRNA) 194, 195, 393
 siRNA 353, 355, 356, 372
 Sitting drop vapor diffusion method 181, 184
 SJL mice 259
 Smallpox
 Amerindians 8
 Antonin plague 6
 Space group 186, 187
 Species demarcation 47, 51, 52
 Specific pathogen-free (SPF) 306, 308–310
 Stable signal peptide (SSP) 158, 161, 163–165, 169
 Stellate (Ito) cells 291
 Stem cells 294, 295, 416
 Structure activity relationship (SAR) 373
 Structure–function assays
 CCHFV 229
 tecVLPs 229–230
 Subcutaneous (s.c.) 261, 269, 280, 283, 287
 Subtilisin kexin isozyme-1/site-1 protease (SKI-1/S1P) 158, 180, 372
 Sudan ebolavirus 339
 Sudan virus (SUDV) 270–274, 276, 277
 Surveillance
 clinical 55
 ELISA 56, 57, 60–63, 67, 68, 71, 73, 74
 GIS 89–91, 93, 94
 mosquito trapping methods 92
 of rodent-borne viruses (roboviruses) 101
 Syncytium formation 158, 163

T

Tai Forest Virus (TAFV) 339
 Taxonomy
 demarcation criteria 44, 46–48
 TCID₅₀ 273, 275, 377, 388
 TEV cleavage 183
 TEV protease 181, 190, 193
 TIM-3 263
 Tissue biopsies 281, 286, 287

Tissue culture infectious doses for 50% of the cultures (TCID₅₀) 280, 377
 Tissue factor (TF) 406, 407, 409–413, 415, 416
 Tomahawk Trap 102
 Total Internal Reflection Fluorescence (TIRF) microscopy 210, 212
 Transcriptome 81, 280
 Transferrin receptor (TfR1) 114, 116, 120, 124, 127, 169
 Trapping methods 91, 101, 102, 104, 105, 108, 912
 Trypan blue exclusion assay 298
 Tumorigenicity 315, 317, 322
 TurboFISH 204
 Tyro3/Axl/Mer (TAM) 136

U

Unformulated Candid #1 Bulk Vaccine 311, 313

V

Vaccine potency 326
 Vascular Leak Assessment 260, 263, 264
 Vascular leakage 257, 259, 264, 280, 281
 vCB21R-LacZ vaccinia virus 159, 161, 162, 164
 Vectors
 Moloney murine leukemia virus (MoMLV) 119, 137, 394–396, 400
 mosquito 8, 10, 11, 14, 15, 18, 57, 257
 retroviral 152
 rodent 10, 12, 14, 17
 tick 10, 14, 17, 18, 23, 257
 vesiculoviruses 325, 394
 Vero C76 310, 314, 325, 326
 Viral entry 113, 114, 120–122, 135–138, 352, 371, 383
 Viral hemorrhagic fever (VHF) 4, 10, 12–18, 24, 33, 44, 48, 55–75, 101, 257–265, 269–271, 279–288, 291, 294, 393, 405
 Viral RNA detection 202
 Viral seed
 Master Viral Seed (MVS) 315–317, 323, 324, 326
 Working Viral Seed (WVS) 306
 Viral titration 318, 319, 326
 Virus budding 219
 Virus classification 44
 Virus entry 114, 121, 122, 126–129, 140, 141, 158, 373, 374, 394
 Virus isolation 58, 59, 64, 65, 68, 72, 73, 82, 107
 Virus replication 10, 80, 351
 Virus titers 142, 153, 259–262, 265, 300, 334, 357
 Virus yield inhibition assay 381, 382
 Virus–Antibody Immune Complexes 331–336
 Virus-like particle (VLP) 115, 116, 170, 174, 175, 177, 178, 209, 211, 212
 Virus-like particle (VLP) budding assay 209–211, 387
 Virus-like particles (VLP) 341

Volumes of blood allowed for withdrawal.....288
 VP40vTF7-3 vaccinia virus 161, 164
 Vulnerability 4, 9–12, 18–20

W

West Nile virus 12, 51
 Western blot (WB), 63, 64, 68, 71, 72, 74, 75,
 82, 147, 153, 175, 211, 212, 354, 355, 361, 362, 366,
 368, 384–386, 414
 Working Cell Seed (WCS) 310, 314, 315
 World Health Organization (WHO)
 Department of Pandemic and Epidemic Diseases
 (PED).....20

X

X-ray structure.....179–187
 XTT assay213

Y

Yellow fever virus (YFV).....12, 14, 15, 57,
 257, 269

Z

Zaire ebolavirus..... 339
 Zika virus.....12
 ZMapp270
 Z-mediated viral minigenome (MG) replication and
 transcription assay
 in vitro RNA transcription223
 plasmid transfection.....224
 renilla luciferase assay225
 Zoonotic diseases..... 11, 14
 Zoonotic viruses 11, 14, 18, 33, 56, 57,
 108, 135, 137